Development of Synthetic Methods and Electrochemical Cells Based on Organic Electron Transfer Reactions

A Thesis

Submitted for the Degree of

DOCTOR OF PHILOSOPHY

By

MASILAMANI SHANMUGARAJA

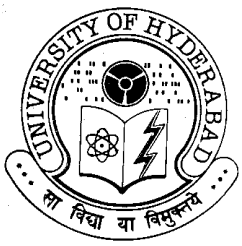

SCHOOL OF CHEMISTRY

UNIVERSITY OF HYDERABAD

HYDERABAD-500 046

INDIA

OCTOBER 2018

Dedicated to

My Father S. Masilamani

And

My Mother M. Chandra

Contents

Chapter 1

General Introduction on Electron Transfer Reactions

Chapter 2

Synthetic Methods based on Electron Transfer Reactions Using Oxygen Adsorbed Carbon Materials and *p*-Doped Polythiophene

Chapter 3

Studies on the Reaction of Amines with Quinones, Viologen and halo compounds

Chapter 4

Development of Electrochemical cell exploiting reversible electron transfer reaction between tertiary amine donors and *p*-chloranil acceptors

School of Chemistry
University of Hyderabad
Central University P.O.
Hyderabad 500046
India

STATEMENT

I hereby declare that the matter embodied in this thesis is the result of investigations carried out by me in the School of Chemistry, University of Hyderabad, Hyderabad, under the supervision of **Professor M. Periasamy**.

In keeping with the general practice of reporting scientific observations, due acknowledgment has been made wherever the work described is based on the findings of other investigators.

Hyderabad

October 2018

MASILAMANI SHANMUGARAJA

School of Chemistry
University of Hyderabad
Central University P.O.
Hyderabad 500046
India

DECLARATION

I, **MASILAMANI SHANMUGARAJA** hereby declare that this thesis entitled "**Development of Synthetic Methods and Electrochemical Cells Based on Organic Electron Transfer Reactions**" submitted by me under the guidance and supervision of **Professor M. Periasamy** is a bonafide research work which is also free from plagiarism. I also declare that it has not been submitted previously in part or in full to this University or any other University or Institution for the award of any degree or diploma. I hereby agree that my thesis can deposit in Shodganga/INFLIBNET.

A report on plagiarism statistics from the University Librarian is enclosed.

Date:

Name:

Signature of the Student:

Regd. No.:

Signature of the Supervisor:

School of Chemistry
University of Hyderabad
Central University P.O.
Hyderabad 500046
India

CERTIFICATE

This is to certify that the thesis entitled "**Development of Synthetic Methods and Electrochemical Cells Based on Organic Electron Transfer Reactions**" submitted by **Mr. Masilamani Shanmugaraja** bearing registration number **10CHPH23** in partial fulfillment of the requirements for award of Doctor of Philosophy in the School of Chemistry is a bonafide work carried out by him under my supervision and guidance.

This thesis is free from plagiarism and has not been submitted previously in part or in full to this or any other University or Institution for the award of any degree or diploma. Further the student has two publications before the submission of his thesis.

Parts of this thesis have been published in the following two publications:

1. Periasamy, M.; **Shanmugaraja, M**.; Obula Reddy, P.; Ramusagar, M.; Ananda Rao, G. ***J. Org. Chem.*, 2017**, *82*, 4944.
2. Periasamy, M.; Obula Reddy, P.; **Shanmugaraja, M.** ***Chemistryselect.***, **2017**, *2*, 7615.

He has also made presentations in the following conferences:

1. Synthetic Transformations Using Molecular Oxygen Adsorbed Carbon Materials; Selected as **Best Poster Presentation** in the *Chemfest-2018* held at School of Chemistry, University of Hyderabad, INDIA,
2. Borane Lewis Base Complexes by the Reaction of Oxidatively Doped Polymers with Sodium Borohydride and Lewis Bases; Poster Presentation in the *Chemfest-2018* held at School of Chemistry, University of Hyderabad, INDIA.

Further the student has passed the following courses towards fulfillment of coursework requirement for Ph.D.

	Course	Title	Credits	Pass/Fail
1.	CY-801	Research Proposal	3	Pass
2.	CY-806	Instrumental Methods B	3	Pass
3.	CY-841	Reactive Intermediates and Synthesis in Organic Chemistry	3	Pass
4.	CY-844	Organometallic and Bioinorganic Chemistry	3	Pass

Hyderabad
Date:

Prof. M. Periasamy
(Thesis Supervisor)

Dean
School of Chemistry
University of Hyderabad
Hyderabad 500 046
INDIA

Acknowledgements

I take immense pleasure in expressing my heartfelt gratitude and indebtedness to my thesis supervisor **Prof. M. Periasamy** for his constant guidance, inspirations, encouragements and support throughout my tenure here.

I extend my heartfelt thanks to Prof. D. Basavaiah, Prof. M. V. Rajasekharan, Prof. M. Durga Prasad and Prof. T. P. Radhakrishan Deans, School of Chemistry, for providing all the necessary facilities to carry out my research work. I am thankful to my doctoral committee members Prof. D. B. Ramachary and Prof. R. Nagarajan for their generous support.

I would like to thank Prof. S. Muthusubramaniam, School of Chemistry, Madurai Kamaraj University, for his inspiring teaching and also supervised my M.Sc., project work during my M.Sc., Chemistry in MKU. I also thank all the other faculty members of the chemistry department for their excellent teaching. I take this opportunity to thank Prof. R. Anantharam, Dr. S. Sevaga Pandian, Dr. T. Sugumaran, Dr. M. Meenakshisundaram, Dr. P. Velusamy, Dr. A. Vanangamudi and Dr. T. Bhupathi Ganesh for inspiring teaching during my B.Sc., Chemistry in ANJA College.

I wish to thank my senior colleague Dr. Mallesh Beesu for his help during the initial stages of my research. I extend my sincere thanks to my past and present labmates Dr. P. Vairaprakash, Dr. Shaik Anwar, Dr. S. Selva Ganesan, Dr. Sakilam Satishkumar, Dr. M. Nagaraju, Dr. Mallesh Beesu, Dr. N. Sanjeeva Kumar, Dr. Guru Brahmam, Dr. Manasi Dalai, Dr. A. Laxman, Dr. P. Obula Reddy, Dr. A. Edukondalu, Mr. M. Ramusagar, Mr. V. Harish, Mr. G. Ananda rao, Mr. B. Uday Kumar, Mr. I. Satyanarayana, Mr. L. Mohan, Mr. E. Ramesh, Mr. Yesu and Mr. Srinivas for creating a pleasant working atmosphere.

All the research scholar of the school of chemistry has been extremely helpful, I thank them all. I specially thank Dr. Viji, Dr. Vignesh, Dr. Santhanam, Dr. Ramesh, Dr. Prakash, Dr. Sudalai kumar, Dr. Ramkumar, Dr. Srinu, Mr. Prabahar, Mrs. Tamilarasi, Mr.

Sakthivel, Mr. Satish, Mr. Tamilarasan, Mr. Arumugam and A to Z are to mention. I also thank all my Tamil friends of University of Hyderabad.

All the non-teaching staff of the School has been helpful, I thank them all. Mr. S. Thurabuddin, Mr. Kumar, Mr. Shetty, Mr. S. Satyanarayana, Mrs. Vijaya Lakshmi, Mr. V. Bhaskar Rao, Mr. Asia Parwez, Mr. Vijaya Bhaskar, Mr. Mr. A. Dilip Kumar Mr. B. Anandam, Mr. Durgesh and Mr. Abraham.

I specially thank all of my M.Sc classmates for their help and thoughtful discussion during my M.Sc., days. Dr. S. Manojveer, Dr. B. Muthuramalingam, Dr. Kannan, Dr. Sankar, Dr. Bharathi Raja, Dr. Ganapathi, Dr. Suresh, Dr. Sivraman, Dr. Pandiyarajan, Dr. Solai selvi, Mrs. Sudha are few to mention.

I wish to express my gratitude and acknowledge the contribution of my parents Mr. S. Masilamani and Mrs. M. Chandra for their support, affections and caring throughout my life. I always thank my sisters Mrs. M. Malathi and Mrs. A. Selvakumari for their affections and caring. I especially thank my wife and life partner S. Anubala for her patience, affection and caring, all the time. I also thank my children Ishani and Arivas for their unconditional love and they always make me happy.

I wish to extend my sincere thanks to the University authorities for providing all the necessary facilities for this work especially for providing EPR and Impedance instrument.

Finally, I would like to thank the UGC, New Delhi for the financial support during my tenure. Also, financial assistance from the research grant of DST-SERB and DST-JC BOSE National fellowship of Prof. M. Periasamy is gratefully acknowledged.

MASILAMANI SHANMUGARAJA

Abbreviations

Ac	acetyl
AC	activated carbon
Al	aluminium
anhyd.	anhydrous
aq.	aqueous
Ar	aryl
Bn	benzyl
BQ	1,4-benzoquinone
br	broad (in spectroscopy)
Bu	butyl
CAN	ceric ammonium nitrate
CAS	ceric ammonium sulphate
CB	carbon black
CT	charge transfer
DABCO	1,4-diazabicyclo[2.2.2]octane
DDQ	2,3-dichloro-5,6-dicyano-p-benzoquinone
DiPrBA	*N*,*N*-diisopropylbenzamide
DIPEA	*N, N*-diisopropylethylamine
d	doublet (in spectroscopy)
DMF	*N*,*N*-dimethylformamide
DMSO	dimethyl sulfoxide
EC	ethylene carbonate
EPR	electron paramagnetic resonance
ET	electron transfer
equiv	equivalent
Et	ethyl
FF	fill factor
h	hour(s)
IR	infrared
J	coupling constant (in NMR spectroscopy)
m	multiplet (in spectroscopy)

Me	methyl
min	minute(s)
mp	melting point
NMP	N-methyl-2-pyrrolidone
NMR	nuclear magnetic resonance
NQ	1,4-naphthaquinone
PC	propylene carbonate
PEO	polyethylene oxide
PMMA	poly(methyl methacrylate)
PTMA	poly(2,2,6,6-tetramethylpiperidinyloxy-4-yl methacrylate)
Nu	nucleophile
Ph	phenyl
$PhNEt_2$	*N,N*-diethylaniline
ppm	parts per million
Pr	propyl
q	quartet (in spectroscopy)
ref	reference number
rt	room temperature
s	singlet (in spectroscopy)
sec	secondary
SET	single electron transfer
soln	solution
SS	stainless steel
T	temperature
TEMPO	(2,2,6,6-tetrmethylpiperidin-1-yl)oxyl
t	tertiary
t	triplet (in spectroscopy)
THF	tetrahydrofuran
TMPDA	*N,N,N',N'*-tetramethylethylenediamine
TPA	triphenylamine
TMS	trimethylsilyl
UV	ultraviolet

Abstract

This thesis entitled "**Development of Synthetic Methods and Electrochemical cells Based on Organic Electron Transfer Reactions**" comprises of four chapters. The first chapter describes the **General Introduction** and **References** on electron transfer reactions in organic chemistry. The second, the third and fourth chapter is subdivided into four sections namely **Introduction**, **Results and Discussion**, **Conclusions** and **Experimental Section** along with **References**. The work described in this thesis is exploratory in nature.

The second chapter describes studies on the reaction of oxygen adsorbed carbon materials and p-doped polythiophene with $NaBH_4$ and amine donors. The reaction of molecular oxygen adsorbed carbon black (CB) with triphenylphosphine (Ph_3P) in presence of benzoic acid gives the triphenylphosphine oxide ($Ph_3P=O$) in 52% yield. Whereas molecular oxygen adsorbed activated carbon (AC) gave 54% yield of $Ph_3P=O$ but in the case of graphite no $Ph_3P=O$ formation was observed (Scheme 1).

Scheme 1

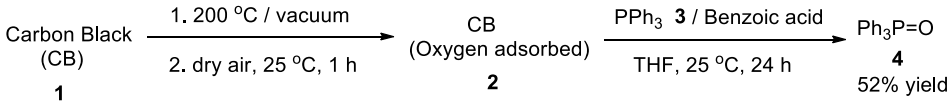

Oxidation of alkyl boranes using molecular oxygen adsorbed carbon black (CB) in presence of NaOH gave the corresponding alcohols or aldehydes in 53-86% yield. Similar reaction with molecular oxygen adsorbed activated carbon (AC) gave the corresponding alcohols or aldehydes in 68-99% yield (Scheme 2). The molecular oxygen adsorbed carbon materials are expected to react with NaOH to give the HOO^-Na^+ species for the oxidation of organoboranes.

Scheme 2

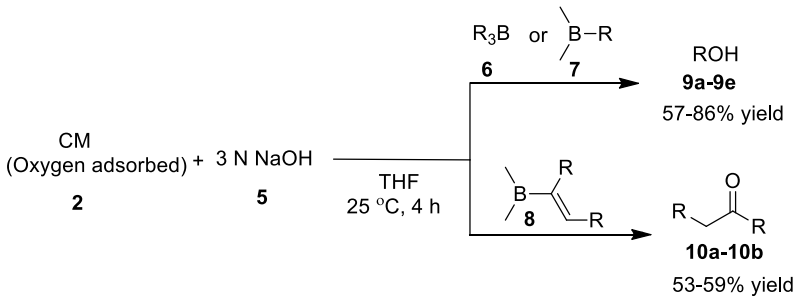

The reaction of oxygen adsorbed carbon materials with $NaBH_4$ in THF leads to slow evolution of hydrogen gas indicating the formation of the AC*-O-O-BH_3 which could react with Ph_3P or amine to give the Ph_3P:BH_3 or amine:BH_3 complex. Under optimized conditions, the oxygen adsorbed carbon black gave the Ph_3P:BH_3 complex in 35-73% yield. In the case of oxygen adsorbed activated carbon, the Ph_3P:BH_3 complex was obtained in 21-77% yield. Similarly, the reaction of oxygen adsorbed carbon black with $NaBH_4$ in the presence of pyridine gave pyridine:BH_3 complex in 52% yield (Scheme 3). Also, the reaction of oxygen adsorbed activated carbon with benzylamine gave benzaldehyde in 30% yield *via* the formation of amine radical cations.

Scheme 3

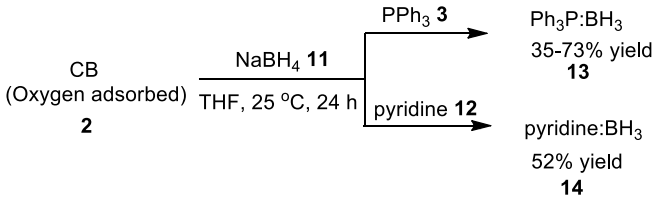

A simple method was developed for estimating the doping levels in polythiophene radical cation salt **16** using $NaBH_4$. For example, the reaction of polythiophene salt **16** with $NaBH_4$ and PPh_3 in THF gave the Ph_3P:BH_3 complex in up to 1.70 mmol (34-72% yield).

Accordingly, it can be concluded that a minimum of approximately 1.7 mmol of radical cation sites are present in 1 g of $PT^{(.+)}{}_m\ nCl^-$. Whereas the reaction of $NaBH_4$ and polythiophene salt **16** in presence of pyridine afforded the pyridine:BH_3 complex in 35-79% yield (Scheme 4).

Scheme 4

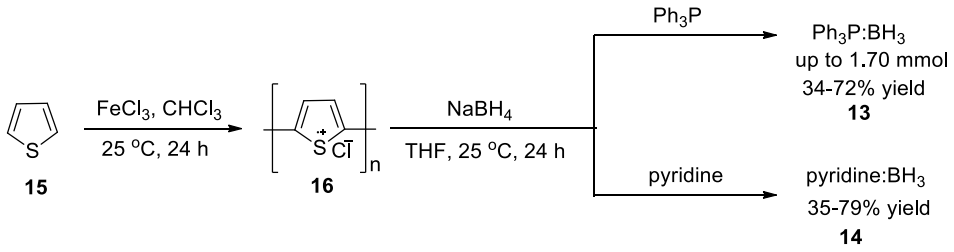

In the third chapter, we have described the studies on electron transfer reaction of amine donors with acceptors like quinones, halomethane and viologen derivatives. The reaction of secondary amine like piperidine with quinones gave the corresponding diamagnetic aminoquinone *via* the formation radical cation and radical anion intermediates (Scheme 5). The intermediacy of radical ion pair was confirmed by epr spectroscopy.

Scheme 5

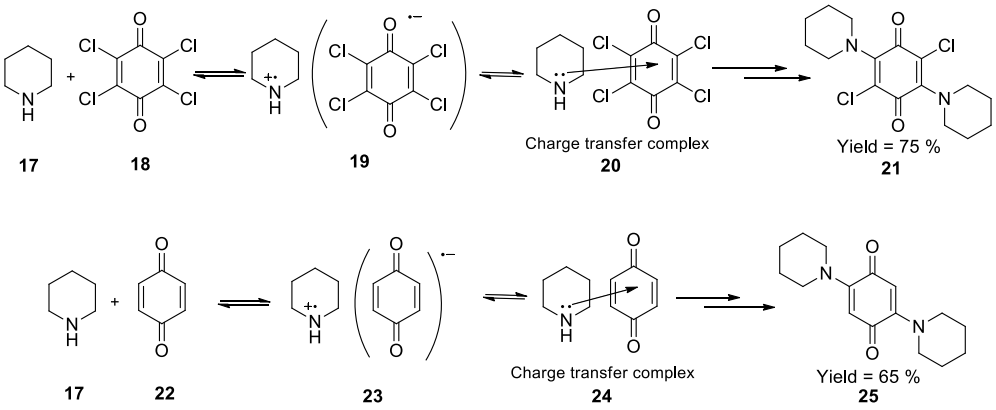

Similarly, the reaction of tertiary amines and *p*-chloranil gave the corresponding charge transfer complexes *via* initially formed radical cation-anion pair as revealed by epr spectroscopic studies (Scheme 6).

Scheme 6

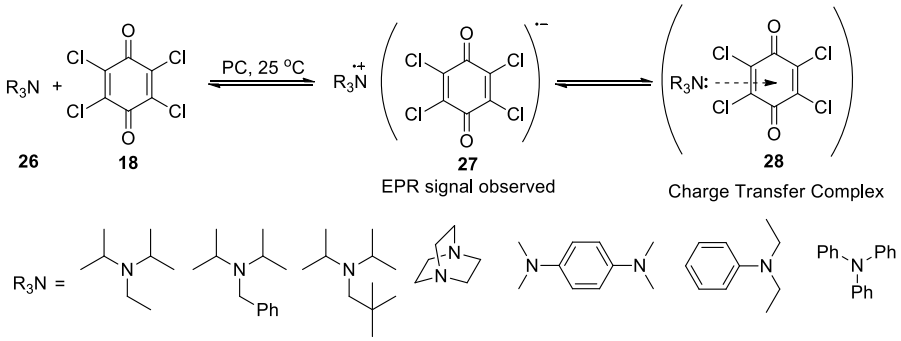

A simple, convenient method was developed to synthesize polymer containing amine as a pendant group through transesterification of PMMA (polymethyl methacrylate) **29** using 4-hydroxy-2,2,6,6-tetramethylpiperidine **30**. The polymeric amine **31** is readily converted to the corresponding TEMPO derivative **32** by oxidation with *m*-CPBA (Scheme 7).

Scheme 7

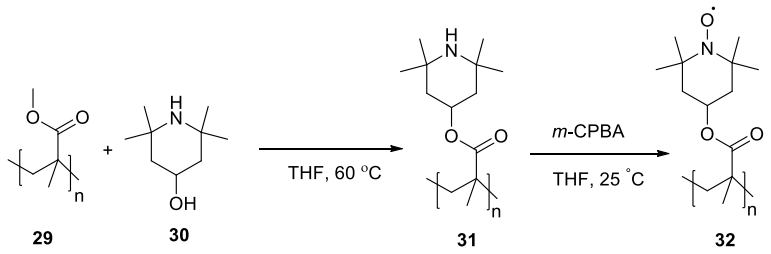

The sterically hindered polymeric 2,2,6,6-tetramethylpiperidine reacts with *p*-chloranil to give the radical ion intermediates followed by charge transfer complex. The radical ion intermediates gave triplet in epr spectroscopy corresponding to the presence of amine radical cation (Scheme 8).

Scheme 8

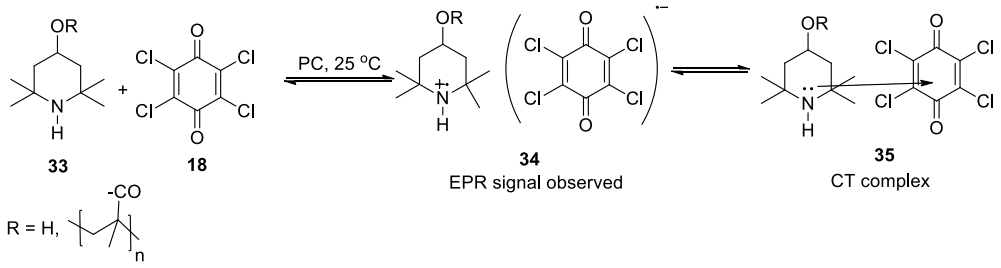

Similar electron transfer reaction using sterically hindered *N, N*-diisopropylethylamine and the polymeric derivative of 2,2,6,6-tetramethylpiperidine with dichloromethane CH_2Cl_2, dibromomethane CH_2Br_2 and chloroform $CHCl_3$ gave the radical ion intermediates as revealed by epr spectroscopy (Scheme 9).

Scheme 9

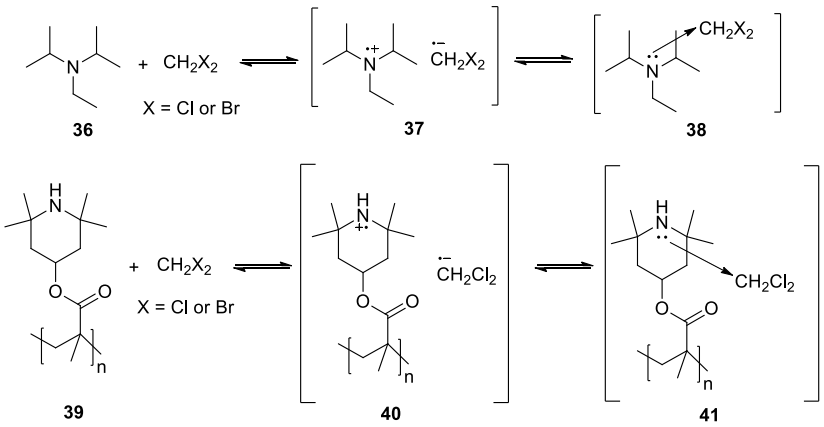

Electron transfer reaction of the benzyl viologen **43** acceptor with various readily accessible amine donors were also studied. The paramagnetic intermediates formed in the reaction were confirmed through epr spectroscopy (Scheme 10).

Scheme 10

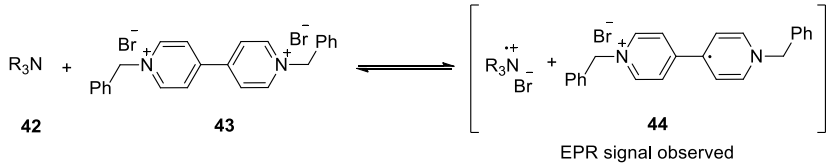

In the fourth chapter, research efforts toward the construction of an electrochemical cell based on the reversible electron transfer reaction of tertiary amines with *p*-chloranil are described. The electrochemical cell was readily constructed using tertiary amine as an electron donor and quinone as an electron acceptor by coating propylene carbonate PC, titanium dioxide TiO_2 and poly(ethylene oxide) PEO paste on aluminium foil and graphite sheet current collector (Scheme 11).

Scheme 11

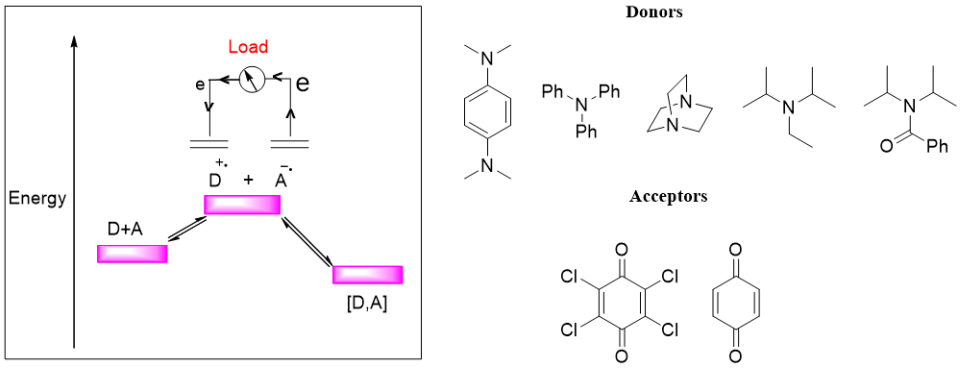

The results are presented and discussed considering the intermediates and mechanisms involved in these transformations.

Note: Scheme numbers and compound numbers given in this abstract are different from those given in the chapters.

Chapter 1

General Introduction on Electron Transfer Reactions

1.1 Introduction

Electron transfer reactions involving the transfer of an electron from donor to an acceptor are very important in chemistry and biology.[1] These reactions can occur both thermally and photochemically.[2] The electrochemical reaction take place by single electron transfer (SET) processes. The SET process also occurs in many biological transformations involving photosynthesis,[3] cytochromes,[4] ferredoxin,[5] rubredoxin[6] etc. The electron transfer reactions are also very important in the functions of semiconductors,[7] conducting polymers[8] and photovoltaics.[9] A brief review on the organic electron transfer reactions would facilitate the discussion.

1.1.1 Redox reactions through electron transfer

Ceric ammonium nitrate, $(NH_4)_2[Ce(NO_3)_6]$ (CAN) is a unique one electron oxidant.[10] Oxidation of benzyl alcohol **1** with CAN **2** gives radical cation which in presence of water affords benzaldehyde **3** in 87% yield (Scheme 1).[11]

Scheme 1

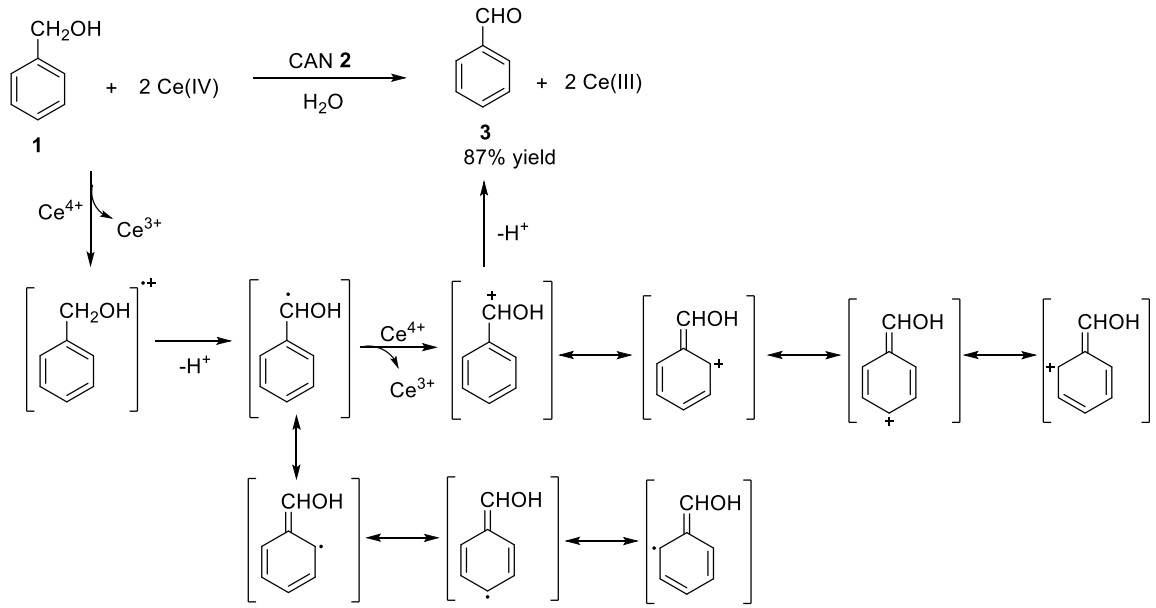

Oxidation of primary and secondary benzylic alcohols **4** with catalytic amount of CAN and stoichiometric amount of $NaBrO_3$ gives the corresponding aldehydes or ketones **5** in good yields (Scheme 2).[12]

Scheme 2

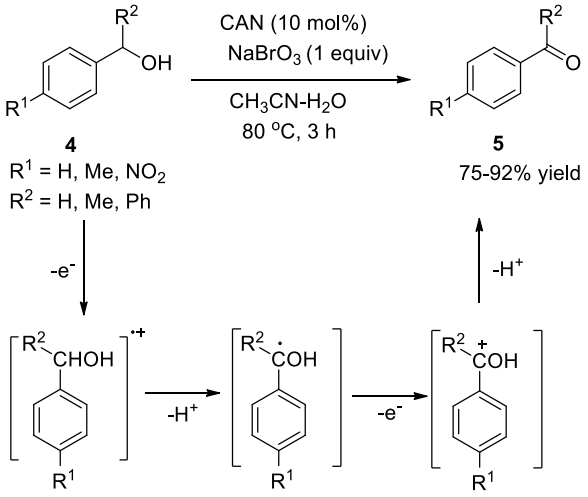

Reaction of 1,4-dimethoxy-2,3,5,6-tetramethyl benzene **6** with CAN in presence of isotopically enriched water gives isotopically labelled duroquinone **7** through a SET process (Scheme 3).[13]

Scheme 3

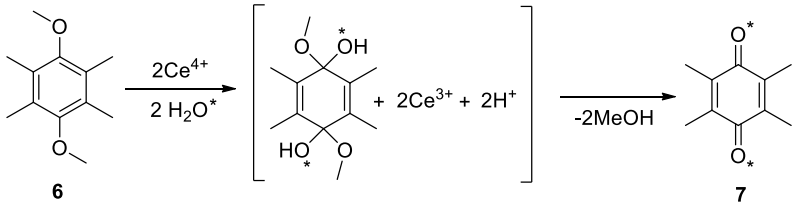

Reaction of naphthalene derivatives with ceric ammonium sulphate (CAS) **9** gives the corresponding naphthoquinones **10** and **11** in moderate to good yields (up to 95 yield).[14] The transformation involves radical cations and rearrangements were observed when the 1, 4-positions was substituted with D or Ph group.[14]

Scheme 4

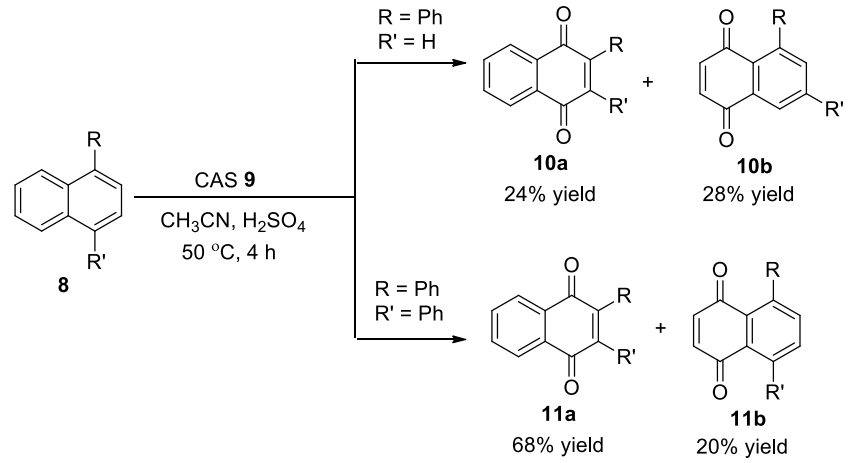

Mechanism:

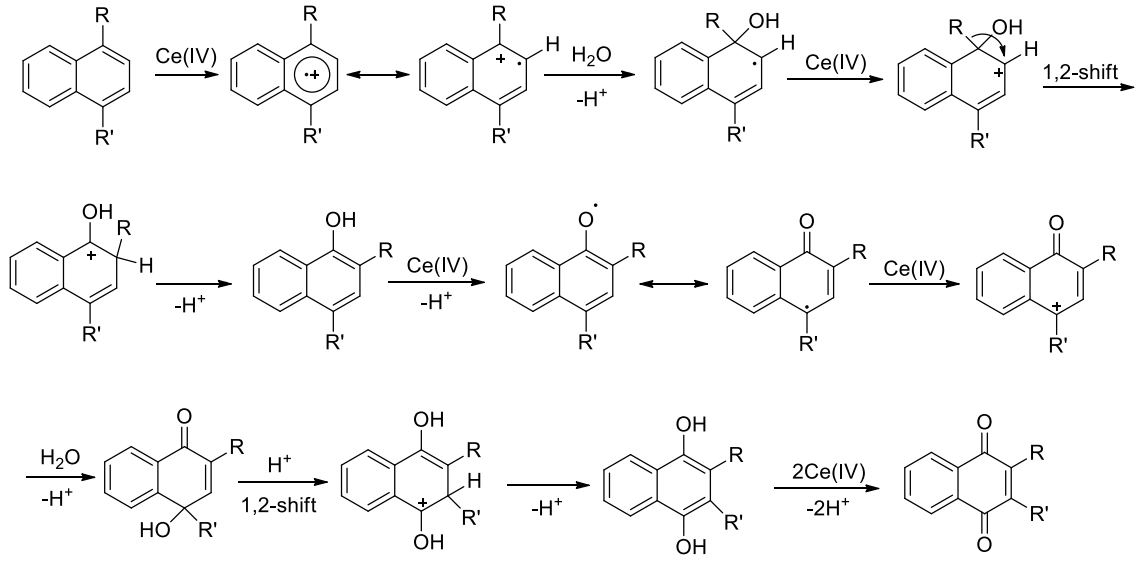

Recently, several organic transformations were reported using ceric ammonium nitrate (CAN) which go through single electron transfer reactions. Some of the reactions are outlined in Chart 1.

Chart 1

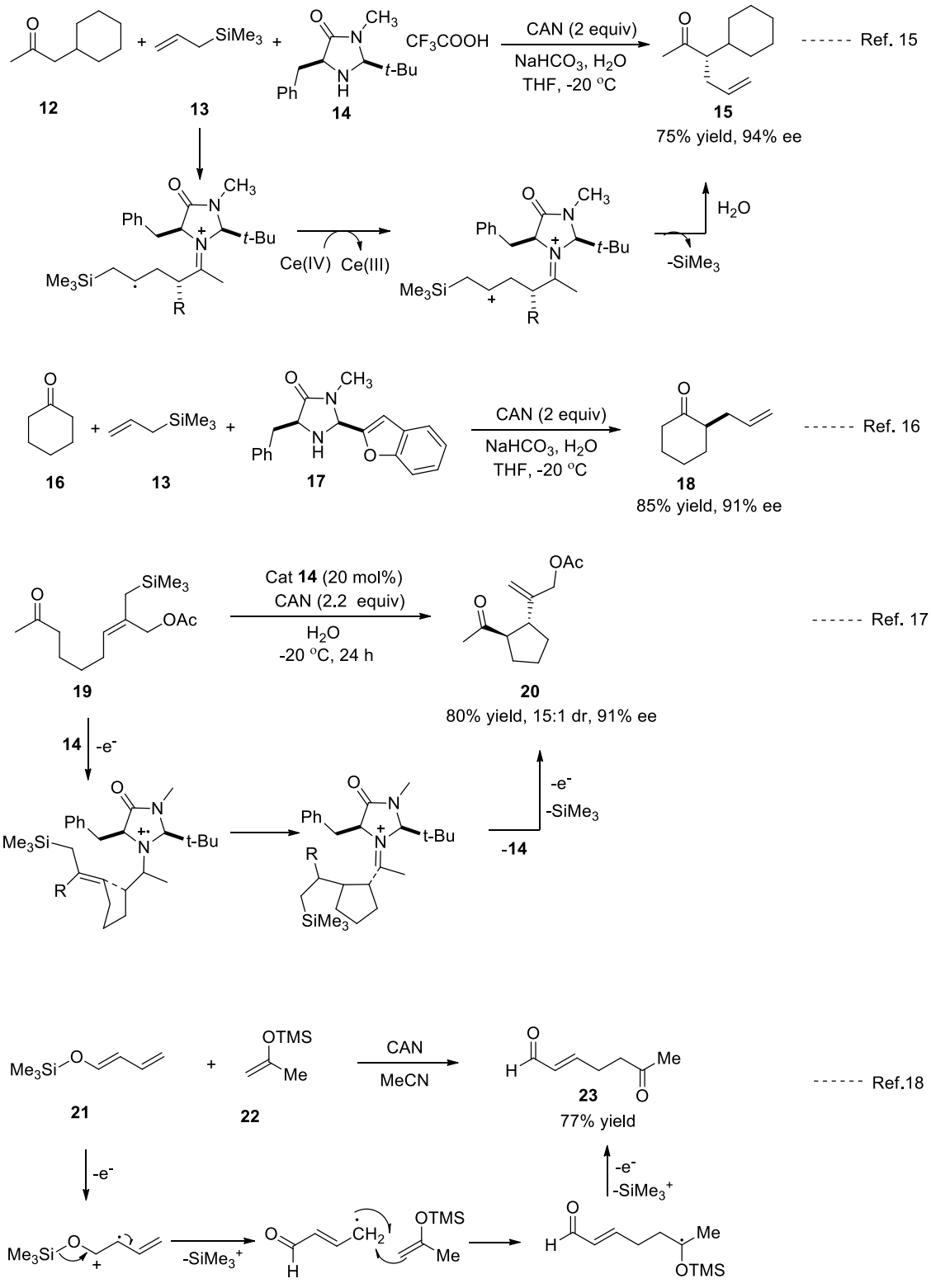
CAN (2 equiv)
NaHCO3, H2O
THF, -20 °C
Ref. 15
12
13
14
15
75% yield, 94% ee
Ce(IV) Ce(III)
H2O
-SiMe3
16
17
18
85% yield, 91% ee
Ref. 16
Cat 14 (20 mol%)
CAN (2.2 equiv)
H2O
-20 °C, 24 h
19
20
80% yield, 15:1 dr, 91% ee
Ref. 17
14 -e-
-e-
-SiMe3
-14
CAN
MeCN
21
22
23
77% yield
Ref.18
-SiMe3+

Chart 1 (continued.)

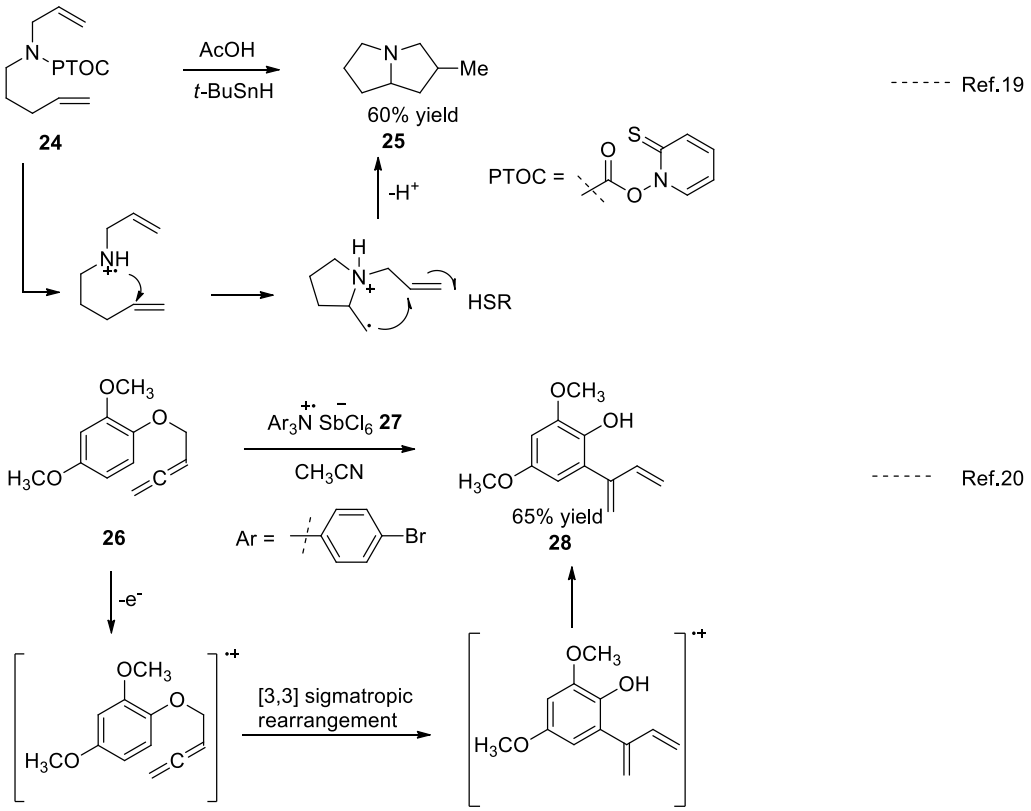

1.1.2 Electrochemical reactions through electron transfer

Kolbe reaction is an anodic oxidation of carboxylate leading to the formation of hydrocarbon dimers *via* the intermediacy of alkyl radicals (Scheme 5).[21]

Scheme 5

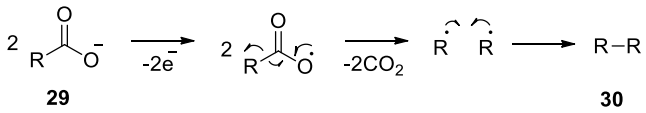

A number of natural products were synthesized *via* anodic oxidation of organic compounds (chart 2).

Chart 2

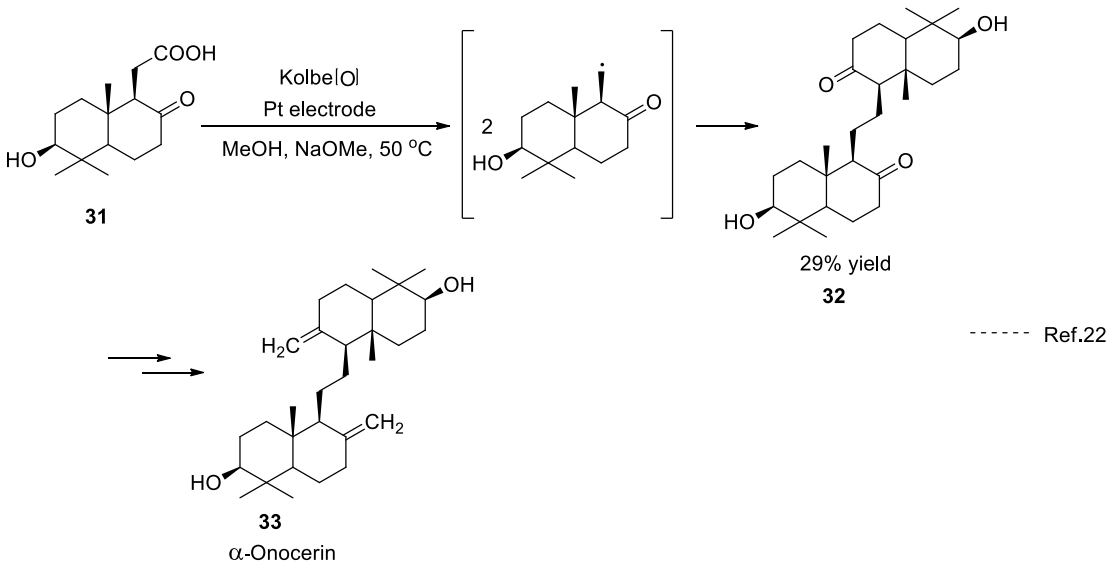

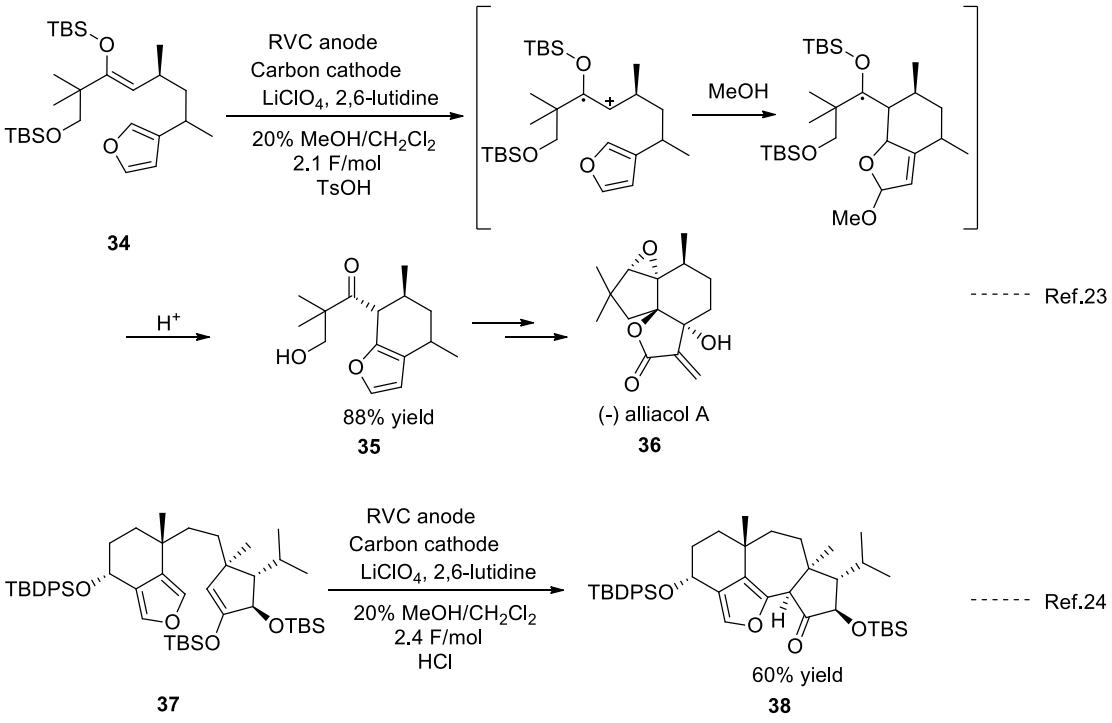

The electrochemical oxidation is also an important tool for C-H functionalization and nucleophilic functionalization of arenes (Chart 3).

Chart 3

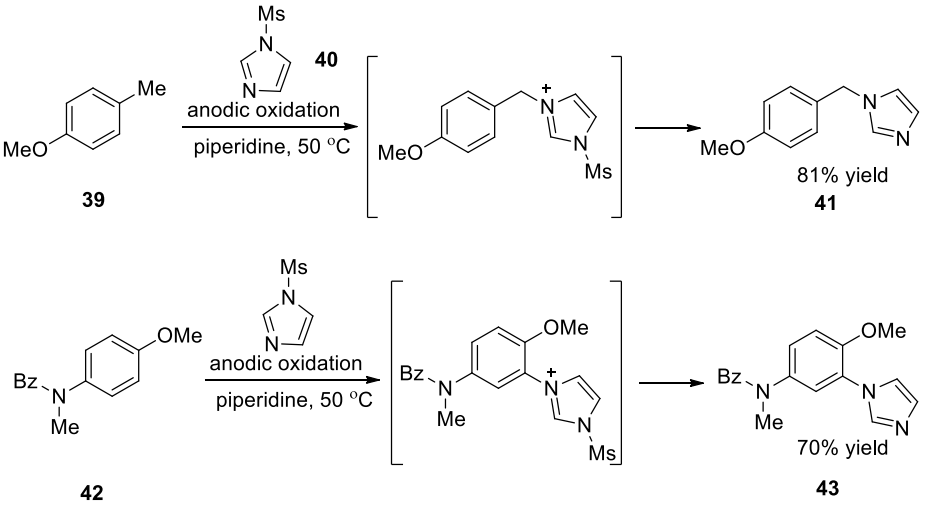
Ms
N
N
40
Me
MeO
anodic oxidation
piperidine, 50 °C
39
MeO
N
N
Ms
MeO
N
N
81% yield
41
Ref.25
Ms
N
N
OMe
Bz
N
Me
anodic oxidation
piperidine, 50 °C
42
OMe
Bz
N
Me
N
N
Ms
OMe
Bz
N
Me
N
N
70% yield
43

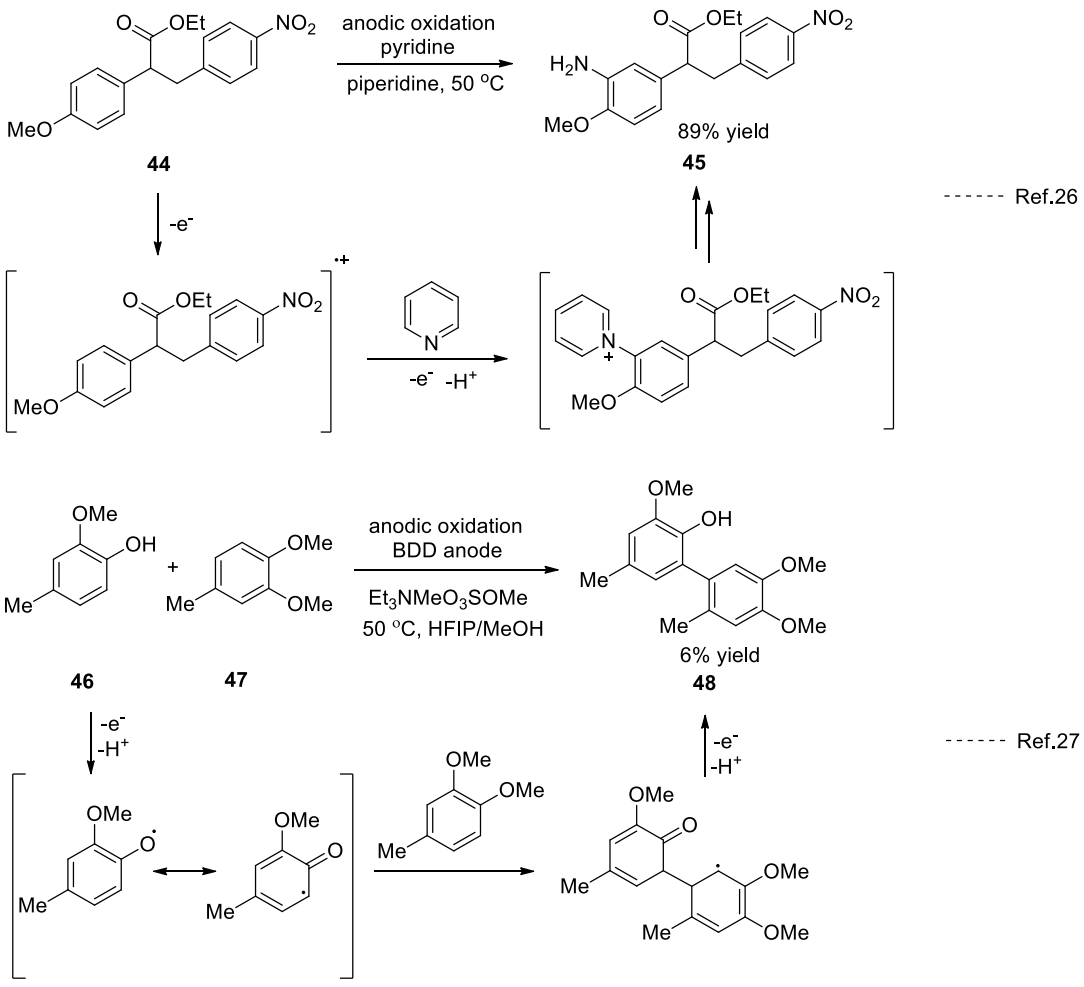
O
OEt
NO2
MeO
anodic oxidation
pyridine
piperidine, 50 °C
44
H2N
MeO
89% yield
45
Ref.26
-e-
O
OEt
NO2
MeO
•+
N
-e- -H+
O
OEt
NO2
N+
MeO
OMe
OH
Me
+
OMe
Me
anodic oxidation
BDD anode
Et3NMeO3SOMe
50 °C, HFIP/MeOH
OMe
OH
Me
OMe
Me
OMe
6% yield
46
47
48
-e-
-H+
OMe
O•
Me
OMe
O
Me
OMe
Me
-e-
-H+
OMe
O
Me
OMe
Me
OMe
Ref.27

Chart 3 (continued.)

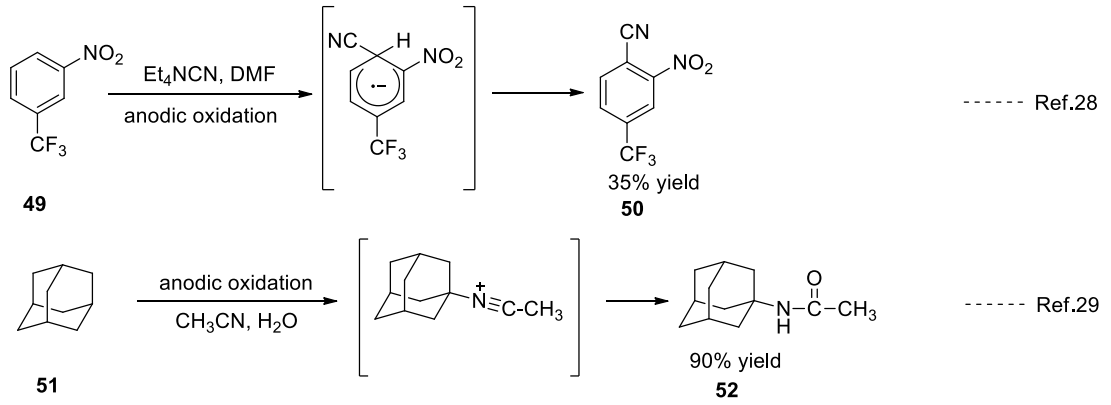

Also, the anodic oxidation was widely used in the oxidation of allylic systems (Chart 4).

Chart 4

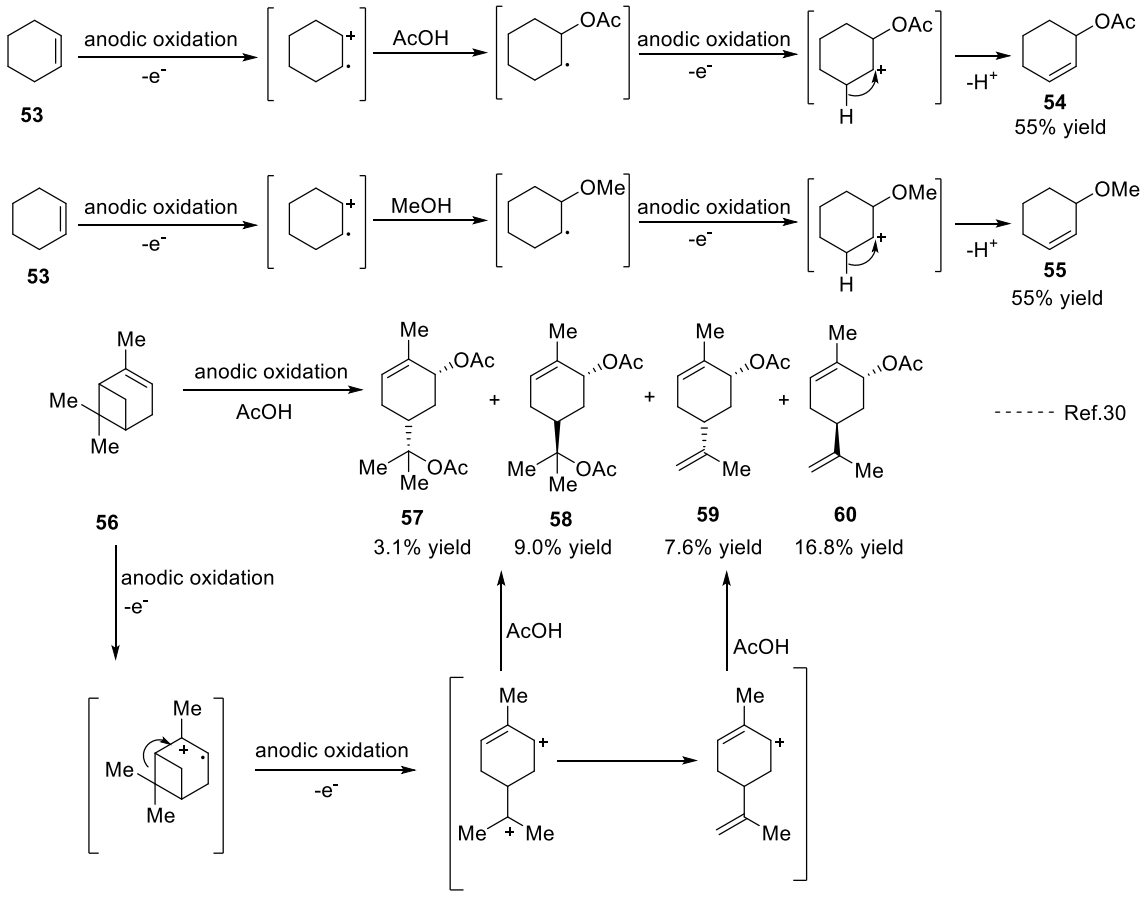

Chart 4 (Continued.)

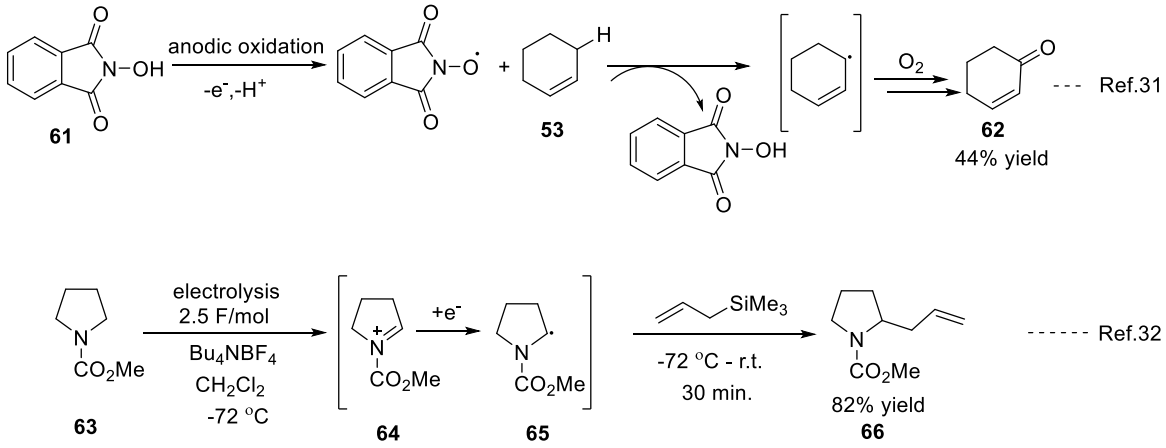

Similarly, cathodic reduction of organic compounds was also widely used in organic synthesis, especially for reductive coupling of carbonyl compounds (Chart 5).

Chart 5

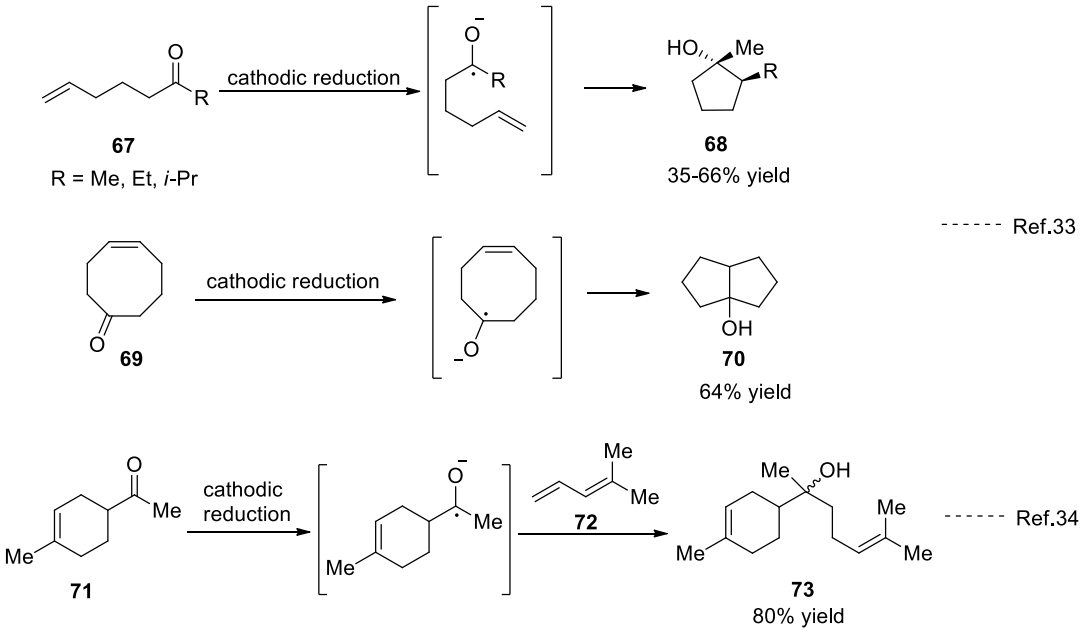

1.1.3 Photochemical electron transfer reactions

Photochemical reactions are performed by absorption of visible or ultraviolet light. For example, a metal complex, such as $Ru(bpy)_3Cl_2$ absorbs light at 452 nm with a high molar extinction coefficient (ε = 14,600 M^{-1} cm^{-1}) and it is widely used as a photo catalyst

in organic synthesis. Some important photochemical electron transfer reactions are shown in Chart 6.

Chart 6

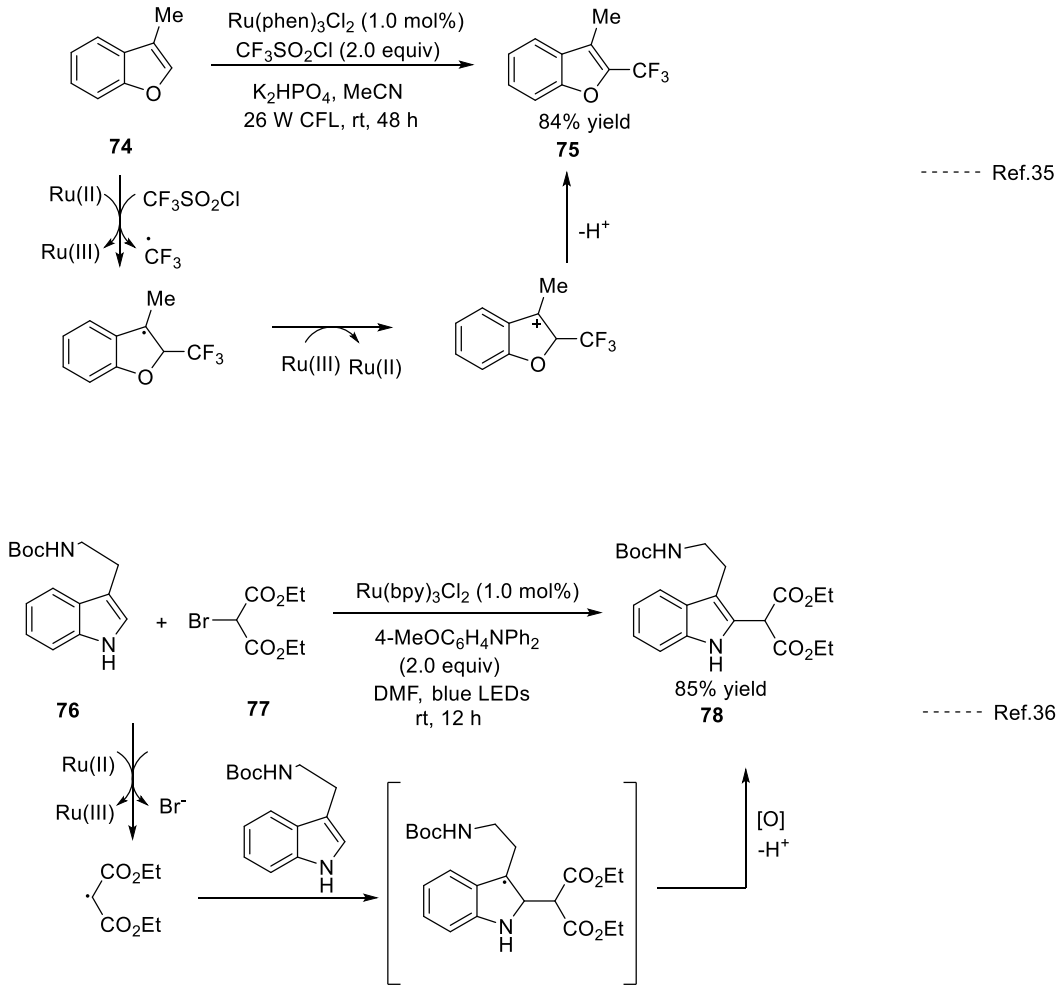

Chart 6 (continued.)

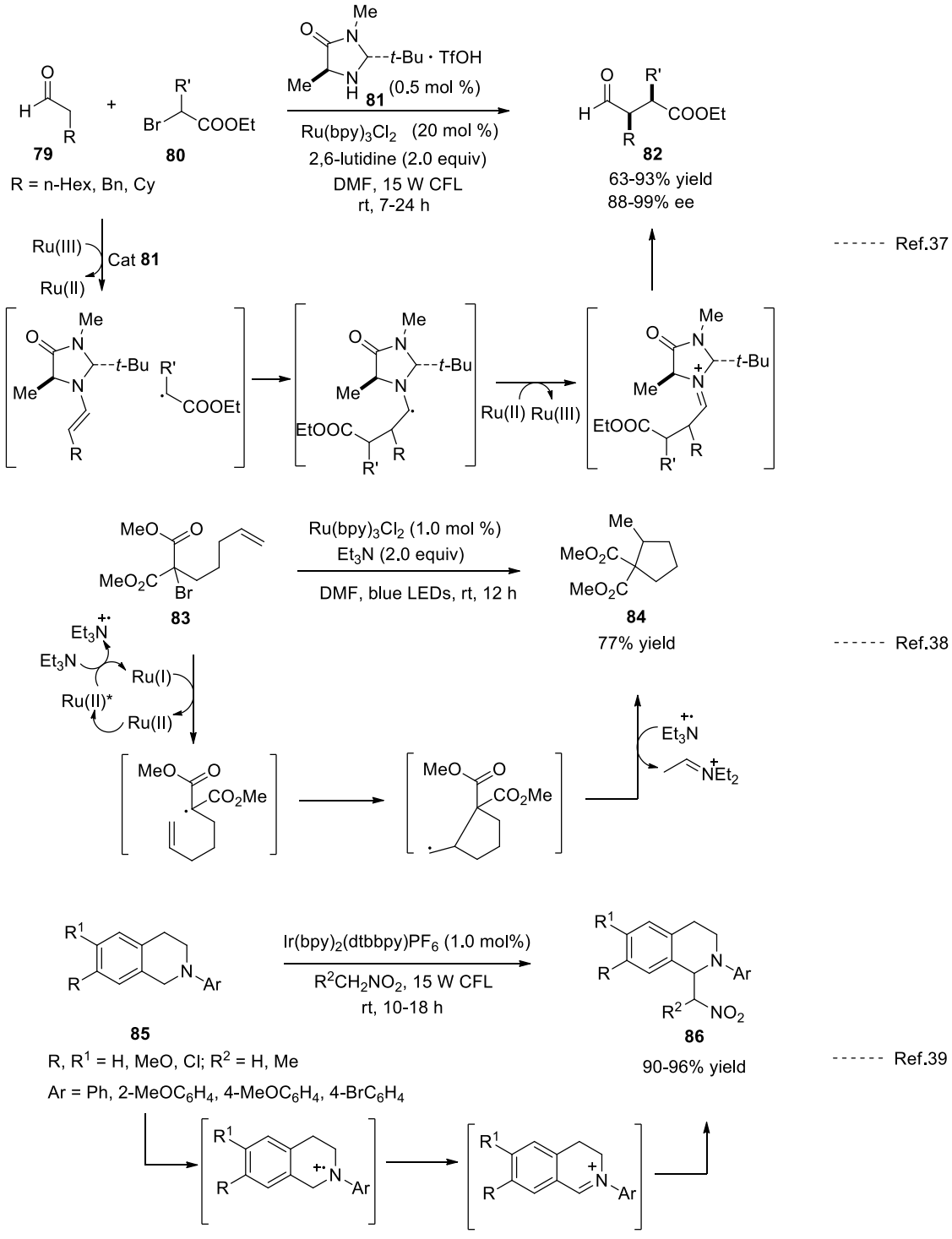

Chart 6 (continued.)

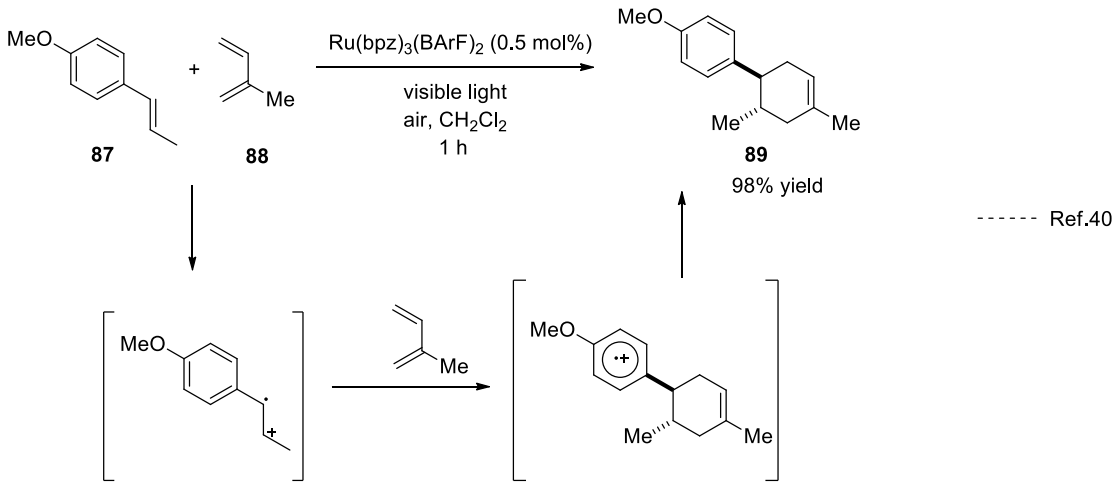

1.1.4 SET reactions in organic chemistry

In the 1970s, there were several reports on the formation of the radical cation/radical anion pair intermediates in several popular organic reactions. A brief review of the literature would facilitate the discussion.

1.1.4.1 SET reactions in aromatic nucleophilic substitution reaction

The unimolecular aromatic nucleophilic substitution ($S_{RN}1$) reaction involves SET process. The halide (X) substituent in aromatic compound **90** is replaced by a nucleophile through free radical intermediates leading to the substitution product **91** (Scheme 6).

Scheme 6

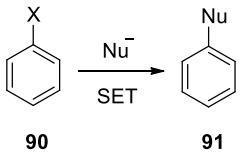

For example, the reaction of iodobenzene **92** with KNH_2 in liquid ammonia gives the substitution product **96** through a SET mediated S_NAr reaction (Scheme 7).[41]

Scheme 7

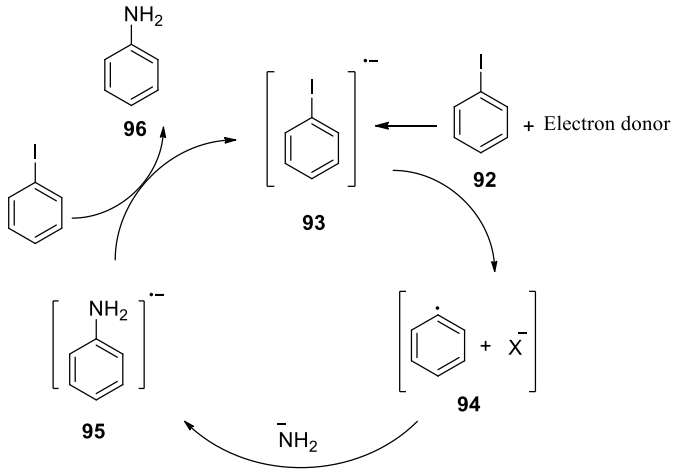

1.1.4.2 SET reactions in acyloin condensation

Other major reactions which involve single electron transfer are acyloin condensation and Birch reduction. For example, the reaction of carboxylic ester **97** with sodium proceeds through single electron transfer from Na to an ester and gives a radical anion **98**. The dimerized compound **98** gives 1,2-diketone **99** which again undergoes further SET process to afford the acyloin product **102** (Scheme 8).[42]

Scheme 8

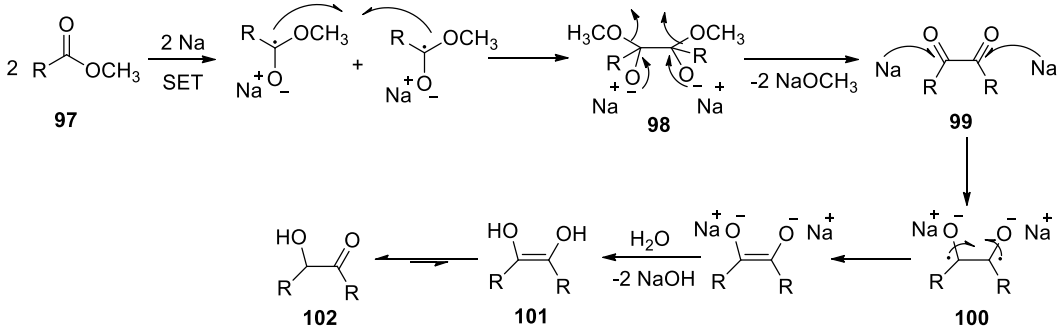

1.1.4.3 SET reactions in Birch reduction

The Birch reduction of substituted benzenes to the corresponding unconjugated cyclohexadienes using Na metal in liquid ammonia involves single electron transfer sequence of reactions (Scheme 9).[43]

Scheme 9

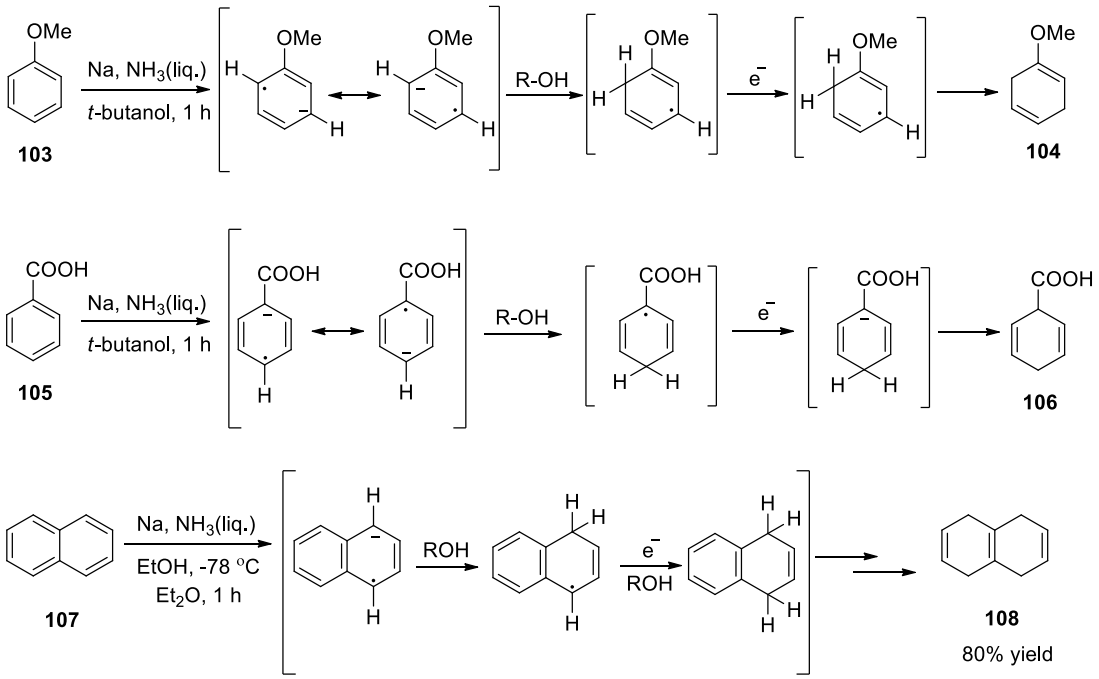

1.1.4.4 SET reactions in Grignard reagent formation

Organomagnesium reagents (RMgX) are very important in organic synthesis. The reaction of an organic halide with magnesium results in Grignard reagent through a SET process (Scheme 10).[44]

Scheme 10

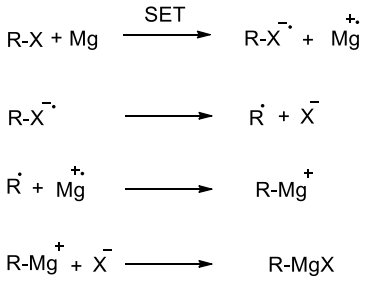

Aldehyde or ketone reacts with organomagnesium halide (Grignard reagent) to form secondary or tertiary alcohol. Polar and SET mechanisms are possible in Grignard reactions (Scheme 11).[45,46]

Scheme 11

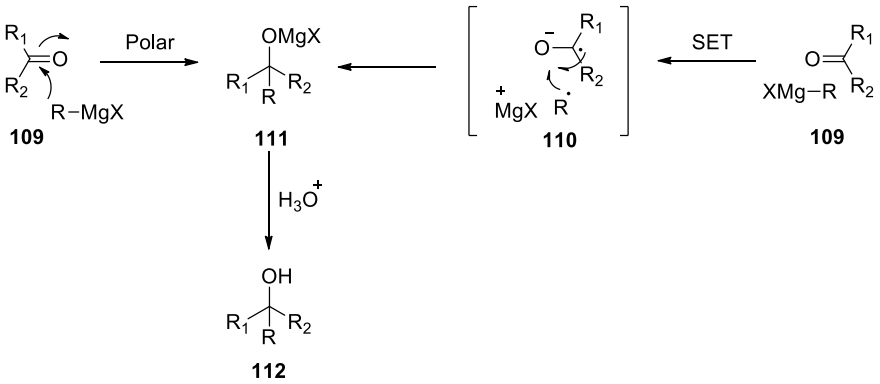

The benzophenone **113** reacts with *t*-butyl magnesium chloride **114** to give the benzophenone ketyl radical anion **115** and alkyl radical **116** which combine to afford tertiary alcohol **117** or to give a pinacol **118** and hydrocarbon **119** (Scheme 12).

Scheme 12

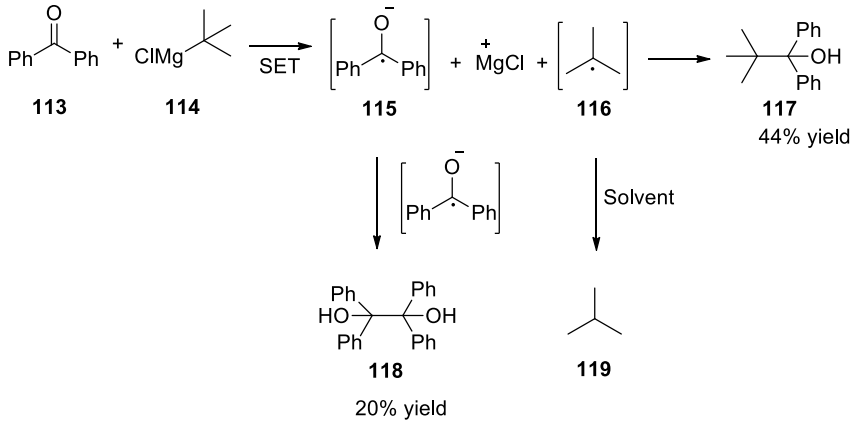

The reaction of neopentylmagnesium chloride **120** with benzophenone **113** gives the corresponding alcohol **121** and pinacol **118** (Scheme 13). EPR spectral analysis confirms that the reaction goes *via* a SET mechanism.[47]

Scheme 13

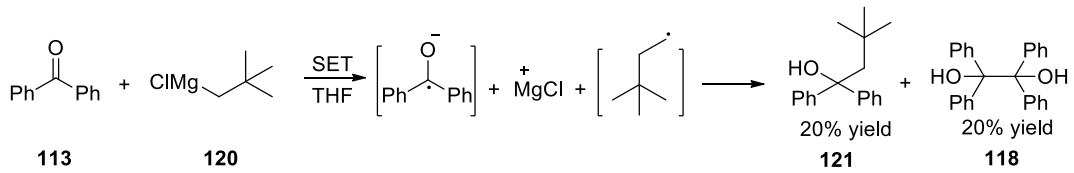

Ashby and coworkers investigated the single electron transfer (SET) pathway in Grignard reactions, reduction of primary halide by metal hydrides, Aldol condensation, Meerwein-Pondorff-Varley reduction, Cannizzaro reaction and Claisen condensation reaction. Evidences were presented for mechanisms involving radical intermediates (Chart 7).[48a]

Chart 7

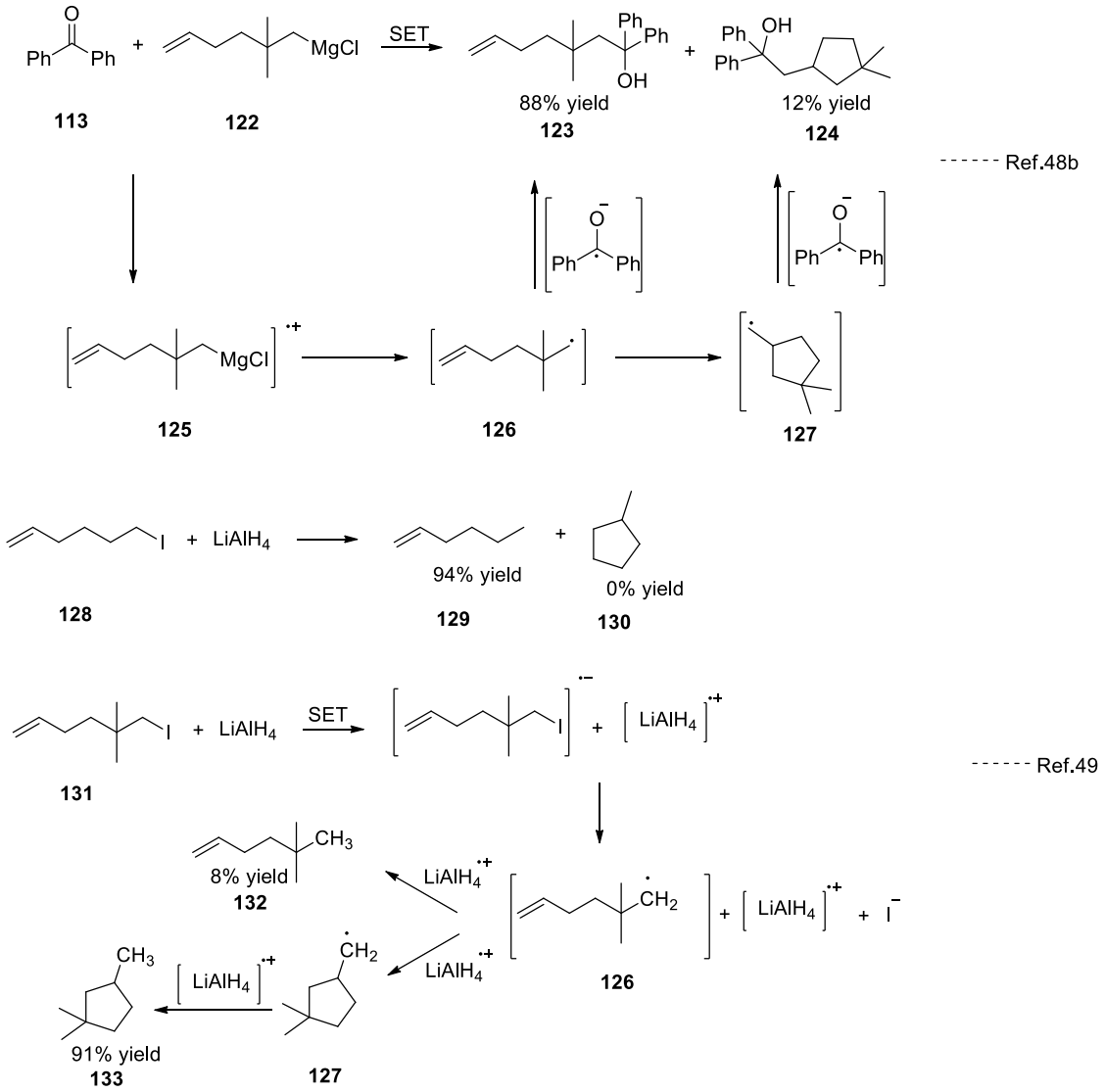

Chart 7 (continued.)

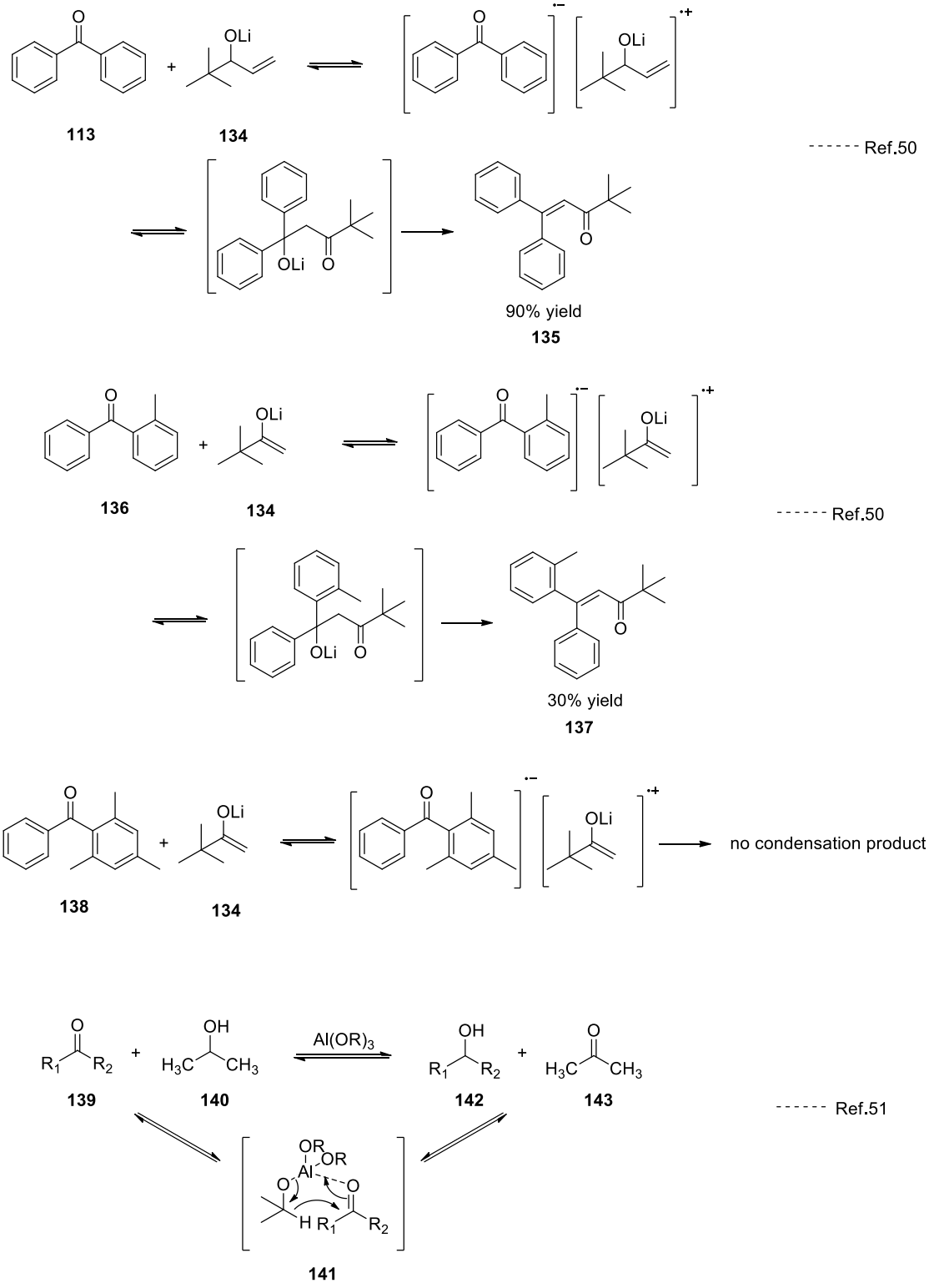

Chart 7 (continued.)

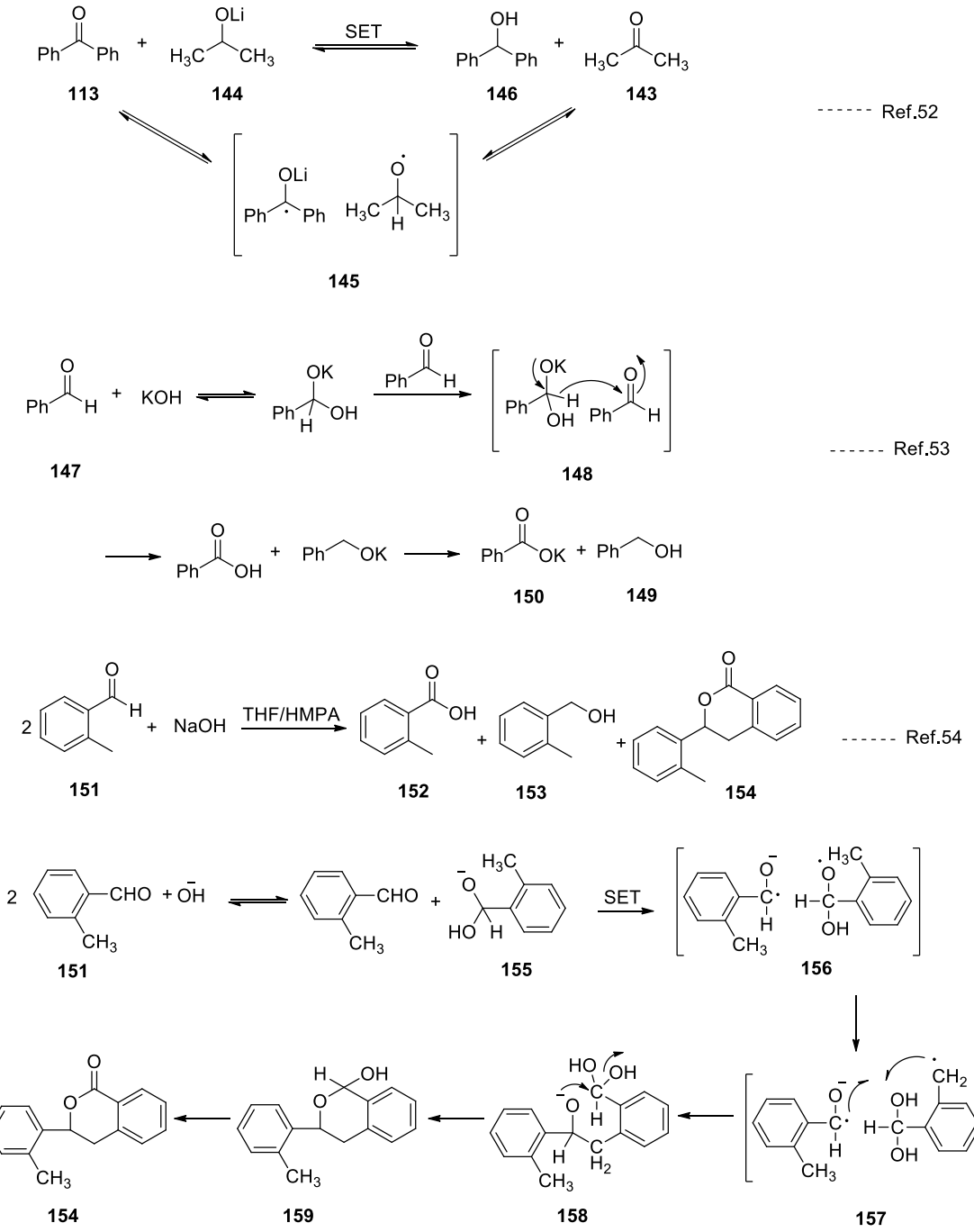

Chart 7 (continued.)

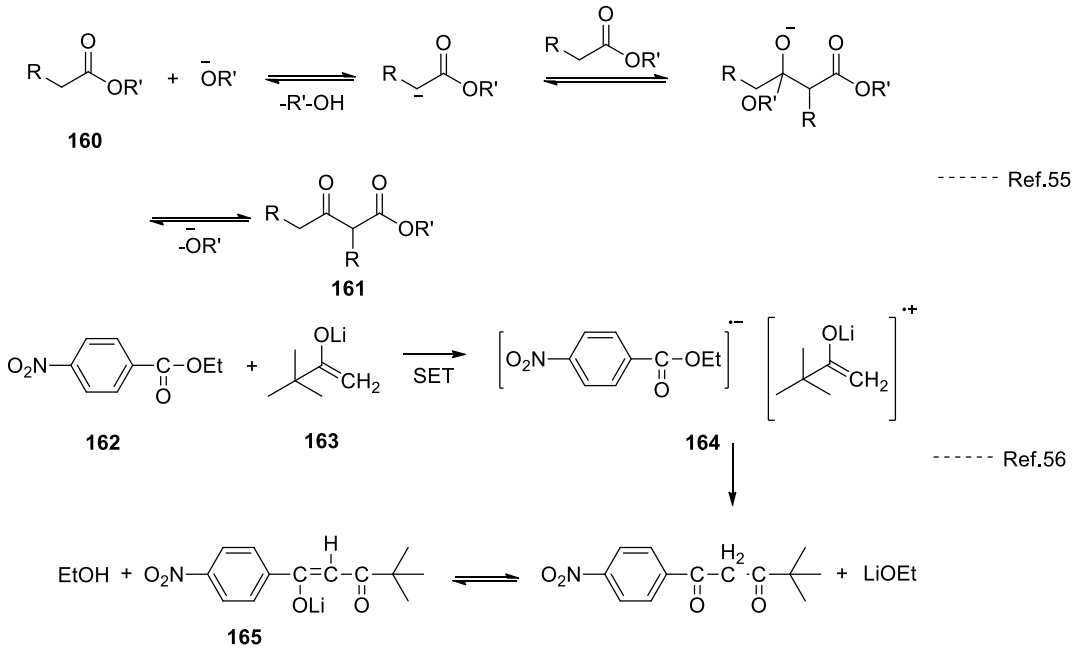

1.1.5 SET Process in Organic Donor and Acceptor System

The formation of charged species can take place in two sequential single electron transfer (SET) processes or in a concerted two electron transfer process (polar mechanism) (Scheme 14).

Scheme 14

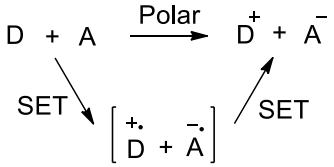

Mulliken's charge transfer theory,[57] Taube's outer sphere/inner sphere mechanism[58] and R. A. Marcus two state non adiabatic theory[59] are the most important concepts developed to rationalize electron transfer reactions.

The charge or electron transfer from one molecule (donor) to the other molecule (acceptor) results in the formation of charge transfer (CT) complex. The electron donors

should have low ionization potential and the electron acceptors should have high electron affinities. Charge transfer complexes have a neutral ground state and there is a partial electron transfer from donor to an acceptor molecule.

Mulliken *et al.*[60] proposed that the diffusive interaction of electron rich donor (D) with an electron acceptor (A) gives a reversible CT complex [D, A] (Scheme 15).

Scheme 15

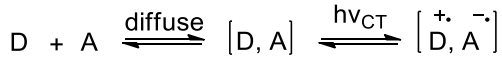

The energy levels of HOMO and LUMO play important role in electron transfer reactions. The LUMO of the electrophilic reagents (acceptor) such as NO_2^+ and Br^+ are lower than the HOMO of aromatic molecules (donor) leading to electrophilic substitution reactions. For example, benzene reacts with NO_2^+ to form nitrobenzene **167** *via* the formation of the radical intermediate **166** (Scheme 16).[61]

Scheme 16

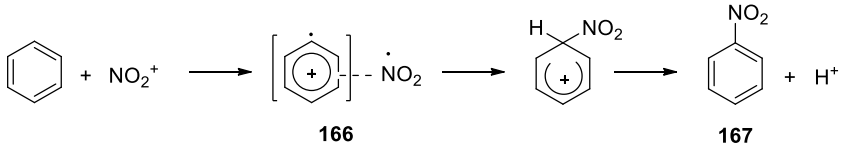

166 167

Taube proposed that both outer-sphere and inner-sphere processes are involved in inorganic electron transfer reactions. The halides could promote the inner-sphere electron transfer *via* bridging effects. Taube *et al.*[62] also reported that in the reaction of chromium complex **168** with cobalt complex **169**, the electron transfer from Cr(II) to Co(III) takes place *via* a bridged intermediate **170** resulting in the green chromium complex **171** and cobalt complex **172** (Scheme 17). The electron transfer is accompanied by the transfer of chloride ligand and this process takes place *via* inner-sphere electron transfer.

Scheme 17

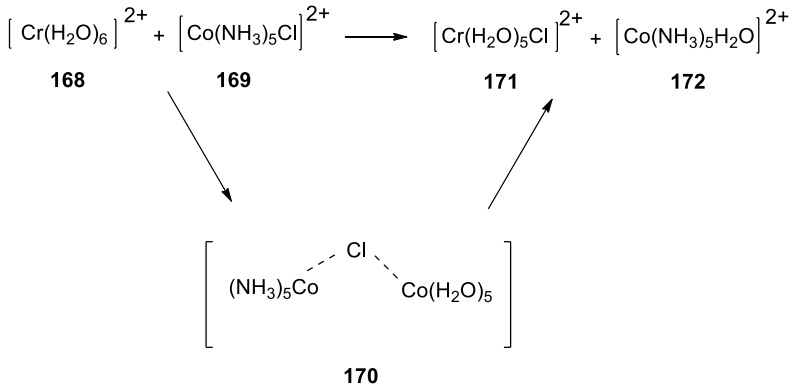

In outer-sphere electron transfer, organic compounds can accept or loose an electron without undergoing structural changes like bond cleavage or bond formation. For example, nitrobenzene **167** can accept one electron to form nitrobenzene radical anion **173** without undergoing any structural change (Scheme 18).[63]

Scheme 18

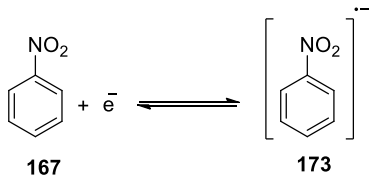

Marcus described the mechanism of electron transfer between an electron donor (D) and an electron acceptor (A) through an outer-sphere precursor complex (D/A) **174**. The precursor complex **174** then reorganizes toward a transition state in which electron transfer takes place to form a successor complex ($D^{+\cdot}/A^{-\cdot}$) **175** that can dissociate to give the corresponding ion pairs **176** (Scheme 19).[64]

Scheme 19

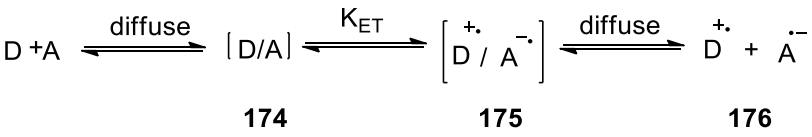

We have decided to investigate the electron transfer reaction of oxygen adsorbed carbon materials, polythiophene radical cation salts, quinones, halomethanes and viologen acceptors. We have also constructed electrochemical cells based on quinone acceptors and amine donors. The results are described in Chapters 2-4.

1.2 References

1 (a) Kornblum, N.; Michel, R. E.; Kerber, R. C. *J. Am. Chem. Soc.* **1966**, *88*, 5662. (b) Kerber, R. C.; Urry, G. W.; Kornblum, N. *J. Am. Chem. Soc.* **1965**, *87*, 4520. (c) Russell, G. A.; Danen, W. C. *J. Am. Chem. Soc.* **1966**, *88*, 5663. (d) Marcus, R. A.; Sutin, N. *Biochim. Biophys. Acta*. **1985**, *811*, 265. (e) Marcus, R. A. *J. Chem. Phys.* **1957**, *26*, 867. (f) Marcus, R. A. *Discuss. Faraday Soc.* **1960**, *29*, 21. (g) Marcus, R. A. *J. Chem. Phys.* **1965**, *43*, 679. (h) Marcus, R. A. *J. Phys. Chem.* **1968**, *72*, 891. (i) Marcus, R. A. *Ann. Rev. Phys. Chem.* **1964**, *15*, 155. (j) Newton, M. D.; Sutin, N. *Ann. Rev. Phys. Chem.* **1984**, *35*, 437. (k) Miller, J. R.; Calcaterra, L. T.; Closs, G. L. *J. Am. Chem. Soc.* **1984**, *106*, 3047. (l) Eberson, L. *J. Am. Chem. Soc.* **1983**, *105*, 3192. (m) Panteleeva, E. V.; Vaganova, T. A.; Shteiogarts, V. D. *Tetrahedron Lett*. **1955**, *36*, 8465. (n) Rossi, R. A.; Pierini, B. A.; Penenory, A. B. *Chem. Rev.* **2003**, *103*, 71 and references cited therein.

2 (a) Kestner, N, R.; Logan, J.; Jortner, J. *J. Phys. Chem.* **1996**, *100*, 19740. (b) Penfield, K. W.; Miller, J. R.; Row, M. N. P.; Cotsaris, E.; Oliver, A. M.; Hush, N. S. *J. Am. Chem. Soc.* **1987**, *109*, 5061. (c) Meyer, T. J. *Acc. Chem. Res.* **1978**, *11*, 94. (d) Hush, N. S. *Electrochemica Acta.* **1968**, *13*, 1005. (e) Hopfield, J. J. *Proc. Nat. Acad. Sci. USA.* **1974**, *71*, 3640. (f) Blankenship, R. E.; Parson, W. W. *Ann. Rev. Biochem.* **1978**, *47*, 635. (g) Poole, J. S.; Hadad, C. M.; Platz, M. S.; Fredin, Z. P.; Pickard, L.; Guerrero1, E. L.; Kessler, M.; Chowdhury, G.; Kotandeniya, D.; Gates, K. S. *Photochemistry and Photobiology*. **2002**, *75*, 339. (h) Schuster, O. I.; Brisimitzakis, A.

C. *Tetrahedron Lett*. **1982**, *23*, 4531. (i) Cossy, J.; Belotti, D. *Tetrahedron.* **2006**, *62*, 6459. (j) Hoffmann, N. *Journal of Photochemistry and Photobiology C: Photochemistry Reviews.* **2008**, *9*, 43.

3 (a) Hsiao, C.; Chou, I. C.; Okafor, C. D.; Bowman, J. C.; O'Neill, E. B.; Athavale, S. S.; Petrov, A. S.; Hud, N. V.; Wartell, R. M.; Harvey, S. C.; Williams, L. D. *Nature Chemistry.* **2013**, *5*, 525. (b) Bobst, A. M. *Proc. Nat. Acad. Sci. USA.* **1971**, *68*, 541. (c) Sjulstok, E.; Olsen, J. M. H.; Solov'yov, I. A. *Scientific Reports.* **2015**, *5*, 18446. (d) Grimes, C. J.; Piszkiewicz, D.; Fleischer, E. B. *Proc. Nat. Acad. Sci. USA.* **1974**, *71*, 1408.

4 (a) Cenas, N.; Anuservicius, Z.; Bironaite, D.; Bachmanova, G. I.; Archakov, A.; Ollinger, K. *Archives of Biochemistry and Biophysics*, **1994**, *315*, 400. (b) Hill, B. C. *J. Biol. Chem.* **1994**, *269*, 2419. (c) Grimes, C. J.; Piszkiewicz, D.; Fleischer, E. B. *Proc. Nat. Acad. Sci. USA.* **1974**, *71*, 541.

5 (a) Batie, C. J.; Kamin, H. *J. Biol. Chem.* **1984**, *259*, 11976. (b) Moreno, C. G.; Julvez, M. M; Medina, M.; Hurley, J. K.; Tollin. G. *Biochimie*, **1998**, *80*, 837.

6 Hagelueken, G.; Wiehlmann, L.; Adams, T. M.; Kolmar, H.; Heinz, D. W.; Tummler, B.; Schubert, W. D. *Proc. Nat. Acad. Sci. USA.* **2007**, *104*, 12276.

7 (a) Koval, C. A.; Howard, J. N. *Chem. Rev.* **1992**, *92*, 411. (b) Lewis, N. S. *J. Phy. Chem. B.* **1998,** *102*, 4843. (c) Corvan, J. R. C.; Whitten, D.G.; McLendon, G.L. *Chemical Physics.* **1993**, *176*, 377. (d) Tvrdy, K.; Frantsuzovc, P. A.; Kamata, P. V. *PNAS*, **2011**, *108*, 29.

8 Zhang, N.; Samanta, S. R.; Rosen, B. M.; Percec, V. *Chem. Rev.* **2014**, *114*, 5848.

9 (a) Lewis, N. S.; Nocera, D. G. *Proc. Nat. Acad. Sci. USA.* **2006**, *103*, 15729. (b) Gratzel, G. *Inorg. Chem.* **2005**, *44*, 6841.

10 Sridharan, V.; Mene´ndez, J. C. *Chem. Rev.* **2010**, *110*, 3805.

11 Trahanovsky, W. S.; Young, L. B.; Brown, G. L. *J. Org. Chem.* **1967**, *32*, 3865.

12 Ho, T. L. *Synthesis*. **1978**, *12*, 936.

13 Jacob, P.; Callery, P. S.; Shulgin A. T.; Castagnoli, N. *J. Org. Chem.* **1976**, *41*, 3627.

14 (a) Periasamy, M.; Bhatt, M. V. *Tetrahedron Letters*. **1977**, *27*, 2357. (b) Bhatt, M. V.; Periasamy, M. *Tetrahedron.* **1994**, *50*, 3575. (c) Bhatt, M. V.; Periasamy, M. *J. Chem. Perkin Trans.2* **1993**, 1811. (d) Periasamy, M.; Bhatt, M. V. *Synthesis.***1977**, *5*, 330. (e) Periasamy, M.; Bhatt, M. V. *Tetrahedron Letters*. **1978**, *46*, 4561.

15 Beeson, T. D.; Mastracchio, A.; Hong, J. B.; Ashton, K.; MacMillan, D. W. C. *Science*, **2007**, *316*, 582.

16 Mastracchio, A.; Warkentin, A. A.; Walji, A. M.; MacMillan, D. W. C. *Proc. Natl. Acad. Sci*. **2010**, *107*, 20648.

17 (a) Pham, P. V.; Ashton, K.; MacMillan, D. W. C. *Chem. Sci.*, **2011**, *2*, 1470. (b) Conrad, J. C.; Kong, J.; Laforteza, B. N.; MacMillan, D. W. C. *J. Am. Chem. Soc.* **2009**, *131*, 11640.

18 Paolobelli, A. B.; Latini, D.; Ruzziconi, R. *Tetrahedron Letters*. **1993**, *34*, 721.

19 Newcomb, M.; Deeb, T. M. *J. Am. Chem. Soc.* **1987**, *109*, 3163.

20 Dhanalekshmi, S.; Venkatachalam, C. S.; Balasubramanian, K. K. *J. Chem. Soc. Chem. Comm.* **1994**, 511.

21 Kolbe, H. *Annalen der chemie und pharmacie.* **1848**, *64*, 339.

22 Stork, G.; Davies, J. E.; Meisels, A. *J. Am. Chem. Soc.* **1959**, 5516.

23 Mihelcic, J.; Moeller, K. D. *J. Am. Chem. Soc.* **2004**, *126*, 9106.

24 Hughes, C. C.; Miller, A. K.; Trauner, D. *Org. Lett.*,**2005**, *7*, 3425.

25 Morofuji, T.; Shimizu, A.; Yoshida, J. I. *J. Am. Chem. Soc.* **2014**, *136*, 4496.

26 Morofuji, T.; Shimizu, A.; Yoshida, J. I. *J. Am. Chem. Soc.* **2013**, *135*, 5000.

27 Kirste, A.; Elsler, B.; Schnakenburg, G.; Waldvogel, S. R. *J. Am. Chem. Soc.* **2012**, *134*, 3571.

28 Gallardo, I.; Guirado, G.; Marquet, J. *Chem. Eur. J.* **2001**, *7*, 1759.

29 Koch, V. R.; Miller, L. L. *J. Am. Chem. Soc.* **1973**, 8631.

30 Shono, T.; Ikeda, A. *J. Am. Chem. Soc.* **1972**, 7892.

31 Masui, M.; Hara, S.; Ueshima, T.; Kawaguchi, T.; Ozaki, S. *Chem. Pharm. Bull.* **1983**, *31*, 4209.

32 Yoshida, J. I.; Kataoka, K.; Horcajada, R.; Nagaki, A. *Chem. Rev.* **2008**, *108*, 2265.

33 Shono, T.; Mitani, M. *J. Am. Chem. Soc.* **1971**, 5284.

34 (a) Shono, T.; Kashimura, S.; Mori, Y.; Hayashi, T.; Soejima, T.; Yamaguchi, Y. *J. Org. Chem.* **1989**, *54*, 6001. (b) Shono, T. *Tetrahedron.* **1984**, *40*, 811.

35 Nagib, D. A.; MacMillan, D. W. C. *Nature.* **2011**, *480*, 224.

36 Furst, L.; Matsuura, B. S.; Narayanam, J. M. R.; Tucker, J. W.; Stephenson, C. R. J. *Org. Lett.* **2010**, *12*, 3104.

37 Nicewicz, D. A.; MacMillan, D. V. C. *Science*. **2008,** *322*, 77.

38 Tucker, J. W.; Nguyen, J. D.; Narayanam, J. M. R.; Krabbe, S. W.; Stephenson, C. R. J. *Chem. Commun.* **2010**, *46*, 4985.

39 Condie, A. G.; Gonzalez-Gomez, J. C.; Stephenson, C. R. J. *J. Am. Chem. Soc.* **2010**, *132*, 1464.

40 Lin, S.; Ischay, M. A.; Fry, C. G.; Yoon, T. P. *J. Am. Chem. Soc.* **2011**, *133*, 19350.

41 Kim, J. K.; Bunnett, J. F. *J. Am. Chem. Soc.* **1970**, *92*, 7463.

42 Finley, K. T. *Chem. Rev.* **1964**, *64*, 573.

43 (a) Birch, A. J. *J. Chem. Soc.***1944**, 430. (b) Birch, A. J. *J. Chem. Soc.* **1945**, 809.

44 Ashby, E. C.; Oswald, J. *J. Org. Chem.* **1988**, *53*, 6068.

45 Ashby, E. C.; Lopp, I. G.; Buhler, J. D. *J. Am. Chem. Soc.* **1975**, *97*, 1964.

46 Blicke**,** F. F.; Powers, L. D. *J. Am. Chem. Soc.* **1929**, *51*, 3378.

47 Blomberg, **C.;** Mosher, H. S. *J. Organometal. Chem.* **1968**, *13*, 519.

48 (a) Ashby, E. C. *Acc. Chem. Res.* **1988**, *21*, 414. (b) Ashby, E. C.; Bowers, J.; Depriest, R. *Tetrahendron Letters*. **1980**, *21*, 3541.

49 Ashby, E. C.; DePriest, R. N.; Goel, A. B. *Tetrahedron Letters.* **1981**, *22*, 1763.

50 Ashby, E. C.; Argyropoulos, J. N. *J. Org. Chem.* **1986**, *51*, 472.

51 Shiner, V. J.; Whittaker, D. *J. Am. Chem. Soc.* **1963**, *85*, 2337.

52 Ashby, E. C.; Argyropoulos, J. N. *J. Org. Chem.* **1986**, *51*, 3593.

53 Swain, C. G.; Powell, A. L.; Sheppard, W. A.; Morgan, C. R. *J. Am. Chem. Soc.* **1979**, *101*, 3576.

54 Ashby, E. C.; Coleman, D.; Gamasa, M. *J. Org. Chem.* **1987**, *52*, 4079.

55 a) Royals, E. E. *J. Am. Chem. Soc.* **1948**, *70*, 489. b) Zook, K. D.; Mcaleer, W. J.; Horwin, L. *J. Am. Chem. Soc.* **1946**, *68*, 2404. c) Baker, R. B.; Reid, E. E. *J. Am.*

Chem. Soc. **1929**, *51*, 1567. d) Soloway, S. B.; Laforge, F.B. *J. Am. Chem. Soc.* **1947**, *69*, 1244. e) Cohen, H.; Shubart, R. *J. Org. Chem.* **1973**, *38*, 4079.

56 Ashby, E. C.; Park, W. S. *Tetrahendron Letters*. **1983**, *24*, 1667.

57 a) Mulliken, R. S. *J. Chem. Phys.* **1955**, *23*, 397. b) Mulliken, R. S. *J. Am. Chem. Soc.* **1950**, *72*, 600. c) Mulliken, R. S. *J. Phys. Chem.* **1952**, *56*, 801. d) Reid, C.; Mulliken, R. S. *J. Am. Chem. Soc.* **1956**, *76*, 3869.

58 a) Taube, H. *J. Am. Chem. Soc.* **1942**, *64*, 161. b) Taube, H. *J. Am. Chem. Soc.* **1943**, *65*, 1876. c) Hochhauser, I. L.; Taube, H. *J. Am. Chem. Soc.* **1947**, *69*, 1582. d) Taube, H. *J. Am. Chem. Soc.* **1947**, *69*, 1418. e) Taube, H. *J. Am. Chem. Soc.* **1948**, *70*, 1216 f) Taube, H. *J. Am. Chem. Soc.* **1948**, *70*, 3928. g) Rich, R. L.; Taube, H. *J. Phys. Chem.* **1954**, *58*, 6. h) Rich, R. L.; Taube, H. *J. Am. Chem. Soc.* **1954**, *76*, 2608. i) Taube, H.; Myers, H.; Rich, R. L. *J. Am. Chem. Soc.* **1953**, *75*, 4118. j) Taube, H.; Myers, H. *J. Am. Chem. Soc.* **1954**, *76*, 2103. k) Saffir, P.; Taube, H. *J. Am. Chem. Soc.* **1960**, *82*, 13. l) Taube, H.; Gould, E. S. *Acc. Chem. Res.* **1969**, *2*, 321. m) Nordmeyer, F. R.; Taube, H. *J. Am. Chem. Soc.* **1968**, *90*, 1162. n) French, J. E.; Taube, H. *J. Am. Chem. Soc.* **1969**, *91*, 6951. o) Endicott, J. F.; Taube, H. *Inorg. Chem.* **1965**, *4*, 437. p) Stritar, J. A.; Taube, H. *Inorg. Chem.* **1969**, *8*, 2281. q) Hammershoi, A.; Geselowitz, D.; Taube, H. *Inorg. Chem.* **1984**, *23*, 979. r) Ford, P. C.; Rudd, D. P.; Gaunder, R.; Taube, H. *J. Am. Chem. Soc.* ***1968***, *90*, 1187.

59 a) Marcus, R. A. *J. Chem. Phys.* **1952**, *20*, 359. b) Marcus, R. A. *J. Chem. Phys.* **1957**, *26***,** 872. c) Marcus, R. A. *Can. J. Chem.* **1959**, *37***,** 155. d) Marcus, R. A. *Annu. Rev. Phys. Chem.* **1964**, *15***,** 155. e) Marcus, R. A. *J. Chem. Phys.* **1965**, *43***,** 2654. f)

Marcus, R. A. *J. Chem. Phys.* **1965**, *43***,** 3477. g) R. **A.** *Electrochim. Acta* **1968***, 13***,** 995. h) Marcus, R. A. *J. Chem. Phys.* **1984**, *81***,** 5613.

60 Mulliken, R. S. *J. Am. Chem. Soc.* **1952**, *74*, 811.

61 Nagakura, S. *Mol. Cryst. Liq. Cryst.* **1985**, *126*, 9.

62 Taube, H.; Mayers, H.; Rich, R. L. *J. Am. Chem. Soc.* **1953**, *75*, 4118.

63 Wagenknecht, J. H. *J. Org. Chem.* **1977***, 42*, 1836.

64 a) Marcus, R. A. *J. Chem. Phys.* **1956**, *24*, 966. b) Marcus, R. A. *Angew. Chem. Int. Ed.* **1993**, *32*, 1111.

Chapter 2

Synthetic Methods Based an Electron Transfer Reactions using Oxygen Adsorbed Carbon Materials and *p*-Doped Polythiophene

2.1 Introduction

2.1.1 Carbon materials

Carbon materials are useful for a wide variety of applications such as electrochemical electrodes, medical implants, electrochemical capacitors, high-performance materials and fuel cells.[1] The heat treatment of carbon material at inert atmosphere decreases the content of heteroatoms and increasees the carbon contents.[2,3] The conversion of an organic macromolecular system (e.g. wood, coal, nutshell etc.) to a macro-atomic carbon atoms through elimination of methanol, carbon monoxide, water and carbon dioxide by progressive heating is called carbonization process.[4]

Recently, the production of pyrolysis gas from woody biomass were investigated in this laboratory. The charcoal is a byproduct in this carbonization process from the woody biomass at 450 °C-500 °C. Therefore, we became interested in the development of organic synthetic methods based on readily accessible activated carbon.

Activated carbon is widely used in electrochemical capacitors (supercapacitors) for electricity storage with potential for use in electric vehicles. Activated carbon act as semiconductor with narrow band gap (34 meV) with potential for use in harvesting IR portion of the solar spectrum.[5] Our interest is to study the electron transfer reactions in organic transformations. Therefore, a brief review on the properties and nature of carbon material for application in organic transformation would facilitate the discussion.

2.1.2 Various forms of carbon

The main allotropic forms of pure carbon are graphite and diamond. However, there is immense interest on other new forms of pure carbon such as fullerenes or buckyballs and carbon nanotubes (CNTs).[6] Amorphous forms of carbon mainly consist of coal, charcoal and carbon black. Charcoal is produced by heating organic materials to a high temperature in the absence of air.[7] It has large surface area and it can absorb gases to form new materials. Carbon black is also the purest form of carbon. It is obtained by incomplete burning of some natural oil and heavy petroleum products with limited supply of air.[8] Carbon black is very soft powder and it is used for making carbon paper, inks and paints. The strength of the rubber is increased by the addition of carbon black. Graphite is the most stable allotrope of carbon and soft in nature.[9] Graphite conducts electricity due to delocalization of electrons.

2.1.3 Surface characterization and properties of activated carbons

The surface characteristics of carbon materials and chemistry of their surface is depending on the amount of heteroatom incorporated into the carbon matrix. The heteroatom like oxygen is responsible for the presence of various acidic functional groups such as carboxyl, carbonyl, phenol, quinone and lactones and also presence of unsaturated sites in the matrix of activated carbon (Figure 1).[10]

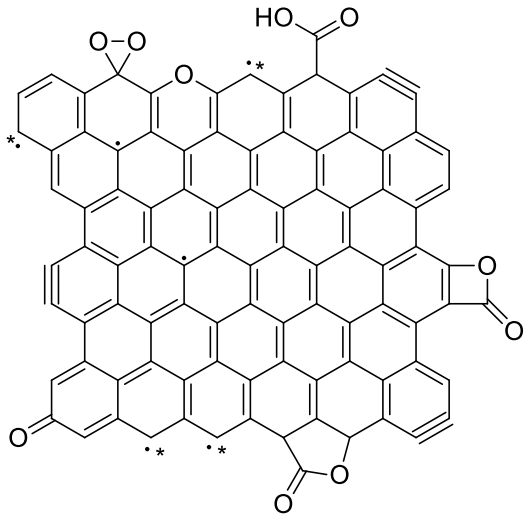

Figure 1. Surface groups present in the Carbon Material. It indicates the presence of σ (*) and π (•) electrons at the zigzag sites and the presence of triple bonds at the armchair sites.

Carbon materials contains: (a) bulk atoms that are neutral (b) surface atoms that are the real adsorption atoms and (c) corner atoms that are very reactive and even react with metals. It is well known that chemical treatment of carbon materials increases the concentration of surface oxygen functional groups. It has been reported[11] that the oxygen acquires a partial negative charge upon chemisorptions. The carbon materials have a free-flowing sp^2-π -electrons, which make them potential catalyst for electron transfer reactions such as oxygen reduction reaction (ORR) to generate super oxide radical.[12] This super oxide radical bound to carbon material acts as an oxidant (Scheme 1).[13]

Scheme 1

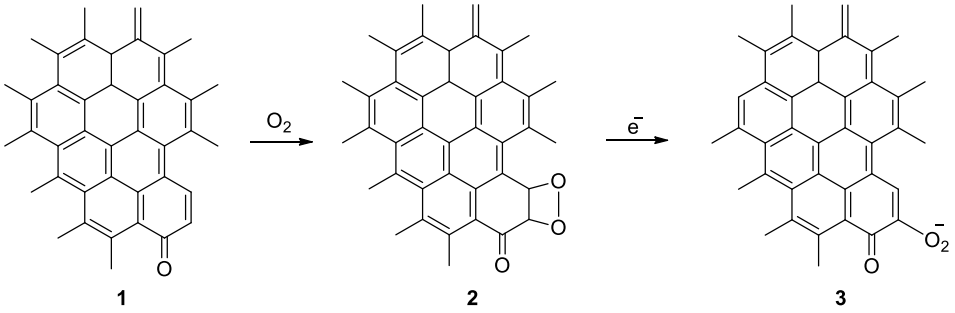

It is of our interest to design experiments for practical use of the reactive intermediate **4** in the oxygen adsorbed activated carbon in synthetic transformations (Scheme 2).

Scheme 2

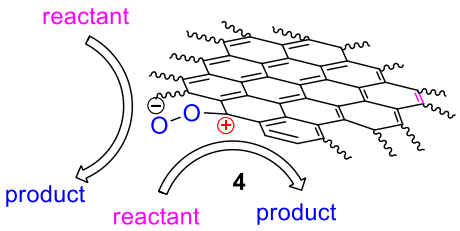

We have investigated the molecular oxygen doped carbon materials for use in the development of new synthetic methods involving reaction with reducing agents and with electron rich compounds and amines. The results are discussed in the next section.

2.2 Results and Discussion

The properties of carbon materials and their surface depend on the heteroatom present and the nature of the materials and methods used for the preparation.[14] Further, it was suggested that the heteroatom (like oxygen) free graphene edge sites in carbon materials are neither hydrogen terminated nor free radicals. Instead, the edge sites are aryne-like armchair sites **5** and carbene-like zigzag sites **6** with triplet ground state. The available evidence points to predominantly carbene-like zigzag sites **6** (Figure 2)**.**[15]

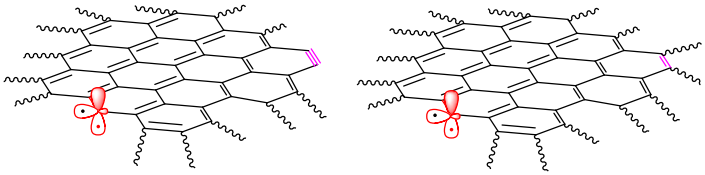

Figure 2. Surface characteristics edge sites in the carbon materials.

The aryne-like sites undergo trimerization to give benzenoid aggregates under ambient atmospheric conditions and expected to give phenolic groups upon reaction with moisture.[16] However, the magnetic properties and chemisorptions with molecular oxygen reported for the carbon materials are in accordance with the proposal that graphene edge sites are carbene-like with triplet ground state **6**.[15]

It has been reported that chemisorption of molecular oxygen by activated carbon fibre materials leads to formation of negatively charged oxygen (C-O-$O^{\delta-}$) species.[16,17]Accordingly, we envisaged the formation of such species **4** through electron transfer from the carbon radical site in **7** formed by the reaction of molecular oxygen with activated carbon **6** (Scheme 3).

Scheme 3

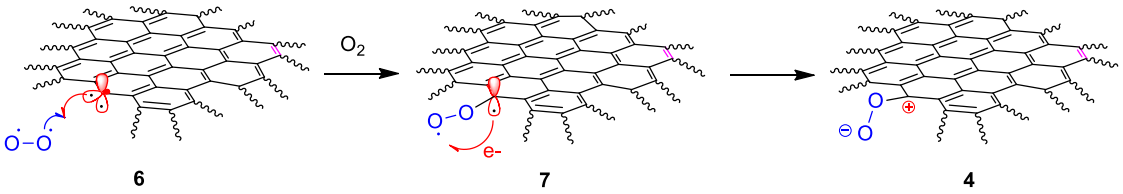

2.2.1 Reactions of molecular oxygen adsorbed carbon materials with Ph_3P

Table 1. Adsorption of molecular oxygen on carbon materials[a]

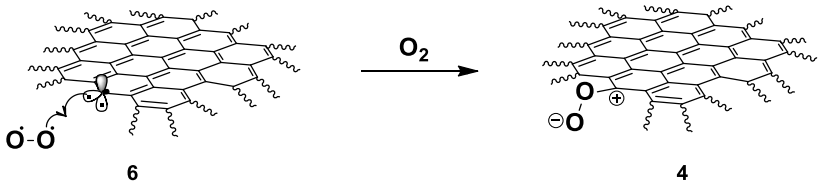

Entry	CM 6 (g)	Oxygen adsorbed CM 4 (g)	O_2, mmol
1	AC (1)	1.034	1.06
	CB (1)	1.053	1.65
	Gr (1)	1.000	-
2	AC (2)	2.071	2.22
	CB (2)	2.078	2.43
3	AC (3)	3.092	2.88
	CB (3)	3.119	3.72
4	AC (4)	4.120	3.75
	CB (4)	4.152	4.75
5	AC (5)	5.175	5.46
	CB (5)	5.190	5.93
	Gr (5)	5.006	0.19
6	AC (10)	10.203	6.34
	CB (10)	10.236	7.37
	Gr (10)	10.013	0.41
7	AC (15)	15.312	9.75

[a]Carbon materials were heated at 200 °C under high vacuum for 2 h and brought to 25 °C under N_2. The dry oxygen was passed through carbon materials for 1 h at 25 °C.

Initially, we have performed several experiments to assess the extent of adsorption of molecular oxygen on carbon materials. The results are summarized in Table 1. The activated carbon (AC) and carbon black (CB) react with molecular oxygen, whereas in the case of graphite (Gr), there was no oxygen or little oxygen gets adsorbed (Table 1).

The carbon material was preheated to 200 °C under high vacuum and brought to room temperature under N_2 atmosphere. Then, the oxygen was passed to the resulting carbon material. The difference in the weight of carbon material before and after oxygen adsorbed indicates that the approximate amount of oxygen molecule gets adsorbed (Table 1).

The carbon skeleton of the oxygen adsorbed intermediate **4** is expected to behave like electron acceptor and the negatively charged oxygen is expected to undergo reaction with proton donors. So, such species are expected to react with proton containing compounds like benzoic acid **8** to give the corresponding hydroperoxide intermediate **9** (Scheme 4).

Scheme 4

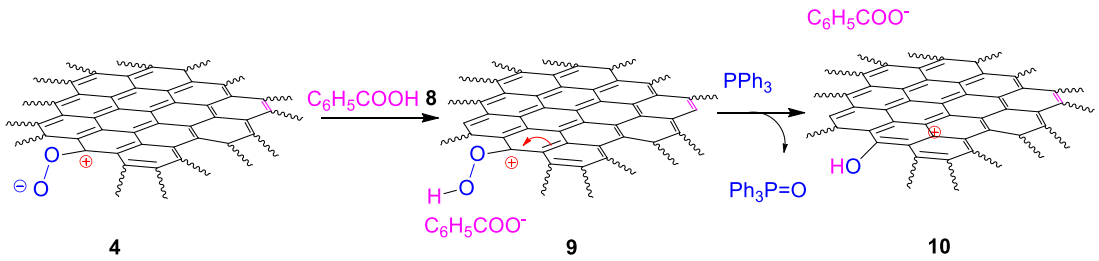

To examine this possibility, we have carried out the reaction of the carbon material with Ph_3P and benzoic acid. We have observed that, in the case of carbon black (CB) without using any proton source or an acid, the triphenylphosphine oxide, $Ph_3P{=}O$ was formed in 17% yield (Table 2, entry 1).

Table 2: Reaction of molecular oxygen adsorbed carbon material **4** with benzoic acid and Ph_3P [a]

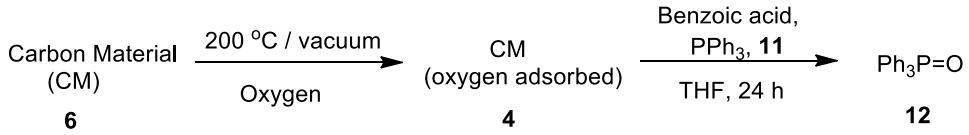

Entry	CM (g)	Benzoic acid (mmol)	Ph_3P (mmol)	THF (mL)	$Ph_3P=O$ Yield (%)[b]
1	CB (5)	0	10	150	17
2	CB (5)	10	10	150	47
3	CB (10)	20	10	150	52
4	AC (5)	10	10	20	54
5	Gr (5)	0	10	20	0
6	Gr (5)	10	10	20	trace
7	Gr (5)	20	10	20	6
8[c]	AC (5)	10	10	20	52
9[c]	CB (5)	10	10	150	45

[a]The carbon material was heated at 200 °C under high vacuum for 2 h and brought to 25 °C under N_2 and dry oxygen was passed through carbon material for 1 h at 25 °C. The reactions were performed with oxygen adsorbed carbon material, benzoic acid and PPh_3 at 25 °C. [b]Isolated yield. [c]The reaction was carried out with re-oxidized carbon material.

The formation of $Ph_3P=O$ was slightly increased with an increase in the amount of either carbon material or benzoic acid. Therefore, an increase in the amount of carbon black and benzoic acid gives the $Ph_3P=O$ in 52% yields (Table 2, entry 3). A further increase in the amount of carbon black leads to moderate increase in the $Ph_3P=O$ product.

Here, the carbon black needs more solvent during the reaction and this limits the use of carbon black in this reaction. Whereas in the case of graphite, without using benzoic acid the formation $Ph_3P=O$ product was not observed (Table 2, entry 5). Further, we have observed that the addition of benzoic acid gives $Ph_3P=O$ in 6% yield (Table 2, entry 7). Further increase in the amount of graphite did not enhance the yield of $Ph_3P=O$. In the case of activated carbon, the $Ph_3P=O$ was isolated in 54% yield (Table 2, entry 4). We have also observed that the carbon material isolated after the reaction with PPh_3 can be reused after vacuum treatment at 200 °C and re-adsorption of molecular oxygen.[18] Reaction using such re-oxidized activated carbon and carbon black with Ph_3P in THF gave the $Ph_3P=O$ product in 52% and 45% yield (Table 2, entry 8 and 9). The results clearly indicate that the molecular oxygen chemisorbed on carbon black and activated carbon but it is only physisorbed on graphite.

2.2.2 Reactions of molecular oxygen adsorbed carbon materials with alkylboranes

Next, we have studied the utilization of the oxygen adsorbed carbon intermediate **4** in organic transformations. The reactive peroxide present in the oxygen adsorbed carbon material **4** can be used for the oxidation of alkylboranes. The organoboranes are readily accessible *via* hydroboration of alkenes and alkynes using easy to handle $NaBH_4/I_2$ reagent system.[19,22] The molecular oxygen itself could oxidize trialkyl borane to the corresponding hydroperoxide or alcohols.[20] However, the preferred reagent for the oxidation of organoboranes is the $HOO^- Na^+$ species produced *in situ* in the reaction of NaOH with H_2O_2. We have envisaged that the oxygen adsorbed intermediate like **4** would react with NaOH to give the species like **13** which could give the $HOO^- Na^+$ species **14** for oxidation of organoboranes *via* the formation of the corresponding borate complex

(Scheme 5).[20] However, there is also a possibility that the peroxy species **13** itself could also oxidize organoboranes in a similar way (Scheme 5).

Scheme 5

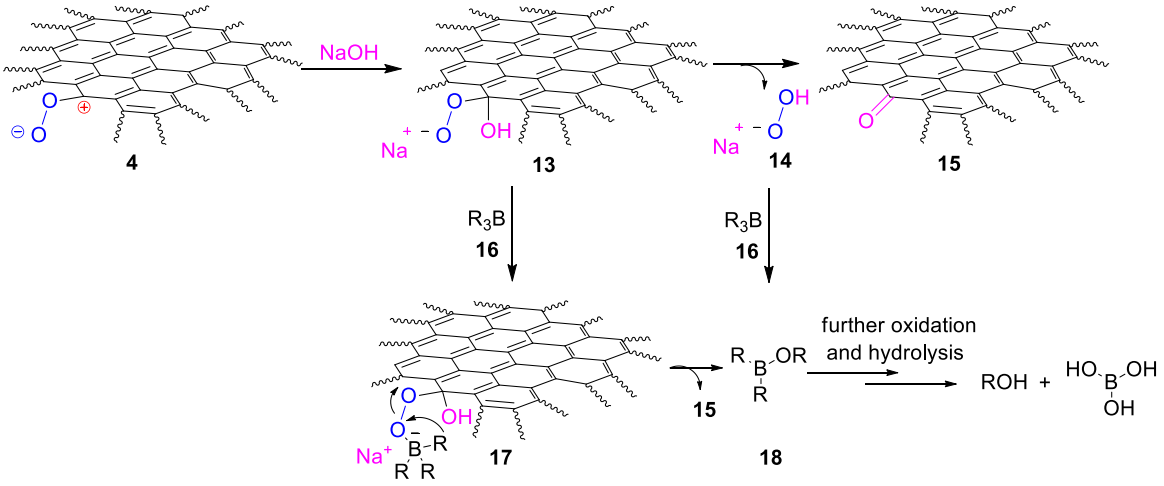

In order to examine this, we have performed a series of experiments on the oxidation of organoboranes prepared using the $NaBH_4/I_2$ reagent system (Scheme 6).

Scheme 6

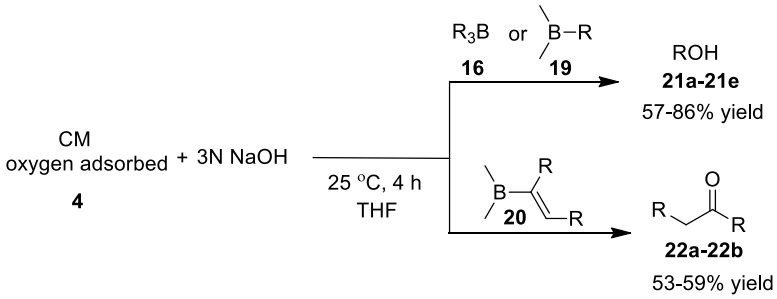

We have observed that trialkylboranes **16a** and **16b** prepared by using hydroboration of 1-decene and norbornene with the $NaBH_4$-I_2 in THF react with a mixture of oxygen adsorbed carbon black **4** and 3N NaOH to give the corresponding alcohol **21a** and **21b** in 85% and 57% yield (Table 3, entry 1 and 2).

Table 3. Reaction of molecular oxygen adsorbed carbon materials **4** with aq. NaOH and alkylboranes[a]

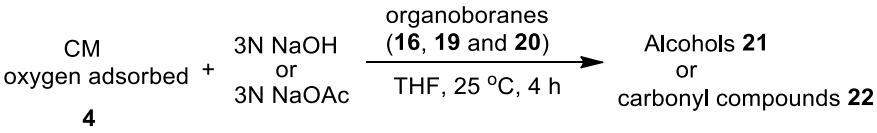

Entry	CM (g)	Alkylboranes (16, 19, 20)	Products (21, 22)	Yield (%)[e]
1[b]	CB (5)	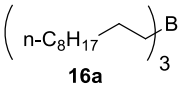 **16a**	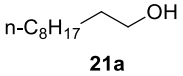 **21a**	85
2[b]	CB (5)	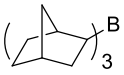 **16b**	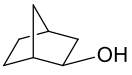 **21b**	57
3[c]	CB (5)	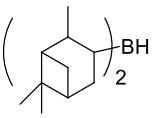 **19a**	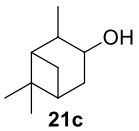 **21c**	71
4[c]	CB (5)	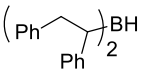 **19b**	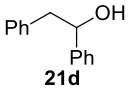 **21d**	86
5[c, f]	CB (5)	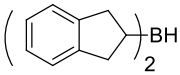 **19c**	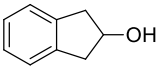 **21e**	80
6[d,g]	CB (5)	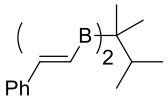 **20a**	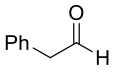 **22a**	53
7[d,f,g]	CB (5)	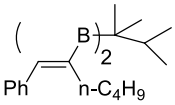 **20b**	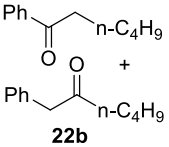 **22b**	59

8 [c,h]	CB (5)	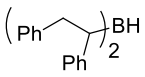 **19b**	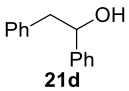 **21d**	82
9 [c,i]	-	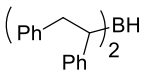 **19b**	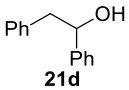 **21d**	<5%

[a]The carbon black was heated at 200 °C under high vacuum for 2 h and brought to 25 °C under N_2 and the dry oxygen was passed through carbon materials for 1 h at 25 °C. Oxidations of organoboranes were carried out with oxygen adsorbed carbon black and aq. 3N NaOH or 3N NaOAc. [b]The reactions were carried out with trialkylboranes (10 mmol). [c]The reactions were carried out with dialkylboranes (10 mmol). [d]The reactions were carried out with alkenylboranes (10 mmol). [e]Isolated yield. [f]Ratio of isomers based on ^{13}C NMR spectrum of the product mixture. [g]The reaction was carried out using aq. NaOAc. [h]Reaction was carried out with molecular oxygen re-adsorbed carbon black. [i]Reaction was performed without molecular oxygen adsorbed carbon black.

The reaction of dialkylboranes **19a-c** prepared by using $NaBH_4$-I_2 in THF, react with the mixture of carbon black and 3N NaOH to give the corresponding alcohols **21c, 21d** and **21e** in 71%, 86% and 80% yield, respectively (Table 3, entries 3-5). Further, the alkenylborane **20a**, prepared by hydroboration using thexylborane, which in turn prepared *in situ* by the reaction of tetramethyl ethylene and the borane gas generated by the reaction of I_2 with *n*-Bu_4NBH_4, upon reaction with oxygen adsorbed carbon black **4** and 3N NaOAc gave the phenylacetaldehyde **22a** in 53% yield (Table 3, entry 6). Whereas, the reaction using the alkenylborane **20b** gives the corresponding regioisomeric mixture **22b** in 59% yield (Table 3**,** entry 7).

The carbon black used for this oxidation could be recovered by filtration, dried at 200 ^0C and re-adsorbed with molecular oxygen. The recovered and re-adsorbed carbon black and 3N NaOH oxidize the dialkylborane **19b** to give the alcohol **21d** in 82% yield (Table 3, entry 8). Also, when the oxidation was performed using dialkylborane **19b** without using molecular oxygen adsorbed carbon black only trace (<5%) amount of alcohol **21d** was obtained (Table 3, entry 9) indicating the role of carbon black in these transformations.

2.2.3 Reaction of sodium borohydride with molecular oxygen adsorbed carbon material and lewis bases

Diborane is one of most important reagent in organic synthesis. Diborane itself is difficult to handle and relatively inert towards olefins. So, it is normally utilized in the form of its complexes such as BH_3:THF, BH_3:SMe_2 and BH_3:NR_3. Many reagent systems have been developed for the generation of diborane gas.[21] Previously, simple methods for generation of diborane gas from I_2/$NaBH_4$, I_2/*n*-Bu_4NBH_4 and $PhCH_2Cl$/*n*-Bu_4NBH_4 reagent systems were reported from this laboratory.[22]

We have observed that the reaction of oxygen adsorbed carbon material **4** with $NaBH_4$ in THF or diglyme lead to slow hydrogen gas evolution. Accordingly, we have envisaged the formation of the AC*-O-O-BH_3 complex **23** as shown in Scheme 7.

Scheme 7

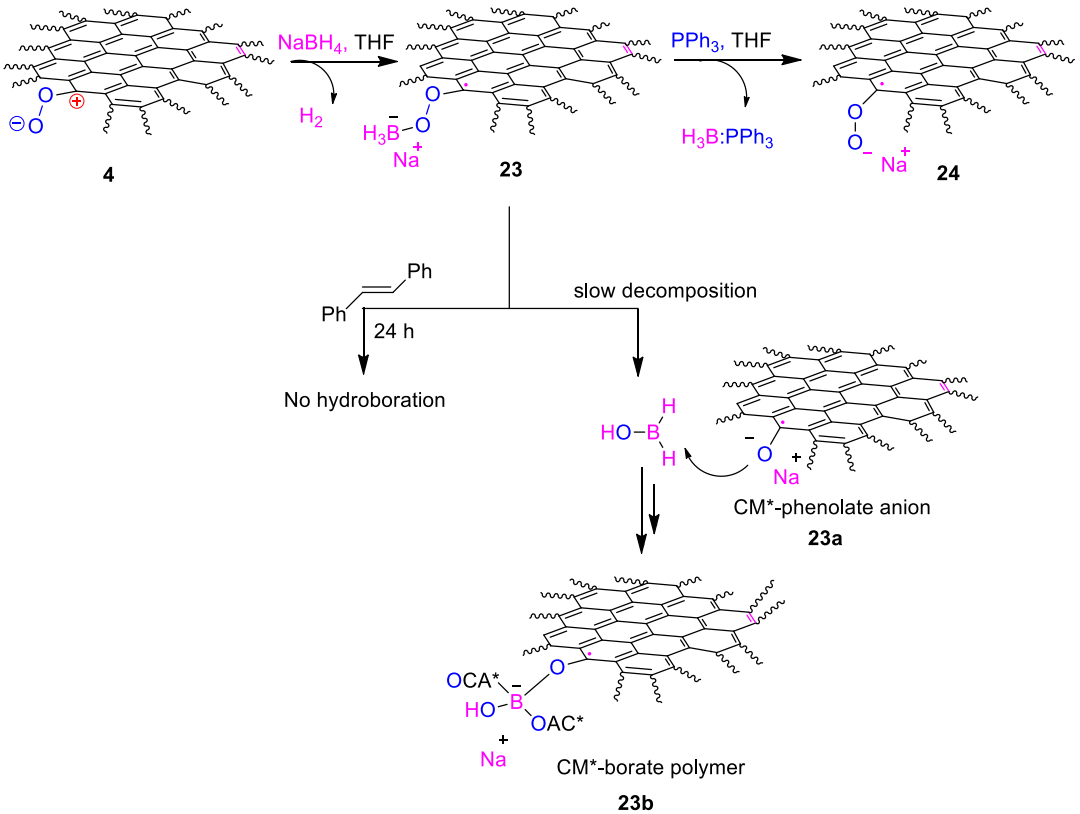

To examine this, we have carried out the hydroboration reaction of stilbene with the intermediate **23** in THF at 25 °C for 24 h. There was no hydroboration observed. Presumably, the reaction of the olefin with the borane complex **23** may be slow and the intermediate **23** may not be stable for longer time to react with olefin or further decomposed to AC* borate polymer (Scheme 7). However, when the reaction of the borane complex **23** was carried out with Ph_3P, the $Ph_3P{:}BH_3$ complex was obtained in 35% yield (Table 4, entry 1).

Table 4. Reaction of $NaBH_4$ with Ph_3P with increasing amount of carbon material (CM).[a]

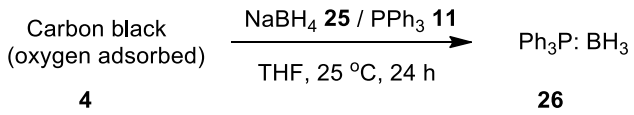

Entry	CM (g)	THF (mL)	$Ph_3P{:}BH_3$ 26 Yield (%)[b]
1	CB (1)	30	35
2	CB (2)	70	54
3	CB (4)	120	62
4	CB (5)	150	69
5	CB (10)	300	73
6[c]	CB (5)	150	65

[a]The reactions were carried out by using $NaBH_4$ (5 mmol) and PPh_3 (5 mmol) at 25°C. [b]Isolated yield. [c]The reaction was performed with molecular oxygen re-adsorbed carbon black.

We have carried out several reactions using different solvents in order to improve the yields and THF turned out to be the best solvent for this transformation. The $Ph_3P{:}BH_3$ was obtained in up to 73% yield, when the reaction was carried out with more amount of oxygen adsorbed carbon black (Table 4). It was found that similar reactions using oxygen adsorbed activated carbon gave 21-77% yield.

Whereas, oxygen adsorbed graphite gave the $Ph_3P:BH_3$ complex only in 9-23% yield, in accordance with reports that molecular oxygen is mainly physisorbed on the surface of graphite.[11,15]

We have also observed that the recovered carbon black remained after reaction with $NaBH_4$ and Ph_3P further reacts with benzoic acid and Ph_3P to give the $Ph_3P{=}O$ in 22% yield. This transformation can be rationalized as shown in Scheme 8.

Scheme 8

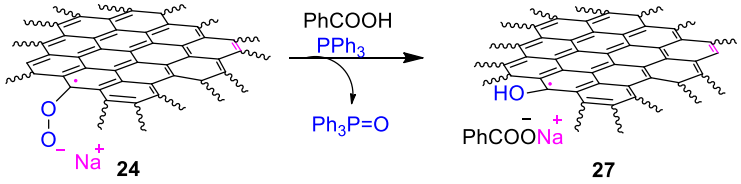

2.2.4 Reaction of molecular oxygen adsorbed carbon black with $NaBH_4$ and amines

We have then turned our attention towards the reaction of pyridine with the AC*-O-O-BH_3 intermediate **23** (Scheme 9).

Scheme 9

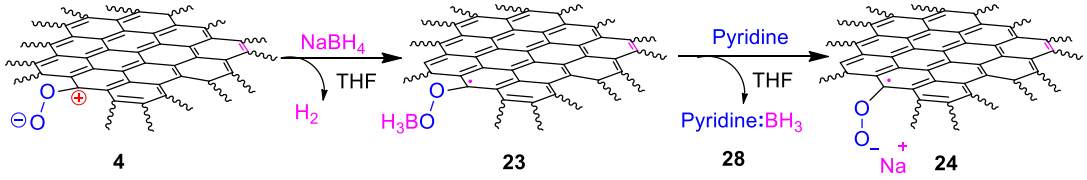

We have found that the reaction of pyridine with $NaBH_4$ in the presence of oxygen adsorbed carbon materials in THF gives the pyridine:BH_3 complex **28** in 42% yield using activated carbon (2 g) and in 52% yield using carbon black (2 g) (Table 5, entry 1 and 2).

We have also performed these experiments using increased amount of carbon material (5 g) in order to improve the yields of pyridine:BH_3 **28** complex. However, there was no further improvement, but there was a slight decrease in the yield of pyridine: BH_3

complex **28** (Table 4, entries 3 and 4). Further, the yields of pyridine:BH_3 complex produced here are relatively low compared to the yields of Ph_3P:BH_3.

Table 5. Reaction of molecular oxygen adsorbed carbon materials with $NaBH_4$ and pyridine[a]

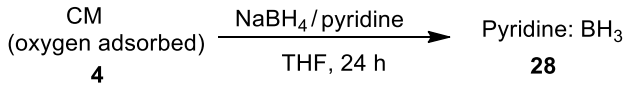

Entry	CM (g)	THF (mL)	Pyrdine:BH_3 complex 28 Yield (%)[b]
1	AC (2)	15	42
2	CB (2)	70	52
3	AC (5)	25	40
4	CB (5)	150	48

[a]The reactions were performed by using $NaBH_4$ (5 mmol) and pyridine (5 mmol) at 25 °C. [b]Isolated yield.

We have also performed the reaction of molecular oxygen adsorbed carbon black with other amines, which are expected to form complexes with borane. The results are summarized in Table 6. The reaction of morpholine **29** with $NaBH_4$ and oxygen adsorbed carbon black in THF gave the morpholine:BH_3 **33** in 43% yield (Table 6**,** entry 1). Similarly, different amine:borane complexes **34-36** were prepared using the amines **30-32** and oxygen adsorbed carbon black (Table 6). The low yields of amine:BH_3 complexes compared to the Ph_3P:BH_3, resulting may be a slow decomposition of the peroxy borane species **23** or the amine borane products may further react with the peroxy species present in the carbon byproduct **24** leading to a reduction in yields.

Table 6. Reaction of molecular oxygen adsorbed carbon black with $NaBH_4$ and amines.[a]

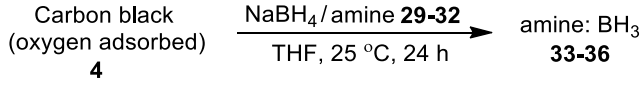

Entry	CB (g)	Amine 29-32	Amine:BH_3 33-36	Yield(%)
1	CB (5)	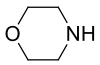 **29**	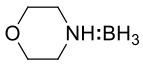 **33**	43
2	CB (5)	 **30**	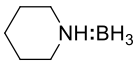 **34**	58
3	CB (5)	 **31**	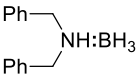 **35**	42
4	CB (5)	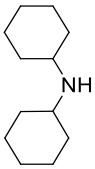 **32**	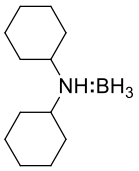 **36**	51

[a]The reactions were carried out by using $NaBH_4$ (5 mmol) and amine (5 mmol) at 25 °C.[b]Isolated yield.

We have also examined the proposed AC*-O-O-BH_3 intermediate **23** for hydroboration reaction of α-methyl styrene **37** in THF but there was no hydroboration (Scheme 10).

Scheme 10

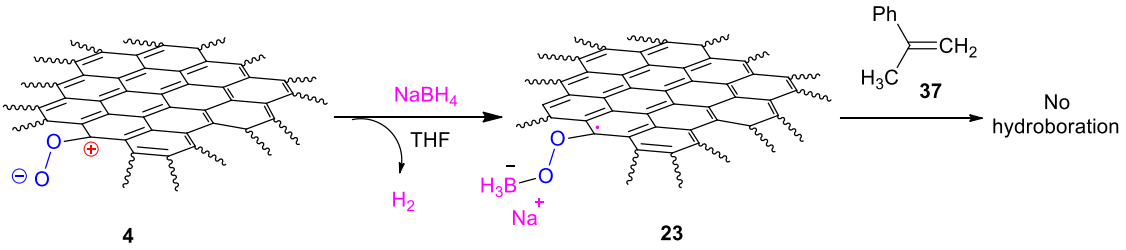

The pyridine:BH_3 complex **28** is useful for hydroboration of olefin at elevated temperatures.[23] Recently it was reported that pyridine:BH_3 complex **28** hydroborates olefins at room temperature under activation by I_2.[24] We have found that the pyridine:BH_3 complex **28** is useful for hydroboration of α-methyl styrene **37**. After oxidation using oxygen adsorbed AC/NaOH, the corresponding alcohol **38** was obtained in 86% yield (Scheme 11).

Scheme 11

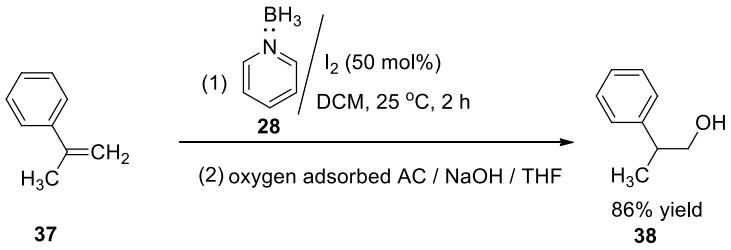

2.2.5 Reaction of oxygen adsorbed activated carbon with benzylamine derivatives

We have observed that benzylamine give benzaldehyde **45** in 30% yield upon reaction with molecular oxygen adsorbed activated carbon. In the case of dibenzylamine **39b**, benzaldehyde was obtained in 25% yield after work up. However, the NMR spectra obtained for the crude product mixture before work up and chromatography revealed the presence of both the imine and benzaldehyde products (Scheme 12). Presumably, the reaction may give amine radical cation followed by the formation of imine, which after

reaction with water yields benzaldehyde. We have also observed that the epr spectrum recorded after addition of amines to oxygen adsorbed activated carbon indicated the presence of paramagnetic species.

Scheme 12

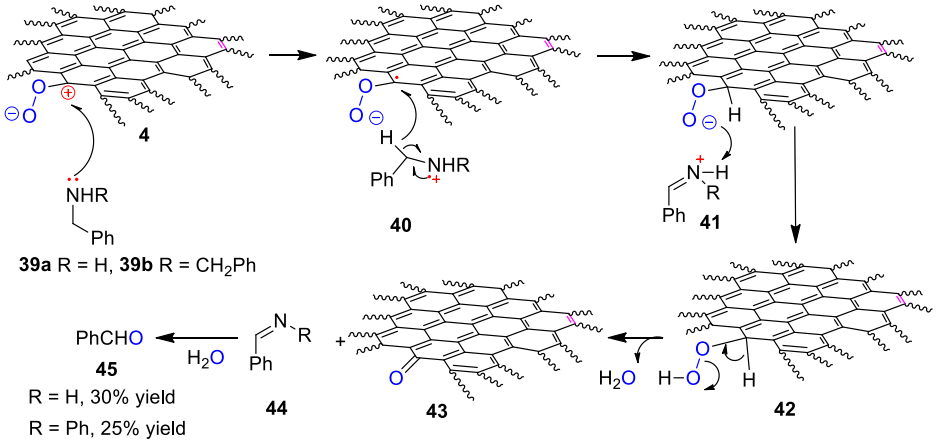

Similarly, it has been observed in this laboratory that the oxygen adsorbed carbon material **4** react with the electron donors like *N*-phenyl tetrahydroisoquinoline **46** and nucleophilic reagents like nitromethane, pyrrole and TMSCN gave the corresponding coupled product **49** in 67-89% yield through the intermediacy of the corresponding radical cation and iminium ion intermediates (Scheme 13).[25]

Scheme 13

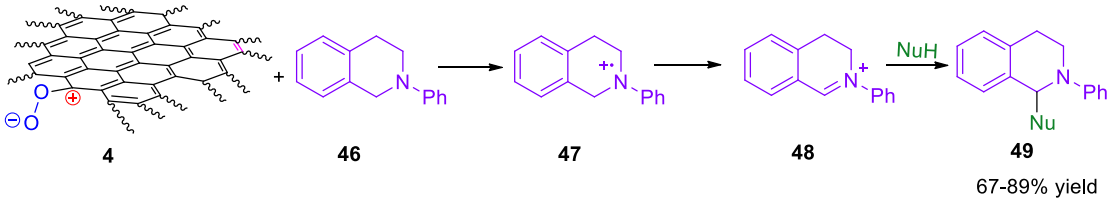

Also, it was found that the 2-naphthol **50** undergoes oxidative coupling reactions in the presence of oxygen adsorbed carbon material **4** to give the bi-2-naphthol **52** (BINOL) in 95% yield *via* the corresponding radical intermediates (Scheme 14).[26]

Scheme 14

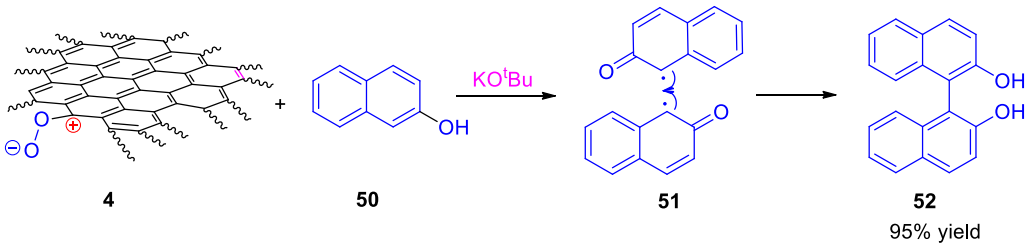

4 **50** **51** **52**

95% yield

2.2.6 Evidence for presence of paramagnetic species through epr spectroscopy

EPR spectra were recorded for the activated carbon samples at various stages and the spectra are presented below.

2.2.6.1 EPR spectrum of commercial carbon material

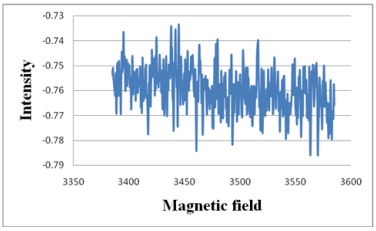

2.2.6.2. EPR spectrum of vacuum dried carbon material

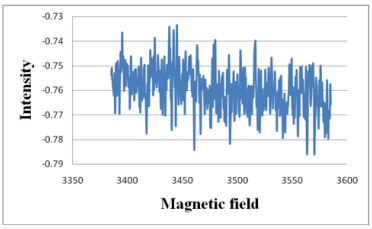

2.2.6.3. EPR spectrum of oxygen doped carbon material

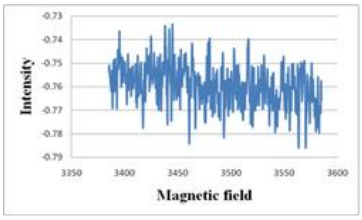

2.2.6.4. EPR spectrum of residual activated carbon (Scheme **4**)

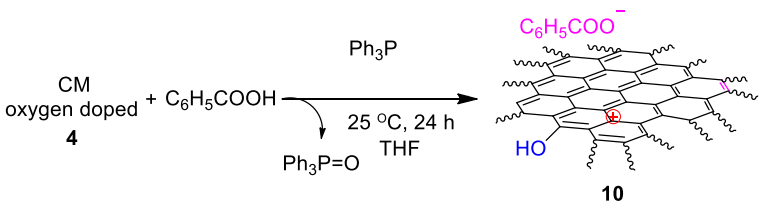

2.2.6.5. EPR spectrum of paramagnetic species **23b** (Scheme **7**)

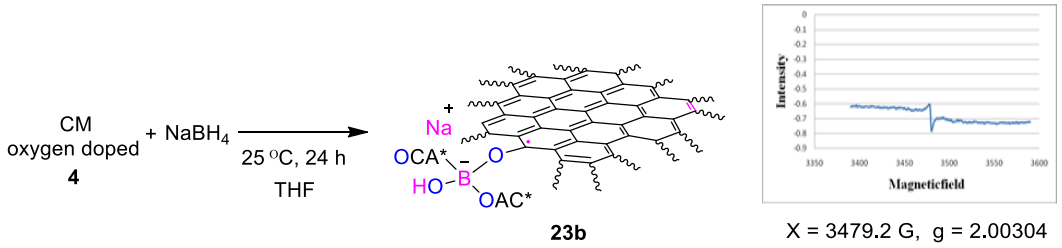

X = 3479.2 G, g = 2.00304

2.2.6.6. EPR spectrum of paramagnetic species **24** (Scheme **7**)

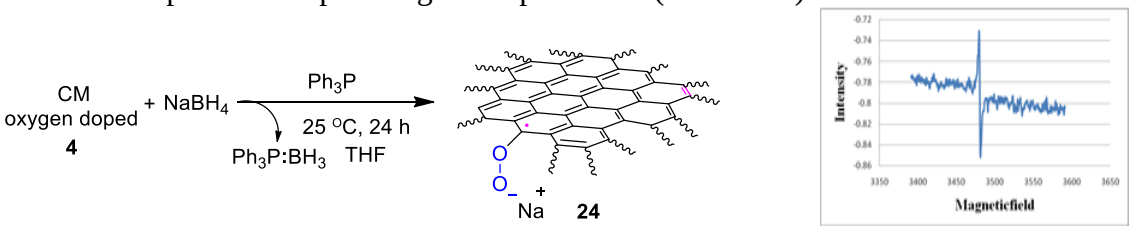

X = 3480.0 G, g = 2.00209

2.2.6.7. EPR spectrum of paramagnetic species **27** (Scheme **8**)

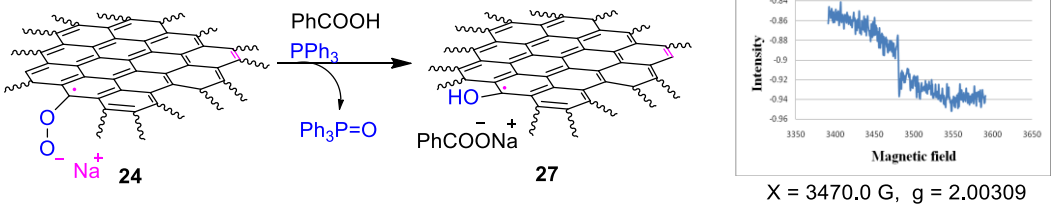

X = 3470.0 G, g = 2.00309

2.2.6.8. EPR spectrum of paramagnetic species **24** (Scheme **9**)

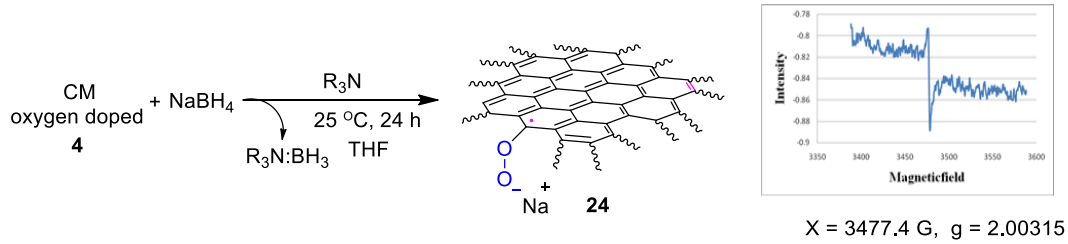

X = 3477.4 G, g = 2.00315

The epr signals observed are in accordance with the paramagnetic species present in residual activated carbon samples.

2.2.7 Synthesis of p-doped polythiophene (PT) and estimation of radical cation site present in p-doped polythiophene.

Electroactive conducting polymers have proven applications in several technologies such as solar cells, display devices, gas sensors and actuators.[27] It is relatively easy to process these polymers to make the devices and their chemically tunable property makes them useful in electronic devices.[28] These polymers are redox-active and their conductivity can be changed by doping the polymer. The physical properties of these conductive polymers depend on the type of the dopant used.

Polythiophene (PT) and its derivatives are good conducting polymers. Optical properties of polythiophenes can be varied by pre-functionalization of monomer.[29,30] Polythiophene derivatives are easy to process and they form a thin film with good optical properties.[31,32] The higher stability and longer life of polythiophene derivatives are suitable for various applications.[33]

Previously, we have discussed the preparation of Lewis base borane complexes using carbon material and borohydride reagent system. Hence, we have undertaken the studies to estimate the doping level in polythiophene radical cation salts using $NaBH_4$. Also, we have envisaged a simple method for generation of Lewis base-borane complexes. The advantage of this method is that we can recover the polythiophene by simple filtration and re-oxidize the polythiophene using $FeCl_3$ to prepare the polymer radical cation salts for reuse in the preparation of Lewis base borane complexes.

We have prepared the polythiophene radical cation salts **54** from thiophene **53** through a slightly modified literature procedure.[34] The dark-brown precipitate of

polythiophene obtained in the reaction was further washed with methanol to remove the residual oxidant. During this procedure the color of the polymer changes from dark-brown to brown. The PT powder was dried in a vacuum at 50 ^{o}C for 12 h (Scheme 15).

Scheme 15

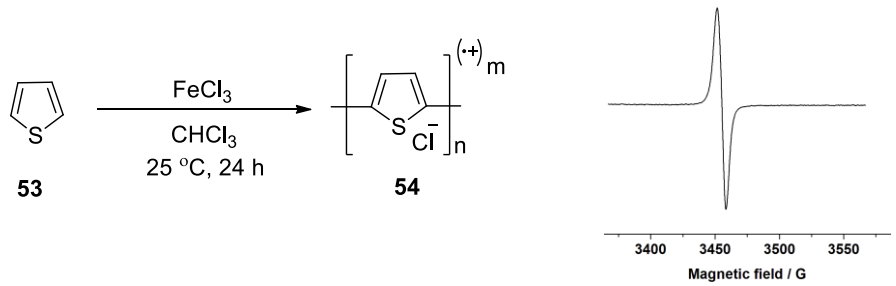

The synthesized polythiophene radical cation salts were confirmed by FT-IR spectroscopy. The presence of paramagnetic sites was confirmed by epr spectroscopy. The polymer exhibits single epr signal with g value of 2.0026 (Scheme 15).[35]

2.2.8 Preparation of lewis base borane complexes using the polythiophene radical cation salts/$NaBH_4$ reagent system.

Earlier reports[36-40] indicate that there are three different structures possible in polythiophene. The structure **55** is a neutral polymer and the removal of an electron from structure **55** leads to form radical cation polymer **56**. This radical cation polymer **56** also called as polaron and it is stabilised by resonance. Removal of an electron from structure **56** gives a bipolaron **57** (Scheme 16). The polaron and bipolaron are formed directly through an oxidation of the thiophene monomer. Previous report[41] shows that the radical cation present in the polythiophene could delocalize into the rings. The repeating unit of cation radical in polythiophene could approximately six monomer units. The planarity of polythiophene gets twisted and delocalisation of the radical cation present in the polymer gets reduced beyond six thiophene rings.

Scheme 16

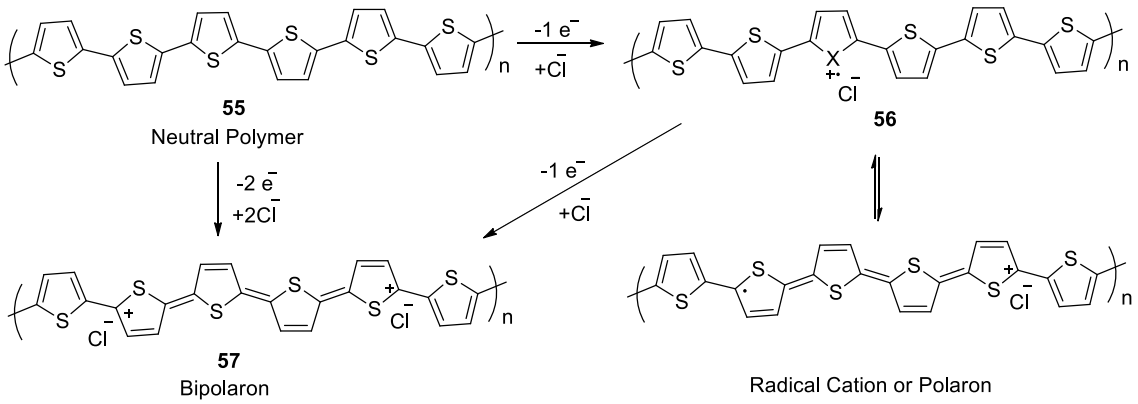

The polythiophene radical cation salts **54** react with $NaBH_4$ with slow evolution of hydrogen gas. Accordingly, the reaction of polythiophene radical cation, $PT^{(.+)}{}_m$ nCl^- $NaBH_4$ and PPh_3 may be visualized by initial formation of a polymer-$NaBH_4$ complex that decomposes to H_2 and borane followed by the formation of $Ph_3P{:}BH_3$ complex. Hence, we have performed the reaction of $NaBH_4$ and Ph_3P with 1 g of polymeric radical cation salts in THF at 25 °C.

Scheme 17

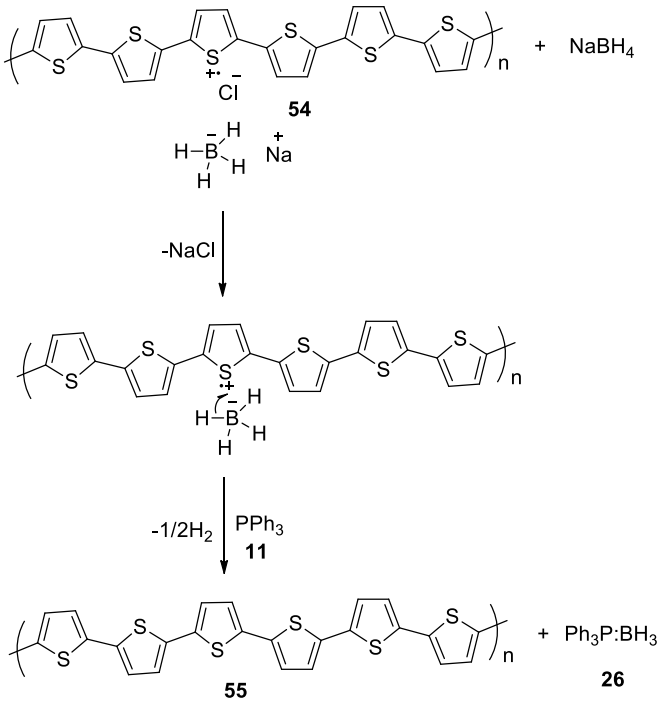

A tentative mechanism for the formation of $Ph_3P{:}BH_3$ complexes can be considered involving the reduction of polythiophene cation radical salts by $NaBH_4$ through single electron transfer (SET) process to give neutral polymer and $Ph_3P{:}BH_3$. The possible mechanism is outlined in Scheme 17.

2.2.9 Estimation of the number of radical cation sites present in polythiophene

We have observed that the reaction of 1 g of $PT^{(.+)}{}_m\ nCl^-$ **54** with $NaBH_4$ (1 mmol) and PPh_3 **11** (1 mmol) gives the $Ph_3P{:}BH_3$ **26** in 0.72 mmol (Table 7, entry 1). When the reaction was carried out using higher amounts of $NaBH_4/Ph_3P$ with 1 g of $PT^{(.+)}{}_m\ nCl^-$ **54**, higher yields of $Ph_3P{:}BH_3$ **26** was obtained (Table 7, entries 2-5).

There was no significant change observed, when the reaction was performed using more than 5 mmol each of $NaBH_4$ and Ph_3P. Accordingly, it can be concluded that a minimum of approximately 1.7 mmol of radical cation sites are present in 1 g of $PT^{(.+)}{}_m\ nCl^-$ **47**. However, the actual number of radical cation salts present is expected to be slightly more than this as the yields are of isolated yields and hence about 5% loss during isolation could be expected. The recovered[42] $PT^{(.+)}{}_m\ nCl^-$ **54** (1 g), after oxidation with $FeCl_3$ (Scheme 15), reacts with $NaBH_4$ (1 mmol)/PPh_3 (1 mmol) to give the $Ph_3P{:}BH_3$ in 0.71 mmol (Table 7, entry 6) without significant change from the freshly prepared sample, illustrating the recyclability of the polymer used.

Table 7. Reaction of polythiophene radical cation salts 54 with $NaBH_4$ and PPh_3[a]

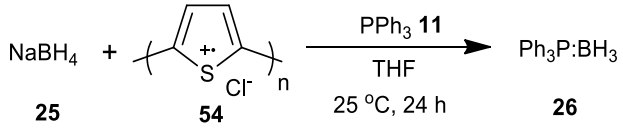

Entry	Polythiophene radical cation salts (1 g)	$NaBH_4$ (mmol)	PPh_3 **11** (mmol)	H_3B:PPh_3 **26** Yield (mmol)[b]
1	**54**	1	1	0.72
2	**54**	2	2	1.22
3	**54**	3	3	1.50
4	**54**	4	4	1.64
5	**54**	5	5	1.70
6[c]	**54**	1	1	0.71

[a]The reactions were performed with polythiophene radical cation salts **54** (1 g), $NaBH_4$ and PPh_3 in THF at 25 °C. [b]Isolated H_3B:PPh_3 complex in mmol. [c]Reaction was performed with re-oxidized polymer radical cation salts.

We have also analyzed the polymer radical cation salts $PT^{(.+)}_m$ nCl^- **54** by UV-Visible spectroscopy before and after the reaction with $NaBH_4$ and PPh_3. Broad absorptions with longer wavelength (red shift) was observed for the polymer before reaction with $NaBH_4$ and PPh_3. The wavelength of absorption gets decreased or move to shorter wavelength after reaction with $NaBH_4$ and PPh_3 (Figure 3). The color of the polymer $PT^{(.+)}_m$ nCl^- **54** also gets changed from dark brown to brown.

The shift in the UV-Visible absorptions spectrum to lower wavelength (blue shift) after the reaction with $NaBH_4$ and PPh_3 for polymer sample **54** indicate that the effective

conjugation present in the polymer or the polymer cation radical sites present in the polymer gets lowered.

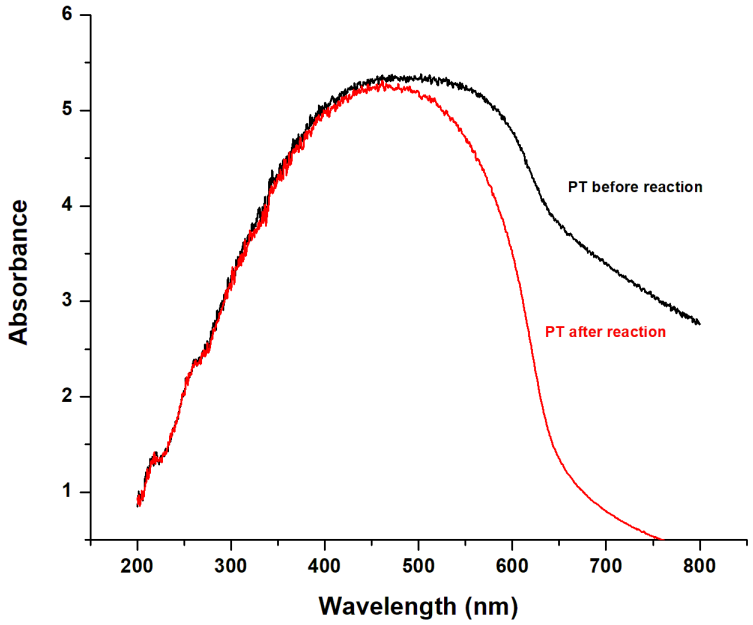

Figure 3. UV-Visible spectrum of polymer **54** powder sample before (black line) and after (red line) reaction with $NaBH_4$ and PPh_3.

The epr studies also indicate that there was a decrease in the radical cation spin density present in the polymer salts (Figure 4). However, the epr studies indicates that the some of the radical cation remains after the reaction with $NaBH_4$ and PPh_3. The epr signals became weak, but not totally absent (Figure 4). Earlier, it was reported that the neutral thiophene polymers react with molecular oxygen to give paramagnetic species.[43] Therefore, formation of small amounts of paramagnetic species by the reaction of polymer with O_2 during the work up procedure cannot be ruled out in these cases.

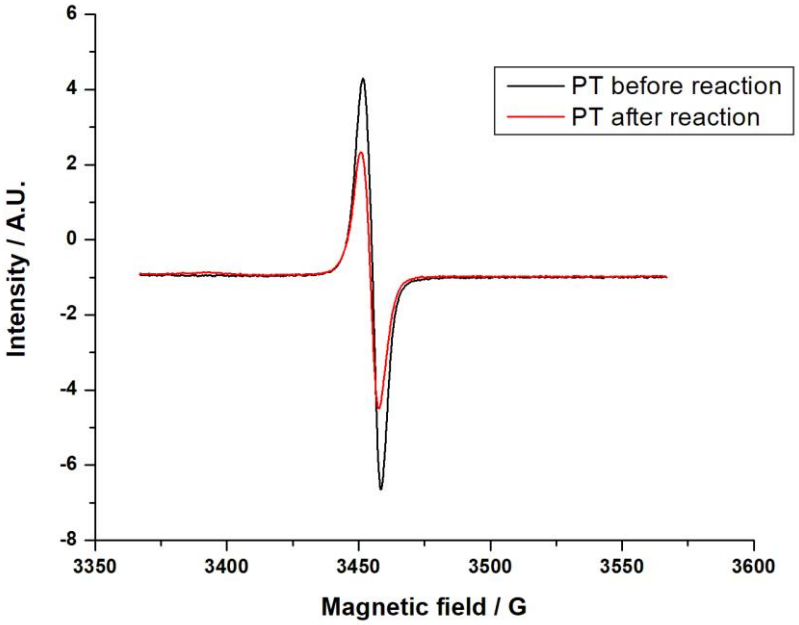

Figure 4. EPR of PT **54** before (black line) and after (red line) reaction with $NaBH_4$ and PPh_3.

The $Ph_3P{:}BH_3$ complex is very stable and hence it is not useful for synthetic applications. However, the amines like pyridine form relatively more reactive borane complexes and hence are useful for hydroboration of olefins at elevated temperatures or at room temperature under activation by I_2.[24] Therefore, we have decided to investigate the reaction of $NaBH_4$ with the polymer radical cation salts in the presence of pyridine.

We have found that the reaction of polythiophene radical cation salts **54** (1 g) with $NaBH_4$ and pyridine in THF gives the pyridine:BH_3 **28** complex. The results are summarized in Table 8. The reaction using PT radical cation **54** (1 g) using 1 mmol each of $NaBH_4$/pyridine gave the pyridine:BH_3 **28** complex in 35% yield based on the presence of 1.7 mmol of radical cation sites in 1 g of PT radical cation **54** (Table 8, entry 1). Similarly, the reaction of PT radical cation **54** with 2 and 3 mmol each of $NaBH_4$ and pyridine gives the pyridine:BH_3 **28** complex in 63% and 79% respectively (Table 8, entry 2 and 3).

Table 8. Reaction of polythiophene radical cation salts 54 with $NaBH_4$ and Pyridine[a]

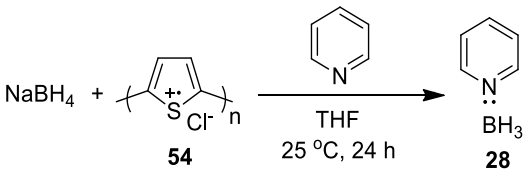

Entry	Polythiophene radical cation (1 g)	$NaBH_4$ (mmol)	Pyridine (mmol)	Pyridine:BH_3 **28** Yield (mmol)[b]	Pyridine:BH_3 **28** Yield[c] (%)
1	**54**	1	1	0.59	35
2	**54**	2	2	1.08	63
3	**54**	3	3	1.35	79

[a]The reactions were performed with polythiophene radical cation salts **54** (1 g), $NaBH_4$ and pyridine in THF at 25 °C. [b]Isolated pyridine:BH_3 complex in mmol. [c]Yields based on mmol of radical cation sites in 1 g polymer and approximately 1.7 mmol of radical cation sites are present in PT **54**.

In these transformations, the borane "BH_3" moiety seems to be extracted by the Ph_3P or pyridine Lewis bases while the radical cation borohydride complex decomposes (Scheme 17). It was of interest to us to examine whether the borohydride complex could hydroborate olefins. Accordingly, we have carried out an experiment using α-methyl styrene with polymer radical cation salts and $NaBH_4$ in THF but there was no hydroboration. Presumably, the olefin is not nucleophilic enough to react with polymer radical cation – borohydride complex. However, we have observed that the pyridine:BH_3 complex **28** prepared in this way readily hydroborates α-methyl styrene under iodine activation. After $NaOH/H_2O_2$ oxidation the corresponding alcohol was obtained in 84% yield.

It was also observed in this laboratory that the reaction of polymers such as poly-*N*-methylpyrrole ($NMPPY^{(.+)}_m$ nCl^-) **54a** and poly(*N*-methylaniline) ($PNMA^{(.+)}_m$ nCl^-) **54b**

radical cation salts with $NaBH_4$ (1 mmol) and PPh_3 (1 mmol) gave the $Ph_3P{:}BH_3$ **26** in 0.62 mmol and 0.68 mmol (Scheme 18). The results indicate that a minimum of approximately 1.35 mmol of radical cation sites are present in 1 g $NMPPY^{(\cdot+)}{}_m$ nCl^- **54a** and also a minimum of 1.60 mmol of radical cation sites are present in 1 g of $PNMA^{(\cdot+)}{}_m$ nCl^- **54b (**Scheme 18).[44]

Scheme 18

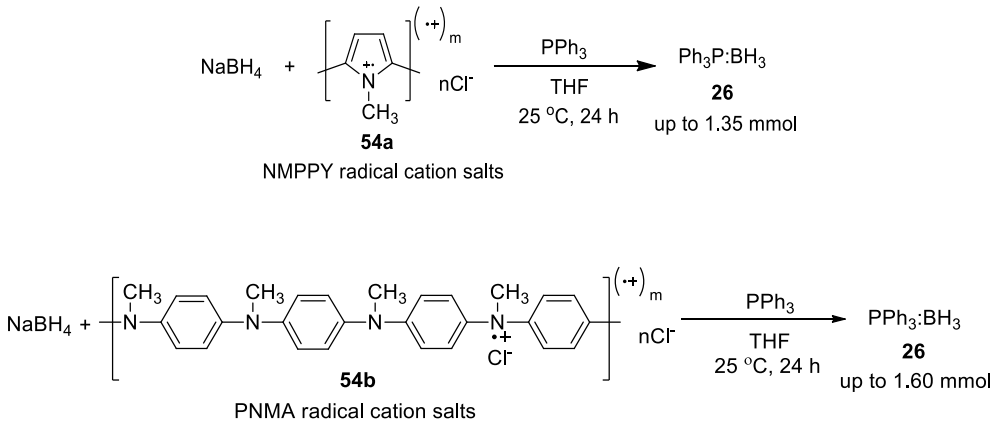

Next, we have studied the reaction of amine nucleophiles with various electron acceptors like quinones, vilologens and halo compounds. The results are described in the chapter 3.

2.3 Conclusions

Convenient methods have been developed for practical use of molecular oxygen adsorbed carbon materials **4**. The molecular oxygen adsorbed carbon black reacts with benzoic acid and Ph_3P to give $Ph_3P{=}O$ in 52% yield. Also, oxidation of organoboranes were performed using readily available oxygen adsorbed carbon materials **4**. These organic transformations were also performed by exploiting the negative charge present in the oxgen end.

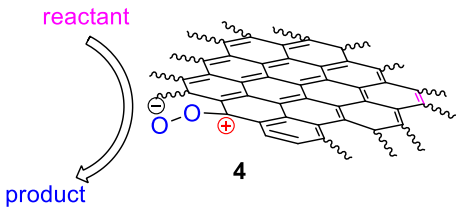

The electron defficiency present in the carbon skeleton of the carbon materials **4** was utilized for the preparation of Lewis base:borane complexes using $NaBH_4$ and Ph_3P or pyridine. The $Ph_3P{:}BH_3$ and amine:BH_3 complexes are prepared in moderate to good yields upon reaction of oxygen adsorbed carbon material with $NaBH_4/Ph_3P$ and $NaBH_4$/amine reagent systems. We have observed bezylamine gives benzaldehyde *via* radical cation intermediates upon reaction with molecular oxygen adsorbed carbon materials.

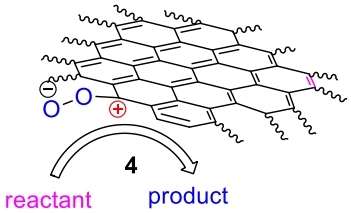

A simple method for estimating doping levels in polymer was developed. Accordingly, it can be concluded that a minimum of approximately 1.7 mmol of radical cation sites are present in 1 g of the $PT^{(.+)}{}_m\ nCl^-$ salt.

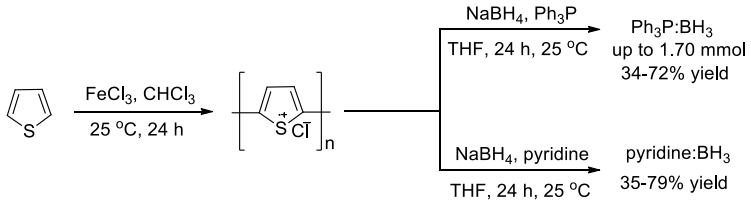

Convenient methods for the preparation of $Ph_3P{:}BH_3$ and pyridine borane and other amine borane complexes were developed.

2.4 Experimental Section

2.4.1 General Informations

IR (KBr) and IR (neat) spectra were recorded on JASCO FT-IR spectrophotometer model-5300. The NMR spectra ^{1}H (400 MHz) and ^{13}C (100 MHz) were recorded on Bruker-Avance-400 spectrometers chloroform-d as solvent. Chemical shifts are expressed in δ downfield with respect to the signal of internal standard tetramethylsilane (δ = 0 ppm). Coupling constants *J* are in Hz. Thin layer chromatography tests were carried out on pre-coated glass plates using silica gel-GF_{254} containing 13% calcium sulfate as binder. The spots were visualized by UV light or exposure to iodine. Gravity column chromatography was used for the separation of compounds using silica gel (100-200 mesh) as stationary phase. All the glasswares were pre-dried at 100-120 °C in an air-oven for 4 h, assembled in hot condition and cooled under a stream of dry nitrogen. Unless otherwise mentioned, all the operations and transfer of reagent were carried out using standard syringe-septum technique recommended for handling air sensitive reagents and organometallic compounds.

In all experiments, a round bottom flask of appropriate size with a side arm, a side septum, a magnetic stirring bar, a condenser and a connecting tube attached to a mercury bubbler was used. The outlet of the mercury bubbler was connected to the atmosphere by a long tube. All dry solvents and reagents used were distilled from appropriate drying agents. As a routine practice, all organic extracts were washed using saturated NaCl solution (brine) and dried over Na_2SO_4 or K_2CO_3 and concentrated on Heidolph-EL-rotary evaporator.

$FeCl_3$ and benzoic acid supplied by E-Merck (India) was used as received. Thiophene, Activated Carbon, Carbon Black, Graphite, norborene, tetramethylethylene, benzylzmine and dibenzylamine were purchased from Aldrich and used as received. $NaBH_4$, PPh_3 and NaOH were supplied by E-Merck (India) was used as received.

Dichloromethane was distilled using calcium hydride under nitrogen. The THF solvent supplied by commercial sources, India were kept over sodium-benzophenone ketyl then freshly distilled before use. Toluene also kept over sodium-benzophenone ketyl, distilled and stored over sodium wire.

2.4.2 General Procedure for reaction of molecular oxygen doped activated charcoal with Ph_3P in presence of benzoic acid

In a 50 mL RB flask, carbon black (10 g) was heated at 200 °C under high vacuum for 2 h. The carbon black was brought to room temperature under nitrogen atmosphere and passed molecular oxygen for 1 h. To this, Ph_3P (2.62 g 10 mmol) and benzoic acid (1.221 g, 10 mmol) in THF were added. The reaction mixture was further stirred for 24 h. The reaction mixture was filtrated and the organic layer was separated. The solvent was evaporated under reduced pressure and the crude product $Ph_3P{=}O$ was purified by silica gel column chromatography using hexane and ethyl acetate as eluent.

Triphenylphosphine oxide $Ph_3P{=}O$ (12)

Yield **:** 0.501 g (54%); White solid

IR (KBr) **:** (cm^{-1}) 3073, 3046, 1599, 1489, 1435, 1308, 1188, 1117, 1002.

^{1}H NMR **:** (400 MHz, $CDCl_3$, δ ppm) 7.67-7.62 (m, 1H), 7.52-7.48 (m, 1H), 7.43-7.40 (m, 1H).

^{13}C NMR **:** (100 MHz, $CDCl_3$, δ ppm) 133.0, 132.1, 132.0, 131.9, 128.5, 128.4.

^{31}P NMR : (162 MHz, $CDCl_3$ δ ppm) 29.3

2.4.3 General procedure for reaction of molecular oxygen adsorbed carbon materials with alkylboranes (16a-16b and 19a-19c)

In a 50 mL RB flask, activated carbon (5 g) and 3N NaOH (10 mL) in THF 15 mL were stirred for about 4 h. To this reaction mixture, the alkylboranes was added dropwise for 20 min at 0 °C and further stirred for 4 h. The reaction mixture was filtered and the organic layer was separated. The aqueous layer was extracted with ether (2 x 10 mL). The solvent was evaporated and the crude products were purified on silica gel column chromatography using hexane: ethyl acetate (95:5) as eluent.

2.4.4 Preparation of trialkylborane (16a-16b)

$NaBH_4$ (0.151 g, 4 mmol) was taken in a two-necked RB flask and dry THF (10 mL) was added. The RB flask placed at -30 °C and iodine (0.51 g, 2 mmol) in THF (10 mL) was added slowly during 10 min. After the evolution of hydrogen gas ceased, the reaction mixture was further stirred for 1 h at -30 °C. A solution of olefin (10 mmol) was added under nitrogen atmosphere. The reaction mixture was brought to 25 °C and further stirred for 4 h at the same temperature to give trialkylborane. The solution was added dropwise to activated carbon (5 g) and 3N NaOH (10 mL) mixture in THF 15 mL for 20 min at 0 °C and stirred for 4 h. The reaction mixture was filtered and the organic layer was separated and the aqueous layer was

extracted with ether (2 x 10 mL). The solvent was evaporated and the crude products were purified on silica gel column chromatography using hexane: ethyl acetate (95:5) as eluent.

Decan-1-ol (21a)

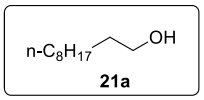

21a

Yield **:** 0.672 g (85%) colorless liquid.

IR (neat) **:** (cm^{-1}) 3332, 2925, 2855, 1462, 1377, 1122, 1055, 723.

^{1}H NMR **:** (400 MHz, $CDCl_3$, δ ppm) 3.65 (t, *J* = 6.0 Hz, 2H), 1.59-1.56 (m, 2H), 1.40-1.28 (m, 14H), 0.91-0.87 (m, 3H);

^{13}C NMR **:** (100 MHz, $CDCl_3$, δ ppm) 63.1, 32.8, 31.9, 29.6, 29.4, 29.3, 25.7, 24.9, 22.6, 14.1.

***exo*-Bicyclo [2.2.1] heptan-2-ol (21b)**

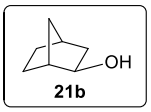

21b

Yield **:** 0.319 g (57%); White solid.

IR (KBr) **:** (cm^{-1}) 3430 (br), 3024, 2935, 2869, 1597, 1495, 1450, 1066, 1042, 755, 741, 702.

^{1}H NMR **:** (400 MHz, $CDCl_3$, δ ppm) 3.68-3.66 (m, 1H), 2.18-2.08 (m, 2H), 1.59-1.51 (m, 2H), 1.42-1.35 (m, 2H), 1.29-1.22 (m, 1H), 1.05-1.03 (m, 1H), 0.98-0.96 (m, 2H)

^{13}C NMR **:** (100 MHz, $CDCl_3$, δ ppm) 74.6, 44.1, 42.1, 35.4, 34.4, 28.1, 24.4.

2.4.5 Preparation of dialkylborane (19a-19c)

The $NaBH_4$ (0.190 g, 5 mmol) was taken in a two-necked RB flask and dry THF (10 mL) was added. The RB flask placed at -30 °C and iodine (0.635 g, 2.5 mmol) in THF (10 mL) was added slowly during 10 min. After the evolution of hydrogen gas ceased, the reaction mixture was further stirred for 1 h at -30 °C. A solution of olefin (10 mmol) was

added under nitrogen atmosphere. The reaction mixture was brought to 25 °C and further stirred for 4 h at the same temperature to give dialkylborane. The solution was added dropwise to activated carbon (5 g) and 3N NaOH (10 mL) mixture in THF 15 mL for 20 min at 0 °C and stirred for 4 h. The reaction mixture was filtered and the organic layer was separated and the aqueous layer was extracted with ether (2 x 10 mL). The solvent was evaporated and the crude products were purified on silica gel column chromatography using hexane: ethyl acetate (95:5) as eluent.

2, 6, 6-Trimethyl-bicyclo [3.1.1] heptan-3-ol (21c)

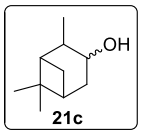

21c

Yield **:** 1.095 g (71%); colorless liquid.

IR (neat) **:** (cm^{-1}) 3327, 2905, 1147, 1055, 808, 692.

^{1}H NMR **:** (400 MHz, $CDCl_3$, δ ppm) 4.18-3.92 (m, 1H), 2.51-2.47 (m, 1H), 2.37-2.34 (m, 1H), 1.79-1.17 (m, 8H), 1.12 (d, *J* = 7.4 Hz, 3H), 1.03 (d, *J* = 9.8 Hz, 1H) 0.91 (s, 3H).

^{13}C NMR **:** (100 MHz, $CDCl_3$, δppm) 71.6, 47.8, 47.7, 41.7, 39.0, 38.1, 34.3, 27.6, 23.6, 20.7.

1, 2-Diphenyl-ethanol (21d)

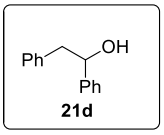

21d

Yield **:** 1.705 g (86%); White soild.

mp **:** 62-63 °C; (lit.[2] mp 63-64 °C)

IR (KBr) **:** (cm^{-1}) 3329, 3078, 3026, 2922, 1039, 696.

^{1}H NMR **:** (400 MHz, $CDCl_3$, δ ppm) 7.38-7.21 (m, 10H), 4.92-4.89 (m, 1H), 3.09-2.98 (m, 2H), 1.95 (s, 1H).

^{13}C NMR **:** (100 MHz, $CDCl_3$, δ ppm) 143.8, 138.1, 129.5, 128.5, 128.4, 127.6, 126.6, 125.9, 75.3, 46.1.

Indan-2-ol (21e)

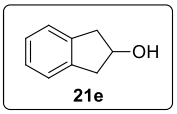

21e

Yield **:** 1.072 g (80%); White solid

IR (KBr) **:** (cm^{-1}) 3281, 3076, 2934, 1554, 1485, 1415, 1379, 1147, 1055, 808, 692.

^{1}H NMR **:** (400 MHz, $CDCl_3$, δ ppm) mixture of isomers (α:β 1:9)

^{13}C NMR **:** (100 MHz, $CDCl_3$, δ ppm) 140.8, 126.6, 126.5, 73.1, 42.6 (major isomer)

2.4.6 General procedure for reaction of molecular oxygen adsorbed carbon materials with alkenylboranes (20a and 20b)

In a 50 mL RB flask, activated carbon (5 g) and 3N NaOAc (10 mL) in THF 15 mL stirred for about 4 h. To this reaction mixture, alkenylboranes **20a** and **20b** was added dropwise for 20 min at 0 °C and further stirred for 4 h. The reaction mixture was filtered and organic layer was separated. The aqueous layer was extracted with ether (2 x 10 mL). The solvent was evaporated and the crude products were purified on silica gel column chromatography using hexane:ethyl acetate (98:2) as eluent.

2.4.7 Preparation of dialkenyl(thexyl)borane (20a and 20b)

n-Bu_4NBH_4 (0.190 g, 5 mmol) was taken in a two-necked RB flask and added dry toluene (5 mL) followed by iodine (0.635 g, 2.5 mmol) in toluene (10 mL). The generated diborane was carried off through a side tube and bubbled through a solution of tetramethyl

ethylene (5 mmol) for 15 min. The reaction mixture was brought to 25 °C and further stirred for 4 h. In another two-necked RB flask the alkyne (10 mmol) in dry THF (10 mL) was taken and cooled to 0 °C under nitrogen atmosphere. The thexylborane in toluene prepared as above was added through a cannula under nitrogen atmosphere. The contents were further stirred for 4 h at 0 °C. The solution was added dropwise to activated carbon (5 g) and 3N NaOAc (10 mL) mixture in THF 15 mL for 20 min at 0 °C and stirred for 4 h. The reaction mixture was filtered and the organic layer was separated and the aqueous layer was extracted with ether (2 x 10 mL).The solvent was evaporated and the crude products were purified on silica gel column chromatography using hexane: ethyl acetate (98:2) as eluent.

2-Phenylacetaldehyde (22a)

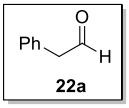

22a

Yield : 0.636 g (53%); colorless liquid.

IR (neat) : (cm^{-1}) 3061, 3029, 1923, 1723, 1602, 1495, 1452, 1131, 950, 750, 701.

^{1}H NMR : (400 MHz, $CDCl_3$, δ ppm) 9.79 (s, 1H), 7.41-7.10 (m, 5H), 3.70 (s, 2H);

^{13}C NMR : (100 MHz, $CDCl_3$, δ ppm) 199.5, 131.8, 129.6, 129.0, 128.1, 127.4, 50.6.

1-Phenyl-hexan-2-one; 1-phenyl-hexan-1-one (22b)

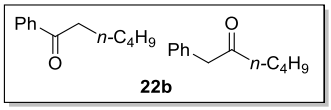

22b

Yield : 1.038 g (59%); colorless liquid.

IR (neat) : (cm^{-1}) 3060, 2960, 2940, 1675, 1600, 1450, 1350, 1220, 950, 760, 700.

^{1}H NMR : (400 MHz, $CDCl_3$, δ ppm) mixture of isomers (60:40).

^{13}C NMR **:** (100 MHz, $CDCl_3$, δ ppm) 208.6, 200.6, 137.1, 134.4, 132.8, 128.8, 128.6, 128.5, 128.0, 126.9, 50.1, 41.7, 38.5, 31.5, 25.8, 24.7, 22.5, 22.2, 13.9, 13.8.

2.4.8 General Procedure for reaction of activated carbon and $NaBH_4$ with PPh_3

In a 50 mL RB flask, carbon black (5 g), and $NaBH_4$ (0.19 g, 5 mmol) in THF (25 mL) were taken added under nitrogen atmosphere. To this reaction mixture PPh_3 (1.31 g, 5 mmol) was added and the contents were stirred for about 24 h. The reaction mixture was filtered and the organic layer was separated. The solvent was evaporated under reduced pressure and the crude product was purified on silica gel column chromatography using hexane as eluent to isolate pure $Ph_3P{:}BH_3$ as white solid.

$Ph_3P{:}BH_3$ complex (26)

Yield **:** 1.06 g (69%); White solid

$Ph_3P{:}BH_3$
26

IR (KBr) **:** (cm^{-1}) 3057, 2372, 2344, 1478, 1435, 1314, 1177, 1106, 1056, 733.

^{1}H NMR **:** (400 MHz, $CDCl_3$, δ ppm) 7.63-7.60 (m, 1H), 7.53-7.50 (m, 1H), 7.46-7.43(m, 1H)

^{13}C NMR **:** (100 MHz, $CDCl_3$, δ ppm) 133.2, 133.1, 131.1, 129.4, 128.8, 128.7

^{31}P **:** (162 MHz, $CDCl_3$, δ ppm) 21.5

^{11}B **:** (128.3 MHz, $CDCl_3$, δ ppm) -37.8

2.4.9 General procedure for reaction of carbon materials and $NaBH_4$ with pyridine

In a 50 mL RB flask, carbon black (5 g) and $NaBH_4$ (0.19 g, 5 mmol) were taken and THF (15 mL) was added under nitrogen atmosphere. To this, pyridine (0.4 ml, 5 mmol) was added and the contents were stirred for 24 h. The contents were filtered and the solvent was evaporated under reduced pressure to afford the crude product. The crude product was purified on silica gel column chromatography using hexane: ethylacetate (90:10) as eluent to isolate pure pyridine:BH_3 complex **28** as colorless liquid.

Pyridine:BH_3 complex (28)

Yield **:** 0.242 g (52%); Colorless liquid

IR (neat) **:** (cm^{-1}) 2964, 2832, 2750, 2712, 2531, 2460, 2400, 2062, 1419, 1304, 1145.

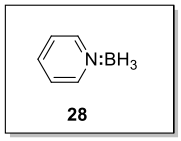

28

^{1}H NMR **:** (400 MHz, $CDCl_3$, δ ppm) 8.52 (s, 2H), 7.91 (s, 1H), 7.50-7.48 (s, 2H).

^{13}C NMR **:** (100 MHz, $CDCl_3$, δ ppm) 147.3, 134.3, 125.4.

^{11}B NMR : (128.3 MHz, $CDCl_3$, δ ppm) -11.4

2.4.10 General Procedure for reaction of activated carbon and $NaBH_4$ with amine

In a 50 mL RB flask, carbon black (5 g) and $NaBH_4$ (0.19 g, 5 mmol) were taken and THF (15 mL) was added under nitrogen atmosphere. To this, amine (5 mmol) was added and the contents were stirred for 24 h. The contents were filtered and the solvent was evaporated under reduced pressure to afford the crude product. The crude product was purified on silica gel column chromatography using hexane:ethylacetate as eluent to isolate coressopnding amine:BH_3 complex.

Morpholine:BH_3 complex (33)

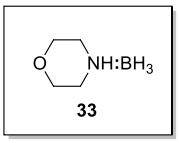

33

Yield **:** 0.215 g (43%); White solid

IR (KBr) **:** (cm^{-1}) 3194, 2969, 2854, 1419, 1369, 1254, 1139, 1041, 904, 843, 734.

^{1}H NMR **:** (400 MHz, $CDCl_3$, δ ppm) 4.36 (s, 1H), 3.97-3.94 (d, *J* = 12.0 Hz, 2H), 3.62-3.55 (t, *J* = 4.0 Hz, 2H), 3.11-3.08 (d, *J* = 12.0 Hz, 2H), 2.85-2.76 (m, 2H).

^{13}C NMR **:** (100 MHz, $CDCl_3$, δ ppm) 65.7, 51.9.

^{11}B NMR : (128.3 MHz, $CDCl_3$ δ ppm) -16.1

Piperidine:BH_3 complex (34)

Yield **:** 0.287 g (58%); White solid

IR (KBr) **:** (cm^{-1}) 3221, 2936, 2849, 2349, 2350, 2273, 1463, 1364, 1276, 1161, 1123, 1057.

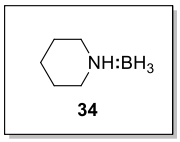

34

^{1}H NMR **:** (400 MHz, $CDCl_3$, δ ppm) 3.80 (brs, 1H), 3.23 (d, *J* = 8.0 Hz, 2H), 2.53-2.47 (m, 2H), 1.78- 1.48 (m, 6H).

^{13}C NMR **:** (100 MHz, $CDCl_3$, δppm) 53.3, 25.3, 22.5.

^{11}B NMR : (128.3 MHz, $CDCl_3$ δppm) -15.0.

Dibenzyl amine:BH_3 complex (35)

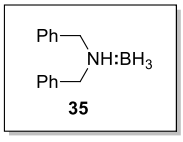

35

Yield **:** 0.443 g (42%); Colorless liquid

IR (neat) **:** (cm^{-1}) 3189, 2969, 2936, 2860, 2372, 2323, 2263, 1457, 1424, 1380, 1282, 1232, 1161.

^{1}H NMR **:** (400 MHz, $CDCl_3$, δ ppm) 7.39-7.31 (m, 4H), 7.21-7.19 (m, 6H), 4.02-3.99 (m, Hz, 4H).

^{13}C NMR **:** (100 MHz, $CDCl_3$, δ ppm) 139.3, 128.9, 128.7, 128.2, 58.4

^{11}B NMR : (128.3 MHz, $CDCl_3$ δ ppm) -14.4

Dicyclohexyl amine:BH_3 complex (36)

Yield **:** 0.497 g (51%); White solid

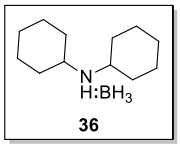

36

IR (KBr) **:** (cm^{-1}) 3200, 3030, 2936, 2372, 2328, 2301, 2273, 1495, 1457, 1413, 1347, 1161.

^{1}H NMR **:** (400 MHz, $CDCl_3$, δ ppm) 2.84-2.83 (m, 4H), 1.89-1.78 (m, 6H), 1.66-1.59 (m, 6H), 1.32-1.24 (m, 6H).

^{13}C NMR **:** (100 MHz, $CDCl_3$, δ ppm) 60.6, 30.8, 29.6, 25.6, 25.3, 25.2

^{11}B NMR : (128.3 MHz, $CDCl_3$ δppm) -19.4

2.4.11 Procedure for the hydroboration/oxidation of α-methyl styrene using pyridine:BH_3 complex with I_2 activation

The pyridine:BH_3 (0.186 g, 2 mmol) was added to 5 ml of dcm. I_2 (0.24 g, 1 mmol) was dissolved in dcm and added slowly at 0 ^{o}C. After the gas evolution, the solution was stirred to rt and α-methyl styrene (0.26 ml, 2 mmol) was added. The mixture was stiired at rt for 2 h. The solution was cooled to 0 ^{o}C, the activated carbon (5 g), NaOH (5 ml) and THF (5 ml) were added. The mixture was further stirred at rt for 4h. The mixture was filtered and the organic layer was separated and the aqueous layer was extracted with ether (2 x 10 mL). The

solvent was evaporated and the crude product was purified by column chromatography on silica gel column using hexane/ethyl acetate (90:10) as eluent to isolate the alcohol 38.

2-Phenylpropanol (38)

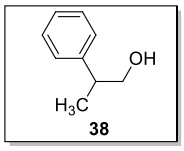

Yield **:** 0.234 g (86%); Colorless liquid

IR (neat) **:** (cm^{-1}) 3336, 3032, 2954, 1603, 1492, 1032, 756.

^{1}H NMR **:** (400 MHz, $CDCl_3$, δppm) 7.36-7.29 (m, 5H), 3.70 (d, *J* = 8 Hz, 2H), 2.96-2.93 (m, 1H), 1.59 (s, 1H); 1.29 (d, *J* = 8 Hz, 3H).

^{13}C NMR **:** (100 MHz, $CDCl_3$, δppm) 143.7, 128.6, 127.5, 126.7, 68.7, 42.4, 17.6

2.4.12 General procedure for oxidation of benzylamine derivatives with activated carbon

In a 25 mL RB flask, activated carbon (1 g) heated at 200 °C under high vacuum (0.001 mm of Hg) for 2 h. After the RB flask was brought to room temperature under nitrogen atmosphere, the contents were saturated with dry air for 1 h. To this benzylamine derivatives (1 mmol) in THF solvent was added. The reaction mixture was further stirred for 24 h. After that, the reaction mixture was filtered and the organic layer was evaporated. Then the NMR was recorded for the crude compound to show the formation of both imine and benzaldehyde. The crude reaction mixture was washed several times with EtOAc and H_2O. The organic layer extracts with EtOAc, washed with brine and then dried over anhyd.Na_2SO_4. Evaporate solvent under vacuum and the crude mixture was chromatographed on silicagel using hexane:ethyl acetate (90:10) as an eluent to give pure benzaldehyde.

2.4.13 General procedure for preparation of polythiophene 54

Thiophene (24 mmol) was taken in $CHCl_3$ (130 mL) under N_2 atmosphere. Then anhydrous $FeCl_3$ (55 mmol) was added slowly in portions from a solid addition flask over a period of 1 h. The mixture was stirred for 24 h at 25 °C. The dark-brown precipitate of polythiophene was formed. The polymer was separated by filtration and washed several times with $CHCl_3$. The polymer was further washed with methanol to remove the residual oxidant. The color of the polymer was changed from dark-brown to brown. The polythiophene powder was dried in a vacuum at 50 °C for 12 h.

Yield : 2.3 g, Brown solid

IR (KBr) : (cm^{-1}) 3468, 3062, 1490, 1437, 778 695.

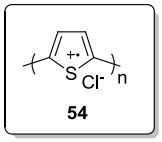

54

2.4.14 General procedure for reaction of polythiophene radical cation salts with $NaBH_4$ with PPh_3

In a 50 mL RB flask, polymer (1 g) and $NaBH_4$ (0.037 g, 1 mmol) in THF (20 mL) were added under nitrogen atmosphere. To this reaction mixture PPh_3 (0.262 g, 1 mmol) was added and the contents were stirred for 24 h. The reaction mixture was filtered and the organic layer was separated. The solvent was evaporated under reduced pressure and the crude product was purified on silica gel column chromatography using hexane/ethyl acetate (98:2) as eluent to isolate pure $Ph_3P{:}BH_3$ as a white solid.

2.4.15 General procedure for reaction of polythiophene radical cation salts and $NaBH_4$ with Pyridine

In a 50 mL RB flask polymer radical cation, $NaBH_4$ and THF (20 mL) were added under nitrogen atmosphere. To this, pyridine was added and the contents were stirred for 24 h. The contents were filtered and the solvent was evaporated under reduced pressure to afford the crude product of corresponding pyridine:BH_3 complex. The crude product was purified on silica gel column chromatography using hexane/ethyl acetate as eluent to isolate 79% yield of pure pyridine:BH_3 complex **28** as colorless liquid.

2.5 References

1 a) Zhai, Y.; Dou, Y.; Zhao, D.; Fulvio, P.F.; Mayes, R.T.; Dai, S. *Adv.Mater.* **2011**, *23*, 4828. (b) Srivastava, M.; Kumar, M.; Singh, R.; Agrawal, U. C.; Garg, M. O. *J. Sci. and Ind. Res.* **2009**, *68*, 93. (c) Chung, D. D. L. *J. Mat. Sci.* **2004**, *39*, 2645.

2 Franklin R. E. *Acta Crystallogr*. **1950**, *3*, 107.

3 Franklin R. E. *Acta Crystallogr*. **1951**, *4*, 252.

4 Jagtoyen, M.; Derbyshire, F.; Rimmer, S.; Rathbone, R. *Fuel.* **1995**, *74*, 610.

5 a) Kastening, B.; Hahn, M.; Kremeskotter, J. *J. Electroanal. Chem*. **1994**, *374*, 159. b) Müllier, M.; Kastening, B. *J. Electroanal. Chem*. **1994**, *374*, 149. c) Chung D. D. L; Wang, S. *Smart Mater. Struct.* **1999**, *8*, 161.

6 (a) Dresselhaus, M. S.; Dresselhaus, G. *Annu. Rev. Mater. Sci.* **1995**, *25*, 487. (b) Varshney, K. Inter. *J. Eng. Res. and Gen. Sci.* **2014**, *2*, 660.

7 Alkhatib, A. J.; Zailaey, K. A.; *Eur. Sci. Journ.* **2015**, *11*, 50.

8 (a) Schobert, H. *Chem. Rev.* **2014**, *114*, 1743. (b) Saha, A.; Nikova, A.; Venkataraman, P.; John, V. T.; Bose, A. *Mater. Interfaces.* **2013**, *5*, 3094. (c) Ma, P. C.; Liu, M. Y.; Zhang, H.; Wang, S. Q.; Wang, R.; Wang, K.; Wong, Y. K.; Tang, B. Z.; Hong, S. H.; Paik, K. W.; Kim, J. K. *App. Mat. Inter*. **2009**, *1*, 1090.

9 Chung, D. D. L. *J. Mat. Sci.* **2002**, *37*, 1475.

10 (a) Menendez, J. A.; Phillips, J.; Xia, B.; Radovic, L. R. *Langmuir* **1996**, *12*, 4404. (b) Zhou, Y.; Wei, L.; Yang, J.; Sun, Y.; Zhou, L. *J. Chem. Eng. Data* **2005**, *50*, 1068. (c) Hallum, J. V.; Drushel, H. V. *Phys. Chem.* **1958**, *62*, 110.

11 Sumanasekera, G. U.; Chen, G.; Takai, K.; Joly, J.; Kobayashi, N.; Enoki, T.; Eklund, P. C. *J. Phys. Condens. Matter*, **2010**, *22*, 334208.

12 Shin, D.; Jeong, B.; Mun, B. S.; Jeon, H.; Shin, H.-J.; Baik, J.; Lee, J. *J. Phys. Chem. C* **2013**, *117*, 11619.

13 Yeager E. *Electrochem. Acta.* **1984**, *29*, 1527.

14 a) Giannozzi, P.; Car, R.; Scoles, G. *J. Chem. Phy*, **2003**, *118*. 1003. b) Su, C.; Loh, K. P. *Acc. Chem. Res.* **2013**, *46*, 2275.

15 a) Radovic, L. R.; Bockrath, B. *J. Am. Chem. Soc.* **2005**, *127*, 5917. b) Radovic, L. R. *J. Am. Chem. Soc.* **2009**, *131*, 17166. c) Hu, X.; Zhou, Z.; Lin, Q.; Wu,Y.; Zhang, Z. *Chem. Phys. Lett.* **2011**, *503*, 287.

16 Zhang, I.; Liu, X.; Blume, R.; Zhang, A.; Schlögl, R.; Su, D. S. *Science* **2008**, *322*, 53.

17 a) Yeager E. *J Mol Catal* **1986**, *38*, 5. b) Wilshire, J.; Sawyer, D. T. *Acc. Chem. Res*. **1979**, *12*, 105. c) Sawyer, D. T.; Valentine, J. S. *Acc. Chem. Res*. **1981**, *14*, 393. d) Kim, S. U.; Liu, Y.; Nash, K. M.; Zweier, J. L.; Rockenbauer, A.; Villamena, F. A. *J. Am. Chem. Soc*. **2010**, *132*, 17157.

18 Re-use of oxidized activated carbon: After completion of the reaction using carbon material, the resulting carbon materials were filtered and washed several times with organic solvents (THF followed by acetone) to remove trace amount of organic products. Then, the sample was heated at 200 °C under high vacuum for 2 h and brought to rt under N_2. The dry oxygen was adsorbed by passing it through the carbon material for 1 h. This oxygen adsorbed activated carbon sample was reused for synthetic transformations.

19 (a) Periasamy, M.; Thirumalaikumar, M. *J. Organomet. Chem.*, **2000**, *609*, 137. (b) Prasad, A.S.B.; Kanth, J. V. B.; Periasamy, M. *Tetrahedron.*, **1992**, *48*, 4623. (c) Narayana, C.; Periasamy, M. *Tetrahedron Lett.*, **1985**, *26*, 1757.

20 Brown, H. C.; Organic Synthesis via Boranes, Wiley Interscience, The John Wiley & Sons Inc., New York, **1975**.

21 Freeguard, G. F.; Long, L. H. *Chem. Ind.* **1965**, 471.

22 a) Narayana, C.; Periasamy, M. *J. Organomet. Chem.* **1987**, *323*, 145. (b) Periasamy, M.; Muthukumaragopal, G. P.; Sanjeevakumar, N. *Tetraheron Lett*. **2007**, *48*, 6966. (c) Narayana, C.; Periasamy, M. *Chem. Commun.* **1987**, 1857. (d) Periasamy, M.; Kishan Reddy, Ch.; Bhaskar Kanth, J. V. *J. Indian Inst. Sci*. **1994**, *74*, 149. (e) Anwar, S.; Periasamy, M. *Tetraherdon: Asymmetry* **2006**, *17*, 3244. (f) Bhaskar Kanth, J, V.; Periasamy, M. *J. Org. Chem*. **1991**, *56*, 5964. (g) Kanth, J. V. B.; Periasamy, M. *J. Chem. Soc. Chem. Commun.*, **1990**, 1145. (h) Reddy, Ch. K.; Kanth, J. V. B.; Periasamy, M. *Synth. Commun*. **1994**, *243*, 313. (i) Reddy, Ch. K.; Periasamy, M. *Tetrahedron Lett.* **1990**, *31*, 1919. (j) Reddy, Ch. K.; Periasamy, M. *Tetrahedron Lett.* **1989**, *30*, 5663. (k) Reddy, Ch. K.; Periasamy, M. *Tetrahedron* **1992**, *48*, 8329. (l) Periasamy, M. *Current Science* **1995**, *68*, 883.

23 (a) Hawthorne. M. F.; *J. Org. Chem.* **1958**, *23*, 1788. (b) Brown, H. C.; Murray, K. J.; Murray, L. J.; Snover, J. A.; Zweifel, G. *J. Am. Chem. Soc.* **1960**, *82*, 4241.

24 Clay, J. M.; Vedejs, E. *J. Am. Chem. Soc.* **2005**, *127*, 5766.

25 Rao, A. G. Ph.D. Thesis **2018**, School of Chemistry, University of Hyderabad.

26 Ramusagar, M. Ph.D. Thesis **2018**, School of Chemistry, University of Hyderabad.

27 a) Hemandez, S.C.; Chaudhari, D.; Chen, W.; Myung, N.; Mulchandani, A. Interscience, **2007**, 19, 2125. b) Mabrrok, M.F.; Person, C.; Petty, M.C. *Sensors and Acuator B: chemical.* **2006**, 115, 547.

28 Novak, P. *Electrochimia Acta*. **1992**, 37, 1227.

29 Berggren, M.; Gustafsson, G.; Inganäs, O.; Andersson, M. R.; Wennerström, O.; Hjertberg ,T. *Appl. Phys. Lett.* **1994**, *65*, 1489.

30 Chan, H. S.; Ng, S. C. *Prog. Polymer. Sci.* **1998**, *23*, 1167.

31 Cai, W.; Gong, X.; CaO, Y. *Sol.Energy.Mater.Sol.Cells*, **2010**, *94*, 114.

32 Scharber, C. M.; Muhlbacher, D.; Koppe, M.; Denk, P.; Waldauf, C.; Heeger, A. J.; Brabec, C. J. *Adv. Mater.* **2006**, *18*, 789.

33 Cremer, J.; Bauerle, P.; Wienk, M. M.; Janssen, R. A. J. *Chem.Mater.* **2006**, *18*, 5832.

34 Gok, A.; Omustova, M.; Yavuz, A. G. *Synthetic Metals*. **2007**, *157*, 23.

35 a) Demirboga, B.; Onal, A.M. *Journal of Physics and Chemistry of Solids.* **2000**, *61*, 907. b) Wang, C.; Benz, M. E.; Legoff, E.; Schindler, J. L.; llbritton-Thomas, J.; Kanatzidis, M. G. *Chem. Mater.* **1994**, *6*, 401.

36 Pron, A.; Rannou, P. *Prog. Polym. Sci.* **2002**, *27*, 135.

37 Bredas, J. L.; Street, G. B. *Acc. Chem. Res.* **1985**, *18*, 309.

38 Bertho, D.; Jouanin, C. *Physical Review B.* **1987**, *35*, 626.

39 Bredas, J. L. Wudl, F.; Heeger, A. *J. Solid State Comm.* **1987**, *63*, 577.

40 Lazzaroni, R.; Logdlund, M.; Stafstrom, S.; Salaneck, W. R.; Bredas, J. L. *J. Chem. Phy*. **1990**, *93*, 4433.

41 Finchou, D.; Horowitz, G.; Garnier, F. *Synthetic Metals.* **1990**, *39*, 125.

42 Re-use of re-oxidized polymer: After the reaction, the resulting polymers were filtered and washed several times with organic solvents (THF followed by acetone) to remove trace amounts of organic products. Then, the polymer was dried under high vacuum. The recovered polymer was oxidized with $FeCl_3$, following the same procedure mentioned in the experimental section. The re-oxidized polymer was reused for the preparation of lewis base borane complexes.

43 Abdou, M. S. A.; Ortino, F. P.; Son, Y.; Holdcroft, S. *J. Am. Chem. Soc.* **1997**, *119*, 4518.

44 (a) Ramusagar, M. Ph.D. Thesis **2018**, School of Chemistry, University of Hyderabad. (b) Suresh, S. Ph.D. Thesis **2016**, School of Chemistry, University of Hyderabad.

Chapter 3

Studies on the Reaction of Amines with Quinones, Viologens and halo compounds

3.1 Introduction

Aliphatic and aromatic, primary, secondary and tertiary amines are known to react with *p*-chloranil in dioxane/2-propanol to produce blue to purple color. Generally, aliphatic amines gives red colour and other amines give different colours as shown in Table 1. Accordingly, *p*-chloranil was used to detect the presence of amines.[1]

Table 1. The colours of chloranil-amine adducts

Amine	Colour of adduct produced with chloranil
n-Butylamine	Red
Benzylamine	Red
Aniline	Violet
N-Methylaniline	Blue-green
N,N-Dimethylaniline	Blue
p-Nitroaniline	Orange
Diphenylamine	Blue-green

3.1.1 SET reactions in quinone chemistry

The quinone – hydroquinone redox couple has been studied over many years.[2] Quinone redox system also plays major roles in biology.[3] Quinones undergoes $2H^+/2e^-$ reduction in aqueous solution (or) in protic solvents.[4] The redox process of hydroquinone-quinone is a sequence of proton and electron transfer (Figure 1). In the first step,

deprotonation leads to a phenoxide ion which is transformed into a phenoxy radical by a one-electron oxidation. Then dissociation of the second OH group generates the radical anion semiquinone followed by a second one-electron oxidation to give benzoquinone **2**. All intermediates are resonance stabilized.

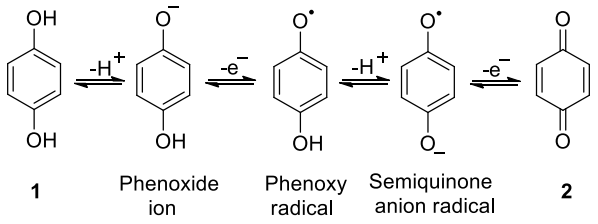

Figure 1. The redox process of hydroquinone-quinone system.

In nonaqueous (or) aprotic conditions, the quinone reduction proceeds through two consecutive single electron reductions (Fig 2).

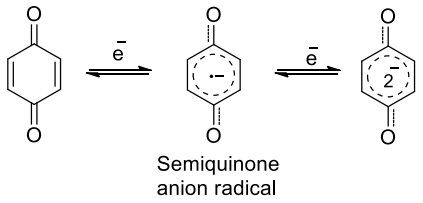

Figure 2. Quinone reduction in aprotic medium.

3.1.1.1 Addition and substitution reaction of quinones with amines

Preparation of various addition products of 1,4- benzoquinone **2** with different substituted anilines **3** was reported (Scheme 1).[5]

Scheme 1

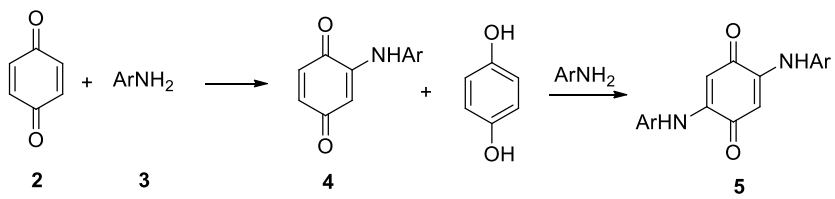

Reaction of *p*-chloranil **6** with aniline to give corresponding amino quinone **10** as a product.[6] A mechanism involving the formation of aminoquinone through outer (π)-complex **8** and inner (σ)-complex **9** was proposed (Scheme 2).

Scheme 2

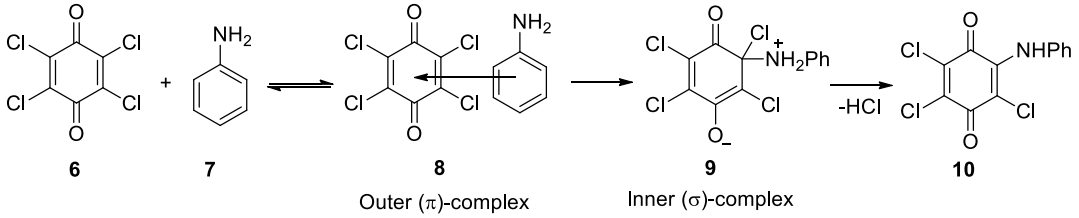

p-Chloranil **6** reacts with *n*-butyl amine **11** by electron transfer from *n*-butylamine **11** to *p*-chloranil **6** followed by substitution reaction to give the product **14** (Scheme 3).[7]

Scheme 3

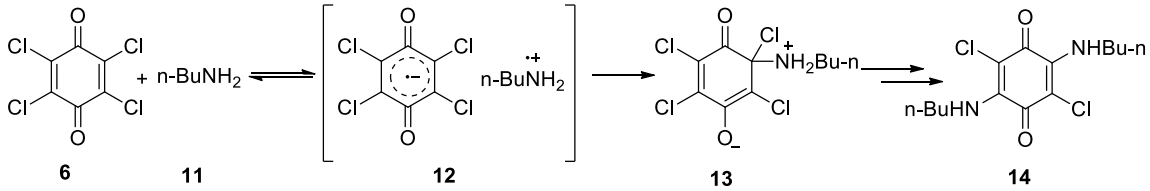

Pyrolidine **11a** was also reported to react with *p*-chloranil **6** to give mono and disubstituted aminoquinone **15** and **16** (Scheme 4).[8]

Scheme 4

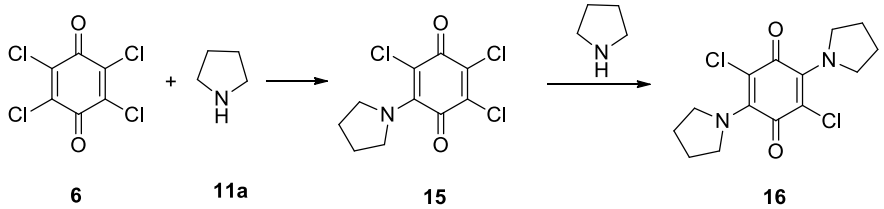

The hydride transfer from dihydroflavins **17** to 2,3-dichloro-5,6-dicynao-*p*-benzoquinone (DDQ) **18** was reported.[9] In this case, the back electron transfer is relatively slow and the proton transfer occurs within the radical ion pair complex **19** (Scheme 5).

Scheme 5

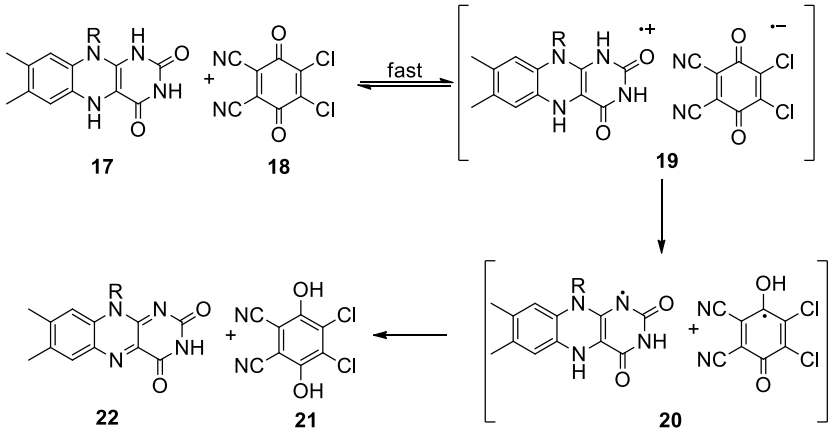

The reaction between *p*-chloranil **6** and diclofenac **23** leads to the charge transfer complex **24**. This CT complex is readily converted to radical ion pairs **25** in methanol solvent (Scheme 6).[10]

Scheme 6

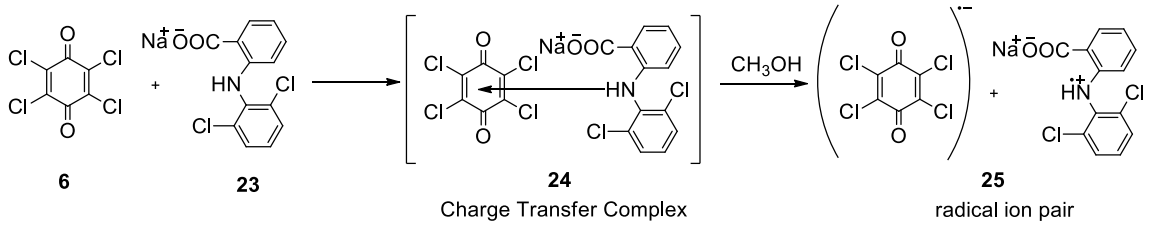

Tertiary amines are excellent electron donors and they strongly interact with electron acceptors. For example, DABCO **26** reacts with *p*-chloranil **6** in benzene solvent to give DABCO-chloranil 1:1 complex. The reaction of *p*-chloranil or *p*-bromanil with DABCO gives paramagnetic species **28** in benzene or in THF solvent (Scheme 7).[11]

Scheme 7

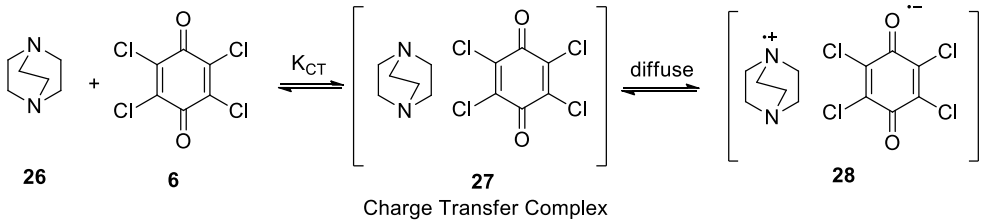

The reaction of 2,2,6,6-tetramethylbenzo[1,2-*d*;4,5-*d'*]bis[1,3]dioxole (TMDO) **29** with DDQ **18** in polar solvents like acetonitrile or propylene carbonate leads to radical ion pairs **30**. The electron transfer from TMDO to DDQ is fast in polar solvents (Scheme 8).[12]

Scheme 8

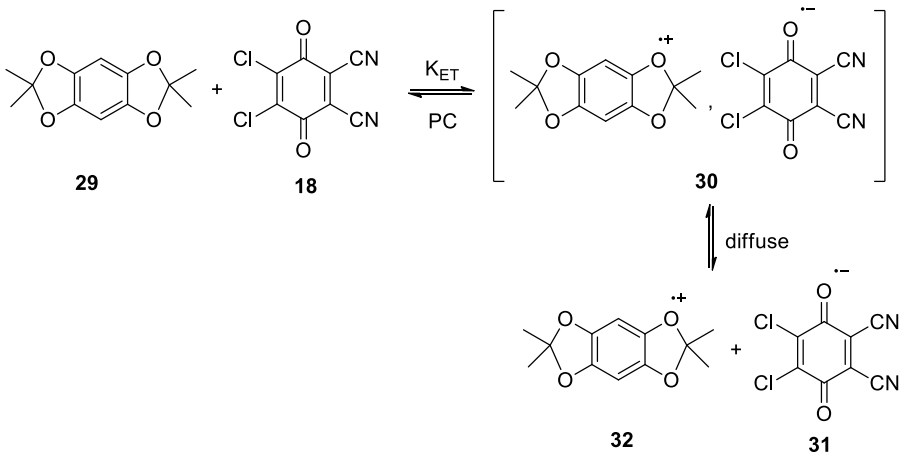

We have decided to investigate the elctron transfer reaction of quinones with amine donors. The mechanism and intermediates formed in these electron transfer reactions are discussed in the next section.

3.2 Results and Discussion

3.2.1 Reaction of secondary amine with quinone acceptors

Piperidine **33** reacts with 1,4- benzoquinone **2** in DCM solvent to give paramagnetic species by electron transfer from piperidine **33** to 1,4- benzoquinone **2**. The intensity of the epr signal decreases with time. We have also observed similar epr pattern in PC solvent with stronger signal. The reaction of piperidine with *p*-chloranil **6**, 1,4-naphthaquinone **34** and 2,3-dichloronaphthaquinone **35** also gave similar results in epr spectroscopic studies (Figure 3).

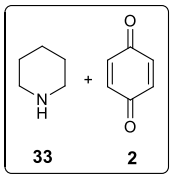

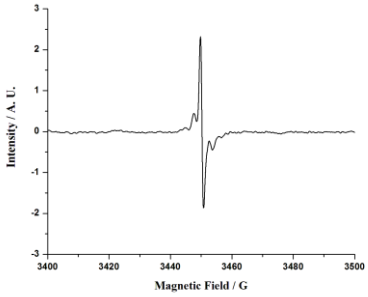

(a) at 5 min

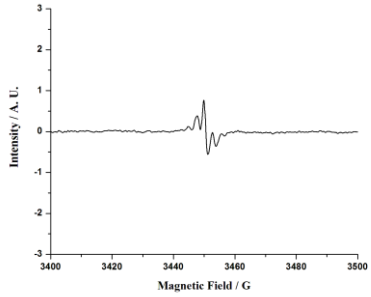

(b) at 1 h

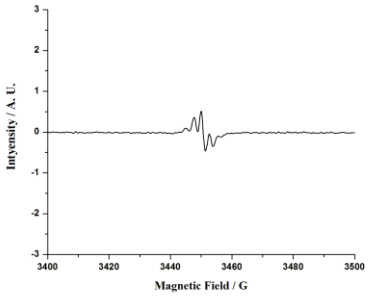

(c) at 2 h

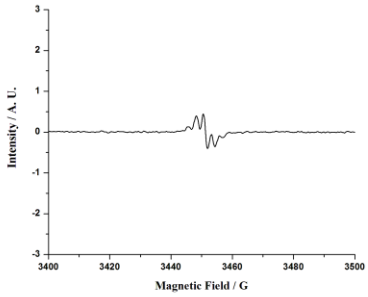

(d) at 6 h

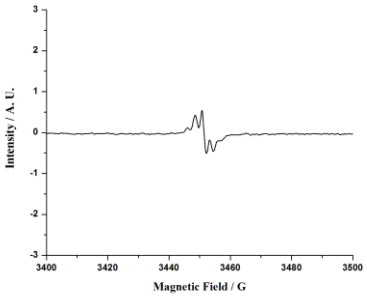

(e) at 12 h

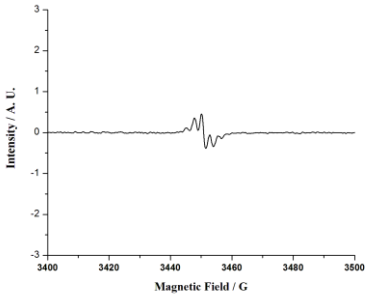

(f) at 24 h

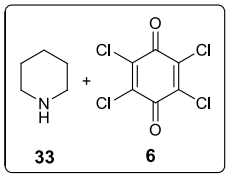

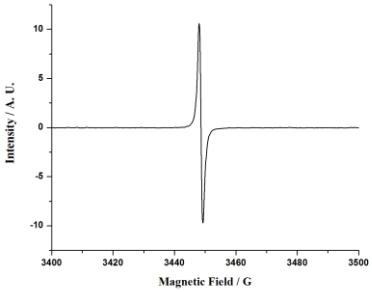

(a) at 5 min

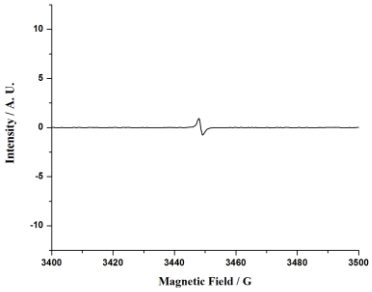

(b) at 1 h

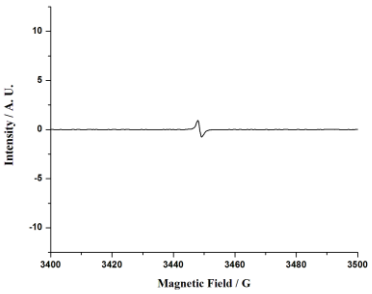

(c) at 2 h

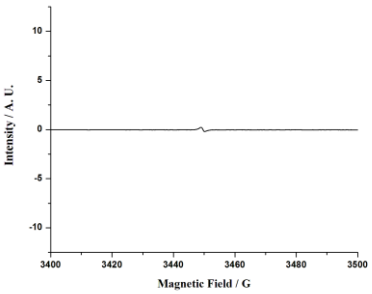

(a) at 6 h

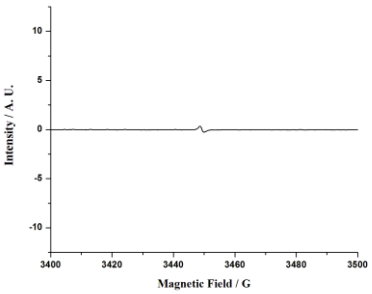

(b) at 12 h

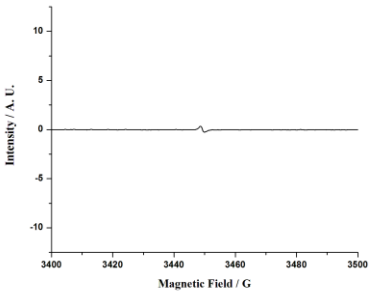

(c) at 24 h

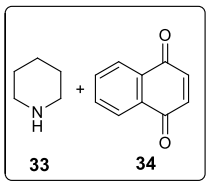

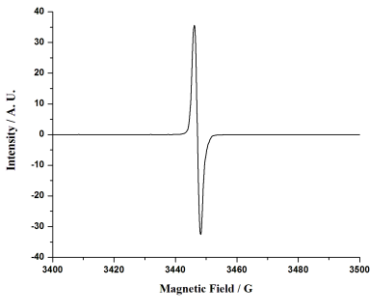

(a) at 5 min

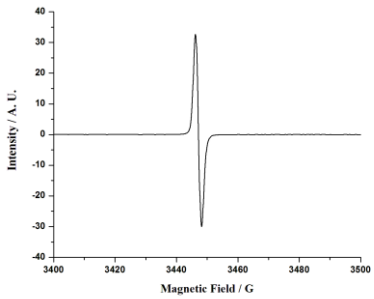

(b) at 1 h

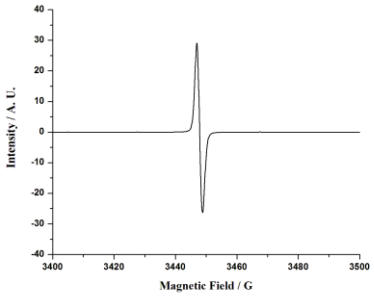

(c) at 2 h

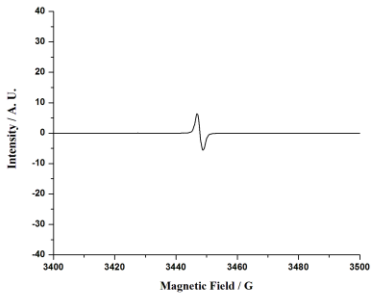

(d) at 6 h

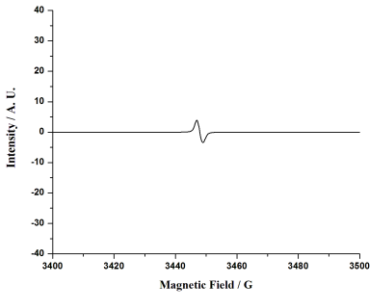

(b) at 12 h

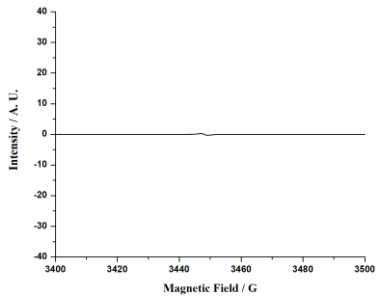

(c) at 24 h

Figure 3. EPR spectra of pipridine **33** with quinones (0.05 mmol) and (0.05 mmol) in CH_2Cl_2 solvent at 25 ^oC.

The reaction finally leads to the formation of diamagnetic 2, 5-di-piperidin-1-yl-[1,4] benzoquinone product **38** (Scheme 9).

Scheme 9. Electron transfer reaction of benzoquinone **2** with piperidine **33**

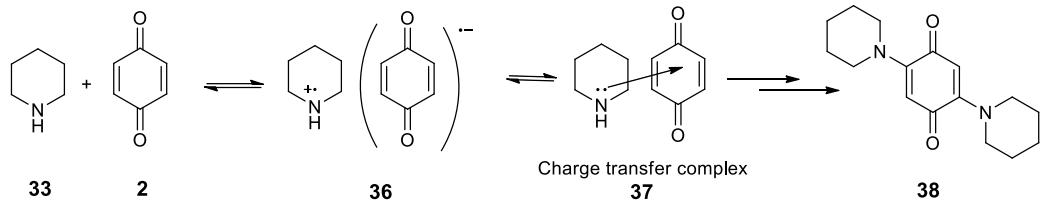

A possible mechanism for the formation aminoquinone is outlined in Scheme 10.

Scheme 10

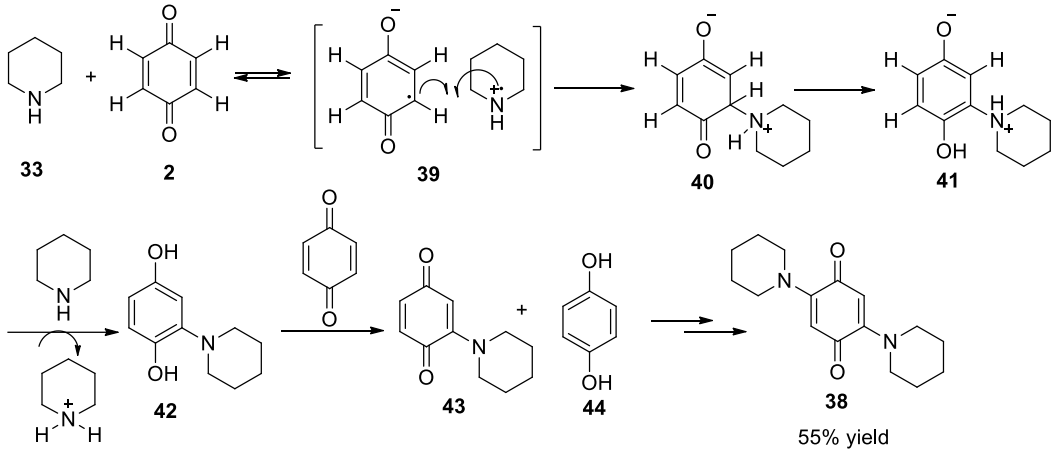

Similar reaction of *p*-chloranil **6** with piperidine **33** gave the ion radical pairs **45** followed by charge transfer complex **46** with subsequent formation of the diamagnetic 2, 5-dichloro-3,6-di-piperidin-1-yl-[1,4] benzoquinone product **47** (Scheme 11).

Scheme 11

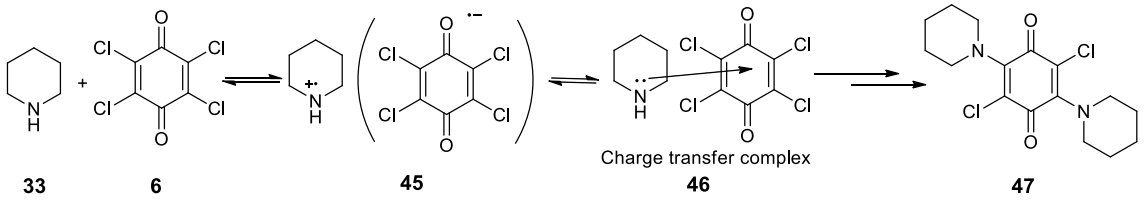

A possible mechanism for the formation of aminoquinone **47** is outlined in Scheme 12.

Scheme 12

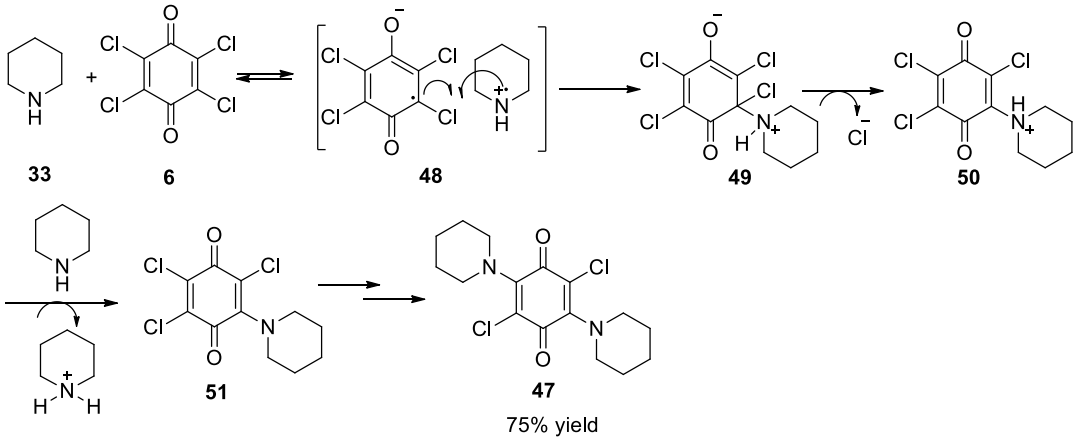

Similarly, the reaction of piperidine **33** with 1,4-naphthaquinone **34** and 2,3-dichloronaphthaquinone **35** results in aminoquinone derivatives **54** and **55** through the formation of paramagnetic intermediates **52** and the charge transfer complex **53** (Scheme 13).

Scheme 13

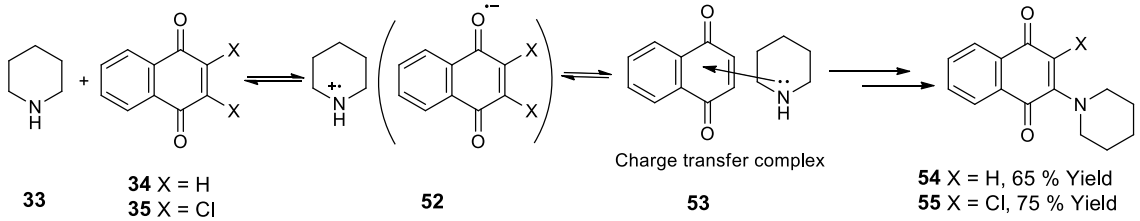

Recently, it was reported that the reaction of pyrrolidine **11a** with *p*-chloranil **6** gives the corresponding mono substituted aminoquinone **15** through polar or ionic intermediate **56** (Scheme 14).[13]

Scheme 14

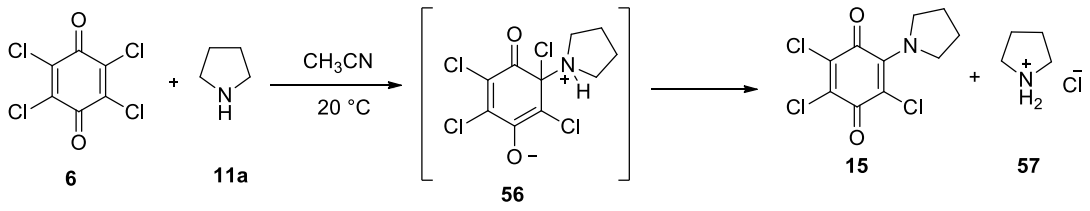

It was also reported that the formation C-C bond by the reaction of amine with quinones through polar pathway is several orders of magnitude faster than that expected for single electron transfer (SET) process. However, the epr data were not discussed by these authors. Also, there was no discussion on the formation of charge transfer or electron transfer complexes in the reaction between amines and quinones.

We have observed epr signal in accordance with the formation of paramagnetic intermediates upon mixing the secondary amine with quinones. Our results clearly indicate that electron transfer *via* initial cross exchange process to give the radical ion pair **45** with subsequent formation of charge transfer complex **46** and the aminoquinone product **47** with time (Scheme 15).

Scheme 15

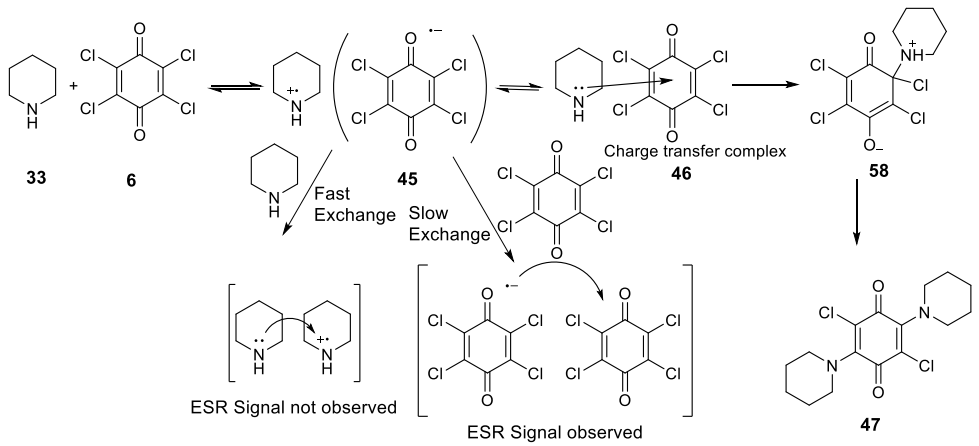

Hence, the electron transfer reaction, the radical ion intermediates and charge transfer complexes cannot be ruled out in this transformations (Scheme 15).

3.2.2 Reaction of tertiary amines with quinone acceptors

The reaction of secondary amine and quinones lead to the aminoquinone derivatives *via* radical intermediates and charge transfer complexes. We have then turned our attention towards the reaction of tertiary amines with *p*-chloranil.

We have observed that the reaction of *N*, *N*-diisopropylethylamine **59** (DIPEA) with *p*-chloranil **6** in PC solvent gave paramagnetic species detected by EPR spectroscopy with g value of 2.0037 (Figure 4)**.** The electron transfer complex was stable up to 24 h but the intensity of the epr signal decreased with time in PC solvent (Figure 4).

The rapid formation of electron transfer and charge transfer complex was observed upon mixing of DIPEA **59** with *p*-choranil **6** in PC solvent. The mixture turns to bright green immediately. Similarly, the reaction using *p*-chloranil **6** with tertiary amines like 1,4-diazabicyclo[2.2.2]octane (DABCO) **26**, *N*, *N*'-tetramethyl-1,4-phenylenediamine (TMPDA) **60**, *N*,*N*-diethylaniline ($PhNEt_2$) **61** and triphenylamine (TPA) **62** also gives paramagnetic intermediates as revealed by epr spectroscopy. The epr spectrum recorded at different time intervals are shown in Figure 4.

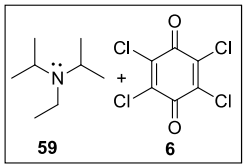

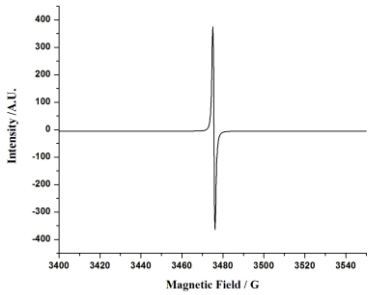

(a) at 5 min

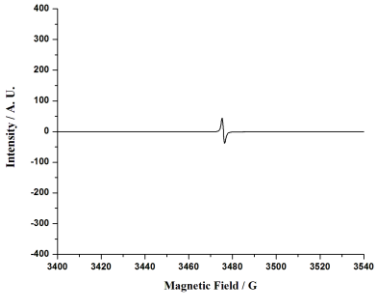

(b) at 1 h

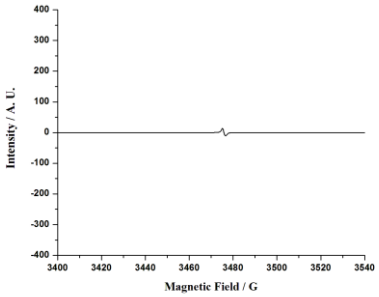

(c) at 2 h

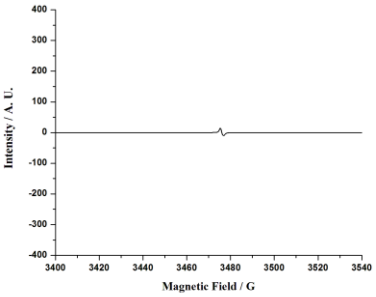

(d) at 6 h

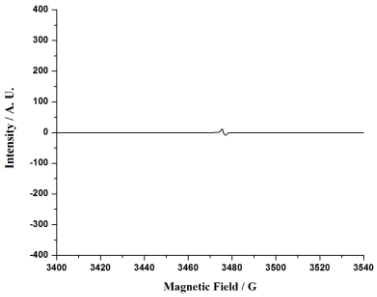

(e) at 12 h

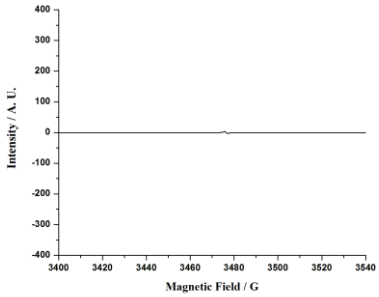

(f) at 24 h

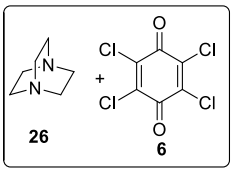

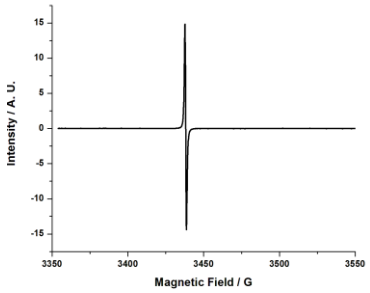

(a) at 5min

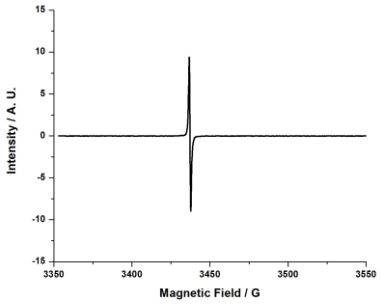

(b) at 1 h

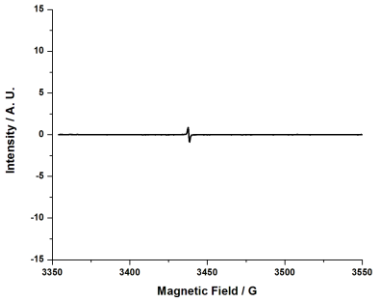

(c) at 6 h

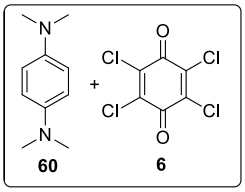

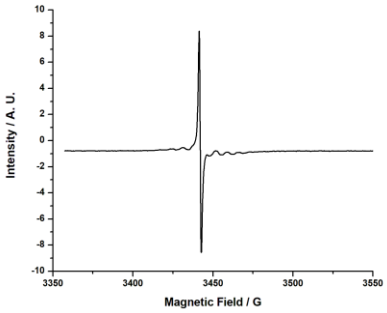

(a) at 5min

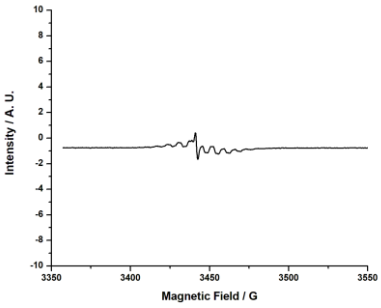

(b) at 1 h

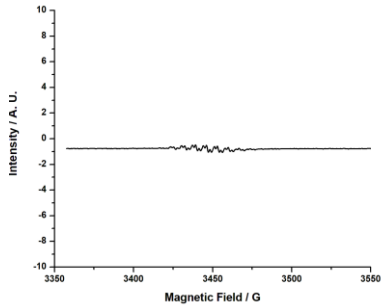

(c) at 6 h

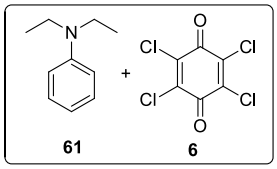

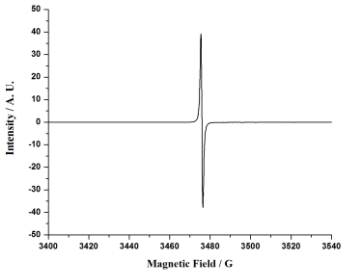

(a) at 5 min

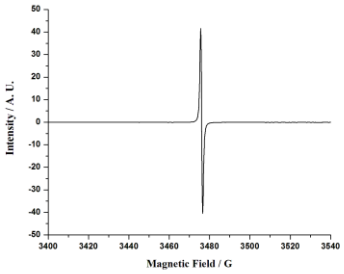

(b) at 1 h

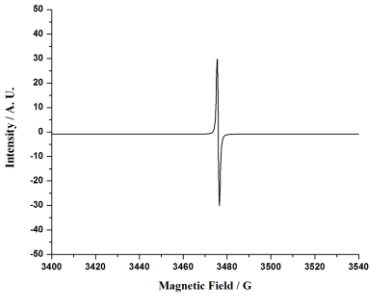

(c) at 2 h

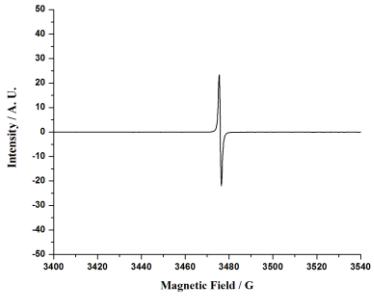

(d) at 6 h

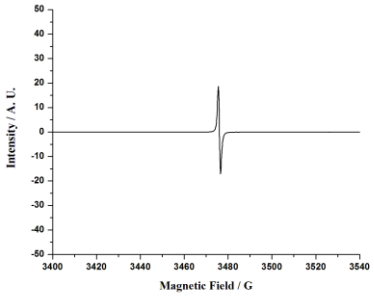

(e) at 12 h

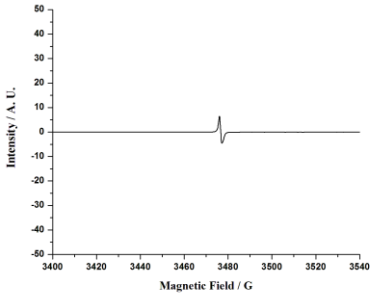

(f) at 24 h

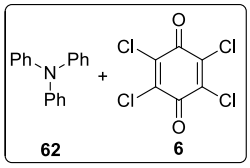

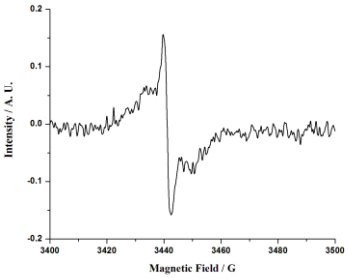

(a) at 5min

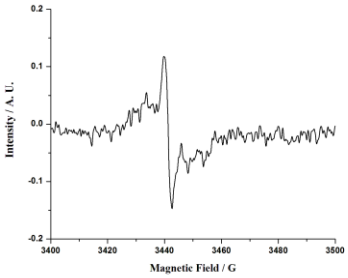

(b) at 1 h

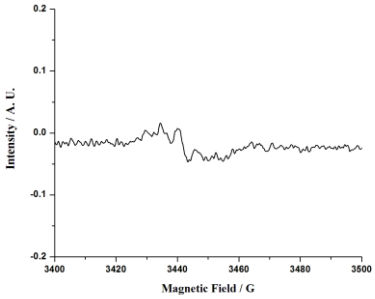

(c) at 6 h

Figure 4. EPR spectra of *p*-chloranul **6** (0.05 mmol) and tertiary amine (0.05 mmol) in PC solvent at 25 ºC.

The reaction of DIPEA **59** with *p*-chloranil **6** gave the amine radical cation and quinone radical anion pairs **63** followed by charge transfer complex **64 (**CT 1). The epr signal is mainly due to the presence of quinone radical anion **65** which may react with neutral *p*-chloranil to give the corresponding CT complex, CT 2. The amine radical cation would undergo fast exchange of electron with the neutral amine and hence does not exhibit epr signal (Scheme 16). Similarly, the other amine donors also react with *p*-chloranil to give radical ion intermediates followed by charge transfer complexes.

Scheme 16

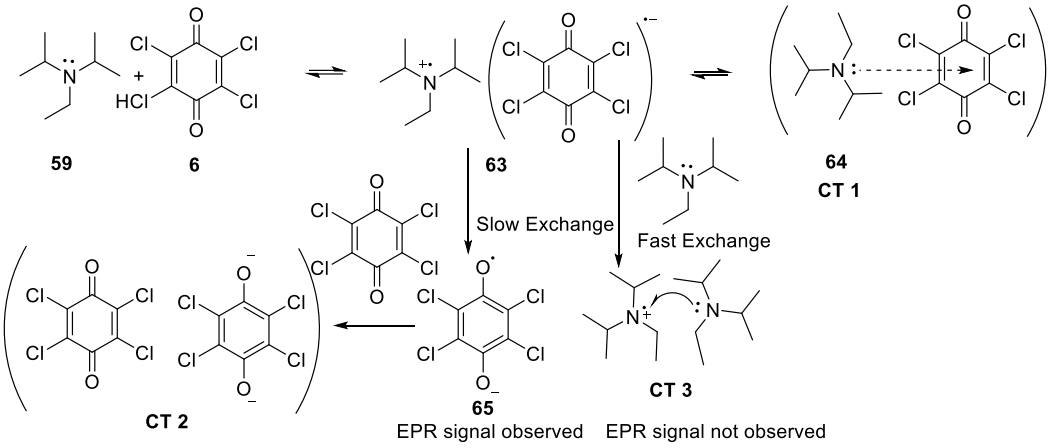

The reaction of *N*,*N*-diethylaniline ($PhNEt_2$) **61** with *p*-chloranil **6** gave paramagnetic intermediates. Presumably, the initially formed amine radical cations are slowly coupled to give the tetraethylbenzidine product **68** besides the formation of a small amount (<5%) of the corresponding hydroquinone (Scheme 17).

Scheme 17

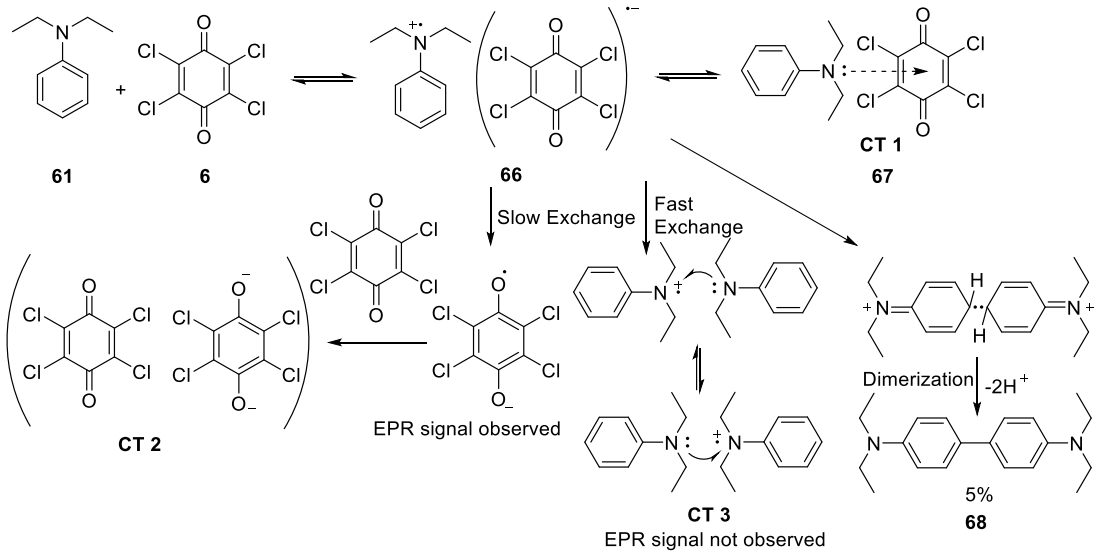

Similarly, the reaction of DIPEA **59** with *p*-chloranil **6** in gamma butyrolactone (GBL) solvent gives paramagnetic intermediates which was also confirmed by epr spectroscopy (Figure 5).

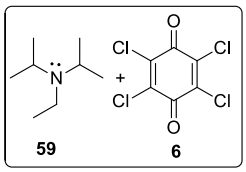

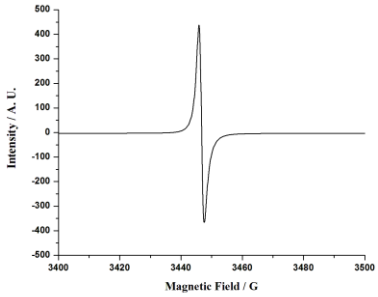

(a) at 5 min

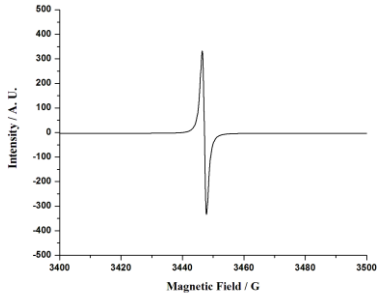

(b) at 1 h

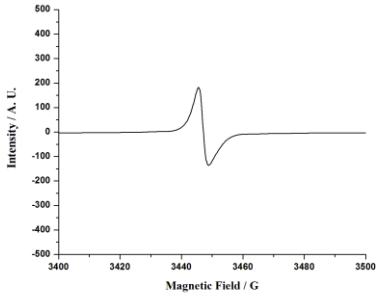

(c) 2 h

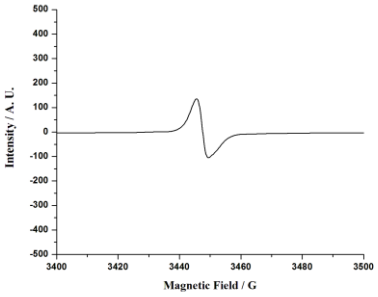

(d) at 12 h

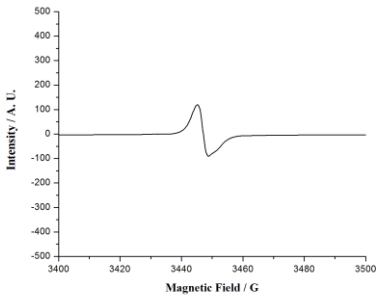

(e) at 24 h

Figure 5. EPR spectra of *p*-chloranul **6** (0.05 mmol) and DIPEA **59** (0.05 mmol) in GBL solvent at 25 ^{o}C.

In all the cases, we have observed a single signal in the epr spectrum. Earlier, it was reported[8] that the line broadening was observed in the epr spectra of naphthalene radical ion by the addition of excess of naphthalene. The rate constants for electron transfer between naphthalene radical ion and naphthalene are in the range 10^{7}-10^{9} liters mole^{-1} sec.$^{-1}$

Such single line broadening was also reported[14,15] in the case of 2,3-dichloro-5,6-dicyano-1,4-benzoquinone (DDQ) radical anion **31** with DDQ **18** with a fast exchange rate constant of 2.5 x 10^9 M^{-1} S^{-1} and activation energy of 1.6 kcal mol^{-1} at 23 ˚C. The electron is transferred from HOMO of donor amine to the LUMO of *p*-chloranil acceptor. Electron transfer leads to the formation amine radical cation and quinone radical anion. But, in epr spectrum, we have observed only one peak for the paramagnetic complex. This indicates that there is a fast self- exchange of electron between neutral amine with amine radical cation.

J. K. Kochi *et al* reported self-exchange and cross exchange reactions between 2,2,6,6-tetramethylbenzo[1,2-d:4,5-d']bis[1,3]dioxole **29** (TMDO) donor with 2,3-dichloro-5,6-dicyano-p-benzoquinone **18** (DDQ) acceptor in CH_2Cl_2 (Scheme 18).[12]

Scheme 18

(1) Cross exchange electron transfer process

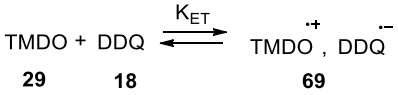

(2) Self-exchange electron transfer process

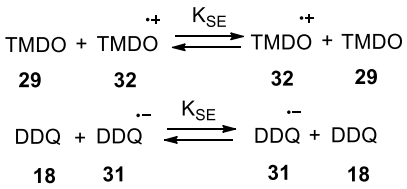

Hence, the line-broadening of epr signals observed for the intermediates obtained from DIPEA **59** and *p*-chloranil **6** can be explained by considering the electron exchange phenomenon.

It was reported that the reaction of *p*-chloranil **6** with 1,4-diazabicyclo[2.2.2]octane, DABCO **26** gives 1:1 charge transfer complex.[11] The formation

of the charge transfer complex was also confirmed by UV-Visible spectroscopy and the absorption band at 450 nm of DABCO-chloranil system was assigned to the chloranil anion radical. Also, the formation of charge transfer complex between electron deficient DDQ with electron rich π-system like cyclic enol ethers was reported.[13b] The charge transfer absorbance band at 589 nm in UV-Visible spectroscopy indicates the formation of charge transfer complex between DDQ and cyclic enol ethers system.

We have also examined the formation of charge transfer complex in the reaction of DIPEA **59** with *p*-chloranil **6** by UV-Visible spectroscopy (Figure 6). The color change was not observed for this diluted solution.

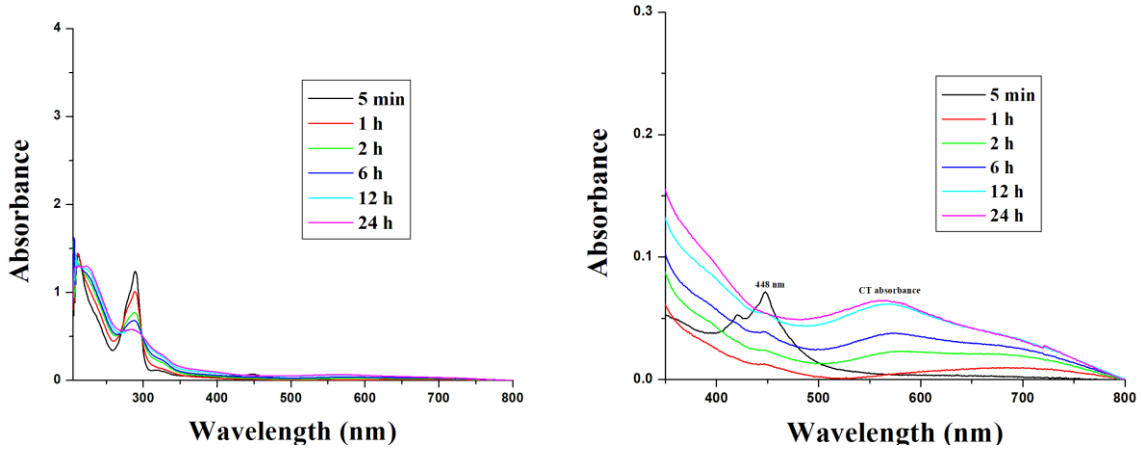

(a) (b)

Figure 6. a) UV-Vis spectra of a mixture of DIPEA **59** (1 x 10^{-3} mol L^{-1}) and *p*-chloranil **6** (1 x 10^{-4} mol L^{-1}) in PC at 25 °C. b) Expanded UV-Visible spectrum.

However, the characteristic absorbance band for chloranil anion radical was observed at 448 nm in 5 minutes and no charge transfer absorption band appears at that time. The new absorbance band developed slowly with time beyond 500 nm can be assigned to the absorption of the charge transfer (CT) complex **64**, because neither *p*-chloranil **6** nor DIPEA **59** absorbed in this region. The UV-Visible spectrum is shown in

Figure 6. We have also recorded the UV-Visible spectrum of solution of *N*, *N*-diethylaniline **61** ($1x10^{-3}$) and triphenyl amine **62** ($1x10^{-3}$) with *p*-chloranil **6** ($1x10^{-4}$) at different time intervals. The results are shown in Figure 7.

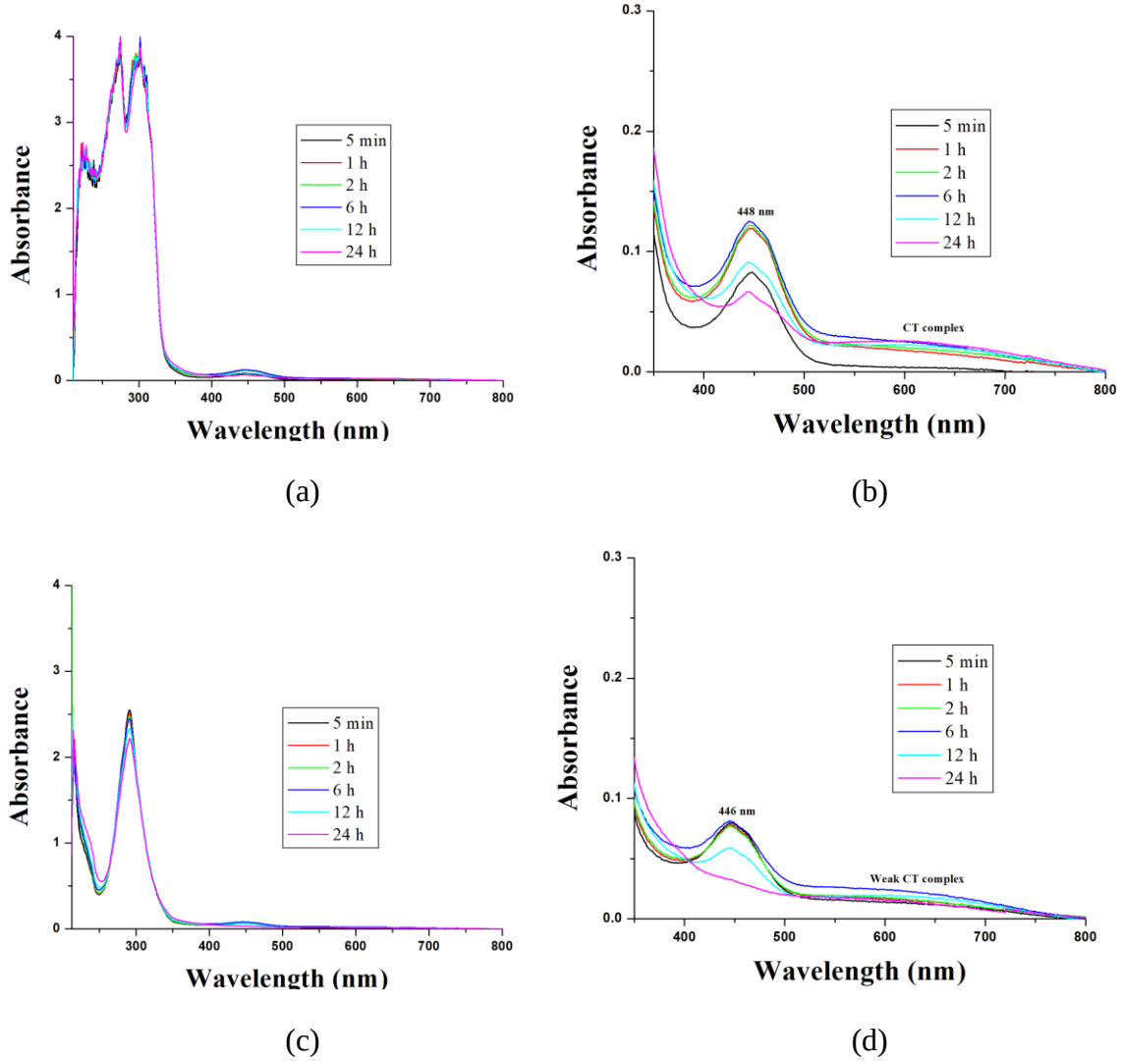

Figure 7. (a) and (c) UV-Vis spectra of a mixture of $PhNEt_2$ **61** (1×10^{-3} mol L^{-1}) and TPA **62** (1×10^{-3} mol L^{-1}) with *p*-chloranil **6** (1×10^{-4} mol L^{-1}) in PC at 25 °C. (b) and (d) Expanded UV-Visible spectrum.

We have also performed the reaction of DIPEA **59** with weak acceptors such as 1,4-benzoquinone (BQ) **2** and naphthoquinone (NQ) **34** also gave weak epr signal corresponding to paramagnetic intermediates formed in the reaction (Figure 8).

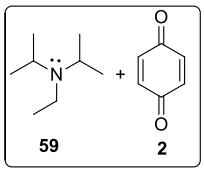

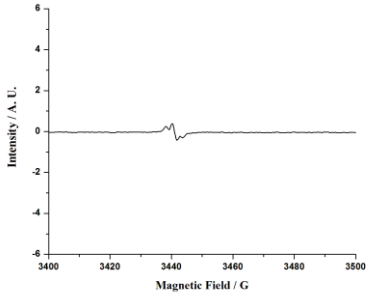

(a) at 5 min

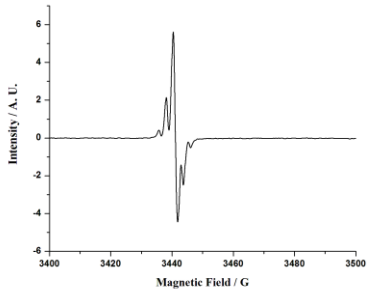

(b) at 2 h

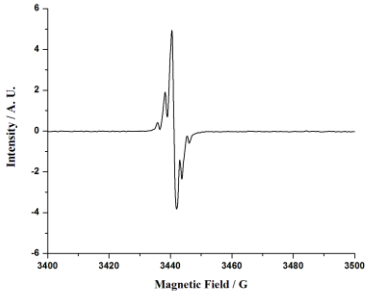

(c) at 6 h

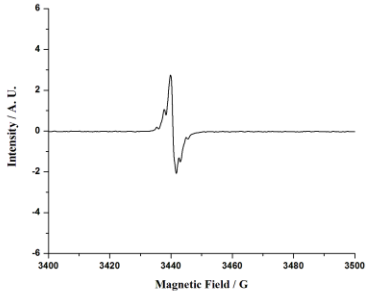

(d) at 12 h

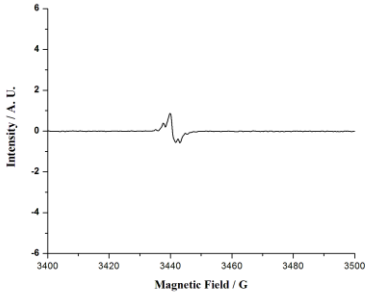

(e) at 24 h

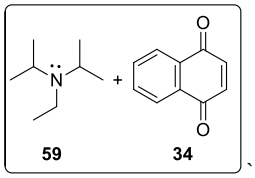

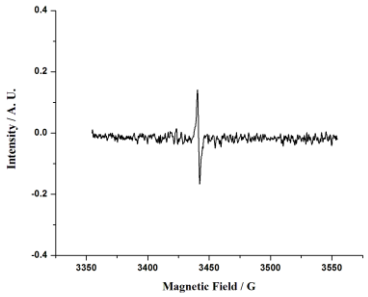

(a) at 5 min

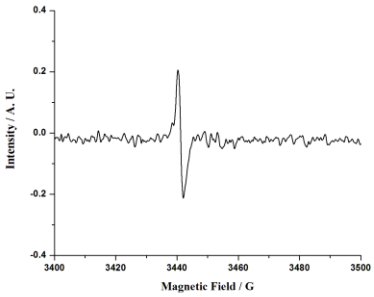

(b) at 2 h

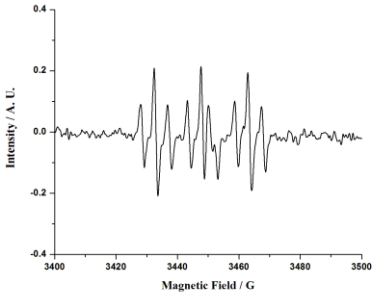

(d) at 6 h

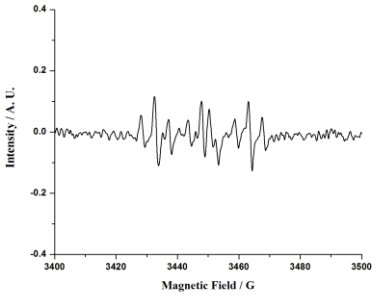

(d) at 12 h

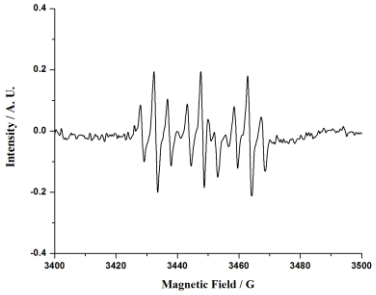

(e) at 24 h

Figure 8. EPR spectra of 1,4- benzoquinone **2** and naphthoquinone **34** (0.05 mmol) with DIPEA **59** (0.05 mmol) in PC solvent at 25 ºC.

It was reported that use of polar solvents in the bimolecular interaction of DDQ **18** with TMDO **29** increases the diffusive separation of radical ion pairs (Scheme 19). [5]

Scheme 19

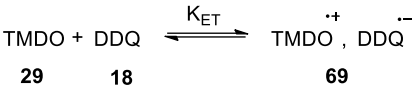

Hence, we have also reacted the amine DIPEA **59** with *p*-chloranil **6** (1:1 ratio) under neat condition. Interestingly, addition of drop of polar solvents like PC or *N*-methyl pyrrolidone (NMP) to the paramagnetic complex leads to increase in the strength of epr signal. The results are shown in Figure 9.

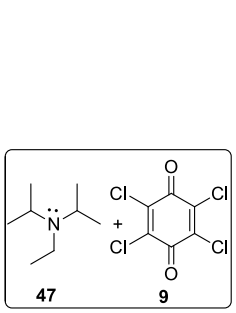

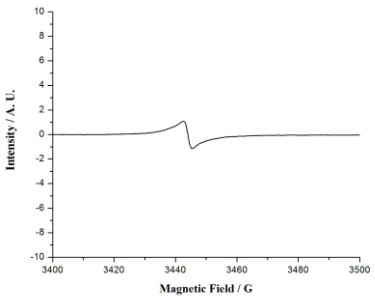

(a) at 5 min

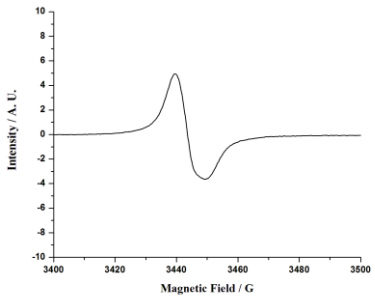

(b) at1 h

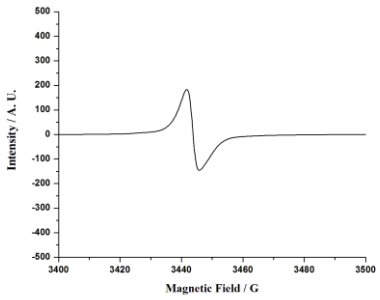

(c)

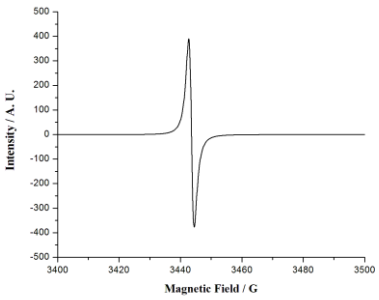

(d) at 1 h

Figure 9. EPR spectra of *p*-chloranil **6** (0.05 mmol) and DIPEA **59** (0.05 mmol) in neat condition at 25 ºC (a) at 5min (b) at 1 h (Intensity 10 to -10) (c) After addition of NMP (d) at 1 h (Intensity 500 to -500).

Presumably, the addition of polar solvents increases the concentration of paramagnetic intermediates due to the diffusive separation of ion pairs leading to more intense epr signal.

The nature of the paramagnetic species observed in the reaction and the reason for the decrease in epr signal intensity with time is not clearly understood. Presumably, a diamagnetic 1, 4-addition product could be formed as the reactivity of the tertiary amine and secondary amine is expected to be similar or the initially formed ion pair intermediates are slowly converted to the charge transfer complex that may lead to decrease in epr signal intensity (Scheme 20).

Scheme 20

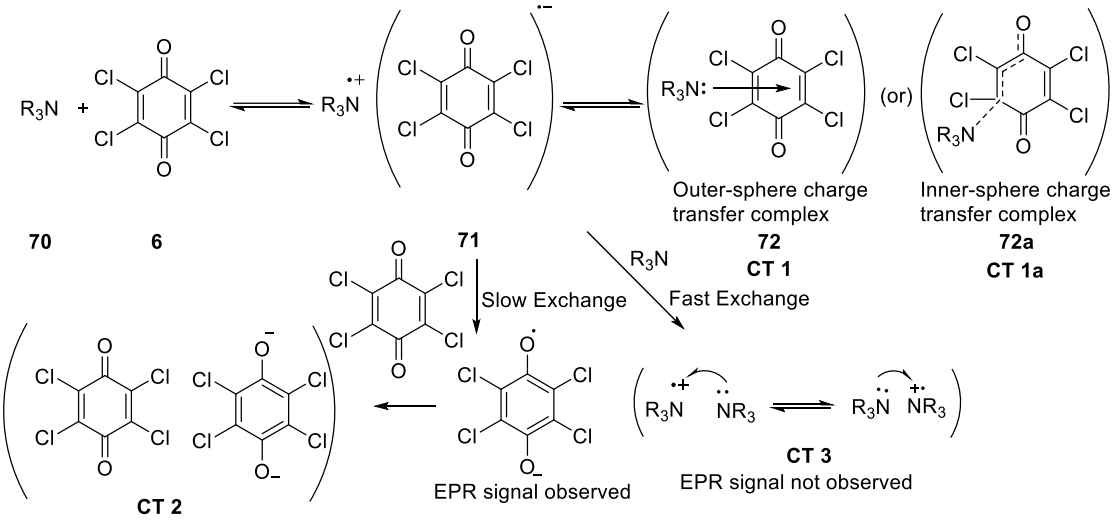

3.2.3 Reaction of tertiary amine with *p*-chloranil 6 under neat condition

We have also reacted *N, N*-diisopropylethylamine **59** (DIPEA) with *p*-chloranil **6** under the neat condition (without solvent)**.** The paramagnetic species formed were detected by epr spectroscopy with g value of 2.0031. In this case, an increase in the epr signal was observed with time. Presumably, the electron transfer reaction of *p*-chloranil and DIPEA will be slower under neat condition. Also, the reaction of DIPEA derivatives like *N*-benzyl-*N*-isopropylpropan-2-amine **73**, *N, N*-diisopropyl-2, 2-dimethylpropan-1-amine **74** and *N,N*-diethylaniline **61** with *p*-chloranil **6** gave the paramagnetic

intermediates under neat condition. The epr signal changes with time are shown in Figure 10.

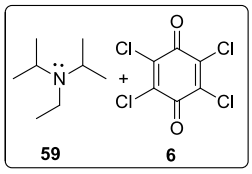

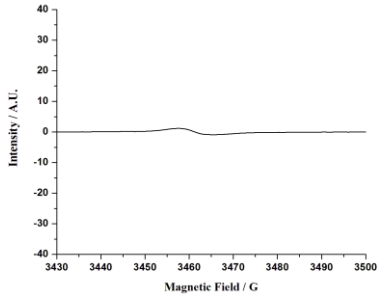

(a) at 5 min

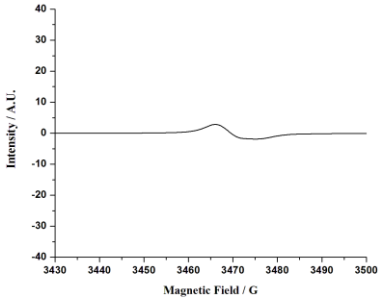

(b) at1 h

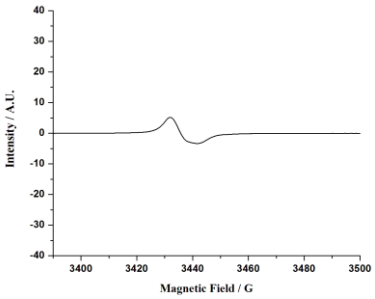

(c) at 2 h

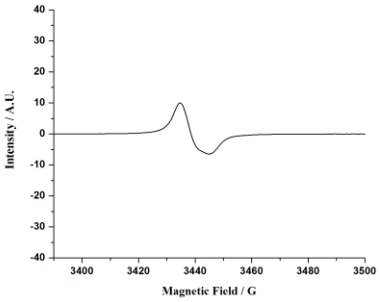

(d) at 6 h

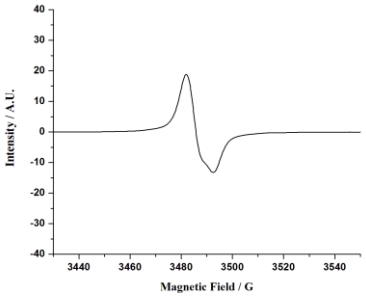

(e) at 12 h

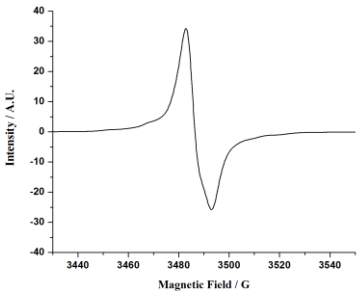

(f) at 24 h

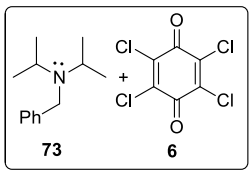

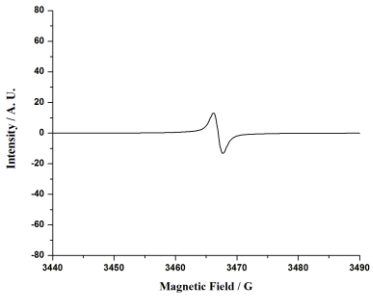

(a) at 5 min

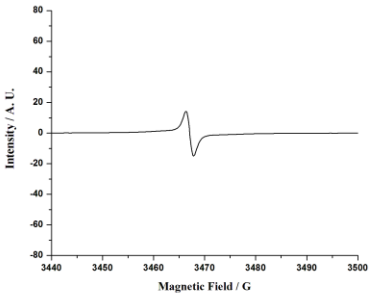

(b) at1 h

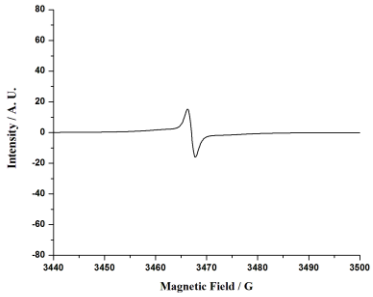

(c) at 2 h

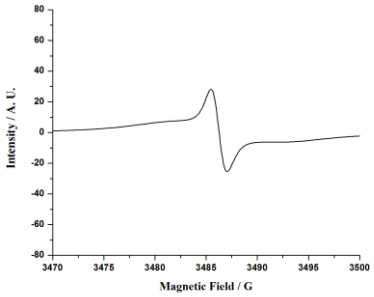

(d) at 6 h

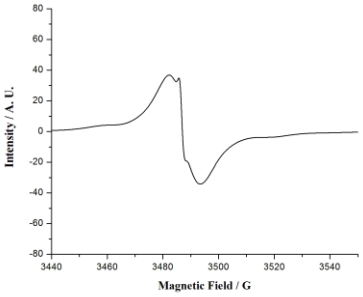

(e) at 12 h

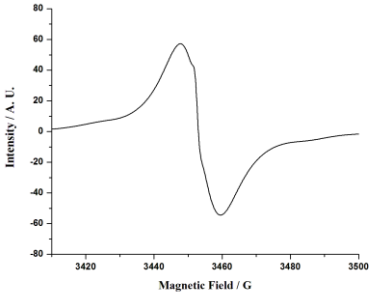

(f) at 24 h

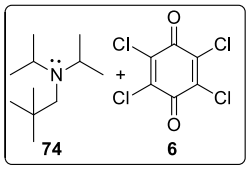

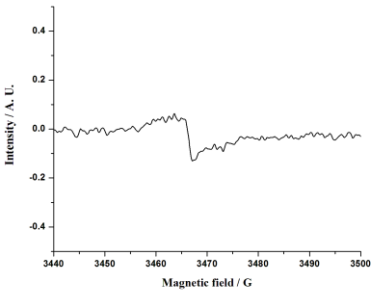

(a) at 5 min

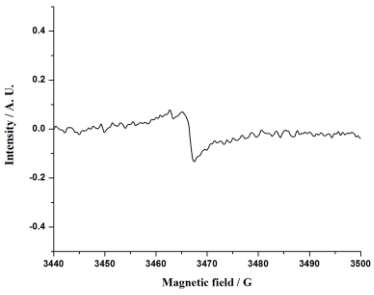

(b) at1 h

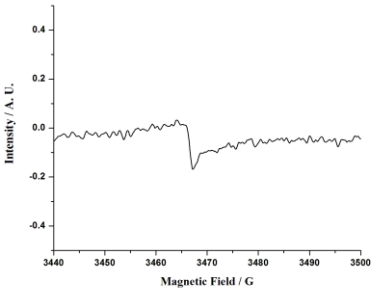

(c) at 2 h

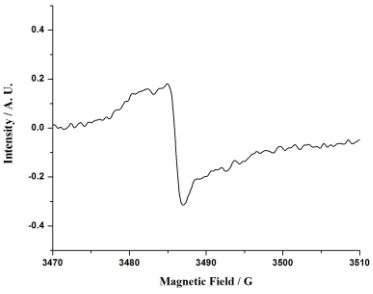

(d) at 6 h

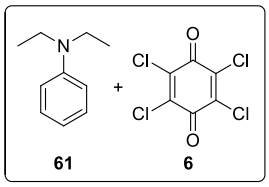

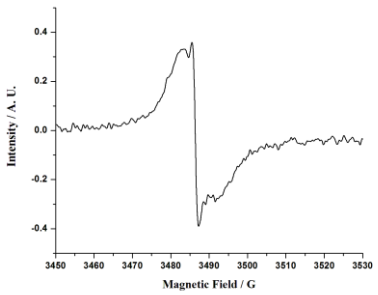

(e) at 12 h

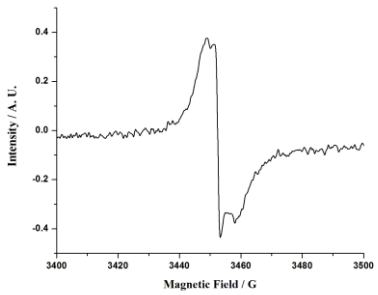

(f) at 24 h

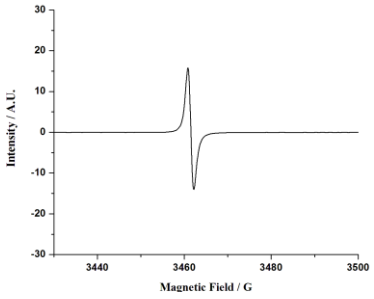

(a) at 5 min

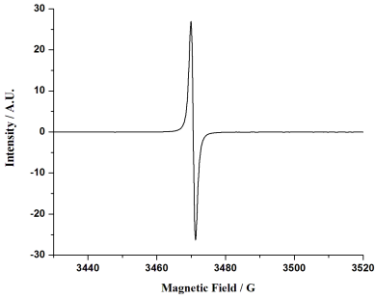

(b) at1 h

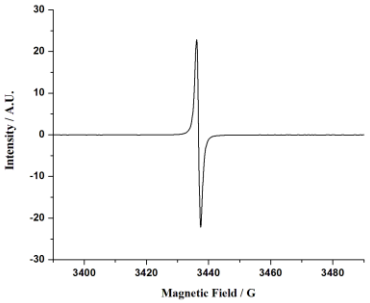

(c) at 2 h

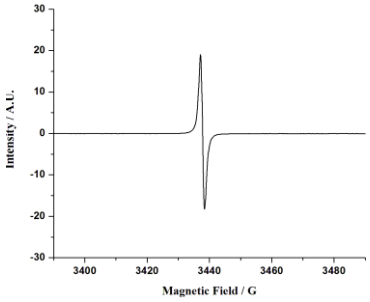

(d) at 6 h

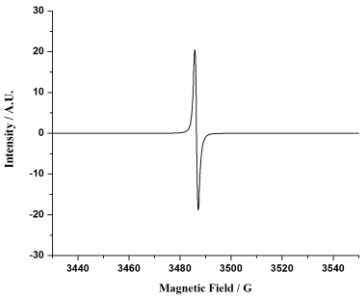

(e) at 12 h

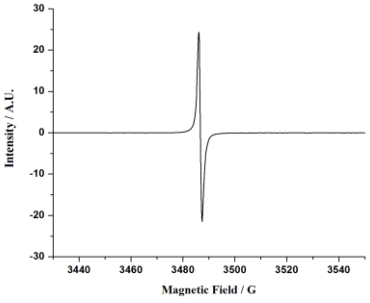

(f) at 24 h

Figure 10. EPR spectra of *p*-chloranil **6** (0.05 mmol) and amine (0.05 mmol) in neat condition at 25 ºC.

Interestingly, the epr signal strength increased with time, whereas under solvent condition (Figure 4) the signal strength decreased with time. Presumably, the formation of radical ion pairs is slow under neat condition. However, the epr signal at 5 minutes in PC is much stronger (DIPEA **59**, Figure 4) indicating the presence of more amounts paramagnetic species in the polar solvent.

3.2.4 Reaction of 2,2,6,6-tetramethylpiperidine derivatives 76 with *p*-chloranil

Synthesis of polymeric amine

We have synthesized polymers containing amine as a pendant group through transesterification of PMMA (polymethylmethacrylate) **75** using 4-hydroxy-2,2,6,6-tetramethylpiperidine **76a**. The polymer **76b** is also readily converted to the corresponding TEMPO derivative **77** (Scheme 21). The prepared radical polymer PTMA **69** was characterized by epr spectroscopy with g value of 2.0063 (Figure 11). The epr of prepared PTMA radical is in accordance with the reported epr signal.[16]

Scheme 21

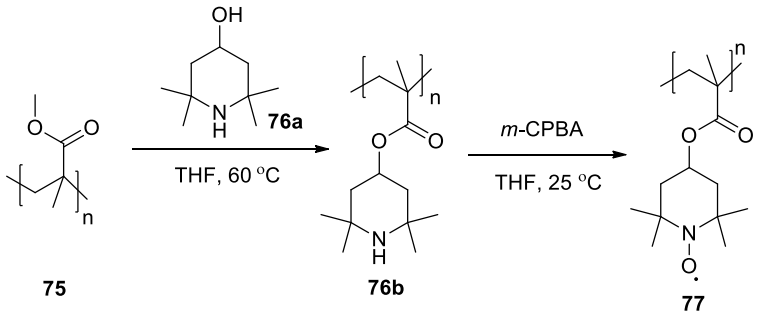

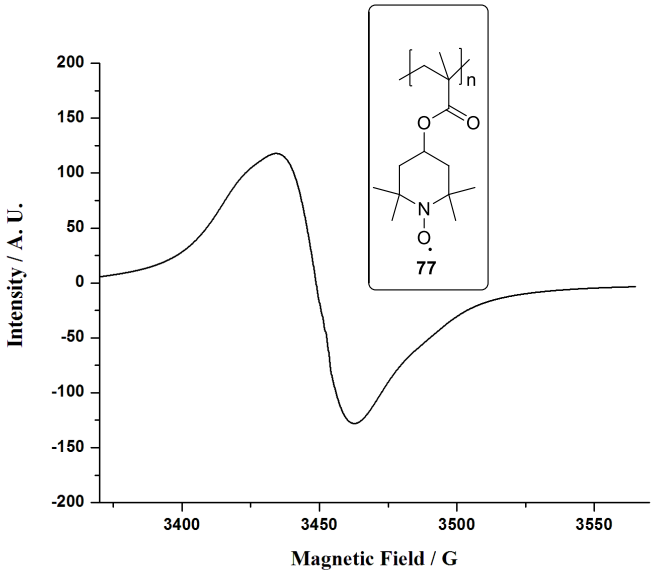

Figure 11. EPR spectra of synthesized PTMA radical polymer **77**

The present method for the preparation of PTMA radical polymer **77** is simple and convenient compared to the methods available in the literature.[17] Previously, the PTMA **77** was synthesized by the polymerization of 2,2,6,6-tetramethylpiperidine methacrylate monomer **79** followed by the oxidation of the precursor secondary amine polymer **76b** (Scheme 22).[18] An advantage of the present method is that commercially available PMMA samples with different molecular weight can be utilized in the preparation of different polymeric derivatives.

Scheme 22

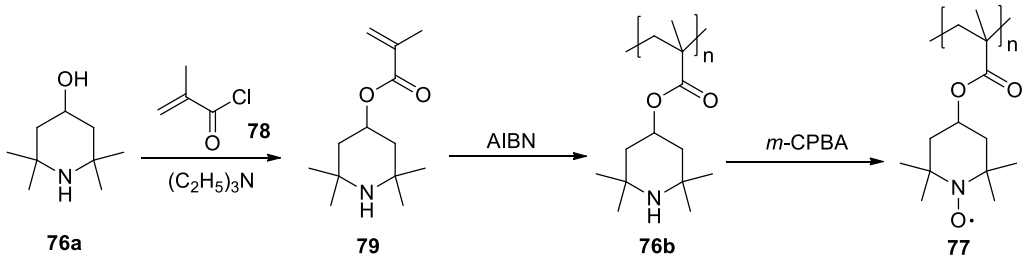

The PTMA **77** has the nitroxide radical 2,2,6,6- tetramethyl-1-piperidinyloxy (TEMPO) as repeating unit. TEMPO possesses good chemical stability because of

resonance structures and steric protection of the radical center. TEMPO and PTMA **77** polymer exhibit reversible oxidation-reduction behavior in aprotic solvents. On oxidation of the nitroxide radical, the p-type doping occurs in a reversible manner and the oxoammonium cation is formed. The existence of such a redox couple of radical makes PTMA **77** an attractive cathode-active material for use in lithium batteries.[19] As PTMA **77** is an electrical insulator, the addition of a suitable conductive material in the cathode composition is essential for effective transport of charges.[20] The PTMA **77** is thermally stable at high temperature. This radical concentration remains unchanged for over one year under ambient conditions. This polymer displays appropriate solubility in organic solvents.

We have also observed that the reaction of sterically hindered 2,2,6,6-tetramethylpiperidine derivatives **76** with *p*-chloranil **6** in PC solvent gave the paramagnetic species **80** (Scheme 23).

Scheme 23

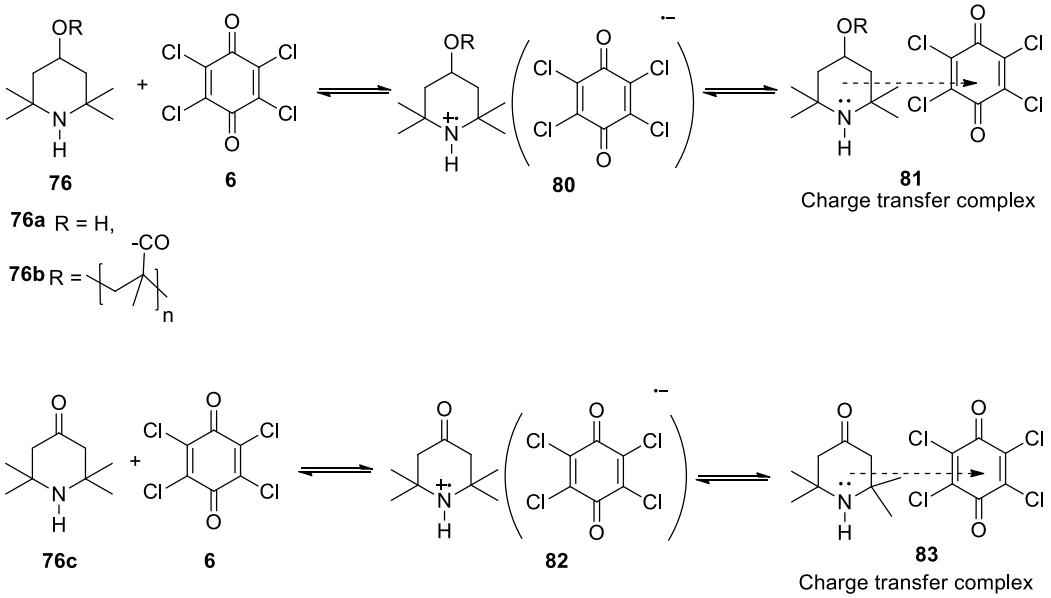

Interestingly, the reaction of the polymeric amine derivative **76b** with *p*-chloranil **6** gave moderately stable paramagnetic intermediates. In all these cases, we observed a triplet signal in the epr spectroscopy corresponding to amine radical cation (Figure 12).

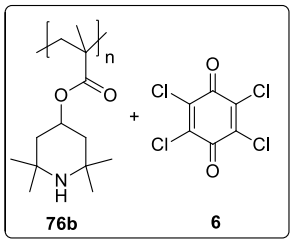

76b **6**

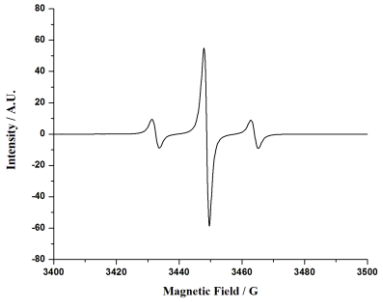

(a) at 5 min

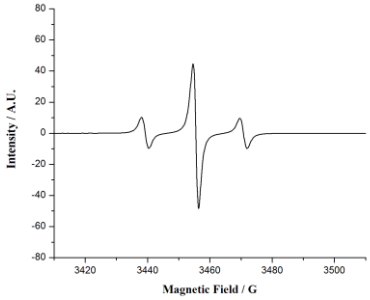

(b) at1 h

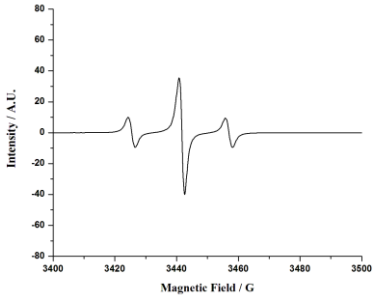

(c) at 2 h

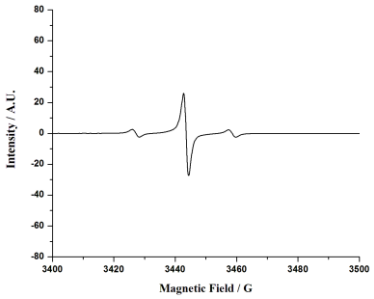

(d) at 6 h

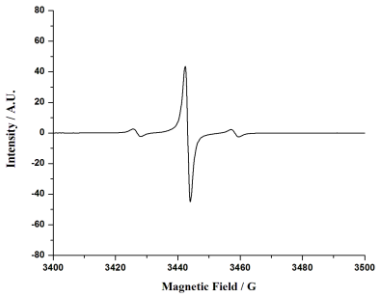

(e) at 12 h

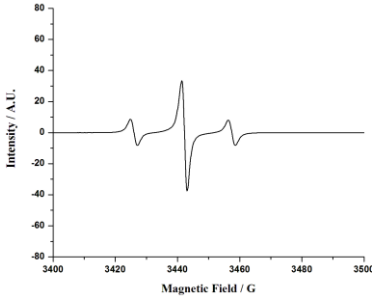

(f) at 24 h

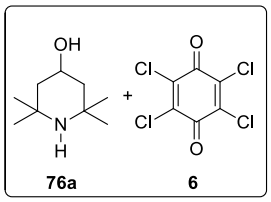

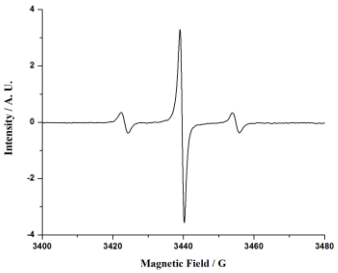

(a) at 5 min

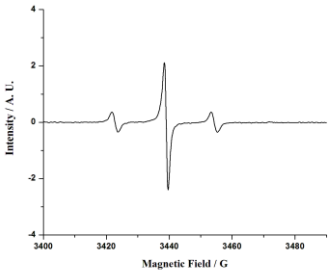

(b) at1 h

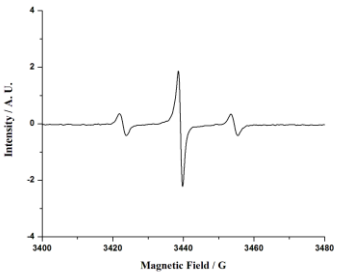

(c) at 2 h

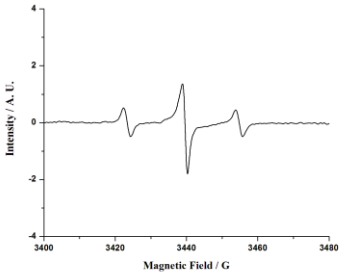

(d) at 6 h

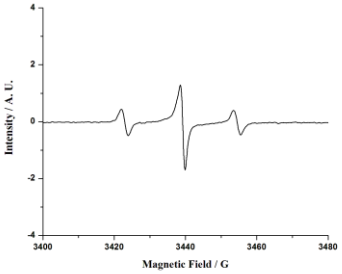

(e) at 12 h

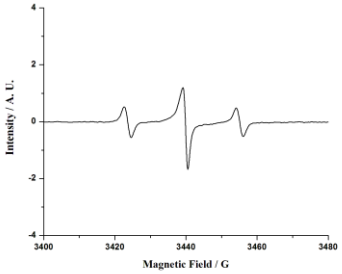

(f) at 24 h

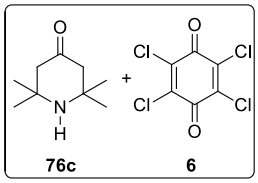

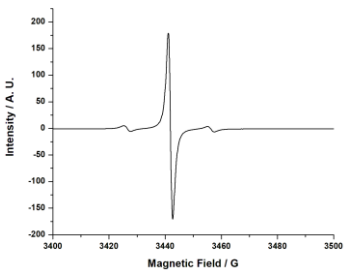

(a) at 5 min

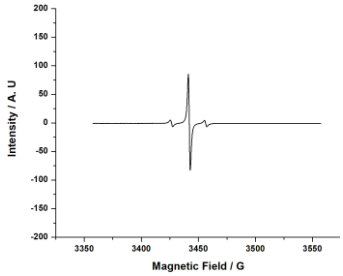

(b) at1 h

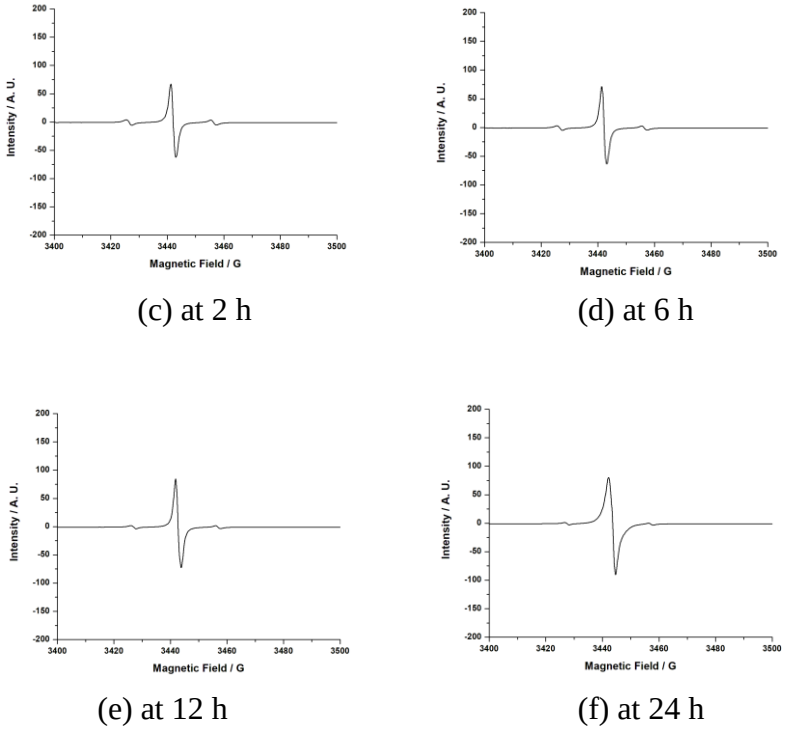

Figure 12. EPR spectra of *p*-chloranul **6** (0.05 mmol) and 2,2,6,6-tetramethylpiperidine derivatives **76a, 76b** and **76c** (0.05 mmol) in PC solvent at 25 ^{o}C.

However, even in the reaction of sterically hindered 2,2,6,6-tetramethylpiperidine with *p*-chloranil decrease in the strength of epr signal was observed with time. Presumably, complex formed here is outer-sphere in nature and not affected by the steric hindrance by the methyl groups.

Scheme 24

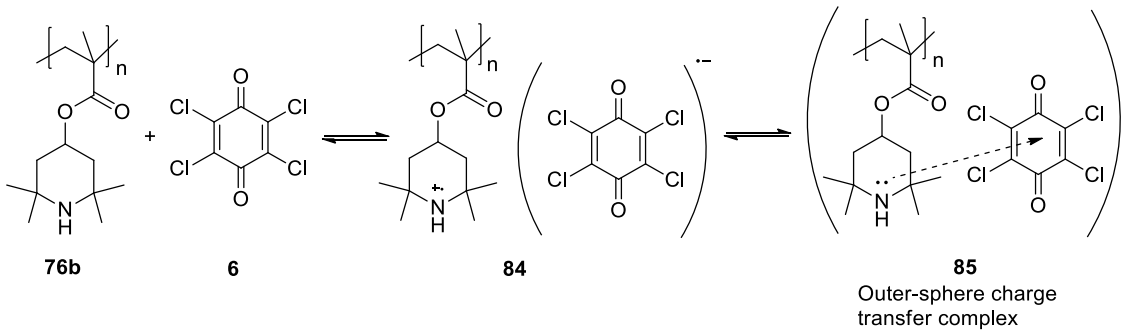

The charge-transfer complex **96** of *N,N,N',N'*-tetramethyl-*p*-phenylenediamine (TMPDA) **4** with *p*-chloranil **12** was reported.[21] It was proposed that such complex interchanges reversibly with radical ion pairs (Scheme 25).[22] Also, in solid state the TMPDA-*p*-chloranil complex was diamagnetic in nature.[23] We have observed that in this case also the epr signal strength decreases with time in PC solvent (Figure 4).

Scheme 25

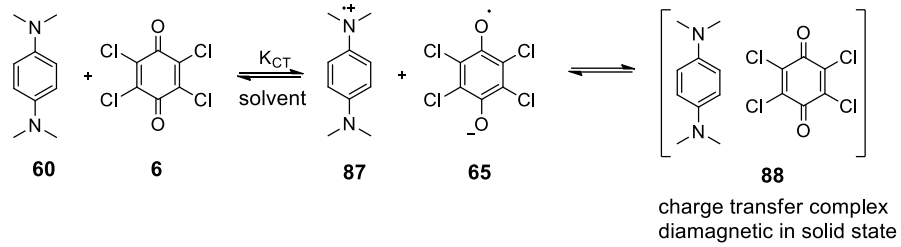

3.2.5 EPR Studies of aminoquinone

The aminoquinones **(38**, **47**, **54** and **55**) were prepared by the reaction of piperidine with corresponding quinone in CH_2Cl_2 solvent. We have already discussed that the aminoquinones are formed by electron transfer mechanism and the paramagnetic intermediates were confirmed by epr spectroscopy.

Scheme 26

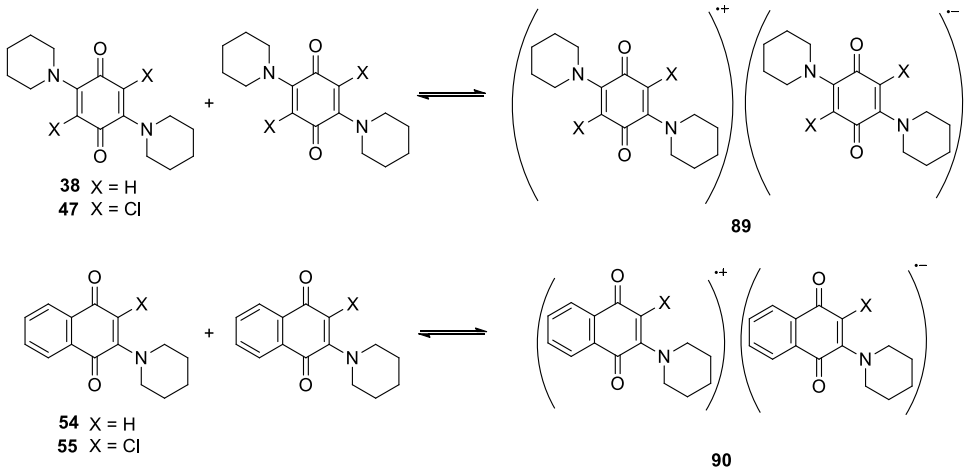

The aminoquinones behave as both donor and acceptor when present in the same molecule. Interestingly, we observed a weak epr signal for aminoquinones in the solid state but did not observe epr signal when aminoquinone was dissolved in CH_2Cl_2 solvent (Scheme 26). Presumably, one of the aminoquinone molecule acts as a donor and another acts as an acceptor in solid state leading to single, broad and weak epr signals (Figure 13). Presumably, the epr signal observed may be in contact between donor site with acceptor site in the solid state which might disappear in solvent and hence no epr signal in solution.

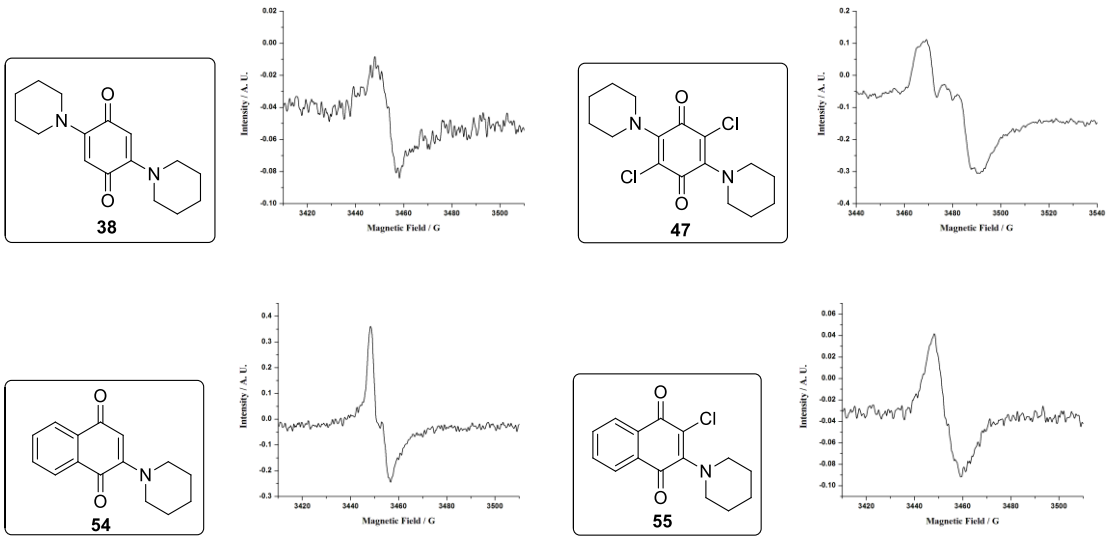

Figure 13. EPR spectra of aminoquinone in solid state at 25 ^{o}C (The aminoquinone solid (5 mg) was taken into epr tube and epr spectrum was recorded).

3.2.6 Attempt towards the electron transfer reaction of amines with halo compound acceptors

We have already discussed the results of the reaction of amines with quinone acceptors. The electron transfer readily takes place from donor amine to acceptor quinone leading to the formation of corresponding radical cation – anion pair as confirmed by epr spectral analysis.

Electron donor acceptor complexes and charge transfer interactions of amines with tetrahalomethanes were reported.[24] For example, DABCO **26** and quinuclidine **91** gives 1:l donor-acceptor (DA) complex with tetrahalomethanes. Also, crystal structures were reported for the of 1:l complex of DABCO and quinuclidine with CBr_4 **92**. The photochemical reaction of the DABCO-CBr_4 charge transfer complex leads to formation of radical ion intermediates (Scheme 27).

Scheme 27

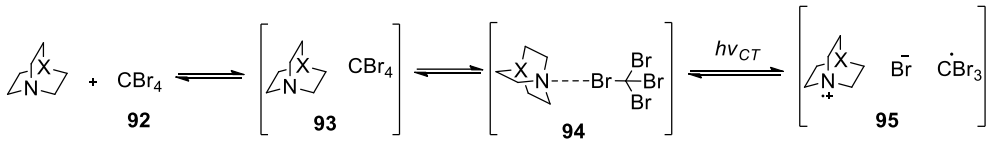

X= N DABCO **(26)**
X= CH Quinuclidine **(91)**

Similarly, electron donor acceptor complexes and charge transfer complexes of carbon tetrabromide, CBr_4 **92** and bromoform, $CHBr_3$ **96** with various donors such as halides, pseudohalide anions, aromatic hydrocarbons and aromatic compounds containing nitrogen and oxygen centers were reported.[25] Hence, we have studied the electron transfer reaction of sterically hindered amines with halometahne.

We have observed a weak epr signal for ion-pairs when the amine and halo compounds are reacted together. Previously, de Meijere *et al.* prepared the triisopropyl radical cation by the oxidation of triisopropylamine with SbF_5 in CH_2Cl_2 solution at 195K which gave the hyperfine epr spectrum.[26] They also noted that this radical cation has unusual thermodynamic and kinetic stability.[26] Also, these authors concluded that trialkylamine with at least two isopropyl substituents would lead to nearly planar structure for the corresponding radical cation, thus making it more stable.

We have briefly studied the electron transfer interaction of amines such as DIPEA **59**, 2,2,6,6-tetramethylpiperidin-4-ol **76a** and polymeric 2,2,6,6-tetramethylpiperidine

derivative **76b** with halo compounds like CH_2Cl_2 **97**, CH_2Br_2 **98** and $CHCl_3$ **99** by epr spectroscopy.

The reaction of DIPEA **59** and dichloromethane CH_2Cl_2 **97,** CH_2Br_2 **98** and $CHCl_3$ **99** at room temperature gave very weak epr signals in epr spectroscopy (Figure 12). In these cases, we have scanned the spectra 10 times to get a clear epr signal. The epr spectrum with different time intervals are shown in Figure 14.

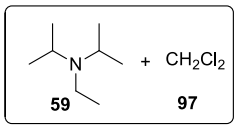

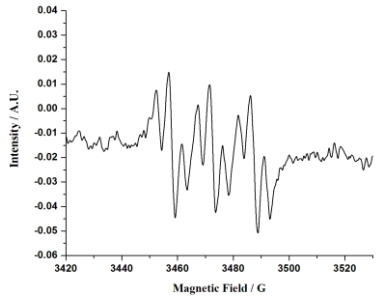

(a) at 5 min

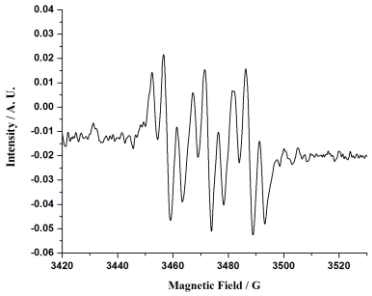

(b) at 1 h

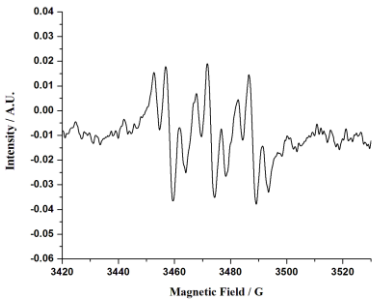

(c) at 6 h

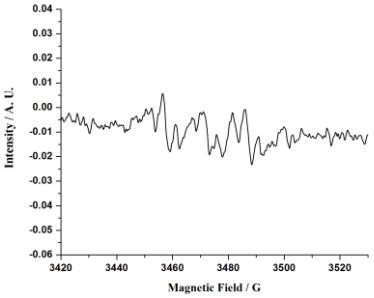

(d) at 12 h

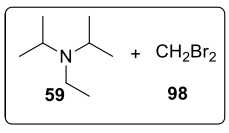

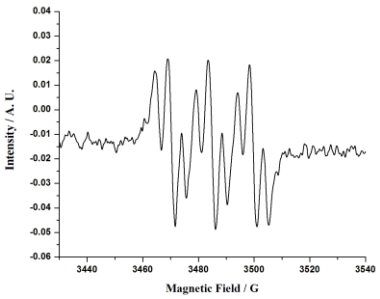

(a) at 5 min

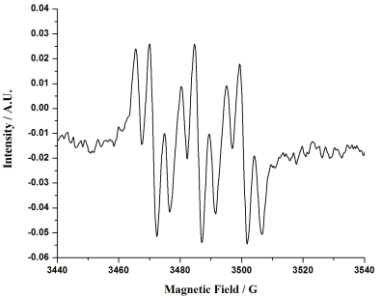

(b) at 1 h

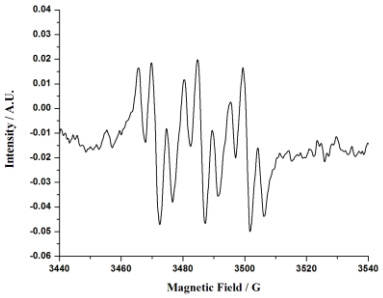

(c) at 2 h

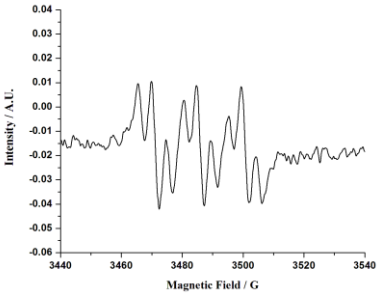

(d) at 6 h

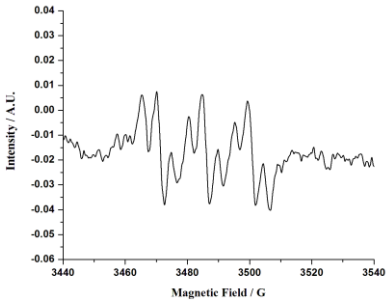

(e) at 12 h

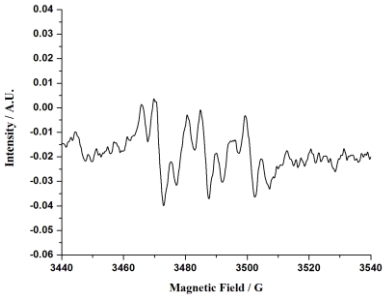

(f) at 24 h

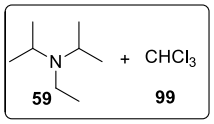

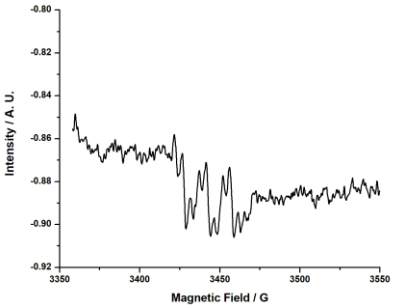

(a) at 5 min

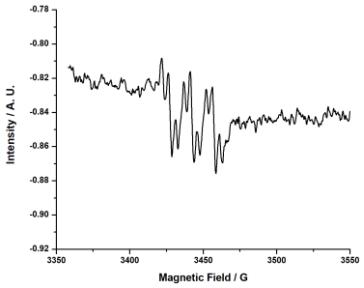

(b) at 1 h

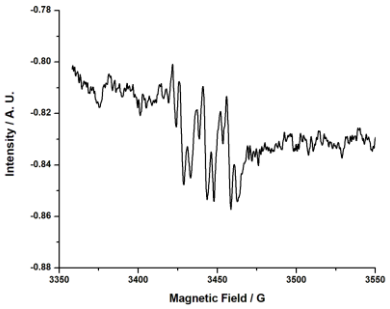

(c) at 2 h

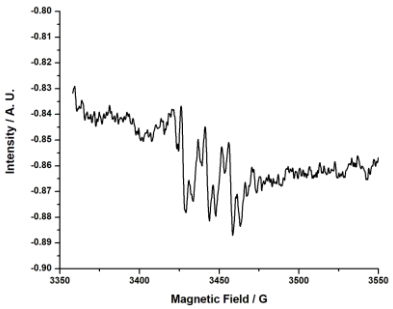

(d) at 6 h

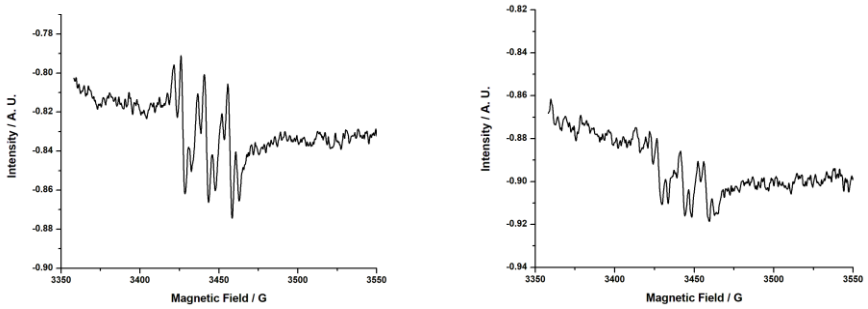

(e) at 12 h (f) at 24 h

Figure 14. EPR spectra of DIPEA **59** and CH_2Cl_2 **97,** CH_2Br_2 **98** and $CHCl_3$ **99** at 25 ^oC (Number of scans = 10).

The epr signal observed here due to the presence of amine radical cation and the signal due to the dichloromethane, dibromomethane and chloroform radical anions were not observed. Presumably, these radical anions may undergo fast exchange with the corresponding neutral species and hence do not give epr signal (Scheme 28).

Scheme 28

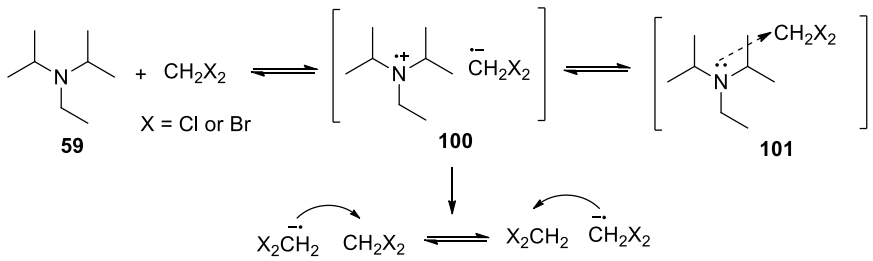

In all these cases, weak hyperfine splitting was also observed in epr spectroscopy. The reaction of *N, N*-diisopropylethylamine, DIPEA **59** with acceptors such as CH_2Cl_2 **97**, CH_2Br_2 **98** and $CHCl_3$ **99** gives a weak hyperfine splitting by the interaction of the radical cation present on nitrogen with two methylene β – protons of ethyl or isopropyl substituent of the radical cation.

We have also performed reaction with other donor amines *N, N*-diethyl aniline **61** and triphenyl amine **62** with halo compounds, but we did not observe the presence of

paramagnetic intermediates. Presumably, these relatively weak amines do not undergo electron transfer reactions with CH_2X_2 compounds.

Also, we have observed that the sterically hindered amine 2,2,6,6-tetramethylpiperidin-4-ol **76a** reacts with CH_2Cl_2 **97**, CH_2Br_2 **98** and $CHCl_3$ **99** to give a triplet signal in epr spectroscopy indicating the formation of corresponding 2,2,6,6-tetramethylpiperidin-4-ol radical cation (Figure 15).

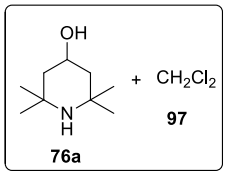

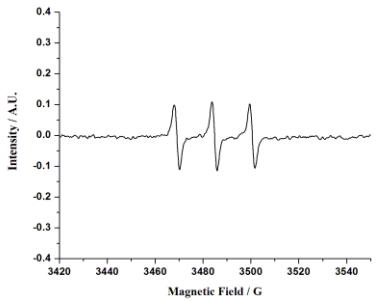

(a) at 5 min

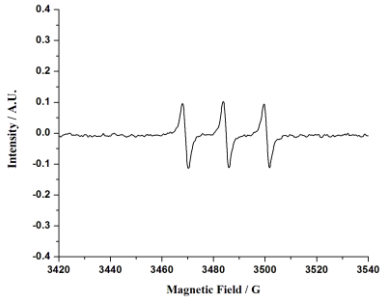

(b) at 1 h

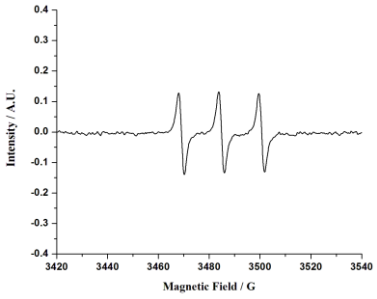

(c) at 2 h

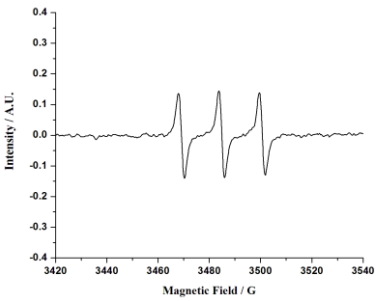

(d) at 6 h

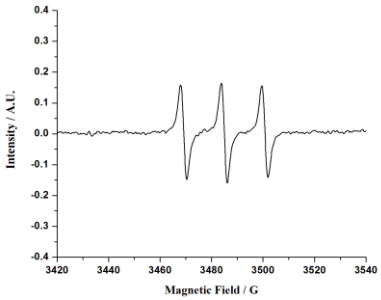

(e) at 12 h

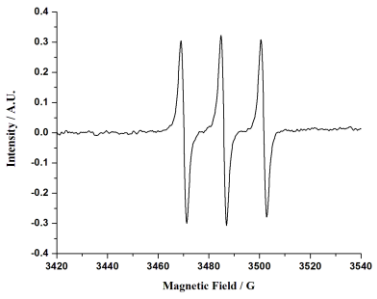

(f) at 24 h

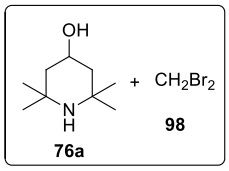

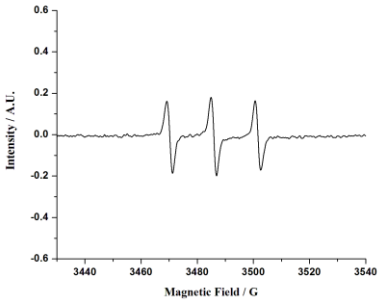

(a) at 5 min

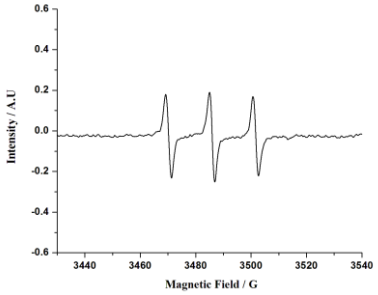

(b) at 1 h

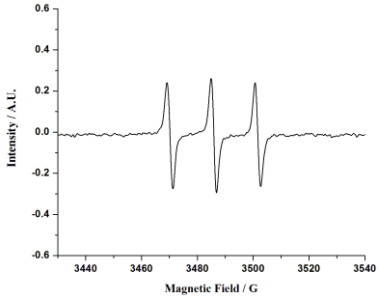

(c) at 2 h

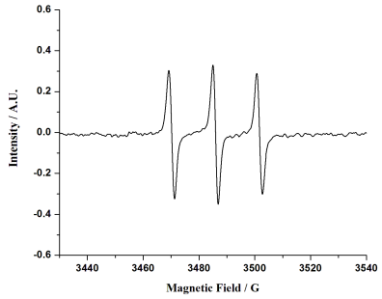

(d) at 6 h

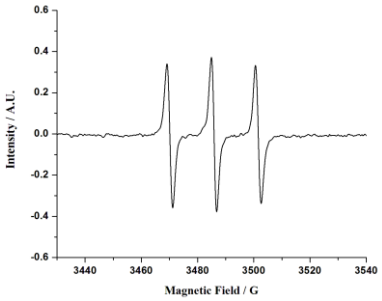

(e) at 12 h

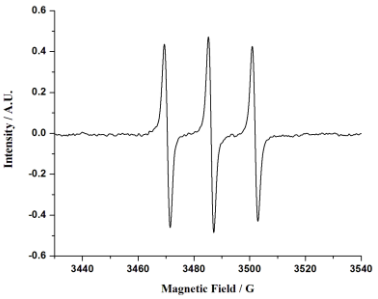

(f) at 24 h

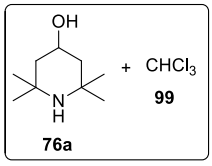

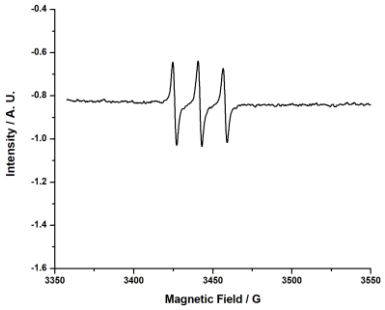

(a) at 5 min

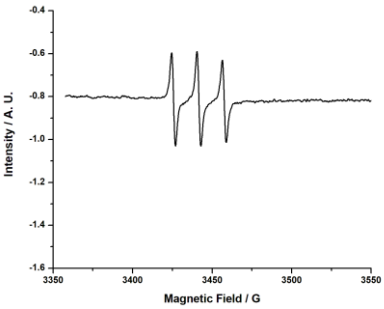

(b) at 1 h

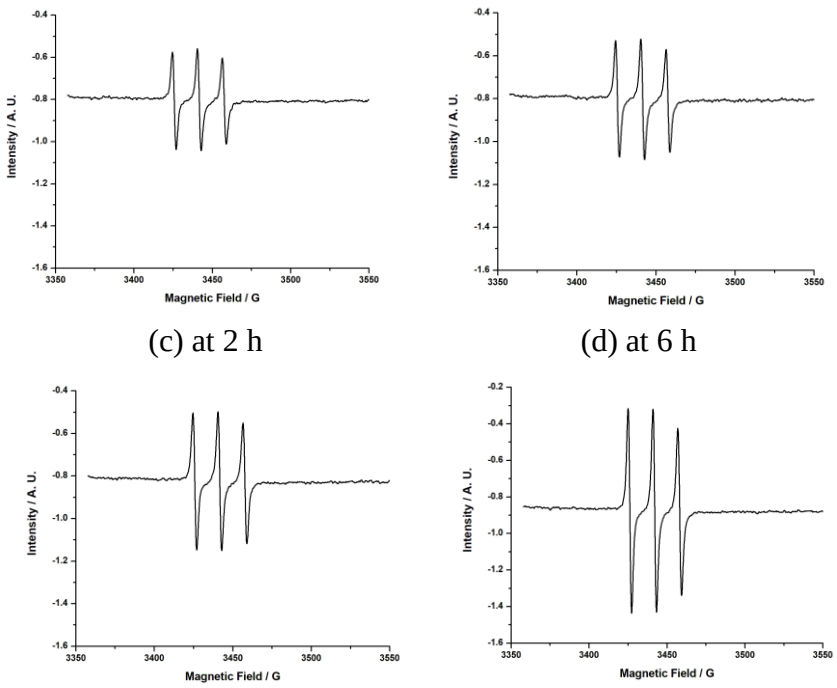

(c) at 2 h (d) at 6 h

(e) at 12 h (f) at 24 h

Figure 15. EPR spectra of 2,2,6,6-tetramethylpiperidin-4-ol **76a** and CH_2Cl_2 **97,** CH_2Br_2 **98** and $CHCl_3$ **99** at 25 ^oC (Number of scans = 5).

Hence, the electron transfer reaction of 2,2,6,6-tetramethylpiperidin-4-ol **76a** with halomethane can be rationalized by the formation of ion radical pairs followed by charge transfer complex **103** (Scheme 29). Interestingly, the epr signal strength increases with time. As expected, the reaction with sterically hindered amine may be slow with more amounts of paramagnetic species formed with time (Figure 15). However, formation of charge transfer complex of the type **103** is equilibrium with paramagnetic radical ion cannot be ruled out.

Scheme 29

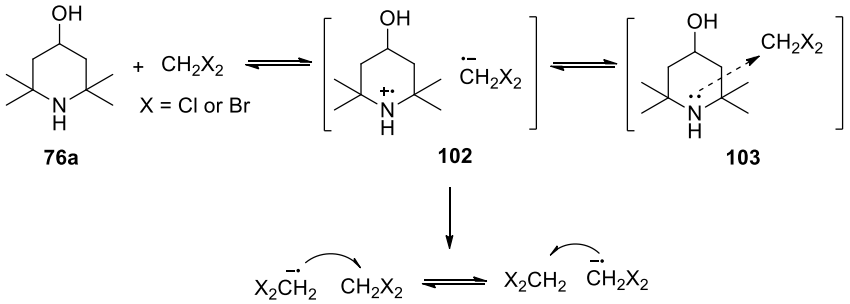

We have also carried out similar electron transfer reaction with polymeric derivative of 4-hydroxy-2,2,6,6-tetramethylpiperidine **76b** with CH_2Cl_2 **97** and CH_2Br_2 **98** and obtained evidence for paramagnetic species with triplet epr signal (Figure 16). In these cases also, subsequent formation of the corresponding charge transfer complexes of the type **105** cannot be ruled out.

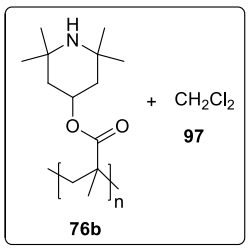

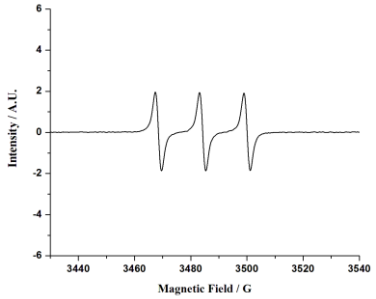

(a) at 5 min

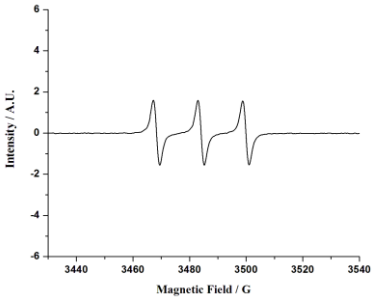

(b) at 1 h

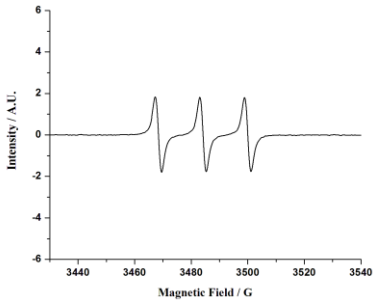

(c) at 2 h

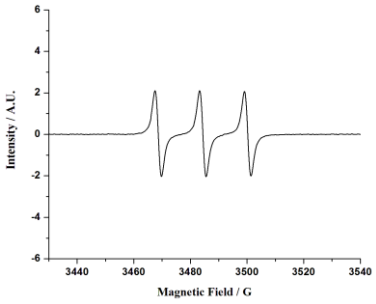

(d) at 6 h

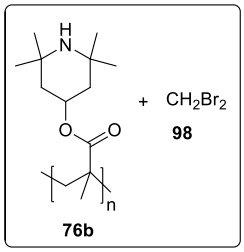

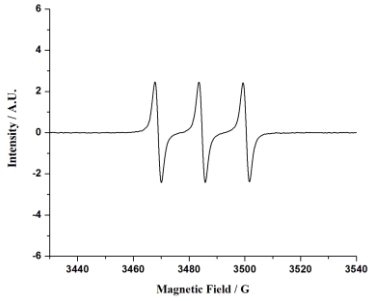

(e) at 12 h

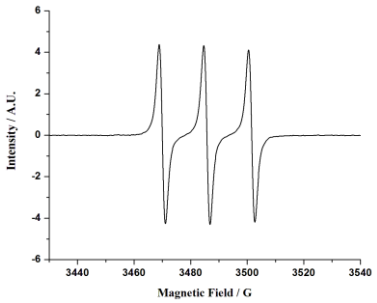

(f) at 24 h

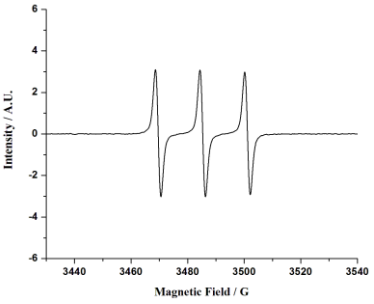

(a) at 5 min

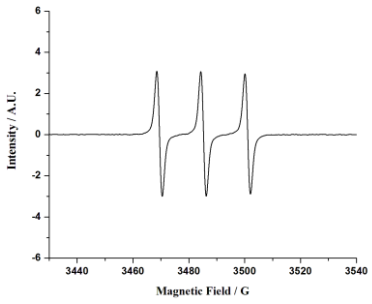

(b) at 1 h

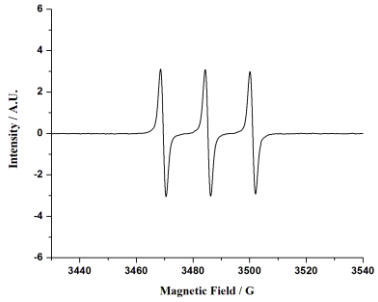

(c) at 2 h

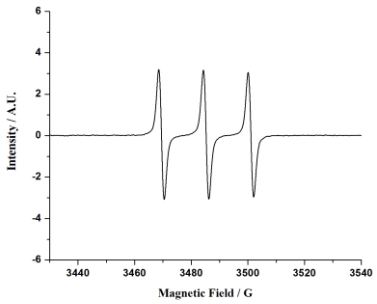

(d) at 6 h

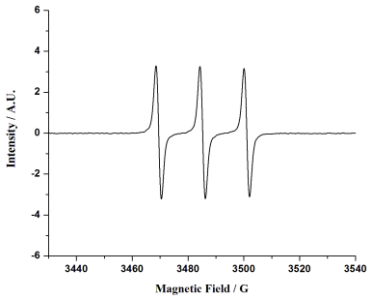

(e) at 12 h

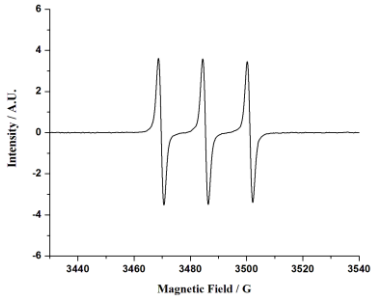

(f) at 24 h

Figure 16. EPR spectra of polymeric 4-hydroxy-2,2,6,6-tetramethylpiperidine **76b** and CH_2Cl_2 **97** and CH_2Br_2 **98** at 25 ^oC (Number of scans = 5).

The electron transfer reaction may be rationalized as outlined in Scheme 30.

Scheme 30

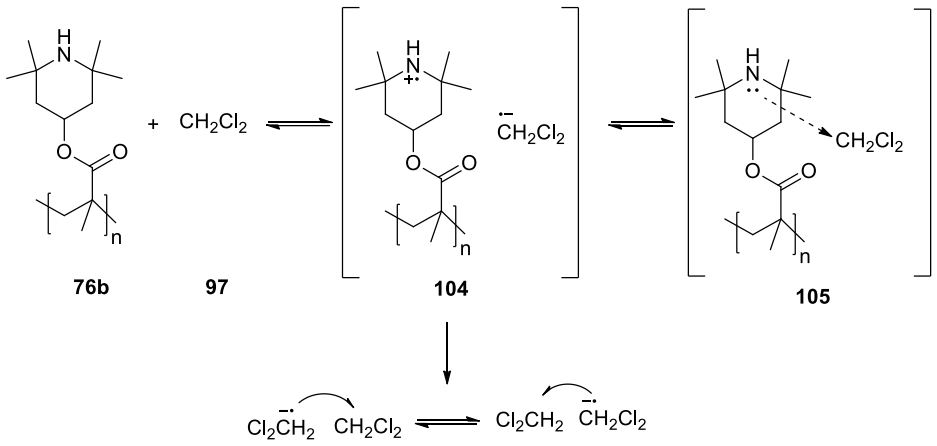

76b **97** **104** **105**

The reaction of 4-hydroxy-2,2,6,6-tetramethylpiperidine **76a** and polymeric derivative of 4-hydroxy-2,2,6,6-tetramethylpiperidine **76b** with CH_2Cl_2 **97**, CH_2Br_2 **98** and $CHCl_3$ **99** gives triplet in epr spectroscopy but there is no hyperfine splitting due to absence of β – hydrogen in the corresponding amine radical cation.

3.2.7 Preliminary studies on electron transfer reaction of amines with viologen acceptors

Viologens are 1,1'-disubstituted-4,4'-bipyridinium salts. Michaelis first reported the electrochemical behaviour of this class of compounds which possess excellent photoelectrochromic properties.[27] The viologens are electron acceptors and are widely used as herbicides and for electron mediation in photosynthesis,[28] in electrochromic display devices,[29] in organic electrical conductors,[30] in chemically modified electrodes,[31] for solar energy storage and photocatalytic reduction of water to hydrogen.[32] The viologens were originally investigated as redox indicators in biological studies. Their electrochemically reversible behaviour and the marked colour change between the

oxidation states, make the viologens as favored candidates for electrochemical display devices as alternative to LEDs and LCDs.[29] The viologens exist in three main oxidation states as shown in Figure 17.

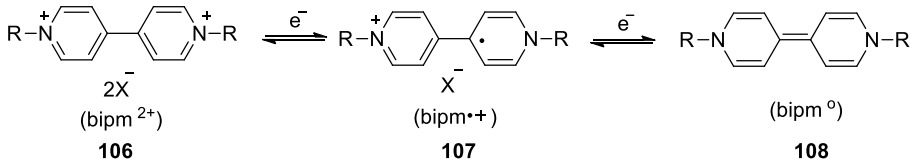

Figure 17. Three common bipyridinium redox states.

Reductive electron transfer to viologen dications **106** gives stable radical cations **107** (Figure 15) due to electron delocalization throughout the π-framework of the bipyridyl nucleus. Whereas the bipyridinium dication salts are normally not coloured, the viologen radical cations are intensely coloured, with high molar absorption coefficients. This is due to charge transfer between the +1 and 0 valent nitrogens.

The reaction of viologen derivatives with amine gives a rapid color change by the formation of electron transfer and charge transfer between viologen derivatives and amine, which is useful for the detection of amines.[33] The reaction of viologen molecules with *N*, *N*-dimethylformamide (DMF) generates an organic dopant for molybdenum disulfide (MoS_2) in metal-oxide-semiconductor field-effect-transistor (MOSFET).[34] Polyviologen are well known material useful as an interfacial layer and cathode buffer layer in polymer solar cell.[35]

Previously, we have studied the electron transfer reaction of an acceptor *p*-chloranil with donor amines. Hence, preliminary studies were undertaken on reaction of amine donors with other acceptors such as viologen derivatives. Hence, we have decided to examine the possibility of electron transfer reaction between viologen acceptor with readily accessible amines. We have prepared a series of viologen derivatives **111** by the

reaction between 4,4'-bipyridyl **109** and alkyl halide **110** in DMF solvent following a closely related reported procedure (Scheme 31).[36]

Scheme 31

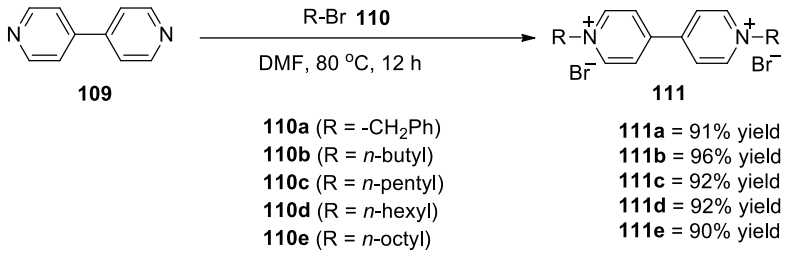

We have also synthesized the 1, 4-dipyridyl benzene **115** *via* preparation of synthesizing 1, 4- phenylenediboronic acid **113** followed by Suzuki coupling with 4-bromo pyridine **114** (Scheme 32).[37]

Scheme 32

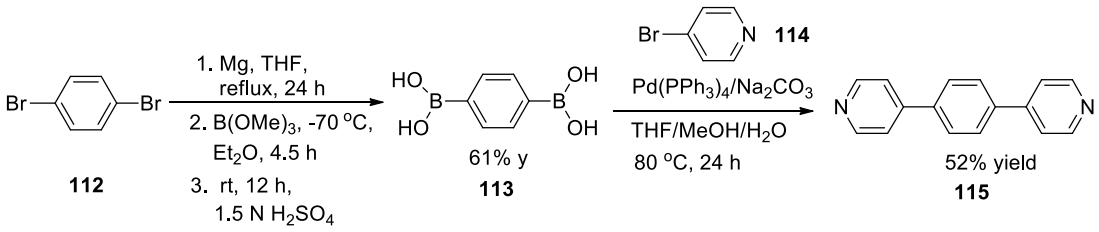

Similarly, the 1,4-dipyridyl benzene **115** was readily converted to extended viologen **116** by reaction with 1-bromo butane in DMF solvent (Scheme 33).

Scheme 33

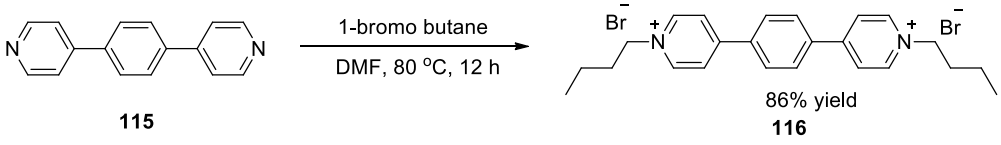

We have investigated the reaction of the viologen salt such as benzyl viologen **111a** with various readily accessible electron donor amines to examine the electron transfer by epr studies. The epr studies of viologen compound with different amines were

carried out by PC and methanol solvent. In the case of reaction of benzyl viologen **111a** with amines like diphenyl amine **118**, *N*, *N*-diethyl aniline **61** and triphenyl amine **62** no epr signal was observed (Table 2, entries 2, 8 and 10). The reason may be the weak donor nature of amines as the lone pair of electrons on the nitrogen atom are delocalised in the aromatic ring, which is unavailable for electron transfer to viologen acceptors. Also, it indicates that viologen is a weak acceptor and it can interact only with strong amines.

Table 2. EPR of benzyl viologen **102a** with various amines in methanol solvent[a]

Entry	Acceptor	Donor	EPR spectra
1	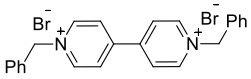 **111a**	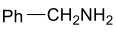 **117**	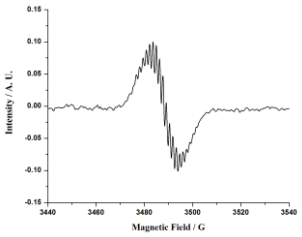
2	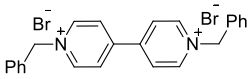 **111a**	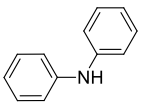 **118**	No signal observed
3	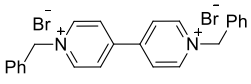 **111a**	 **59**	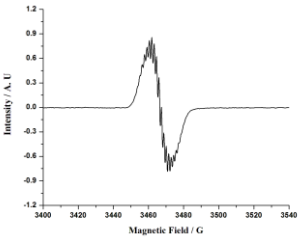
4	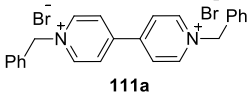 **111a**	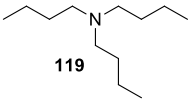 **119**	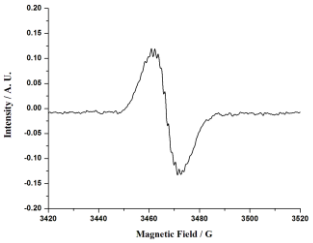

5	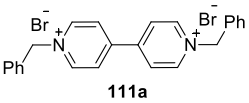 **111a**	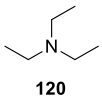 **120**	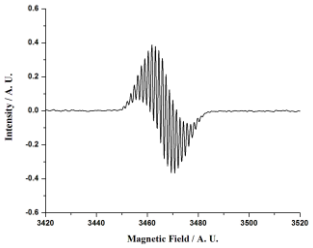
6	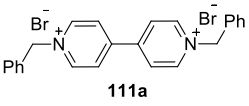 **111a**	 **26**	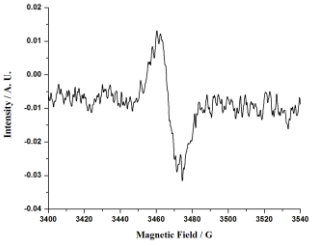
7	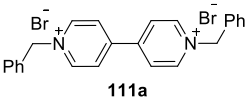 **111a**	 **121**	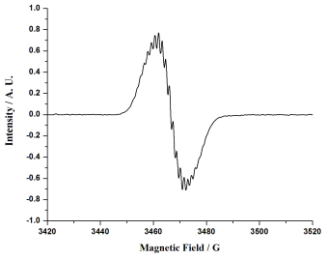
8	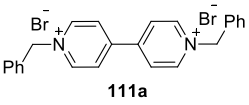 **111a**	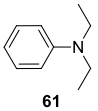 **61**	No signal observed
9	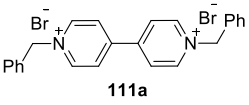 **111a**	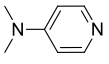 **122**	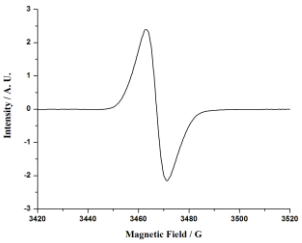
10	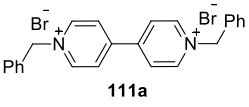 **111a**	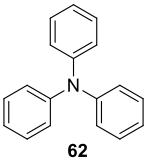 **62**	No signal observed

[a]EPR experiment were carried out by mixing amine (0.2 mmol) with benzyl viologen **111a** (0.2 mmol) in methanol. The mixture was taken into epr tube and recorded the spectra at 25 °C.

Similarly, we have studied the reaction of benzylviologen **111a** with different amines in PC solvent. In this case, we have observed weak epr signal in the reaction of benzylamine **117**, *N, N*-diisopropylethylamine **59** and triethyamine **120** with benzyl viologen acceptor (Table 3, entries 1,3,5). The weak epr signal or no signal also indicates that the paramagnetic intermediates are formed to lesser extent due to heterogeneous nature of the reaction due to poor solubility of viologen in PC solvent. Alternatively, the reason for weak epr signal may be also due to disproportionation of the viologen radical cation to give back the starting viologen (Scheme 34).

Scheme 34

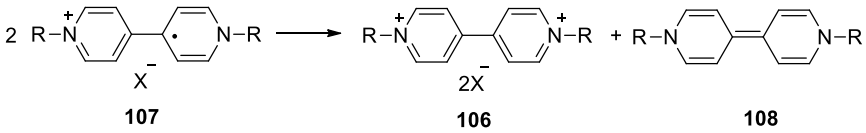

Table 3. EPR of benzyl viologen with various amines in PC solvent[a]

Entry	Donor	Donor	ESR spectra
1	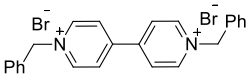 **111a**	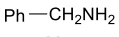 **117**	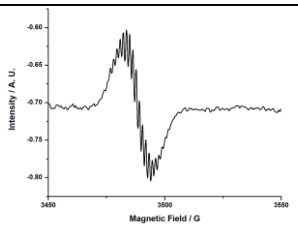
2	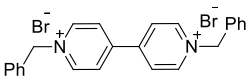 **111a**	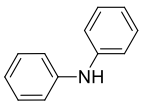 **118**	No signal observed
3	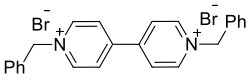 **111a**	 **59**	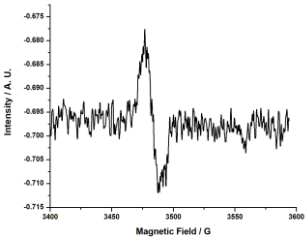

4	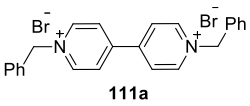 **111a**	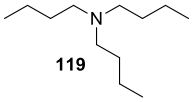 **119**	No signal observed
5	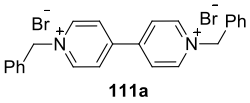 **111a**	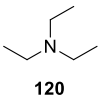 **120**	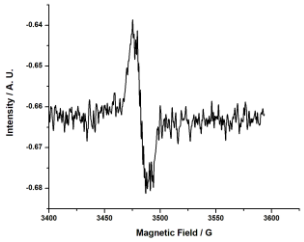
6	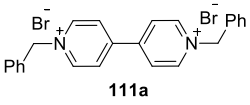 **111a**	 **26**	No signal observed
7	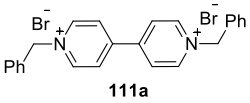 **111a**	 **121**	No signal observed
8	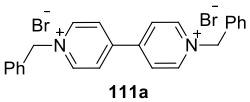 **111a**	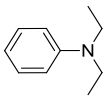 **61**	No signal observed
9	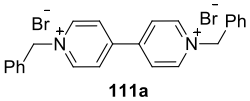 **111a**	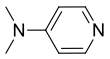 **122**	No signal observed
10	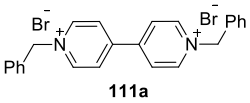 **111a**	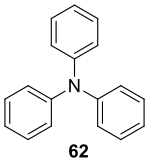 **62**	No signal observed

[a]EPR experiment were carried out by mixing amine (0.2 mmol) with benzyl viologen **111a** (0.2 mmol) in PC. The mixture was taken into epr tube and recorded the spectra at 25 °C.

Electrochemistry of viologen were reported extensively.[38] The high resolution epr spectra of photochemically generated viologen radical cation derivatives in ethanol-water system has been also reported.[39]

Here also, we have observed a epr signal only for viologen radical cation formed in the reaction of benzyl viologen with amines. The amine radical cation formed after electron transfer to viologen would undergo fast electron exchange with the neutral amine and hence may not show epr signal (Scheme 35).

Scheme 35

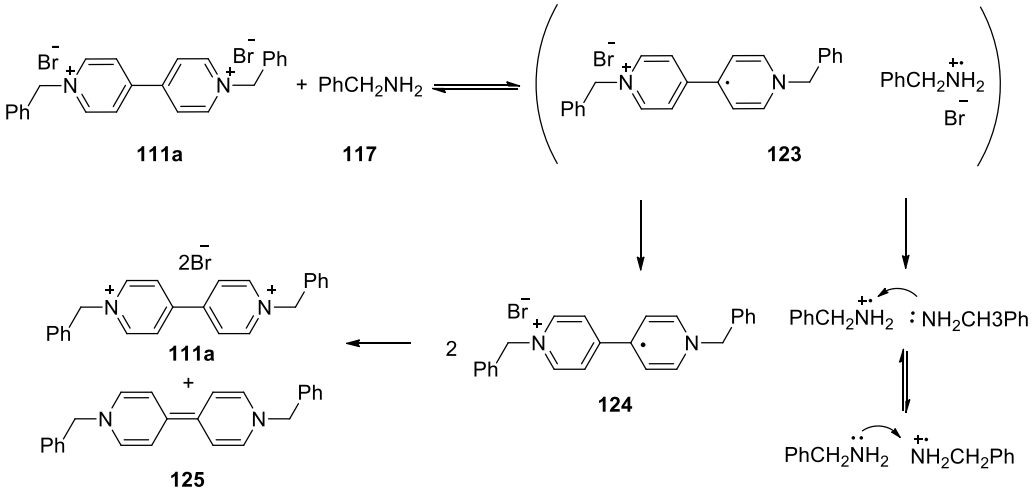

We have investigated the electron transfer reaction of acceptors like quinones, halomethanes and viologens with amine donors. Also, we proposed tentative mechanisms for the formation of paramagnetic intermediates in these reactions in accordance with epr spectroscopic studies. Among the acceptors studied, *p*-chloranil which has a very high electron affinity (EA=2.78 eV) gives strong epr signals with donor amines. The electrochemistry of quinone is also well studied and hence we have selected the *p*-chloranil as an acceptor for studies on the construction of organic electrochemical cell

based on electron transfer reaction with tertiary amines. The results are discussed in the next chapter.

3.3 Conclusions

We have investigated the electron transfer reaction of quinones with piperidine. The corresponding aminoquinone was formed in good yield (55% to 75%) *via* the corresponding radical ion intermediates. The formation of paramagnetic intermediates were confirmed by epr spectroscopy.

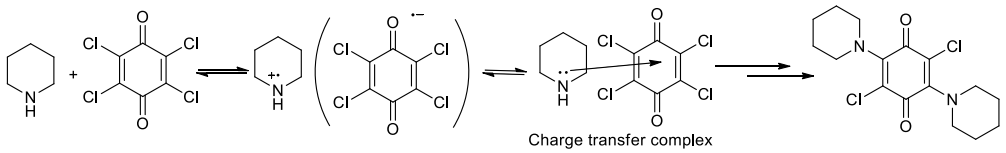

We have also studied the reaction of tertiary amines like *N, N*-disopropylethylamine, *N, N*-diethylaniline, triphenylamine, *N*-benzyl-*N*-isopropylpropan-2-amine and *N, N*-diisopropyl-2, 2-dimethylpropan-1-amine with *p*-chloranil acceptor. We have observed that electron transfer from amine donor to quinone acceptor was fast. The formation of ion pair intermediates and charge transfer complexes were confirmed by epr and UV-Visible spectroscopic studies. The epr analysis of the intermediates formed in PC solvents indicate that the initially formed ion pair by electron transfer from donor to acceptor are converted to charge transfer complexes in equilibrium with small amounts of radical ions. The epr signal corresponds to the presence of quinone radical anion and the amine radical cation signal does not apperar as it undergoes fast self-exchange with another amine.

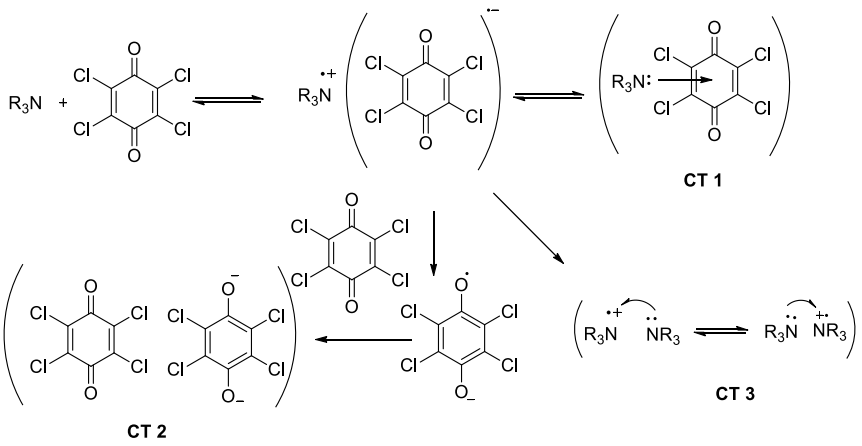

We have developed a simple method for the preparation of polymers containing amine as a pendant group through the reaction of PMMA (polymethylmethacrylate) and 4-hydroxy-2,2,6,6-tetramethylpiperidine. The sterically hindered polymeric 2,2,6,6-tetramethyl-4-piperidinol product reacts with *p*-chloranil to give radical ion intermediates followed by charge transfer complex. The radical ion intermediates gave triplet signal in epr spectroscopy which corresponds to the presence of amine radical cation. Similar results were also obtained in the reaction of 4-hydroxy-2,2,6,6-tetramethylpiperidine and 2,2,6,6-tetramethylpiperidin-4-one with *p*-chloranil.

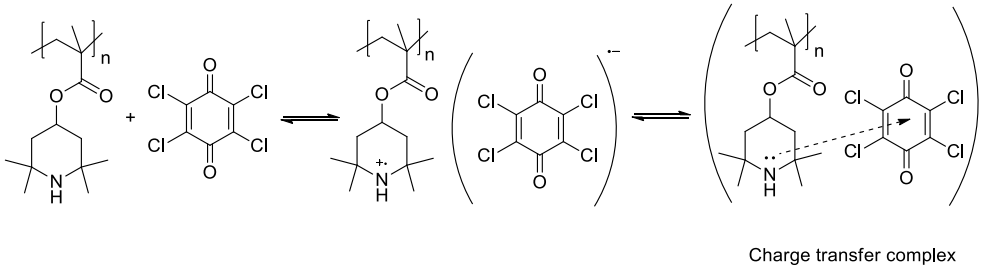

We have briefly studied the reaction between *N*, *N*-diisopropyl ethylamine, DIPEA with CH_2Cl_2, CH_2Br_2 and $CHCl_3$. The formation of paramagnetic intermediates were confirmed by epr spectroscopy. The epr signal with very weak hyperfine splitting for the

nitrogen radical cation was observed. We have also investigated the reaction of 2,2,6,6-tetramethylpiperidin-4-ol and polymeric 2,2,6,6-tetramethylpiperidine derivatives with CH_2Cl_2, CH_2Br_2 and $CHCl_3$. Similar paramagnetic intermediates with triplet epr signal were observed. The results indicate that the halogenated solvents also behave like acceptor in the presence of strong amine donors.

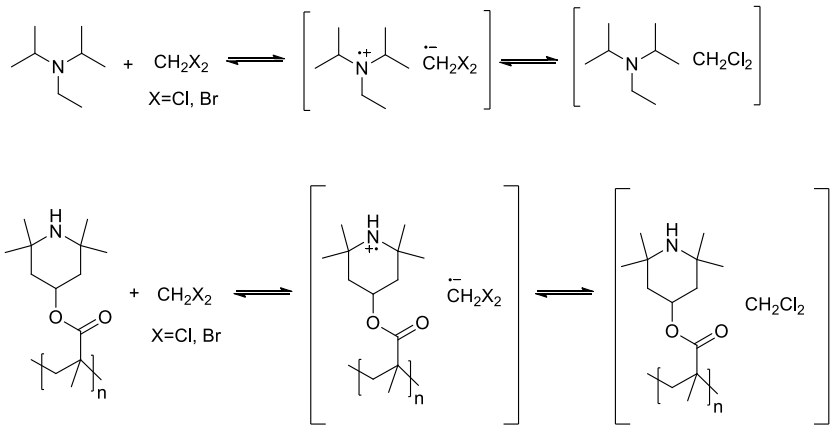

We have also studied the reaction of viologen acceptors with different amines. Again, the formation of paramagnetic intermediates was confirmed by epr spectroscopy. The releatively weak aromatic amine donors did not undergo electron transfer reaction with viologen derivatives.

3.4 Experimental Section

3.4.1 General Informations

IR (KBr) and IR (neat) spectra were recorded on JASCO FT-IR spectrophotometer model-5300. The NMR spectra ^{1}H (400 MHz) and ^{13}C (100 MHz) were recorded on Bruker-Avance-400 spectrometers chloroform-d as solvent. Chemical shifts are expressed in δ downfield with respect to the signal of internal standard tetramethylsilane (δ = 0 ppm). Coupling constants *J* are in Hz. EPR spectra was recorded on a Bruker-ER073 instrument equipped with an EMX micro X source for X band measurement using Xenon 1.1b.60 software provided by the manufacturer. Thin layer chromatography tests were carried out on pre-coated glass plates using silica gel-GF_{254} containing 13% calcium sulfate as binder. The spots were visualized by UV light or exposure to iodine. Gravity column chromatography was used for the separation of compounds using silica gel (100-200 mesh) as stationary phase. All the glasswares were pre-dried at 100-120 °C in an air-oven for 4 h, assembled in hot condition and cooled under a stream of dry nitrogen.

In all experiments, a round bottom flask of appropriate size with a side arm, a side septum, a magnetic stirring bar, a condenser and a connecting tube attached to a mercury bubbler was used. The outlet of the mercury bubbler was connected to the atmosphere by a long tube. All dry solvents and reagents used were distilled from appropriate drying agents. As a routine practice, all organic extracts were washed using saturated NaCl solution (brine) and dried over Na_2SO_4 or K_2CO_3 and concentrated on Heidolph-EL-rotary evaporator.

p-Chloranil, *N, N*-diisopropylethylamine (DIPEA), 1,4-diazabicyclo[2.2.2]octane (DABCO), diisopropylamine, benzyl bromide, *m*-CPBA, dibenzylamine and *N*-methylpyrolidine were purchased from Avra chemicals (India). *P*-benzoquinone (BQ), 1,4-naphthaquinone, 2,3-dichloronaphthaquinone, triphenylamine (TPA), *N,N'*-tetramethyl-1,4-phenylenediamine (TMPDA), PMMA, 4-hydroxy-2,2,6,6-tetramethylpiperidine, 2,2,6,6-tetramethylpiperidin-4-one, propylene carbonate and 4,4'-bipyridyl were purchased from Sigma Aldrich. CH_2Cl_2, CH_2Br_2, $CHCl_3$, tributylamine, trimethylamine and *N*,*N*-diethylaniline were purchased from Merck, India.

3.4.2 General procedure for preparation of aminoquinones

In a 50 mL RB flask, corresponding quinones (5 mmol) was dissolved in DCM (30 mL) solvent and piperidine (10 mmol) was slowly added for 5 min. The reaction mixture was stirred at room temperature for 12 h. Then the reaction mixture was concentrated under reduced pressure and 100 mL of ether was added to precipitate out the polar impurities and it was removed by filtration. The filtrate was diluted with water and the organic layer was separated. The organic layer was washed with saturated NaCl solution and the solvent was evaporated under reduced pressure. The residue was chromatographed on a silica gel (100-200) column to isolate the corresponding aminoquinones.

2,5-di-piperidin-1-yl-[1,4] benzoquinone 38

Yield : 0.754 g (55%); Brown solid

mp : 167-170 °C

IR (KBr) : (cm^{-1}) 2926, 1621, 1545, 1216, 1189, 756.

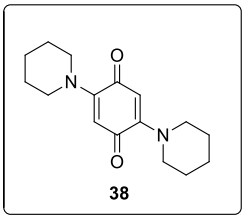

38

^{1}H NMR ($CDCl_3$) : (400 MHz, $CDCl_3$, δ ppm) 5.53 (s, 2H), 3.54 (s, 8H), 1.60-1.71 (m, 12H).

^{13}C NMR ($CDCl_3$) : (100 MHz, $CDCl_3$, δ ppm) 182.5, 153.2, 105.5, 50.4, 25.8, 24.3.

2,5-dichloro-3,6-di-piperidin-1-yl-[1,4] benzoquinone 47

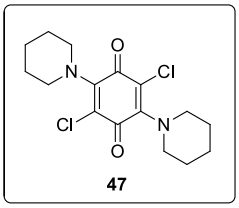

47

Yield : 1.283 g (75%); Dark brown solid

mp : 110-115 °C

IR (KBr) : (cm^{-1}) 2926, 1685, 1605, 1470, 745.

^{1}H NMR : (400 MHz, $CDCl_3$, δ ppm) 3.49 (s, 8H), 1.7 (s, 12H)

^{13}C NMR : (100 MHz, $CDCl_3$, δ ppm) 176.0, 149.3, 116.9, 53.2, 26.9, 24.0

2-piperidin-1-yl-[1,4] naphthaquinone 54

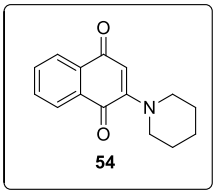

54

Yield : 0.783 g (65%); Black solid

mp : 82-85 °C

IR (KBr) : (cm^{-1}) 2941, 1675, 1559, 1243, 780.

^{1}H NMR : (400 MHz, $CDCl_3$, δ ppm) 8.02-7.95 (m, 2H), 7.66-7.60 (m, 2H), 6.00 (s, 1H), 3.48 (s, 4H), 1.7 (s, 6H)

^{13}C NMR : (100 MHz, $CDCl_3$, δ ppm) 183.5, 183.4, 154.1, 133.7, 132.9, 132.5, 132.2, 126.5, 125.4, 110.4, 50.4, 25.7, 24.3

2-chloro-3-(piperidin-1-yl)naphthalene-1,4-dione 55

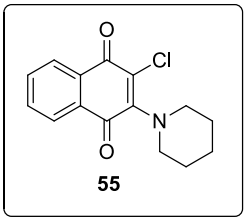

55

Yield : 1.031 g (75%); Orange solid

mp : 89-92 °C

IR (KBr) : (cm^{-1}) 2933, 1645, 1557, 1276, 717.

^{1}H NMR : (400 MHz, $CDCl_3$, δ ppm) 8.19-8.22 (m, 1H), 8.11-8.13 (d, 1H), 7.91-8.0 (d, 1H), 7.81-7.83 (m, 1H), 3.54-3.56 (m,4H), 1.73-1.78 (m, 6H)

^{13}C NMR : (100 MHz, $CDCl_3$, δ ppm) 182.0, 176.0, 150.8, 134.6, 133.9, 131.7, 131.5, 127.8, 126.8, 52.9, 26.8, 24.1.

3.4.3 Procedure for preparation of N-benzyl-N-isopropylpropan-2-amine 73

In an oven dried RB flask *N, N*-disopropyl amine (10 mmol, 1.14 ml) was dissolved in CH_3CN solvent. Then potassium carbonate, K_2CO_3 (50 mmol, 6.9 g) was mixed with the above solution. Then benzyl bromide (10 mmol, 1.2 ml) was added slowly to the mixture and it was heated to around 70 °C for 12 h. Then the reaction was filtered and the filtrate was evaporated under reduced pressure. Then it was dissolved in DCM and water was added to the reaction mixture. The organic layer was separated, dried over Na_2SO_4 and evaporated. The corresponding crude product was purified by column chromatography on silica gel (100-200) using hexane and ethyl acetate as eluent to isolate pure amine **73** as product.

N-benzyl-N-isopropylpropan-2-amine 73

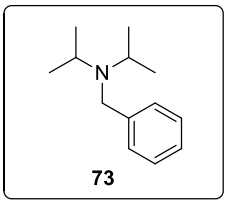

73

Yield : 1.432 g (75%); Colorless liquid

IR (neat) : (cm^{-1}) 3083, 2962, 2869, 1601, 1493, 1256, 1177, 1024, 952, 820, 750, 694.

^{1}H NMR : (400 MHz, $CDCl_3$, δ ppm) 7.44-7.42 (m, 2H), 7.34-7.30 (m, 2H), 7.25-7.21 (m, 1H), 3.69 (S, 2H), 3.10-3.03 (m, 2H), 1.07-1.06 (m, 12H)

^{13}C NMR : (100MHz, $CDCl_3$, δ ppm) 143.2, 127.9, 127.8, 126.1, 48.9, 47.7, 20.7

3.4.4 Procedure for the preparation of N, N-diisopropyl-2, 2-dimethylpropan-1-amine 74

In an oven dried RB flask, N, N-diisopropylpivalamide (20 mmol) was taken in THF solvent cooled to 0 °C under N_2 atmosphere and $NaBH_4$ (50 mmol, 2 g) was added. Iodine (25 mmol, 6.35 g) in THF (10 ml) was addend slowly during 15 min. Then, the reaction was refluxed for 12 h. The reaction was quenched with water. The solvent was evaporated and residue was taken in dry ether. 3N NaOH solution added to this and amine was extracted in to ether. The organic layer was washed with brine and dried over anhydrous Na_2SO_4. The organic layer was evaporated to get crude amine which was purified by column chromatography on silica gel (100-200) using hexane and ethyl acetate as eluent to isolate pure amine **74** as product.

N, N-diisopropyl-2, 2-dimethylpropan-1-amine 74

Yield : 1.710 g (50%) Colorless liquid

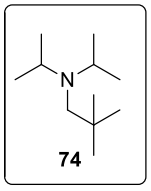

74

IR (neat) : (cm^{-1}) 2967, 2811, 1477, 1468, 1209, 1152, 1113, 1046, 990, 713.

^{1}H NMR : (400 MHz, $CDCl_3$, δ ppm) 3.02-2.90 (m, 2H), 2.20 (S, 2H), 1.0-0.9 (m, 12H), 0.88-0.87 (m, 9H).

^{13}C NMR : (100 MHz, $CDCl_3$, δ ppm) δ: 57.3, 49.0, 32.4, 28.8, 21.3.

3.4.5 Procedure for preparation of PTMA polymer 77

In an oven dried RB flask, PMMA **75** (5 mmol, 0.5 g) was dissolved in THF solvent. Then, 4-hydroxy-2,2,6,6-tetramethylpiperidine **76a** (6.3 mmol, 1 g) was added to the dissolved polymer. Then the mixture was heated to around 70 °C for 2 h. Then the reaction was distilled out to get a crude polymer. The polymer was dissolved in DCM and water was added to the reaction mixture. After work up, the organic layer was separated, dried over Na_2SO_4 and evaporated to give the 79% yield of polymer **76b**.

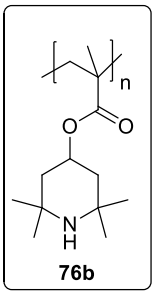

76b

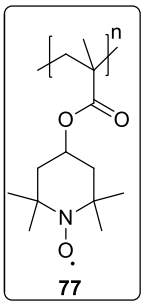

77

The polymer **76b** (4 mmol, 0.906 g) was dissolved in THF solvent. The *m*-chloroperoxybenzoic acid, *m*-CPBA (7 mmol, 1.2 g) in THF solvent was added slowly at 0 °C. The reaction mixture was slowly changed to red colour and it was further stirred at rt for 18 h. Then the solvent was removed under reduced pressure. Then the crude polymer was dissolved in DCM. Then 10% of sodium sufite and 5% sodium bicarbonate were added to remove excess *m*-CPBA. The organic layer was separated, dried over Na_2SO_4 and evaporated to give the 84% yield of polymer **77**.

3.4.6 General Procedure for the preparation of viologen derivatives

In an oven dried RB flask, 4, 4'-Bipyridyl **109** (5 mmol) was added and dissolved in DMF (30 mL) solvent. The corresponding aryl or alkyl bromide **110** (12 mmol) was slowly

added for 5 min. The reaction mixture was heated at 80 °C for 24 h. Then the reaction mixture was cooled to room temperature and the resulting yellowish solids were filtered. The solids were poured into dehydrated diethyl ether for washing. The corresponding viologen powder product was collected and dried. The dried product was washed twice with diethyl ether to remove the reactants. Then the resulting viologen salts **111** were dried in vacuum at room temperature.

1,1'-Dibutyl-4,4'-bipyridinium dibromide 111b

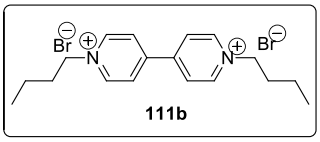

111b

Yield : 2.05 g (96%);

IR (KBr) : (cm^{-1}) 2931, 1638, 1501, 1238, 1178, 832.

^{1}H NMR : (400 MHz, D_2O, δ ppm) 9.07-9.05 (d, 4H), 8.49-8.48 (d, 4H), 4.75 4.70 (t, 4H), 2.02-1.99 (m, 4H), 1.36-1.34 (m, 4H), 0.94-0.89 (t, 6H)

^{13}C NMR : (100 MHz, D_2O, δ ppm) 150.0, 145.5, 127.0, 62.0, 32.6, 18.8, 12.7.

1,1'-Dipentyl-4,4'-bipyridinium dibromide 111c

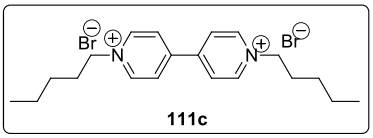

111c

Yield : 2.10 g (92%);

IR (KBr) : (cm^{-1}) 2931, 1638, 1506, 1232, 1178, 832.

^{1}H NMR : (400 MHz, D_2O, δ ppm) 9.06-9.04 (d, 4H), 8.49-8.47 (d, 4H), 4.74-4.66 (t, 4H), 2.02 (m, 4H), 1.31-1.29 (m, 8H), 0.83-0.80 (t, 6H)

^{13}C NMR : (100 MHz, D_2O, δ ppm) 150.0, 145.4, 12.9, 62.2, 30.3, 27.4, 21.4, 13.0.

1,1'-Dihexyl-4,4'-bipyridinium dibromide 111d

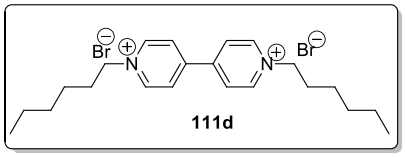

111d

Yield : 2.23 g (92%);

IR (KBr) : (cm^{-1}) 2926, 1638, 1512, 1232, 1178, 832.

^{1}H NMR : (400 MHz, D_2O, δ ppm) 9.08 (d, 4H), 8.52 (d, 4H), 4.69 (t, 4H), 2.04 (m, 4H), 1.32 (m,12H), 0.83-0.81 (t, 6H)

^{13}C NMR : (100 MHz, D_2O, δ ppm) 150.0, 145.4, 127.0, 62.3, 34.6, 30.6, 24.9, 21.8, 13.2.

1,1'-Dioctyl-4,4'-bipyridinium dibromide 111e

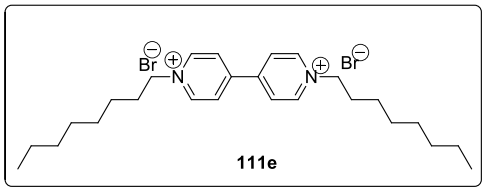

111e

Yield : 2.30 g (90%);

IR (KBr) : (cm^{-1}) 2915, 1638, 1512, 1238, 1172, 832.

^{1}H NMR : (400 MHz, D_2O, δ ppm) 9.08 (d, 2H), 8.51 (d, 2H), 4.69 (t, 4H), 2.04 (m, 4H), 1.32-1.21 (m, 20H), 0.80 (t, 6H)

^{13}C NMR : (100 MHz, D_2O, δ ppm) 150.0, 145.4, 127.0, 62.3, 30.9, 30.6, 28.1, 28.0, 25.2, 22.0, 13.4.

3.4.7 Procedure for the preparation of 1, 4-phenylenediboronic acid 113

To a suspension of magnesium (2.30 g, 95.80 mmol) in dry THF was added dropwise solution of *p*-dibromobenzene **112** (7.5 g 28.5 mmol) in dry THF (30ml) about 20 minutes under the N_2 atmosphere. The reaction mixture was heated to reflux for 2.5 h and then cooled to -70 ^{0}C. Then the solution of $B(OMe)_3$ (14.2 mL, 127.2 mmol) in dry diethyl ether (15 ml) was added dropwise to the reaction mixture about 30 minutes and the reaction mixture was stirred for 4.5 h at -70 ^{0}C. The reaction mixture was brought to room temperature and then further stirred for 10 h. Then 1.5 N H_2SO_4 (80 mL) was added and stirred for 25 minutes. The

reaction mixture was extracted with diethyl ether (3X100 ml) and then the organic layer was dried over anhydrous Na_2SO_4. The organic layer was concentrated under reduced pressure to obtain white solid product. The crude product was chromatographed on silica gel (100-200) column using ethyl acetate as eluent to obtain the pure 1, 4-phenylenediboronic acid **113**.

1, 4-phenylenediboronic acid 113

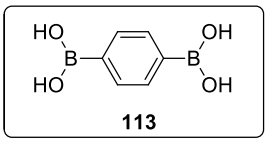

113

Yield : 2.90 g (61%);

IR (KBr) : (cm^{-1}) 3287, 1517, 1347, 1123, 1013, 800.

^{1}H NMR : (400 MHz, DMSO, δ ppm) 8.06 (s, 4H), 7.21 (s, 4H)

^{13}C NMR : (100 MHz, DMSO, δ ppm) 136.2, 133.5.

3.4.8 Purification of 4-bromopyridine 114

4-Bromopyridine hydrochloride salt (2.0 g) was dissolved in 50 mL aqueous solution of NaOH (0.008 g/mL) and the reaction mixture was stirred for 20 minutes. The organic layer was extracted with CH_2Cl_2 (3X100mL) and concentrated in vacuum to afford a pale yellow oil of 4-bromopyridine **114**.

3.4.9 Procedure for the preparation of 1, 4-dipyridylbenzene 115

4-bromopyridine **114** (0.6 mL, 6 mmol) and $Pd(PPh_3)_4$ (0.346 g , 0.3 mmol) was taken in THF solvent (40 ml) under N_2 atmosphere. Then the solution of 1,4-phenylenediboronic acid **113** (0.5 g, 3.0 mmol) and Na_2CO_3 (0.63 g, 6.0 m mol) in ethanol (5 ml) and distilled water (5 mL) was added under N_2 atmosphere. The reaction mixture was stirred under the N_2 at 80 °C for 24 h and then cooled to room temperature. The organic layer was extracted with diethyl ether and washed with brine solution. The organic layer was

separated and dried with anhydrous Na_2SO_4 and concentrated in vacuum to get a white solid 1, 4-dipyridylbenzene **115**.

1, 4-dipyridylbenzene 115

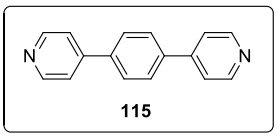

Yield : 0.35 g (52%);

IR (KBr) : (cm^{-1}) 3073, 1594, 1479, 1227, 1041, 805.

^{1}H NMR : (400 MHz, $CDCl_3$, δ ppm) 8.73-8.69 (m, 4H), 7.80-7.76 (m, 4H), 7.58-7.28 (m, 4H)

^{13}C NMR : (400 MHz, $CDCl_3$, δ ppm) 151.8, 148.7, 140.1, 129.1, 122.9.

3.4.10 Procedure for the preparation of extended viologen 116

The procedure for preparation of extended vilogen **116** is similar to the general procedure discussed in the section **3.4.6** using 1, 4-dipyridylbenzene **115** and butyl bromide**.**

4, 4'-(1,4-phenylene)bis(1-butylpyridin-1-ium) bromide 116

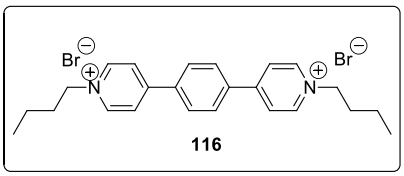

Yield : 0.22 g (86%);

IR (KBr) : (cm^{-1}) 3101, 2958, 1627, 1506, 1172, 832.

^{1}H NMR : (400 MHz, D_2O, δ ppm) 8.83-8.81 (d, 4H), 8.32-8.30 (d, 4H), 8.06-8.05 (d, 4H), 4.56-4.52 (t, 4H), 1.96-1.93 (m, 4H), 1.34-1.29 (m, 4H), 0.90-0.87 (t, 6H).

^{13}C NMR : (100 MHz, D_2O, δ ppm) 154.9, 144.3, 136.9, 129.1, 125.4, 61.0, 32.6, 18.8, 12.7.

3.5 References

1 (a) Smith, R. E.; Davis W.R. *Anal. Chem.* **1904**, *56*, 2345. (b) Chapyshev, S. V.; Ibata, T. *Mendeleev. Comm.* **1994**, *4*, 109.

2 Guin, P. S.; Das, S.; Mandal, P. C. *International journal of Electrochemistry*. **2011**, *2011*, 1.

3 a) Efremov, R. G.; Baradaran, R.; Sazanov, L. A. *Nature,* **2010**, *465*, 441. b) Nohl, H.; Jordan, W.; Youngman, R. J. *Adv. Free. Radical. Biol.* **1986**, *2*, 211.

4 Patai, S.; Rappoport, Z.; *Eds. Electrochemistry of Quinones.* Wiley: New York, **1988**, *2*, 719.

5 Suida, H. and Suida, W. *Justus Liebigs Ann. Chem.* ***1918****, 416,* 113.

6 Nogami, T.; Yoshihara, K.; Hosoya, H.; Nagakura, S. *J. Phys. Chem.* **1969**, *73*, 2670.

7 Yamaoka, T.; Nagakura, S. *Bull. Chem. Soc. Japan.* **1971**, *44*, 2971.

8 (a) Smith, R. E.; Davis W.R. *Anal. Chem.* **1904**, *56*, 2345. (b) Chapyshev, S. V.; Ibata, T. *Mendeleev. Comm.***1994**, *4*, 109.

9 Fukuzumi, S.; Kitano, T. *Chemical Physics*. **1993**, *176*, 337.

10 Ciapina, E. G.; Santini, A. O.; Weinert, P. L.; Gofardo, M. A.; Pezza, H. R.; Pezza, L. *Ecl. Quim.* **2005**, *30*, 29.

11 Sersen, F.; Koscal, S.; Banacky, P.; Krasnec, L. *Coll. Czech. Chem. Comm*. **1977**, *42*, 2173.

12 Sun, D.; Rosokha, S. V.; Kochi, J. K. *J. Phys. Chem. B.* **2007**, *111*, 6655.

13 (a) Guo, X.; Mayr, H. *J. Am. Chem. Soc.* **2014**, *136*, 11499. (b) Guo, X.; Mayr, H. *J. Am. Chem. Soc.* **2013**, *135*, 12377.

14 Ward, R. L.; Weissman, S. I. *J. Am. Chem. Soc*. **1957**, *79*, 2086.

15 (a) Rosokha, S. V.; Kochi, J. K. *J. Am. Chem. Soc*, **2007**, *129*, 3683. (b) Rosokha, S. V.; Newton, M. D.; Jalilov, A. S.; Kochi, J. K. *J. Am. Chem. Soc*. **2008**, *130*, 1944.

16 (a) Nishide, H.; Suga, T. *Electrochem. Soc. Interface. Winter*. **2005**, *14*, 32. (b) Nishide, H.; Iwasa, S.; Pu, Y-J.; Suga, T.; Nakahara, K.; Satoh, M. *Electrochimica Acta*. **2004**, *50*, 827.

17 (a) Lopez-Pena, H. A.; Hernandez-Munoz, L. S.; Frontana-Urine, B. A.; Gonzalez, F. J.; Frontana, C.; Cardoso, J. *J. Phy. Chem. B.* **2012**, *116*, 5542. (b) Guo, W.; Yin, Y-X.; Xin, S.; Guo, Y-G.; Wan, L-J. *Energy. Environ. Sci*. **2012**, *5*, 5221.

18 Li, H.; Zou, Y.; Xia, Y. *Electrochimica Acta*, **2007**, *15*, 77.

19 Nakahara, K.; Iriyama, J.; Iwasa, S.; Suguro, M.; Saton, M.; Cairns, E. J. *Journal of Power Sources.* **2007**, *165*, 398.

20 Kim, J.; Ahn, J.; Cheruvally, G.; Chauhan, G.S.; Choi, J.; Kim, D.; Ahn, H.; Lee, S.H.; Song, C. E. *Met. Mater. Int.* **2009**, *15*, 77.

21 a) Nagakura, S. *Mol. Cryst. Liq. Crtst*. **1985**, *126*, 9. b). Nogami, T.; Yamaoka, T.; Yoshihara, K.; Nagakura, S. *Bull. Chem. Soc. Japan*. **1971**, *44*, 380. c) Sato, Y.; Kinoshita, M.; Sano, M.; Akamatu, H. *Bull. Chem. Soc. Japan*. **1970**, *43*, 2370 d) Foster, R.; Thomson, J. *Trans. Faraday. Soc*. **1962**, *58*, 860.

22 a) Lu, J. M.; Rosokha, S. V.; Lindeman, S. V.; Neretin, I. S.; Kochi, J. K. *J. Am. Chem. Soc.* **2005**, *127*, 1797. b) Lu, J. M.; Rosokha, S. V.; Lindeman, S. V.; Neretin, I. S.; Kochi, J. K. *J. Am. Chem. Soc*. **2006**, *128*, 16708.

23 Soos, Z.G.; Keller, H. J.; Ludolf, K.; Queckborner, J.; Wehe, D. *J. Chem. Phys*. **1981**, *74*, 5287.

24 Blackstock, S. C.; Lorand, J. P.; Kochi, J. K. *J. Org. Chem.* **1987**, *52*, 1451.

25 Rosokha, S. V.; Neretin, I. S.; Rosokha, T. Y.; Hecht, J.; Kochi, J. K. *Heteroatom Chemistry.* **2006**, *17*, 449.

26 de Meijere, A.; Chaplinski, V.; Gerson, F.; Merstetter, P.; Haselbach, E. *J. Org. Chem*. **1999**, *64*, 6951.

27 Michaelis, L.; Hill, E. S. *J. Gen. Phisol.* **1933**, *16*, 859.

28 Yonemoto, E. H.; Saupe, G.B.; Schmehi, R. H.; Hubig, S. M.; Riley, R. L.; Iverson, B. L.; Mallouk, T.E. *J. Am. Chem. Soc.* **1994**, *116*, 4786.

29 Bird, C. L.; Kuhn, A. T.; *Chem. Soc. Rev*. **1981**, *10*, 49.

30 Porter, W.W.; Vaid, T. P. *J. Org. Chem*, **2005**, *70*, 5028.

31 Lezna, R. O.; Centeno, S. A. *Langmuir*. **1996**, *12*, 591.

32 Gratzel, M. *Acc. Chem. Res*. **1981**, *14*, 376.

33 Wang, Y.; Xu, S.; Gao, F.; Chen, Q.; Ni, B-B.; Ma,Y. *Supramolecular Chemistry.* **2013**, *25*, 344.

34 Fukui, A.; Miura, K.; Ichimiya, H.; Tsurusaki, A.; Kariya, K.; Yoshimura, T.; Ashida, A.; Fujimura, N.; Kiriya D. *AIP Advances.* **2018**, *8*, 055313-1.

35 (a) Jo, M. Y.; Ha, Y. E.; Kim, J. H. *Solar Energy Materials & Solar Cells.* **2012**, *107*, 1. (b) Do, T. T.; Hong, H. S.; Ha, Y. E.; Park, C-Y.; Kim J. H. *Macromolecular Research.* **2015**, *23*, 177.

36 Kakibe, T.; Ohno, H. *J. Mater. Chem*. **2009**, *19*, 4960, 10.

37 Esteruelas, M. A.; Fernandez, I.; Gomez-Gallego, M.; Martin-Ortiz, M.; Molina, P.; Olivan, M.; Oton, F.; Sierra, M. A.; Valencia, M. *Dalton. Trans*. **2013**, *42*, 3597.

38 (a) Bird, C. L.; Kuhn, A. T. *Chem. Soc. Rev.* **1981**, *10*, 49. (b) Lukac, S.; Harbour, J. R. *J. Am. Chem. Soc.* **1983**, *105*, 4248.

39 Johnson, C. S.; Gutowsky, H. S. *The Journ. Chem. Phy*. **1963**, *39*, 58.

Chapter 4

Development of Electrochemical cell exploiting reversible electron transfer reaction between tertiary amine donors and *p*-chloranil acceptor

4.1 Introduction

In the previous chapter, we have already discussed that electron transfer readily takes place from donor amines to acceptor quinones resulting the formation corresponding radical cation – anion pair (Scheme 1).

Scheme 1

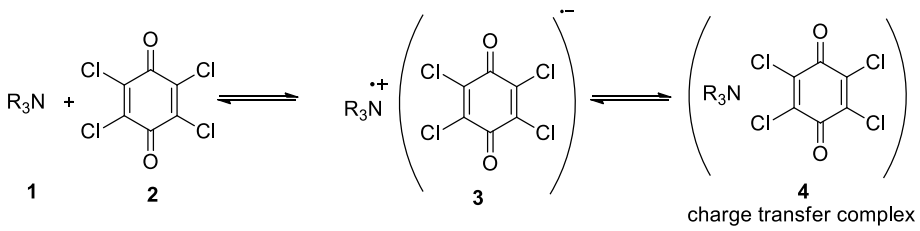

We have also observed that the reaction of tertiary amines with *p*-chloranil gives radical cation-anion pair first followed by formation charge transfer complex (CT complex) in equilibrium with the ion pair (Scheme 2). These reversible reactions take place at ambient temperature conditions in the ground state of the donor and acceptor. Accordingly, energy barrier or activation energy for the formation of the ions and ions is overcome by surrounding heat (Figure 1).

Scheme 2

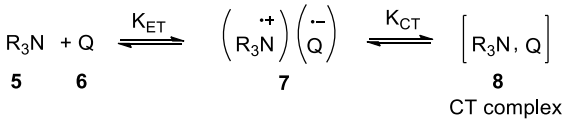

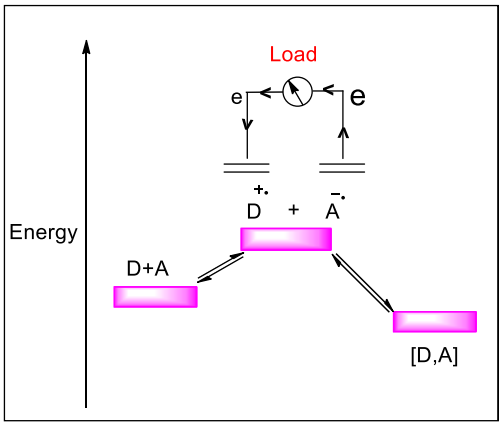

Figure 1. Ground state electron transfer between organic electron donor (D) and acceptor (A) - Construction of an electricity harvesting cell.

We have envisaged the construction of an electrochemical cell that could transport the charge carriers (i.e. electron in $Q^{-\cdot}$ and the hole in $R_3N^{+\cdot}$) formed in such reactions to produce electricity (Figure 1). The difference between such ground state electron transfer process in such cells and the electron transfer involved in donor/acceptor photovoltaic or solar cell is that in the later case the electron transfer from a donor to an acceptor takes place after photoexcitation of the electron from the ground state to excited state. Accordingly, a brief review of reports on the construction of various types of solar cells including donor/acceptor organic photovoltaic cells would facilitate the discussion of the present results.

4.1.1 Photovoltaic cell

Electrochemical cell which produce electric current through chemical reactions are called voltaic or galvanic cell. In a photovoltaic cell or solar cell, the light or solar energy is converted into electrical energy and produces an electric current in the circuit. Solar cells are made up of semiconductors which absorb light in the visible region. The research on solar cell

focused mainly on technologies involving the silicon and other inorganic semiconductors, dyes, perovskites and organic donor/acceptor molecules.

4.1.2 Silicon solar cell

Silicon (Si) solar cell consists of n-type Si and p-type Si semiconductor material. The Addition of atoms (boron or gallium) having one electron less than silicon in their outer energy level produce a p-type silicon. Addition of atoms (phosphorus or arsenic) having one electron more than silicon in their outer energy level produce an n-type silicon. When sunlight (photons) strikes the solar cell the electrons ejected from the silicon moves to the n-type layer and holes moves to the p-type layer. The produced electron and holes will move to the electrodes to produce electricity (Figure 2).

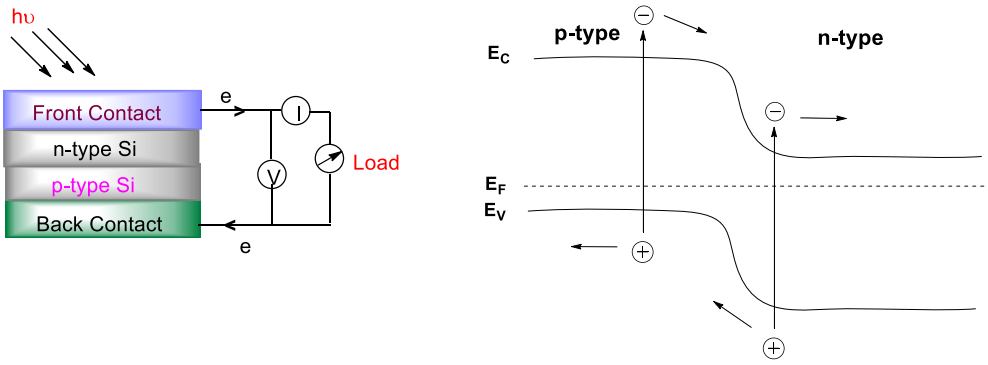

a) b)

Figure 2. (a) Schematic diagram for crystalline silicon solar cell. (b) Energy level diagram for crystalline silicon solar cell (E_V-Valance band energy level, E_F-Fermi energy level and E_C-Conduction band energy level)

In 1954, scientists in Bell laboratory produced the first practical photovoltaic cell based on silicon semiconductor material with 6% efficiency.[1] The crystalline solar cell

requires complex fabrication process and high production cost even though the efficiency of single crystal silicon solar cell reached up to 25%.[2] At present, amorphous silicon (a-Si), cadmium telluride (CdTe), copper indium gallium selenide (CIGS) and gallium arsenide (GaAs) materials are used in thin film solar cells.

4.1.3 Thin film solar cell or Inorganic solar cell

Thin film solar cells also called as second generation solar cells are made by placing one or more thin layers of photovoltaic material on glass or metal current collector.

4.1.3.1 Amorphous silicon solar cells (a-Si)

Amorphous silicon (a-Si) is an allotrope of silicon and widely used in thin film technology. The absorption of solar radiation by amorphous silicon is 40 times more than that of single crystal silicon solar cell. The thin layer of silicon is coated using a gaseous mixture of silane and hydrogen on transparent conductive oxide (TCO) glass. The basic electronic structure of amorphous silicon solar cell is p-i-n junction (Figure 3).

The efficiency of amorphous silicon solar cell is around 5-7% and lower than that of crystalline solar cell.[3] The efficiency of amorphous silicon solar cell was improved to 10% by stacking the two or more cells together with micro crystalline silicon (μ-c-Si) solar cell. This type of stacking improve the performance of the cell (Figure 3b).

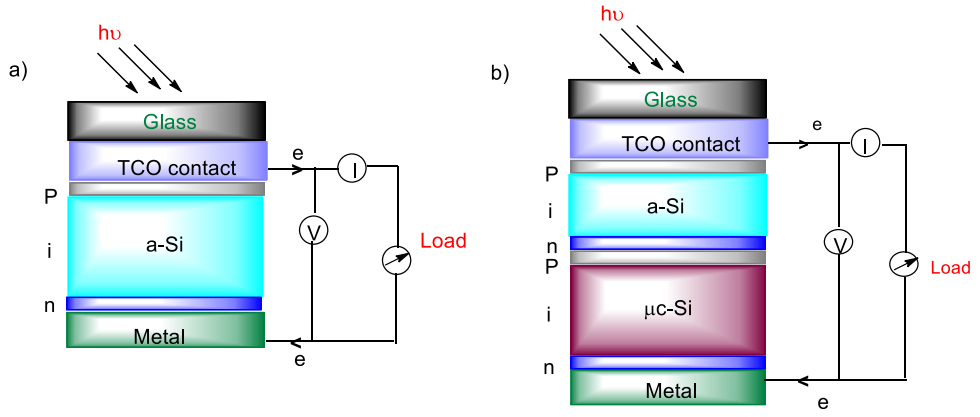

Figure 3. (a) Schematic diagram for thin film amorphous silicon solar cell. (b) Tandem a-Si and µ-c-Si solar cell.

4.1.3.2 Cadium-telluride (CdTe) thin film solar cell

This cell is a simple heterojunction contains p-type CdTe and n-type CdS semiconductors (Figure 4 a).

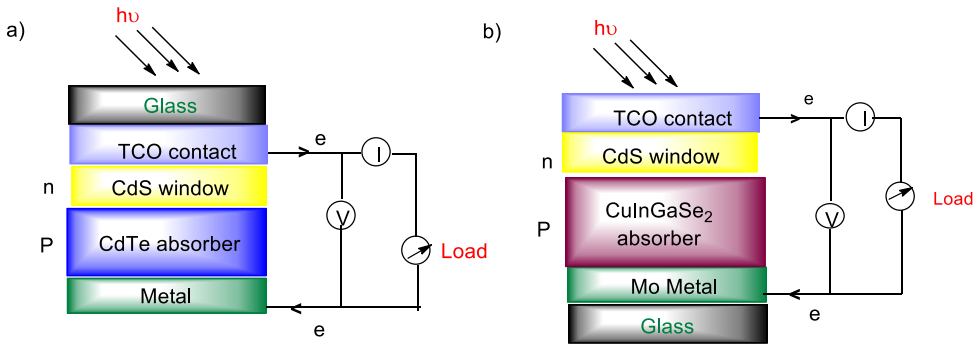

Figure 4. (a) Schematic diagram for thin film CdTe solar cell. (b) Thin film $CuInGaSe_2$ (CIGS) solar cell.

The efficiency of CdTe solar cell varies between 10-16%.[4,5] However, the rare abundance of tellurium and toxicity of cadmium are the main disadvantage of this cell.

4.1.3.3 Copper indium gallium selenide (CIGS) thin film solar cell

The fabricating process of CIGS thin film cell is similar to that of CdTe process but the light conversion efficiency is higher than that of CdTe cell (Figure 4 b). This material absorbs sunlight effectively because it has high absorption coefficient. The efficiency of CIGS solar cell was around 20% and higher than that of other thin film cell.[6]

4.1.4 Dye-sensitized solar cell (DSSC)

In 1968, Gerischer and co-workers[7] developed the electrolytic cell using the p-type perylene organic dyes and with n-type zinc oxide (ZnO). The modern DSSC was invented by O' Regan and Grätzel[8] in 1991. The use of mesoporous titanium dioxide (TiO_2) as photoanode and the electrolyte containing iodide/triiodide redox shuttle leads to the DSSC with up to 12% efficiency. The cell was further improved by the introduction of N3 (cis-Bis(isothiocyanato)-bis(2,2'-bipyridyl-4,4'-dicarboxylato ruthenium(II)) dye with efficiency of around 10%.

The DSSC was fabricated by coating TiO_2 on the conductive glass plate. Then the plates were soaked into the organic dye solution. The redox electrolyte couple was drop coated on the organic dye layer and the counter electrode was fixed above the fabricated conductive glass. When the solar radiation (light) strikes the dye molecule and it goes to excited state. The photo induced electron is injected to the conduction band of mesoporous TiO_2. The oxidized dye molecule gets regenerated by electron donation from the electrolyte I^-/I_3^- redox couple. The holes move towards the counter electrode to complete the electronic circuit (Figure 5).

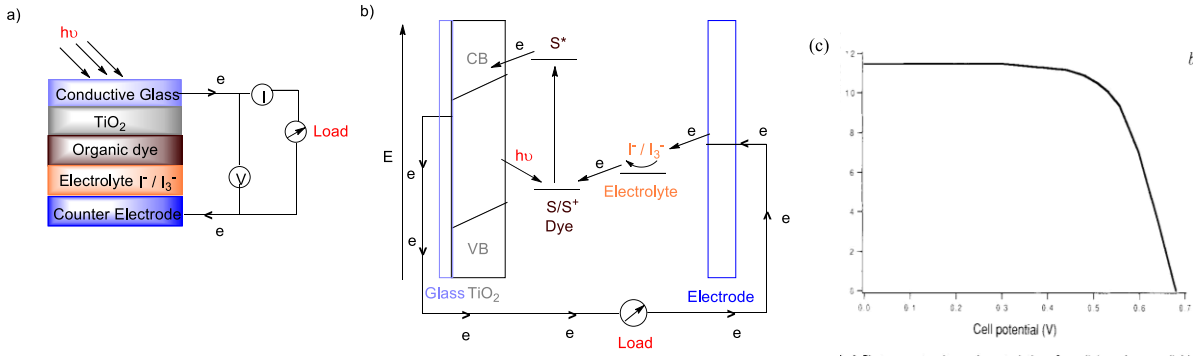

Figure 5. (a) Schematic diagram for DSSC solar cell. (b) Energy level diagram of liquid DSC based on mesoporous TiO_2 photoanode and I^-/I_3^- redox couple (c) Typical current voltage curve for DSSC (Cell efficiency = 7.12% with FF = 0.684, Reference. 8).

In last two decades research efforts were undertaken to improve the performance of DSSC by designing the organic dye molecules with high extinction coefficient and also with modified redox shuttle[9-13] like cobalt (II/III), copper (I/II), ferrocene (Fc)/ferrocinium (Fc^+), Nickel (III/IV), TEMPO/$TEMPO^+$. The redox shuttle can reduce the electron-hole recombination process with efficient electron transport properties.[14-21]

It was reported that the highest efficiency of 13% observed for the cobalt (II/III) electrolyte used in the DSSC.[22] The first solid-state dye-sensitized solar cell (sDSSC) using 2,2',7,7'-tetrakis(*N*,*N*-dimethoxyphenylamine)-9,9'-spirobifluorene (spiro-OMeTAD) as hole transporting material (HTM) was also reported. [23] The efficiency of the DSSC was improved to 7.2% by the use of spiro-OMeTAD with the addition of cobalt complex (p-type dopant).[24] The sDSSC was further improved by using other hole transporting material like poly(3-hexylthiophene-2,5-diyl) (P3HT).[25] But, the efficiency is lower than that of liquid DSSC.[26,27]

The decrease in efficiency is due to the higher recombination rate and intrinsic properties of spiro-OMeTAD with TiO_2.

4.1.5 Perovskite solar cell

The perovskite (ABX_3) is hybrid inorganic/organic material with efficient light harvesting structure. The construction of perovskite solar cell is similar to that of dye-sensitized solar cell as shown in Figure 6. In 2009, the first perovskite solar cell was reported with methylammonium lead iodide ($CH_3NH_3PbI_3$) which gave 3.81% power conversion efficiency.[28]

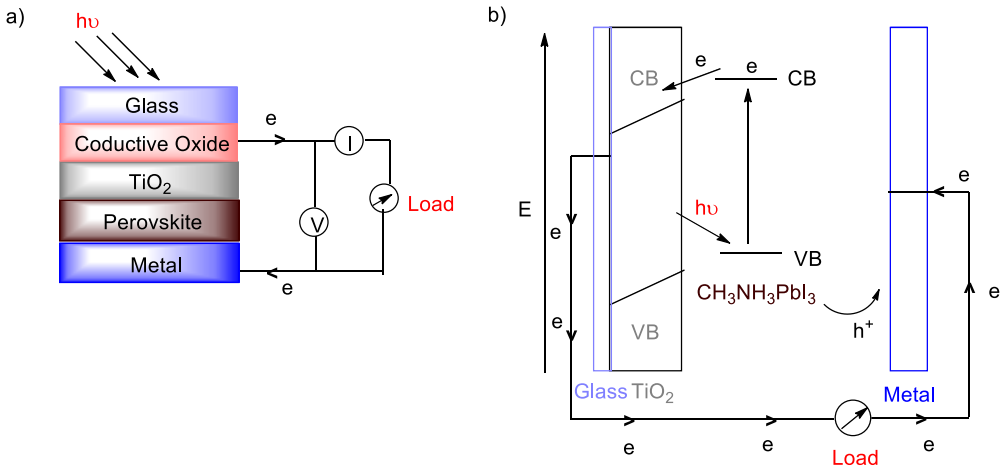

Figure 6. (a) Schematic diagram for perovskite solar cell (b) Energy level diagram of perovskite solar cell without hole transport material.

The iodide redox couple degrades the perovskite that leads to the lower efficiency. The replacement of the liquid electrolyte with solid-state p-type semiconductor spiro-OMeTAD as a hole transport material (HTM) improves the efficiency to 9.7%.[29]

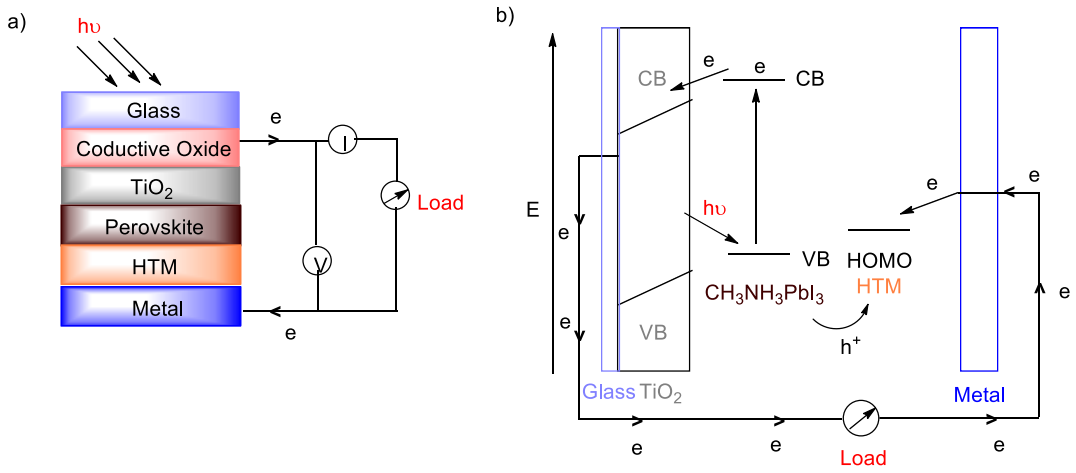

Figure 7. (a) Schematic diagram for perovskite solar cell. (b) Energy level diagram of perovskite solar cell with hole transport material.

Recent reports[30] on mixed lead halogen perovskite solar cell indicated that the efficiency was improved to 20.7%. Some of the hole transporting materials used for the studies on perovskite solar cell are listed in Figure 8. The research efforts on the perovskite solar cells are still under progress.[31-35]

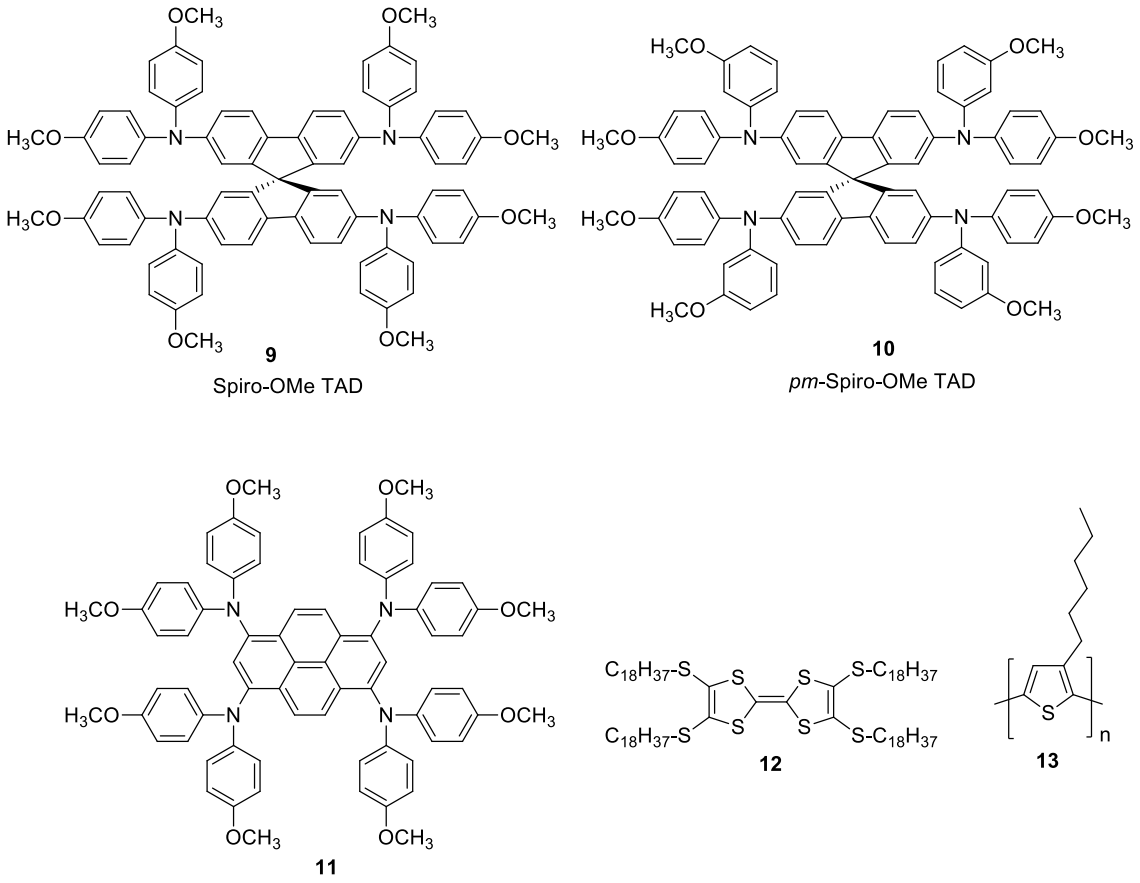

Figure 8. Hole Transporting Material (HTM) used in perovskite solar cell.

4.1.6 Organic solar cell

The organic photovoltaics or solar cells are flexible devices with low manufacturing cost compared to the rigid inorganic solar cells. In organic solar cells, upon excitation of organic material creates positive charge on the donor layer (p-type) and negative charge on the acceptor layer (n-type) like p-n junction.

The operating mechanism of the organic solar cell is almost similar to that of the inorganic solar cell. The photo excitation of the light harvesting organic material produces an exciton (coupled electron-hole pair). The field splits the exciton into the charge carrier (separated electron-hole pair) which then moves to the respective electrodes to produce

electricity. Some typical donor and acceptors used in the organic solar cells are shown in Figure 9.

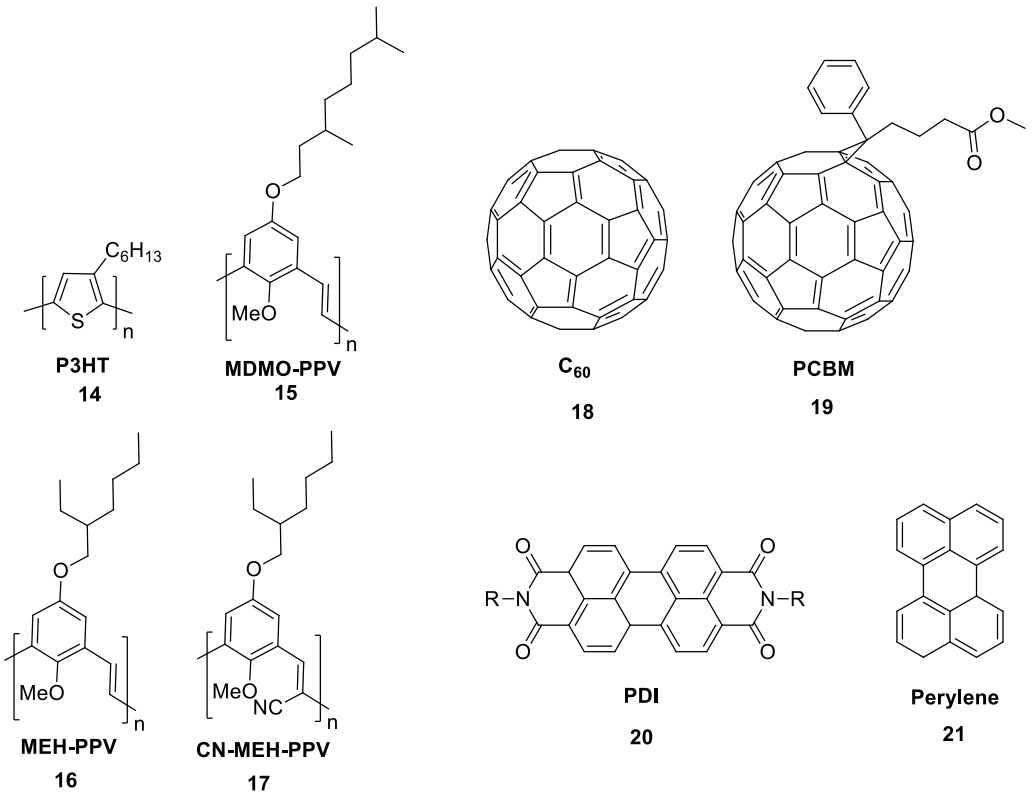

Figure 9. Major donor polymers and acceptors used in the organic solar cells.

4.1.6.1 Single layer organic solar cell

The cell was made by sandwiching an organic material between the two metal conductors having high work function such as ITO and low work function such as aluminum, magnesium or calcium (Figure 10). The organic material absorbs the light which excites the electrons to the LUMO and leaves holes in the HOMO. The potential created by the different work functions of the metals splits the exciton pair. The electrons move to the positive electrode and holes to the negative electrode. The magnesium phthalocyanine (MgPc) used in the single layer solar cell (Al/MgPc/Ag) produces 0.01% efficiency.[36]

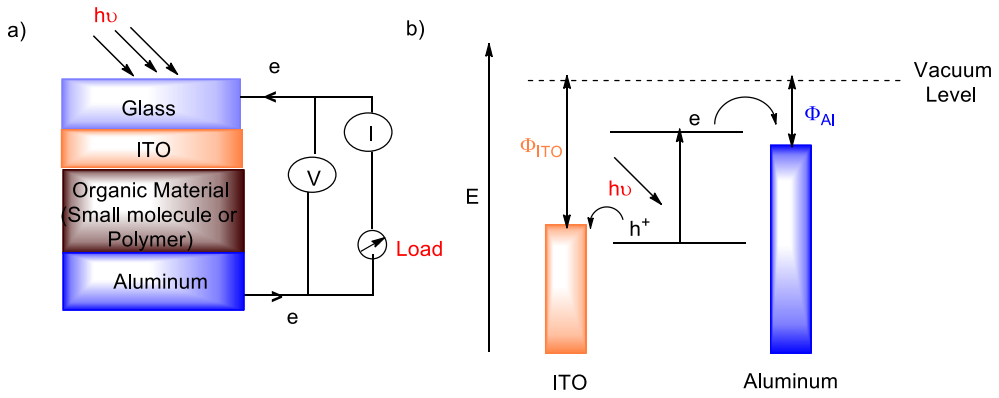

Figure 10. (a) Schematic diagram for single layer organic solar cell (b) Energy level diagram for organic solar cell.

The single layer cell using poly-3-methyl thiophene gave 0.15% power conversion efficiency.[37] Another single layer cell using the conjugated polymer polyacetylene gave 0.3% efficiency.[38] These types of cells produces low quantum efficiency (<1%) and less than 1% power conversion efficiency.

4.1.6.2 Bilayer or Planar donor-acceptor heterojunction

Bilayer cells are constructed by sandwiching two different layers contains donor and acceptor between two conductive electrodes (Figure 11 a). The difference in electron affinity and ionization energy of two layers could generate the electrostatic forces at the interface. The layers having high electron affinity and ionization energy are called as electron acceptor and electron donor, respectively. Tang *et al.* investigated copper phthalocyanine (CuPc) as an electron donor and perylene tetracarboxylic derivative as an acceptor in two layer organic cell which gave 1% power conversion efficiency.[39]

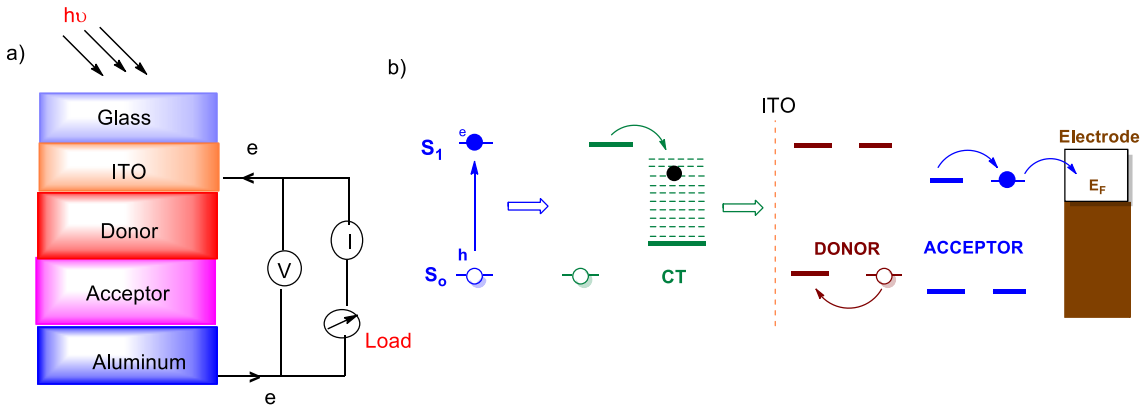

Figure 11. (a) Schematic diagram for Bilayer organic solar cell (b) Energy level diagram for bilayer organic solar cell.

Perylene amide derivatives are chemically stable and have high electron affinity. Sariciftci and co-workers reported[40] that the use of C_{60}/MEH-PPV in double layer cell gave 0.04% power conversion efficiency. Here, C_{60} acts as an acceptor and poly (2-methoxy-5-(2'-ethylhexyloxy- 1,4-phenylene-vinylene), MEH-PPV as a donor. The bilayer cell with donor polymer poly (p-phenylenevinylene), PPV and acceptor C_{60} produces around 9% power conversion efficiency. [41]

4.1.6.3 Bulk heterojunction solar cell

In organic photovoltaics the layer thickness is important for effective absorption of light. The increase of layer thickness increases the exciton diffusion pathway in the donor-acceptor interface. The exciton has shorter life time and it recombines before reaching the electrodes if thickness of the layer is more. In bulk-heterojunction cell, the exciton diffusion pathway is minimized by placing a mixture of electron donor and acceptor blend and it also increases the light absorption efficiency. The light absorbing layer of bulk heterojunction

solar cell consists a blend of donor and acceptor materials. In bulk heterojunction the donor and acceptor are mixed together and deposited over the ITO electrode (Figure 12a).

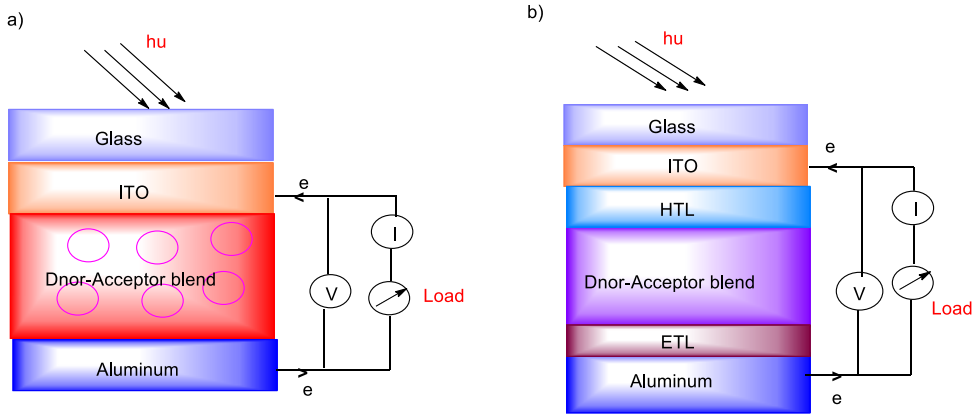

Figure 12. (a) Schematic diagram for Bulk heterojunction solar cell (b) Use of buffer HTL and ETL layers

The active layer consists of conjugated donor and fullerene based acceptor. The efficiency of polymer photovoltaic cell (single layer cell) was improved by the introduction of fullerene based derivatives in bulk heterojunction. The cell with blend polymer MEH-PPV donor and fullerene acceptor as the heterojunction was reported.[42] The device using Ca/MEH-PPV/PCBM/ITO gave 2.9% power conversion efficiency. It was reported that the introduction of poly (3-octylthiophene) P3OT in place of polymer MEH-PPV improved the quantum efficiency as well as power conversion efficiency.[43]

Recently, it was reported[44] that the higher power conversion efficiency of 11% was obtained using thiophene based PTB7-Th polymer and $PC_{71}BM$ as an acceptor. The use of donor MEH-PPV polymer and acceptor CN-PPV polymer in polymer/polymer blend heterojunction cell gave power conversion efficiency of 1% under monochromatic light.[45] It was found that the cell efficiency improved by incorporating hole conducting material such as

PEDOT:PSS.[46] The organic bulk heterojunction was further improved by sandwiching the active layer between the electron and hole transport material.[47,48]

We have decided to examine the possibility of constructing an organic electrochemical cell with ground state electron transfer using readily accessible donor amines and acceptor quinones. The radical cation - radical anion intermediates formed in the reaction could lead to generation of electric current. To construct the cell, we have chosen the readily accessible aluminum foil (Al) and stainless steel or graphite as electrodes/current collectors.

4.2 Results and Discussion

Organic charge transfer complexes and electron transfer reactions from organic donors and acceptors were known for more than 60 years.[49] In recent years, attention was turned towards mostly solid state high conductivity or superconductivity of organic charge transfer salts. For instance, the highly conductive donor-acceptor complex of TTF-TCNQ was called as organic metal.[50] Recent reports reveal that these complexes have interesting and important semiconductor properties useful in the construction of electronic devices.[51]

The charge transfer complexes formed from the donor and acceptor in solution have entirely different properties compared to that of the parent compounds. Mechanistic schemes were proposed involving the formation of charge transfer (CT) complex followed by equilibrium involving formation of radical cation and anion pairs, dissociated ions in such organic electron transfer reactions (eq. 1).[52a] The electron transfer kinetics were reconciled with an electron transfer process and formation of paramagnetic intermediates (eq. 2) without involving initial formation of a CT complex in a manner analogous to self-exchange (SE) of the $D/D^{\cdot+}$ and $A/A^{\cdot-}$ based on two state model.[52b,c] Formation of radical cation and anion pairs followed by slow formation of CT complex was also considered in polar solvent (eq. 3).[52a] The epr spectroscopic results obtained in present work (chapter 3) are in accordance with the initial formation of paramagnetic intermediates followed by formation of diamagnetic CT complexes (eq. 3).

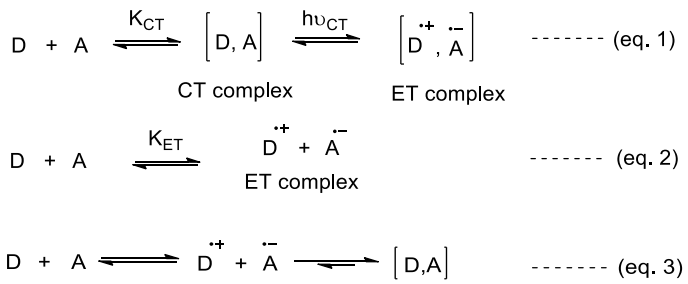

In 1966, it was reported[53] that conductometric titration could be carried out by titrating a donor solution with an acceptor and the conductivity pass through a maximum when the donor and acceptor were present in the stoichiometry required for the formation of the CT complex.

Surprisingly, there was no attempt on the development of an electrochemical device based on transport of charges in these radical cation and anion pair species to the electrodes and regenerating the donor and acceptor for further electron transfer reaction. If the electron transfer from the amine donor to the quionone acceptor could happen reversibly, then the device would be useful in converting the heat around it continuously to electricity. Therefore, we have decided to construct the electrochemical cell using *p*-chloranil acceptor with amine or amide donors.

4.2.1 Construction of donor and acceptor electrochemical cell

We have selected the readily accessible acceptor quinones and donor amines to construct the electrochemical cell which can produce electricity from the surrounding heat without using visible light (Figure 13). We have already discussed that a variety of readily accessible, inexpensive and simple tertiary amine donors react with quinone acceptors like 1,4-benzoquinone**,** *p*-chloranil**,** 1, 4-naphthoquinone and 2,3-dichloro-1,4-naphthoquinone to give paramagnetic intermediates.

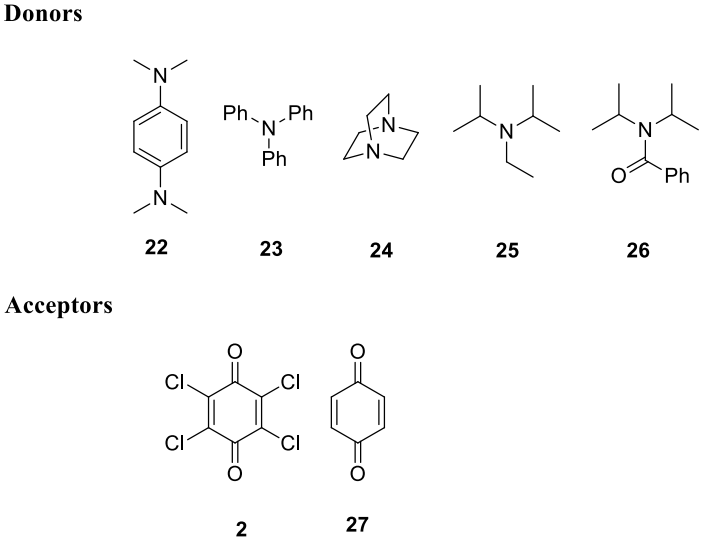

Figure 13. Donors and acceptors used in the electrochemical cell studies.

We have selected the highly electron deficient *p*-chloranil **2** as acceptor for detailed studies as it acts as an acceptor even with tertiary amides (Figure 13). Also, we have selected the donors like *N,N'*-tetramethyl-1,4-phenylenediamine (TMPDA) **22**, triphenylamine (TPA) **23**, 1,4-diazabicyclo[2.2.2]octane (DABCO) **24**, *N*, *N*-diisopropylethylamine (DIPEA) **25** and *N*,*N*-diisopropylbenzamide (DiPrBA) **26** for the construction of the electrochemical cell (Figure 13).

4.2.1.1 Two Layer Cell Configuration

After extensive experimentation, we have found that the cells can be easily constructed by making donor and acceptor pastes using TiO_2, polyethylene oxide (PEO) and propylene carbonate (PC) for coating on commercially available Al (0.2mm x 5cm x 5cm) and SS (SS 304, 0.05mm x 5cm x 5cm) foils or graphite sheet (0.4mm x 5cm x 5cm). Initially, a simple two layer cell was constructed using Al and SS foils. The mixture of TiO_2, *p*-chloranil, PC, EC and PEO was coated on Al foil and the mixture of TiO_2, amines, PC, EC and PEO was coated on SS foil. The foils were then sandwiched to construct the electrochemical cell. The configuration of this two layers electrochemical

cell is almost similar to the bi-layer in organic solar cell[54] but the electron transport would have contributions from both ionic conduction and also through exchange reactions involving $D/D^{\cdot+}$ and $A^{\cdot-}/A$ with formation of corresponding charge transfer complexes (CT 1, CT 2 and CT 3). The current (I) and voltage (V) characteristics observed for the cells using different amines are summarized in the experimental section in Table ES1 (ES: Experimental Section), entries 1-3.

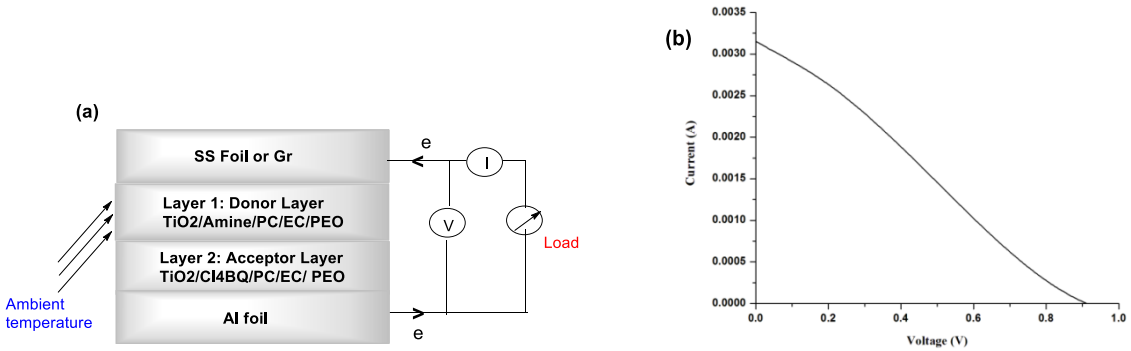

At 28^{0}C, With SS Foil Cathode

DIPEA	Pmax=0.756mW/FF=0.263
DABCO	Pmax=0.665mW/FF=0.233
TPA	Pmax=0.306mW/FF=0.254

With Graphite Cathode:

DIPEA	Pmax=1.415mW/FF=0.235
DABCO	Pmax=0.139mW/FF=0.194
TPA	Pmax=0.794mW/FF=0.240

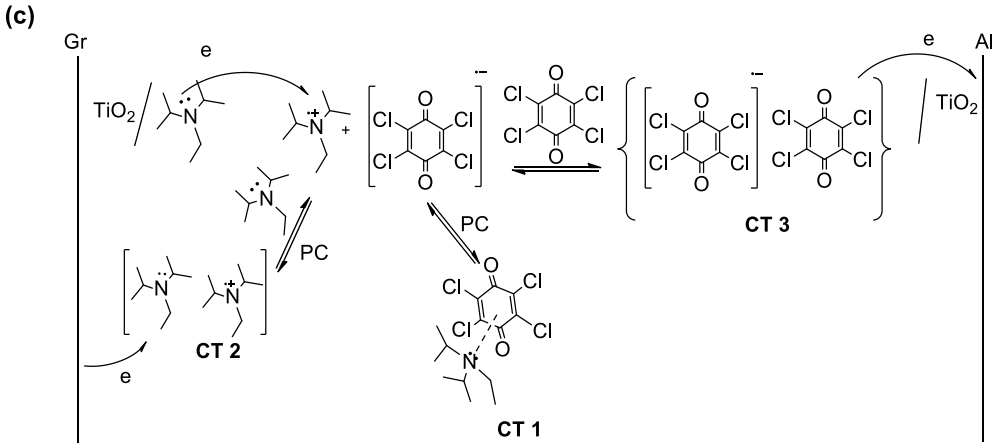

Figure 14. (a) Schematic diagram of cell with two layer configuration (b) Representative IV curve for the two layer cell (Table ES1, entry 1, DIPEA donor). (c) Tentative mechanism for electron transport via $D/D^{\cdot+}$ and $A^{\cdot-}/A$ exchange reactions.

The representative IV curve for this cell is shown in Figure 14b for the cell in (Pmax = 0.756 mW, FF=0.263). Similarly, the cells prepared using amines DABCO and TPA with *p*-chloranil gave power output of 0.665 mW with FF=0.233 and 0.306 mW with FF=0.254, respectively.

However, visible holes were formed on the SS foil indicating corrosion, probably due to the formation of Fe^{2+}-amine species by the reaction of SS foil with the amine radical cation present in the reaction mixture. We then constructed the cell with similar configuration using Al foil (0.2mm x 5cm x 5cm) anode and graphite (0.4mm x 5cm x 5cm) cathode. The results obtained are summarized in the experimental section in Table ES1, entries 4-6. The cells constructed did produce power in these cases (Table ES1, Figure 14), but there was only very little or no power output after 24 h. A possibility is that ionic conduction may lead to the deposition of the radical ion pairs on the respective electrodes which may not dissolve back into the solution preventing reversible equilibrium necessary for continued power generation. Also, the formation of amine-*p*-chloranil CT complex to more extent may lead to reduction in power output, especially if this complex precipitates out of the PC solution.

4.2.1.2 Multi-layer cell configuration

We have then decided to construct multi-layer cell to improve the performance of the cell. Recently, there were several reports[55-61] that the stability of the solar cells improved by coating additional buffer layers or electrode interfacial layer using metal oxides like TiO_2.

Accordingly, we have constructed the cells in two different configurations (Figure 15a and 15b) by coating TiO_2/PEO on both electrodes, followed by coating of Cl_4BQ/PEO on TiO_2/PEO/Al and TiO_2/PEO/Gr. Then, the Cl_4BQ/Amine/PC/PEO (Figure 15a) or

Cl_4BQ/Amine/PC/TiO_2/PEO pastes (Figure 15b) coated above the Cl_4BQ/PEO layers. The results are summarized in Table ES2, entries 1-10.

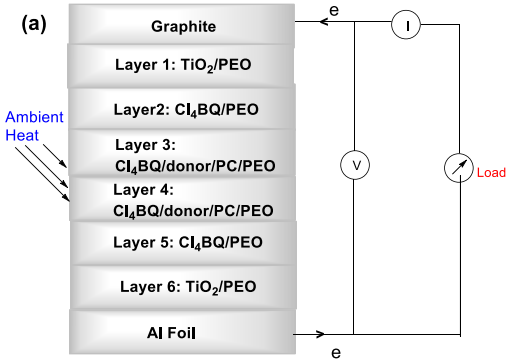

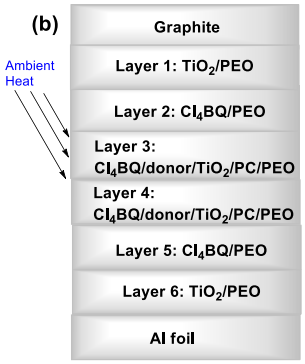

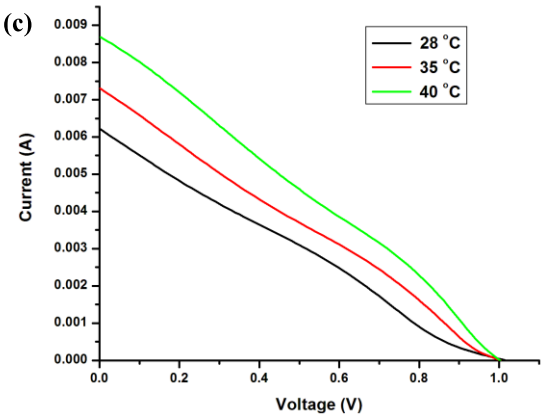

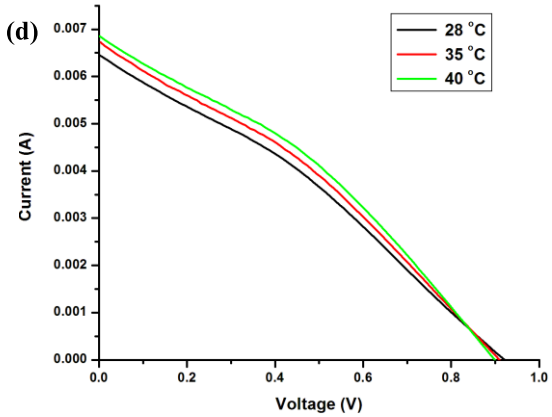

1 h after packing

Donor	**Pmax/mW/FF(40 °C)**	**Donor**	**Pmax/mW/FF(40 °C)**
TMPDA	1.469/0.221	TMPDA	3.099/0.261
TPA	1.333/0.255	TPA	0.375/0.245
DABCO	5.492/0.313	DABCO	6.155/0.206
DIPEA	5.695 /0.296	DIPEA	8.147/0.347
DiPrBA	2.198/0.260	DiPrBA	4.193/0.295

48 h after packing

Donor	**Pmax/mW/FF(40 °C)**	**Donor**	**Pmax mW/FF(40°C)**
TMPDA	0.790/0.309	TMPDA	1.822/0.250
TPA	0.428/0.285	TPA	0.142/0.256
DABCO	**2.320/0.267**	DABCO	1.216/0.249
DIPEA	2.228 /0.347	**DIPEA**	**2.057/0.334**
DiPrBA	1.047/0.261 (35 °C)	DiPrBA	2.969/0.273

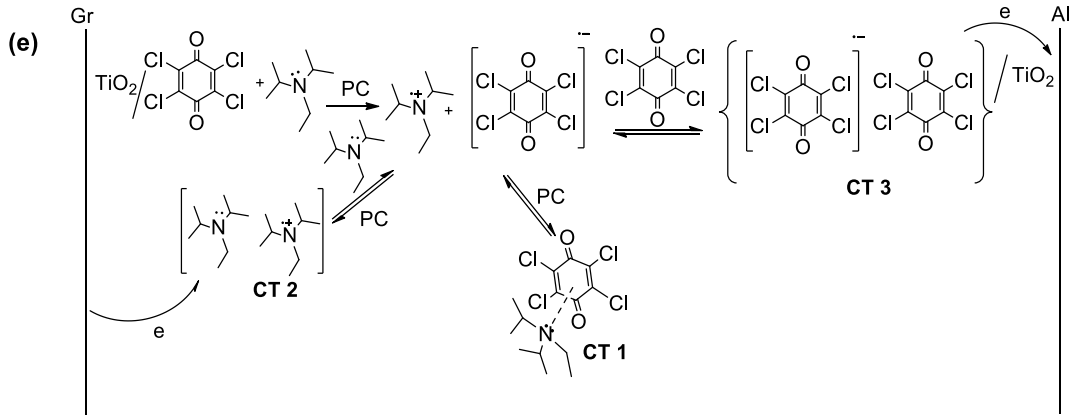

Figure 15. (a) Schematic diagram of multi-layer with Cl_4BQ/donor/PC/PEO configuration and (b) Schematic diagram of multi-layer with Cl_4BQ/donor/PC/TiO_2/ PEO configuration (c) Representative IV curve for the cell (Table ES2, entry 3, DABCO donor) after 48 h packing (d) Representative IV curve for the cell (Table ES2, entry 9, DIPEA donor) after 48 h packing (e) Tentative mechanism for electron transport to the electrodes via D/D.+ and A-/A exchange reactions.

The IV-data were recorded after 1 h and 48 h after packing. The higher power outputs (Pmax) were observed 1 h after packing compared to that observed after 48 h. Presumably, the power output becomes less as the initially formed amine radical cations and *p*-chloranil anions are converted to the corresponding charge transfer complex (CT 1) (Figure 15e). The complexes CT 2 and CT 3 may also contribute to the conduction. The data for the cells with similar configuration with additional TiO_2 in PC layer (Figure 15b) are summarized in Table ES2, entries 6-10.

The data (Table ES2) indicate that increase in the temperature of the cell (from 28 °C to 40 °C) increases the power output due to increase in the rate of electron transfer between the donor-acceptor and also dissociation of formed charge transfer complexes into radical ion pairs. Also, the increase in temperature would help in crossing the activation energy barrier for transport of ions to the electrodes and hence would improve the conductance.

The TiO_2 rutile and TiO_2 and anatase were reported to have very high electron affinities of 4.8eV and 5.1eV, respectively.[62a,b] It was also reported that the TiO_2 surface could donate or accept electrons depending on the nature of the adsorbed molecules.[62c] Accordingly, it was of interest to us to examine whether the donors used in the cell experiments could produce power by interaction with TiO_2 without using *p*-chloranil. Indeed, this was observed and diisopropylbenzamide gave slightly higher power upon interaction with TiO_2 (Figure 16). Presumably, the interactions outlined in Figure 16c may also play a role in the reaction and transport of charge carriers using *p*-chloranil.

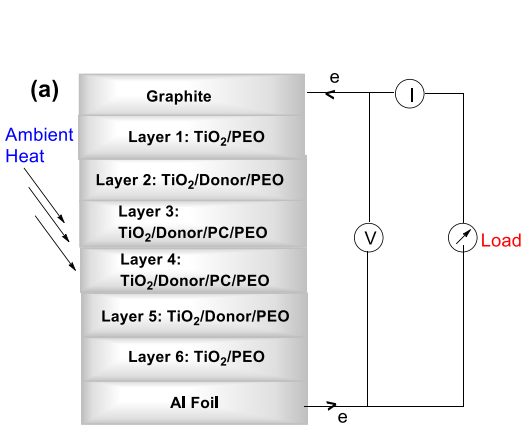

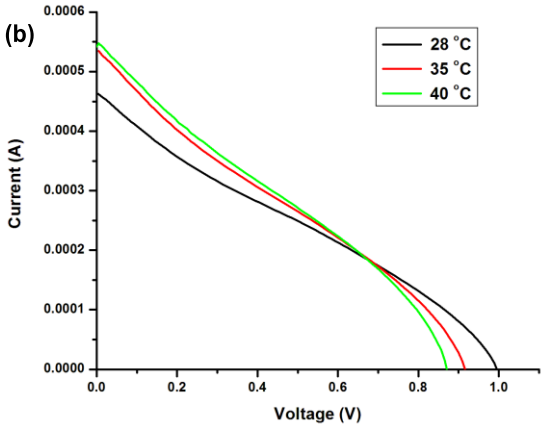

1 h after packing

Donor	**Pmax/mW/FF(40°C)**
TPA	0.004/0.270
DABCO	0.026/0.092
DIPEA	0.005/0.281
DiPrBA	0.235/0.283

48 h after packing

Donor	**Pmax/mW/FF(40°C)**
TPA	0.003/0.287
DABCO	0.019/0.136
DIPEA	0.005/0.305
DiPrBA	**0.136/0.289**

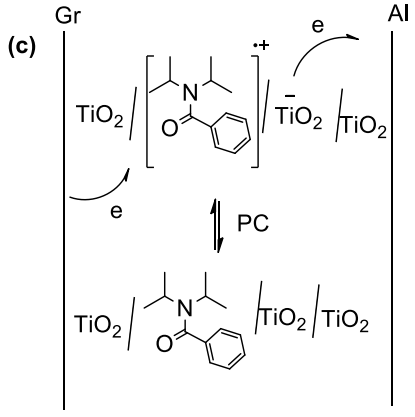

Figure 16. (a) Schematic diagram of multi-layer cell with TiO_2/donor without Cl_4BQ (b) Representative IV curve for the cell (Table ES3, entry 4, DiPrBA donor) (c) Tentative mechanism for electron transport.

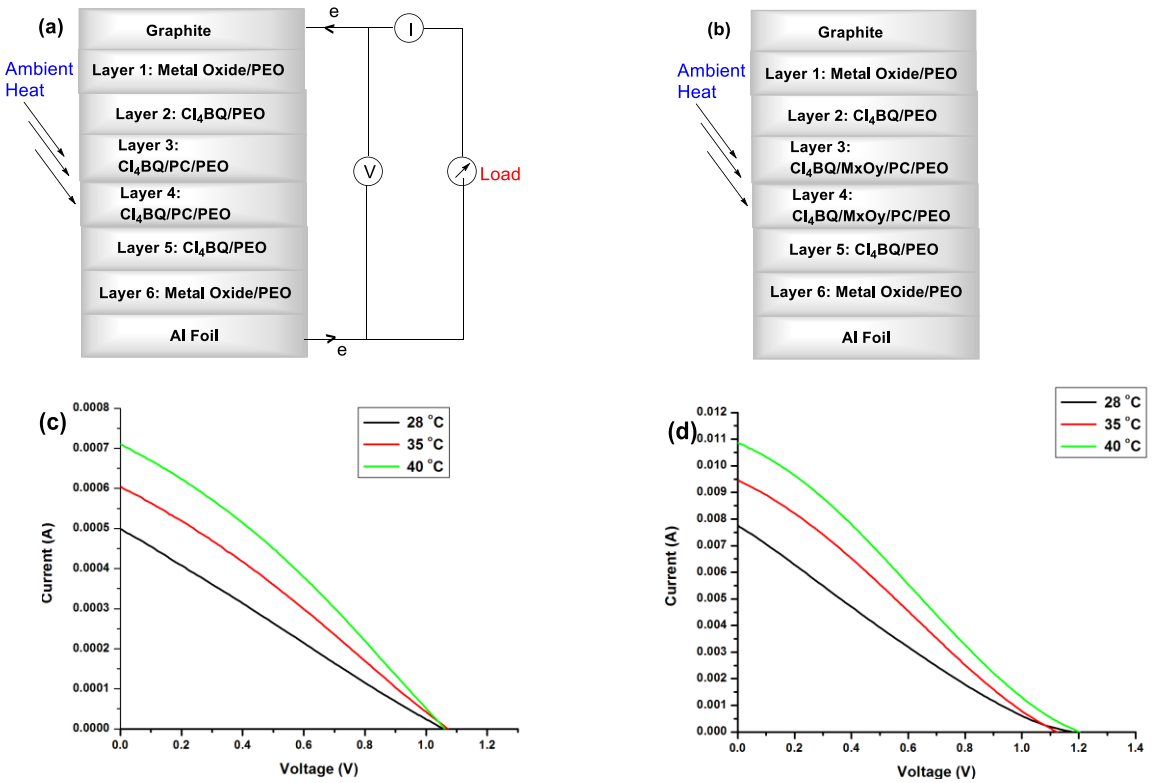

1 h after packing

MxOy	**Pmax/MW/FF(40 °C)**
TiO_2	1.181/0.270
ZnO	0.492/0.266
Al_2O_3	1.276/0.206

1 h after packing

MxOy	**Pmax/mW/FF(40 °C)**
TiO_2	3.639/0.261
ZnO	0.584/0.227
Al_2O_3	0.848/0.233

48 h after packing

MxOy	**Pmax/MW/FF(40 °C)**
TiO_2	**0.228/0.303**
ZnO	0.272/0.260
Al_2O_3	1.049/0.203

48 h after packing

MxOy	**Pmax/mW/FF(40 °C)**
TiO_2	**3.376/0.258**
ZnO	0.366/0.195
Al_2O_3	1.226/0.286

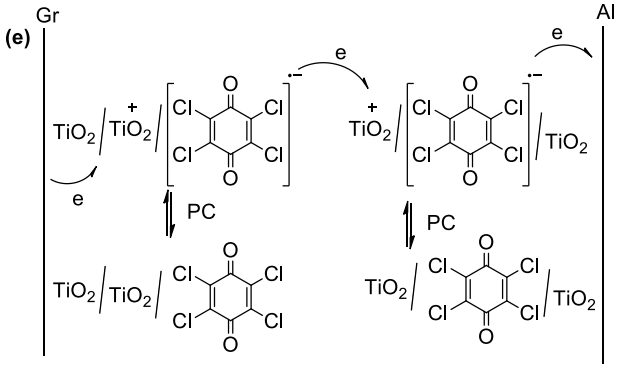

Figure 17. (a) Schematic diagram of multi-layer cell with metal oxide in edge layers (b) multi-layer cell with metal oxide in edge layers and also in PC layer (c) Representative IV curve for the cell (Table ES4, entry 1, TiO_2 donor) (d) Representative IV curve for the cell (Table ES4, entry 4, TiO_2 donor) (e) Tentative mechanism for electron transport.

Previously, there were also reports on the formation paramagnetic intermediates when *p*-chloranil was adsorbed on the surface of TiO_2.[63] Such intermediates may play a role in the electron transport at the interfaces, thus improving the performance of the device. The TiO_2 sample used in the present studies did not give paramagnetic species with *p*-chloranil. However, we have also constructed the cell without using other donors. Interestingly, the cells constructed using the metal oxides TiO_2, Al_2O_3 and ZnO in the configurations shown in Figure 17a and 17b without using donor amines or amide did produce power with TiO_2 giving higher power when it is present in the middle PC layers (Figure 17b). The results indicate that the metal oxides transfer electron to *p*-chloranil as visualized in Figure 17e. This may also play a role in the transport of charges in the cells using donors.

We have observed that in the cells constructed using different donors and *p*-chloranil acceptor (Figure 15 and Figure 17), the power output decreases with time. Possibly, the chloranil radical anion may get deposited on the Al electrode and the *p*-chloranil may not fully dissolve back in the PC solvent (only 0.03 g *p*-chloranil soluble in 1 mL PC), thus preventing the reversible formation of amine or amide radical cation and *p*-chloranil radical anion.

The *p*-chloranil has a very high electron affinity (EA) of 2.78eV.[64] Interestingly, it was reported that anion radicals of molecules with lower electron affinity are solvated to more extent.[64a] Therefore, we have carried out experiments using *p*-benzoquinone (BQ) which has lower electron affinity (EA=1.91eV) to examine whether the chloranil anion radical can transfer electron to BQ to form the corresponding radical anion for further electron transport to the Al electrode. Also, the BQ is more soluble in PC solvent (0.1 g BQ soluble in 1 mL PC) which may be also helpful. We have carried out experiments by

constructing the cell in two different configurations, Figure 18a and 18b. Some improvements were observed in the power outputs, but still the Pmax values decreased with time (Figure 18a and 18b). Presumably, the more soluble BQ accepts electrons from *p*-chloranil anion radical effectively for transporting to the Al electrode improving the power output to some extent. The results of cells 18a and 18b are summarized in Table ES 5, entries 1-10.

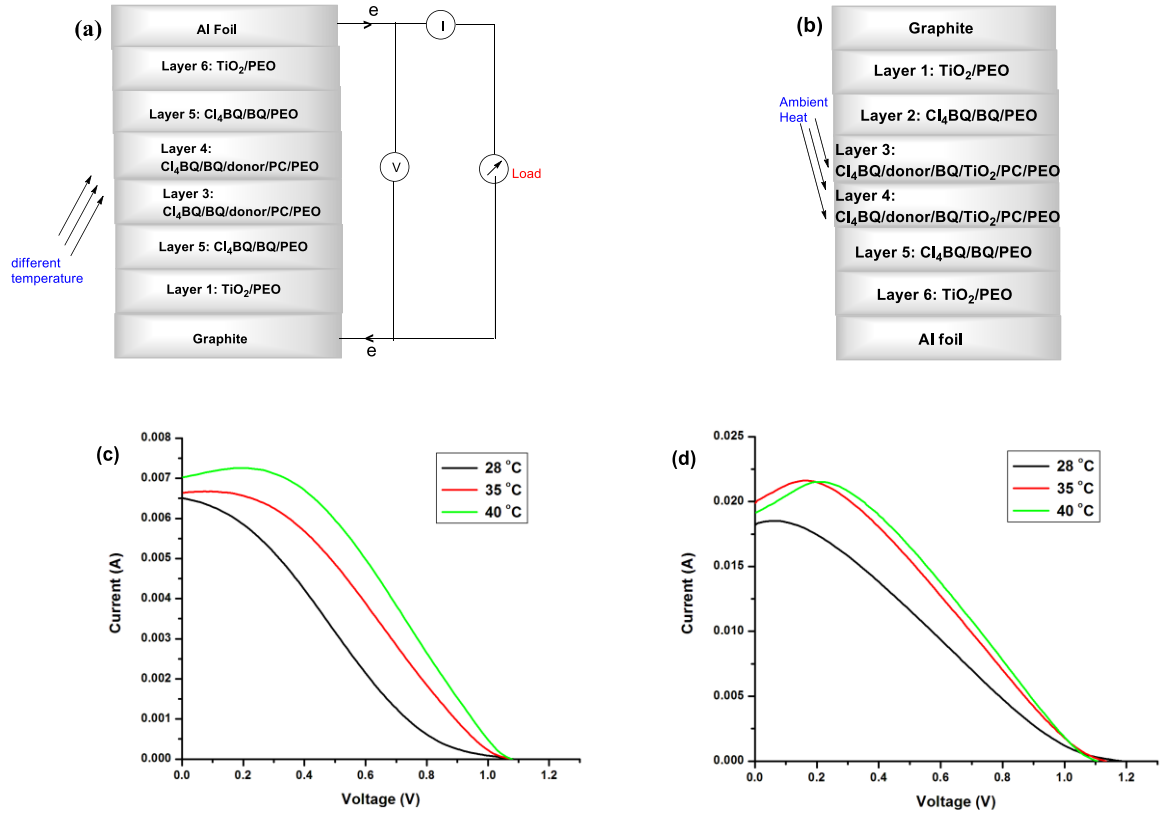

1 h after packing

Donor	**Pmax(mW)/FF(40 °C)**	**Donor**	**Pmax(mW)/FF(40 °C)**
TMPDA	2.175/0.276	TMPDA	1.614/0.282
TPA	1.752/0.240	TPA	0.939/0.219
DABCO	5.391/0.391	DABCO	4.806/0.432
DIPEA	8.229/0.229	DIPEA	11.74/0.296
DiPrBA	1.714/0.243	DiPrBA	1.871/0.232

48 h after packing

Donor	**Pmax(mW)/FF(40 °C)**	**Donor**	**Pmax(mW)/FF(40 °C)**
TMPDA	1.205/0.273	TMPDA	1.299/0.263
TPA	1.216/0.240	TPA	0.728/0.219
DABCO	**3.023/0.399**	DABCO	3.776/0.434
DIPEA	2.074/0.231	**DIPEA**	**8.338/0.394**
DiPrBA	1.534/0.258	DiPrBA	1.411/0.243

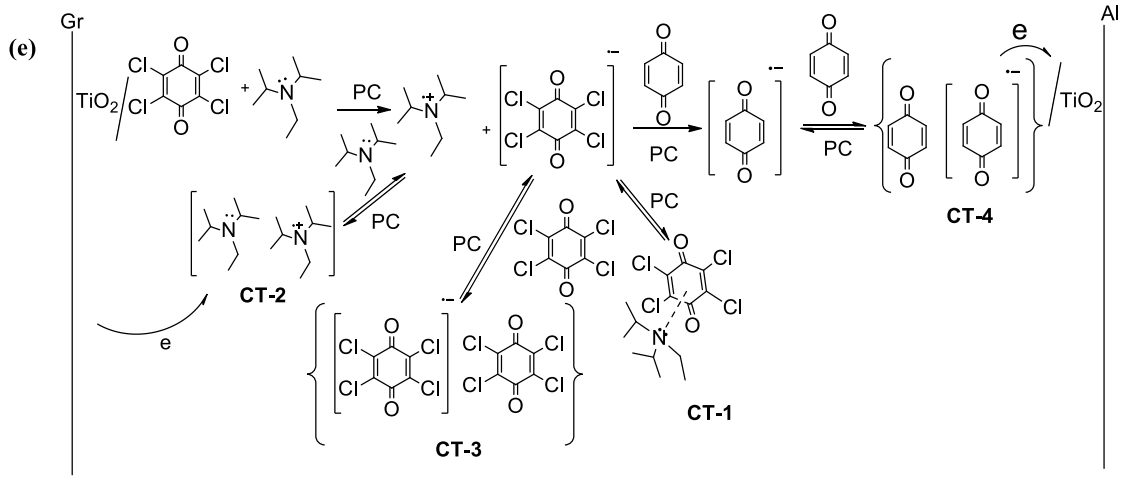

Figure 18. (a) Schematic diagrams of multi-layer cell using BQ along with *p*-chloranil without TiO_2 in PC layer (b) multilayer cell using BQ along with *p*-chloranil with TiO_2 in PC layer (c) Representative IV curve for the cell (Table ES5, entry 3, DABCO donor) and (d) Representative IV curve for the cells (Table ES5, entry 9, DIPEA donor) (e) Tentative mechanism for electron transport to the electrodes via D/D.+ and A-/A exchange reactions.

As discussed in Chapter 3, epr spectral studies indicated that the radical ions are transformed to charge transfer complexes with time. This could account for the reduction of current and Pmax values with time as the concentration of radical ions would be lesser with time. One way to prevent the formation of such charge transfer complexes is to remove the charges from the radical ions by using the cells to charge a rechargeable battery. The results obtained on the performance of the cells while charging a rechargeable Ni-Cd battery is summarized in Table 1.

The performance of the cells with configurations as in Figures 18a and 18b using BQ improved when the cells were used for charging batteries (Table 1, entries 3 and 4)

compared to cells with configurations without using BQ (Figures 15a and 15b, Table 1, entries 1 and 2) indicating that the BQ may transport the electron from the *p*-chloranil radical anion as it is formed thus preventing the formation of the corresponding CT complex which otherwise would reduce the concentration of radical ions with time. The electron acceptor BQ would accept electron from the *p*-chloranil radical anion as the corresponding anion radical formed from these compounds with lower EA are expected to interact with solvents to more extent, preventing the formation of CT complex. In case of DABCO (Table 1, entry 5) there was not much power output was observed. This may be due to the formation of stronger charge transfer complex with *p*-chloranil thus preventing the reversible reaction for charge transport. The donor DIPEA gives higher power output for longer time in these configurations compared to other donors. This may be due to the formation of more amount of radical ion pairs in case reaction of DIPEA with *p*-chloranil as revealed by epr spectroscopic studies. Further, it is sterically hindered and hence formation of CT 1 complex may be also difficult.

Table 1. Performance of Cells by Charging Ni-Cd Battery after packing.[a]

entry	Figure/Donor	Pmax/mW/FF at 40 °C/1 h	Pmax/mW/FF at 40 °C/48 h	Pmax/mW/FF at 40 °C/144 h
1[b]	15(a)/DIPEA	8.988/0.300	2.893/0.473	1.738/0.391
2[b]	15(b)/DIPEA/TiO_2	7.626/0.286	2.911/0.437	2.027/0.366
3[c]	18(a)/DIPEA/BQ	17.49/0.189	13.46/0.239	14.57/0.260
4[c]	18(b)/DIPEA/BQ/TiO_2	13.21/0.172	12.77/0.270	10.65/0.277
5[c]	18(b)/DABCO/BQ/TiO_2	4.022/0.413	2.733/0.316	1.291/0.160
6[c]	18(b)/TMPDA/BQ/TiO_2	1.883/0.279	0.620/0.249	0.373/0.248
7[c]	18(b)/TPA/BQ/TiO_2	0.985/0.255	0.855/0.231	0.698/0.218
8[c]	18(b)/DiPrBA/BQ/TiO_2	2.606/0.238	1.660/0.234	0.592/0.223

[a]After packing the cell was connected immediately to charge a Ni-Cd battery through Zener diode and disconnected while carrying out the IV-curve measurement (Table ES6 and ES7). The battery connection was removed from the cell after 48 h. [b]Configuration without BQ. [c]Configuration with BQ.

Also, charging the rechargeable battery would lead to removal of charges from the radical ions, resulting in the recycling of the neutral species for continuous reactions. The donors TMPDA, TPA and DiPrBA which are relatively weak donors and also produce lower power output as concentration of radical ion formed may also be lower (Table 1, entries 6, 7 and 8).

In recent years, there have been several reports on the conversion of low-grade waste heat (<130 $^{\circ}$C) to electricity by thermally regenerative electrochemical cycles.[65a,b] A thermoelectrochemical device based on ferrocene-iodine redox couple was also reported, but the device produced only $\mu W/m^2$ power with respect to the electrode surface area.[65c] The power density of the cell in this case was calculated by using the amount of power produced with respect to the electrode surface area. The cell constructed from the donor DIPEA (Table 1, entry 3) gave power density at 40 °C was 0.5384 mW/cm^2 or 5.384 W/m^2 (13.46 mW (Pmax)/25 cm^2 (electrode surface area)). The methods reported in the literature for construction of the devices are very complex compared to methods described here. In the present case, the device utilizes very inexpensive materials that are already manufactured in large scale. Further, since there are established methods are available for heating air at even below 0 $^{\circ}$C to 40 $^{\circ}$C using solar radiation and methods available for storing solar heat in simple chemicals like aq. NaOH, $CaCl_2$ and methods are also available for using these solar heat stored materials for heating the air to 40 $^{\circ}$C to 60 $^{\circ}$C,[66] the present low/ambient heat harvesting electricity producing cell device has potential for use 24x7 in all seasons, day and night.

4.3 Conclusions

We have developed a simple method and device for constructing the electrochemical cell based on ground state electron transfer reaction of amine or amide donor and *p*-chloranil acceptor in various configurations. These low/ambient heat harvesting electricity producing and air cooling cells can be readily stacked.

The present case, the device utilizes very inexpensive materials and hence has potential for household, automobile and large scale applications. However, long term performance of this cell device remains to be established and there is plenty of scope for further research and developments to improve the performance of this device. Accordingly, the low/ambient heat to electricity converting electrochemical system disclosed here has the potential to meet the increasing energy requirements without having to burn fossil fuels. Systematic studies are required for improving the stability of the cells with different electron donors, acceptors and electron transporters. Additional studies may be also required for studies on corrosion of electrodes by radical ions formed.

4.4 Experimental Section

4.4.1 General Information

P-Chloranil, N, N-diisopropylethylamine (DIPEA), 1,4-diazabicyclo[2.2.2]octane (DABCO), *P*-benzoquinone (BQ),and TiO_2 were purchased from Avra chemicals (India). Triphenylamine (TPA), *N,N'*-tetramethyl-1,4-phenylenediamine (TMPD), propylene carbonate (PC), ethylene carbonate (EC) and polyethylene oxide (PEO) were purchased from Sigma Aldrich. Netural alumina (Al_2O_3) was purchased from SRL chemicals, India. Zinc oxide (ZnO) was purchased from E-Merck, India. The metal oxides were heated at 150 °C in a vacuum oven for 2 h before use. PC and EC were always kept under molecular sieves. *N, N*-diisopropylbenzamide was prepared from the literature procedure. Graphite sheet (0.4mm thickness, 5cm x 5cm, Resistivity, $\rho = 2x10^{-4}\Omega.m$) was purchased from Falcon Graphite Industries, Hyderabad, India. Aluminium Foil (0.2mm thickness, 5cm x 5cm, Resistivity, $\rho = 2x10^{-5}\Omega.m$) and Stainless steel (0.4mm thickness, 5cm x 5cm, Resistivity, $\rho = 5x10^{-4}\Omega.m$) were purchased from Aluminium Enterprises and Rasik Metals, Hyderabad, India. EPR spectra was recorded on a Bruker-ER073 instrument equipped with an EMX micro X source for X band measurement using Xenon 1.1b.60 software provided by the manufacturer. Electrical measurements were carried out by ZAHNER instrument using CIMPS software. The current-voltage curve was drawn using Origin software.

4.4.2 Procedure for preparation of diisopropyl benzamide

In an oven dried RB flask, the diisopropyl amine (20 mmol) in dry dichloromethane (60 mL) solvent was taken and triethylamine (2.1 mL, 21 mmol) was added slowly at room temperature with constant stirring. Then the reaction mixture was stirred for 1 h and corresponding benzoyl chloride (20 mmol) was added at 0^{o} C. Then the reaction mixture was brought to room temperature and it stirred for 8 h. The mixture was quenched with saturated ammonium chloride solution and the organic layer was separated. The organic layer was extracted with dichloromethane (2x50 mL). The combined organic extracts were washed with saturated NaCl solution (15 mL) and dried over anhydrous Na_2SO_4. Then the solvent was evaporated to get the crude product. The corresponding crude amide product was purified by column chromatography on silica gel (100-200) using hexane and ethyl acetate as eluent to isolate pure amide product.

***N, N*-diisopropylbenzamide**

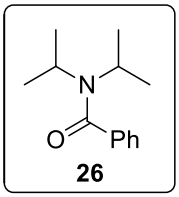

26

Yield : 3.48 g (85%).

IR (neat) :(cm^{-1}) 2970, 2937, 1627, 1446, 1342, 1222, 1156, 1041, 739.

^{1}H NMR :(400 MHz, $CDCl_3$, δ ppm): 7.36 (m, 3H), 7.31 (m, 2H), 3.75 (s, 2H), 1.35 (s, 12H).

^{13}C NMR :(100 MHz, $CDCl_3$, δ ppm) 171.0, 138.9, 128.5, 128.4, 125.5, 50.8, 45.7, 20.7.

4.4.3 Preparation of Electrochemical Cells

Simple solution processing and casting techniques were followed for the construction of the cell device.

Table ES1. Cell Configuration 1

The PEO (0.2 g) was dissolved in dichloromethane and mixed with TiO_2 (1 g) powder. DCM was removed to obtain a paste. The *p*-chloranil (0.5 g), PC (0.5 g) and EC (0.5 g) were added to the above made paste and it was cast over the Al (0.2mm thickness, 5x5 cm^2). The layer was dried in air at room temperature overnight. Similarly, PEO (0.2 g), TiO_2 (1 g) powder, donor amine (2 mmol), PC (0.5 g) and EC (0.5 g) were mixed and cast above SS (0.05 mm thickness, 5x5 cm^2) or Graphite (0.4 mm thickness, 5x5 cm^2). The layer was dried in air at room temperature overnight. The cell was prepared by sandwiching the coated Al/SS or Al/Gr layers. The rim of the cell prepared in this way was sealed all around using TiO_2/PEO paste, then with commercial adhesive Bondfix (India) and covered with cellophane tape.

Table ES2. Cell Configuration 2

The PEO (0.05 g) was dissolved in dichloromethane and mixed with TiO_2 (0.5 g) powder. DCM was removed to obtain a paste for coating on Al or Graphite foils. After 1 h, Cl_4BQ (0.1 g)/PEO (0.05 g) in DCM was coated on TiO_2/PEO/Al and TiO_2/PEO/Gr and dried. The Cl_4BQ (0.025 g)/donor (0.1g) /PC (0.5 g)/PEO (0.05 g) slurry was prepared and casted above the coated layer on Al and Graphite and dried in air at room temperature overnight. The cell was prepared by sandwiching the coated Al/Gr layers. The rim of the cell

prepared in this way was sealed all around using TiO_2/PEO paste, then with commercial adhesive Bondfix (India) and covered with cellophane tape.

Table ES2. Cell Configuration 3

The PEO (0.05 g) was dissolved in dichloromethane and mixed with TiO_2 (0.5 g) powder. DCM was removed to obtain a paste for coating on Al or Graphite foils. After 1 h, Cl_4BQ (0.1 g)/PEO (0.05 g) in DCM was coated on TiO_2/PEO/Al and TiO_2/PEO/Gr and dried. The Cl_4BQ (0.025 g)/donor (1 mmol)/PC (0.5 g)/TiO_2 (0.25 g)/PEO (0.05 g) slurry was prepared and casted above the coated layer on Al and Graphite and dried in air at room temperature overnight. The cell was prepared by sandwiching the coated Al/Gr layers. The rim of the cell prepared in this way was sealed all around using TiO_2/PEO paste, then with commercial adhesive Bondfix (India) and covered with cellophane tape.

Table ES3. Cell Configuration 4

The PEO (0.05 g) was dissolved in dichloromethane and mixed with TiO_2 (0.5 g) powder. DCM was removed to obtain a paste for coating on Al and Graphite foils. After 1 h, TiO_2 (0.25 g)/donor (1 mmol)/PEO (0.05 g) in DCM was coated on TiO_2 (0.5 g)/PEO/Al and TiO_2 (0.5 g)/PEO/Gr and dried. The donor (1 mmol)/TiO_2 (0.25 g)/PC (0.5 g)/PEO(0.05 g) slurry was prepared and casted above the coated layer on Al and Graphite and dried in air at room temperature overnight. The cell was prepared by sandwiching the coated Al/Gr layers. The rim of the cell prepared in this way was sealed all around using TiO_2/PEO paste, then with commercial adhesive Bondfix (India) and covered with cellophane tape.

Table ES4. Cell Configuration 5

The PEO (0.05 g) was dissolved in dichloromethane and mixed with metal oxide (0.5 g) powder. DCM was removed to obtain a paste for coating on Al or Graphite foils. After 1 h, Cl_4BQ (0.1 g)/PEO (0.05 g) in DCM was coated on metal oxide/PEO/Al and metal oxide/PEO/Gr and dried. The Cl_4BQ (0.025 g)/PC (0.5 g)/PEO (0.05 g) slurry was prepared and casted above the coated layer on Al and Graphite and dried in air at room temperature overnight. The cell was prepared by sandwiching the coated Al/Gr layers. The rim of the cell prepared in this way was sealed all around using TiO_2/PEO paste, then with commercial adhesive Bondfix (India) and covered with cellophane tape.

Table ES4. Cell Configuration 6

The PEO (0.05 g) was dissolved in dichloromethane and mixed with metal oxide (0.5 g) powder. DCM was removed to obtain a paste for coating on Al or Graphite foils. After 1 h, Cl_4BQ (0.1 g)/PEO (0.05 g) in DCM was coated on metal oxide (0.5 g)/PEO/Al and metal oxide (0.5 g)/PEO/Gr and dried. The Cl_4BQ (0.025 g)/metal oxide (0.5 g)/PC (0.5 g)/PEO(0.05 g) slurry was prepared and casted above the coated layer on Al and Graphite and dried in air at room temperature overnight. The cell was prepared by sandwiching the coated Al/Gr layers. The rim of the cell prepared in this way was sealed all around using TiO_2/PEO paste, then with commercial adhesive Bondfix (India) and covered with cellophane tape.

Table ES5. Cell Configuration 7

The PEO (0.05 g) was dissolved in dichloromethane and mixed with TiO_2 (0.5 g) powder. DCM was removed to obtain a paste for coating on Al or Graphite foils. After 1 h, Cl_4BQ (0.1 g)/BQ (0.1 g)/PEO (0.05 g) in DCM was coated on TiO_2/PEO/Al and

TiO_2/PEO/Gr and dried. The Cl_4BQ (0.025 g)/donor (0.1g)/BQ (0.1 g)/PC (0.5 g)/ BQ (0.1 g)/PEO (0.05 g) slurry was prepared and casted above the coated layer on Al and Graphite and dried in air at room temperature overnight. The cell was prepared by sandwiching the coated Al/Gr layers. The rim of the cell prepared in this way was sealed all around using TiO_2/PEO paste, then with commercial adhesive Bondfix (India) and covered with cellophane tape.

Table ES5. Cell Configuration 8

The PEO (0.05 g) was dissolved in dichloromethane and mixed with TiO_2 (0.5 g) powder. DCM was removed to obtain a paste for coating on Al or Graphite foils. After 1 h, Cl_4BQ (0.1 g)/BQ (0.1 g)/PEO (0.05 g) in DCM was coated on TiO_2/PEO/Al and TiO_2/PEO/Gr and dried. The Cl_4BQ (0.025 g)/donor (1 mmol)/PC (0.5 g)/BQ (0.1 g)/TiO_2 (0.25 g)/PEO (0.05 g) slurry was prepared and casted above the coated layer on Al and Graphite and dried in air at room temperature overnight. The cell was prepared by sandwiching the coated Al/Gr layers. The rim of the cell prepared in this way was sealed all around using TiO_2/PEO paste, then with commercial adhesive Bondfix (India) and covered with cellophane tape.

Table ES6. Cell Configuration 9

The PEO (0.05 g) was dissolved in dichloromethane and mixed with TiO_2 (0.5 g) powder. DCM was removed to obtain a paste for coating on Al or Graphite foils. After 1 h, Cl_4BQ (0.1 g)/PEO (0.05 g) in DCM was coated on TiO_2/PEO/Al and TiO_2/PEO/Gr and dried. The Cl_4BQ (0.025 g)/donor (0.1g) /PC (0.5 g)/PEO (0.05 g) slurry was prepared and casted above the coated layer on Al and Graphite and dried in air at room temperature

overnight. The cell was prepared by sandwiching the coated Al/Gr layers. The rim of the cell prepared in this way was sealed all around using TiO_2/PEO paste, then with commercial adhesive Bondfix (India) and covered with cellophane tape. After packing the cell was connected immediately to charge a Ni-Cd battery through a Zener diode. It was disconnected while carry out the IV-curve measurement.

Table ES6. Cell Configuration 10

The PEO (0.05 g)was dissolved in dichloromethane and mixed with TiO_2 (0.5 g) powder. DCM was removed to obtain a paste for coating on Al or Graphite foils. After 1 h, Cl_4BQ (0.1 g)/PEO (0.05 g) in DCM was coated on TiO_2/PEO/Al and TiO_2/PEO/Gr and dried. The Cl_4BQ (0.025 g)/donor (1 mmol)/PC (0.5 g)/TiO_2 (0.25 g)/PEO (0.05 g) slurry was prepared and casted above the coated layer on Al and Graphite and dried in air at room temperature overnight. The cell was prepared by sandwiching the coated Al/Gr layers. The rim of the cell prepared in this way was sealed all around using TiO_2/PEO paste, then with commercial adhesive Bondfix (India) and covered with cellophane tape. After packing the cell was connected immediately to charge a Ni-Cd battery through a Zener diode. It was disconnected while carry out the IV-curve measurement.

Table ES7. Cell Configuration 11

The PEO (0.05 g) was dissolved in dichloromethane and mixed with TiO_2 (0.5 g) powder. DCM was removed to obtain a paste for coating on Al or Graphite foils. After 1 h, Cl_4BQ (0.1 g)/BQ (0.1 g)/PEO (0.05 g) in DCM was coated on TiO_2/PEO/Al and TiO_2/PEO/Gr and dried. The Cl_4BQ (0.025 g)/donor (0.1g)/BQ (0.1 g)/PC (0.5 g)/ BQ (0.1 g)/PEO (0.05 g) slurry was prepared and casted above the coated layer on Al and Graphite

and dried in air at room temperature overnight. The cell was prepared by sandwiching the coated Al/Gr layers. The rim of the cell prepared in this way was sealed all around using TiO_2/PEO paste, then with commercial adhesive Bondfix (India) and covered with cellophane tape. After packing the cell was connected immediately to charge a Ni-Cd battery through a Zener diode. It was disconnected while carry out the IV-curve measurement.

Table ES7. Cell Configuration 12

The PEO (0.05 g) was dissolved in dichloromethane and mixed with TiO_2 (0.5 g) powder. DCM was removed to obtain a paste for coating on Al or Graphite foils. After 1 h, Cl_4BQ (0.1 g)/BQ (0.1 g)/PEO (0.05 g) in DCM was coated on TiO_2/PEO/Al and TiO_2/PEO/Gr and dried. The Cl_4BQ (0.025 g)/donor (1 mmol)/PC (0.5 g)/BQ (0.1 g)/TiO_2 (0.25 g)/PEO (0.05 g) slurry was prepared and casted above the coated layer on Al and Graphite and dried in air at room temperature overnight. The cell was prepared by sandwiching the coated Al/Gr layers. The rim of the cell prepared in this way was sealed all around using TiO_2/PEO paste, then with commercial adhesive Bondfix (India) and covered with cellophane tape. After packing the cell was connected immediately to charge a Ni-Cd battery through a Zener diode. It was disconnected while carry out the IV-curve measurement.

Table ES1. Cell Experiments – Two Layer Configuration

Cell Configuration 1

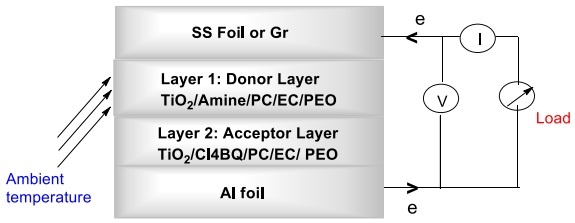

Entry	SS (or Gr)/Layers/Al	Voc (V)	Isc (mA)	Vmax (V)	Imax (mA)	Pmax (mW)	Fill Factor
1 1638A	SS----- Layer1: TiO_2(1g) + DIPEA(2mmol,0.34ml) + PC(0.5g)+EC(0.5g)+ PEO(0.2g) Layer2: TiO_2(1g)+ Cl_4BQ(2 mmol,0.5g) + PC(0.5g)+EC(0.5g)+ PEO(0.2g) Al-------	0.912	3.150	0.419	1.805	0.756	0.263
2 1639A	SS----- Layer1: TiO_2(1g) + DABCO(2mmol,0.22g) + PC(0.5g)+EC(0.5g)+ PEO(0.2g) Layer2: TiO_2(1g)+ Cl_4BQ(2 mmol,0.5g) + PC(0.5g)+EC(0.5g)+ PEO(0.2g) Al-------	0.723	3.942	0.358	1.860	0.665	0.233
3 1638	SS----- Layer1:TiO_2(1g)+TPA(2mmol,0.5g)+PC(0.5g)+ EC(0.5g)+ PEO(0.2g) Layer2:TiO_2(1g)+Cl_4BQ(2mmol,0.5g)+PC(0.5g) + EC(0.5g)+ PEO(0.2g) Al-------	0.833	1.446	0.396	0.778	0.306	0.254
4 1634	Gr---------- Layer1: TiO_2(1g) + DIPEA(2mmol,0.34ml) + PC(1g)+ PEO(0.2g) Layer2: TiO_2(1g)+ Cl_4BQ(2 mmol,0.5g) + PC(1g)+ PEO(0.2g) Al----------	1.152	5.237	0.507	2.795	1.415	0.235
5 1661A	Gr---------- Layer1: TiO_2(1g) + DABCO (2mmol,0.22g) + PC(1g)+ PEO(0.2g) Layer2: TiO_2(1g)+ Cl_4BQ(2 mmol,0.5g) + PC(1g)+ PEO(0.2g) Al----------	1.070	0.671	0.446	0.313	0.139	0.194
6 1634A	Gr---------- Layer1: TiO_2(1g) + TPA(2mmol,0.5g) + PC(1g)+ PEO(0.2g) Layer2: TiO_2(1g)+ Cl_4BQ(2 mmol,0.5g) + PC(1g)+ PEO(0.2g) Al----------	1.147	2.882	0.518	1.535	0.794	0.240

[a]Layer 1 was coated above SS electrode and Layer 2 was coated above Al. [c]All the cells were characterized by IV curve measurement.

Table ES2. Cell Experiments: TiO_2 edge layer, Cl_4BQ + donor in PC layers

Cell Configuration 2:

(Without TiO_2 in PC layer)

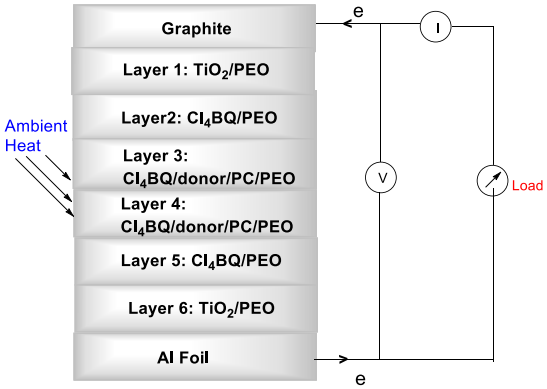

Cell Configuration 3:

(With TiO_2 in PC layer)

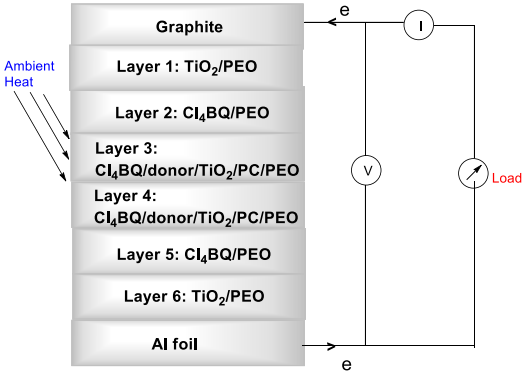

Entry	Cell Configuration	Time after packing	T °C[c]	Voc (V)	Isc (mA)	Vmax (V)	Imax (mA)	Pmax (mW)	Fill Factor
1 2812	Gr---------- Layer1: TiO_2(0.5g) + PEO (0.05g) Layer2: Cl4BQ(0.1g) + PEO (0.05g) Layer3:Cl_4BQ(0.025g)+TMPDA(0.1g) +PC(0.5g) + PEO(0.05g) Layer4:Cl_4BQ(0.025g)+TMPDA(0.1g) +PC(0.5g) + PEO(0.05g) Layer5: Cl4BQ(0.1g)+PEO(0.05g) Layer6: TiO_2(0.5g) + PEO (0.1g) Al----------	1h	28 °C	0.863	6.151	0.395	2.980	1.176	0.221
			35 °C	0.840	6.219	0.422	3.096	1.305	0.255
			40 °C	0.830	6.510	0.434	3.382	1.469	0.272
		48h	28 °C	0.782	2.364	0.353	1.058	0.373	0.202
			35 °C	0.765	3.052	0.332	1.789	0.593	0.254
			40 °C	0.759	3.370	0.370	2.138	0.790	0.309
		96h	28 °C	0.780	1.189	0.431	0.468	0.201	0.218
2 2811	Gr---------- Layer1: TiO_2(0.5g) + PEO (0.05g) Layer2: Cl4BQ(0.1g) + PEO (0.05g) Layer3:Cl_4BQ(0.025g)+TPA(0.1g) +PC(0.5g) + PEO(0.05g) Layer4:Cl_4BQ(0.025g)+TPA(0.1g) +PC(0.5g) + PEO(0.05g) Layer5: Cl4BQ(0.1g)+PEO(0.05g) Layer6: TiO_2(0.5g) + PEO (0.1g) Al----------	1h	28 °C	1.098	3.008	0.561	1.588	0.889	0.269
			35 °C	1.093	3.640	0.547	1.921	1.050	0.264
			40 °C	1.101	4.756	0.536	2.490	1.333	0.255
		48h	28 °C	1.055	1.031	0.510	0.535	0.273	0.251
			35 °C	1.031	1.210	0.524	0.641	0.336	0.266
			40 °C	1.044	1.443	0.555	0.772	0.428	0.285
		96h	28 °C	1.039	0.574	0.495	0.296	0.146	0.246
3 2810	Gr---------- Layer1: TiO_2(0.5g) + PEO (0.05g) Layer2: Cl4BQ(0.1g) + PEO (0.05g) Layer3: Cl_4BQ(0.025g) + DABCO(0.11g) +PC(0.5g) + PEO(0.05g) Layer4:Cl_4BQ(0.025g) + DABCO (0.11g) +PC(0.5g) + PEO(0.05g) Layer5: Cl4BQ(0.1g)+PEO(0.05g) Layer6: TiO_2(0.5g) + PEO (0.1g) Al----------	1h	28 °C	0.907	15.80	0.396	7.541	2.986	0.208
			35 °C	1.052	17.01	0.575	9.478	5.445	0.304
			40 °C	1.039	16.87	0.629	8.727	5.492	0.313
		48h	28 °C	1.017	6.203	0.520	2.986	1.553	0.246
			35 °C	1.004	7.302	0.560	3.349	1.874	0.256
			40 °C	1.003	8.679	0.561	4.137	2.320	0.267

		96h	28 ºC	0.999	4.100	0.469	2.053	0.962	0.235
4 2809	Gr---------- Layer1: TiO_2(0.5g) + PEO (0.05g) Layer2: Cl4BQ(0.1g) + PEO (0.05g) Layer3: Cl_4BQ(0.025g) + DIPEA (0.13g) +PC(0.5g) + PEO(0.05g) Layer4: Cl_4BQ(0.025g) + DIPEA (0.13g) +PC(0.5g) + PEO(0.05g) Layer5: Cl4BQ(0.1g)+PEO(0.05g) Layer6: TiO_2(0.5g) + PEO (0.1g) Al----------	1h	28 ºC	1.110	6.467	0.531	3.244	1.724	0.240
			35 ºC	1.090	6.134	0.536	3.364	1.804	0.270
			40 ºC	1.104	17.43	0.601	9.472	5.695	0.296
		48h	28 ºC	1.030	5.378	0.526	3.132	1.648	0.297
			35 ºC	1.010	6.142	0.561	3.654	2.050	0.330
			40 ºC	0.966	6.448	0.577	3.862	2.228	0.347
		96h	28 ºC	0.975	3.187	0.501	1.881	0.942	0.303
5 2793	Gr---------- Layer1: TiO_2(0.5g) + PEO(0.05g) Layer2: Cl_4BQ(0.1g) + PEO(0.05g) Layer3: Cl_4BQ(0.025g) + DiPrBA (0.1g) +PC (0.5g) +PEO(0.025g) Layer4: Cl_4BQ(0.025g) + DiPrBA(0.1g) + PC (0.5g) +PEO(0.025g) Layer5: Cl_4BQ(0.1g) + PEO(0.05g) Layer6: TiO_2(0.5g) + PEO(0.05g) Al----------	1h	28 ºC	1.181	6.360	0.545	3.116	1.699	0.226
			35 ºC	1.147	7.527	0.534	3.950	2.110	0.245
			40 ºC	1.157	7.317	0.576	3.820	2.198	0.260
		48h	28 ºC	1.074	3.147	0.512	1.608	0.822	0.243
			35 ºC	1.069	3.748	0.532	1.968	1.047	0.261
		96h	28 ºC	0.913	1.620	0.451	0.844	0.380	0.257
6 3012	Gr---------- Layer1: TiO_2(0.5g) + PEO(0.05g) Layer2: Cl_4BQ(0.1g) + PEO(0.05g) Layer3: TMPDA (0.166g) + Cl_4BQ(0.025g) +PC (0.5g) +PEO(0.05g) + TiO_2 (0.25g) Layer4: TMPDA (0.166g) + Cl_4BQ(0.025g) + PC (0.5g) +PEO(0.05g) + TiO_2 (0.25g) Layer5: Cl_4BQ(0.1g) + PEO(0.05g) Layer6: TiO_2(0.5g) + PEO(0.05g) Al----------	1h	28 ºC	0.897	13.56	0.413	6.912	2.855	0.235
			35 ºC	0.883	12.60	0.445	6.717	2.986	0.269
			40 ºC	0.822	14.43	0.394	7.876	3.099	0.261
		48h	28 ºC	0.884	6.98	0.402	3.603	1.449	0.235
			35 ºC	0.877	7.687	0.431	3.905	1.682	0.250
			40 ºC	0.888	8.226	0.464	3.928	1.822	0.250
		96h	40 ºC	0.891	5.079	0.441	2.211	0.975	0.216
7 3011	Gr---------- Layer1: TiO_2(0.5g) + PEO(0.05g) Layer2: Cl_4BQ(0.1g) + PEO(0.05g) Layer3: TPA (0.245g) + Cl_4BQ(0.025g) +PC (0.5g) +PEO(0.05g) + TiO_2 (0.25g) Layer4: TPA (0.245g) + Cl_4BQ(0.025g) + PC (0.5g) +PEO(0.05g) + TiO_2 (0.25g) Layer5: Cl_4BQ(0.1g) + PEO(0.05g) Layer6: TiO_2(0.5g) + PEO(0.05g) Al----------	1h	28 ºC	1.089	1.161	0.543	0.563	0.306	0.242
			35 ºC	1.104	1.229	0.535	0.646	0.345	0.255
			40 ºC	1.085	1.408	0.518	0.724	0.375	0.245
		48h	28 ºC	1.157	0.398	0.549	0.198	0.109	0.236
			35 ºC	1.154	0.501	0.569	0.252	0.143	0.248
			40 ºC	1.144	0.485	0.583	0.244	0.142	0.256
		96h	40 ºC	1.151	0.277	0.540	0.134	0.072	0.226
8 3010	Gr---------- Layer1: TiO_2(0.5g) + PEO(0.05g) Layer2: Cl_4BQ(0.1g) + PEO(0.05g) Layer3: DABCO (0.112g) + Cl_4BQ(0.025g) +PC (0.5g) +PEO(0.05g) + TiO_2 (0.25g) Layer4: DABCO (0.112g) + Cl_4BQ(0.025g) + PC (0.5g) +PEO(0.05g) + TiO_2 (0.25g) Layer5: Cl_4BQ(0.1g) + PEO(0.05g)	1h	28 ºC	0.958	26.75	0.376	12.89	4.846	0.189
			35 ºC	0.968	32.29	0.365	16.18	5.898	0.189
			40 ºC	1.006	29.67	0.685	8.986	6.155	0.206
		48h	28 ºC	0.95	4.173	0.506	1.904	0.963	0.243
			35 ºC	0.942	4.877	0.492	2.246	1.104	0.24
			40 ºC	0.932	5.242	0.517	2.352	1.216	0.249

	Layer6: TiO_2(0.5g) + PEO(0.05g) Al----------	96h	40 ºC	0.929	1.726	0.441	0.840	0.370	0.231
9 3009	Gr---------- Layer1: TiO_2(0.5g) + PEO(0.05g) Layer2: Cl_4BQ(0.1g) + PEO(0.05g) Layer3: DIPEA(0.13g, 0.17ml) + Cl_4BQ(0.025g) +PC (0.5g) +PEO(0.05g) + TiO_2 (0.25g) Layer4: DIPEA(0.13g) + Cl_4BQ(0.025g) + PC (0.5g) +PEO(0.05g) + TiO_2 (0.25g) Layer5: Cl_4BQ(0.1g) + PEO(0.05g) Layer6: TiO_2(0.5g) + PEO(0.05g) Al----------	1h	28 ºC	1.073	25.75	0.623	11.98	7.483	0.271
			35 ºC	1.055	19.77	0.595	13.02	7.741	0.371
			40 ºC	1.042	22.54	0.572	14.26	8.147	0.347
		48h	28 ºC	0.922	6.449	0.476	3.85	1.833	0.308
			35 ºC	0.91	6.727	0.503	3.88	1.95	0.318
			40 ºC	0.899	6.854	0.498	4.131	2.057	0.334
		96h	40 ºC	0.820	2.946	0.424	1.462	0.620	0.257
10 3111	Gr---------- Layer1: TiO_2(0.5g) + PEO(0.05g) Layer2: Cl_4BQ(0.1g) + PEO(0.05g) Layer3: DiPrBA (0.205g) + Cl_4BQ(0.025g) +PC (0.5g) +PEO(0.05g) + TiO_2 (0.25g) Layer4: DiPrBA (0.205g) + Cl_4BQ(0.025g) + PC (0.5g) +PEO(0.05g) + TiO_2 (0.25g) Layer5: Cl_4BQ(0.1g) + PEO(0.05g) Layer6: TiO_2(0.5g) + PEO(0.05g) Al----------	1h	28 ºC	1.032	5.946	0.477	2.014	0.959	0.156
			35 ºC	1.144	8.256	0.518	2.789	1.444	0.153
			40 ºC	1.179	12.06	0.561	7.482	4.193	0.295
		48h	28 ºC	1.165	7.532	0.548	4.148	2.272	0.259
			35 ºC	1.086	9.214	0.558	5.305	2.958	0.296
			40 ºC	1.125	9.679	0.548	5.420	2.969	0.273
		96h	40 ºC	1.169	5.816	0.525	2.987	1.569	0.231

Table ES3. Cell Experiments: Without *p*-chloranil acceptor

Cell Configuration 4

(Without Cl_4BQ)

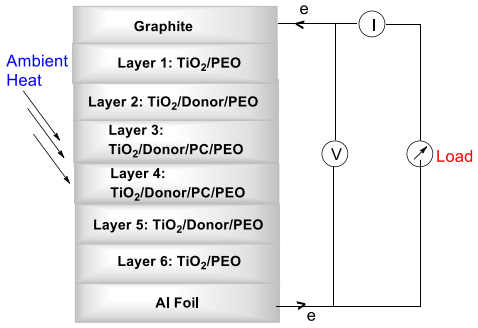

Entry No.	Cell Configuration	Time after packing	T ºC[c]	Voc (V)	Isc (mA)	Vmax (V)	Imax (mA)	Pmax (mW)	Fill Factor
1	Gr---------- Layer1: TiO_2(0.5g) + PEO (0.05g) Layer2: TiO_2 (0.25g)+ TPA (0.245g) + PEO (0.05g) Layer3:TiO_2(0.5g) + TPA (0.245g) + PC	1h	28 ºC	0.776	0.019	0.433	0.009	0.004	0.277
			35 ºC	0.764	0.023	0.445	0.010	0.004	0.268
			40 ºC	0.755	0.024	0.452	0.010	0.004	0.270

	(0.5ml) + PEO(0.05g) Layer4: TiO_2(0.5g) TPA (0.245g) + PC (0.5ml) + PEO(0.05g) Layer5: TiO_2 (0.25g)+ TPA (0.245g) + PEO (0.05g) Layer6: TiO_2(0.5g) + PEO (0.05g) Al----------	48h	28 ºC 35 ºC 40 ºC	0.739 0.727 0.717	0.011 0.015 0.016	0.42 0.396 0.408	0.005 0.007 0.008	0.002 0.003 0.003	0.279 0.279 0.287
2	Gr---------- Layer1: TiO_2(0.5g) + PEO (0.05g) Layer2:TiO_2(0.25g)+DABCO (0.112g) + PEO (0.05g) Layer3:TiO_2(0.5g) + DABCO (0.112g) + PC (0.5ml) + PEO(0.05g) Layer4: TiO_2(0.5g) + DABCO (0.112g) + PC (0.5ml) + PEO(0.05g) Layer5:TiO_2(0.25g)+DABCO (0.112g) + PEO (0.05g) Layer6: TiO_2(0.5g) + PEO (0.05g) Al----------	1h	28 ºC 35 ºC 40 ºC	0.784 0.781 0.787	0.288 0.314 0.366	0.148 0.145 0.151	0.136 0.140 0.176	0.020 0.020 0.026	0.089 0.083 0.092
		48h	28 ºC 35 ºC 40 ºC	0.82 0.818 0.815	0.102 0.156 0.178	0.355 0.382 0.41	0.033 0.038 0.048	0.011 0.014 0.019	0.114 0.114 0.136
3	Gr---------- Layer1: TiO_2(0.5g) + PEO (0.05g) Layer2:TiO_2 (0.25g)+ DIPEA (0.13g) + PEO (0.05g) Layer3:TiO_2(0.5g)+DIPEA(0.13g)+PC(0.5ml)+ PEO(0.05g) Layer4: TiO_2(0.5g)+DIPEA(0.13g)+PC(0.5ml) + PEO(0.05g) Layer5: TiO_2 (0.25g)+ DIPEA (0.13g) + PEO (0.05g) Layer6: TiO_2(0.5g) + PEO (0.05g) Al----------	1h	28 ºC 35 ºC 40 ºC	0.688 0.682 0.68	0.021 0.028 0.028	0.413 0.404 0.401	0.010 0.013 0.013	0.004 0.005 0.005	0.289 0.279 0.281
		48h	28 ºC 35 ºC 40 ºC	0.713 0.692 0.674	0.022 0.027 0.028	0.424 0.408 0.405	0.010 0.013 0.014	0.004 0.005 0.005	0.295 0.294 0.305
4	Gr---------- Layer1: TiO_2(0.5g) + PEO (0.05g) Layer2: TiO_2 (0.25g)+ DiPrBA (0.205g) + PEO (0.05g) Layer3: TiO_2(0.5g) + DiPrBA (0.205g) + PC (0.5ml) + PEO(0.05g) Layer4: TiO_2(0.5g) + DiPrBA (0.205g) + PC (0.5ml) + PEO(0.05g) Layer5: TiO_2 (0.25g)+ DiPrBA (0.205g) + PEO (0.05g) Layer6: TiO_2(0.5g) + PEO (0.05g) Al----------	1h	28 ºC 35 ºC 40 ºC	0.791 1.039 1.021	0.773 0.715 0.814	0.493 0.621 0.61	0.374 0.335 0.385	0.184 0.208 0.235	0.302 0.281 0.283
		48h	28 ºC 35 ºC 40 ºC	0.995 0.916 0.871	0.462 0.534 0.542	0.574 0.554 0.535	0.223 0.242 0.255	0.128 0.134 0.136	0.278 0.274 0.289

Table ES4: Cell Experiments: With and without metal oxides in PC layer

Cell Configuration 5

(With metal oxides (MxOy) without other donors)

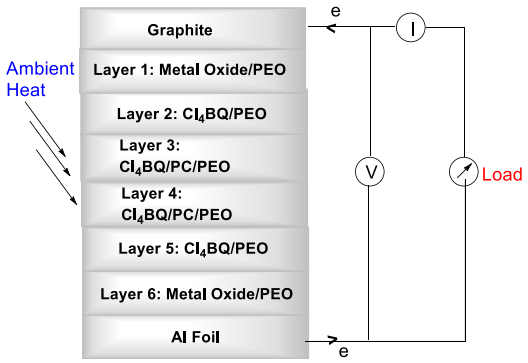

Cell Configuration 6

(With additional metal oxides (MxOy) in PC layers without other donors)

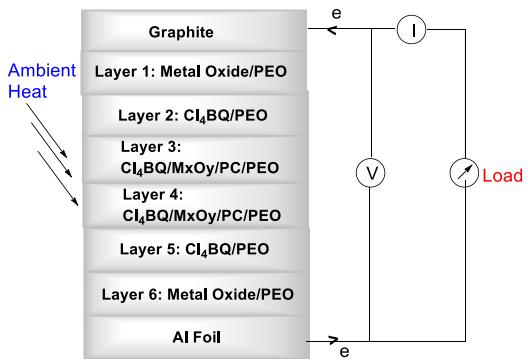

Entry No.	Cell Configuration	Time after packing	T °C[c]	Voc (V)	Isc (mA)	Vmax (V)	Imax (mA)	Pmax (mW)	Fill Factor
1 2815	Gr---------- Layer1: TiO_2(0.5g) + PEO (0.05g) Layer2: Cl_4BQ(0.1g) + PEO (0.05g) Layer3: Cl_4BQ(0.025g) +PC(0.5g) + PEO(0.05g) Layer4: Cl_4BQ(0.025g) +PC(0.5g) + PEO(0.05g) Layer5: Cl_4BQ(0.1g)+PEO(0.05g) Layer6: TiO_2(0.5g) + PEO (0.1g) Al----------	1h	28 °C	1.071	3.503	0.557	1.956	1.089	0.290
			35 °C	1.067	3.786	0.564	2.043	1.153	0.285
			40 °C	1.071	4.084	0.535	2.210	1.181	0.270
		48h	28 °C	1.055	0.498	0.522	0.253	0.132	0.252
			35 °C	1.071	0.604	0.549	0.330	0.181	0.281
			40 °C	1.061	0.710	0.558	0.409	0.228	0.303
		96h	28 °C	0.936	0.449	0.476	0.231	0.110	0.262
2 3053	Gr---------- Layer1: Al_2O_3(0. 5g)+ PEO (0.05g) Layer2: Cl_4BQ(0.1g) + PEO (0.05g) Layer3: Cl_4BQ(0.025g) +PC(0.5g) + PEO(0.05g) Layer4: Cl_4BQ(0.025g) +PC(0.5g) + PEO(0.05g) Layer5: Cl_4BQ(0.1g)+PEO(0.05g) Layer6: Al_2O_3(0.5g) + PEO (0.1g) Al----------	1h	28 °C	1.07	4.871	0.444	1.943	0.862	0.166
			35 °C	1.071	5.66	0.461	2.454	1.131	0.187
			40 °C	1.076	5.756	0.477	2.674	1.276	0.206
		48h	28 °C	1.106	3.296	0.499	1.321	0.658	0.181
			35 °C	1.099	4.588	0.484	2.019	0.976	0.199
			40 °C	1088	4.750	0.485	2.163	1.049	0.203
		96h	40 °C	1.123	3.604	0.469	1.452	0.680	0.168
3 3054	Gr---------- Layer1: ZnO(0.5g) + PEO (0.05g) Layer2: Cl_4BQ(0.1g) + PEO (0.05g) Layer3: Cl_4BQ(0.025g) +PC(0.5g) +	1h	28 °C	0.826	1.889	0.423	0.955	0.403	0.259
			35 °C	0.836	1.963	0.424	1.017	0.431	0.263

	PEO(0.05g) Layer4: Cl_4BQ(0.025g) +PC(0.5g) + PEO(0.05g) Layer5: Cl_4BQ(0.1g)+PEO(0.05g) Layer6: ZnO(0.5g) + PEO (0.1g) Al----------		40 ºC	0.839	2.209	0.44	1.12	0.492	0.266
		48h	28 ºC	0.838	0.872	0.412	0.448	0.184	0.253
			35 ºC	0.846	1.146	0.421	0.595	0.250	0.249
			40 ºC	0.847	1.238	0.415	0.641	0.272	0.260
		96h	40 ºC	0.837	0.831	0.414	0.404	0.167	0.241
4 2871	Gr---------- Layer1: TiO_2(0.5g) + PEO (0.05g) Layer2: Cl4BQ(0.1g) + PEO (0.05g) Layer3:Cl_4BQ(0.025g)+TiO_2(0.25g)+PC(0.5g) + PEO(0.05g) Layer4: Cl_4BQ(0.025g) + TiO_2(0.25g)+PC(0.5g) + PEO(0.05g) Layer5: Cl4BQ(0.1g)+ PEO(0.05g) Layer6: TiO_2(0.5g) + PEO (0.1g) Al----------	1h	28 ºC	1.073	12.62	0.483	6.299	3.043	0.225
			35 ºC	1.059	13.28	0.498	6.888	3.428	0.244
			40 ºC	1.044	13.35	0.509	7.156	3.639	0.261
		48h	28 ºC	1.177	7.753	0.507	3.880	1.965	0.215
			35 ºC	1.124	9.453	0.522	5.334	2.782	0.262
			40 ºC	1.205	10.86	0.539	6.260	3.376	0.258
		96h	28 ºC	1.189	5.731	0.494	2.540	1.255	0.184
5 2923	Gr---------- Layer1: Al_2O_3(0.5g) + PEO (0.05g) Layer2: Cl4BQ(0.1g) + PEO (0.05g) Layer3:Cl_4BQ(0.025g)+ Al_2O_3(0.25g)+PC(0.5g)+ PEO(0.05g) Layer4: Cl_4BQ(0.025g) + Al_2O_3(0.25g)+PC(0.5g) + PEO(0.05g) Layer5: Cl4BQ(0.1g)+ PEO(0.05g) Layer6: Al_2O_3(0.5g) + PEO (0.1g) Al----------	1h	28 ºC	0.999	2.664	0.456	1.265	0.576	0.217
			35 ºC	0.997	3.462	0.464	1.710	0.792	0.230
			40 ºC	1.025	3.551	0.473	1.796	0.848	0.233
		48h	28 ºC	1.052	3.064	0.491	1.568	0.770	0.239
			35 ºC	1.003	3.805	0.503	2.035	1.022	0.268
			40 ºC	0.982	4.367	0.510	2.406	1.226	0.286
		96h	28 ºC	1.070	2.889	0.495	1.485	0.735	0.288
6 2924	Gr---------- Layer1: ZnO(0.5g) + PEO (0.05g) Layer2: Cl4BQ(0.1g) + PEO (0.05g) Layer3:Cl_4BQ(0.025g)+ ZnO (0.25g)+PC(0.5g)+ PEO(0.05g) Layer4: Cl_4BQ(0.025g) + ZnO (0.25g)+PC(0.5g) + PEO(0.05g) Layer5: Cl4BQ(0.1g)+ PEO(0.05g) Layer6: ZnO(0.5g) + PEO (0.1g) Al----------	1h	28 ºC	0.925	1.790	0.440	0.877	0.386	0.233
			35 ºC	0.926	2.274	0.449	1.091	0.489	0.233
			40 ºC	0.945	2.721	0.453	1.292	0.584	0.227
		48h	28 ºC	0.958	0.992	0.438	0.454	0.199	0.210
			35 ºC	0.926	1.491	0.445	0.639	0.284	0.206
			40 ºC	0.931	2.020	0.407	0.900	0.366	0.195
		96h	28 ºC	0.982	0.471	0.453	0.209	0.094	0.204

Table ES5. Cell Experiments: With BQ in Cl_4BQ layer, without and with TiO_2 in PC layer

Cell Configuration 7

(With BQ in Cl_4BQ Layers)

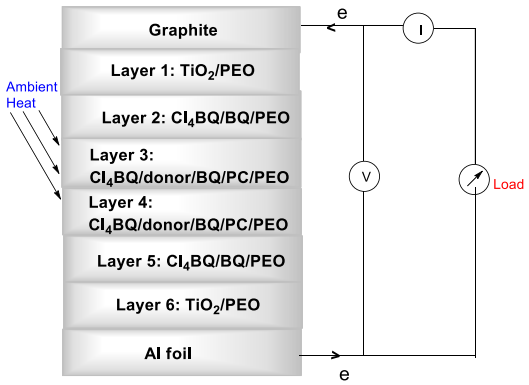

Cell Configuration 8

(With BQ in Cl_4BQ layers and additional TiO_2 using 1mmol donors in PC layers)

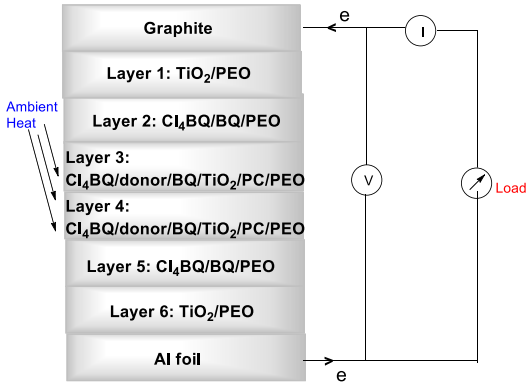

Entry	Cell Configuration	Time after packing	T °C[c]	Voc (V)	Isc (mA)	Vmax (V)	Imax (mA)	Pmax (mW)	Fill Factor
1 2802	Gr---------- Layer1: TiO_2(0.5g) + PEO (0.05g) Layer2: Cl4BQ(0.1g) + BQ(0.1g) + PEO (0.05g) Layer3: Cl_4BQ(0.025g) + TMPDA(0.1g) +PC(0.5g) + BQ(0.1g) + PEO(0.05g) Layer4: Cl_4BQ(0.025g) + TMPDA (0.1g) +PC(0.5g) + BQ(0.1g) + PEO(0.05g) Layer5: Cl4BQ(0.1g)+ BQ(0.1g) + PEO(0.05g) Layer6: TiO_2(0.5g) + PEO (0.1g) Al----------	1h	28 °C	0.761	5.623	0.409	3.537	1.448	0.338
			35 °C	1.051	6.348	0.476	3.234	1.538	0.231
			40 °C	1.044	7.546	0.515	4.223	2.175	0.276
		48h	28 °C	0.917	3.010	0.393	1.386	0.544	0.197
			35 °C	0.911	3.981	0.403	2.050	0.826	0.228
			40 °C	0.904	4.890	0.441	2.734	1.205	0.273
		96h	28 °C	0.865	1.384	0.359	0.600	0.215	0.180
2 2801	Gr---------- Layer1: TiO_2(0.5g) + PEO (0.05g) Layer2: Cl4BQ(0.1g) + BQ(0.1g) + PEO (0.05g) Layer3: Cl_4BQ(0.025g) + TPA(0.1g) +PC(0.5g) + BQ(0.1g) + PEO(0.05g) Layer4: Cl_4BQ(0.025g) + TPA (0.1g) +PC(0.5g) + BQ(0.1g) + PEO(0.05g) Layer5: Cl4BQ(0.1g)+BQ(0.1g) + PEO(0.05g) Layer6: TiO_2(0.5g) + PEO (0.1g) Al----------	1h	28 °C	1.192	5.529	0.534	2.720	1.453	0.220
			35 °C	1.165	6.120	0.541	3.062	1.658	0.233
			40 °C	1.158	6.313	0.548	3.199	1.752	0.240
		48h	28 °C	1.164	3.634	0.483	1.828	0.882	0.209
			35 °C	1.133	4.302	0.522	2.176	1.135	0.233
			40 °C	1.113	4.534	0.523	2.315	1.216	0.240
		96h	28 °C	1.176	3.295	0.453	1.687	0.764	0.197

3 2800	Gr---------- Layer1: TiO_2(0.5g) + PEO (0.05g) Layer2: Cl4BQ(0.1g) + BQ(0.1g) + PEO (0.05g) Layer3: Cl_4BQ(0.025g) + DABCO(0.1g) +PC(0.5g) + BQ(0.1g) + PEO(0.05g) Layer4: Cl_4BQ(0.025g) + DABCO (0.1g) +PC(0.5g) + BQ(0.1g) + PEO(0.05g) Layer5: Cl4BQ(0.1g)+ BQ(0.1g) + PEO(0.05g) Layer6: TiO_2(0.5g) + PEO (0.1g) Al----------	1h	28 ºC	1.113	10.64	0.471	6.310	2.972	0.251
			35 ºC	1.092	11.52	0.532	7.639	4.062	0.323
			40 ºC	1.093	12.63	0.582	9.271	5.391	0.391
		48h	28 ºC	1.086	6.500	0.400	4.224	1.688	0.239
			35 ºC	1.080	6.642	0.514	4.734	2.433	0.339
			40 ºC	1.080	7.024	0.553	5.472	3.023	0.399
		96h	28 ºC	1.072	4.736	0.394	2.839	1.118	0.220
4 2799	Gr---------- Layer1: TiO_2(0.5g) + PEO (0.05g) Layer2: Cl4BQ(0.1g) + BQ(0.1g) + PEO (0.05g) Layer3: Cl_4BQ(0.025g) + DIPEA (0.1g) +PC(0.5g) + BQ(0.1g) + PEO(0.05g) Layer4: Cl_4BQ(0.025g) + DIPEA (0.1g) +PC(0.5g) + BQ(0.1g) +PEO(0.05g) Layer5: Cl4BQ(0.1g)+BQ(0.1g)+ PEO(0.05g) Layer6: TiO_2(0.5g) + PEO (0.1g) Al----------	1h	28 ºC	1.208	26.94	0.457	12.93	5.909	0.182
			35 ºC	1.158	29.95	0.505	14.49	7.321	0.211
			40 ºC	1.146	31.33	0.523	15.75	8.229	0.229
		48h	28 ºC	1.190	6.245	0.499	3.005	1.500	0.202
			35 ºC	1.167	7.108	0.521	3.485	1.816	0.219
			40 ºC	1.155	7.772	0.535	3.880	2.074	0.231
		96h	28 ºC	1.138	4.328	0.502	2.145	1.076	0.219
5 2794	Gr---------- Layer1: TiO_2(0.5g) + PEO(0.05g) Layer2: Cl_4BQ(0.1g) + BQ (0.1g) + PEO(0.05g) Layer3: DiPrBA (0.1g)+Cl_4BQ (0.025g) +PC (0.5g) + BQ(0.1g)+ PEO(0.025g) Layer4: DiPrBA (0.1g)+ Cl_4BQ(0.025g) + PC (0.5g) + BQ(0.1g) + PEO(0.025g) Layer5: Cl_4BQ(0.1g) +BQ(0.1g) + PEO(0.05g) Layer6: TiO_2(0.5g) + PEO(0.05g) Al----------	1h	28 ºC	1.185	4.081	0.544	2.036	1.108	0.229
			35 ºC	1.185	5.255	0.580	2.660	1.544	0.248
			40 ºC	1.185	5.949	0.571	3.000	1.714	0.243
		48h	28 ºC	1.206	2.806	0.534	1.406	0.750	0.222
			35 ºC	1.215	3.722	0.573	1.937	1.109	0.245
			40 ºC	1.215	4.900	0.578	2.653	1.534	0.258
		96h	28 ºC	1.177	2.595	0.507	1.342	0.680	0.223
6 3018	Gr---------- Layer1: TiO_2(0.5g) + PEO (0.05g) Layer2: Cl4BQ(0.1g) + BQ(0.1g) + PEO (0.05g) Layer3: Cl_4BQ(0.025g) + TMPDA(0.164g) +PC(0.5g) + BQ(0.1g) + PEO(0.05g) + TiO_2 (0.25g) Layer4: Cl_4BQ(0.025g) + TMPDA (0.164g) +PC(0.5g) + BQ(0.1g) + PEO(0.05g) + TiO_2 (0.25g) Layer5: Cl4BQ(0.1g)+ BQ(0.1g) + PEO(0.05g) Layer5: TiO_2(0.5g) + PEO (0.1g) Al----------	1h	28 ºC	1.000	3.940	0.470	1.969	0.926	0.235
			35 ºC	0.995	4.655	0.521	2.418	1.259	0.272
			40 ºC	0.986	5.795	0.534	3.023	1.614	0.282
		48h	28 ºC	0.954	3.341	0.415	1.6	0.663	0.208
			35 ºC	0.944	4.631	0.44	2.334	1.026	0.235
			40 ºC	0.936	5.272	0.458	2.835	1.299	0.263
		96h	40 ºC	0.939	2.579	0.398	1.205	0.478	0.198
7 3017	Gr---------- Layer1: TiO_2(0.5g) + PEO (0.05g) Layer2: Cl4BQ(0.1g) + BQ(0.1g) + PEO (0.05g) Layer3: Cl_4BQ(0.025g) + TPA(0.245g) +PC(0.5g) + BQ(0.1g) + PEO(0.05g) + TiO_2	1h	28 ºC	1.185	2.858	0.543	1.303	0.706	0.209
			35 ºC	1.177	3.313	0.552	1.552	0.857	0.220
			40 ºC	1.168	3.667	0.546	1.722	0.939	0.219

	(0.25g) Layer4: Cl_4BQ(0.025g) + TPA (0.245g) +PC(0.5g) + BQ(0.1g) + PEO(0.05g) + TiO_2 (0.25g) Layer5: Cl4BQ(0.1g)+BQ(0.1g) + PEO(0.05g) Layer5: TiO_2(0.5g) + PEO (0.1g) Al----------	48h	28 ºC	1.229	1.857	0.518	0.868	0.450	0.197
			35 ºC	1.218	2.439	0.519	1.171	0.607	0.204
			40 ºC	1.209	2.757	0.556	1.31	0.728	0.219
		96h	40 ºC	1.244	1.437	0.483	0.701	0.338	0.190
8 3016	Gr---------- Layer1: TiO_2(0.5g) + PEO (0.05g) Layer2: Cl4BQ(0.1g) + BQ(0.1g) + PEO (0.05g) Layer3: Cl_4BQ(0.025g) + DABCO(0.166g) +PC(0.5g) + BQ(0.1g) + PEO(0.05g) + TiO2 (0.25g) Layer4: Cl_4BQ(0.025g) + DABCO (0.166g) +PC(0.5g) + BQ(0.1g) + PEO(0.05g) + TiO2 (0.25g) Layer5: Cl4BQ(0.1g)+ BQ(0.1g) + PEO(0.05g) Layer5: TiO_2(0.5g) + PEO (0.1g) Al----------	1h	28 ºC	1.148	8.383	0.561	6.318	3.544	0.368
			35 ºC	1.126	8.687	0.620	7.323	4.542	0.464
			40 ºC	1.147	9.693	0.612	7.850	4.806	0.432
		48h	28 ºC	1.159	6.841	0.492	4.849	2.387	0.301
			35 ºC	1.154	7.903	0.56	6.271	3.51	0.385
			40 ºC	1.147	7.591	0.583	6.482	3.776	0.434
		96h	40 ºC	1.163	6.415	0.478	4.123	1.972	0.264
9 3015	Gr---------- Layer1: TiO_2(0.5g) + PEO (0.05g) Layer2: Cl4BQ(0.1g) + BQ(0.1g) + PEO (0.05g) Layer3: Cl_4BQ(0.025g) + DIPEA (0.13g) +PC(0.5g) + BQ(0.1g) + PEO(0.05g) + TiO2 (0.25g) Layer4: Cl_4BQ(0.025g) + DIPEA (0.13g) +PC(0.5g) + BQ(0.1g) +PEO(0.05g) + TiO2 (0.25g) Layer5: Cl4BQ(0.1g)+BQ(0.1g)+ PEO(0.05g) Layer6: TiO_2(0.5g) + PEO (0.1g) Al----------	1h	28 ºC	1.190	30.09	0.497	15.69	7.788	0.218
			35 ºC	1.136	34.92	0.519	18.22	9.450	0.238
			40 ºC	1.126	35.22	0.526	22.34	11.74	0.296
		48h	28 ºC	1.187	18.23	0.509	11.42	5.816	0.269
			35 ºC	1.134	19.91	0.518	15.02	7.775	0.344
			40 ºC	1.106	19.15	0.543	15.37	8.338	0.394
		96h	40 ºC	1.180	14.63	0.480	9.626	4.618	0.268
10 3019	Gr---------- Layer1: TiO_2(0.5g) + PEO(0.05g) Layer2: Cl_4BQ(0.1g) + BQ (0.1g) + PEO(0.05g) Layer3: DiPrBA (0.205g)+Cl_4BQ (0.025g) +PC (0.5g) + BQ(0.1g)+ PEO(0.025g) + TiO2 (0.25g) Layer4: DiPrBA (0.205g)+ Cl_4BQ(0.025g) + PC (0.5g) + BQ(0.1g) + PEO(0.025g) + TiO2 (0.25g) Layer5: Cl_4BQ(0.1g) + BQ(0.1g) + PEO(0.05g) Layer6: TiO_2(0.5g) + PEO(0.05g) Al----------	1h	28 ºC	1.214	4.470	0.552	2.205	1.216	0.224
			35 ºC	1.206	5.720	0.570	2.846	1.622	0.235
			40 ºC	1.199	6.714	0.577	3.245	1.871	0.232
		48h	28 ºC	1.241	3.403	0.563	1.669	0.939	0.22
			35 ºC	1.247	4.024	0.595	1.977	1.176	0.234
			40 ºC	1.254	4.623	0.616	2.292	1.411	0.243
		96h	40 ºC	1.238	2.734	0.551	1.336	0.736	0.218

Table ES6. Cell Expeiments: Charging Ni-Cd battery with electrochemical cell for charging studies

Cell Configuration 9

(Without TiO_2 in PC layer)

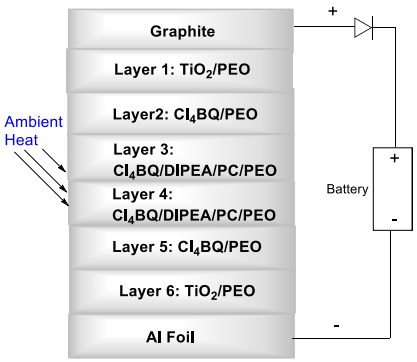

Cell Configuration 10

(With TiO_2 in PC layer)

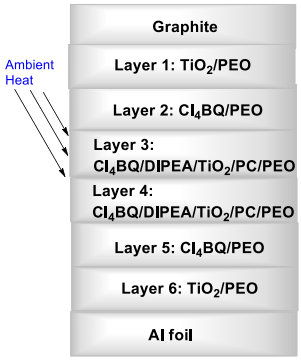

Entry	Cell Configuration	Time after packing	T °C°	Voc (V)	Isc (mA)	Vmax (V)	Imax (mA)	Pmax (mW)	Fill Factor
1 3278	Gr---------- Layer1: TiO_2(0.5g) + PEO (0.05g) Layer2: Cl4BQ(0.1g) + PEO (0.05g) Layer3:Cl_4BQ(0.025g)+DIPEA(0.13g) +PC(0.5g) + PEO(0.05g) Layer4:Cl_4BQ(0.025g)+DIPEA(0.13g) +PC(0.5g) + PEO(0.05g) Layer5: Cl4BQ(0.1g)+PEO(0.05g) Layer6: TiO_2(0.5g) + PEO (0.1g) Al----------	1h	28 °C	1.140	20.95	0.555	11.68	6.485	0.272
			35 °C	1.116	22.84	0.581	13.56	7.882	0.309
			40 °C	1.132	26.48	0.585	15.36	8.988	0.300
		48h	28 °C	0.970	5.605	0.563	3.829	2.154	0.396
			35 °C	0.957	6.364	0.571	4.660	2.659	0.437
			40 °C	0.955	6.414	0.574	5.039	2.893	0.473
		96h	40 °C	0.945	4.204	0.542	2.753	1.491	0.375
		144h	40 °C	0.936	4.752	0.576	3.017	1.738	0.391
2 3279	Gr---------- Layer1: TiO_2(0.5g) + PEO (0.05g) Layer2: Cl4BQ(0.1g) + PEO (0.05g) Layer3:Cl_4BQ(0.025g)+ DIPEA(0.13g) +PC(0.5g) + TiO_2(0.25 g)+PEO(0.05g) Layer4:Cl_4BQ(0.025g)+ DIPEA(0.13g) +PC(0.5g) + TiO_2(0.25 g)+ PEO(0.05g) Layer5: Cl4BQ(0.1g)+PEO(0.05g) Layer6: TiO_2(0.5g) + PEO (0.1g) Al----------	1h	28 °C	1.143	23.50	0.556	12.57	6.992	0.260
			35 °C	1.138	24.38	0.557	13.65	7.600	0.274
			40 °C	1.126	23.69	0.569	13.40	7.626	0.286
		48h	28 °C	0.981	6.314	0.537	4.482	2.405	0.387
			35 °C	0.964	6.576	0.538	4.719	2.538	0.401
			40 °C	0.961	6.935	0.572	5.089	2.911	0.437

		96h	40 ºC	0.911	5.528	0.473	3.756	1.776	0.353
		144h	40 ºC	0.865	6.407	0.506	4.010	2.027	0.366

Table ES7. Cell Expeiments: Charging Ni-Cd battery using electrochemical cell

Cell Configuration 11

(With BQ in Cl_4BQ Layers)

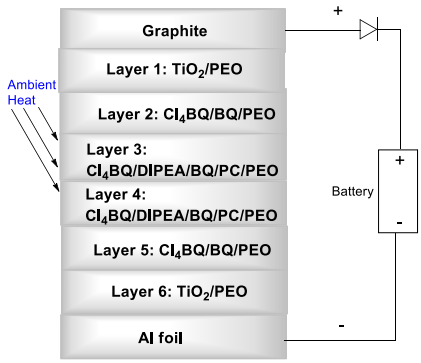

Cell Configuration 12

(With BQ in Cl_4BQ layers and additional TiO_2 in PC layers)

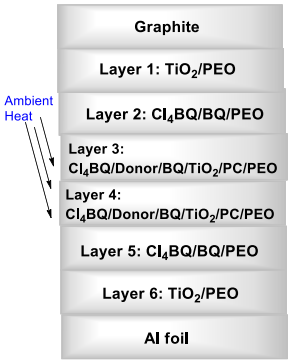

Entry	Cell Configuration	Time after packing	T ºC[c]	Voc (V)	Isc (mA)	Vmax (V)	Imax (mA)	Pmax (mW)	Fill Factor
1 3264	Gr---------- Layer1: TiO_2(0.5g) + PEO (0.05g) Layer2: Cl4BQ(0.1g) +BQ(0.1g)+PEO (0.05g) Layer3:Cl_4BQ(0.025g)+DIPEA(0.13g) +PC(0.5g) + BQ(0.1g)+PEO(0.05g) Layer4:Cl_4BQ(0.025g)+DIPEA(0.13g) +PC(0.5g) + BQ(0.1g)+PEO(0.05g) Layer5: Cl4BQ(0.1g)+ BQ(0.1g)+ PEO(0.05g) Layer6: TiO_2(0.5g) + PEO (0.1g) Al----------	1h	28 ºC	1.176	74.63	0.453	31.18	14.12	0.161
			35 ºC	1.129	76.34	0.485	33.77	16.38	0.190
			40 ºC	1.119	82.96	0.456	38.34	17.49	0.189
		48h	28 ºC	1.177	30.07	0.520	14.33	7.451	0.211
			35 ºC	1.168	44.71	0.529	22.02	11.65	0.223
			40 ºC	1.154	48.90	0.542	24.83	13.46	0.239
		96h	40 ºC	1.190	31.95	0.529	17.49	9.246	0.243
		144h	40 ºC	1.214	46.17	0.549	26.53	14.57	0.260
2 3265	Gr---------- Layer1: TiO_2(0.5g) + PEO (0.05g) Layer2: Cl4BQ(0.1g) + BQ(0.1g)+PEO (0.05g) Layer3:Cl_4BQ(0.025g)+ DIPEA(0.13g) +PC(0.5g) + BQ(0.1g)+ TiO_2(0.25 g)+PEO(0.05g) Layer4:Cl_4BQ(0.025g)+ DIPEA(0.13g) +PC(0.5g) + BQ(0.1g)+ TiO_2(0.25 g)+ PEO(0.05g)	1h	28 ºC	1.132	51.42	0.536	22.93	12.28	0.211
			35 ºC	1.137	56.00	0.510	25.02	12.77	0.200
			40 ºC	1.180	65.18	0.486	27.17	13.21	0.172
		48h	28 ºC	1.143	34.64	0.526	18.04	9.481	0.239
			35 ºC	1.171	35.48	0.530	20.09	10.64	0.256
			40 ºC	1.140	41.54	0.542	23.59	12.77	0.270

	Layer5: Cl4BQ(0.1g)+ BQ(0.1g)+ PEO(0.05g) Layer6: TiO_2(0.5g) + PEO (0.1g) Al----------	96h	28 ºC	1.187	27.10	0.525	15.17	7.962	0.248
		144h	40 ºC	1.198	32.07	0.534	19.96	10.65	0.277
3 3303	Gr---------- Layer1: TiO_2(0.5g) + PEO (0.05g) Layer2: Cl4BQ(0.1g) + BQ(0.1g)+PEO (0.05g) Layer3:Cl_4BQ(0.025g)+ TMPDA (0.164g) +PC(0.5g) + BQ(0.1g)+ TiO_2(0.25 g)+PEO(0.05g) Layer4:Cl_4BQ(0.025g)+ TMPDA (0.164g) +PC(0.5g) + BQ(0.1g)+ TiO_2(0.25 g)+ PEO(0.05g) Layer5: Cl4BQ(0.1g)+ BQ(0.1g)+ PEO(0.05g) Layer6: TiO_2(0.5g) + PEO (0.1g) Al----------	1h	28 ºC	0.906	6.536	0.479	3.428	1.642	0.277
			35 ºC	0.873	7.093	0.461	3.705	1.706	0.276
			40 ºC	0.885	7.614	0.505	3.727	1.883	0.279
		48h	28 ºC	0.811	2.269	0.388	1.182	0.458	0.249
			35 ºC	0.794	2.847	0.373	1.561	0.581	0.257
			40 ºC	0.807	3.084	0.375	1.653	0.620	0.249
		96h	40 ºC	1.019	11.52	0.386	6.450	2.488	0.212
		144h	40 ºC	0.824	1.829	0.446	0.838	0.373	0.248
4 3309	Gr---------- Layer1: TiO_2(0.5g) + PEO (0.05g) Layer2: Cl4BQ(0.1g) + BQ(0.1g)+PEO (0.05g) Layer3:Cl_4BQ(0.025g)+ TPA (0.245g) +PC(0.5g) + BQ(0.1g)+ TiO_2(0.25 g)+PEO(0.05g) Layer4:Cl_4BQ(0.025g)+ TPA (0.245g) +PC(0.5g) + BQ(0.1g)+ TiO_2(0.25 g)+ PEO(0.05g) Layer5: Cl4BQ(0.1g)+ BQ(0.1g)+ PEO(0.05g) Layer6: TiO_2(0.5g) + PEO (0.1g) Al----------	1h	28 ºC	1.166	2.837	0.569	1.411	0.803	0.243
			35 ºC	1.157	3.123	0.563	1.560	0.877	0.243
			40 ºC	1.161	3.332	0.571	1.727	0.985	0.255
		48h	28 ºC	1.237	2.325	0.557	1.182	0.658	0.229
			35 ºC	1.225	3.025	0.565	1.501	0.847	0.229
			40 ºC	1.210	3.063	0.560	1.528	0.855	0.231
		96h	40 ºC	1.266	3.542	0.586	1.765	1.034	0.231
		144h	40 ºC	1.263	2.537	0.558	1.252	0.698	0.218
5 3302	Gr---------- Layer1: TiO_2(0.5g) + PEO (0.05g) Layer2: Cl4BQ(0.1g) + BQ(0.1g)+PEO (0.05g) Layer3:Cl_4BQ(0.025g)+ DABCO(0.112g) +PC(0.5g) + BQ(0.1g)+ TiO_2(0.25 g)+PEO(0.05g) Layer4:Cl_4BQ(0.025g)+ DABCO(0.112g) +PC(0.5g) + BQ(0.1g)+ TiO_2(0.25 g)+ PEO(0.05g) Layer5: Cl4BQ(0.1g)+ BQ(0.1g)+ PEO(0.05g) Layer6: TiO_2(0.5g) + PEO (0.1g) Al----------	1h	28 ºC	1.039	8.589	0.406	6.239	2.532	0.284
			35 ºC	1.032	9.364	0.536	6.713	3.595	0.372
			40 ºC	1.032	9.435	0.574	7.013	4.022	0.413
		48h	28 ºC	1.021	6.912	0.410	3.850	1.579	0.224
			35 ºC	1.021	8.619	0.507	5.107	2.589	0.294
			40 ºC	1.013	8.545	0.505	5.412	2.733	0.316
		96h	40 ºC	0.813	2.280	0.402	1.162	0.466	0.252
		144h	40 ºC	1.014	7.966	0.351	3.685	1.291	0.160
6 3308	Gr---------- Layer1: TiO_2(0.5g) + PEO (0.05g) Layer2: Cl4BQ(0.1g) + BQ(0.1g)+PEO (0.05g) Layer3:Cl_4BQ(0.025g)+ DiPrBA (0.205g) +PC(0.5g) + BQ(0.1g)+ TiO_2(0.25 g)+PEO(0.05g) Layer4:Cl_4BQ(0.025g)+ DiPrBA (0.205g) +PC(0.5g) + BQ(0.1g)+ TiO_2(0.25 g)+ PEO(0.05g) Layer5: Cl4BQ(0.1g)+ BQ(0.1g)+ PEO(0.05g) Layer6: TiO_2(0.5g) + PEO (0.1g) Al----------	1h	28 ºC	1.170	8.195	0.536	4.071	2.181	0.228
			35 ºC	1.154	8.190	0.536	4.110	2.204	0.233
			40 ºC	1.142	9.591	0.537	4.853	2.606	0.238
		48h	28 ºC	1.196	3.458	0.527	1.766	0.929	0.225
			35 ºC	1.196	5.033	0.539	2.563	1.382	0.230
			40 ºC	1.184	5.988	0.541	3.070	1.660	0.234
		96h	40 ºC	1.201	2.703	0.539	1.368	0.736	0.227
		144h	40 ºC	1.172	2.265	0.512	1.156	0.592	0.223

4.5 References

1 Chapin, D. M.; Fuller, C. S.; Pearson, G. L. *J. Appl. Phys.* **1954**, *25*, 676.

2 Green, M. A.; Emery, K.; Hishikawa, Y.; Warta, W.; Dunlop, E. D. *Prog. Photovolt: Res. Appl.* **2012**, *20*, 12.

3 Green, M.A.; Basore, P.A.; Chang, N.; Clugston, D.; Egan, R.; Evans, R.; Ho, J.; Hogg, D.; Jarnason, S.; Keevers, P.; Lasswell, P.; O'Sullian, J.; Schubert, U.; Turner, A.; Wenham, S. R.; Young, T. *Solar Energy. Special issue on thin film photovoltaics*. **2004**, *77*, 857.

4 Corwine, C. R.; Pudov, A. O.; Gloeckler, M.; Demtsu, S. H.; Sites, J. R.; *Solar Energy Materials and Solar Cells.* **2004**, *82*, 481.

5 Green, M. A.; Emery, K.; Hishikawa, Y.; Warta, W.; Dunlop, E. D. *Prog. Photovolt: Res. Appl.* **2011**, 19, 565.

6 Repins, I.; Contreras, M. A.; Egaas, B.; DeHart, C.; Scharf, J.; Perkins, C. L.; To, B.; Noufi, R. *Prog. Photovolt: Res. Appl.* **2008**, *16*, 235.

7 Gerischer, H.; Willig, F.; Schäfer, F.; Gerischer, H.; Willig, F.; Meier, H.; Jahnke, H.; Schönborn, M.; Zimmermann, G.; *Physical and Chemical Applications of Dyestuffs.* **1976**, *61*, 31.

8 O'Regan, B.; Grätzel, M.; *Nature.* **1991**, *353*, 737.

9 Sapp, S. A.; Elliott, C. M.; Contado, C.; Caramori, S.; Bignozzi, C. A. *J. Am. Chem. Soc*. **2002**, *124*, 11215.

10 Hattori, S.; Wada, Y.; Yanagida, S.; Fukuzumi, S. *J. Am. Chem. Soc*. **2005**, *127*,

9648.

11 Feldt, S. M.; Gibson, E. A.; Gabrielsson, E.; Sun, L.; Boschloo, G.; Hagfeldt, A. *J. Am. Chem. Soc.* **2010**, *132*, 16714.

12 Daeneke, T.; Kwon, T.; Holmes, A. B.; Duffy, N. W.; Bach, U.; Spiccia, L. *Nat Chem.* **2011**, *3*, 211.

13 Li, T. C.; Spokoyny, A. M.; She, C.; Farha, O. K.; Mirkin, C. A.; Marks, T. J.; Hupp, J. T. *J. Am. Chem. Soc.* **2010**, *132*, 4580.

14 Boucharef, M.; Din, C. D.; Boumaza, M. S.; Colas, M.; Snaith, H. J.; Ratier, B.; Bouclé, J. *Nanotechnology*. **2010**, *21*, 205203.

15 Zhang, Q.; Dandeneau, C. S.; Zhou, X.; Cao, G. *Adv. Mater.* **2009**, *21*, 4087.

16 Duan, Y.; Fu, N.; Liu, Q.; Fang, Y.; Zhou, X.; Zhang, J.; Lin, Y. *J. Phys. Chem. C* **2012**, *116*, 8888.

17 Du, J.; Qi, J.; Wang, D.; Tang, Z. *Energy Environ. Sci.* **2012**, *5*, 6914.

18 Plank, N. O. V.; Howard, I.; Rao, A.; Wilson, M. W. B.; Ducati, C.; Mane, R. S.; Bendall, J. S.; Louca, R. R. M.; Greenham, N. C.; Miura, H.; Friend, R. H.; Snaith, H. J.; Welland, M. E. *J. Phys. Chem. C.* **2009**, *113*, 18515.

19 Xu, C. K.; Wu, J. M.; Desai, U. V.; Gao, D. *Nano Lett.* **2012**, *12*, 2420.

20 Peiro, A. M.; Ravirajan, P.; Govender, K.; Boyle, D. S.; O'Brien, P.; Bradley, D. D. C.; Nelson, J.; Durrant, J. R. *J. Mater. Chem*. **2006**, *16*, 2088.

21 Desai, U. V.; Xu, C. K.; Wu, J. M.; Gao, D. *Nanotechnology* **2012**, *23*, 205401.

22 Mathew, S.; Yella, A.; Gao, P.; Humphry-Baker, R.; Curchod, B. F. E.; Ashari-Astani, N.; Tavernelli, I.; Rothlisberger, U.; Nazeeruddin, M. K.; Grätzel, M. *Nat.*

Chem. **2014**, *6*, 242.

23 Bach, U.; Lupo, D.; Comte, P.; Moser, J. E.; Weissörtel, F.; Salbeck, J.; Spreitzer, H.; Grätzel, M. *Nature* **1998**, *395*, 583.

24 Burschka, J.; Dualeh, A.; Kessler, F.; Baranoff, E.; Cevey-Ha, N.-L.; Yi, C.; Nazeeruddin, M. K.; Grätzel, M. *J. Am. Chem. Soc.* **2011**, 45, 18042.

25 Leijtens, T.; Ding, I-K.; Giovenzana, T.; Bloking, J. T.; McGehee, M. D.; Sellinger, A. *ACS Nano* **2012**, *6*, 1455.

26 Yang, L.; Xu, B.; Bi, D.; Tian, H.; Boschloo, G.; Sun, L.; Hagfeldt, A.; Johansson, E. M. J. *J. Am. Chem. Soc.* **2013**, *135*, 7378.

27 a) Jiang, K. J.; Manseki, K.; Yu, Y. H.; Masaki, N.; Suzuki, K.; Song, Y. L.; Yanagida, S. *Adv. Funct. Mater*. **2009**, *19*, 2481. b) Yang, L.; Cappel, U. B.; Unger, E. L.; Karlsson, M.; Karlsson, K. M.; Gabrielsson, E.; Sun, L.; Boschloo, G.; Hagfeldt, A.; Johansson, E. M. J. *Phys. Chem. Chem. Phys.* **2012**, *14*, 779. c) Zhang, W.; Zhu, R.; Li, F. Wang, Q.; Liu, B. *J. Phys. Chem. C.* **2011**, *115*, 7038.

28 Kojima, A.; Teshima, K.; Shirai, Y.; Miyasaka, T. *J. Am. Chem. Soc.* **2009**, 131, 6050.

29 Kim, H. S.; Lee, C. R.; Im, J. H.; Lee, K. B.; Moehl, T.; Marchioro, A.; Moon, S. J.; Humphry-Baker, R.; Yum, J. H.; Moser, J. E.; Grätzel, M.; Park, N. G. *Sci. Rep.* **2012**, *2*, 591.

30 Jacobsson, T. J.; Correa-Baena, J. P.; Pazoki, M.; Saliba, M.; Schenk, K.; Gratzel, M.; Hagfeldt, A. *Energy Environ. Sci.*, **2016**, *9*, 1706.

31 Luo, S.; Daoud, W. A. *J. Mater. Chem. A.*, **2015**, *3*, 8992.

32 Niu, G.; Guo, X.; Wang, L. *J. Mater. Chem. A.*, **2015**, *3*, 8970.

33 Yu, Z.; Sun, L. *Adv. Energy Mater*. **2015**, *5*, 1500213.

34 Yin, W-J.; Yang, J-H.; Kang, J.; Yan, Y.; Wei, S-H. *J. Mater. Chem. A*, **2015**, *3*, 8926.

35 a) Snaith, H. J.; Abate, A.; Ball, J. M.; Eperon, G. E.; Leijtens, T.; Noel, N. K.; Stranks, S. D.; Wang, J. T. W.; Wojciechowski, K.; Zhang, W. *J. Phys. Chem. Lett.* **2014,** *5*, 1511. b) Noel, N. K.; Abate, A.; Stranks, S. D.; Parrott, E. S.; Burlakov, V. M.; Goriely, A.; Snaith, H. J. *ACS Nano.* **2014**, *8*, 9815. c) Abate, A.; Saliba, M.; Hollman, D. J.; Stranks, S. D.; Wojciechowski, K.; Avolio, R.; Grancini, G.; Petrozza, A.; Snaith, H. J. Nano Lett. **2014**, *14*, 3247.

36 Ghosh, A. K.; Morel, D. L.; Feng, T.; Shaw, R. F.; Rowe Jr, C. A. *Journal of Applied Physics.* **1974,** *45*, 230.

37 Gelenis, S.; Tourillon, G.; Granier, F. *Thin Solid Films.* 1986, 139, 221.

38 Weinberger, B. R.; Akhtar, M.; Gau, S. C. *Synthetic Metals*. 1982, 4, 187.

39 Tang, C. W. *Appl. Phy. Lett.* **1986**, *48*, 183.

40 Sariciftci, N. S.; Braun, D.; Zhang, C.; Srdanov, V. I.; Heeger, A. J.; Stucky, G.; Wudl, F. *Appt. Phys. Lett.* **1993**, *62*, 585.

41 Halls, J. J. M.; Pichler, K.; Friend, R. H.; Moratti, S. C.; Holmes, A. B. *Appt. Phys. Lett.* **1996**, *68*, 3120.

42 Yu, G.; Gao, J.; Hummelen, J. C.; Wudl, F.; Heeger, A. J. *Science.* **1995**, *270,* 1789.

43 Yu, G.; Wang, J.; McElvain, J.; Heeger, A. J. *Adv. Mater.* **1998**, *10,* 1431.

44 He, Z.; Xiao, B.; Liu, F.; Wu, H.; Yang, Y.; Xiao, S.; Wang, C.; Russell, T. P.; Cao, Y. *Nature Photonics.* **2015,** *9*, 174.

45 Halls, J. J. M.; Walsh, C. A.; Greenham, N. C.; Marseglia, E. A.; Friend, R. H.; Moratti, S. C.; Holmes, A. B. *Nature.* **1995,** *376,* 498.

46 a) Gebeyehu, D.; Maennig, B.; Drechsel, J.; Leo, K.; Pfeiffer, M. *Solar Energy Materials & Solar Cells.* **2003,** *79,* 81. b) Spanggaard, H.; Krebs, F. C.; *Solar Energy Materials & Solar Cells.* **2004,** *83,* 81. c) Gunes, S.; Neugebauer, H.; Sariciftci, N. S. *Chem. Rev.* **2007,** *107,* 1324.

47 a) Hoppe, H.; Sariciftci, N. S. *J. Mater. Res.* **2004**, *19,* 1924. b) Yang, L.; Cappel, U. B.; Unger, E. L.; Karlsson, M.; Karlsson, K. M.; Gabrielsson, E.; Sun, L.; Boschloo, G.; Hagfeldt, A.; Johansson, E. M. J. *Phys. Chem. Chem. Phys.* **2012,** *14*, 779. c) Jeon, N. J.; Lee, H. G.; Kim, Y. C.; Seo, J.; Noh, J. H.; Lee, J.; Seok, S. *J. Am. Chem. Soc.* **2014,** *136,* 7837.

48 a) Huang, Y.; Kramer, E. J.; Heeger, A. J.; Bazan, G. C. *Chem. Rev.* **2014,** *114,* 7006. b) Lu, L.; Zheng, T.; Wu, Q.; Schneider, A. M.; Zhao, D.; Yu, L. *Chem. Rev.* **2015,** *115,* 12666. c) Shivanna, R.; Shoaee, S.; Dimitrov, S.; Kandappa, Sridhar Rajaram, S. K.; Durrant, J. R.; Narayan, K. S. *Energy Environ sci.* **2014**, *7,* 435. d) Nielsen, C. B.; Holliday, S.; Chen, H-Y.; Cryer, S. J.; McCulloch, I. *Acc. Chem. Res.* **2015**, *48,* 2803. e) Sun, D.; Meng, D.; Cai, Y.; Fan, B.; Li, Y.; Jiang, W.; Huo, L.; Sun, Y.; Wang, Z. *J. Am. Chem. Soc.* **2015,** *137,* 11156. f) Deibel, C.; Dyakonov, V. *Rep. Prog. Phys.* **2010**, *73***.** 1.

49 (a) Mulliken, R. S. *J. Am. Chem. Soc.* **1952**, *74*, 811. (b) Mulliken, R. S.; Person, W. B. Wiley: New York, **1969**. (c) Taube, H.; Myers, H. J.; Rich, R. L. *J. Am. Chem. Soc.*

1953, *75*, 4118. (d) Taube, H. *Science.*, **1984**, *226*, 1028. (e) Marcus, R. A. *J. Chem. Phys.* **1956**, *24*, 966. (f) Marcus, R. A. *Angew. Chem., Int. Ed.* **1993**, *32*, 1111.

50 Ferraris, J.; Cowan, D. O.; Walatka, V.; Perlstein, J. H. *J. Am. Chem. Soc.* **1973**, *95*, 948.

51 (a) Goetz, K. P.; Vermeulen, D.; Payne, M. E.; Kloc, C.; McNeilb, L. E.; Jurchescu, O. D. *J. Mater. Chem. C*, **2014**, *2*, 3065. (b) Zhang, J.; Xu,W.; Sheng, P.; Zhao, G.; Zhu, D. *Acc. Chem. Res.* **2017**, *50*, 1654.

52 (a) Rosokha S. V.; Kochi, J. K. *Acc. Chem. Res.*, **2008**, *41*, 641. (b) Sutin, N. *Prog. Inorg. Chem.* **1983**, *30*, 441. (c) Brunschwig, B. S.; Sutin, N. *Coord. Chem. Rev.* **1999**, *187*, 233.

53 Gutmann, F.; Keyzer, H. *Electrochimica Acta.* **1966**, *11*, 555.

54 a) Lee, K. H.; Schwenn, P. E.; Smith, A. R. G.; Cavaye, H.; Shaw, P.W.; James, M.; Krueger,K. B.; Gentle, I. R.; Meredith, P.; Burn, P. L. *Adv. Mater.* **2011,** *23,* 766. b) Hoppea, H.; Sariciftci, N. S. *J. Mater. Res.* **2004**, *19*, 1924.

55 Ardestani, S. S.; Ajeian, R.; Badrabadi, M. N.; Tavakkoli, M. *Solar Energy Materials and Solar Cells.* **2013,** *111*,107.

56 You, J.; Meng, L.; Song, T-B.; Guo, T-F.; Yang, Y.; Chang, W-H.; Hong, Z.; Chen, H.; Zhou, H.; Chen, Q.; Liu, Y.; Marco, N. D.; Yang, Y. *Nature Nanotechnology.* **2016,** *11*, 75.

57 Dong, X.; Fang, X.; Lv, M.; Lin, B.; Zhang, S.; Ding, J.; Yuan, N. *J. Mater. Chem. A.* **2015**, *3*, 5360.

58 Guarnera, S.; Abate, A.; Zhang, W.; Foster, J. M.; Richardson, G.; Petrozza, A.; Snaith, H. J. *J. Phy. Chem. Lett.* **2015,** *6,* 432.

59 Zhao, X.; Park, N-G. *Photonics.* **2015**, *2*, 1139.

60 Sanehira, E. M.; Villers, B. J. T. D.; Schulz, P.; Reese, M. O.; Ferrere, S.; Zhu, K.; Lin, L. Y.; Berry, J. J.; Luther, J. M. *ACS Energy Lett.* **2016,** *1,* 38.

61 Bush, K. A.; Bailie, C. D.; Chen, Y.; Bowring, A. R.; Wang, W.; Ma, W.; Leijtens, T.; Moghadam, F.; McGehee, M. D. *Adv. Mater.* **2016,** *28,* 3937.

62 (a) Scanlon, D. O.; Dunnill, C. W.; John Buckeridge, J.; Shevlin, S. A; Logsdail, A. J.; Woodley, M. C.; Catlow, R. A.; Powell, M. J.; Palgrave, R. G.; Parkin, I. P.; Watson, G.W.; Keal, T. W.; Sherwood, P.; Walsh, A.; Sokol, A. A.; *Nat. Mater.* **2013**, *12*, 798. (b) Xiong, G; Shao R., Droubay T. C.; Joly, A. G; Beck K. M.; Chambers, S. A; Hess W. P.; *Adv. Funct. Mater.* **2007**, *17, 2133*. (c) Martinez, U.; Hammer, B.; *J. Chem. Phys.* **2011**, *134*, 194703.

63 Davidson, R. S.; Slater, M. R. *J. Chem. Soc. Faraday. Trans. 1.* **1976**, *72*, 2416.

64 (a) Shalev, H.; Evans, D, H. *J. Am. Chem. Soc.* **1989**, *111*, 2667. (b) Grimsrud, E. P.; Caldwell, G.; Chowdhury, S.; Kebarle, P. *J. Am. Chem. Soc.* **1985**, *107*, 4627. (c) Heinis, T.; Chowdhury, S.; Scott, S. L.; Kebarle, P. *J. Am. Chem. Soc.* **1988**, *110*, 400. (d) Chowdhury, S.; Heinis, T.; Grimsrud E. P.; Kebarle, P. *J. Phys. Chem.* **1986**, *90*, 2747. (e) Kebarle, P.; Chowdhury, S. *Chem. Rev*. **1987**, *87*, 513.

65 (a) Rahimi, M.; Kim, T.; Gorski, C. A.; Bruce E. Logan. *Journal of Power Sources.*, **2018**, *373*, 95 (b) Rahimi, M.; Zhu, L.; Kowalski, K. L.; Zhu, X.; Gorski, C. A.; Hickner, M. A.; Logan B. E. *Journal of Power Sources*. **2017**, *342*, 956. (c) Anari, E.

H. B.; Romano, M.; Teh, W. X.; Black, J. J.; Jiang, E.; Chen, J.; To, T. Q.; Panchompoo, J.; Aldous, L. *Chem. Comm.* **2016**, *52*, 745.

66 (a) Fumey, F.; Weber, R.; Gatenbein, P.; Daguenet-Frick, X.; Williamson, T.; Dorer, V.; *Energy Procedia*, **2014**, 46, 134 (b) Yu, N.; Wang, R. Z.; Wang, L. *W.; Progress in Energy and Combustion Science*. **2013**, *39, 489*.

Appendix I

(Representative Spectra)

Spectrum No. 1 (Chapter 2, Section 2.4.2), ^{1}H NMR Spectrum (400 MHz, $CDCl_3$)

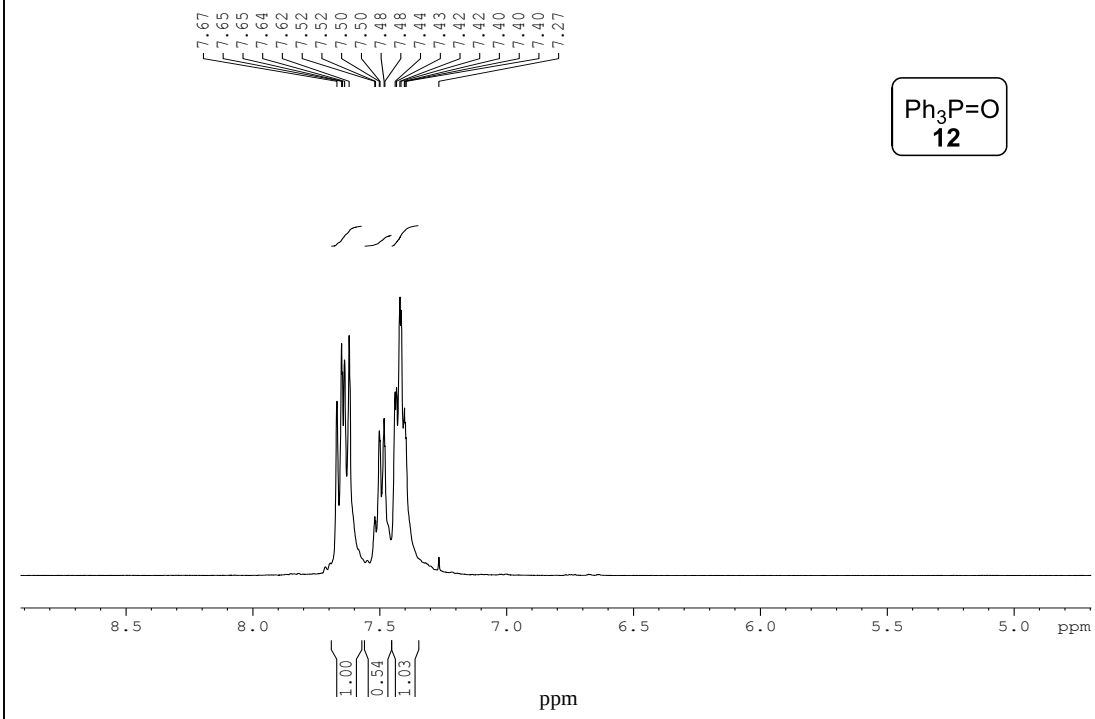

Spectrum No. 2 (Chapter 2, Section 2.4.2), ^{13}C NMR Spectrum (100 MHz, $CDCl_3$)

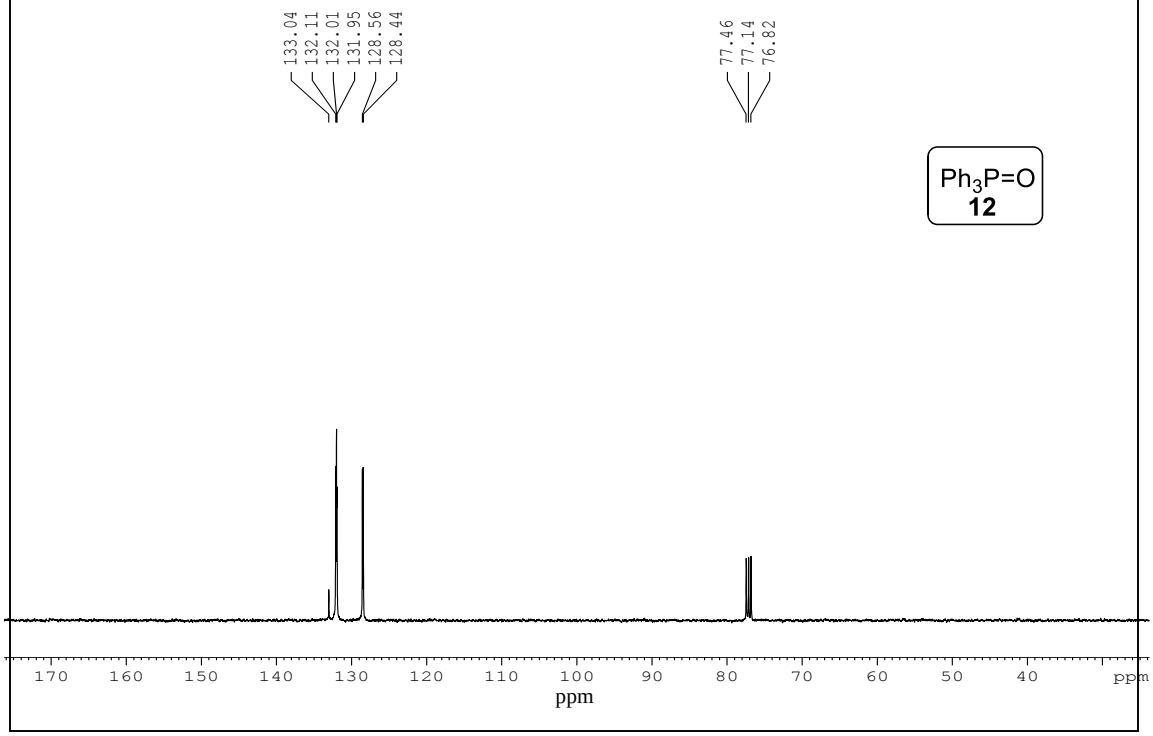

Spectrum No. 3 (Chapter 2, Section 2.4.4), ^{1}H NMR Spectrum (400 MHz, $CDCl_3$)

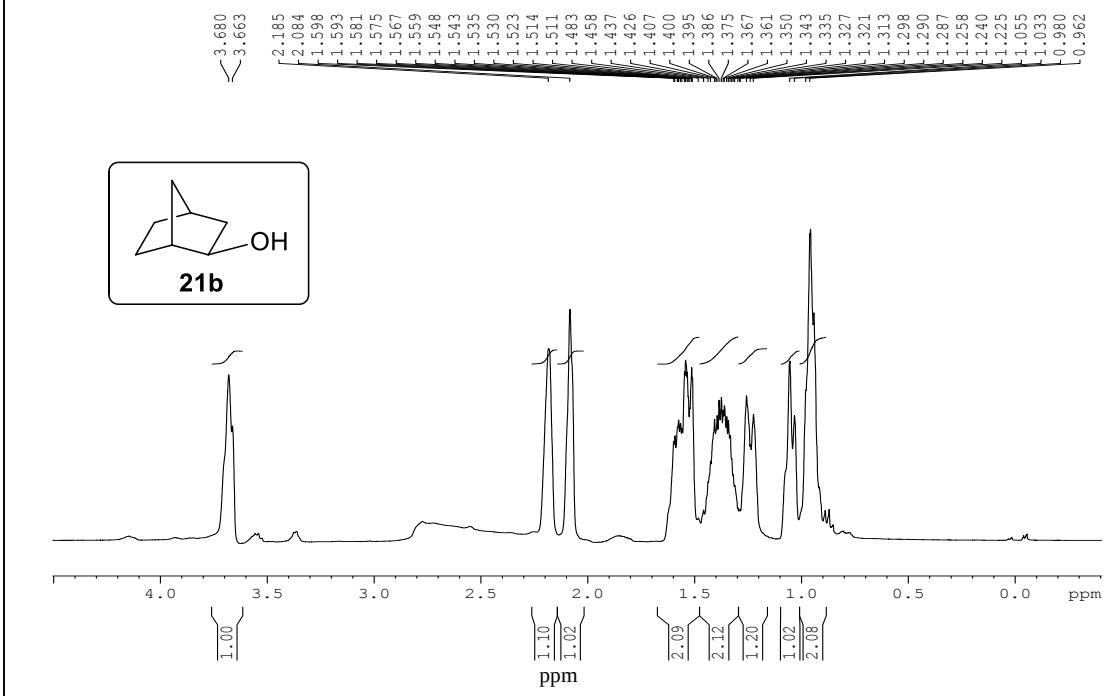

Spectrum No. 4 (Chapter 2, Section 2.4.4), ^{13}C NMR Spectrum (100 MHz, $CDCl_3$)

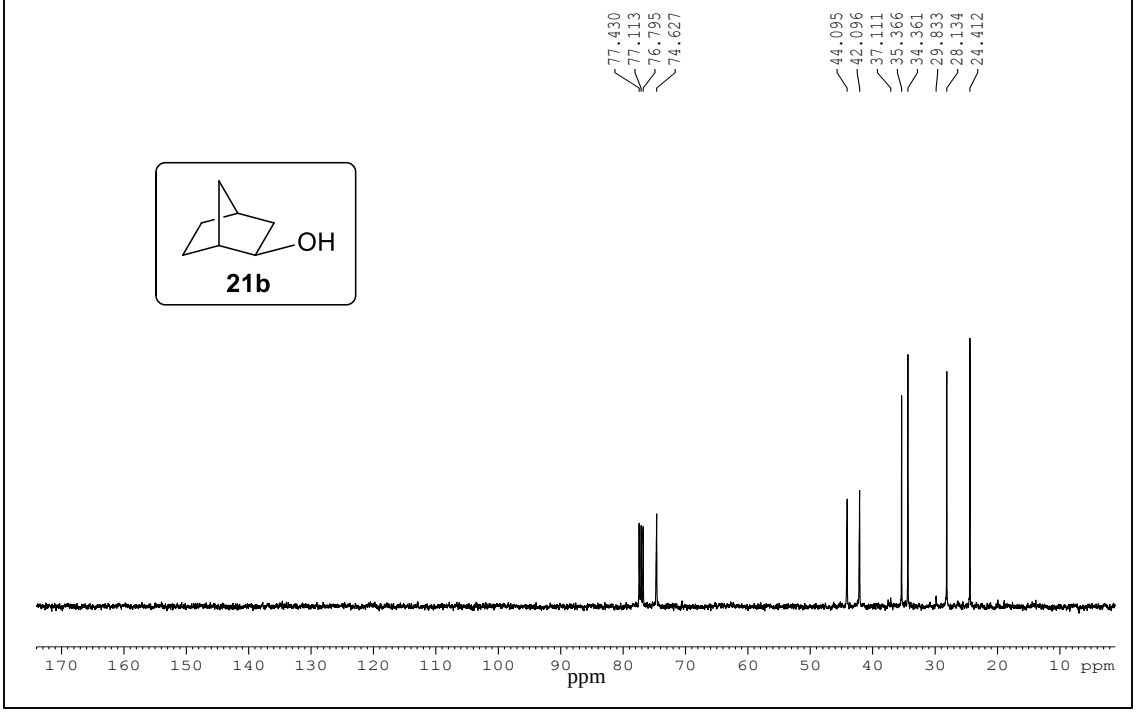

Spectrum No. 5 (Chapter 2, Section 2.4.5), ^{1}H NMR Spectrum (400 MHz, $CDCl_3$)

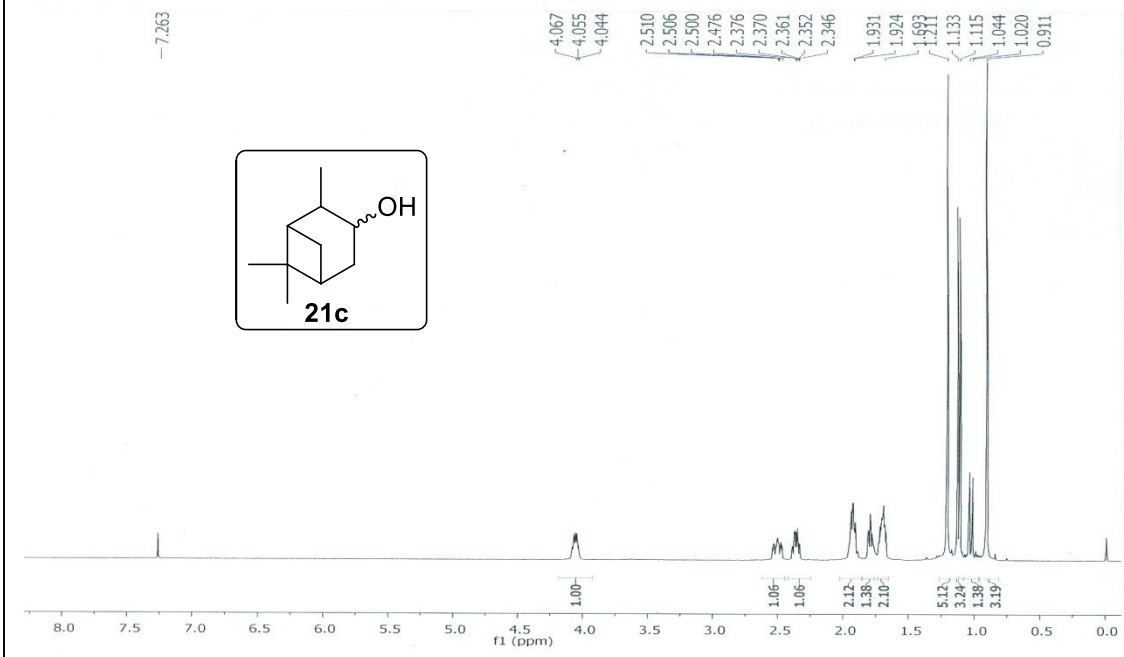

Spectrum No. 6 (Chapter 2, Section 2.4.5), ^{13}C NMR Spectrum (100 MHz, $CDCl_3$)

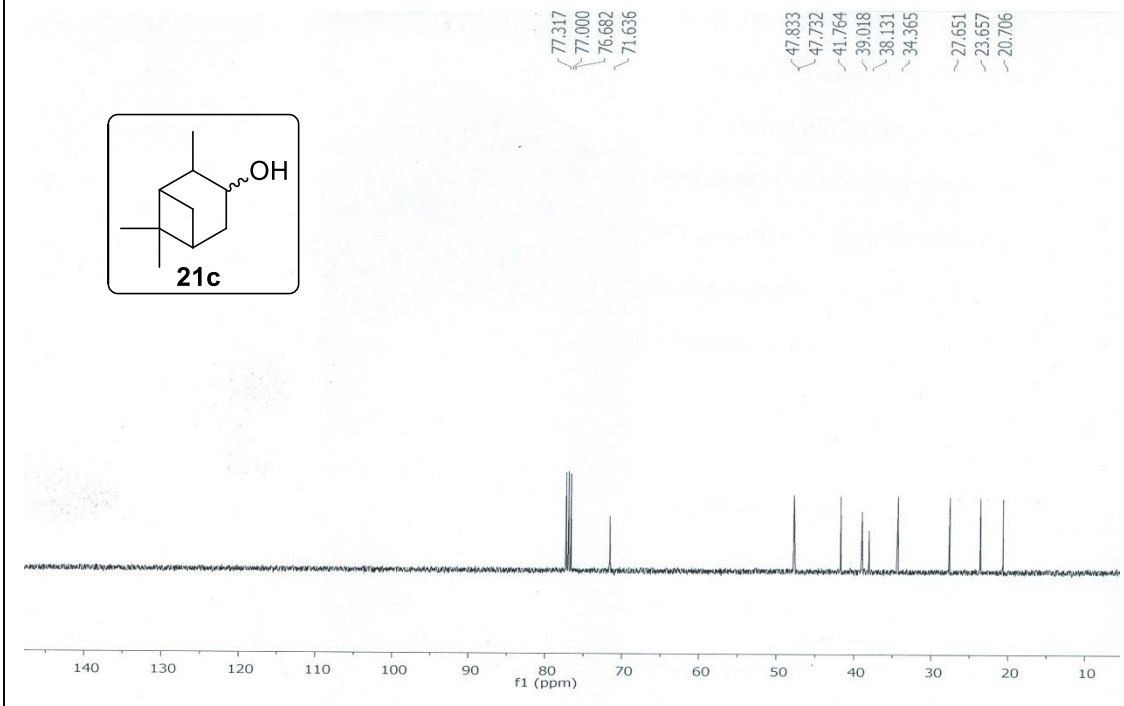

Spectrum No. 7 (Chapter 2, Section 2.4.5), ^{1}H NMR Spectrum (400 MHz, $CDCl_3$)

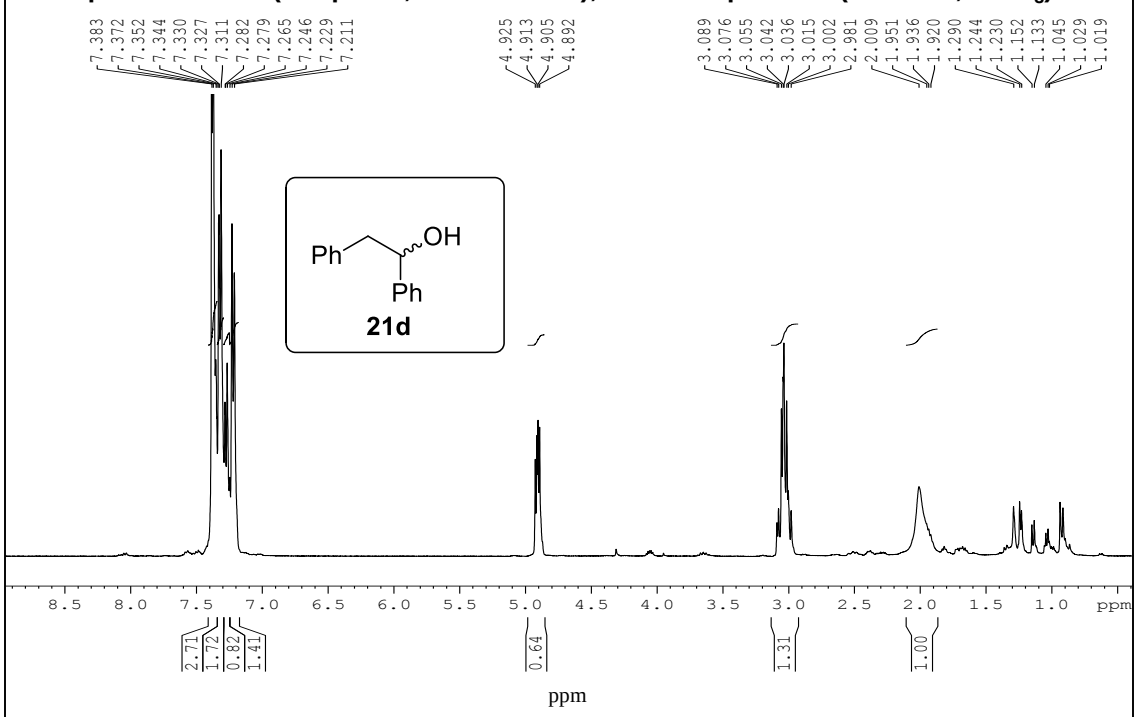

Spectrum No. 8 (Chapter 2, Section 2.4.5), ^{13}C NMR Spectrum (100 MHz, $CDCl_3$)

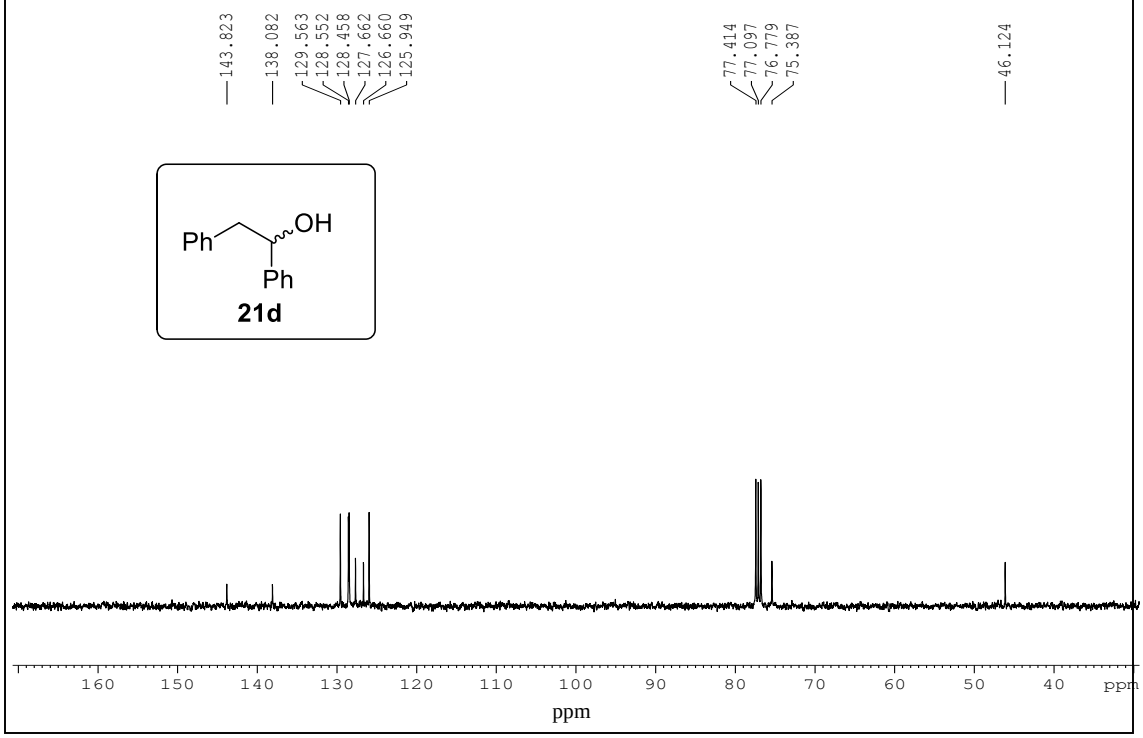

Spectrum No. 9 (Chapter 2, Section 2.4.7), ^{1}H NMR Spectrum (400 MHz, $CDCl_3$)

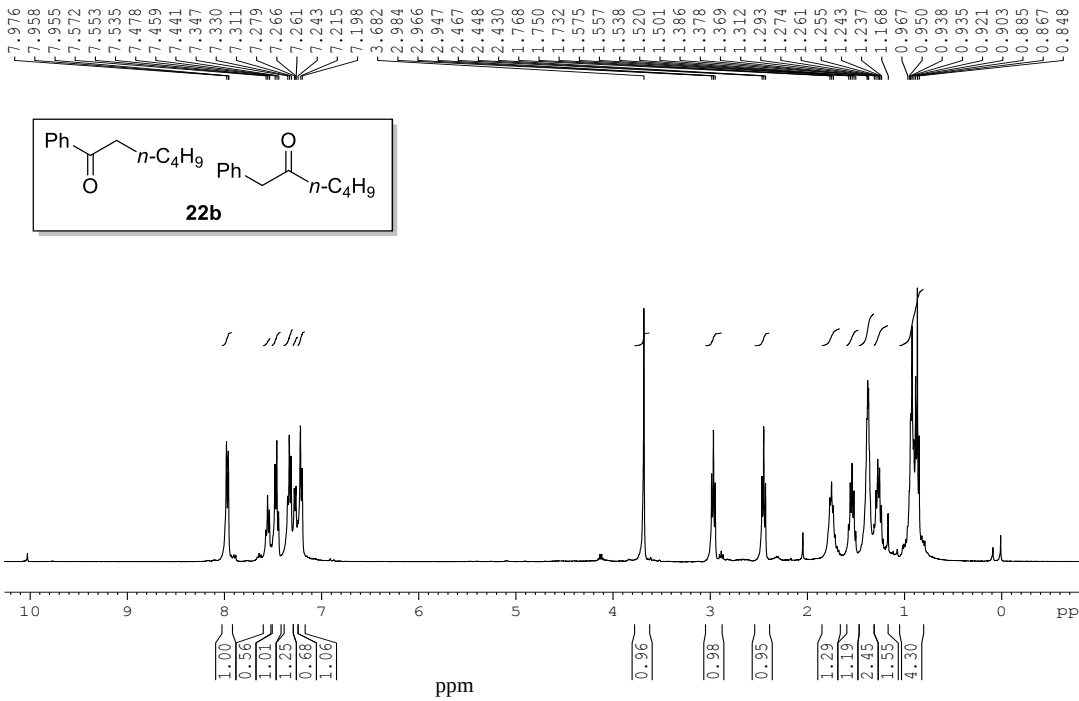

Spectrum No. 10 (Chapter 2, Section 2.4.7), ^{13}C NMR Spectrum (100 MHz, $CDCl_3$)

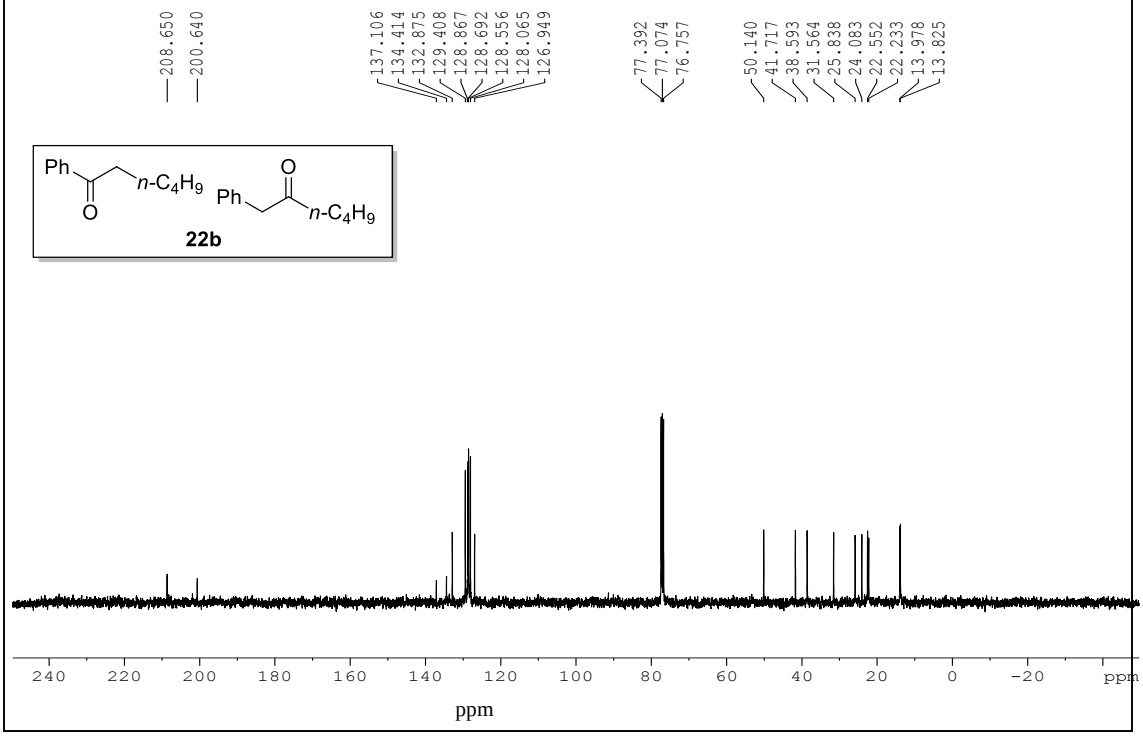

Spectrum No. 11 (Chapter 2, Section 2.4.8), ^{1}H NMR Spectrum (400 MHz, $CDCl_3$)

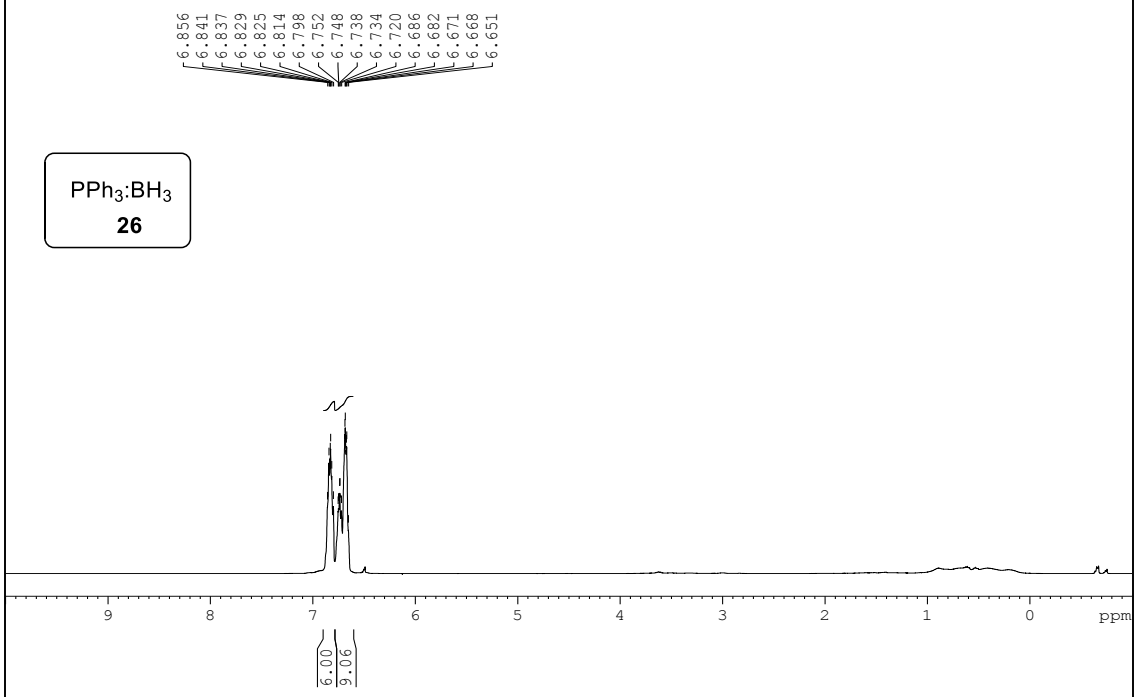

ppm

Spectrum No. 12 (Chapter 2, Section 2.4.8), ^{13}C NMR Spectrum (100 MHz, $CDCl_3$)

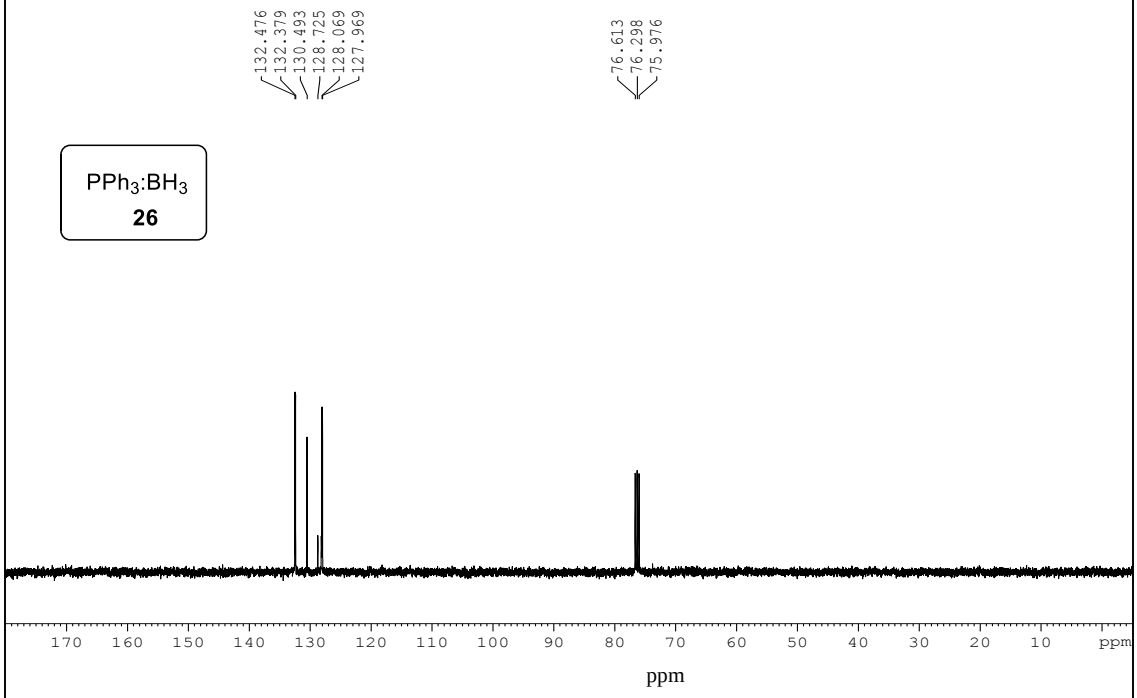

ppm

Spectrum No. 13 (Chapter 2, Section 2.4.8), ^{11}B NMR Spectrum (128.3 MHz, $CDCl_3$)

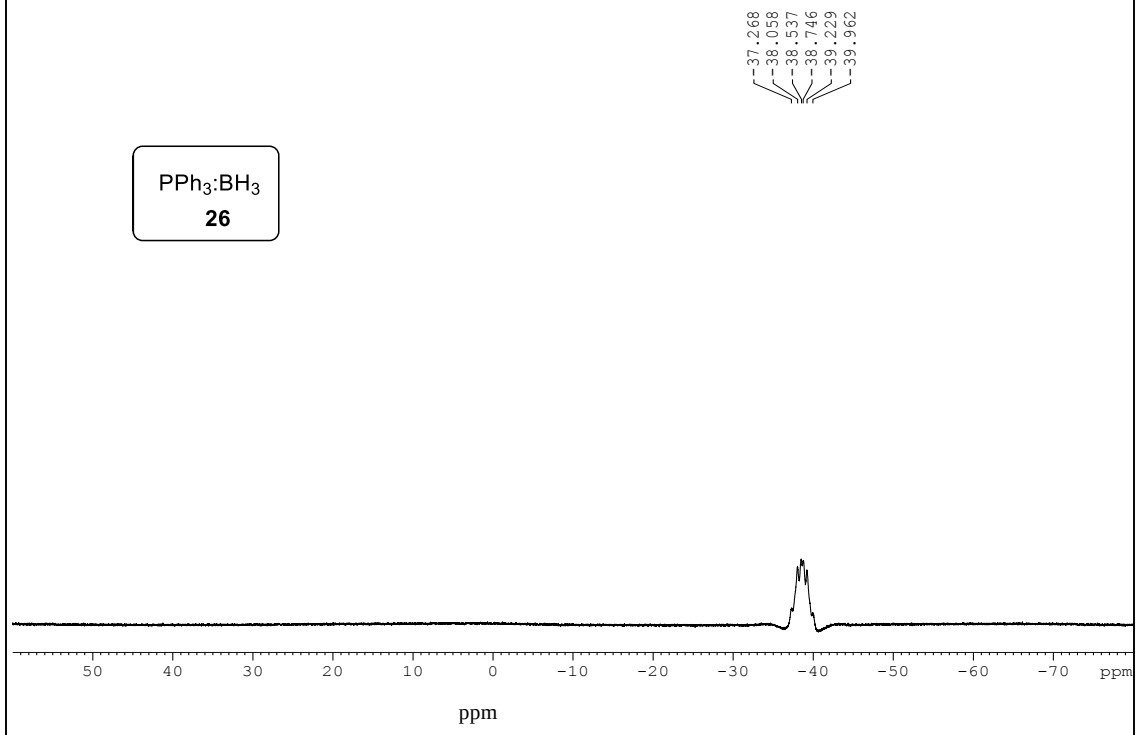

Spectrum No. 14 (Chapter 2, Section 2.4.8), ^{31}P NMR Spectrum (162 MHz, $CDCl_3$)

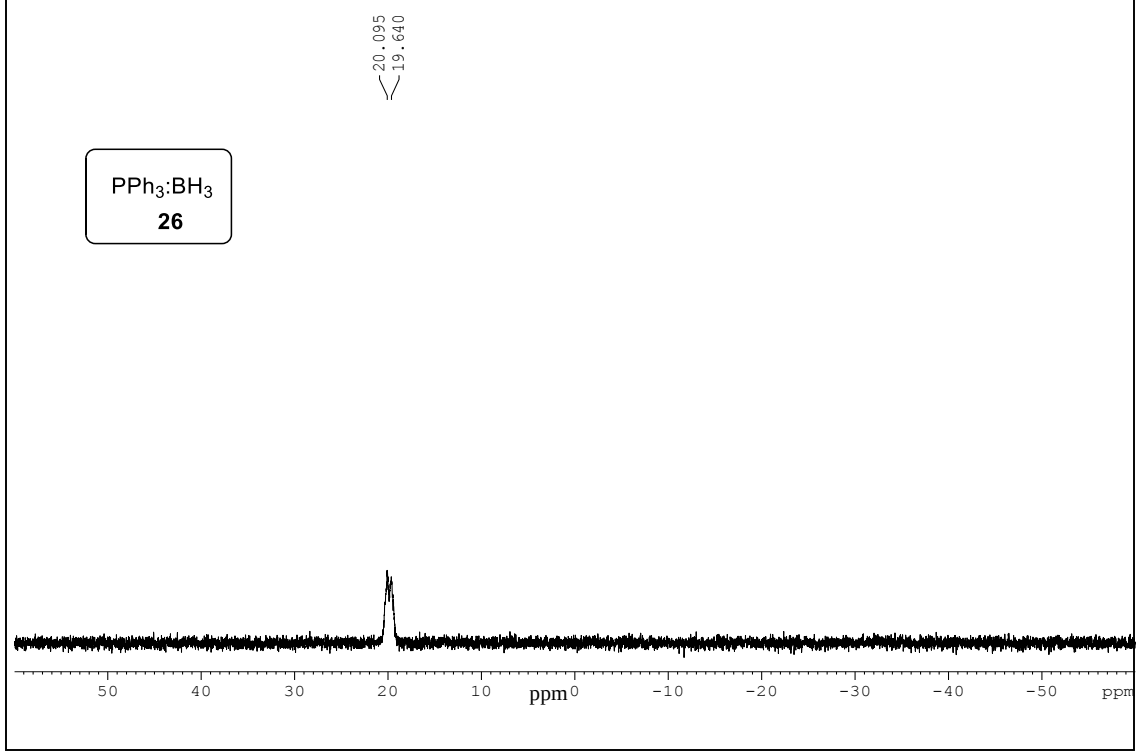

Spectrum No. 15 (Chapter 2, Section 2.4.9), ^{1}H NMR Spectrum (400 MHz, $CDCl_3$)

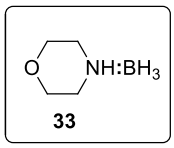

33

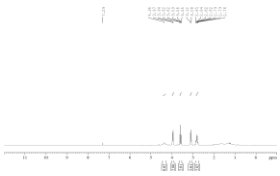

ppm

Spectrum No. 16 (Chapter 2, Section 2.4.9), ^{13}C NMR Spectrum (100 MHz, $CDCl_3$)

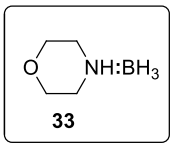

33

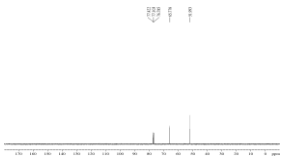

ppm

Spectrum No. 17 (Chapter 2, Section 2.4.9), ^{1}H NMR Spectrum (400 MHz, $CDCl_3$)

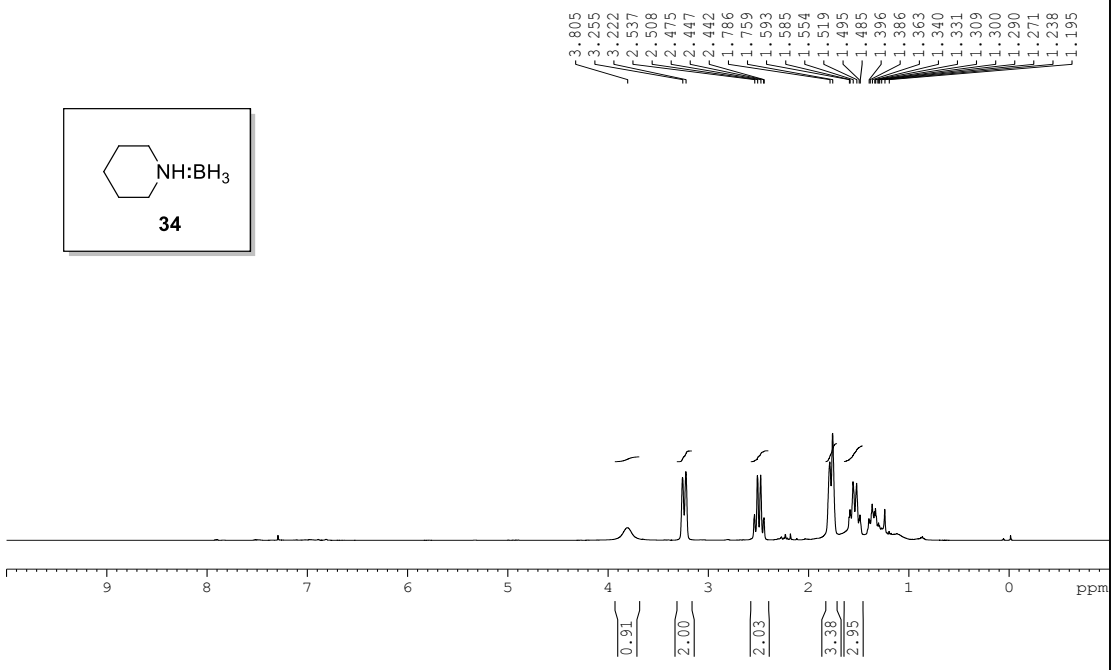

ppm

Spectrum No. 18 (Chapter 2, Section 2.4.9), ^{13}C NMR Spectrum (100 MHz, $CDCl_3$)

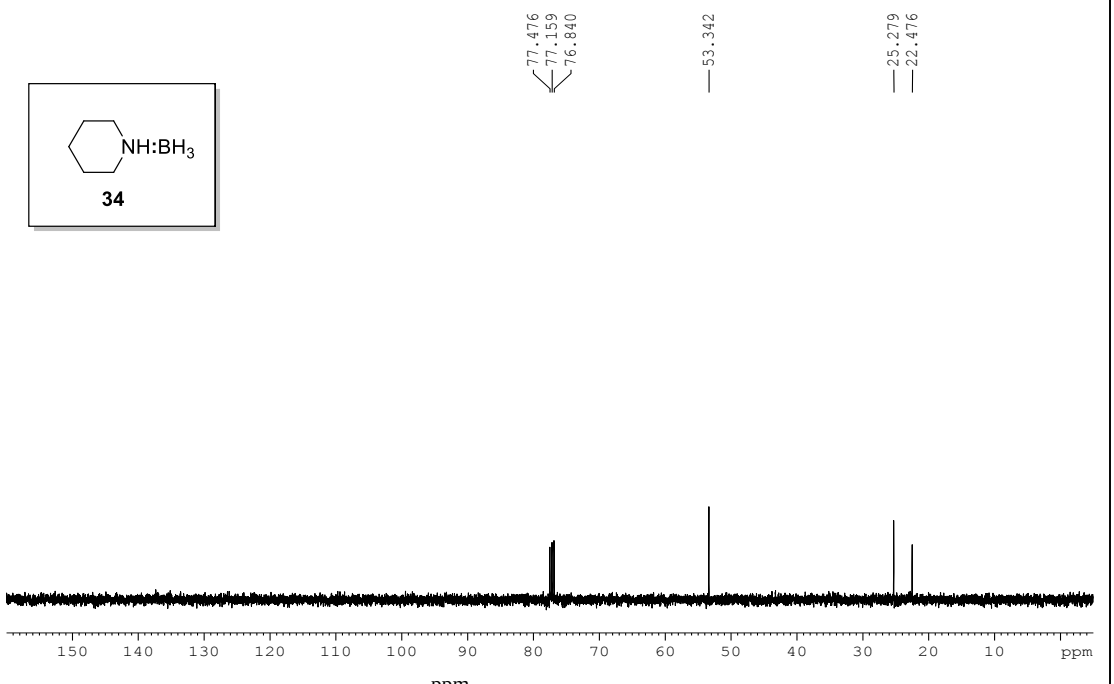

ppm

Spectrum No. 19 (Chapter 2, Section 2.4.10), ^{1}HNMR Spectrum (400 MHz, $CDCl_3$)

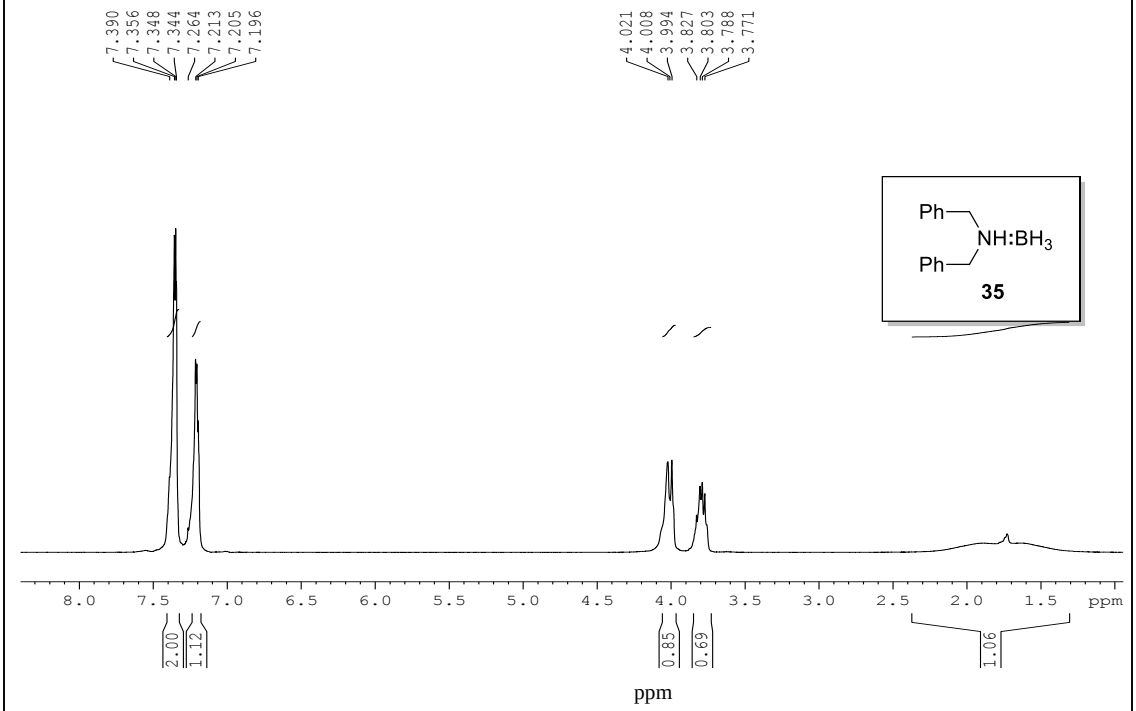

ppm

Spectrum No. 20 (Chapter 2, Section 2.4.10), ^{13}C NMR Spectrum (100 MHz, $CDCl_3$)

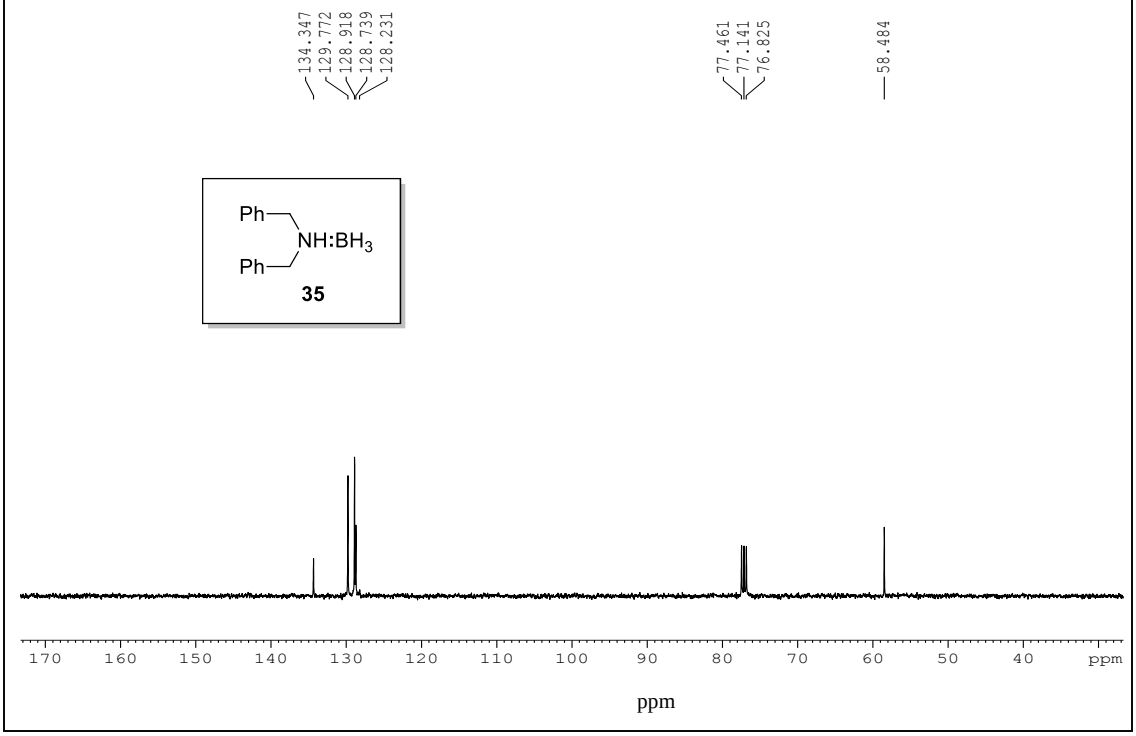

ppm

Spectrum No. 21 (Chapter 2, Section 2.4.9), ^{1}H NMR Spectrum (400 MHz, $CDCl_3$)

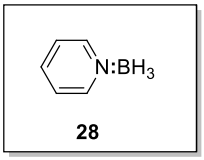

28

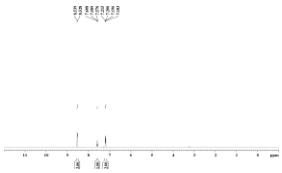

ppm

Spectrum No. 22 (Chapter 2, Section 2.4.9), ^{13}C NMR Spectrum (100 MHz, $CDCl_3$)

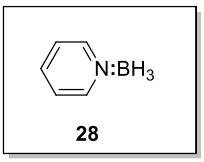

28

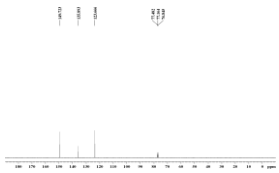

ppm

Spectrum No. 23 (Chapter 2, Section 2.4.10), ^{11}B NMR Spectrum (128.3 MHz, $CDCl_3$)

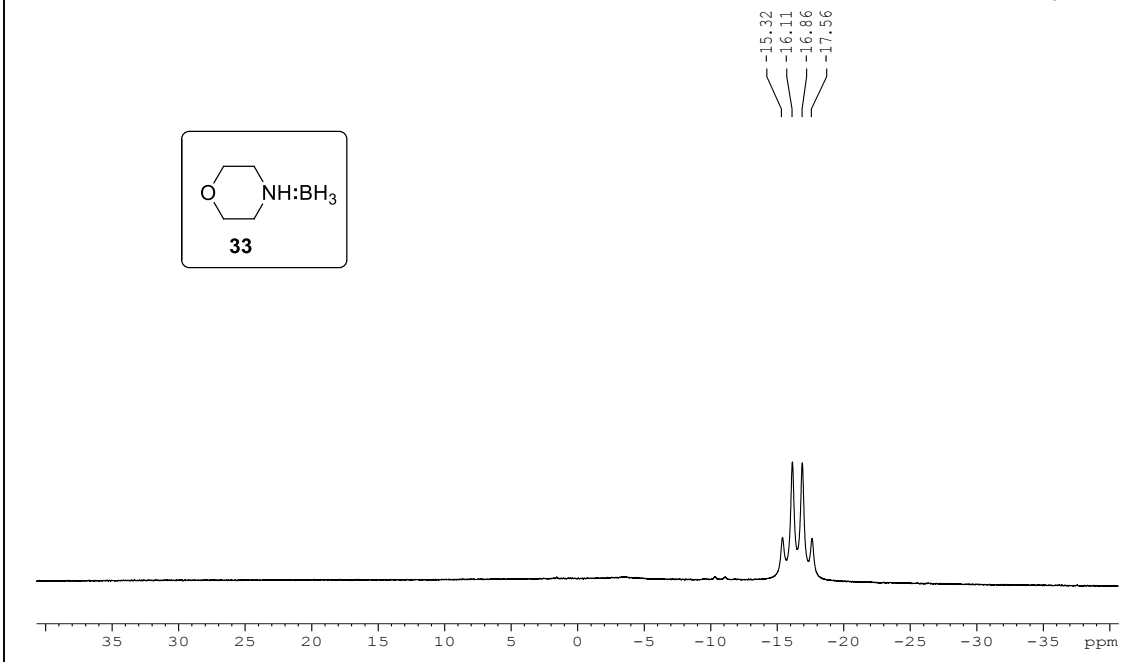

33

ppm

Spectrum No. 24 (Chapter 2, Section 2.4.9), ^{11}B NMR Spectrum (128.3 MHz, $CDCl_3$)

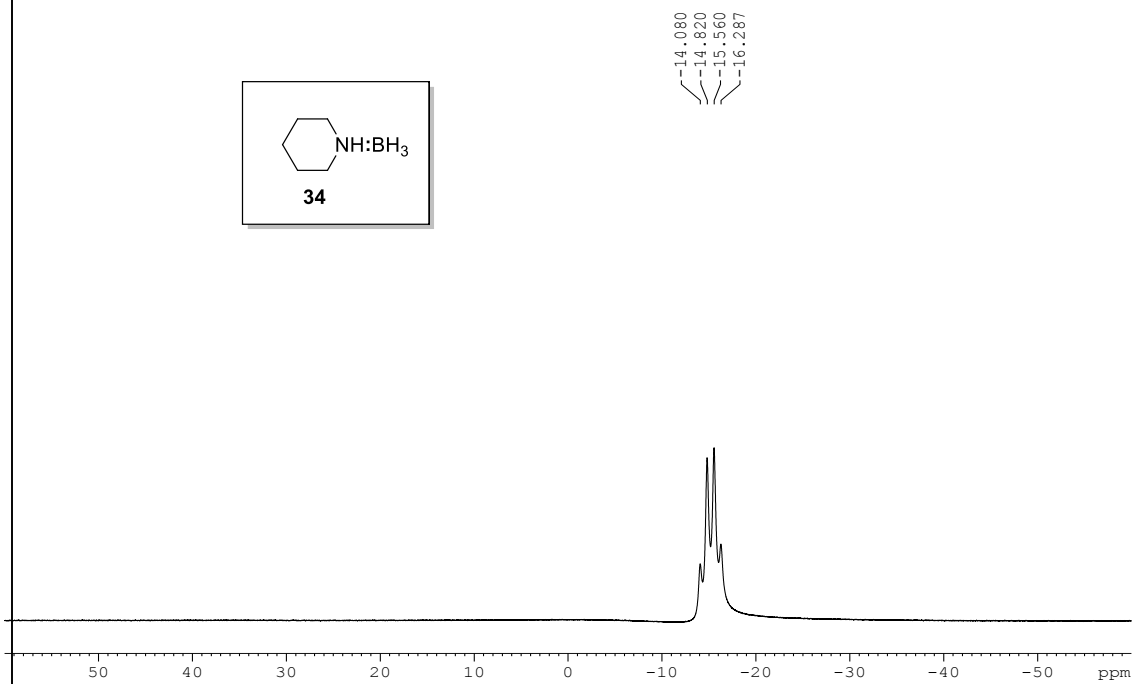

34

ppm

Spectrum No. 25 (Chapter 2, Section 2.4.9), ^{11}B NMR Spectrum (128.3 MHz, $CDCl_3$)

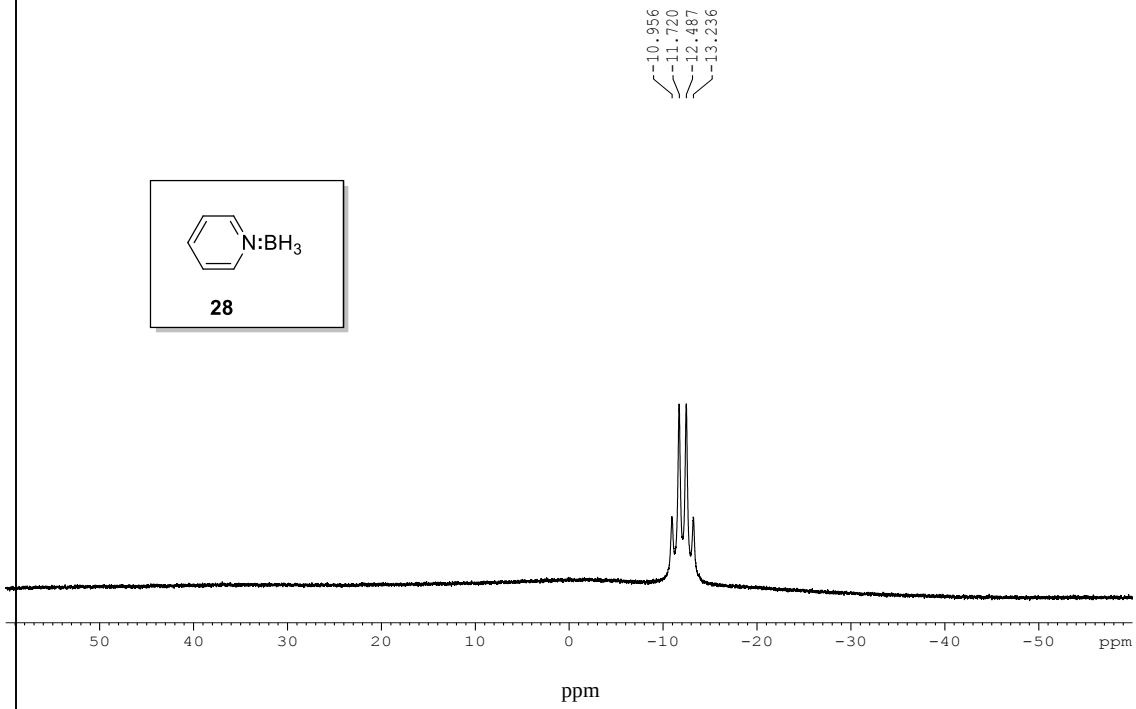

ppm

Spectrum No. 26 (Chapter 2, Section 2.4.10), ^{11}B NMR Spectrum (128.3 MHz, $CDCl_3$)

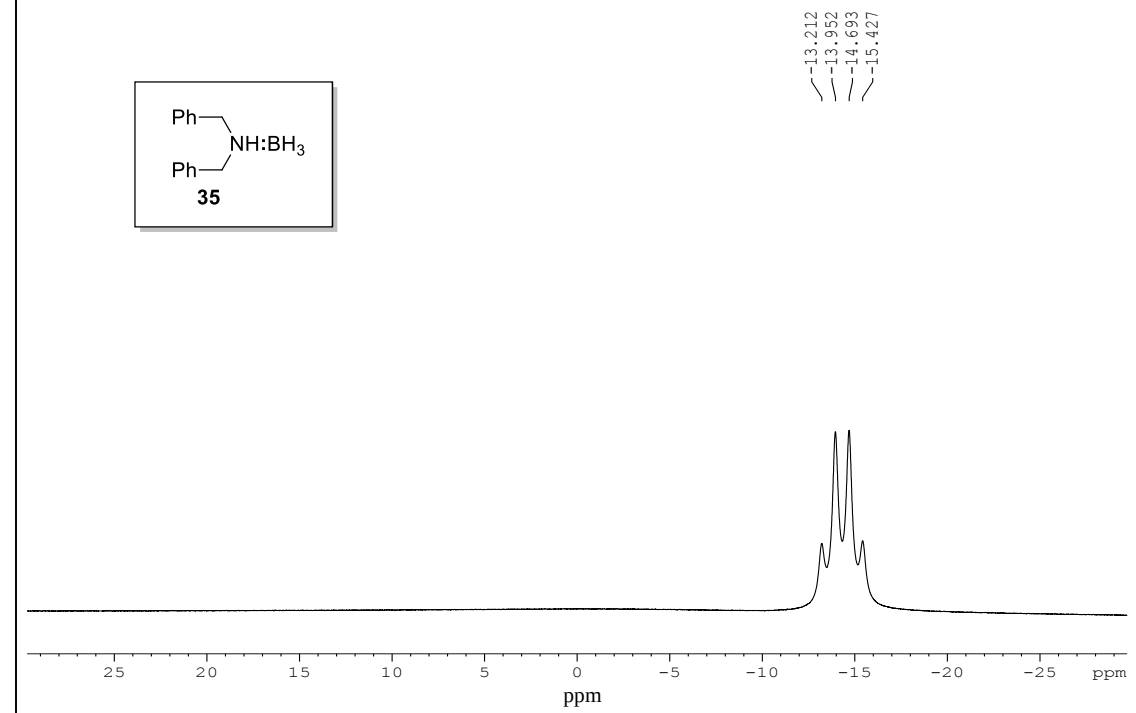

ppm

Spectrum No. 27 (Chapter 3, Section 3.4.2), ^{1}H NMR Spectrum (400 MHz, $CDCl_3$)

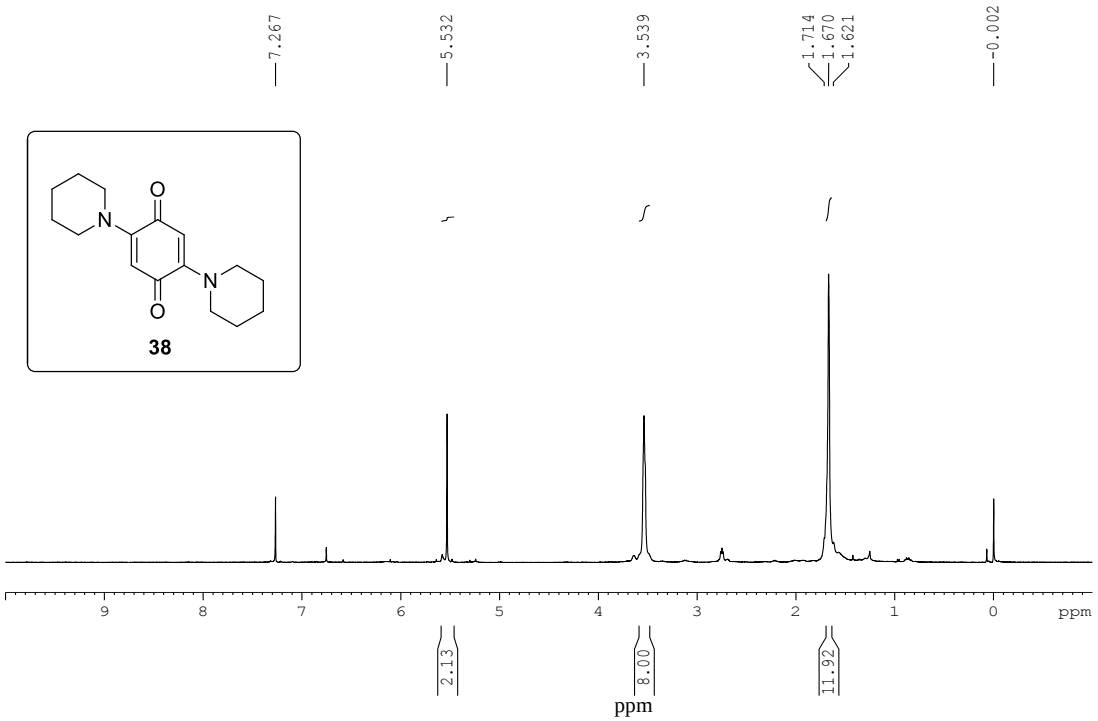

Spectrum No. 28 (Chapter 3, Section 3.4.2), ^{13}C NMR Spectrum (100 MHz, $CDCl_3$)

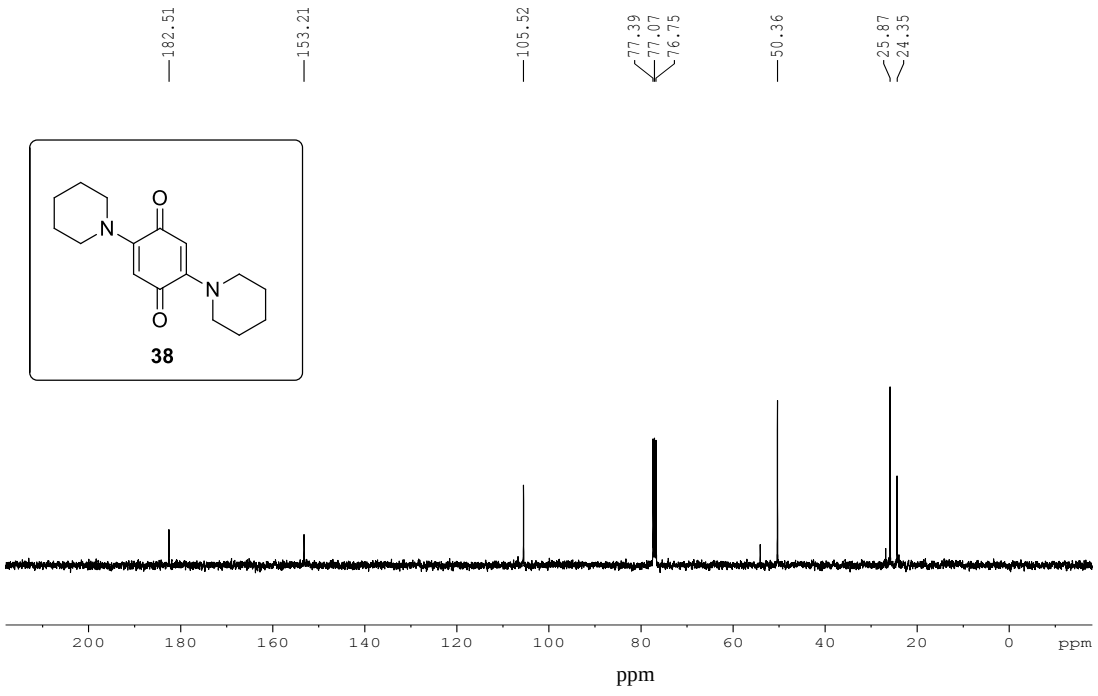

Spectrum No. 29 (Chapter 3, Section 3.4.2), ^{1}H NMR Spectrum (400 MHz, $CDCl_3$)

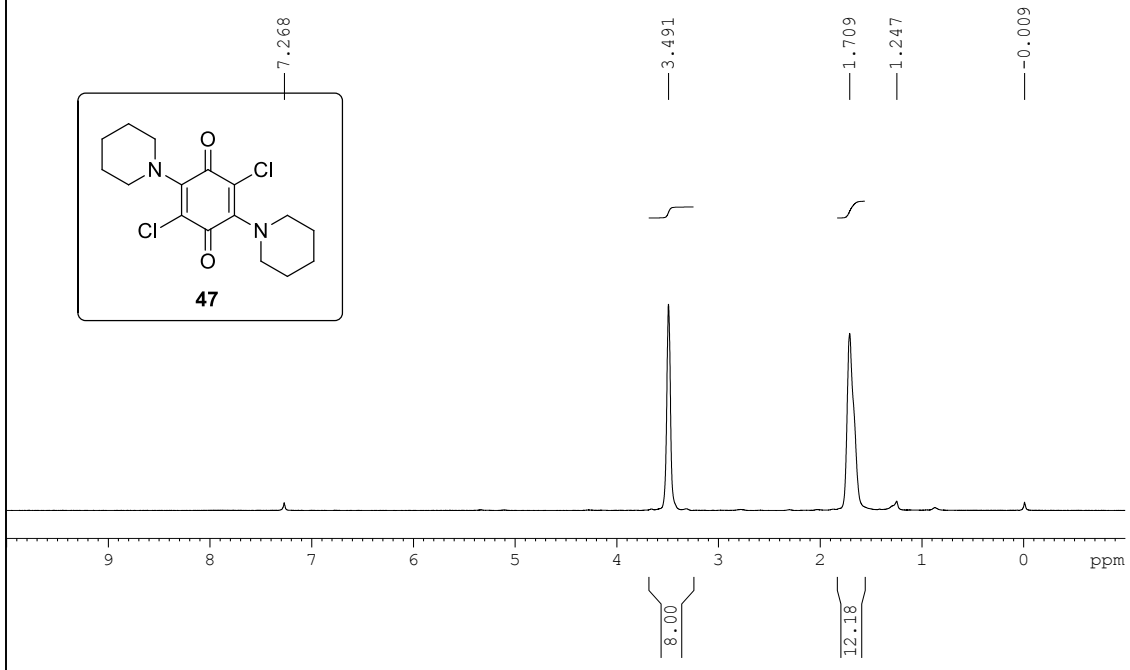

Spectrum No. 30 (Chapter 3, Section 3.4.2), ^{13}C NMR Spectrum (100 MHz, $CDCl_3$)

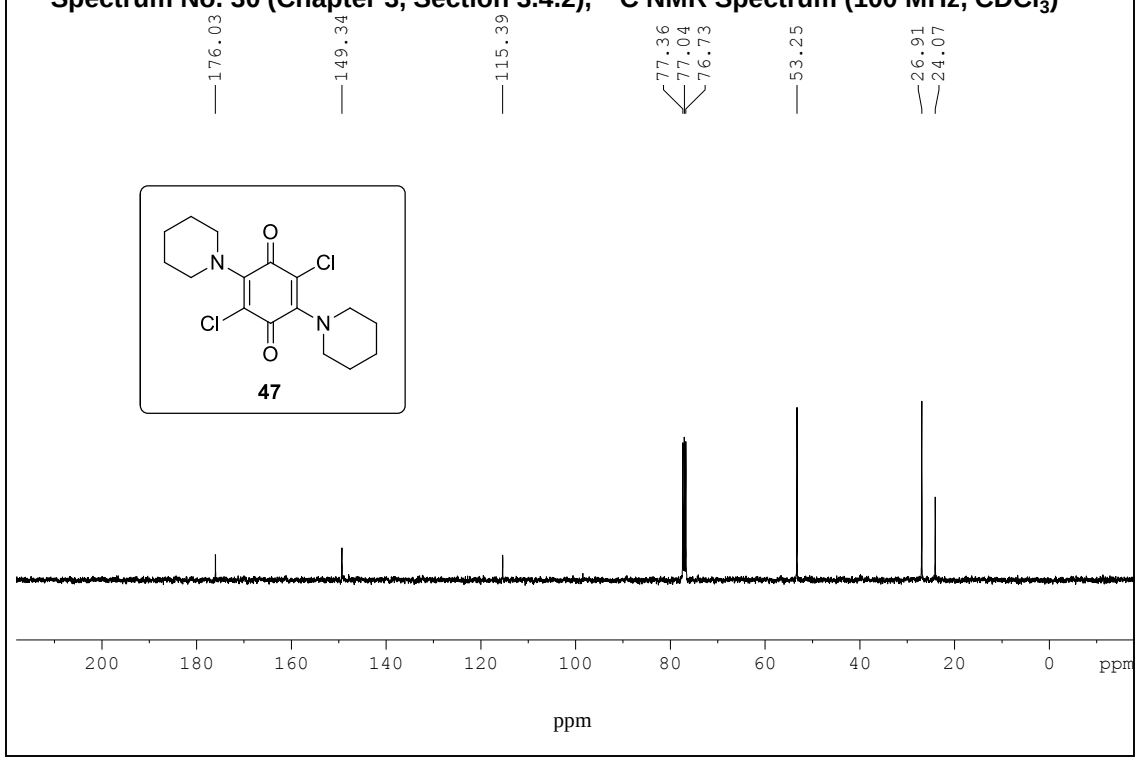

Spectrum No. 31 (Chapter 3, Section 3.4.2), ^{1}H NMR Spectrum (400 MHz, $CDCl_3$)

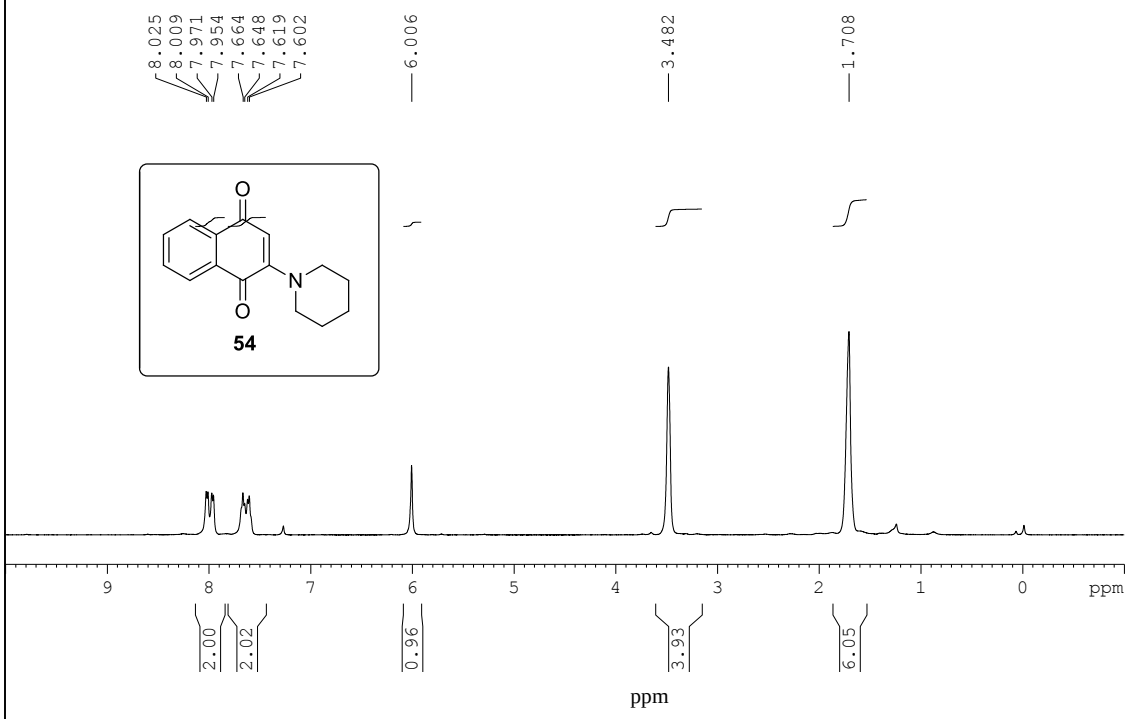

Spectrum No. 32 (Chapter 3, Section 3.4.2), ^{13}C NMR Spectrum (100 MHz, $CDCl_3$)

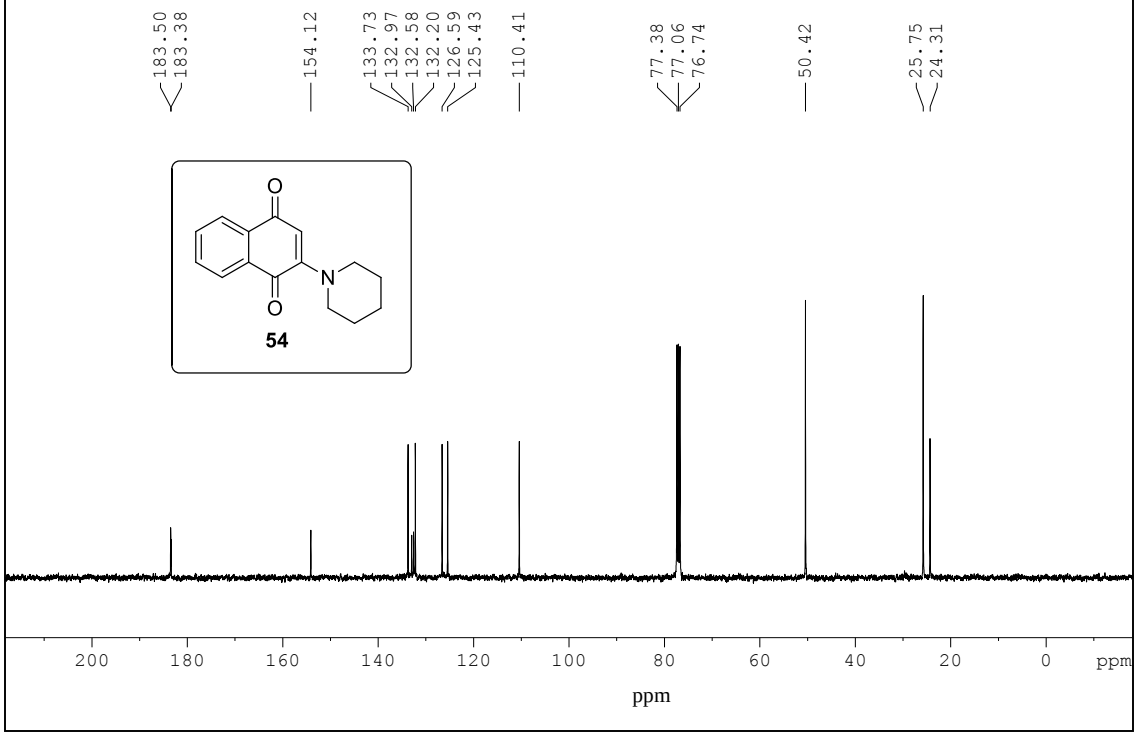

Spectrum No. 33 (Chapter 3, Section 3.4.2), ^{1}H NMR Spectrum (400 MHz, $CDCl_3$)

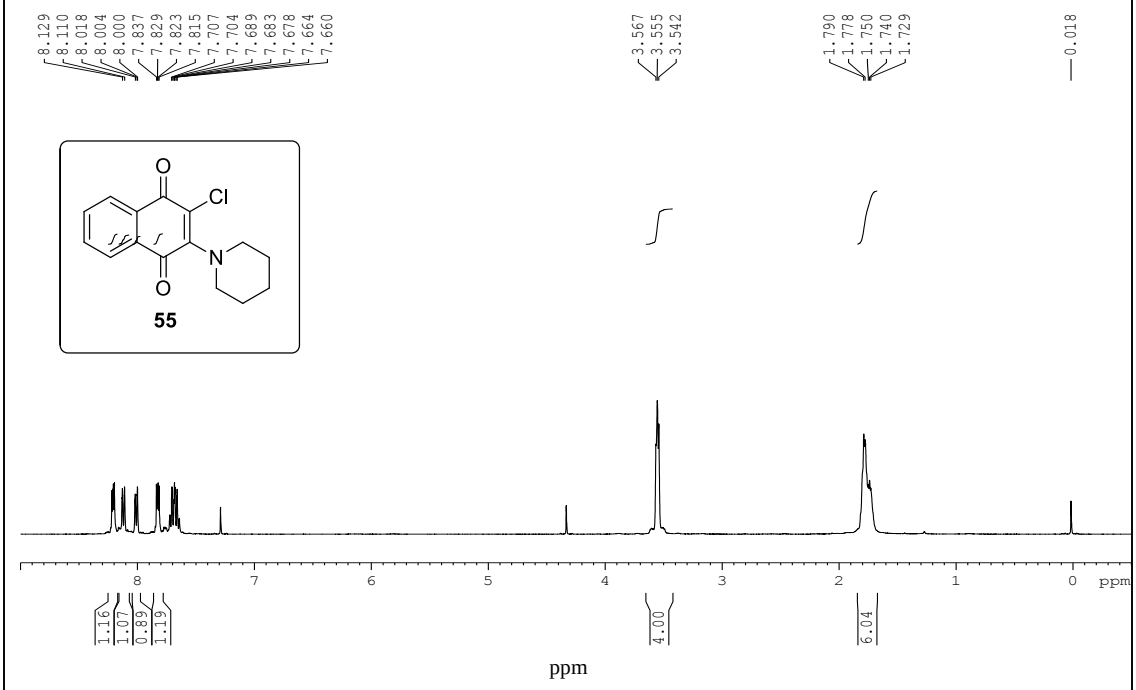

Spectrum No. 34 (Chapter 3, Section 3.4.2), ^{13}C NMR Spectrum (100 MHz, $CDCl_3$)

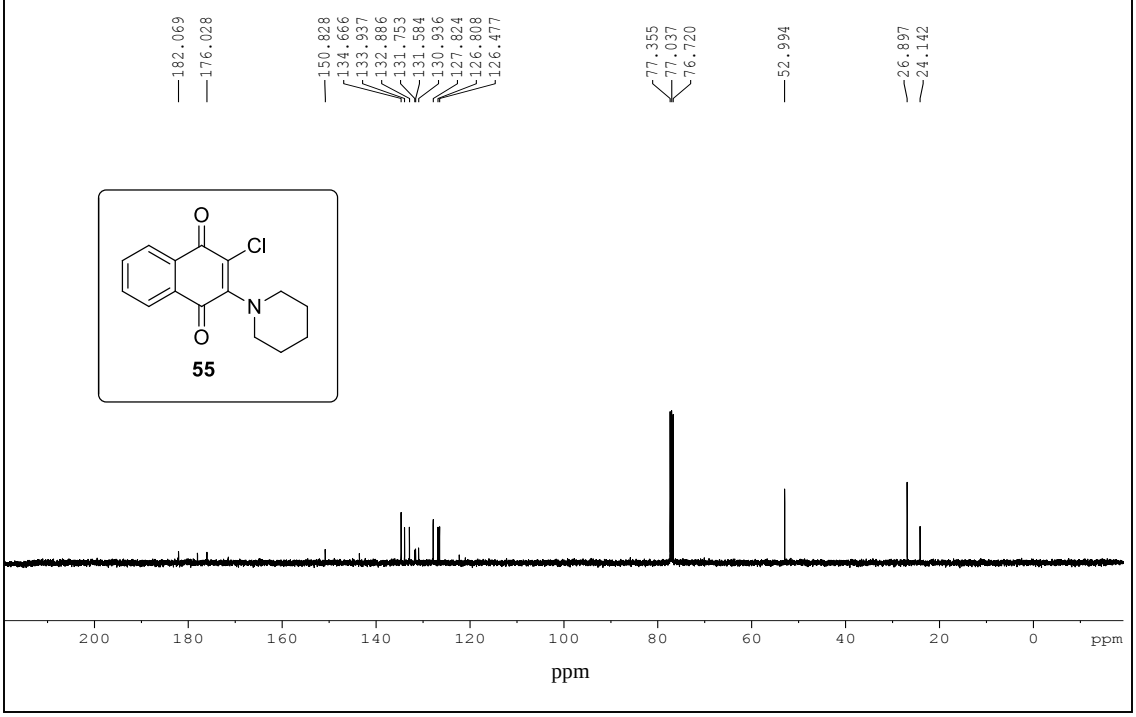

Spectrum No. 35 (Chapter 3, Section 3.4.3), ^{1}H NMR Spectrum (400 MHz, $CDCl_3$)

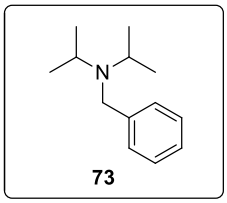

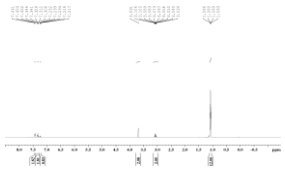

ppm

Spectrum No. 36 (Chapter 3, Section 3.4.3), ^{13}C NMR Spectrum (100 MHz, $CDCl_3$)

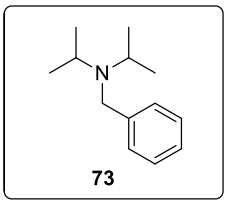

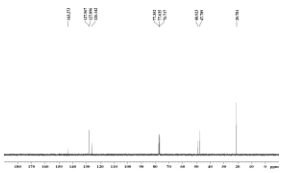

ppm

Spectrum No. 37 (Chapter 3, Section 3.4.4), ^{1}H NMR Spectrum (400 MHz, $CDCl_3$)

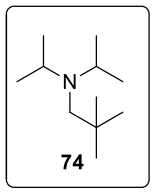

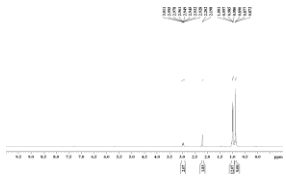

ppm

Spectrum No. 38 (Chapter 3, Section 3.4.4), ^{13}C NMR Spectrum (100 MHz, $CDCl_3$)

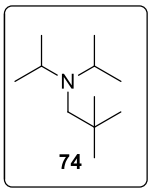

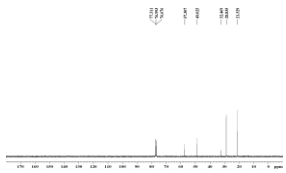

ppm

Spectrum No. 39 (Chapter 3, Section 3.4.9), ^{1}H NMR Spectrum (400 MHz, $CDCl_3$)

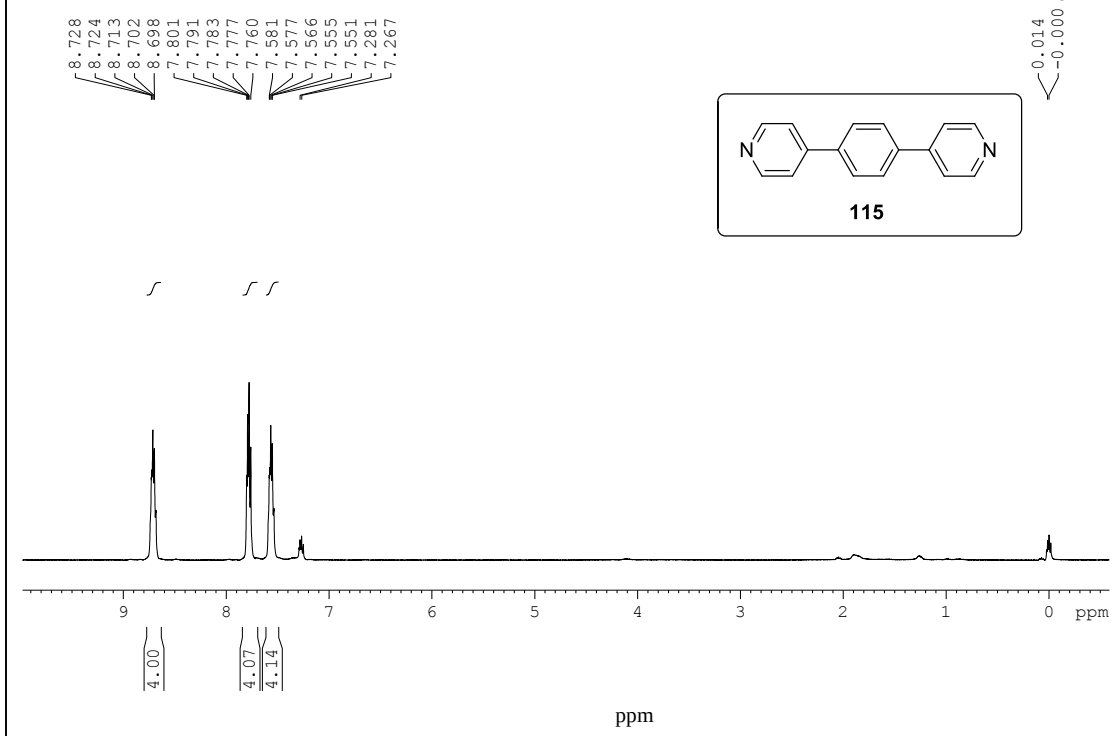

ppm

Spectrum No. 40 (Chapter 3, Section 3.4.9), ^{13}C NMR Spectrum (100 MHz, $CDCl_3$)

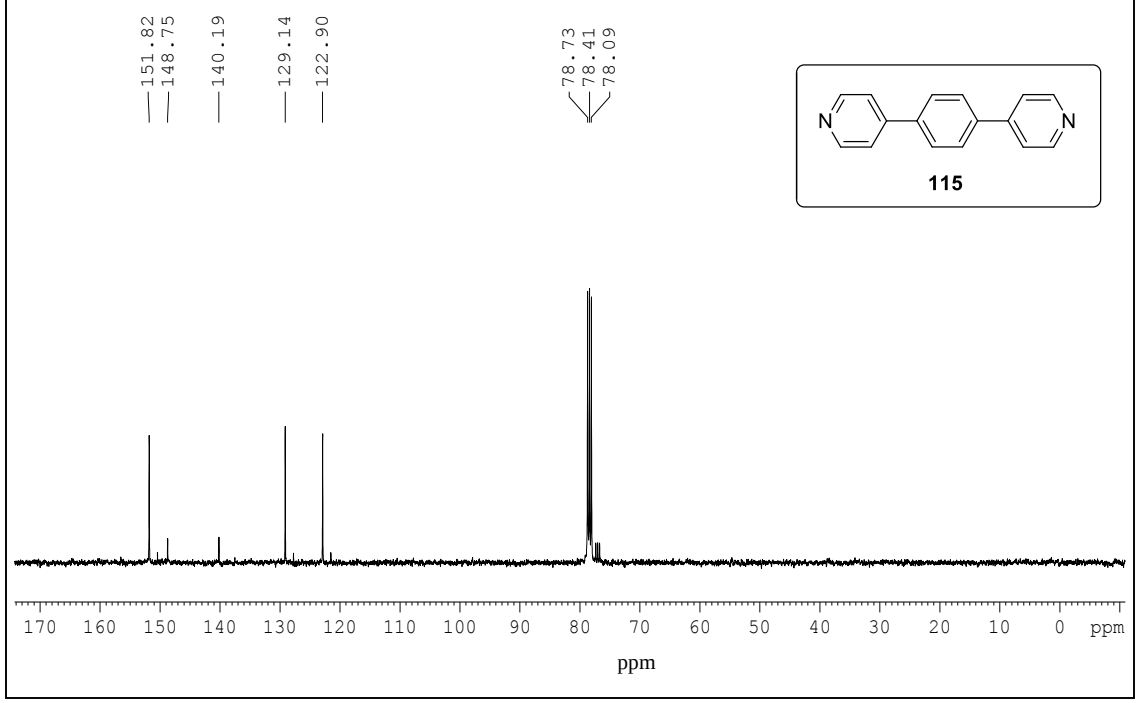

ppm

Spectrum No. 41 (Chapter 3, Section 3.4.10), ^{1}H NMR Spectrum (400 MHz, D_2O)

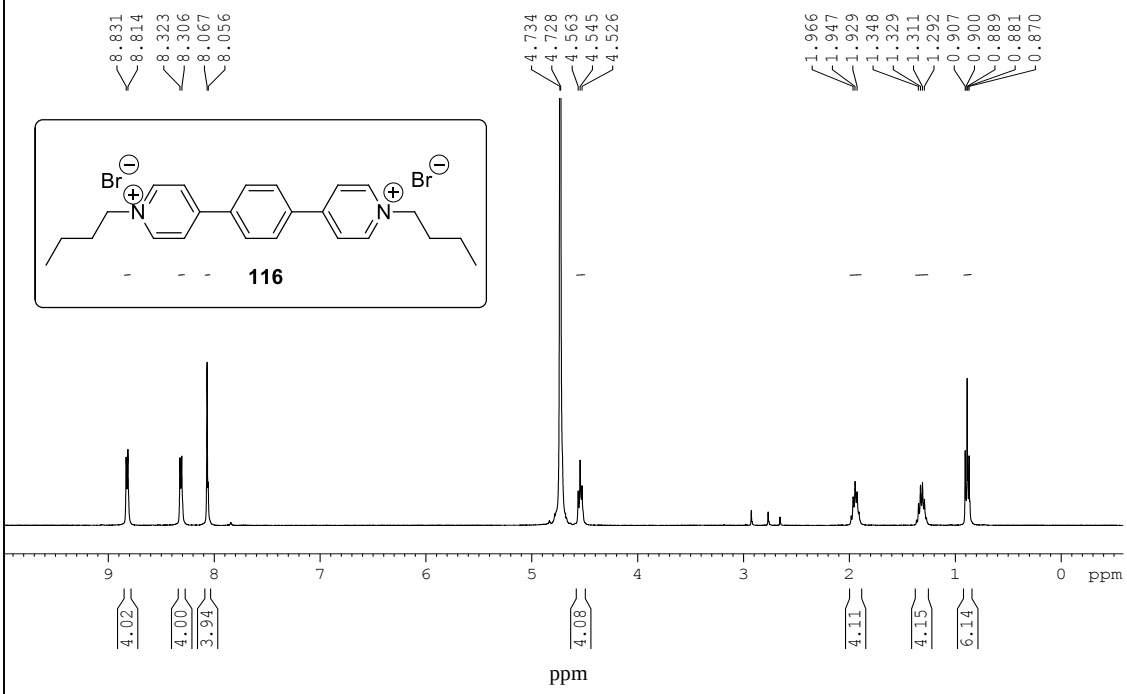

Spectrum No. 42 (Chapter 3, Section 3.4.10), ^{13}C NMR Spectrum (100 MHz, D_2O)

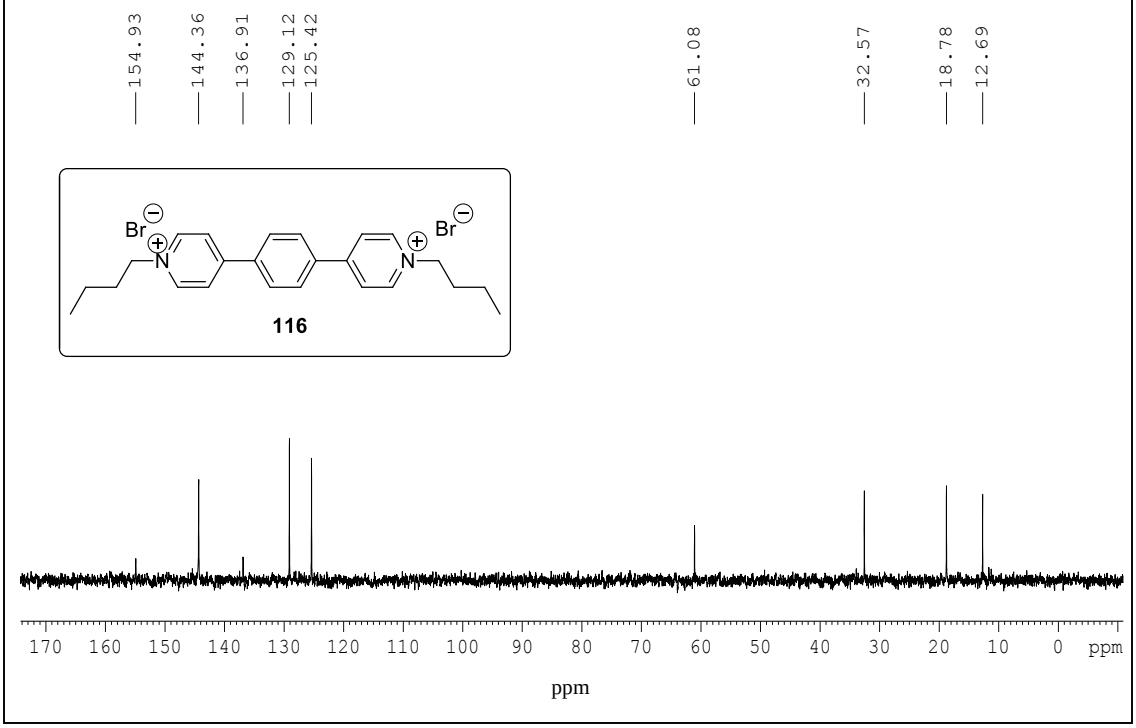

Development of Synthetic Methods and Electrochemical Cells Based on Organic Electron Transfer Reactions

by Shanmugaraja Masilamani

Chapter 1

General Introduction on Electron Transfer Reactions

1.1 Introduction

Electron transfer reactions involving the transfer of an electron from donor to an acceptor are very important in chemistry and biology.[1] These reactions can occur both thermally and photochemically.[2] The electrochemical reaction take place by single electron transfer (SET) processes. The SET process also occurs in many biological transformations involving photosynthesis,[3] cytochromes,[4] ferredoxin,[5] rubredoxin[6] etc. The electron transfer reactions are also very important in the functions of semiconductors,[7] conducting polymers[8] and photovoltaics.[9] A brief review on the organic electron transfer reactions would facilitate the discussion.

1.1.1 Redox reactions through electron transfer

Ceric ammonium nitrate $(NH_4)_2[Ce(NO_3)_6]$ (CAN) is unique one electron oxidant.[10] Oxidation of benzyl alcohol **1** with CAN **2** gives radical cation which in presence of water affords benzaldehyde **3** in 87% yield (Scheme 1).[11]

Scheme 1

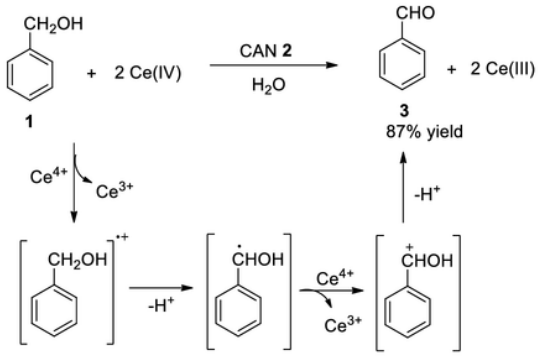

Oxidation of primary and secondary benzylic alcohols **4** with catalytic amount of CAN and stoichiometric amount of $NaBrO_3$ gives the corresponding aldehydes or ketones **5** in good yields (Scheme 2).[12]

Scheme 2

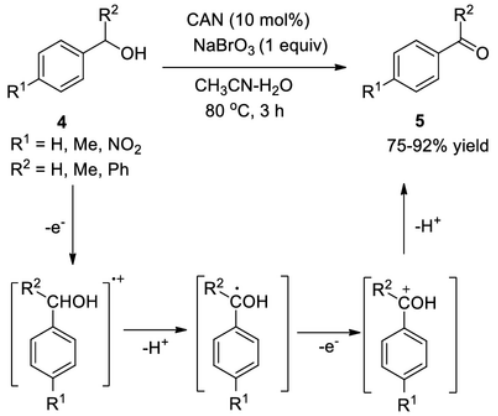

Reaction of 1,4-dimethoxy-2,3,5,6-tetramethyl benzene **6** with CAN in presence of isotopically enriched water gives isotopically labelled duroquinone **7** through a SET process (Scheme 3).[13]

Scheme 3

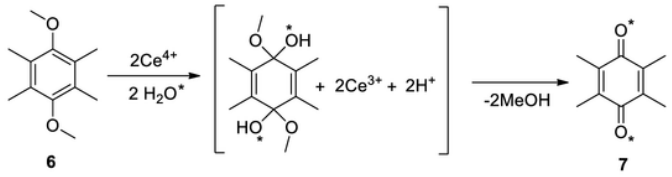

Reaction of naphthalene derivatives with ceric ammonium sulphate (CAS) **9** gives the corresponding naphthoquinones **10** and **11** in moderate to good yields (up to 95 yield).[14] The transformation involves radical cations and rearrangements were observed when the 1, 4-positions was substituted with D or Ph group.[14]

Scheme 4

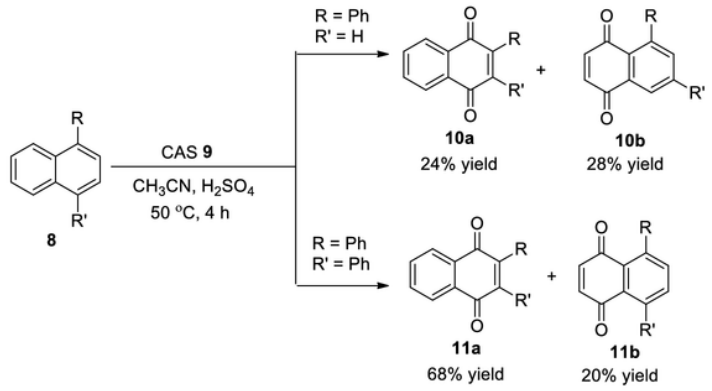

Mechanism:

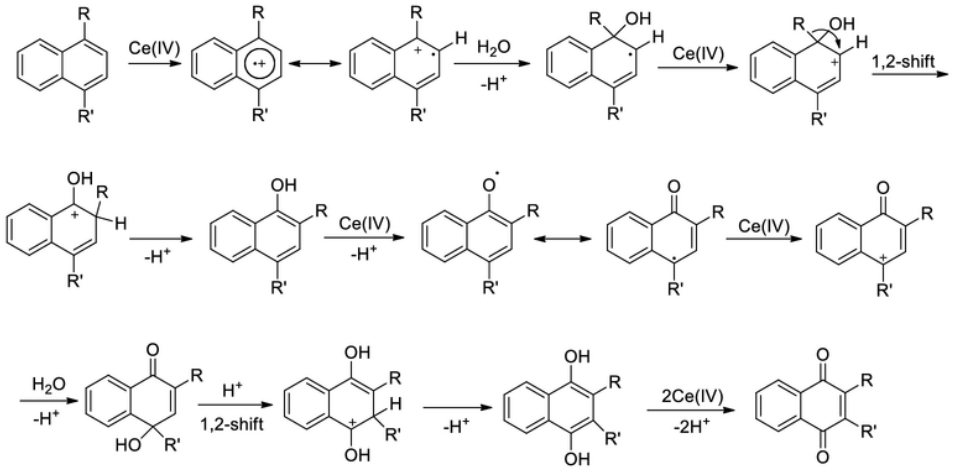

Recently, several organic transformations were reported using ceric ammonium nitrate (CAN) which go through single electron transfer reactions. Some of the reactions are outlined in Chart 1.

Chart 1

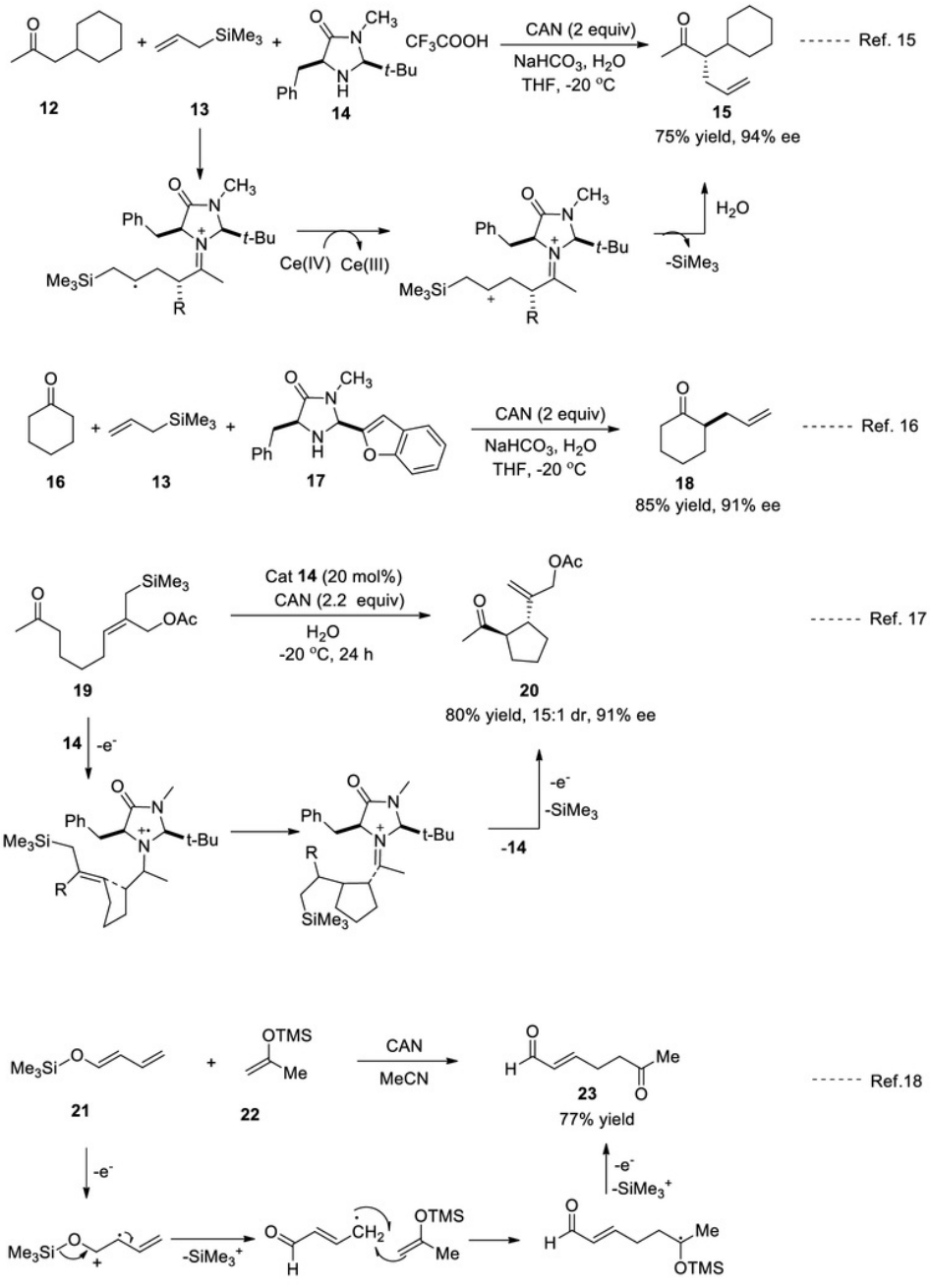
12
13
14
CF3COOH
CAN (2 equiv)
NaHCO3, H2O
THF, -20 °C
15
75% yield, 94% ee
------ Ref. 15
Ce(IV) Ce(III)
H2O
-SiMe3
16
17
18
85% yield, 91% ee
------ Ref. 16
Cat 14 (20 mol%)
CAN (2.2 equiv)
H2O
-20 °C, 24 h
19
20
80% yield, 15:1 dr, 91% ee
------ Ref. 17
14 -e-
-e-
-SiMe3
-14
21
22
CAN
MeCN
23
77% yield
------ Ref.18
-e-
-SiMe3+
-SiMe3+

Chart 1 (continued.)

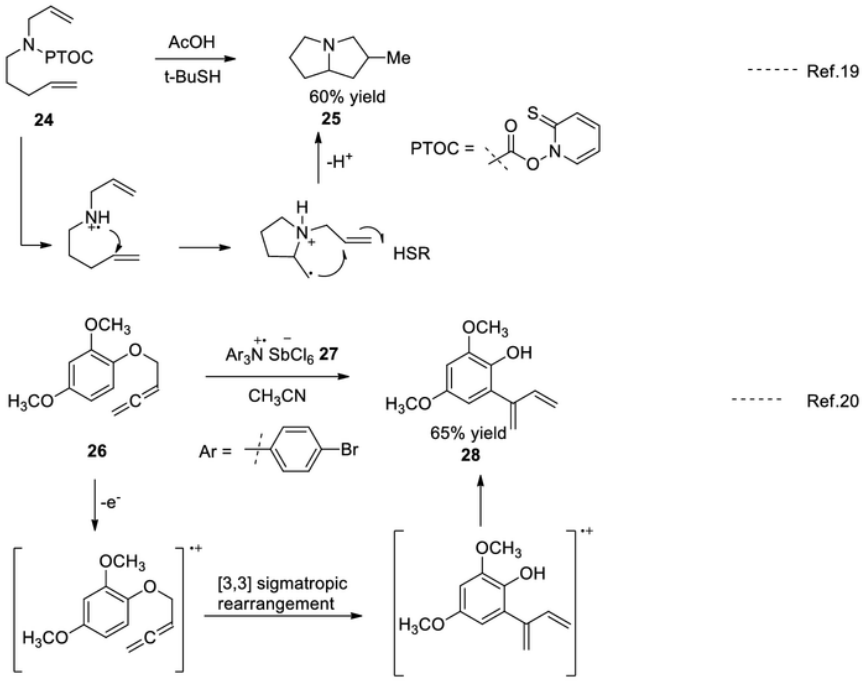

1.1.2 Electrochemical reactions through electron transfer

Kolbe reaction is an anodic oxidation of carboxylate leading to the formation of hydrocarbon dimers *via* the intermediacy of alkyl radicals (Scheme 5).[21]

Scheme 5

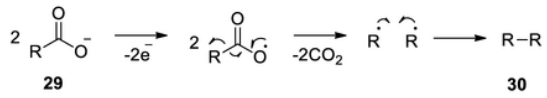

A number of natural products were synthesized *via* anodic oxidation of organic compounds (chart 2).

Chart 2

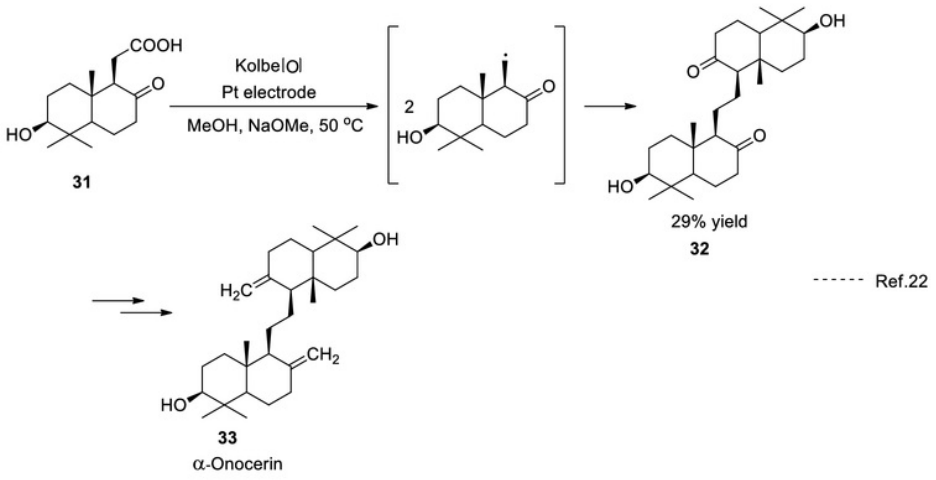

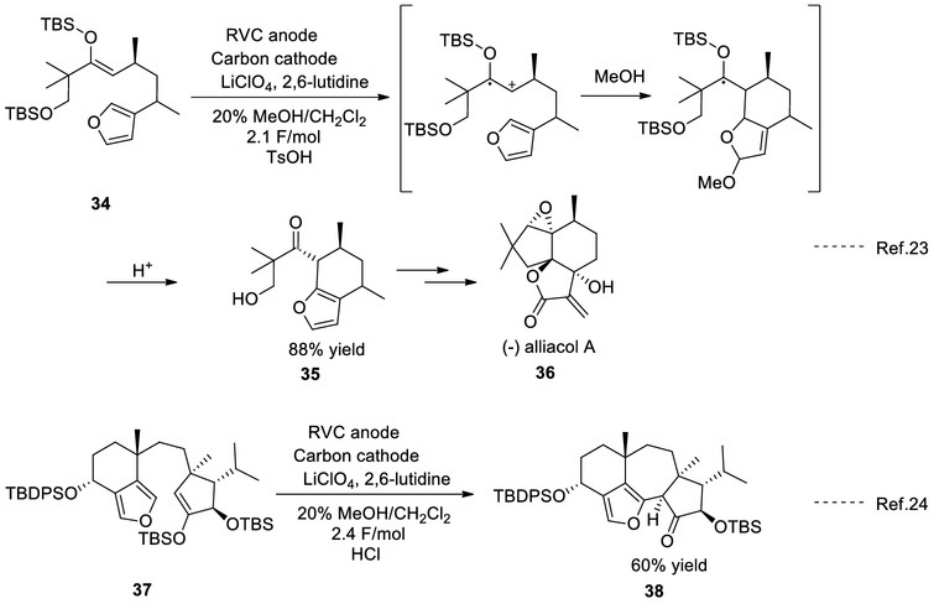

The electrochemical oxidation is also an important tool for C-H functionalization and nucleophilic functionalization of arenes (Chart 3).

Chart 3

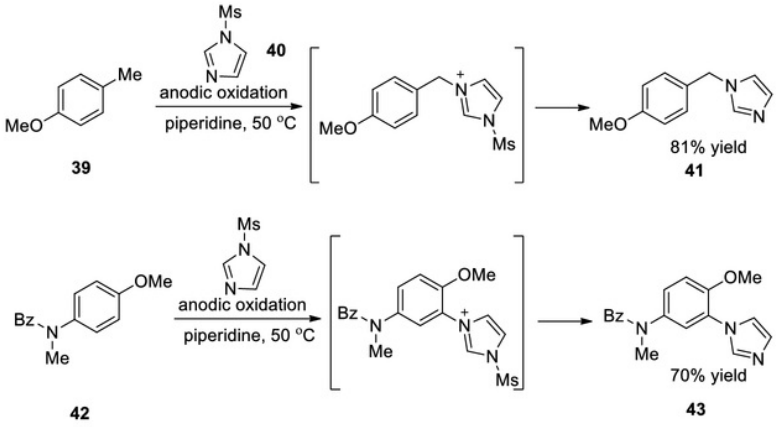
Ms
40
Me
MeO
anodic oxidation
piperidine, 50 °C
39
MeO
Ms
MeO
81% yield
41
Ref.25
Ms
OMe
Bz
N
Me
anodic oxidation
piperidine, 50 °C
42
OMe
Bz
N
Me
Ms
OMe
Bz
N
Me
70% yield
43

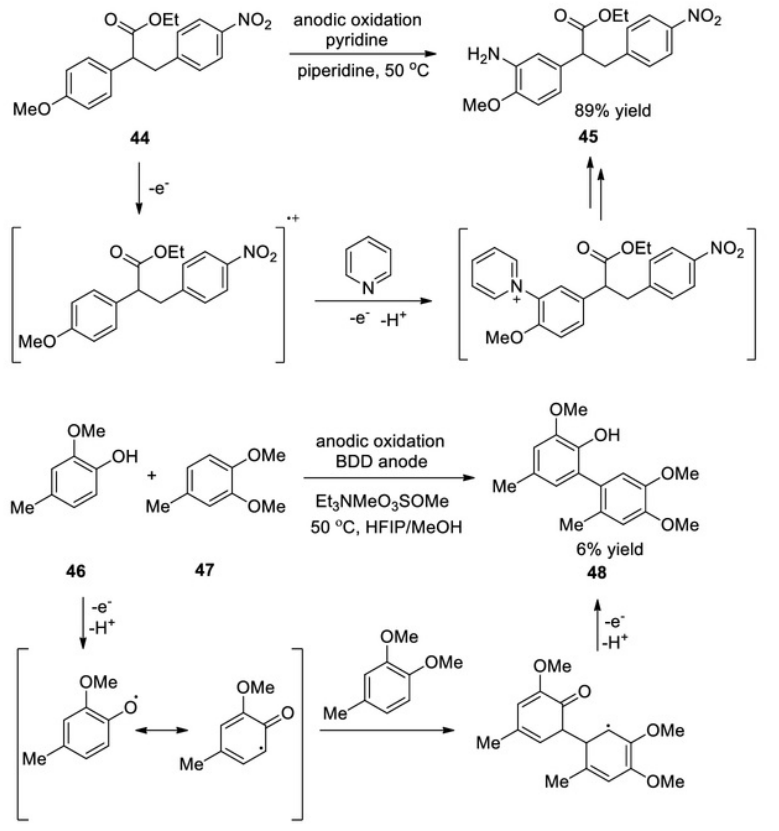
O
OEt
NO2
MeO
anodic oxidation
pyridine
piperidine, 50 °C
44
H2N
MeO
89% yield
45
Ref.26
-e-
-e- -H+
OMe
OH
Me
+
OMe
Me
OMe
anodic oxidation
BDD anode
Et3NMeO3SOMe
50 °C, HFIP/MeOH
OMe
OH
Me
OMe
Me
OMe
6% yield
46
47
48
-e-
-H+
Ref.27
OMe
Me
OMe
O
Me
OMe
Me
OMe

Chart 3 (continued.)

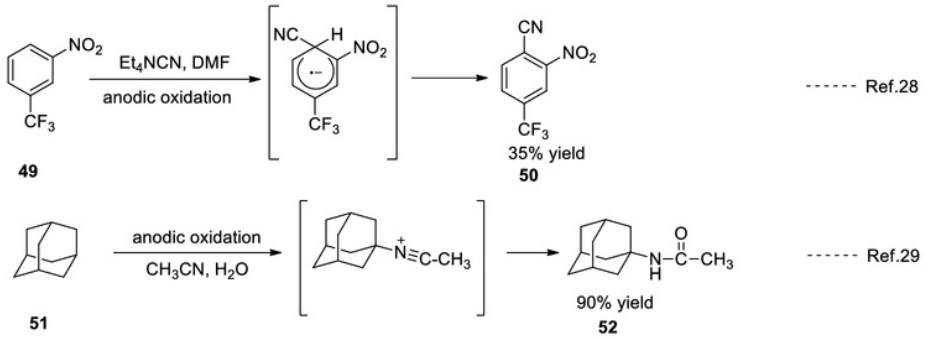

49 50 51 52

Also, the anodic oxidation was widely used in the oxidation of allylic systems (Chart 4).

Chart 4

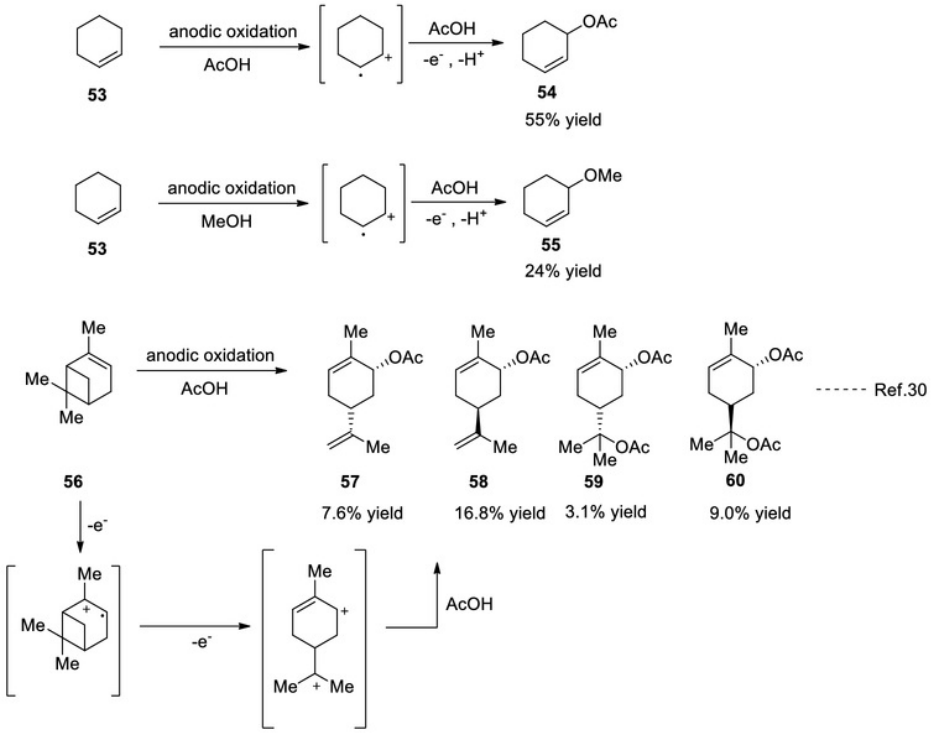

53 54 55% yield

53 55 24% yield

56 57 58 59 60

Chart 4 (Continued.)

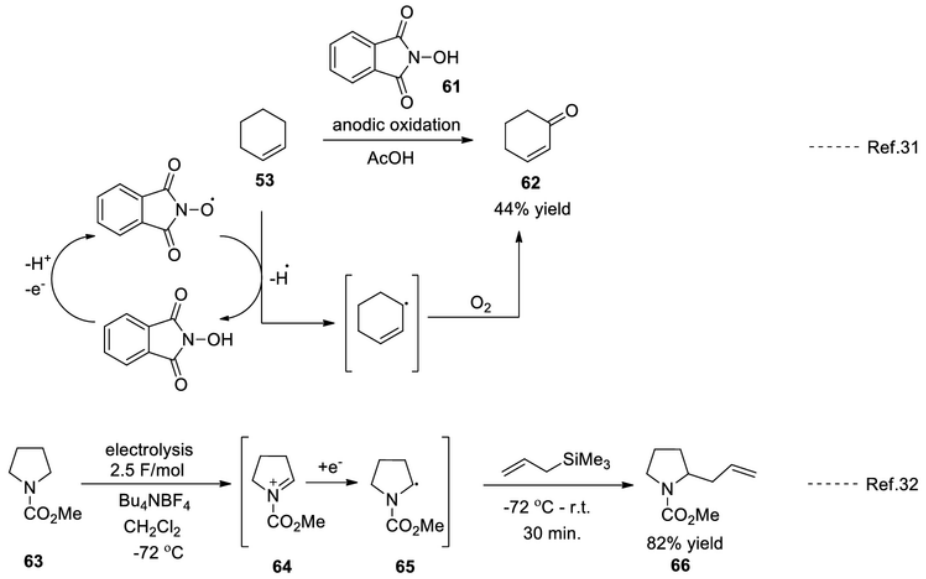

Similarly, cathodic reduction of organic compounds was also widely used in organic synthesis, especially for reductive coupling of carbonyl compounds (Chart 5).

Chart 5

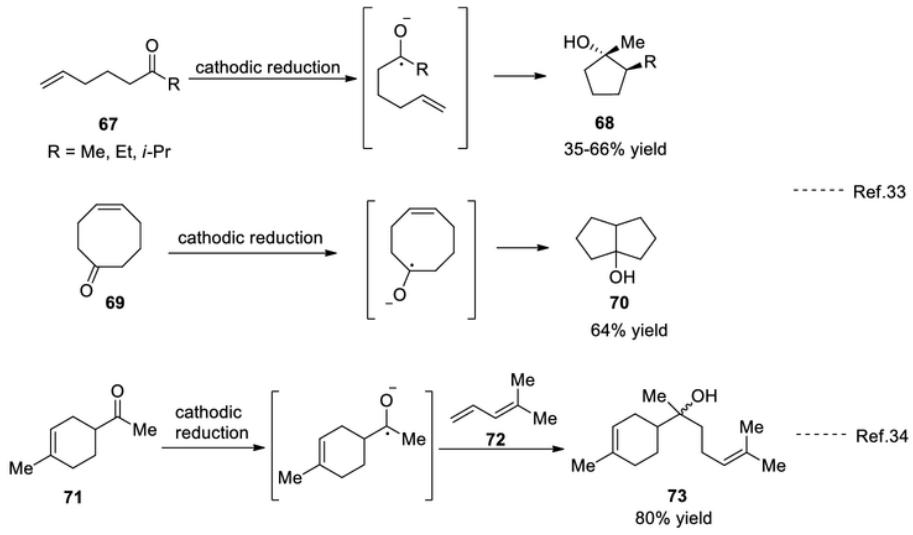

1.1.3 Photochemical electron transfer reactions

Photochemical reactions are performed by absorption of visible or ultraviolet light. For example, a metal complex, such as $Ru(bpy)_3Cl_2$ absorbs light at 452 nm with a high molar extinction coefficient (ε = 14,600 M^{-1} cm^{-1}) and it is widely used as a photo catalyst in organic synthesis. Some important photochemical electron transfer reactions are shown in Chart 6.

Chart 6

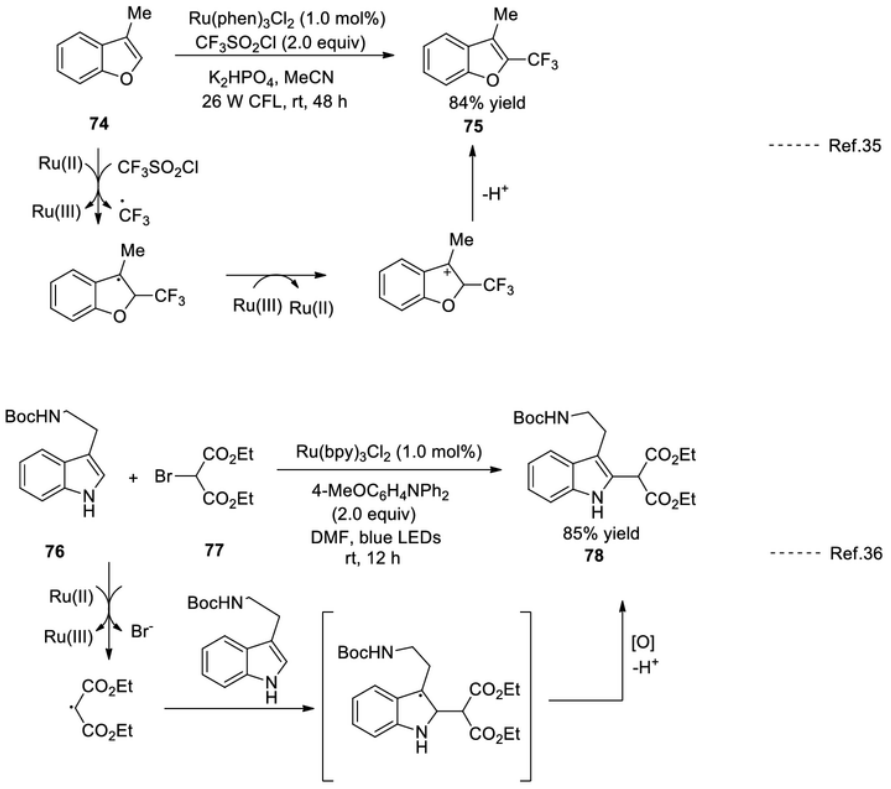

Chart 6 (continued.)

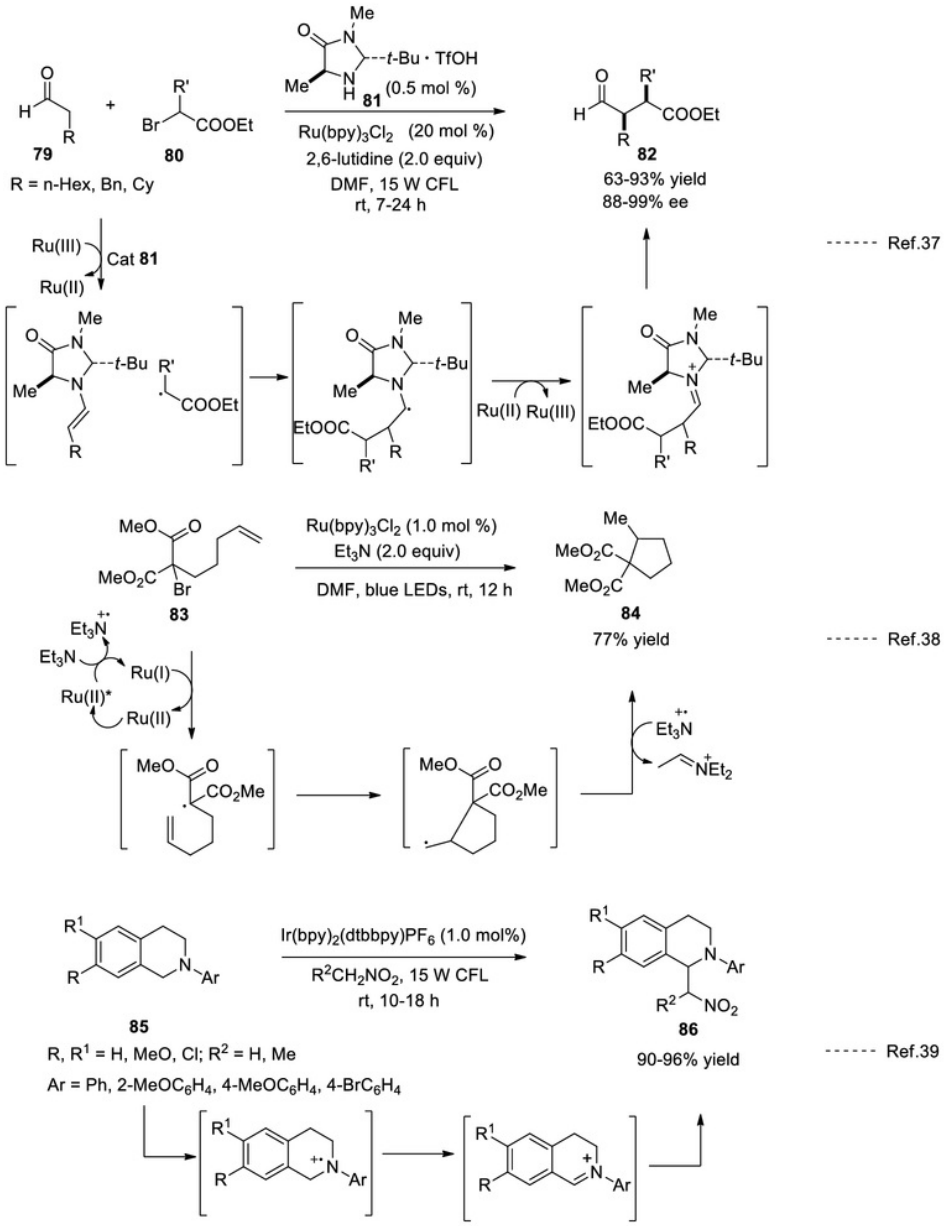

Chart 6 (continued.)

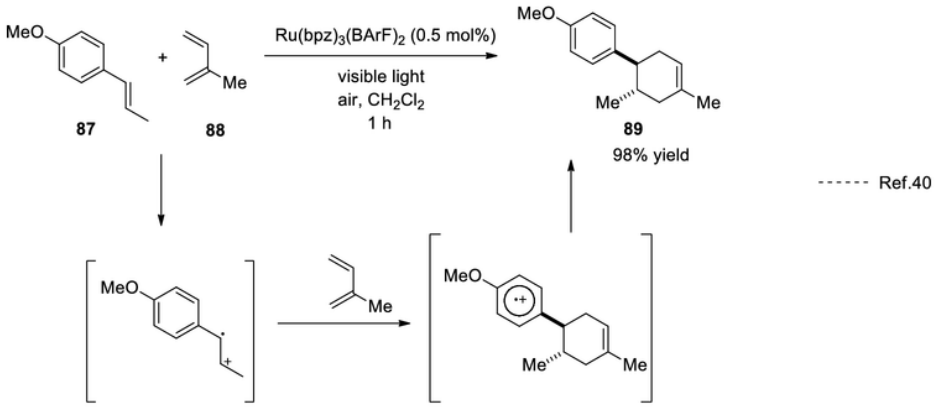

1.1.4 SET reactions in organic chemistry

In the 1970s, there were several reports on the formation of the radical cation/radical anion pair intermediates in several popular organic reactions. A brief review of the literature would facilitate the discussion.

1.1.4.1 SET reactions in aromatic nucleophilic substitution reaction

The unimolecular aromatic nucleophilic substitution ($S_{RN}1$) reaction involves SET process. The halide (X) substituent in aromatic compound **90** is replaced by a nucleophile through free radical intermediates leading to the substitution product **91** (Scheme 6).

Scheme 6

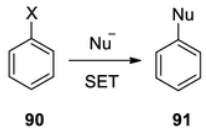

For example, the reaction of iodobenzene **92** with KNH_2 in liquid ammonia gives the substitution product **96** through a SET mediated S_NAr reaction (Scheme 7).[41]

Scheme 7

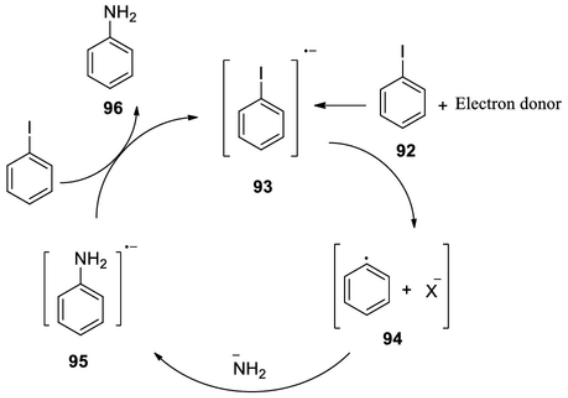

1.1.4.2 SET reactions in acyloin condensation

Other major reactions which involve single electron transfer are acyloin condensation and Birch reduction. For example, the reaction of carboxylic ester **97** with sodium proceeds through single electron transfer from Na to an ester and gives a radical anion **98**. The dimerized compound **98** gives 1,2-diketone **99** which again undergoes further SET process to afford the acyloin product **102** (Scheme 8).[42]

Scheme 8

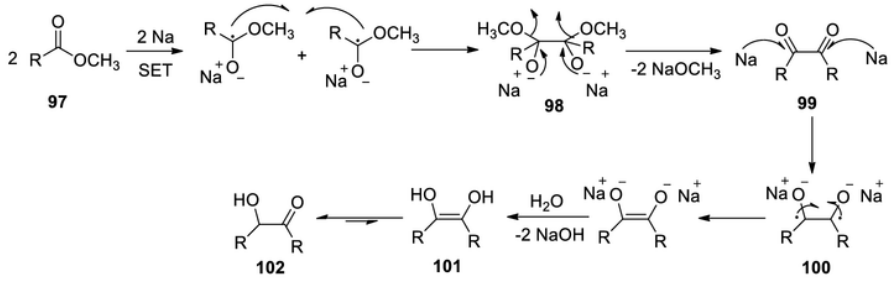

1.1.4.3 SET reactions in Birch reduction

The Birch reduction of substituted benzenes to the corresponding unconjugated cyclohexadienes using Na metal in liquid ammonia involves single electron transfer sequence of reactions (Scheme 9).[43]

Scheme 9

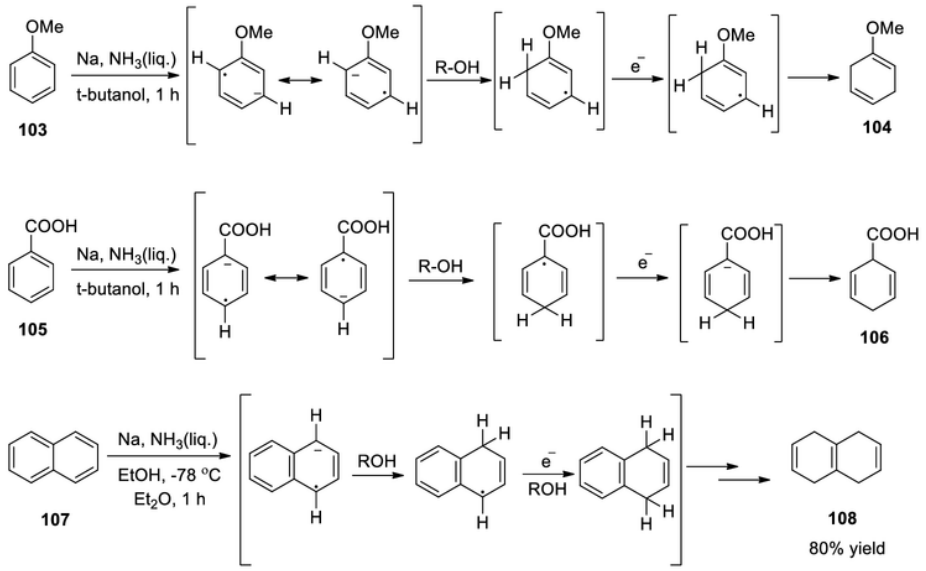

1.1.4.4 SET reactions in Grignard reagent formation

Organomagnesium reagents (RMgX) are very important in organic synthesis. The reaction of an organic halide with magnesium results in Grignard reagent through a SET process (Scheme 10).[44]

Scheme 10

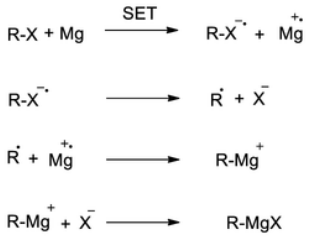

Aldehyde or ketone reacts with organomagnesium halide (Grignard reagent) to form secondary or tertiary alcohol. Polar and SET mechanisms are possible in Grignard reactions (Scheme 11).[45,46]

Scheme 11

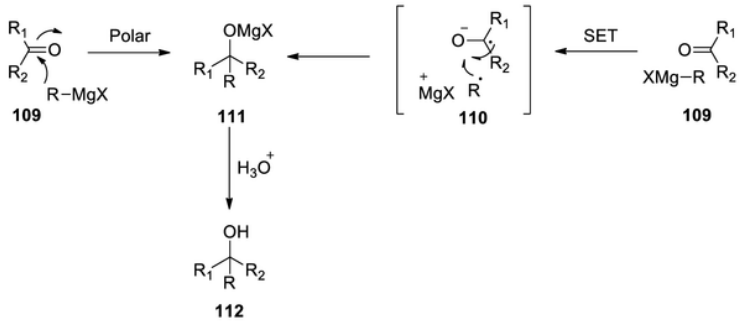

The benzophenone **113** reacts with *t*-butyl magnesium chloride **114** to give the benzophenone ketyl radical anion **115** and alkyl radical **116** which combine to afford tertiary alcohol **117** or to give a pinacol **118** and hydrocarbon **119** (Scheme 12).

Scheme 12

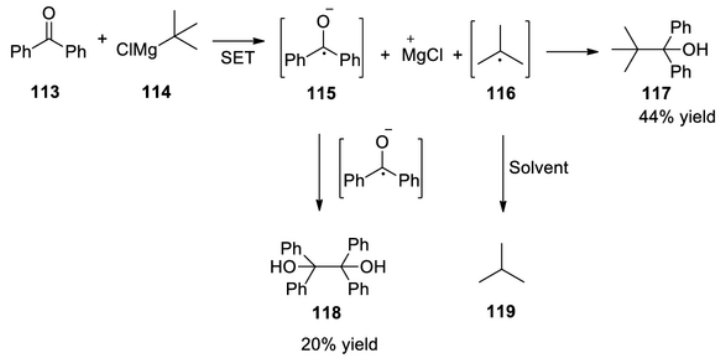

The reaction of neopentylmagnesium chloride **120** with benzophenone **113** gives the corresponding alcohol **121** and pinacol **118** (Scheme 13). EPR spectral analysis confirms that the reaction goes *via* a SET mechanism.[47]

Scheme 13

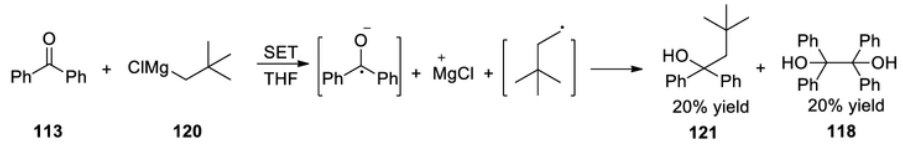

Ashby and coworkers investigated the single electron transfer (SET) pathway in Grignard reactions, reduction of primary halide by metal hydrides, Aldol condensation, Meerwein-Pondorff-Varley reduction, Cannizzaro reaction and Claisen condensation reaction. Evidences were presented for mechanisms involving radical intermediates (Chart 7).[48a]

Chart 7

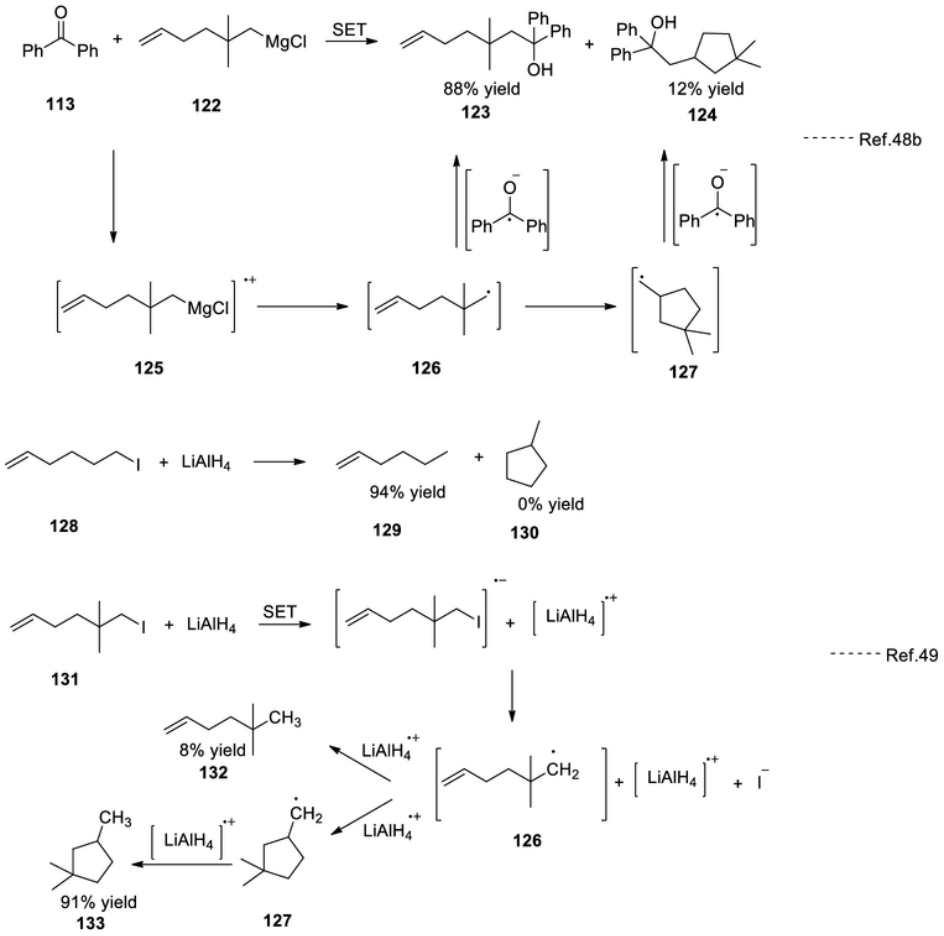

Chart 7 (continued.)

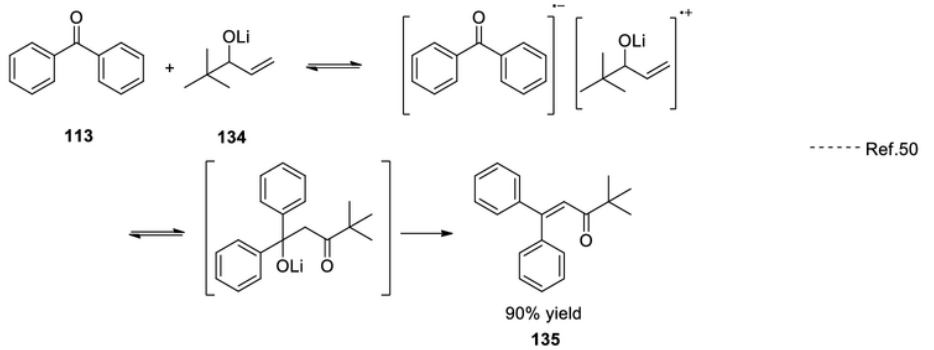

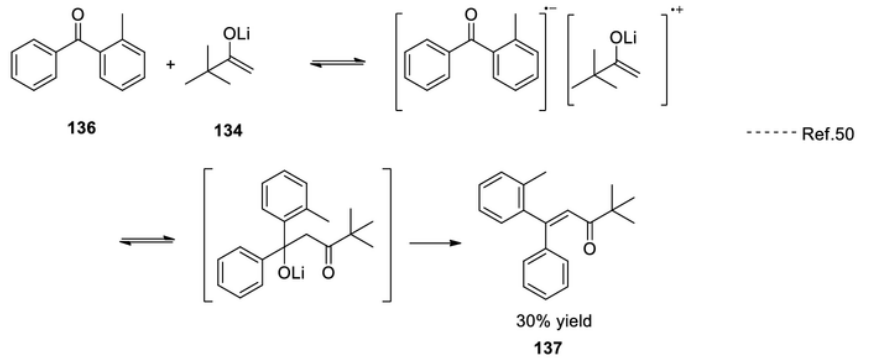

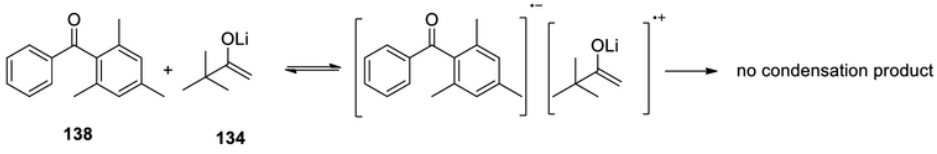

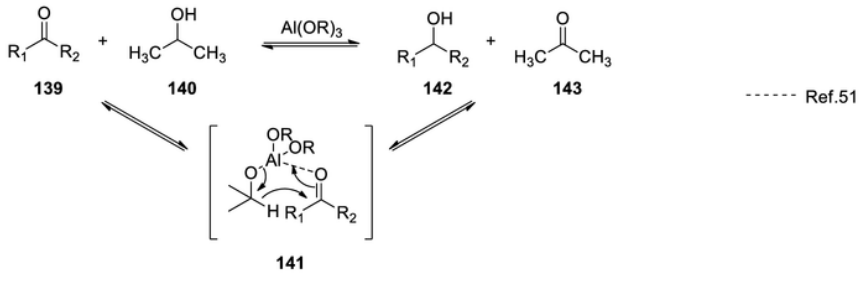

Chart 7 (continued.)

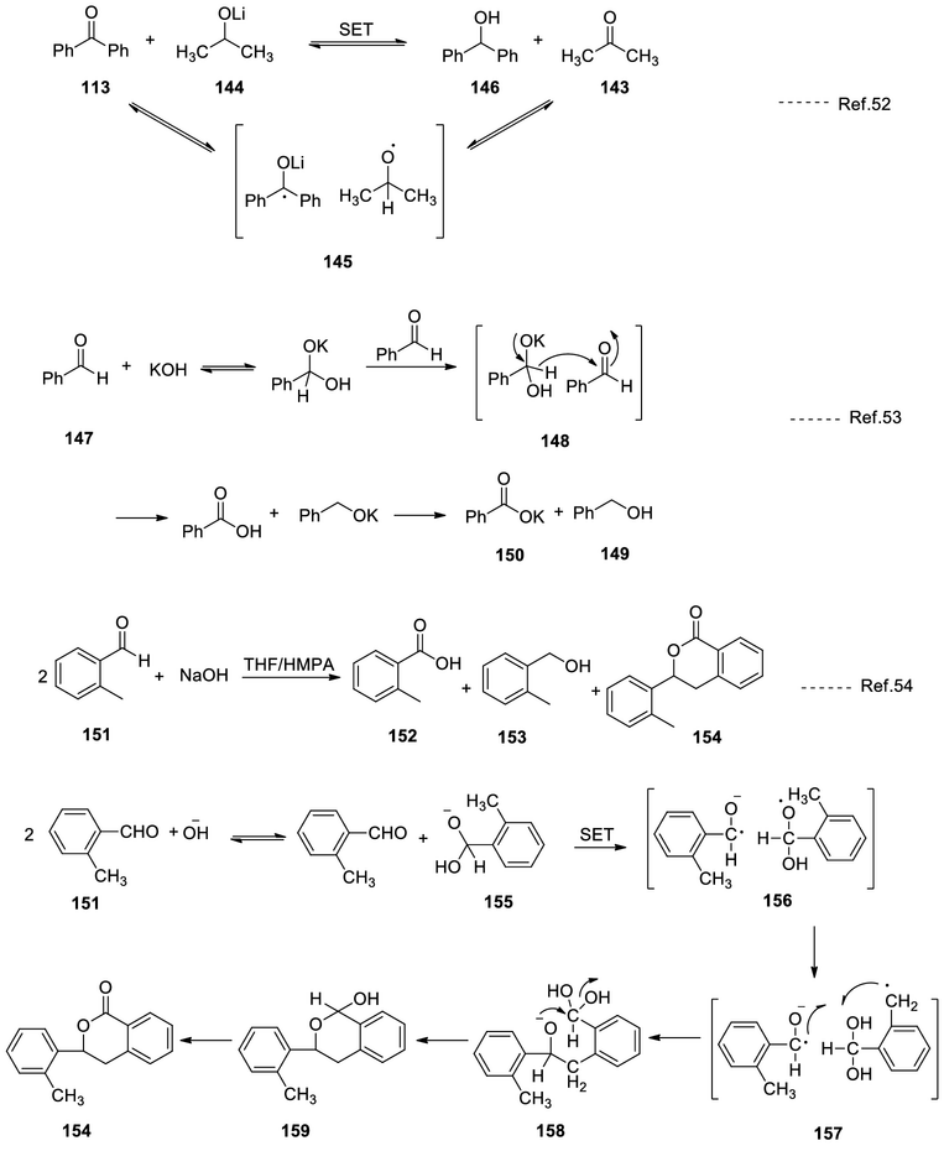

Chart 7 (continued.)

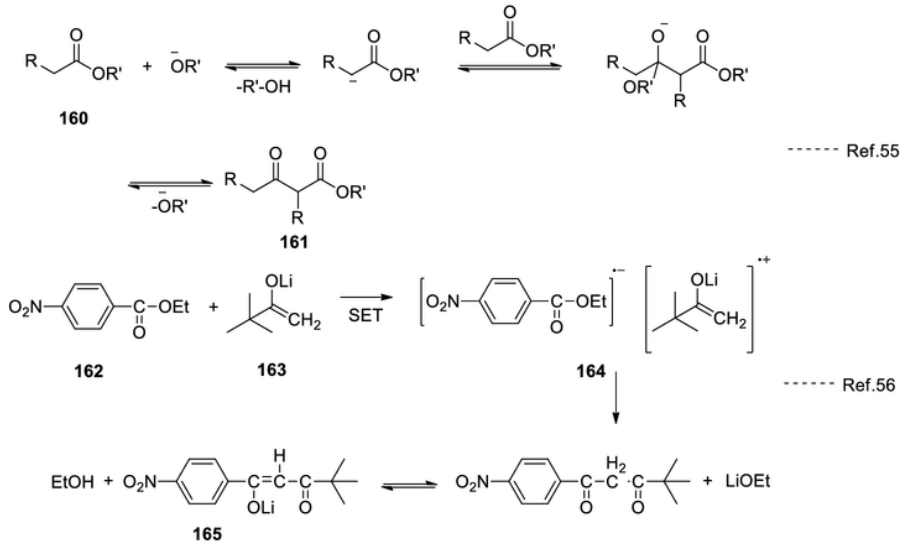

1.1.5 SET Process in Organic Donor and Acceptor System

The formation of charged species can take place in two sequential single electron transfer (SET) processes or in a concerted two electron transfer process (polar mechanism) (Scheme 14).

Scheme 14

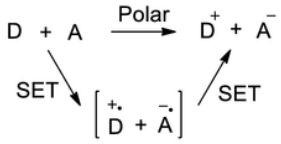

Mulliken's charge transfer theory,[57] Taube's outer sphere/inner sphere mechanism[58] and R. A. Marcus two state non adiabatic theory[59] are the most important concepts developed to rationalize electron transfer reactions.

The charge or electron transfer from one molecule (donor) to the other molecule (acceptor) results in the formation of charge transfer (CT) complex. The electron donors

should have low ionization potential and the electron acceptors should have high electron affinities. Charge transfer complexes have a neutral ground state and there is a partial electron transfer from donor to an acceptor molecule.

Mulliken *et al.*[60] proposed that the diffusive interaction of electron rich donor with an electron acceptor gives a reversible CT complex [D, A] (Scheme 15).

Scheme 15

The energy levels of HOMO and LUMO play important role in electron transfer reactions. The LUMO of the electrophilic reagents (acceptor) such as NO_2^+ and Br^+ are lower than the HOMO of aromatic molecules (donor) leading to electrophilic substitution reactions. For example, benzene reacts with NO_2^+ to form nitrobenzene **167** *via* the formation of the radical intermediate **166** (Scheme 16).[61]

Scheme 16

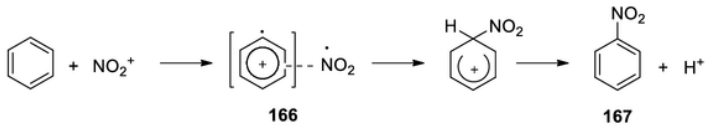

166 167

Taube proposed that both outer-sphere and inner-sphere processes are involved in inorganic electron transfer reactions. The halides could promote the inner-sphere electron transfer *via* bridging effects. Taube *et al.*[62] also reported that in the reaction of chromium complex **168** with cobalt complex **169**, the electron transfer from Cr(II) to Co(III) takes place *via* a bridged intermediate **170** resulting in the green chromium complex **171** and cobalt complex **172** (Scheme 17). The electron transfer is accompanied by the transfer of chloride ligand and this process takes place *via* inner-sphere electron transfer.

Scheme 17

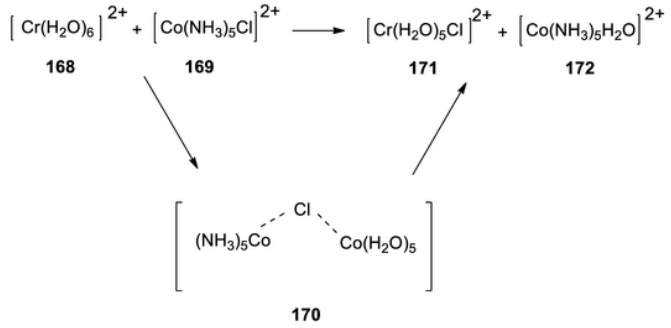

In outer-sphere electron transfer, organic compounds can accept or loose an electron without undergoing structural changes like bond cleavage or bond formation. For example, nitrobenzene **167** can accept one electron to form nitrobenzene radical anion **173** without undergoing any structural change (Scheme 18).[63]

Scheme 18

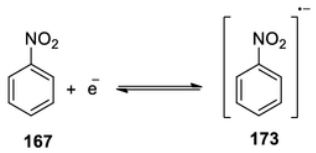

Marcus described the mechanism of electron transfer between an electron donor (D) and an electron acceptor (A) through an outer-sphere precursor complex (D/A) **174**. The precursor complex **174** then reorganizes toward a transition state in which electron transfer takes place to form a successor complex ($D^{+\cdot}/A^{-\cdot}$) **175** that can dissociate to give the corresponding ion pairs **176** (Scheme 19).[64]

Scheme 19

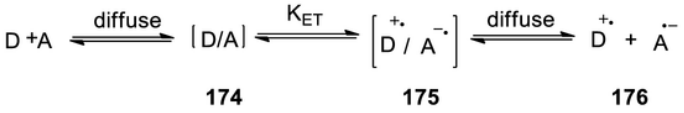

We have decided to investigate the electron transfer reaction of oxygen adsorbed carbon materials, polythiophene radical cation salts, quinones, halomethanes and viologen acceptors. We have also constructed electrochemical cells based on quinone acceptors and amine donors. The results are described in Chapters 2-4.

Chapter 2

Synthetic Methods Based an Electron Transfer Reactions using Oxygen Adsorbed Carbon Materials and *p*-Doped Polythiophene

2.1 Introduction

2.1.1 Carbon materials

Carbon materials are useful for a wide variety of applications such as electrochemical electrodes, medical implants, electrochemical capacitors, high-performance materials and fuel cells.[1] The heat treatment of carbon material at inert atmosphere decreases the content of heteroatoms and increasees the carbon contents.[2,3] The conversion of an organic macromolecular system (e.g. wood, coal, nutshell etc.) to a macro-atomic carbon atoms through elimination of methanol, carbon monoxide, water and carbon dioxide by progressive heating is called carbonization process.[4]

Recently, the production of pyrolysis gas from woody biomass were investigated in this laboratory. The charcoal is a byproduct in this carbonization process from the woody biomass at 450 °C-500 °C. Therefore, we became interested in the development of organic synthetic methods based on readily accessible activated carbon.

Activated carbon is widely used in electrochemical capacitors (supercapacitors) for electricity storage with potential for use in electric vehicles. Activated carbon act as semiconductor with narrow band gap (34 meV) with potential for use in harvesting IR portion of the solar spectrum.[5] Our interest is to study the electron transfer reactions in organic transformations. Therefore, a brief review on the properties and nature of carbon material for application in organic transformation would facilitate the discussion.

2.1.2 Various forms of carbon

The main allotropic forms of pure carbon are graphite and diamond. However, there is immense interest on other new forms of pure carbon such as fullerenes or buckyballs and carbon nanotubes (CNTs).[6] Amorphous forms of carbon mainly consist of coal, charcoal and carbon black. Charcoal is produced by heating organic materials to a high temperature in the absence of air.[7] It has large surface area and it can absorb gases to form new materials. Carbon black is also the purest form of carbon. It is obtained by incomplete burning of some natural oil and heavy petroleum products with limited supply of air.[8] Carbon black is very soft powder and it is used for making carbon paper, inks and paints. The strength of the rubber is increased by the addition of carbon black. Graphite is the most stable allotrope of carbon and soft in nature.[9] Graphite conducts electricity due to delocalization of electrons.

2.1.3 Surface characterization and properties of activated carbons

The surface characteristics of carbon materials and chemistry of their surface is depending on the amount of heteroatom incorporated into the carbon matrix. The heteroatom like oxygen is responsible for the presence of various acidic functional groups such as carboxyl, carbonyl, phenol, quinone and lactones and also presence of unsaturated sites in the matrix of activated carbon (Figure 1).[10]

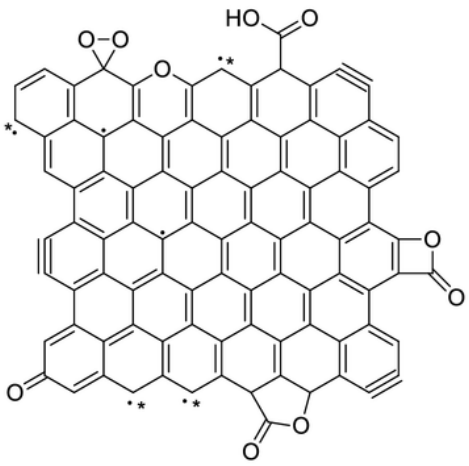

Figure 1. Surface groups present in the Carbon Material. It indicates the presence of σ (*) and π (•) electrons at the zigzag sites and the presence of triple bonds at the armchair sites.

Carbon materials contains bulk atoms that are neutral, surface atoms that are the real adsorption atoms and corner atoms that are very reactive and even react with metals. It is well known that chemical treatment of carbon materials increases the concentration of surface oxygen functional groups. It has been reported[11] that the oxygen acquires a partial negative charge upon chemisorptions. The carbon materials have a free-flowing sp^2 π -electrons, which make them potential catalyst for electron transfer reactions such as oxygen reduction reaction (ORR) to generate super oxide radical.[12] This super oxide radical bound to carbon material acts as an oxidant (Scheme 1).[13]

Scheme 1

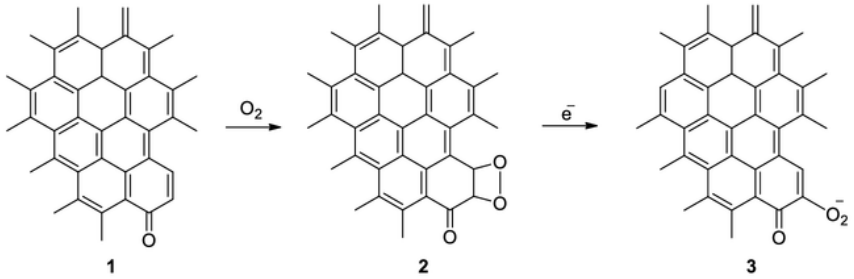

It is of our interest to design experiments for use the reactive intermediate **4** in the oxygen adsorbed activated carbon in synthetic transformations (Scheme 2).

Scheme 2

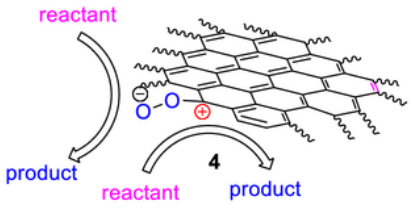

We have investigated the oxygen doped carbon materials for use in the development of new synthetic methods involving reaction with reducing agents and with electron rich compounds and amines. The results are discussed in the next section.

2.2 Results and Discussion

The properties of carbon materials and their surface depend on the heteroatom present and the nature of the materials and methods used for the preparation.[14] Further, it was suggested that the heteroatom (like oxygen) free graphene edge sites in carbon materials are neither hydrogen terminated nor free radicals. Instead, the edge sites are aryne-like armchair sites **5** and carbene-like zigzag sites **6** with triplet ground state. The available evidence points to predominantly carbene-like zigzag sites **6** (Figure 2).[15]

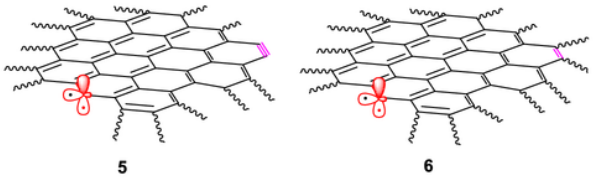

5 **6**

Figure 2. Surface characteristics edge sites in the carbon materials.

The aryne-like sites undergo trimerization to give benzenoid aggregates under ambient atmospheric conditions and expected to give phenolic groups upon reaction with moisture.[16] However, the magnetic properties and chemisorptions with molecular oxygen reported for the carbon materials are in accordance with the proposal that graphene edge sites are carbene-like with triplet ground state **6**.[15]

It has been reported that chemisorption of molecular oxygen by activated carbon fibre materials leads to formation of negatively charged oxygen ($C\text{-}O\text{-}O^{\delta-}$) species.[16,17] Accordingly, we envisaged the formation of such species **4** through electron transfer from the carbon radical site in **7** formed by the reaction of molecular oxygen with activated carbon **6** (Scheme 3).

Scheme 3

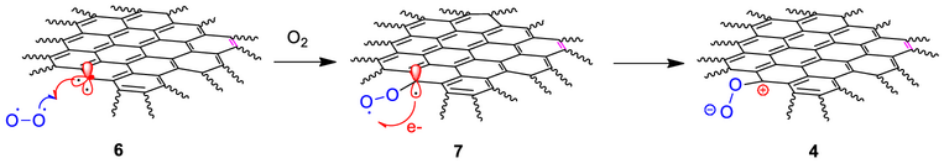

2.2.1 Reactions of Molecular Oxygen Adsorbed Carbon Materials with Ph_3P

Table 1. Adsorption of molecular oxygen on carbon materials[a]

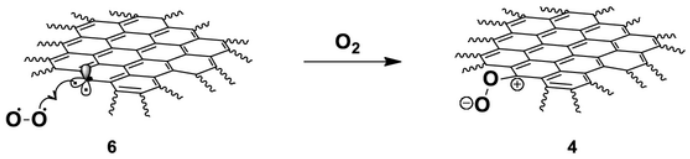

Entry	CM 6 (g)	Oxygen adsorbed CM 4 (g)	O_2, mmol
1	AC (1)	1.034	1.06
	CB (1)	1.053	1.65
	Gr (1)	1.000	-
2	AC (2)	2.071	2.22
	CB (2)	2.078	2.43
3	AC (3)	3.092	2.88
	CB (3)	3.119	3.72
4	AC (4)	4.120	3.75
	CB (4)	4.152	4.75
5	AC (5)	5.175	5.46
	CB (5)	5.190	5.93
	Gr (5)	5.006	0.19
6	AC (10)	10.203	6.34
	CB (10)	10.236	7.37
	Gr (10)	10.013	0.41
7	AC (15)	15.312	9.75

Initially, we have performed several experiments to assess the extent of adsorption of molecular oxygen on carbon materials. The results are summarized in Table 1. The activated carbon (AC) and carbon black (CB) react with molecular oxygen, whereas in the case of graphite (Gr), there was no oxygen or little oxygen gets adsorbed (Table 1).

The carbon material was preheated to 200 °C under high vacuum and brought to room temperature under N_2 atmosphere. Then, the oxygen was passed to the resulting carbon material. The difference in the weight of carbon material before and after oxygen adsorbed indicates that the approximate amount of oxygen molecule gets adsorbed (Table 1).

The carbon skeleton of the oxygen adsorbed intermediate **4** is expected to behave like electron acceptor and the negatively charged oxygen is expected to undergo reaction with proton donors. So, such species are expected to react with proton containing compounds like benzoic acid **8** to give the corresponding hydroperoxide intermediate **9** (Scheme 4).

Scheme 4

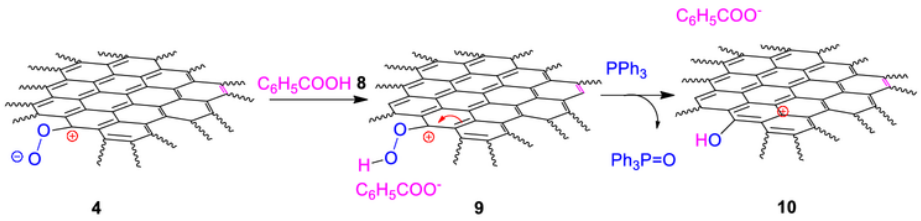

To examine this possibility, we have carried out the reaction of the carbon material with Ph_3P and benzoic acid. We have observed that, in the case of carbon black (CB) without using any proton source or an acid, the $Ph_3P{=}O$ was formed in 17% yield (Table 2, entry 1).

Table 2: Reaction of molecular oxygen adsorbed carbon material **4** with benzoic acid and Ph_3P [a]

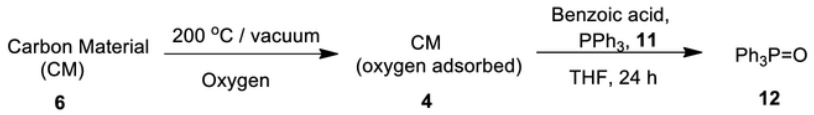

Entry	CM (g)	Benzoic acid (mmol)	Ph_3P (mmol)	THF (mL)	$Ph_3P=O$ Yield (%)[b]
1	CB (5)	0	10	150	17
2	CB (5)	10	10	150	47
3	CB (10)	20	10	150	52
4	AC (5)	10	10	20	54
5	Gr (5)	0	10	20	0
6	Gr (5)	10	10	20	trace
7	Gr (5)	20	10	20	6
8[c]	AC (5)	10	10	20	52
9[c]	CB (5)	10	10	150	45

The formation of $Ph_3P=O$ was slightly increased with an increase in the amount of either carbon material or benzoic acid. Therefore, an increase in the amount of carbon black and benzoic acid gives the $Ph_3P=O$ in 52% yields (Table 2, entry 3). A further increase in the amount of carbon black leads to moderate increase in the $Ph_3P=O$ product.

Here, the carbon black needs more solvent during the reaction and this limits the use of carbon black in this reaction. Whereas in the case of graphite, without using benzoic acid the formation $Ph_3P=O$ product was not observed (Table 2, entry 5). Further, we have observed that the addition of benzoic acid gives $Ph_3P=O$ in 6% yield (Table 2, entry 7). Further increase in the amount of graphite did not enhance the yield of $Ph_3P=O$. In the case of activated carbon, the $Ph_3P=O$ was isolated in 54% yield (Table 2, entry 4). We have also observed that the carbon material isolated after the reaction with PPh_3 can be reused after vacuum treatment at 200 °C and re-adsorption of molecular oxygen.[18] Reaction using re-oxidized activated carbon and carbon black with Ph_3P in THF gave the $Ph_3P=O$ product in 52% and 45% yield (Table 2, entry 8 and 9). The results clearly indicate that the molecular oxygen chemisorbed on carbon black and activated carbon but it is only physisorbed on graphite.

2.2.2 Reactions of Molecular Oxygen Adsorbed Carbon Materials with Alkylboranes

Next, we have studied the utilization of the oxygen adsorbed carbon intermediate **4** in organic transformations. The reactive peroxide present in the oxygen adsorbed carbon material **4** can be used for the oxidation of alkylboranes. The organoboranes are readily accessible *via* hydroboration of alkenes and alkynes using easy to handle $NaBH_4/I_2$ reagent system.[19,22] The molecular oxygen itself could oxidize trialkyl borane to the corresponding hydroperoxide or alcohols.[20] However, the preferred reagent for the oxidation of organoboranes is the $HOO^-\ Na^+$ species produced *in situ* in the reaction of NaOH with H_2O_2. We have envisaged that the oxygen adsorbed intermediate like **4** would react with NaOH to give the species like **13** which could give the $HOO^-\ Na^+$ species **14** for

oxidation of organoboranes *via* the formation of the corresponding borate complex (Scheme 5).[20]

Scheme 5

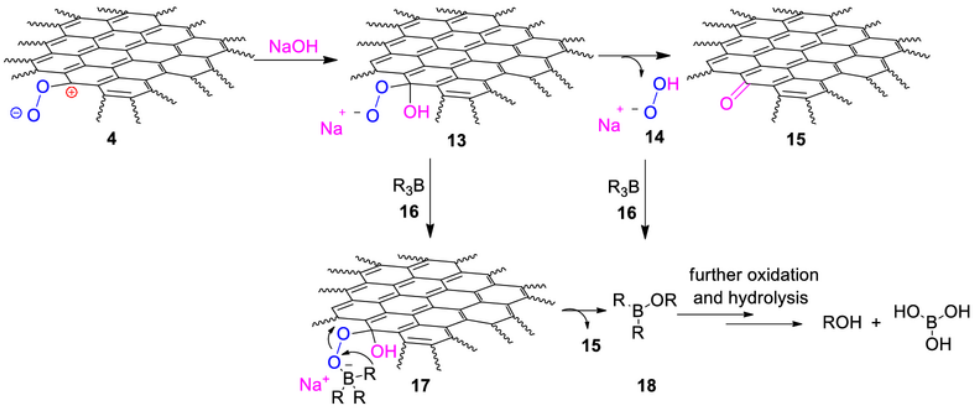

In order to examine this, we have performed a series of experiments on the oxidation of organoboranes prepared using the $NaBH_4/I_2$ reagent system (Scheme 6).

Scheme 6

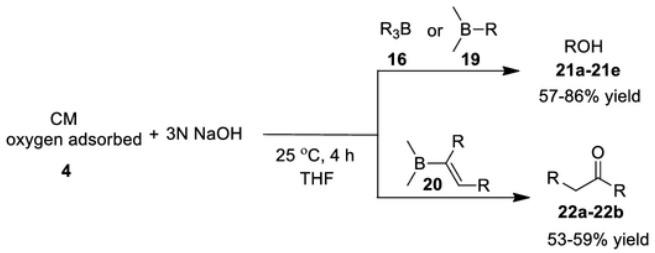

We have observed that trialkylboranes **16a** and **16b** prepared by using hydroboration of 1-decene and norbornene with the $NaBH_4$-I_2 in THF react with a mixture of oxygen adsorbed carbon black **4** and 3N NaOH to give the corresponding alcohol **21a** and **21b** in 85% and 57% yield (Table 3, entry 1 and 2).

Table 3. Reaction of molecular oxygen adsorbed carbon materials **4** with aq. NaOH and alkylboranes[a]

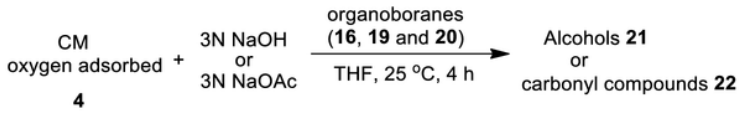

Entry	CM (g)	Alkylboranes (16, 19, 20)	Products (21, 22)	Yield (%)[e]
1[b]	CB (5)	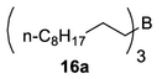 **16a**	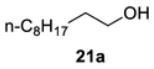 **21a**	85
2[b]	CB (5)	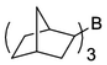 **16b**	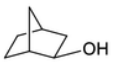 **21b**	57
3[c]	CB (5)	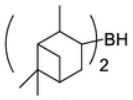 **19a**	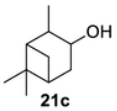 **21c**	71
4[c]	CB (5)	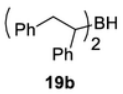 **19b**	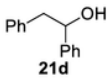 **21d**	86
5[c, f]	CB (5)	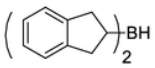 **19c**	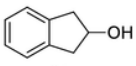 **21e**	80
6[d,g]	CB (5)	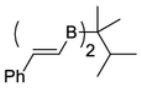 **20a**	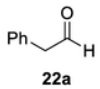 **22a**	53
7[d,f,g]	CB (5)	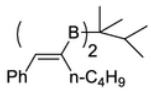 **20b**	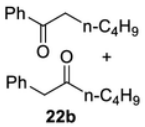 **22b**	59

8 [c,h]	CB (5)	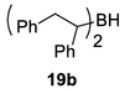 **19b**	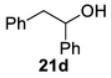 **21d**	82
9 [c,i]	-	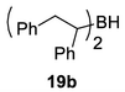 **19b**	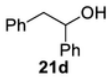 **21d**	<5%

The reaction of dialkylboranes **19a-c** prepared by using $NaBH_4$-I_2 in THF, react with the mixture of carbon black and 3N NaOH to give the corresponding alcohols **21c, 21d** and **21e** in 71%, 86% and 80% yield, respectively (Table 3, entries 3-5). Further, the alkenylborane **20a**, prepared by hydroboration using thexylborane, which in turn prepared *in situ* by the reaction of tetramethyl ethylene and the borane gas generated by the reaction of I_2 with *n*-Bu_4NBH_4, upon reaction with oxygen adsorbed carbon black **4** and 3N NaOAc gave the phenylacetaldehyde **22a** in 53% yield (Table 3, entry 6). Whereas, the reaction using the alkenylborane **20b** gives the corresponding regioisomeric mixture **22b** in 59% yield (Table 3, entry 7).

The carbon black used for this oxidation could be recovered by filtration, dried at 200 ^{0}C and re-adsorbed with molecular oxygen. The recovered and re-adsorbed carbon black and 3N NaOH oxidize the dialkylborane **19b** to give the alcohol **21d** in 82% yield (Table 3, entry 8). Also, when the oxidation was performed using dialkylborane **19b** without using molecular oxygen adsorbed carbon black only trace (<5%) amount of alcohol **21d** was obtained (Table 3, entry 9) indicating the role of carbon black in these transformations.

2.2.3 Reaction of Sodium Borohydride with Molecular Oxygen Adsorbed Carbon Material and Lewis Bases

Diborane is one of most important reagent in organic synthesis. Diborane itself is difficult to handle and relatively inert towards olefins. So, it is normally utilized in the form of its complexes such as BH_3:THF, BH_3:SMe_2 and BH_3:NR_3. Many reagent systems have been developed for the generation of diborane gas.[21] Previously, simple methods for generation of diborane gas from I_2/$NaBH_4$, I_2/*n*-Bu_4NBH_4 and $PhCH_2Cl$/*n*-Bu_4NBH_4 reagent systems were reported from this laboratory.[22]

We have observed that the reaction of oxygen adsorbed carbon material **4** with $NaBH_4$ in THF or diglyme lead to slow hydrogen gas evolution. Accordingly, we have envisaged the formation of the AC*-O-O-BH_3 complex **23** as shown in Scheme 7.

Scheme 7

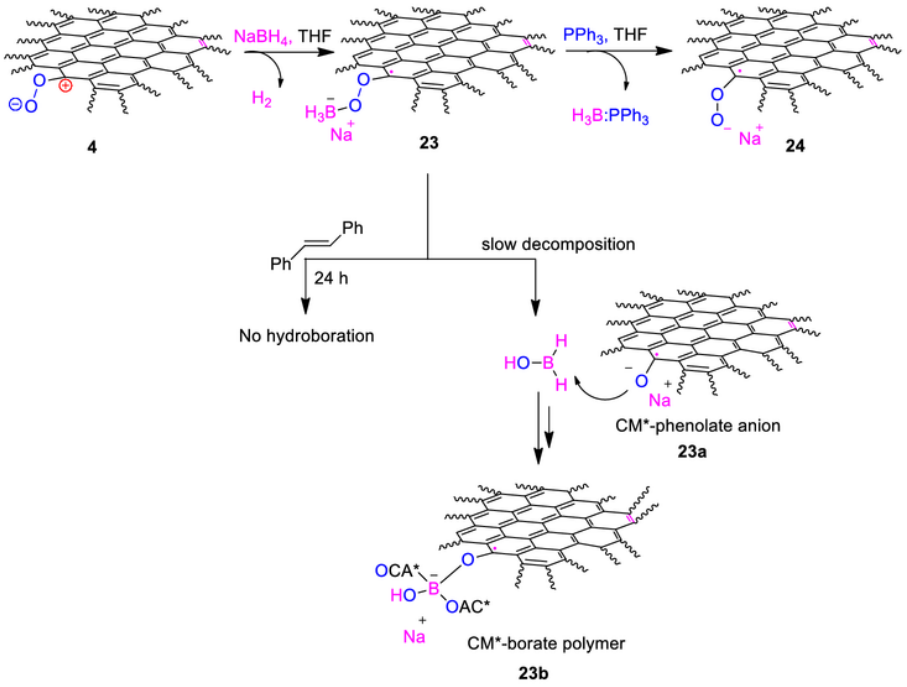

To examine this, we have carried out the hydroboration reaction of stilbene with the intermediate **23** in THF at 25 °C for 24 h. There was no hydroboration observed. Presumably, the reaction of the olefin with the borane complex **23** may be slow and the intermediate **23** may not be stable for longer time to react with olefin or further decomposed to AC* borate polymer (Scheme 7). However, when the reaction of the borane complex **23** was carried out with Ph_3P, the $Ph_3P{:}BH_3$ complex was obtained in 35% yield (Table 4, entry 1).

Table 4. Reaction of $NaBH_4$ with Ph_3P with increasing amount of carbon material (CM).[a]

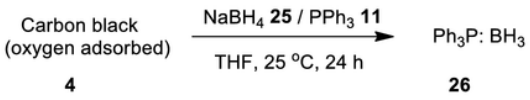

Entry	CM (g)	THF (mL)	$Ph_3P{:}BH_3$ 26 Yield (%)[b]
1	CB (1)	30	35
2	CB (2)	70	54
3	CB (4)	120	62
4	CB (5)	150	69
5	CB (10)	300	73
6[c]	CB (5)	150	65

We have carried out several reactions using different solvents in order to improve the yields and THF turned out to be the best solvent for this transformation. The $Ph_3P{:}BH_3$ was obtained in up to 73% yield, when the reaction was carried out with more amount of oxygen adsorbed carbon black (Table 4). It was found that similar reactions using oxygen adsorbed activated carbon gave 21-77% yield.

Whereas, oxygen adsorbed graphite gave the $Ph_3P:BH_3$ complex only in 9-23% yield, in accordance with reports that molecular oxygen is mainly physisorbed on the surface of graphite.[11,15]

We have also observed that the recovered carbon black remained after reaction with $NaBH_4$ and Ph_3P further reacts with benzoic acid and Ph_3P to give the $Ph_3P{=}O$ in 22% yield. This transformation can be rationalized as shown in Scheme 8.

Scheme 8

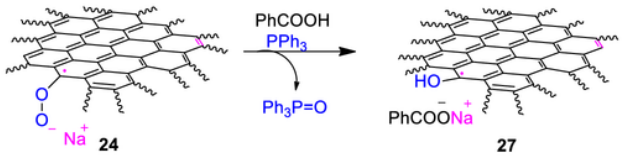

2.2.4 Reaction of Molecular Oxygen Adsorbed Carbon Black with $NaBH_4$ and Amines

We have then turned our attention towards the reaction of pyridine with the AC*-O-O-BH_3 intermediate **23** (Scheme 9).

Scheme 9

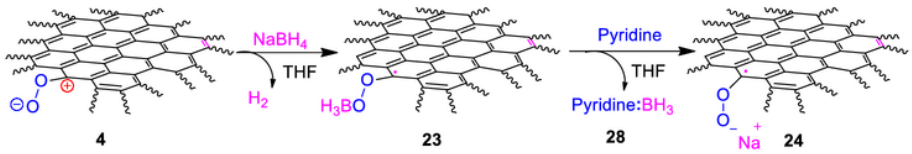

We have found that the reaction of pyridine with $NaBH_4$ in the presence of oxygen adsorbed carbon materials in THF gives the pyridine:BH_3 complex **28** in 42% yield using activated carbon (2 g) and in 52% yield using carbon black (2 g) (Table 5, entry 1 and 2).

We have also performed these experiments using increased amount of carbon material (5 g) in order to improve the yields of pyridine:BH_3 **28** complex. However, there was no further improvement, but there was a slight decrease in the yield of pyridine: BH_3

complex **28** (Table 4, entries 3 and 4). Further, the yields of pyridine:BH_3 complex produced here are relatively low compared to the yields of Ph_3P:BH_3.

Table 5. Reaction of molecular oxygen adsorbed carbon materials with $NaBH_4$ and pyridine[a]

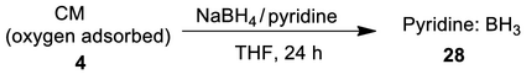

Entry	CM (g)	THF (mL)	Pyrdine:BH_3 complex 28 Yield (%)[b]
1	AC (2)	15	42
2	CB (2)	70	52
3	AC (5)	25	40
4	CB (5)	150	48

We have also performed the reaction of molecular oxygen adsorbed carbon black with other amines, which are expected to form complexes with borane. The results are summarized in Table 6. The reaction of morpholine **29** with $NaBH_4$ and oxygen adsorbed carbon black in THF gave the morpholine:BH_3 **33** in 43% yield (Table 6, entry 1). Similarly, different amine:borane complexes **34-36** were prepared using the amines **30-32** and oxygen adsorbed carbon black (Table 6). The low yields of amine:BH_3 complexes compared to the Ph_3P:BH_3, resulting may be a slow decomposition of the peroxy borane species **23** or the amine borane products may further react with the peroxy species present in the carbon byproduct **24** leading to a reduction in yields.

Table 6. Reaction of molecular oxygen adsorbed carbon black with $NaBH_4$ and amines.[a]

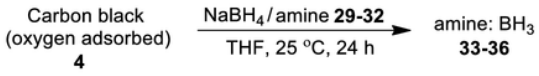

Entry	CB (g)	Amine 29-32	Amine:BH_3 33-36	Yield(%)
1	CB (5)	 **29**	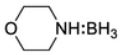 **33**	43
2	CB (5)	 **30**	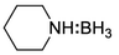 **34**	58
3	CB (5)	 **31**	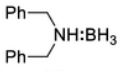 **35**	42
4	CB (5)	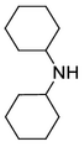 **32**	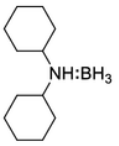 **36**	51

We have also examined the proposed AC*-O-O-BH_3 intermediate **23** for hydroboration reaction of α-methyl styrene **37** in THF but there was no hydroboration (Scheme 10).

Scheme 10

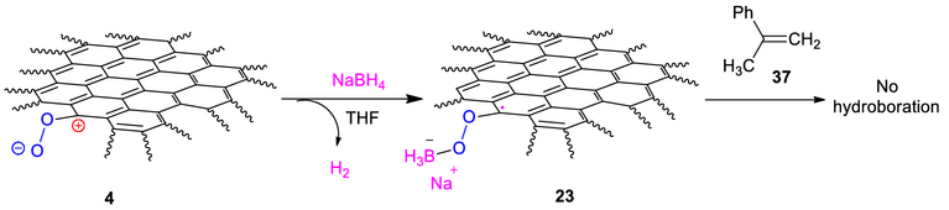

The pyridine:BH_3 complex **28** is useful for hydroboration of olefin at elevated temperatures.[23] Recently it was reported that pyridine:BH_3 complex **28** hydroborates olefins at room temperature under activation by I_2.[24] We have found that the pyridine:BH_3 complex **28** is useful for hydroboration of α-methyl styrene **37**. After oxidation using oxygen adsorbed AC/NaOH, the corresponding alcohol **38** was obtained in 86% yield (Scheme 11).

Scheme 11

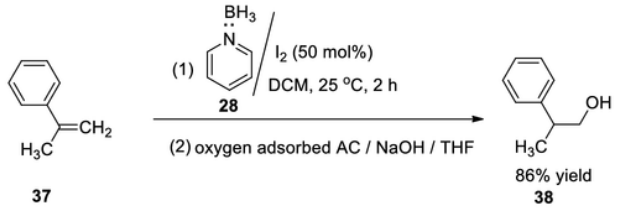

2.2.5 Reaction of Oxygen Adsorbed Activated Carbon with Benzylamine Derivatives

We have observed that benzylamine give benzaldehyde **45** in 30% yield upon reaction with molecular oxygen adsorbed activated carbon. In the case of dibenzylamine **39b**, benzaldehyde was obtained in 25% yield after work up. The NMR spectra obtained for the crude product mixture before work up and chromatography revealed the presence of both the imine and benzaldehyde products (Scheme 12). Presumably, the reaction may

give amine radical cation followed by the formation of imine, which after reaction with water yields benzaldehyde. We have also observed that the epr spectrum recorded after addition of amines to oxygen adsorbed activated carbon indicated the presence of paramagnetic species.

Scheme 12

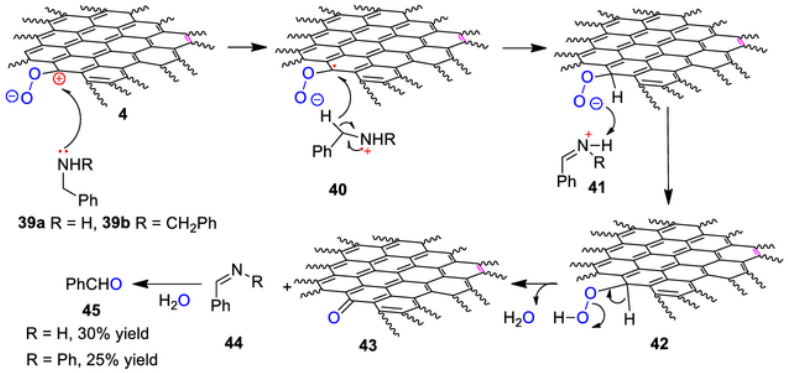

Similarly, it has been observed in this laboratory that the oxygen adsorbed carbon material **4** react with the electron donors like *N*-phenyl tetrahydroisoquinoline **46** and nucleophilic reagents like nitromethane, pyrrole and TMSCN gave the corresponding coupled product **49** in 67-89% yield through the intermediacy of the corresponding radical cation and iminium ion intermediates (Scheme 13).[25]

Scheme 13

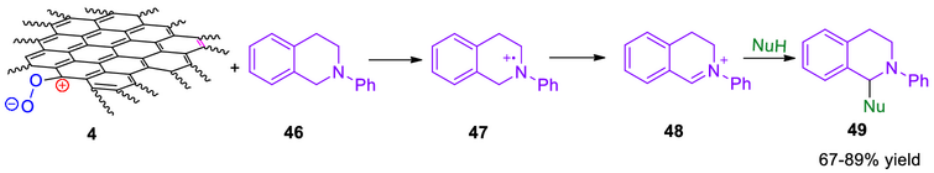

Also, it was found that the 2-naphthol **50** undergoes oxidative coupling reactions in the presence of oxygen adsorbed carbon material **4** to give the bi-2-naphthol **52** (BINOL) in 95% yield *via* the corresponding radical intermediates (Scheme 14).[26]

Scheme 14

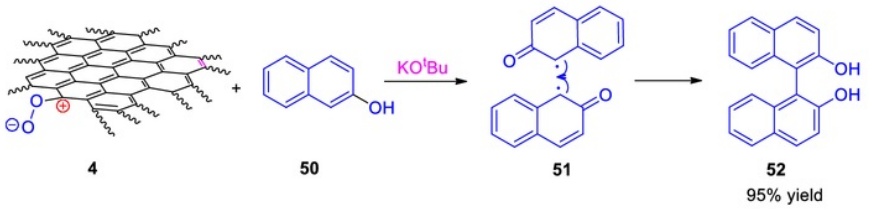

2.2.6 Evidence for Presence of Paramagnetic Species Through EPR Spectroscopy

EPR spectra were recorded for the activated carbon samples at various stages and the spectra are presented below.

2.2.6.1 EPR spectrum of commercial carbon material

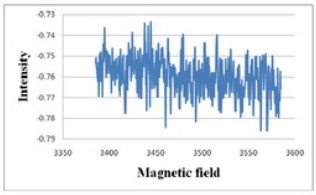

2.2.6.2. EPR spectrum of vacuum dried carbon material

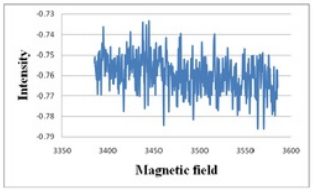

2.2.6.3. EPR spectrum of oxygen doped carbon material

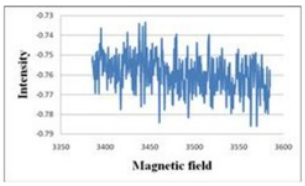

2.2.6.4. EPR spectrum of residual activated carbon (Scheme **4**)

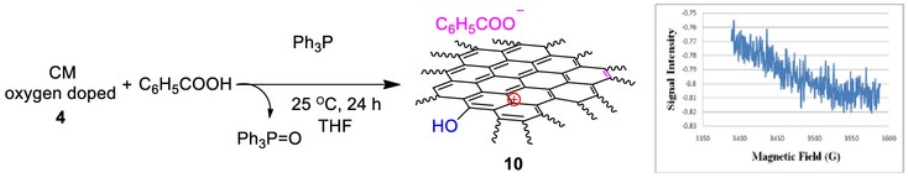

2.2.6.5. EPR spectrum of paramagnetic species **23b** (Scheme **7**)

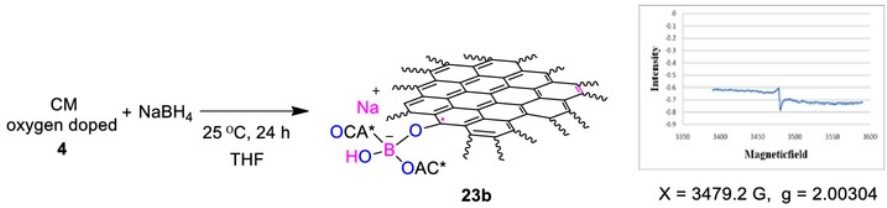

X = 3479.2 G, g = 2.00304

2.2.6.6. EPR spectrum of paramagnetic species **24** (Scheme **7**)

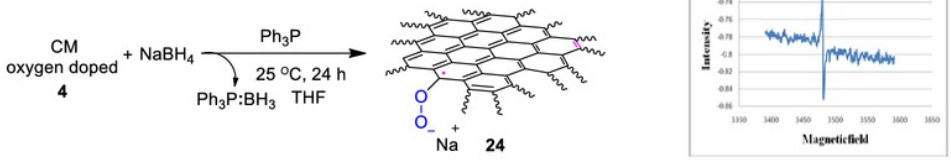

X = 3480.0 G, g = 2.00209

2.2.6.7. EPR spectrum of paramagnetic species **27** (Scheme **8**)

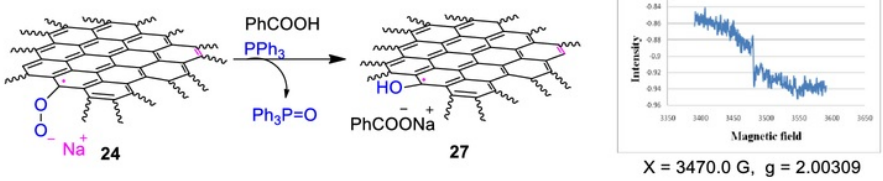

X = 3470.0 G, g = 2.00309

2.2.6.8. EPR spectrum of paramagnetic species **24** (Scheme **9**)

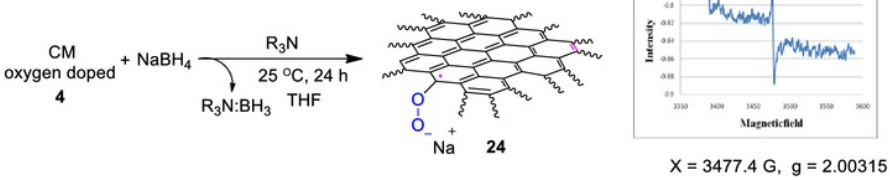

X = 3477.4 G, g = 2.00315

The epr signals observed are in accordance with the paramagnetic species present in residual activated carbon samples.

2.2.7 Synthesis of p-Doped Polythiophene (PT) and Estimation of Radical Cation Site Present in p-Doped Polythiophene.

Electroactive conducting polymers have proven applications in several technologies such as solar cells, display devices, gas sensors and actuators.[27] It is relatively easy to process these polymers to make the devices and their chemically tunable property makes them useful in electronic devices.[28] These polymers are redox-active and their conductivity can be changed by doping the polymer. The physical properties of these conductive polymers depend on the type of the dopant used.

Polythiophene (PT) and its derivatives are good conducting polymers. Optical properties of polythiophenes can be varied by pre-functionalization of monomer.[29,30] Polythiophene derivatives are easy to process and they form a thin film with good optical properties.[31,32] The higher stability and longer life of polythiophene derivatives are suitable for various applications.[33]

Previously, we have discussed the preparation of Lewis base borane complexes using carbon material and borohydride reagent system. Hence, we have undertaken the studies to estimate the doping level in polythiophene radical cation salts using $NaBH_4$. Also, we have envisaged a simple method for generation of Lewis base-borane complexes. The advantage of this method is that we can recover the polythiophene by simple filtration and re-oxidize the polythiophene using $FeCl_3$ to prepare the polymer radical cation salts for reuse in the preparation of Lewis base borane complexes.

We have prepared the polythiophene radical cation salts **54** from thiophene **53** through a slightly modified literature procedure.[34] The dark-brown precipitate of polythiophene obtained in the reaction was further washed with methanol to remove the residual oxidant. The color of the polymer changes from dark-brown to brown. The PT powder was dried in a vacuum at 50 °C for 12 h (Scheme 15).

Scheme 15

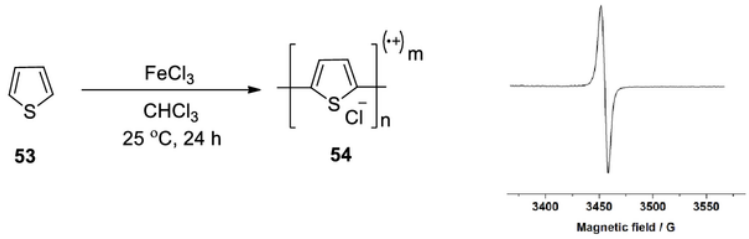

The synthesized polythiophene radical cation salts were confirmed by FT-IR spectroscopy. The presence of paramagnetic sites was confirmed by epr spectroscopy. The polymer exhibits single epr signal with g value of 2.0026 (Scheme 15).[35]

2.2.8 Preparation of Lewis Base Borane Complexes Using the Polythiophene Radical Cation Salts/$NaBH_4$ Reagent System.

Earlier reports[36-40] indicate that there are three different structures possible in polythiophene. The structure **55** is a neutral polymer and the removal of an electron from structure **55** leads to form radical cation polymer **56**. This radical cation polymer **56** also called as polaron and it is stabilised by resonance. Removal of an electron from structure **56** gives a bipolaron **57** (Scheme 16). The polaron and bipolaron are formed directly through an oxidation of the thiophene monomer. Previous report[41] shows that the radical cation present in the polythiophene could delocalize into the rings. The repeating unit of cation radical in polythiophene could approximately six monomer units. The planarity of

polythiophene gets twisted and delocalisation of the radical cation present in the polymer gets reduced beyond six thiophene rings.

Scheme 16

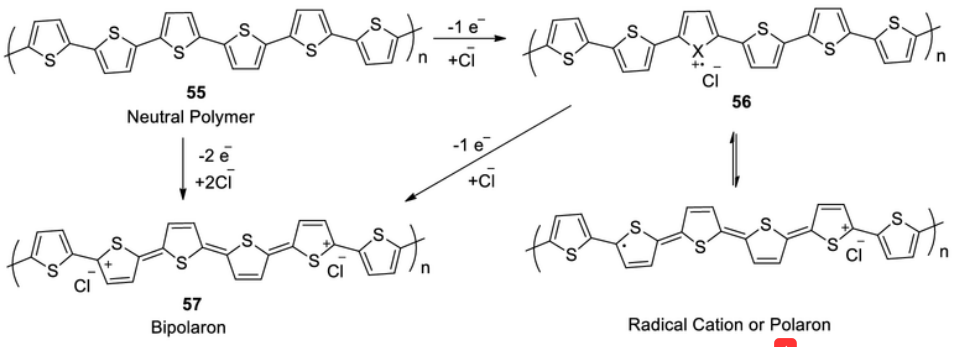

The polythiophene radical cation salts **54** react with $NaBH_4$ with slow evolution of hydrogen gas. Accordingly, the reaction of polythiophene radical cation, $PT^{(.+)}{}_m$ nCl^- $NaBH_4$ and PPh_3 may be visualized by initial formation of a polymer-$NaBH_4$ complex that decomposes to H_2 and borane followed by the formation of $Ph_3P{:}BH_3$ complex. Hence, we have performed the reaction of $NaBH_4$ and Ph_3P with 1 g of polymeric radical cation salts in THF at 25 °C.

Scheme 17

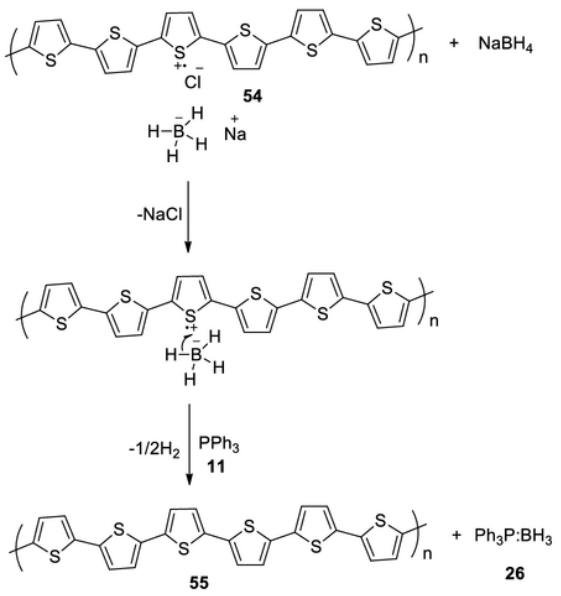

A tentative mechanism for the formation of $Ph_3P:BH_3$ complexes can be considered involving the reduction of polythiophene cation radical salts by $NaBH_4$ through single electron transfer (SET) process to give neutral polymer and $Ph_3P:BH_3$. The possible mechanism is outlined in Scheme 17.

2.2.9 Estimation of the Number of Radical Cation Sites Present in Polythiophene

We have observed that the reaction of 1 g of $PT^{(.+)}_m$ nCl^- **54** with $NaBH_4$ (1 mmol) and PPh_3 **11** (1 mmol) gives the $Ph_3P:BH_3$ **26** in 0.72 mmol (Table 7, entry 1). When the reaction was carried out using higher amounts of $NaBH_4/Ph_3P$ with 1 g of $PT^{(.+)}_m$ nCl^- **54**, higher yields of $Ph_3P:BH_3$ **26** was obtained (Table 7, entries 2-5).

There was no significant change observed, when the reaction was performed using more than 5 mmol each of $NaBH_4$ and Ph_3P. Accordingly, it can be concluded that a minimum of approximately 1.7 mmol of radical cation sites are present in 1 g of $PT^{(.+)}_m$

nCl^- **47**. However, the actual number of radical cation salts present is expected to be slightly more than this as the yields are of isolated yields and hence about 5% loss during isolation could be expected. The recovered[42] $PT^{(.+)}_m$ nCl^- **54** (1 g), after oxidation with $FeCl_3$ (Scheme 15), reacts with $NaBH_4$ (1 mmol)/PPh_3 (1 mmol) to give the $Ph_3P{:}BH_3$ in 0.71 mmol (Table 7, entry 6) without significant change from the freshly prepared sample, illustrating the recyclability of the polymer used.

Table 7. Reaction of polythiophene radical cation salts 54 with $NaBH_4$ and PPh_3[a]

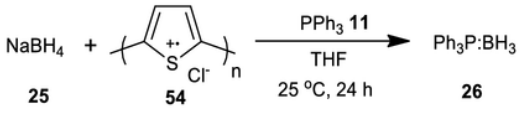

Entry	Polythiophene radical cation salts (1 g)	$NaBH_4$ (mmol)	PPh_3 **11** (mmol)	$H_3B{:}PPh_3$ **26** Yield (mmol)[b]
1	**54**	1	1	0.72
2	**54**	2	2	1.22
3	**54**	3	3	1.50
4	**54**	4	4	1.64
5	**54**	5	5	1.70
6[c]	**54**	1	1	0.71

We have also analyzed the polymer radical cation salts $PT^{(.+)}_m$ nCl^- **54** by UV-Visible spectroscopy before and after the reaction with $NaBH_4$ and PPh_3. Broad

absorptions with longer wavelength (red shift) was observed for the polymer before reaction with $NaBH_4$ and PPh_3. The wavelength of absorption gets decreased or move to shorter wavelength after reaction with $NaBH_4$ and PPh_3 (Figure 3). The color of the polymer $PT^{(.+)}{}_m$ nCl^- **54** also gets changed from dark brown to brown.

The shift in the UV-Visible absorptions spectrum to lower wavelength (blue shift) after the reaction with $NaBH_4$ and PPh_3 for polymer sample **54** indicate that the effective conjugation present in the polymer or the polymer cation radical sites present in the polymer gets lowered.

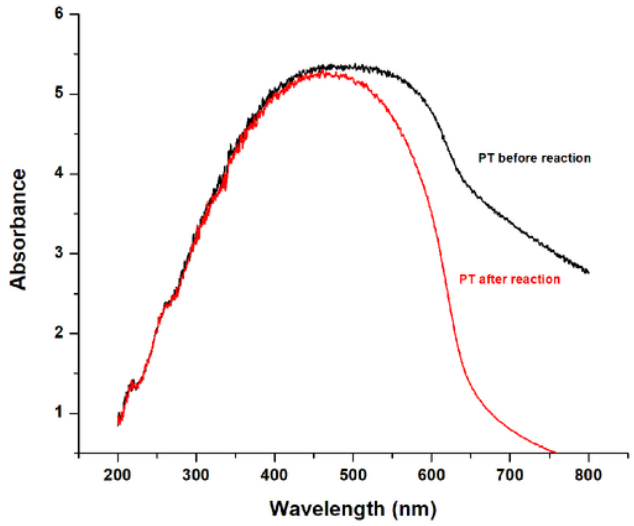

Figure 3. UV-Visible spectrum of polymer **54** powder sample before (black line) and after (red line) reaction with $NaBH_4$ and PPh_3.

The epr studies also indicate that there was a decrease in the radical cation spin density present in the polymer salts (Figure 4). However, the epr studies indicates that the some of the radical cation remains after the reaction with $NaBH_4$ and PPh_3. The epr signals became weak, but not totally absent (Figure 4). Earlier, it was reported that the

neutral thiophene polymers react with molecular oxygen to give paramagnetic species.[43] Therefore, formation of small amounts of paramagnetic species by the reaction of polymer with O_2 during the work up procedure cannot be ruled out in these cases.

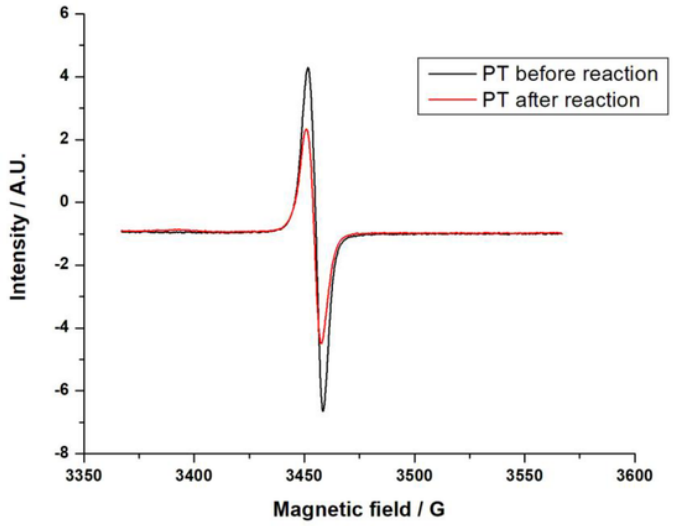

Figure 4. EPR of PT **54** before (black line) and after (red line) reaction with $NaBH_4$ and PPh_3.

The $Ph_3P{:}BH_3$ complex is very stable and hence it is not useful for synthetic applications. However, the amines like pyridine form relatively more reactive borane complexes and hence are useful for hydroboration at room temperature under activation by I_2.[24] Therefore, we have decided to investigate the reaction of $NaBH_4$ with the polymer radical cation salts in the presence of pyridine.

We have found that the reaction of polythiophene radical cation salts **54** (1 g) with $NaBH_4$ and pyridine in THF gives the pyridine:BH_3 **28** complex. The results are summarized in Table 8. The reaction using PT radical cation **54** (1 g) using 1 mmol each

of $NaBH_4$/pyridine gave the pyridine:BH_3 **28** complex in 35% yield based on the presence of 1.7 mmol of radical cation sites in 1 g of PT radical cation **54** (Table 8, entry 1). Similarly, the reaction of PT radical cation **54** with 2 and 3 mmol each of $NaBH_4$ and pyridine gives the pyridine:BH_3 **28** complex in 63% and 79% respectively (Table 8, entry 2 and 3).

Table 8. Reaction of polythiophene radical cation salts 54 with $NaBH_4$ and Pyridine[a]

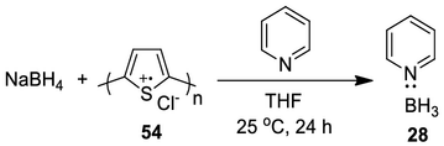

Entry	Polythiophene radical cation (1 g)	$NaBH_4$ (mmol)	Pyridine (mmol)	Pyridine:BH_3 **28** Yield (mmol)[b]	Pyridine:BH_3 **28** Yield[c] (%)
1	**54**	1	1	0.59	35
2	**54**	2	2	1.08	63
3	**54**	3	3	1.35	79

In these transformations, the borane "BH_3" moiety seems to be extracted by the Ph_3P or pyridine Lewis bases while the radical cation borohydride complex decomposes (Scheme 17). It was of interest to us to examine whether the borohydride complex could hydroborate olefins. Accordingly, we have carried out an experiment using α-methyl styrene with polymer radical cation salts and $NaBH_4$ in THF but there was no hydroboration. Presumably, the olefin is not nucleophilic enough to react with polymer radical cation – borohydride complex. However, we have observed that the pyridine:BH_3 complex **28** prepared in this way readily hydroborates α-methyl styrene under iodine

activation. After $NaOH/H_2O_2$ oxidation the corresponding alcohol was obtained in 84% yield.

It was also observed in this laboratory that the reaction of polymers such as poly-*N*-methylpyrrole ($NMPPY^{(\cdot+)}{}_m$ nCl^-) **54a** and poly(*N*-methylaniline) ($PNMA^{(\cdot+)}{}_m$ nCl^-) **54b** radical cation salts with $NaBH_4$ (1 mmol) and PPh_3 (1 mmol) gave the $Ph_3P{:}BH_3$ **26** in 0.62 mmol and 0.68 mmol (Scheme 18). The results indicate that a minimum of approximately 1.35 mmol of radical cation sites are present in 1 g $NMPPY^{(\cdot+)}{}_m$ nCl^- **54a** and also a minimum of 1.60 mmol of radical cation sites are present in 1 g of $PNMA^{(\cdot+)}{}_m$ nCl^- **54b (**Scheme 18).[44]

Scheme 18

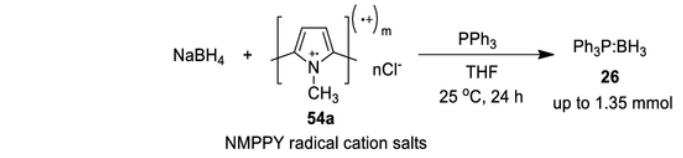

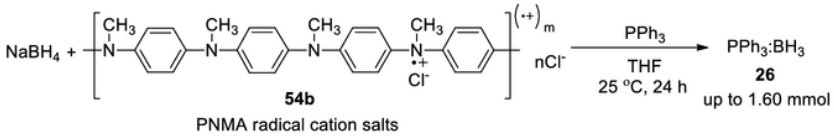

Next, we have studied the reaction of amine nucleophiles with various electron acceptors like quinones, vilologens and halo compounds. The results are described in the chapter 3.

2.3 Conclusions

The molecular oxygen adsorbed carbon black reacts with benzoic acid and Ph_3P to give $Ph_3P{=}O$ in 52% yield. Also, oxidation of organoboranes were performed using readily available oxygen adsorbed carbon materials **4**. These organic transformations were also performed by exploiting the negative charge present in the oxgen end.

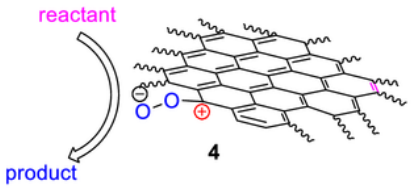

The electron defficiency present in the carbon skeleton of the carbon materials **4** was utilized for the preparation of Lewis base:borane complexes using $NaBH_4$ and Ph_3P or pyridine. The $Ph_3P{:}BH_3$ and amine:BH_3 complexes are prepared in moderate to good yields upon reaction of oxygen adsorbed carbon material with $NaBH_4/Ph_3P$ and $NaBH_4$/amine reagent systems. We have observed bezylamine gives benzaldehyde *via* radical cation intermediates reaction with molecular oxygen adsorbed carbon materials.

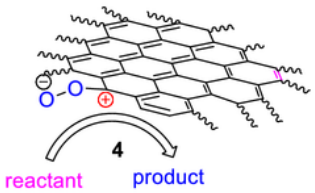

A simple method for estimating doping levels in polymer was developed. Accordingly, it can be concluded that a minimum of approximately 1.7 mmol of radical cation sites are present in 1 g of the $PT^{(.+)}{}_m\ nCl^-$ salt.

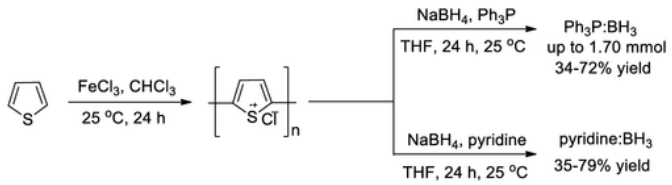

Convenient methods for the preparation of $Ph_3P{:}BH_3$ and pyridine borane and other amine borane complexes were developed.

Chapter 3

Studies on the Reaction of Amines with Quinones, Viologens and halo compounds

3.1 Introduction

Aliphatic and aromatic, primary, secondary and tertiary aminesare known to react with *p*-chloranil in dioxane/2-propanol to produce blue to purple color. Generally, aliphatic amines gives red colour and other amines give different colours as shown in Table 1. Accordingly, *p*-chloranil was used to detect the presence of amines.[1]

Table 1. The colours of chloranil-amine adducts

Amine	Colour of adduct produced with chloranil
n-Butylamine	Red
Benzylamine	Red
Aniline	Violet
N-Methylaniline	Blue-green
N,N-Dimethylaniline	Blue
p-Nitroaniline	Orange
Diphenylamine	Blue-green

3.1.1 SET Reactions in Quinone Chemistry

The quinone – hydroquinone redox couple has been studied over many years.[2] Quinone redox system also plays major roles in biology.[3] Quinones undergoes $2H^+/2e^-$ reduction in aqueous solution (or) in protic solvents.[4] The redox process of hydroquinone-quinone is a sequence of proton and electron transfer (Figure 1). In the first step,

deprotonation leads to a phenoxide ion which is transformed into a phenoxy radical by a one-electron oxidation. Then dissociation of the second OH group generates the radical anion semiquinone followed by a second one-electron oxidation to give benzoquinone **2**. All intermediates are resonance stabilized.

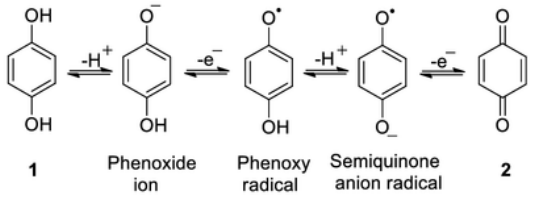

Figure 1. The redox process of hydroquinone-quinone system.

In nonaqueous (or) aprotic conditions, the quinone reduction proceeds through two consecutive single electron reductions (Fig 2).

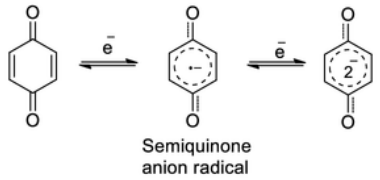

Figure 2. Quinone reduction in aprotic medium.

3.1.1.1 Addition and substitution reaction of quinones with amines

Preparation of various addition products of 1,4- benzoquinone **2** with different substituted anilines **3** was reported (Scheme 1).[5]

Scheme 1

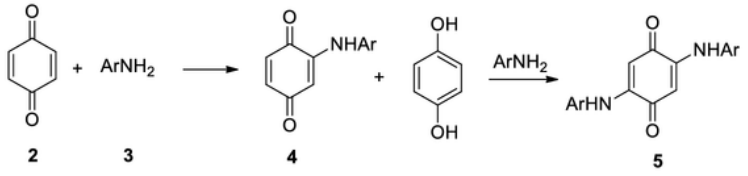

Reaction of *p*-chloranil **6** with aniline to give corresponding amino quinone **10** as a product.[6] A mechanism involving the formation of aminoquinone through outer (π)-complex **8** and inner (σ)-complex **9** was proposed (Scheme 2).

Scheme 2

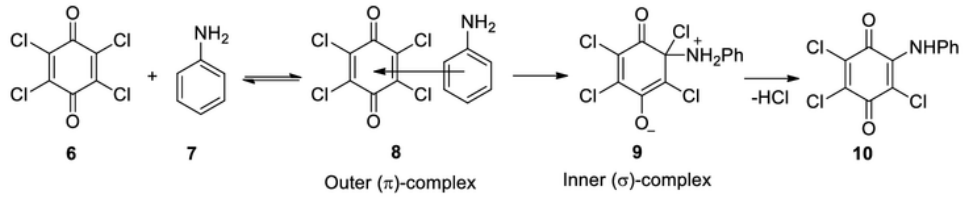

p-Chloranil **6** reacts with *n*-butyl amine **11** by electron transfer from *n*-butylamine **11** to *p*-chloranil **6** followed by substitution reaction to give the product **14** (Scheme 3).[7]

Scheme 3

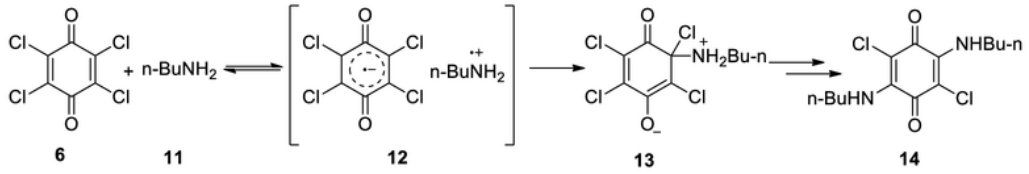

Pyrolidine **11a** was also reported to react with *p*-chloranil **6** to give mono and disubstituted aminoquinone **15** and **16** (Scheme 4).[8]

Scheme 4

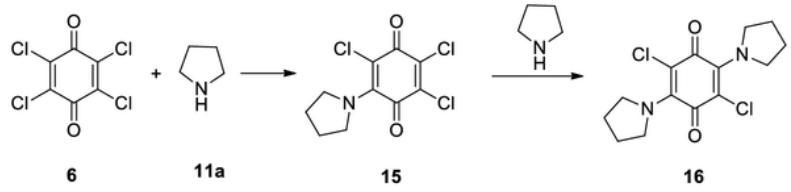

The hydride transfer from dihydroflavins **17** to 2,3-dichloro 5,6-dicynao-*p*-benzoquinone (DDQ) **18** was reported.[9] In this case, the back electron transfer is relatively slow and the proton transfer occurs within the radical ion pair complex **19** (Scheme 5).

Scheme 5

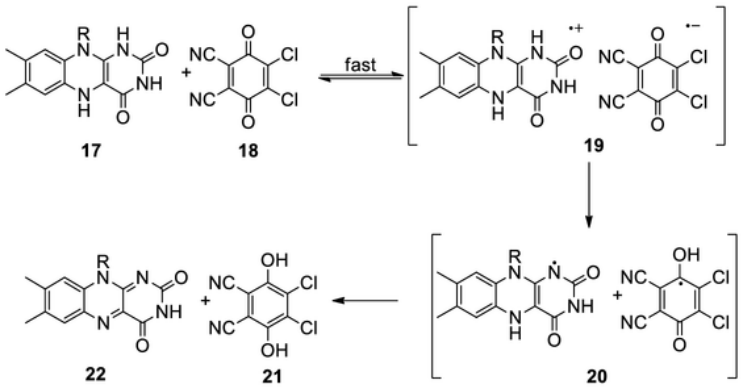

The reaction between *p*-chloranil **6** and diclofenac **23** leads to the charge transfer complex **24**. This CT complex is readily converted to radical ion pairs **25** in methanol solvent (Scheme 6).[10]

Scheme 6

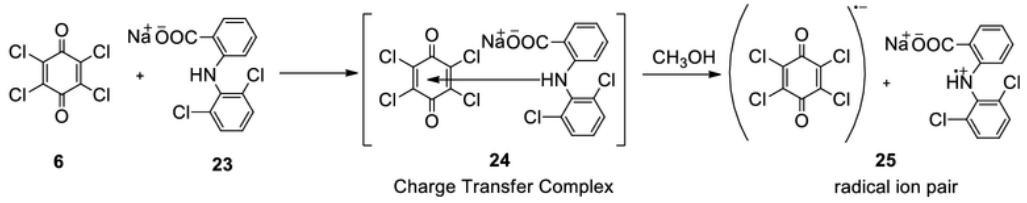

Tertiary amines are excellent electron donors and they strongly interact with electron acceptors. For example, DABCO **26** reacts with *p*-chloranil **6** in benzene solvent to give DABCO-chloranil 1:1 complex. The reaction of *p*-chloranil or *p*-bromanil with DABCO gives paramagnetic species **28** in benzene or in THF solvent (Scheme 7).[11]

Scheme 7

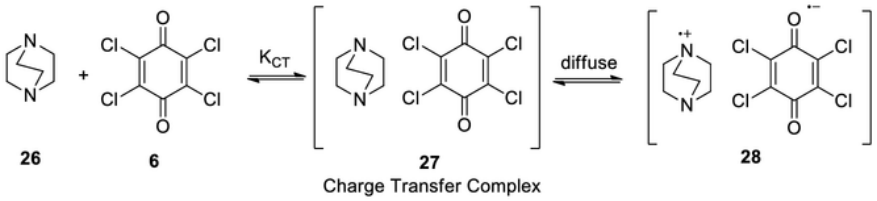

The reaction of 2,2,6,6-tetramethylbenzo [1,2-*d*;4,5-*d'*]bis[1,3]dioxole (TMDO) **29** DDQ **18** in polar solvents like acetonitrile or propylene carbonate leads to radical ion pairs **30**. The electron transfer from TMDO to DDQ is fast in polar solvents (Scheme 8).[12]

Scheme 8

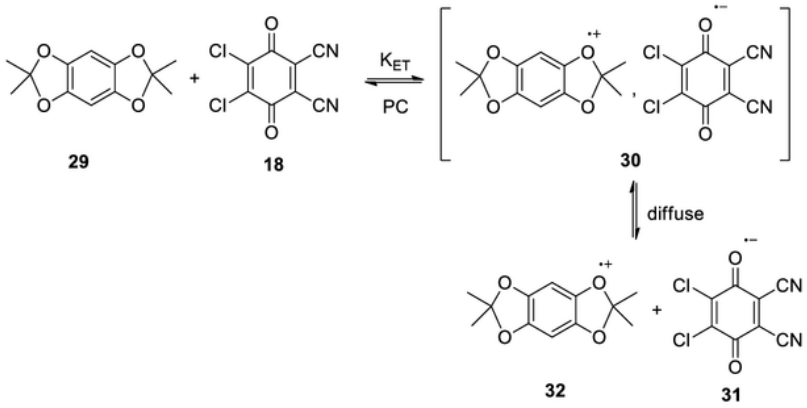

We have decided to investigate the elctron transfer reaction of quinones with amine donors. The mechanism and intermediates formed in these electron transfer reactions are discussed in the next section.

3.2 Results and Discussion

3.2.1 Reaction of secondary amine with quinone acceptors

Piperidine **33** reacts with 1,4- benzoquinone **2** in DCM solvent to give paramagnetic species by electron transfer from piperidine **33** to 1,4- benzoquinone **2**. The intensity of the epr signal decreases with time. We have also observed similar epr pattern in PC solvent with stronger signal. The reaction of piperidine with *p*-chloranil **6**, 1,4-naphthaquinone **34** and 2,3-dichloronaphthaquinone **35** also gave similar results in epr spectroscopic studies (Figure 3).

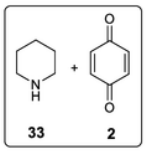

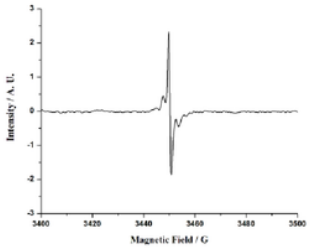

(a) at 5 min

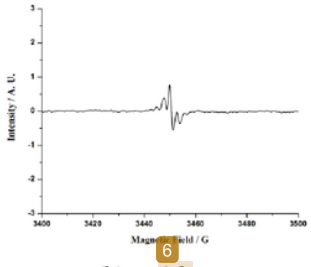

(b) at 1 h

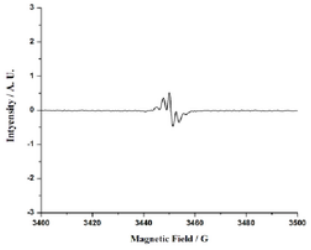

(c) at 2 h

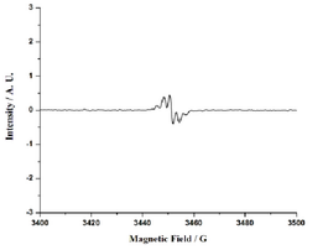

(d) at 6 h

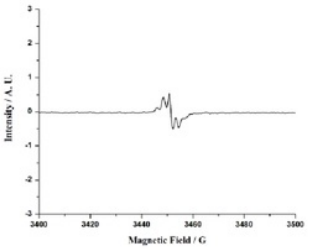

(e) at 12 h

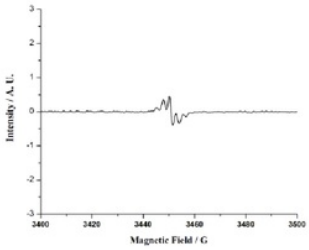

(f) at 24 h

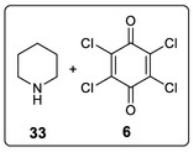

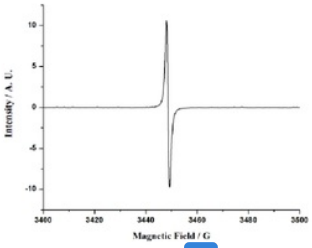

(a) at 5 min

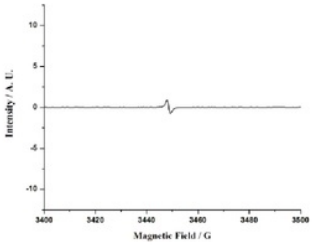

(b) at 1 h

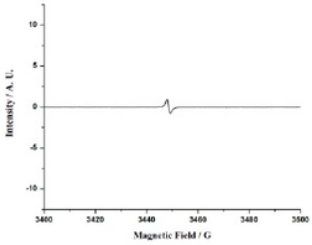

(c) at 2 h

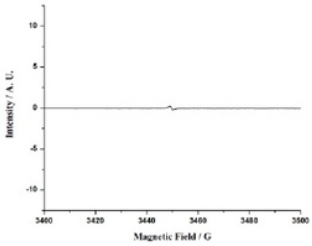

(a) at 6 h

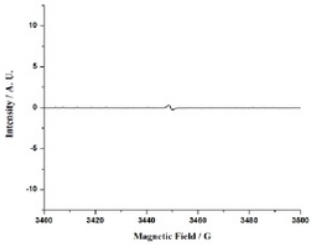

(b) at 12 h

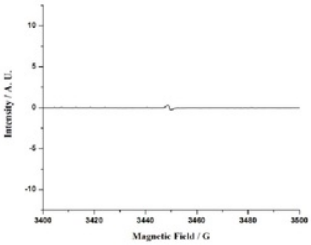

(c) at 24 h

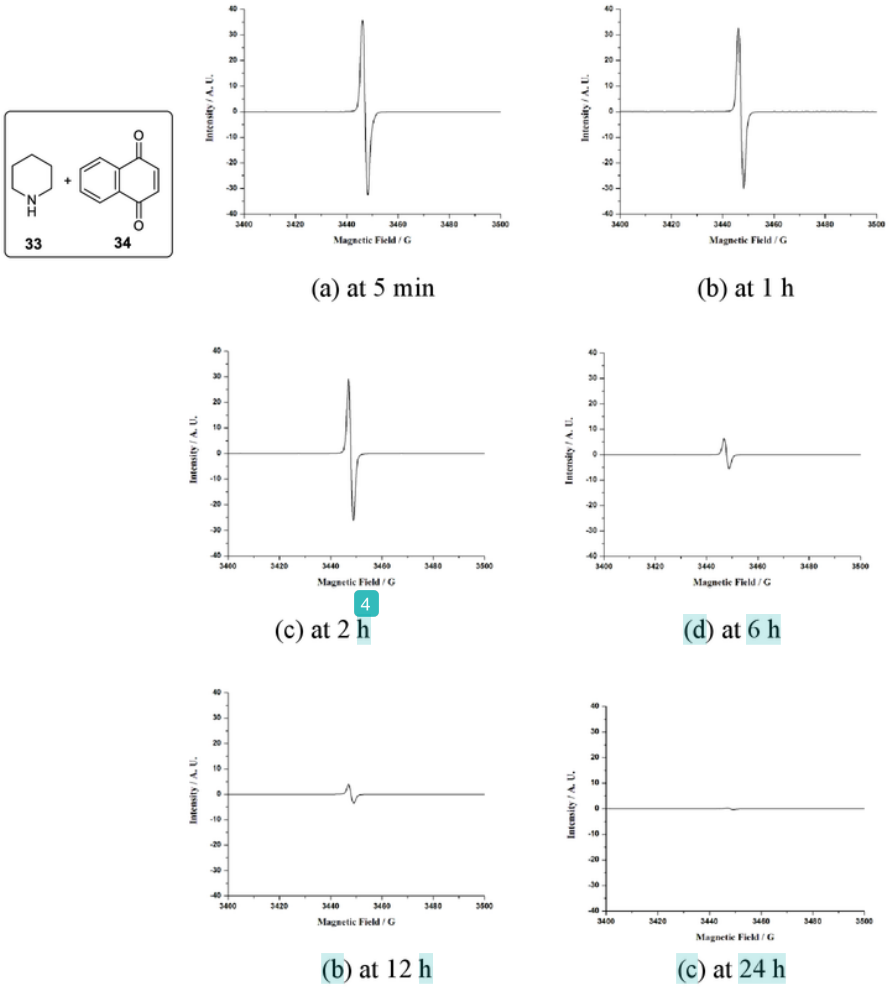

Figure 3. EPR spectra of pipridine **33** with quinones (0.05 mmol) and (0.05 mmol) in CH_2Cl_2 solvent.

The reaction finally leads to the formation of diamagnetic 2, 5-di-piperidin-1-yl-[1,4] benzoquinone product **38** (Scheme 9).

Scheme 9. Electron transfer reaction of benzoquinone **2** with piperidine **33**

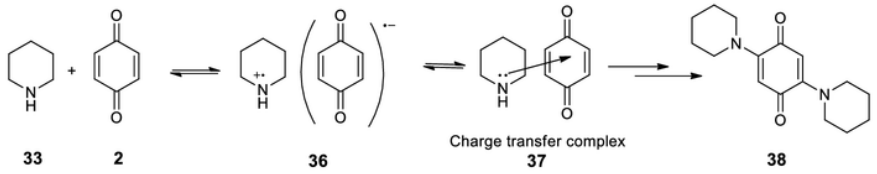

A possible mechanism for the formation aminoquinone is outlined in Scheme 10.

Scheme 10

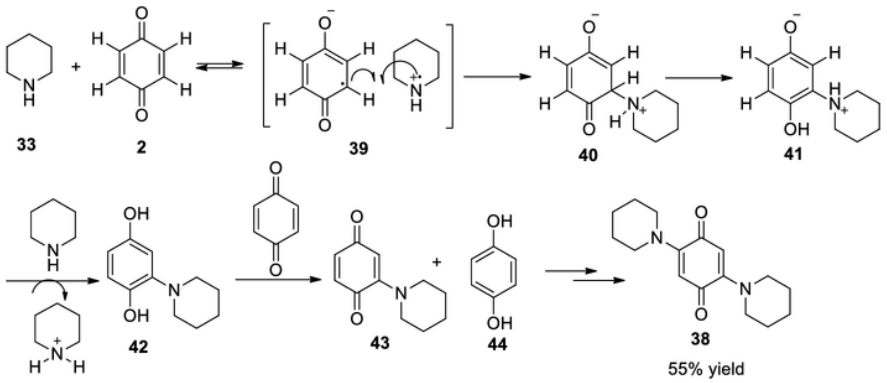

Similar reaction of *p*-chloranil **6** with piperidine **33** gave the ion radical pairs **45** followed by charge transfer complex **46** with subsequent formation of the diamagnetic 2, 5-dichloro-3,6-di-piperidin-1-yl-[1,4] benzoquinone product **47** (Scheme 11).

Scheme 11

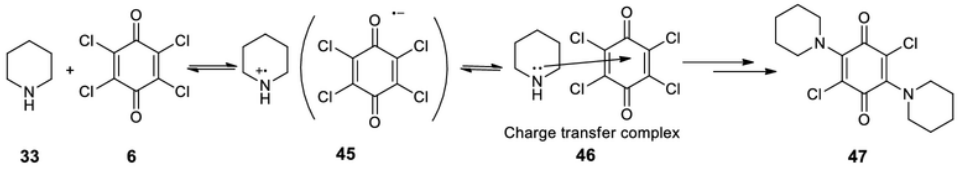

A possible mechanism for the formation of aminoquinone **47** is outlined in Scheme 12.

Scheme 12

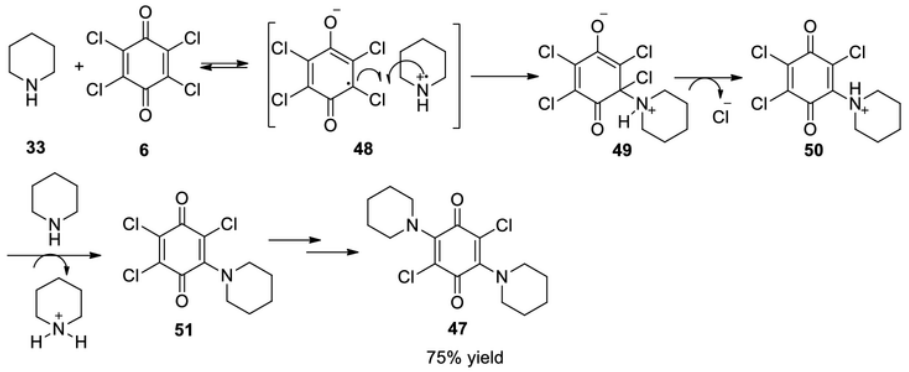

Similarly, the reaction of piperidine **33** with 1,4-naphthaquinone **34** and 2,3-dichloronaphthaquinone **35** results in aminoquinone derivatives **54** and **55** through the formation of paramagnetic intermediates **52** and the charge transfer complex **53** (Scheme 13).

Scheme 13

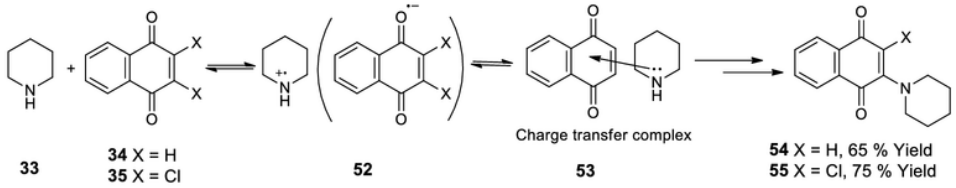

Recently, it was reported that the reaction of pyrrolidine **11a** with *p*-chloranil **6** gives the corresponding mono substituted aminoquinone **15** through polar or ionic intermediate **56** (Scheme 14).[13]

Scheme 14

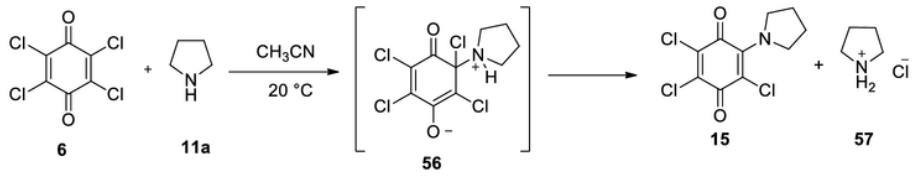

It was also reported that the formation C-C bond by the reaction of amine with quinones through polar pathway is several orders of magnitude faster than that expected for single electron transfer (SET) process. However, the epr data were not discussed by these authors. Also, there was no discussion on the formation of charge transfer or electron transfer complexes in the reaction between amines and quinones.

We have observed epr signal in accordance with the formation of paramagnetic intermediates upon mixing the secondary amine with quinones. Our results clearly indicate that electron transfer *via* initial cross exchange process to give the radical ion pair **45** with subsequent formation of charge transfer complex **46** and the aminoquinone product **47** with time (Scheme 15).

Scheme 15

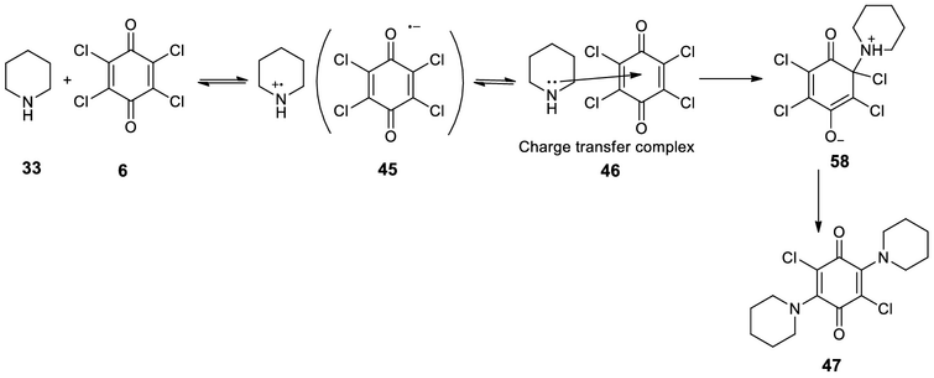

Hence, the electron transfer reaction, the radical ion intermediates and charge transfer complexes cannot be ruled out in this transformations (Scheme 15).

3.2.2 Reaction of tertiary amines with quinone acceptors

The reaction of secondary amine and quinones lead to the aminoquinone derivatives *via* radical intermediates and charge transfer complexes. We have then turned our attention towards the reaction of tertiary amines with *p*-chloranil.

We have observed that the reaction of *N, N*-diisopropylethylamine **59** (DIPEA) with *p*-chloranil **6** in PC solvent gave paramagnetic species detected by EPR spectroscopy with g value of 2.0037 (Figure 4)**.** The electron transfer complex was stable up to 24 h but the intensity of the epr signal decreased with time in PC solvent (Figure 4).

The rapid formation of electron transfer and charge transfer complex was observed upon mixing of DIPEA **59** with *p*-choranil **6** in PC solvent. The mixture turns to bright green immediately. Similarly, the reaction using *p*-chloranil **6** with tertiary amines like 1,4-diazabicyclo[2.2.2]octane (DABCO) **26**, *N, N'*-tetramethyl-1,4-phenylenediamine (TMPDA) **60**, *N,N*-diethylaniline ($PhNEt_2$) **61** and triphenylamine (TPA) **62** also gives paramagnetic intermediates as revealed by epr spectroscopy. The epr spectrum recorded at different time intervals are shown in Figure 4.

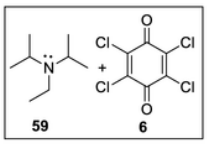

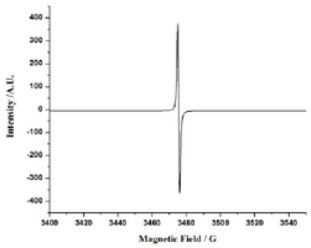

(a) at 5 min

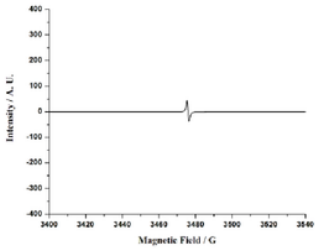

(b) at 1 h

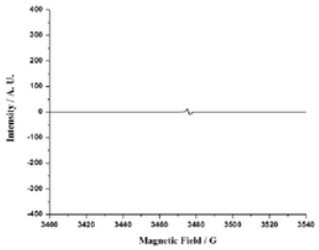

(c) at 2 h

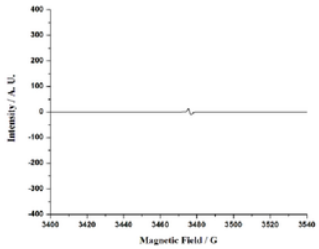

(d) at 6 h

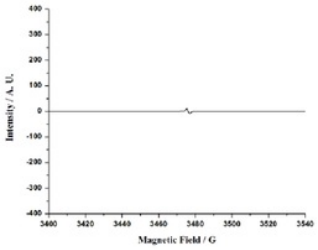

(e) at 12 h

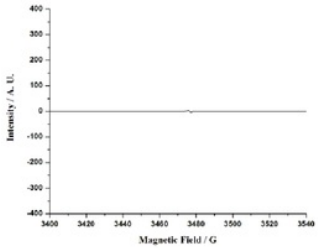

(f) at 24 h

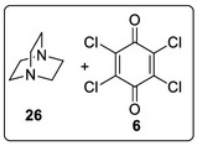

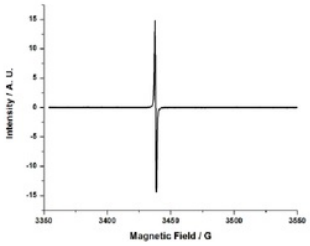

(a) at 5min

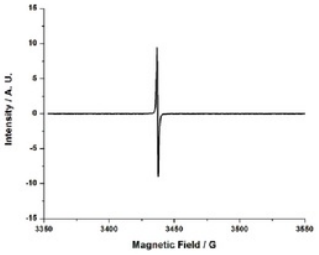

(b) at 1 h

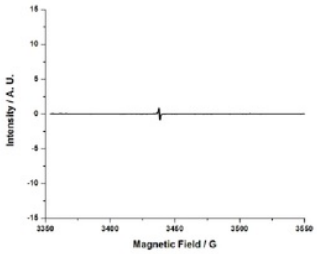

(c) at 6 h

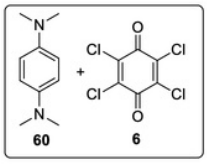

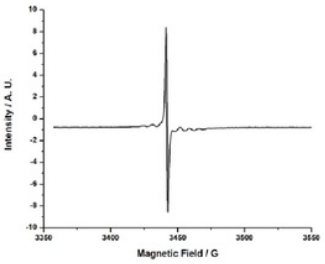

(a) at 5min

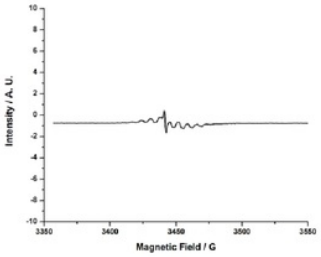

(b) at 1 h

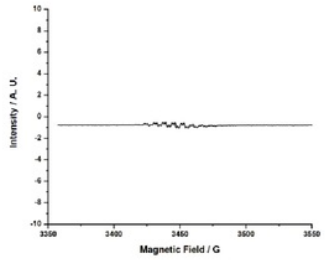

(c) at 6 h

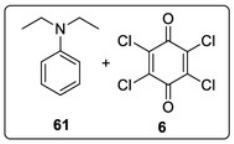

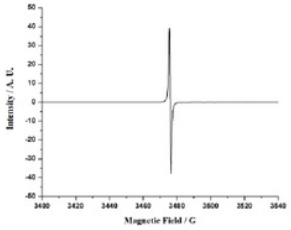

(a) at 5 min

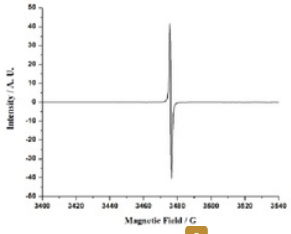

(b) at 1 h

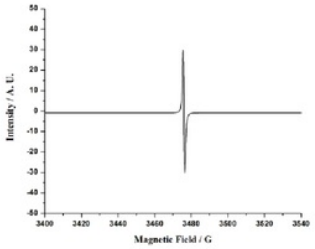

(c) at 2 h

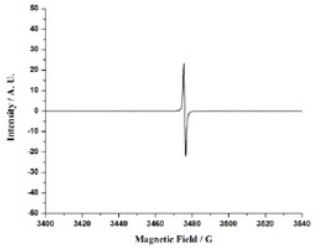

(d) at 6 h

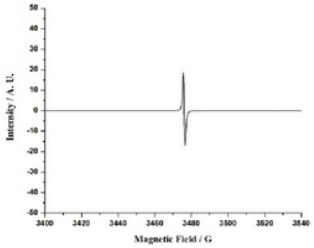

(e) at 12 h

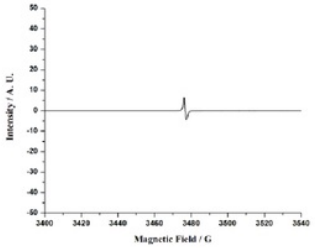

(f) at 24 h

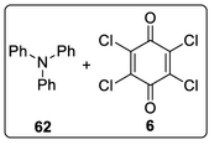

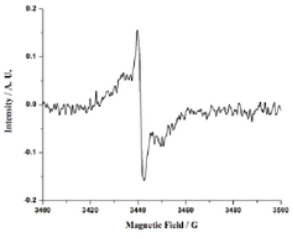

(a) at 5min

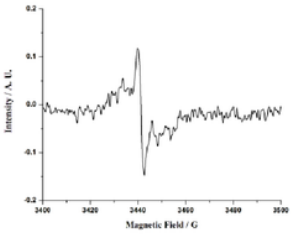

(b) at 1 h

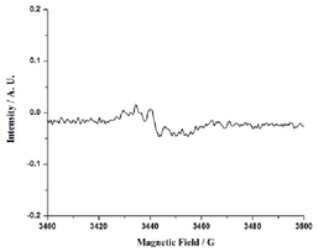

(c) at 6 h

Figure 4. EPR spectra of *p*-chloranul **6** (0.05 mmol) and tertiary amine (0.05 mmol) in PC solvent.

The reaction of DIPEA **59** with *p*-chloranil **6** gave the amine radical cation and quinone radical anion pairs **63** followed by charge transfer complex **64 (**CT 1). The epr signal is mainly due to the presence of quinone radical anion **65** which may react with neutral *p*-chloranil to give the corresponding CT complex, CT 2. The amine radical cation would undergo fast exchange of electron with the neutral amine and hence does not exhibit epr signal (Scheme 16). Similarly, the other amine donors also react with *p*-chloranil to give radical ion intermediates followed by charge transfer complexes.

Scheme 16

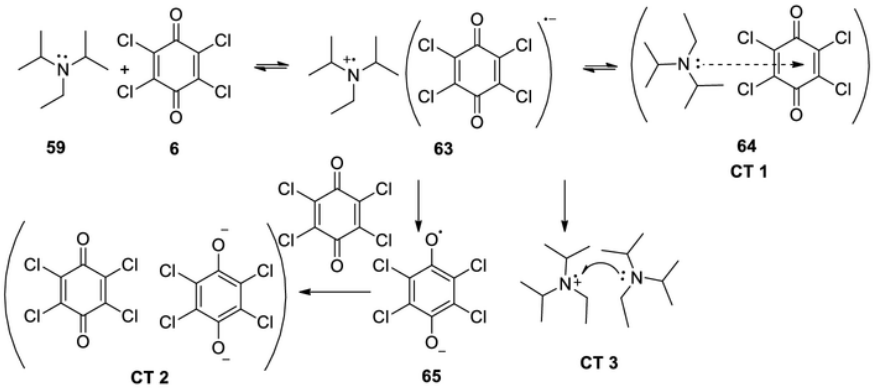

The reaction of *N,N*-diethylaniline ($PhNEt_2$) **61** with *p*-chloranil **6** gave paramagnetic intermediates. Presumably, the initially formed amine radical cations are slowly coupled to give the tetraethylbenzidine product **68** besides the formation of a small amount (<5%) of the corresponding hydroquinone (Scheme 17).

Scheme 17

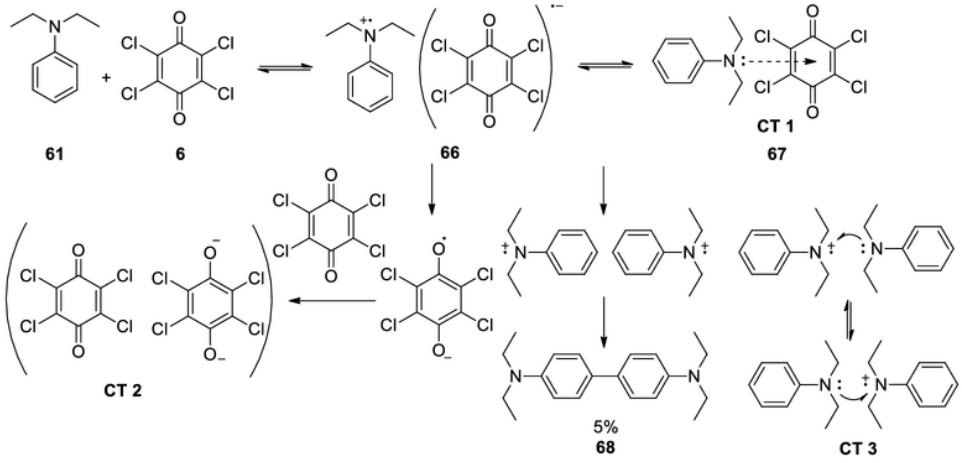

Similarly, the reaction of DIPEA **59** with *p*-chloranil **6** in gamma butyrolactone (GBL) solvent gives paramagnetic intermediates which was also confirmed by epr spectroscopy (Figure 5).

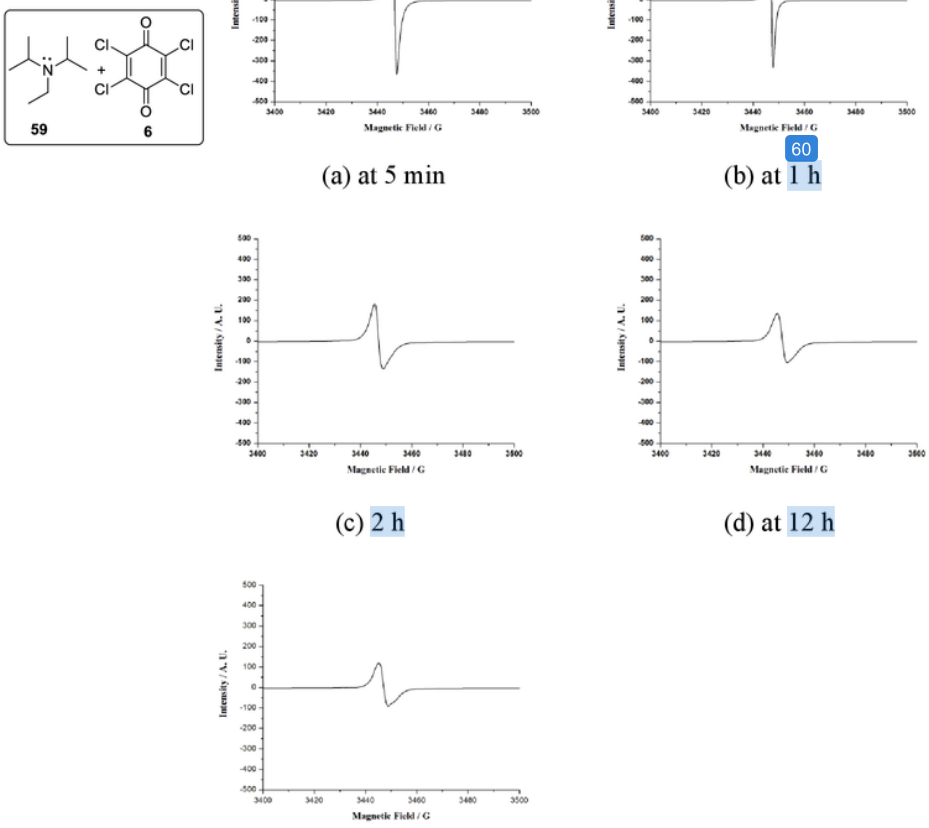

Figure 5. EPR spectra of *p*-chloranul **6** (0.05 mmol) and DIPEA **59** (0.05 mmol) in GBL solvent.

In all the cases, we have observed a single signal in the epr spectrum. Earlier, it was reported[8] that the line broadening was observed in the epr spectra of naphthalene radical ion by the addition of excess of naphthalene. The rate constants for electron transfer between naphthalene radical ion and naphthalene are in the range 10^7-10^9 liters $mole^{-1}$ $sec.^{-1}$

Such single line broadening was also reported[14,15] in the case of 2,3-dichloro-5,6-dicyano-1,4-benzoquinone (DDQ) radical anion **31** with DDQ **18** with a fast exchange rate constant of 2.5 x 10^9 M^{-1} S^{-1} and activation energy of 1.6 kcal mol^{-1} at 23 °C. The electron is transferred from HOMO of donor amine to the LUMO of *p*-chloranil acceptor. Electron transfer leads to the formation amine radical cation and quinone radical anion. But, in epr spectrum, we have observed only one peak for the paramagnetic complex. This indicates that there is a fast self- exchange of electron between neutral amine with amine radical cation.

J. K. Kochi *et al* reported self-exchange and cross exchange reactions between 2,2,6,6-tetramethylbenzo[1,2-d:4,5-d']bis[1,3]dioxole **29** (TMDO) donor with 2,3-dichloro-5,6-dicyano-p-benzoquinone **18** (DDQ) acceptor in CH_2Cl_2 (Scheme 18).[12]

Scheme 18

(1) Cross exchange electron transfer process

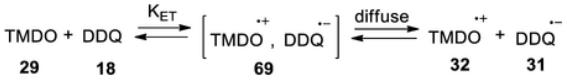

(2) Self-exchange electron transfer process

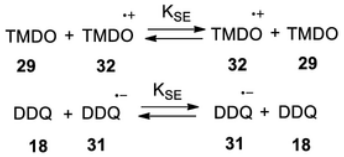

Hence, the line-broadening of epr signals observed for the intermediates obtained from DIPEA **59** and *p*-chloranil **6** can be explained by considering the electron exchange phenomenon.

It was reported that the reaction of *p*-chloranil **6** with 1,4-diazabicyclo[2.2.2]octane, DABCO **26** gives 1:1 charge transfer complex.[11] The formation

of the charge transfer complex was also confirmed by UV-Visible spectroscopy and the absorption band at 450 nm of DABCO-chloranil system was assigned to the chloranil anion radical. Also, the formation of charge transfer complex between electron deficient DDQ with electron rich π-system like cyclic enol ethers was reported.[13b] The charge transfer absorbance band at 589 nm in UV-Visible spectroscopy indicates the formation of charge transfer complex between DDQ and cyclic enol ethers system.

We have also examined the formation of charge transfer complex in the reaction of DIPEA **59** with *p*-chloranil **6** by UV-Visible spectroscopy (Figure 6). The color change was not observed for this diluted solution.

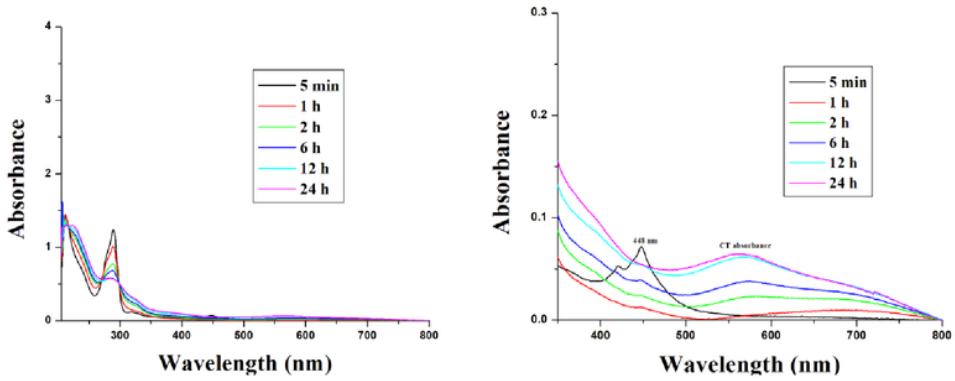

(a) (b)

Figure 6. a) UV-Vis spectra of a mixture of DIPEA **59** (1 x 10^{-3} mol L^{-1}) and *p*-chloranil **6** (1 x 10^{-4} mol L^{-1}) in PC at 25 °C. b) Expanded UV-Visible spectrum.

However, the characteristic absorbance band for chloranil anion radical was observed at 448 nm in 5 minutes and no charge transfer absorption band appears at that time. The new absorbance band developed slowly with time beyond 500 nm can be assigned to the absorption of the charge transfer (CT) complex **64**, because neither *p*-chloranil **6** nor DIPEA **59** absorbed in this region. The UV-Visible spectrum is shown in

Figure 6. We have also recorded the UV-Visible spectrum of solution of *N, N*-diethylaniline **61** ($1x10^{-3}$) and triphenyl amine **62** ($1x10^{-3}$) with *p*-chloranil **6** ($1x10^{-4}$) at different time intervals. The results are shown in Figure 7.

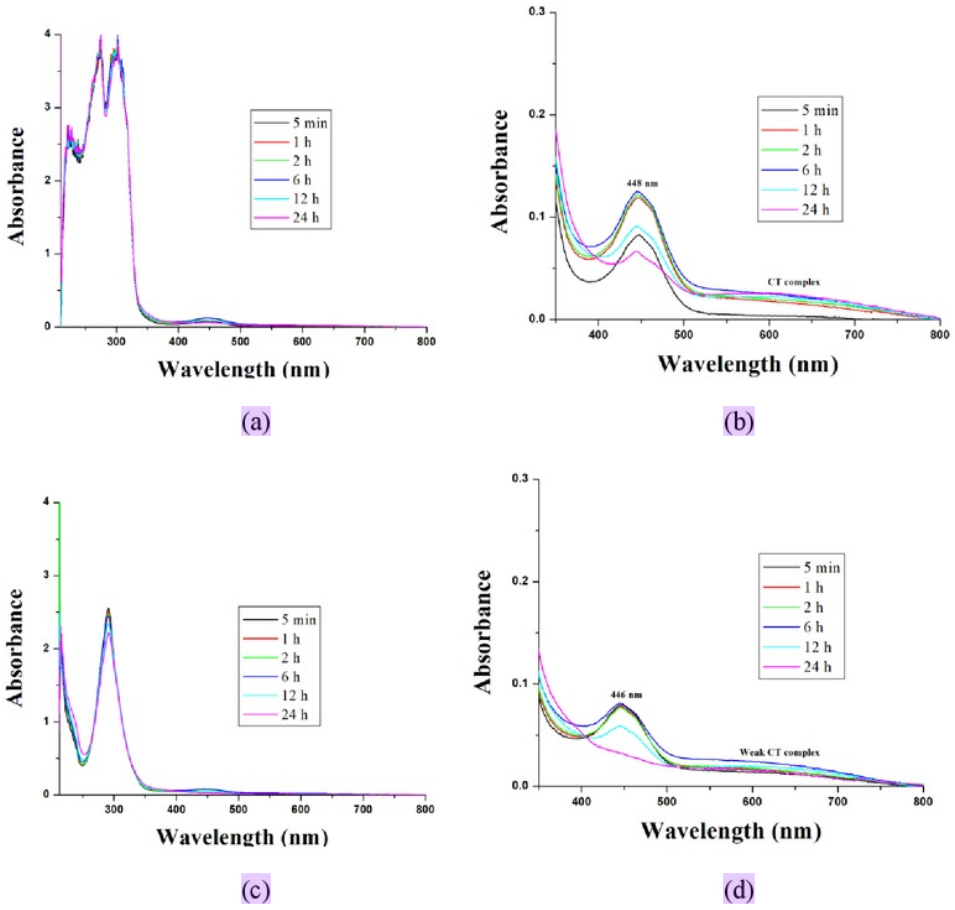

Figure 7. (a) and (c) UV-Vis spectra of a mixture of $PhNEt_2$ **61** (1 x 10^{-3} mol L^{-1}) and TPA **62** (1 x 10^{-3} mol L^{-1}) with *p*-chloranil **6** (1 x 10^{-4} mol L^{-1}) in PC at 25 °C. (b) and (d) Expanded UV-Visible spectrum.

We have also performed the reaction of DIPEA **59** with weak acceptors such as 1,4-benzoquinone (BQ) **2** and naphthoquinone (NQ) **34** also gave weak epr signal corresponding to paramagnetic intermediates formed in the reaction (Figure 8).

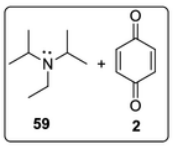

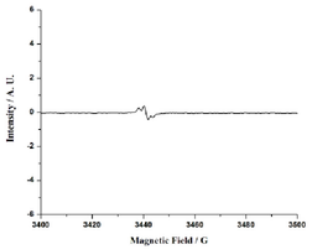

(a) at 5 min

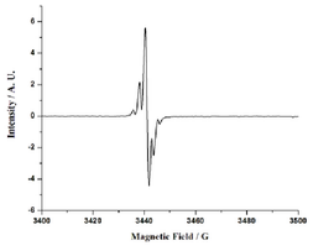

(b) at 2 h

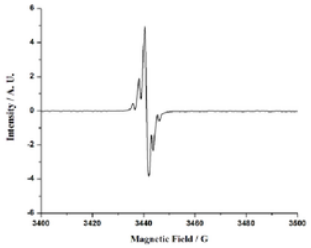

(c) at 6 h

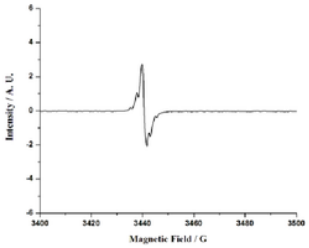

(d) at 12 h

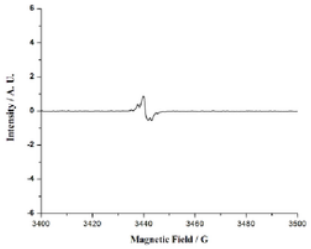

(e) at 24 h

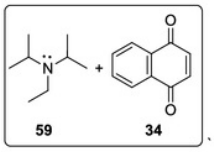

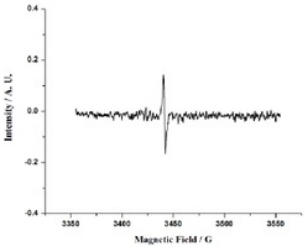

(a) at 5 min

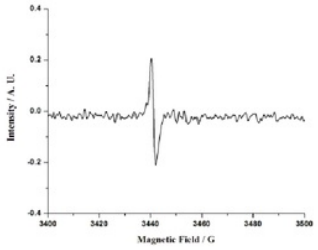

(b) at 2 h

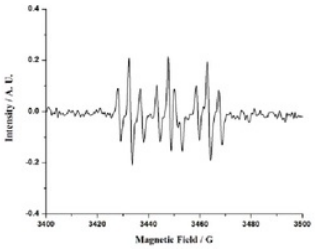

(d) at 6 h

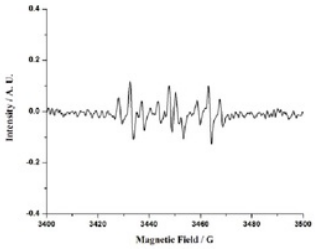

(d) at 12 h

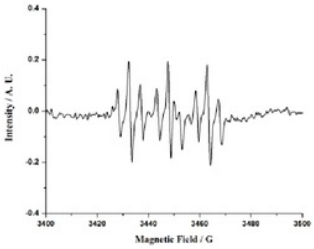

(e) at 24 h

Figure 8. EPR spectra of 1,4- benzoquinone **2** and naphthoquinone **34** (0.05 mmol) with DIPEA **59** (0.05 mmol) in PC solvent.

It was reported that use of polar solvents in the bimolecular interaction of DDQ **18** with TMDO **29** increases the diffusive separation of radical ion pairs (Scheme 19). [5]

Scheme 19

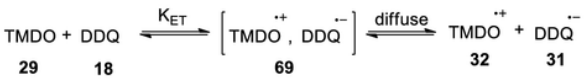

Hence, we have also reacted the amine DIPEA **59** with *p*-chloranil **6** (1:1 ratio) under neat condition. Interestingly, addition of drop of polar solvents like PC or *N*-methyl pyrrolidone (NMP) to the paramagnetic complex leads to increase in the strength of epr signal. The results are shown in Figure 9.

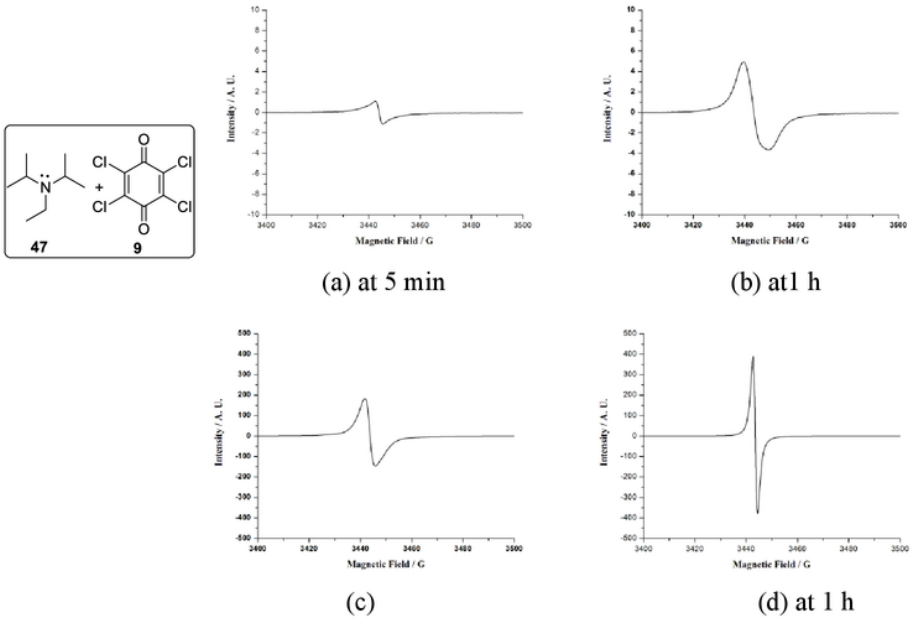

Figure 9. EPR spectra of *p*-chloranil **6** (0.05 mmol) and DIPEA **59** (0.05 mmol) in neat condition (a) at 5min (b) at 1 h (Intensity 10 to -10) (c) After addition of NMP (d) at 1 h (Intensity 500 to -500).

Presumably, the addition of polar solvents increases the concentration of paramagnetic intermediates due to the diffusive separation of ion pairs leading to more intense epr signal.

The nature of the paramagnetic species observed in the reaction and the reason for the decrease in epr signal intensity with time is not clearly understood. Presumably, a diamagnetic 1, 4-addition product could be formed as the reactivity of the tertiary amine and secondary amine is expected to be similar or the initially formed ion pair intermediates are slowly converted to the charge transfer complex that may lead to decrease in epr signal intensity (Scheme 20).

Scheme 20

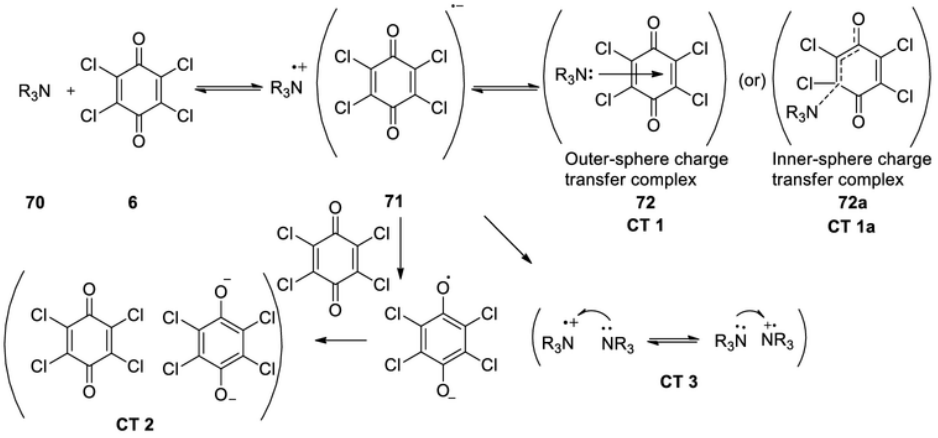

3.2.3 Reaction of tertiary amine with *p*-chloranil 6 under neat condition

We have also reacted *N, N*-diisopropylethylamine **59** (DIPEA) with *p*-chloranil **6** under the neat condition (without solvent)**.** The paramagnetic species formed were detected by epr spectroscopy with g value of 2.0031. In this case, an increase in the epr signal was observed with time. Presumably, the electron transfer reaction of *p*-chloranil and DIPEA will be slower under neat condition. Also, the reaction of DIPEA derivatives like *N*-benzyl-*N*-isopropylpropan-2-amine **73**, *N, N*-diisopropyl-2, 2-dimethylpropan-1-amine **74** and *N,N*-diethylaniline **61** with *p*-chloranil **6** gave the paramagnetic

intermediates under neat condition. The epr signal changes with time are shown in Figure 10.

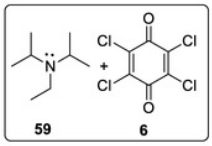

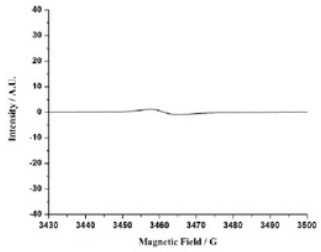

(a) at 5 min

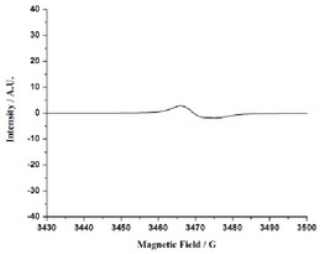

(b) at1 h

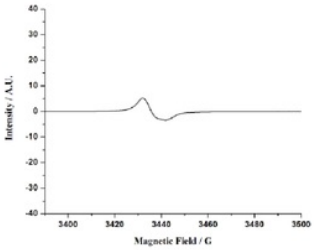

(c) at 2 h

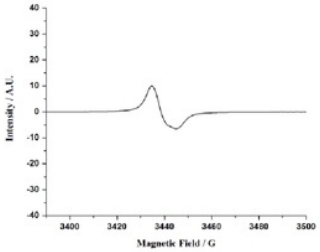

(d) at 6 h

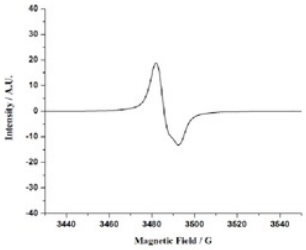

(e) at 12 h

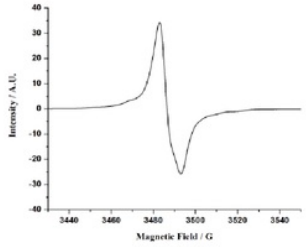

(f) at 24 h

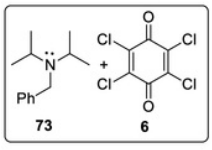

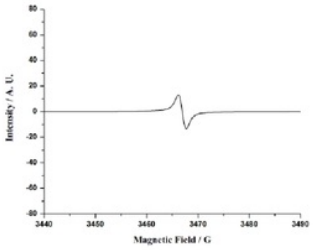

(a) at 5 min

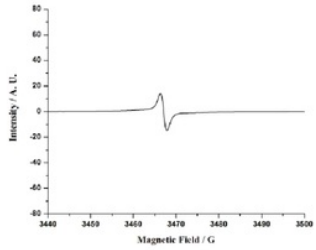

(b) at1 h

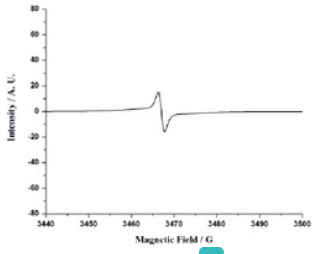

(c) at 2 h

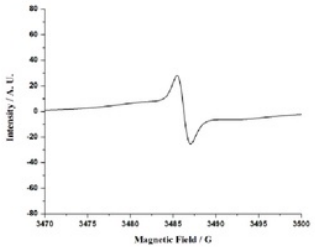

(d) at 6 h

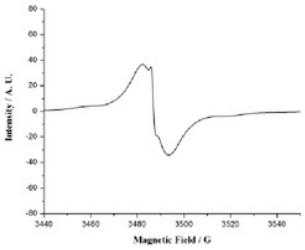

(e) at 12 h

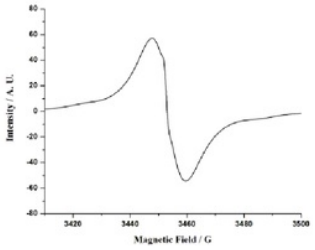

(f) at 24 h

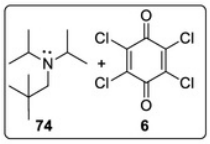

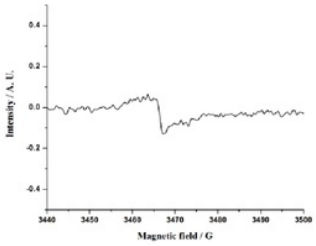

(a) at 5 min

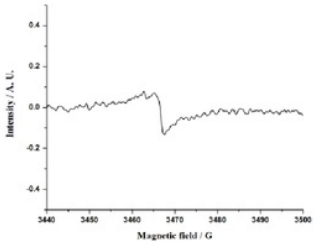

(b) at1 h

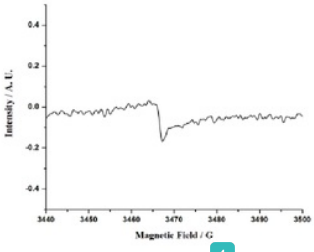

(c) at 2 h

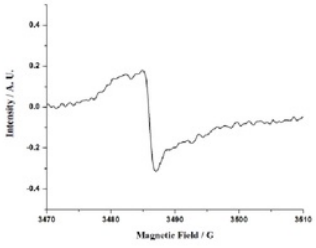

(d) at 6 h

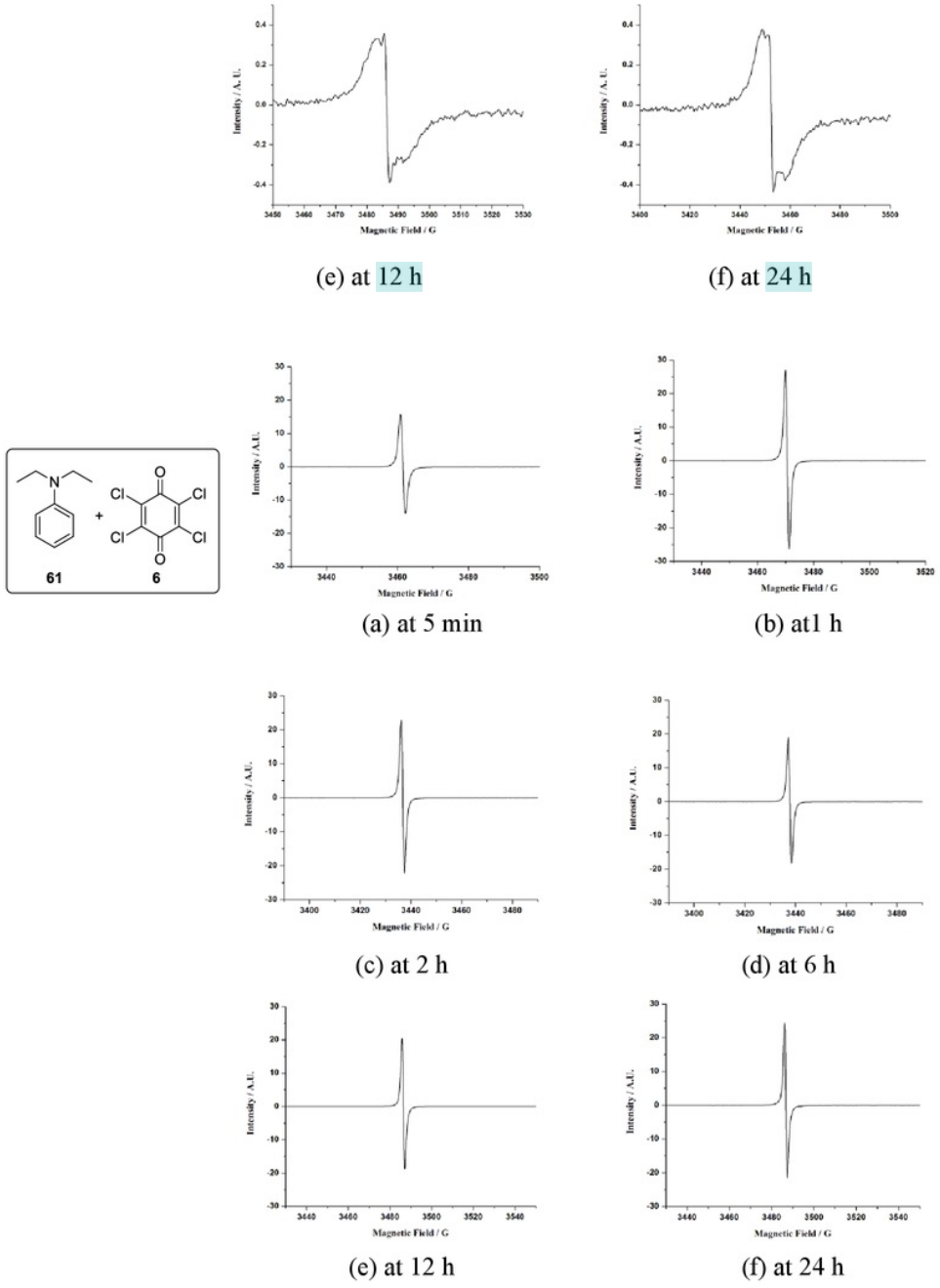

Figure 10. EPR spectra of *p*-chloranil **6** (0.05 mmol) and amine (0.05 mmol) in neat condition.

Interestingly, the epr signal strength increased with time, whereas under solvent condition (Figure 4) the signal strength decreased with time. Presumably, the formation of radical ion pairs is slow under neat condition. However, the epr signal at 5 minutes in PC is much stronger (DIPEA **59**, Figure 4) indicating the presence of more amounts paramagnetic species in the polar solvent.

3.2.4 Reaction of 2,2,6,6-tetramethylpiperidine derivatives 76 with *p*-chloranil

Synthesis of polymeric amine

We have synthesized polymers containing amine as a pendant group through transesterification of PMMA (polymethylmethacrylate) **75** using 4-hydroxy-2,2,6,6-tetramethylpiperidine **76a**. The polymer **76b** is also readily converted to the corresponding TEMPO derivative **77** (Scheme 21). The prepared radical polymer PTMA **69** was characterized by epr spectroscopy with g value of 2.0063 (Figure 11). The epr of prepared PTMA radical is in accordance with the reported epr signal.[16]

Scheme 21

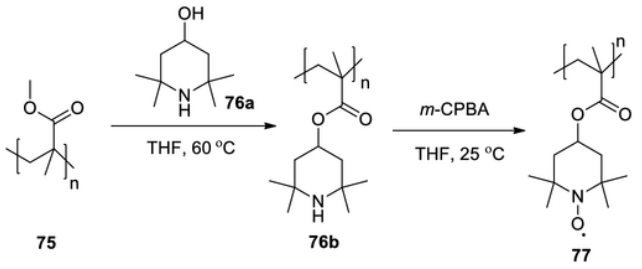

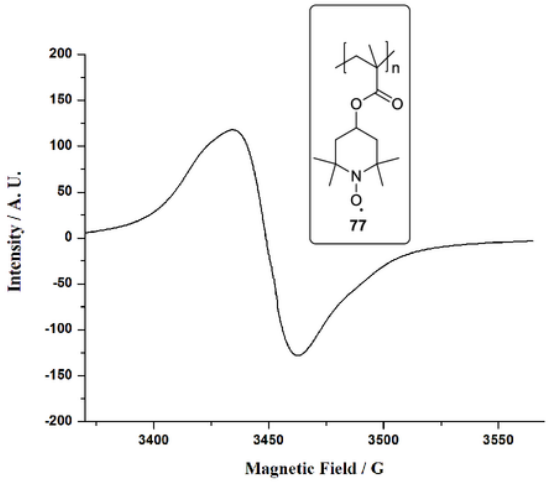

Figure 11. EPR spectra of synthesized PTMA radical polymer **77**

The present method for the preparation of PTMA radical polymer **77** is simple and convenient compared to the methods available in the literature.[17] Previously, the PTMA **77** was synthesized by the polymerization of 2,2,6,6-tetramethylpiperidine methacrylate monomer **79** followed by the oxidation of the precursor secondary amine polymer **76b** (Scheme 22).[18] An advantage of the present method is that commercially available PMMA samples with different molecular weight can be utilized in the preparation of different polymeric derivatives.

Scheme 22

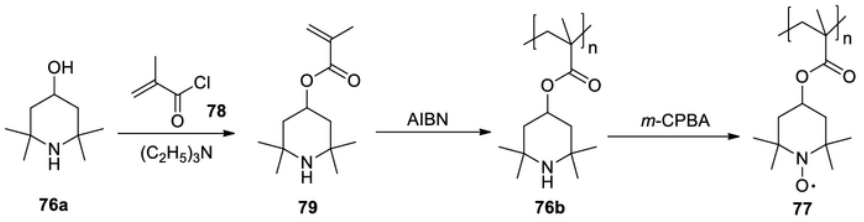

The PTMA **77** has the nitroxide radical 2,2,6,6- tetramethyl-1-piperidinyloxy (TEMPO) as repeating unit. TEMPO possesses good chemical stability because of

resonance structures and steric protection of the radical center. TEMPO and PTMA **77** polymer exhibit reversible oxidation-reduction behavior in aprotic solvents. On oxidation of the nitroxide radical, the p-type doping occurs in a reversible manner and the oxoammonium cation is formed. The existence of such a redox couple of radical makes PTMA **77** an attractive cathode-active material for use in lithium batteries.[19] As PTMA **77** is an electrical insulator, the addition of a suitable conductive material in the cathode composition is essential for effective transport of charges.[20] The PTMA **77** is thermally stable at high temperature. This radical concentration remains unchanged for over one year under ambient conditions. This polymer displays appropriate solubility in organic solvents.

We have also observed that the reaction of sterically hindered 2,2,6,6-tetramethylpiperidine derivatives **76** with *p*-chloranil **6** in PC solvent gave the paramagnetic species **80** (Scheme 23).

Scheme 23

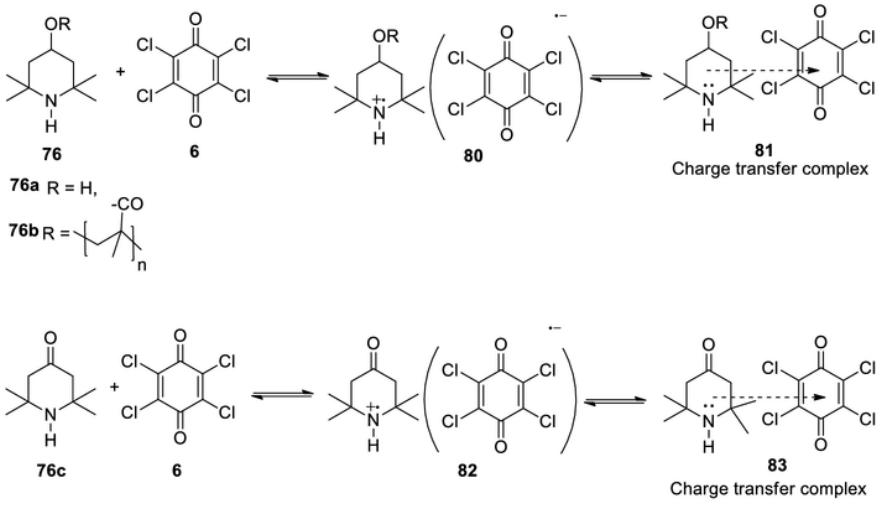

Interestingly, the reaction of the polymeric amine derivative **76b** with *p*-chloranil **6** gave moderately stable paramagnetic intermediates. In all these cases, we observed a triplet signal in the epr spectroscopy corresponding to amine radical cation (Figure 12).

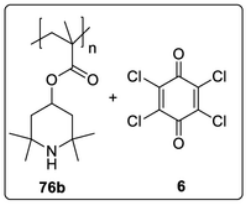

76b 6

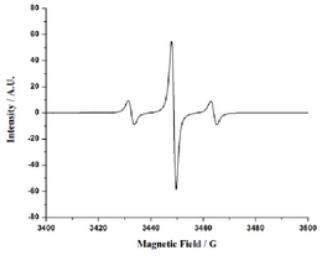

(a) at 5 min

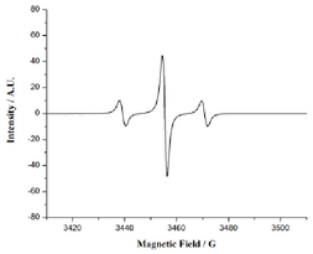

(b) at1 h

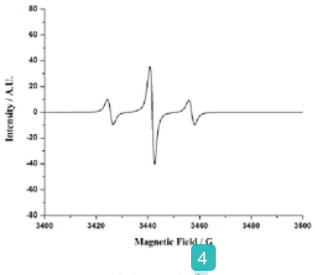

(c) at 2 h

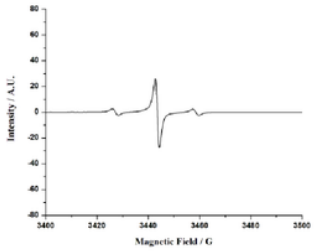

(d) at 6 h

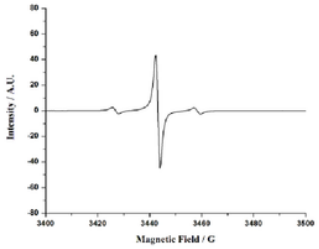

(e) at 12 h

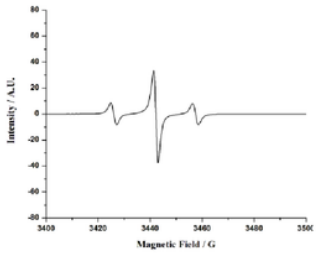

(f) at 24 h

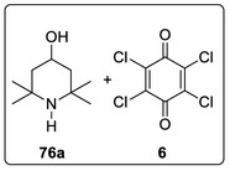

76a 6

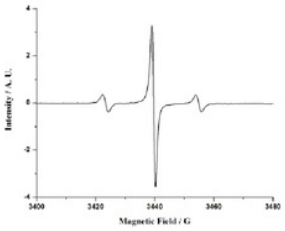

(a) at 5 min

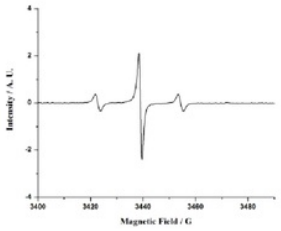

(b) at1 h

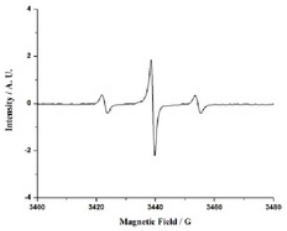

(c) at 2 h

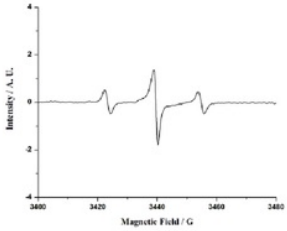

(d) at 6 h

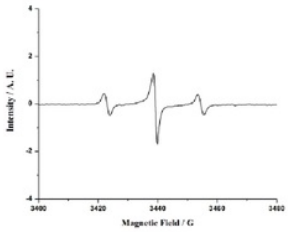

(e) at 12 h

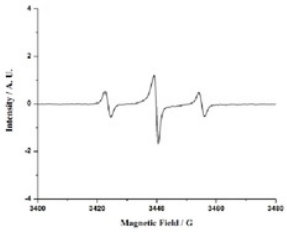

(f) at 24 h

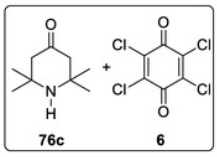

76c 6

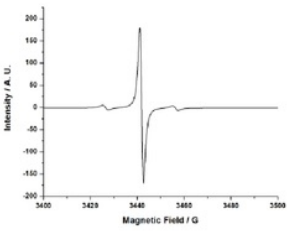

(a) at 5 min

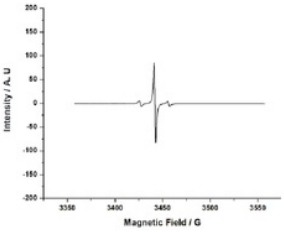

(b) at1 h

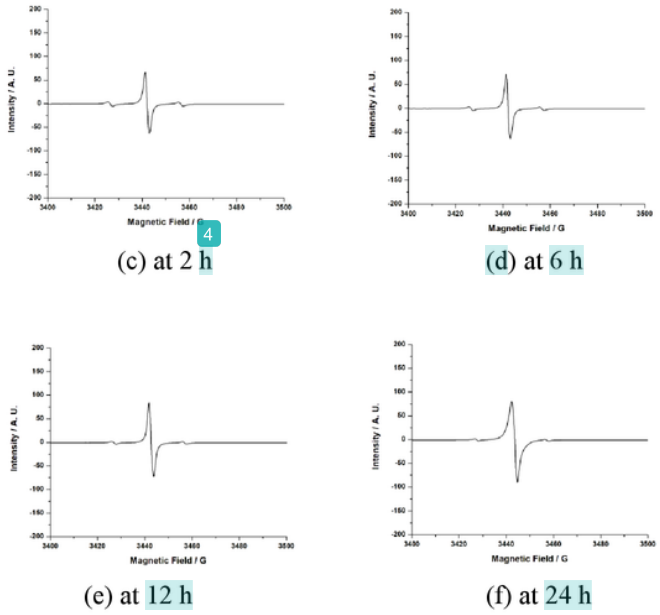

Figure 12. EPR spectra of *p*-chloranul **6** (0.05 mmol) and 2,2,6,6-tetramethylpiperidine derivatives **76a, 76b** and **76c** (0.05 mmol) in PC solvent.

However, even in the reaction of sterically hindered 2,2,6,6-tetramethylpiperidine with *p*-chloranil decrease in the strength of epr signal was observed with time. Presumably, complex formed here is outer-sphere in nature and not affected by the steric hindrance by the methyl groups.

Scheme 24

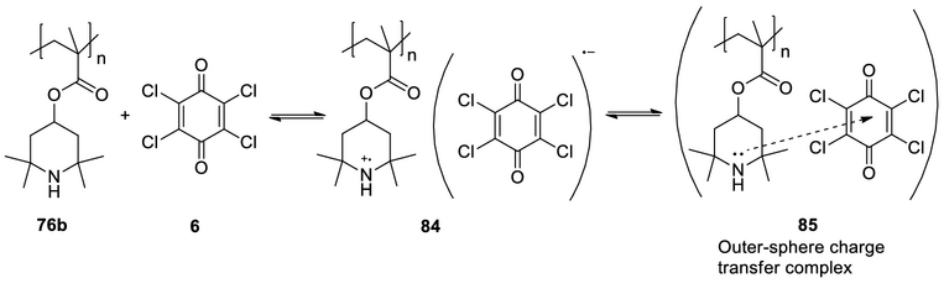

The charge-transfer complex **96** of *N,N,N′,N′*-tetramethyl-*p*-phenylenediamine (TMPDA) **4** with *p*-chloranil **12** was reported.[21] It was proposed that such complex interchanges reversibly with radical ion pairs (Scheme 25).[22] Also, in solid state the TMPDA-*p*-chloranil complex was diamagnetic in nature.[23] We have observed that in this case also the epr signal strength decreases with time in PC solvent (Figure 4).

Scheme 25

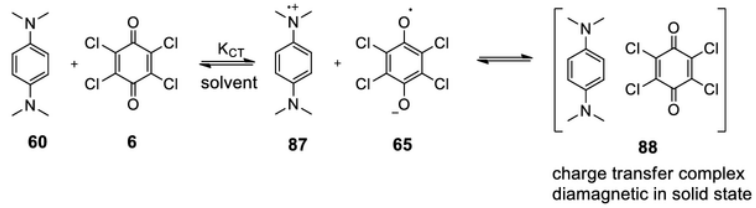

3.2.5 EPR Studies of aminoquinone

The aminoquinones (**38**, **47**, **54** and **55**) were prepared by the reaction of piperidine with corresponding quinone in CH_2Cl_2 solvent. We have already discussed that the aminoquinones are by electron transfer mechanism and the paramagnetic intermediates were confirmed by epr spectroscopy.

Scheme 26

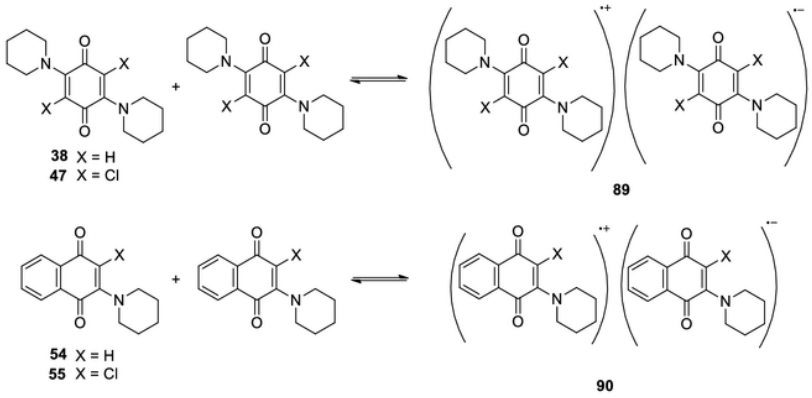

The aminoquinones behave as both donor and acceptor when present in the same molecule. Interestingly, we observed a weak epr signal for aminoquinones in the solid state but did not observe epr signal when aminoquinone was dissolved in CH_2Cl_2 solvent (Scheme 26). Presumably, one of the aminoquinone molecule acts as a donor and another one acts as an acceptor in solid state leading to single, broad and weak epr signals (Figure 13).

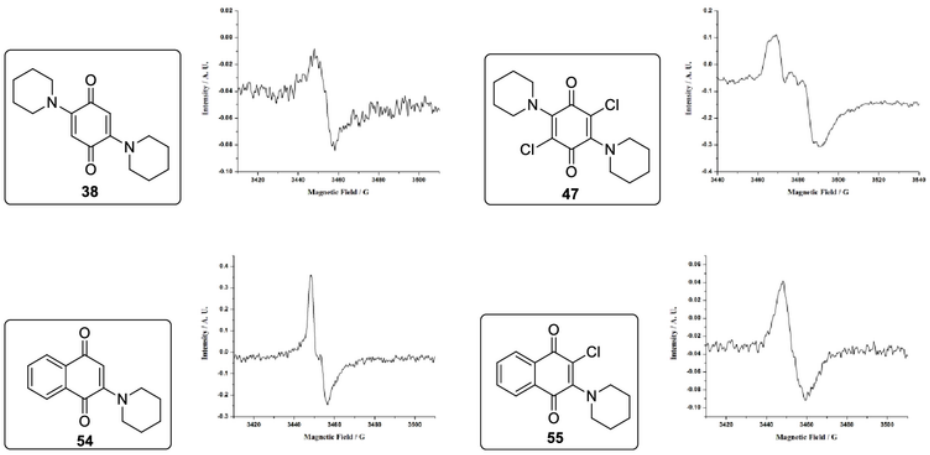

Figure 13. EPR spectra of aminoquinone in solid state (The aminoquinone solid (5 mg) was taken into epr tube and epr spectrum was recorded).

3.2.6 Attempt towards the electron transfer reaction of amines with halo compound acceptors

We have already discussed the results of the reaction of amines with quinone acceptors. The electron transfer readily takes place from donor amine to acceptor quinone leading to the formation of corresponding radical cation – anion pair as confirmed by epr spectral analysis.

Electron donor acceptor complexes and charge transfer interactions of amines with tetrahalomethanes were reported.[24] For example, DABCO **26** and quinuclidine **91** gives 1:1

donor-acceptor (DA) complex with tetrahalomethanes. Also, crystal structures were reported for the of 1:1 complex of DABCO and quinuclidine with CBr_4 **92**. The photochemical reaction of the DABCO-CBr_4 charge transfer complex leads to formation of radical ion intermediates (Scheme 27).

Scheme 27

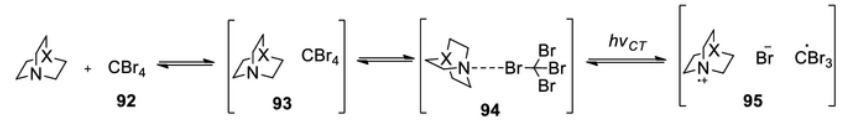

Similarly, electron donor acceptor complexes and charge transfer complexes of carbon tetrabromide, CBr_4 **92** and bromoform, $CHBr_3$ **96** with various donors such as halides, pseudohalide anions, aromatic hydrocarbons and aromatic compounds containing nitrogen and oxygen centers were reported.[25] Hence, we have studied the electron transfer reaction of sterically hindered amines with halometahne.

We have observed a weak epr signal for ion-pairs when the amine and halo compounds are reacted together. Previously, de Meijere *et al.* prepared the triisopropyl radical cation by the oxidation of triisopropylamine with SbF_5 in CH_2Cl_2 solution at 195K which gave the hyperfine epr spectrum.[26] They also noted that this radical cation has unusual thermodynamic and kinetic stability.[26] Also, these authors concluded that trialkylamine with at least two isopropyl substituents would lead to nearly planar structure for the corresponding radical cation, thus making it more stable.

We have briefly studied the electron transfer interaction of amines such as DIPEA **59**, 2,2,6,6-tetramethylpiperidin-4-ol **76a** and polymeric 2,2,6,6-tetramethylpiperidine derivative **76b** with halo compounds like CH_2Cl_2 **97**, CH_2Br_2 **98** and $CHCl_3$ **99** by epr spectroscopy.

The reaction of DIPEA **59** and dichloromethane CH_2Cl_2 **97,** CH_2Br_2 **98** and $CHCl_3$ **99** at room temperature gave very weak epr signals in epr spectroscopy (Figure 12). In these cases, we have scanned the spectra 10 times to get a clear epr signal. The epr spectrum with different time intervals are shown in Figure 14.

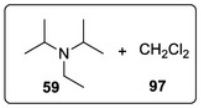

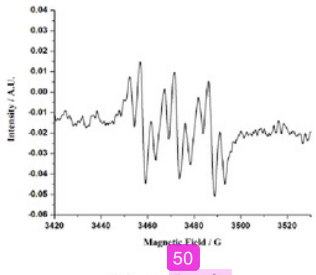

(a) at 5 min

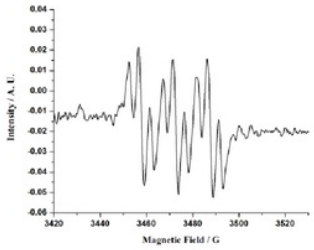

(b) at 1 h

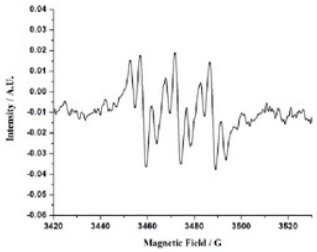

(c) at 6 h

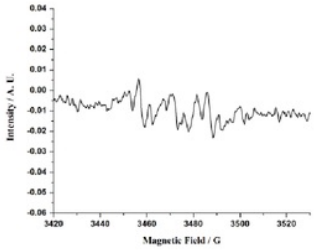

(d) at 12 h

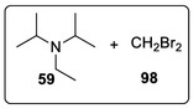

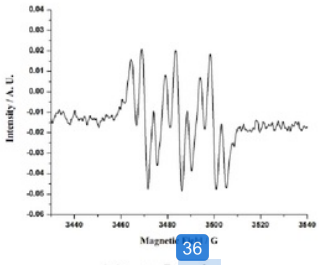

(a) at 5 min

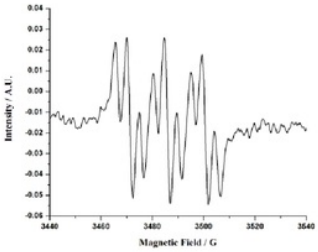

(b) at 1 h

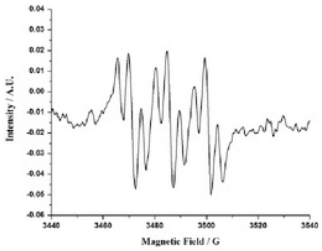

(c) at 2 h

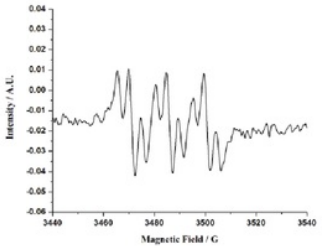

(d) at 6 h

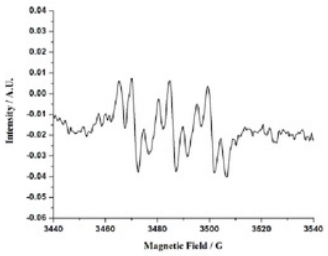

(e) at 12 h

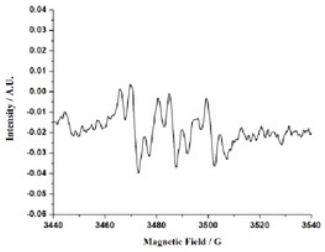

(f) at 24 h

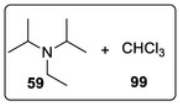

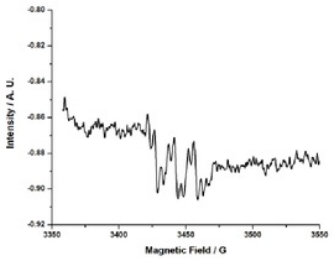

(a) at 5 min

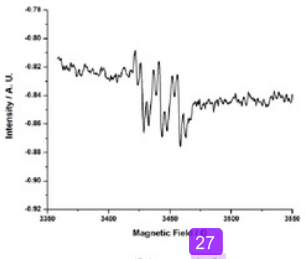

(b) at 1 h

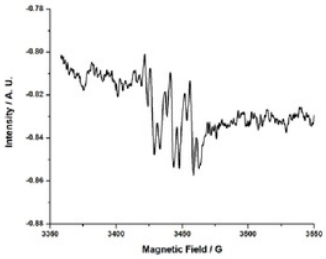

(c) at 2 h

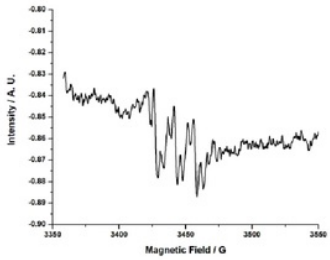

(d) at 6 h

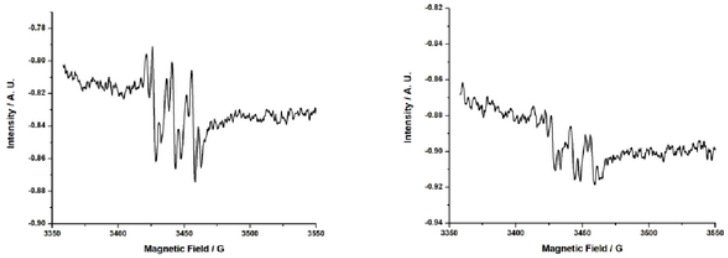

(e) at 12 h (f) at 24 h

Figure 14. EPR spectra of DIPEA **59** and CH_2Cl_2 **97,** CH_2Br_2 **98** and $CHCl_3$ **99** (Number of scans = 10).

The epr signal observed here due to the presence of amine radical cation and the signal due to the dichloromethane, dibromomethane and chloroform radical anions were not observed. Presumably, these radical anions may undergo fast exchange with the corresponding neutral species and hence do not give epr signal (Scheme 28).

Scheme 28

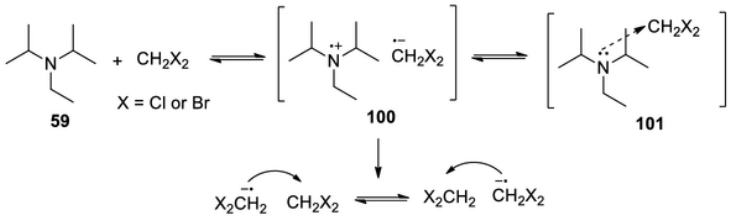

In all these cases, weak hyperfine splitting was also observed in epr spectroscopy. The reaction of *N, N*-diisopropylethylamine, DIPEA **59** with acceptors such as CH_2Cl_2 **97**, CH_2Br_2 **98** and $CHCl_3$ **99** gives a weak hyperfine splitting by the interaction of the radical cation present on nitrogen with two methylene β – protons of ethyl or isopropyl substituent of the radical cation.

We have also performed reaction with other donor amines *N, N*-diethyl aniline **61** and triphenyl amine **62** with halo compounds, but we did not observe the presence of

paramagnetic intermediates. Presumably, these relatively weak amines do not undergo electron transfer reactions with CH_2X_2 compounds.

Also, we have observed that the sterically hindered amine 2,2,6,6-tetramethylpiperidin-4-ol **76a** reacts with CH_2Cl_2 **97**, CH_2Br_2 **98** and $CHCl_3$ **99** to give a triplet signal in epr spectroscopy indicating the formation of corresponding 2,2,6,6-tetramethylpiperidin-4-ol radical cation (Figure 15).

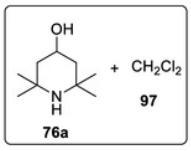

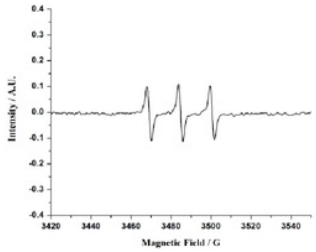

(a) at 5 min

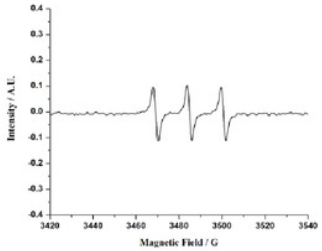

(b) at 1 h

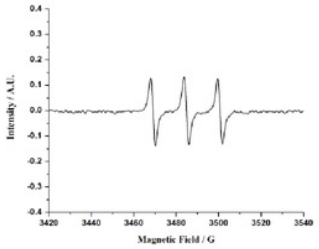

(c) at 2 h

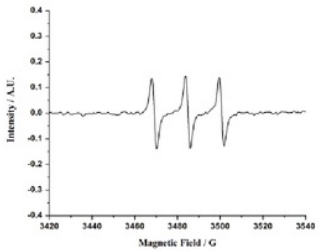

(d) at 6 h

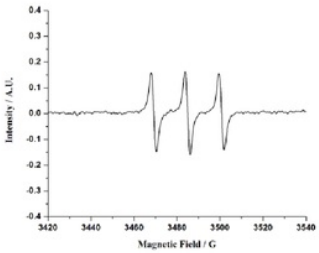

(e) at 12 h

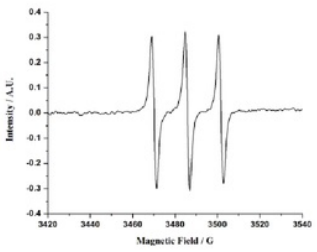

(f) at 24 h

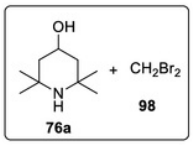

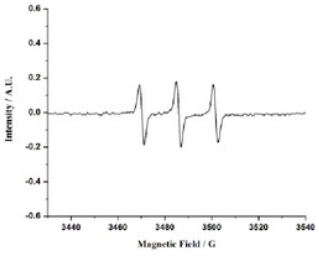

(a) at 5 min

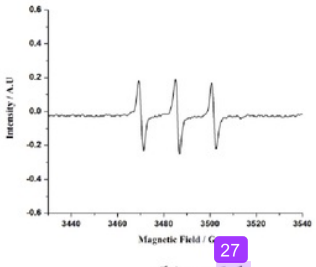

(b) at 1 h

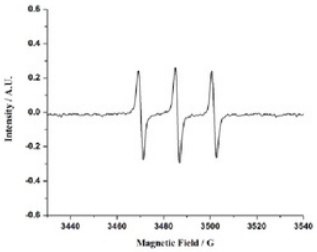

(c) at 2 h

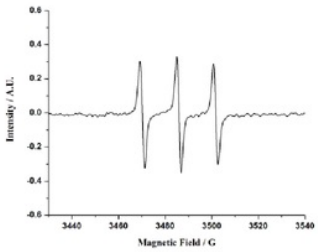

(d) at 6 h

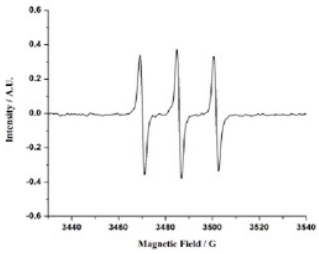

(e) at 12 h

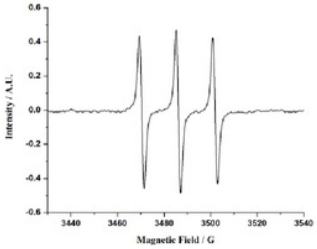

(f) at 24 h

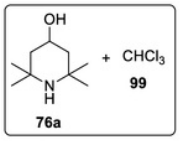

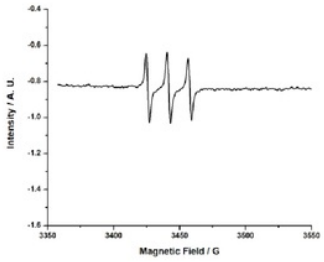

(a) at 5 min

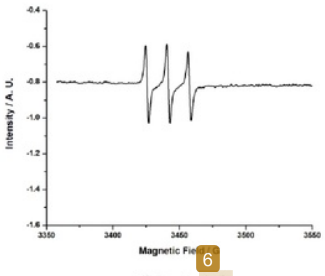

(b) at 1 h

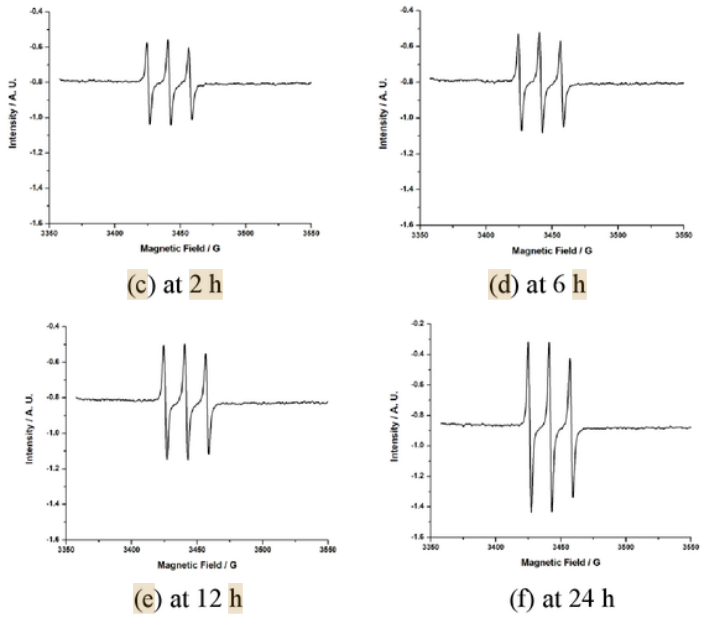

Figure 15. EPR spectra of 2,2,6,6-tetramethylpiperidin-4-ol **76a** and CH_2Cl_2 **97,** CH_2Br_2 **98** and $CHCl_3$ **99** (Number of scans = 5).

Hence, the electron transfer reaction of 2,2,6,6-tetramethylpiperidin-4-ol **76a** with halomethane can be rationalized by the formation of ion radical pairs followed by charge transfer complex **103** (Scheme 29). Interestingly, the epr signal strength increases with time. As expected, the reaction with sterically hindered amine may be slow with more amounts of paramagnetic species formed with time (Figure 15). However, formation of charge transfer complex of the type **103** is equilibrium with paramagnetic radical ion cannot be ruled out.

Scheme 29

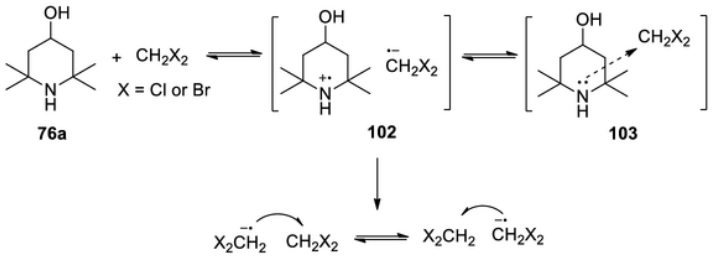

We have also carried out similar electron transfer reaction with polymeric derivative of 4-hydroxy-2,2,6,6-tetramethylpiperidine **76b** with CH_2Cl_2 **97** and CH_2Br_2 **98** and obtained evidence for paramagnetic species with triplet epr signal (Figure 16). In these cases also, subsequent formation of the corresponding charge transfer complexes of the type **105** cannot be ruled out.

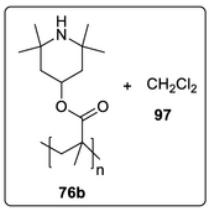

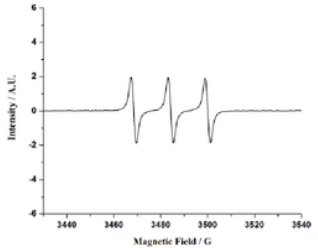

(a) at 5 min

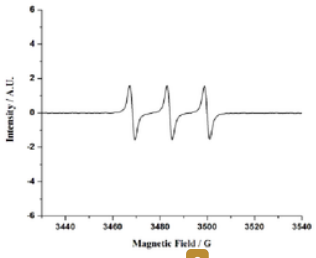

(b) at 1 h

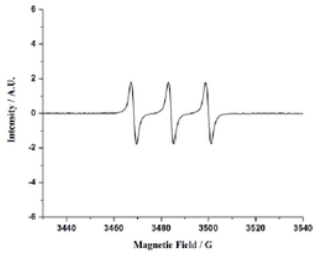

(c) at 2 h

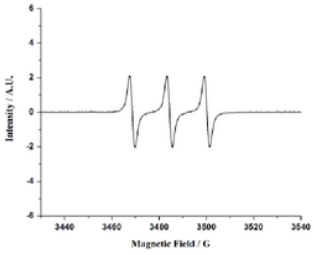

(d) at 6 h

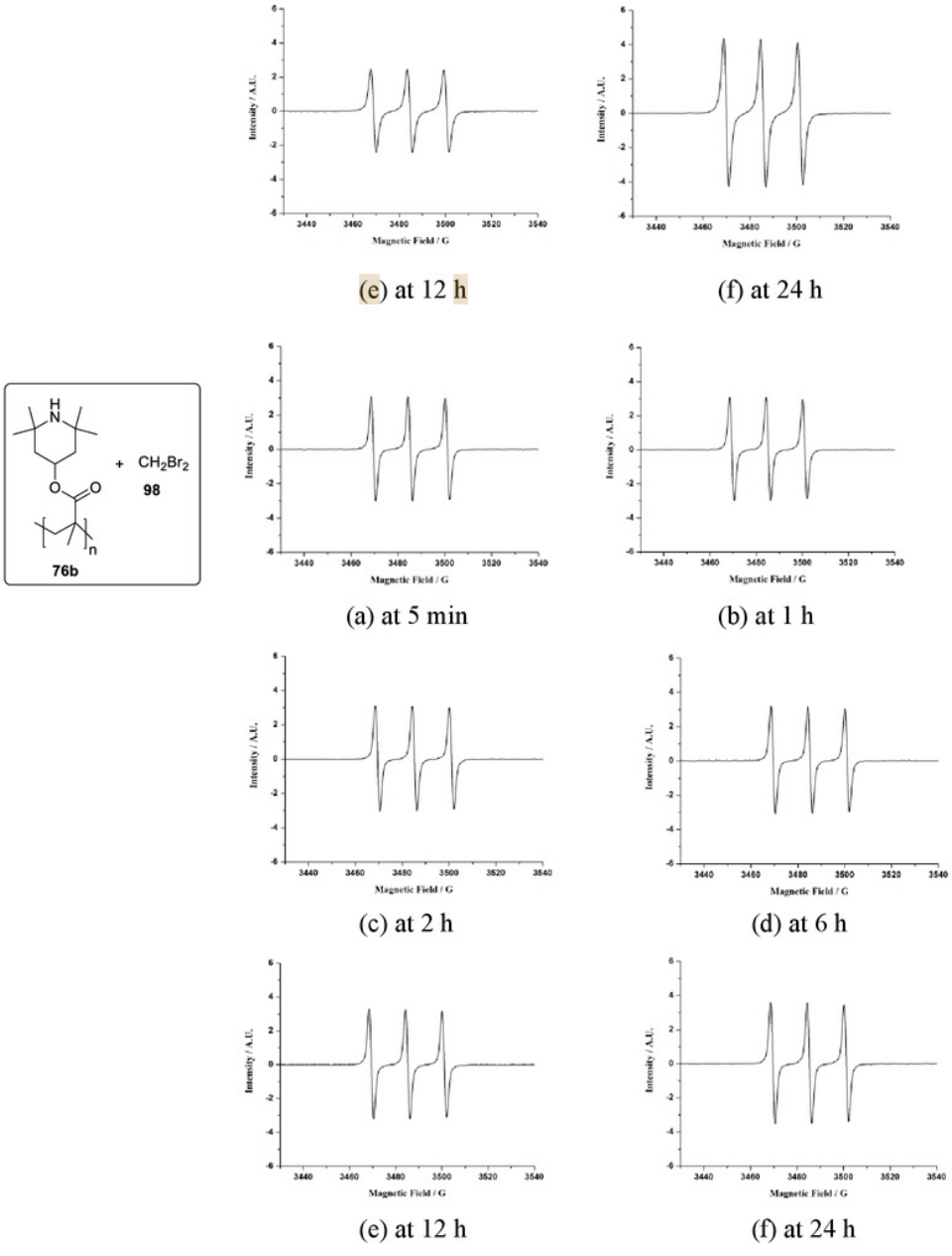

Figure 16. EPR spectra of polymeric 4-hydroxy-2,2,6,6-tetramethylpiperidine **76b** and CH_2Cl_2 **97** and CH_2Br_2 **98** (Number of scans = 5).

The electron transfer reaction may be rationalized as outlined in Scheme 30.

Scheme 30

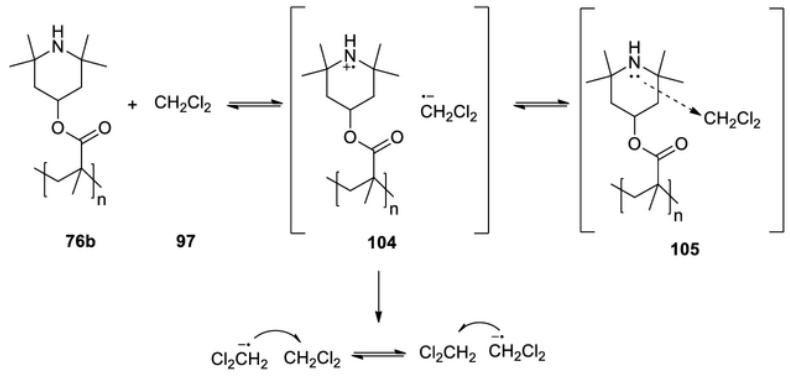

76b **97** **104** **105**

The reaction of 4-hydroxy-2,2,6,6-tetramethylpiperidine **76a** and polymeric derivative of 4-hydroxy-2,2,6,6-tetramethylpiperidine **76b** with CH_2Cl_2 **97**, CH_2Br_2 **98** and $CHCl_3$ **99** gives triplet in epr spectroscopy but there is no hyperfine splitting due to absence of β – hydrogen in the corresponding amine radical cation.

3.2.7 Preliminary studies on electron transfer reaction of amines with viologen acceptors

Viologens are 1,1'-disubstituted-4,4'-bipyridinium salts. Michaelis first reported the electrochemical behaviour of this class of compounds which possess excellent photoelectrochromic properties.[27] The viologens are electron acceptors and are widely used as herbicides and for electron mediation in photosynthesis,[28] in electrochromic display devices,[29] in organic electrical conductors,[30] in chemically modified electrodes,[31] for solar energy storage and photocatalytic reduction of water to hydrogen.[32] The viologens were originally investigated as redox indicators in biological studies. Their electrochemically reversible behaviour and the marked colour change between the

oxidation states, make the viologens as favored candidates for electrochemical display devices as alternative to LEDs and LCDs.[29] The viologens exist in three main oxidation states as shown in Figure 17.

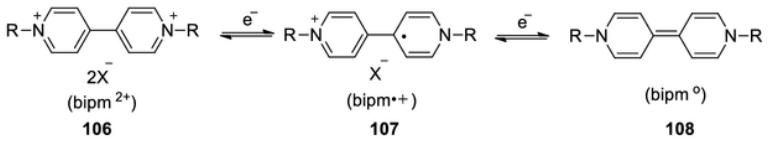

Figure 17. Three common bipyridinium redox states.

Reductive electron transfer to viologen dications **106** gives stable radical cations **107** (Figure 15) due to electron delocalization throughout the π-framework of the bipyridyl nucleus. Whereas the bipyridinium dication salts are normally not coloured, the viologen radical cations are intensely coloured, with high molar absorption coefficients. This is due to charge transfer between the +1 and 0 valent nitrogens.

The reaction of viologen derivatives with amine gives a rapid color change by the formation of electron transfer and charge transfer between viologen derivatives and amine, which is useful for the detection of amines.[33] The reaction of viologen molecules with *N, N*-dimethylformamide (DMF) generates an organic dopant for molybdenum disulfide (MoS_2) in metal-oxide-semiconductor field-effect-transistor (MOSFET).[34] Polyviologen are well known material useful as an interfacial layer and cathode buffer layer in polymer solar cell.[35]

Previously, we have studied the electron transfer reaction of an acceptor *p*-chloranil with donor amines. Hence, preliminary studies were undertaken on reaction of amine donors with other acceptors such as viologen derivatives. Hence, we have decided to examine the possibility of electron transfer reaction between viologen acceptor with readily accessible amines. We have prepared a series of viologen derivatives **111** by the

reaction between 4,4'-bipyridyl **109** and alkyl halide **110** in DMF solvent following a closely related reported procedure (Scheme 31).[36]

Scheme 31

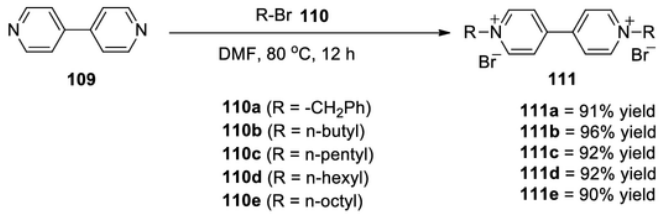

We have also synthesized the 1, 4-dipyridyl benzene **115** *via* preparation of synthesizing 1, 4- phenylenediboronic acid **113** followed by Suzuki coupling with 4-bromo pyridine **114** (Scheme 32).[37]

Scheme 32

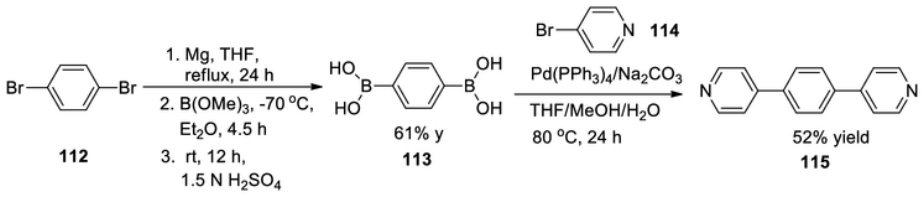

Similarly, the 1,4-dipyridyl benzene **115** was readily converted to extended viologen **116** by reaction with 1-bromo butane in DMF solvent (Scheme 33).

Scheme 33

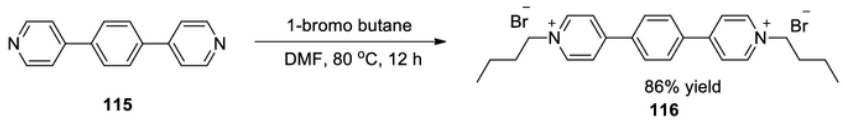

We have investigated the reaction of the viologen salt such as benzyl viologen **111a** with various readily accessible electron donor amines to examine the electron transfer by epr studies. The epr studies of viologen compound with different amines were

carried out by PC and methanol solvent. In the case of reaction of benzyl viologen **111a** with amines like diphenyl amine **118**, *N, N*-diethyl aniline **61** and triphenyl amine **62** no epr signal was observed (Table 2, entries 2, 8 and 10). The reason may be the weak donor nature of amines as the lone pair of electrons on the nitrogen atom are delocalised in the aromatic ring, which is unavailable for electron transfer to viologen acceptors. Also, it indicates that viologen is a weak acceptor and it can interact only with strong amines.

Table 2. EPR of benzyl viologen **102a** with various amines in methanol solvent[a]

Entry	Acceptor	Donor	EPR spectra
1	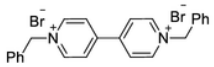 **111a**	$Ph-CH_2NH_2$ **117**	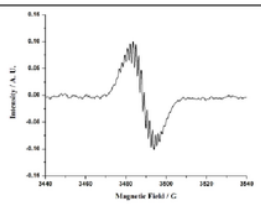
2	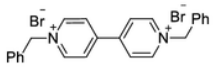 **111a**	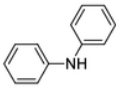 **118**	No signal observed
3	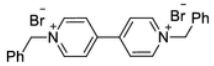 **111a**	 **59**	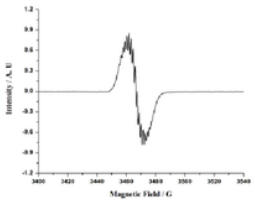
4	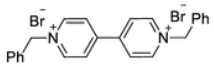 **111a**	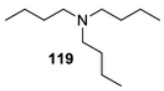 **119**	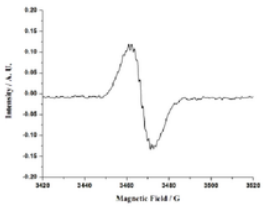

5	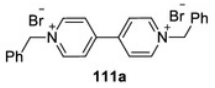 **111a**	 **120**	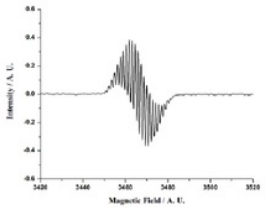
6	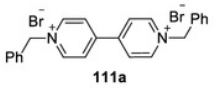 **111a**	 **26**	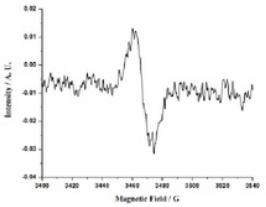
7	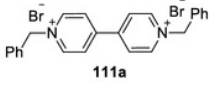 **111a**	 **121**	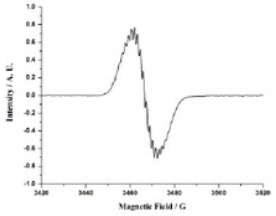
8	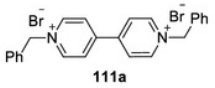 **111a**	 **61**	No signal observed
9	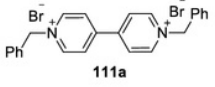 **111a**	 **122**	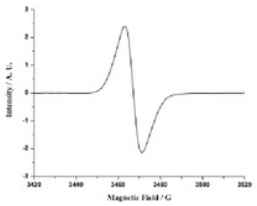
10	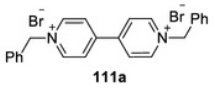 **111a**	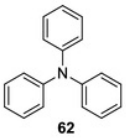 **62**	No signal observed

[a] EPR experiment were carried out by mixing amine (0.2 mmol) with benzyl viologen **111a** (0.2 mmol) in methanol. The mixture was taken into epr tube and recorded the spectra.

Similarly, we have studied the reaction of benzylviologen **111a** with different amines in PC solvent. In this case, we have observed weak epr signal in the reaction of benzylamine **117**, *N, N*-diisopropylethylamine **59** and triethyamine **120** with benzyl viologen acceptor (Table 3, entries 1,3,5). The weak epr signal or no signal also indicates the poor solubility of viologen in PC solvent. The reason for weak epr signal may be also due to the fast disproportionation of the viologen radical cation to give back the starting viologen (Scheme 34).

Scheme 34

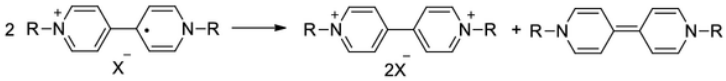

107 **106** **108**

Table 3. EPR of benzyl viologen with various amines in PC solvent[a]

Entry	Donor	Donor	ESR spectra
1	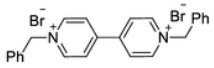 **111a**	$Ph-CH_2NH_2$ **117**	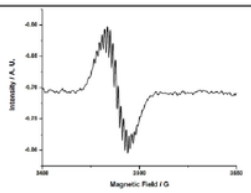
2	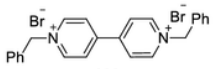 **111a**	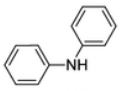 **118**	No signal observed
3	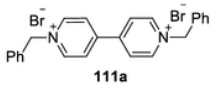 **111a**	 **59**	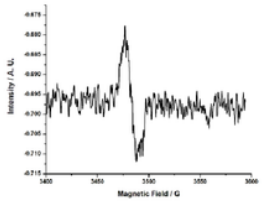

4	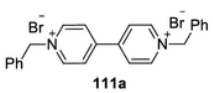 **111a**	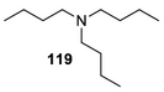 **119**	No signal observed
5	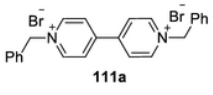 **111a**	 **120**	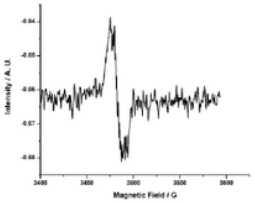
6	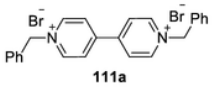 **111a**	 **26**	No signal observed
7	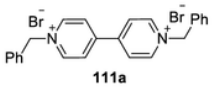 **111a**	 **121**	No signal observed
8	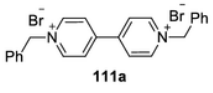 **111a**	 **61**	No signal observed
9	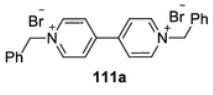 **111a**	 **122**	No signal observed
10	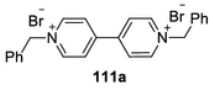 **111a**	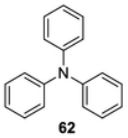 **62**	No signal observed

[a] EPR experiment were carried out by mixing amine (0.2 mmol) with benzyl viologen **111a** (0.2 mmol) in PC. The mixture was taken into epr tube and recorded the spectra.

Electrochemistry of viologen were reported extensively.[38] The high resolution epr spectra of photochemically generated viologen radical cation derivatives in ethanol-water system has been also reported.[39]

Here also, we have observed a epr signal only for viologen radical cation formed in the reaction of benzyl viologen with amines. The amine radical cation formed after electron transfer to viologen would undergo fast electron exchange with the neutral amine and hence may not show epr signal (Scheme 35).

Scheme 35

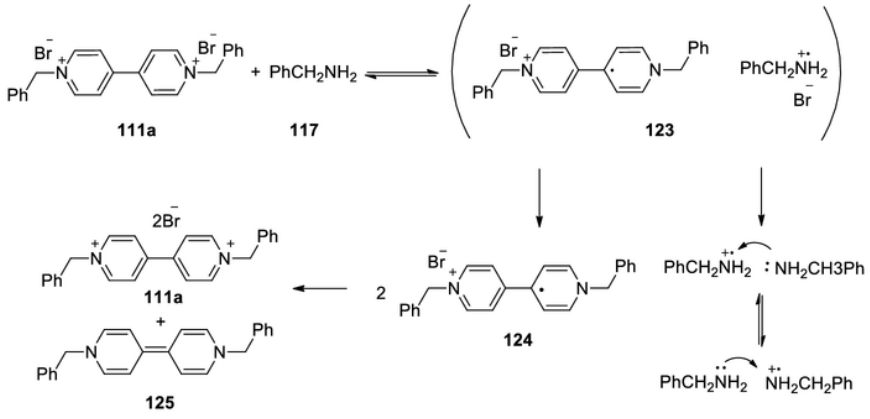

We have investigated the electron transfer reaction of acceptors like quinones, halomethanes and viologens with amine donors. Also, we proposed tentative mechanisms for the formation of paramagnetic intermediates in these reactions in accordance with epr spectroscopic studies. Among the acceptors studied, *p*-chloranil which has a very high electron affinity (EA=2.78 eV) gives strong epr signals with donor amines. The electrochemistry of quinone is also well studied and hence we have selected the *p*-chloranil as an acceptor for studies on the construction of organic electrochemical cell

based on electron transfer reaction with tertiary amines. The results are discussed in the next chapter.

3.3 Conclusions

We have investigated the electron transfer reaction of quinones with piperidine. The corresponding aminoquinone was formed in good yield (55% to 75%) *via* the corresponding radical ion intermediates. The formation of paramagnetic intermediates were confirmed by epr spectroscopy.

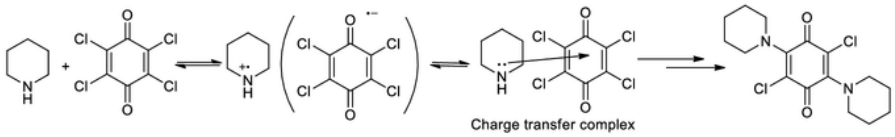

We have also studied the reaction of tertiary amines like *N, N*-disopropylethylamine, *N, N*-diethylaniline, triphenylamine, *N*-benzyl-*N*-isopropylpropan-2-amine and *N, N*-diisopropyl-2, 2-dimethylpropan-1-amine with *p*-chloranil acceptor. We have observed that electron transfer from amine donor to quinone acceptor was fast. The formation of ion pair intermediates and charge transfer complexes were confirmed by epr and UV-Visible spectroscopic studies. The epr analysis of the intermediates formed in PC solvents indicate that the initially formed ion pair by electron transfer from donor to acceptor are converted to charge transfer complexes in equilibrium with small amounts of radical ions. The epr signal corresponds to the presence of quinone radical anion and the amine radical cation signal does not apperar as it undergoes fast self-exchange with another amine.

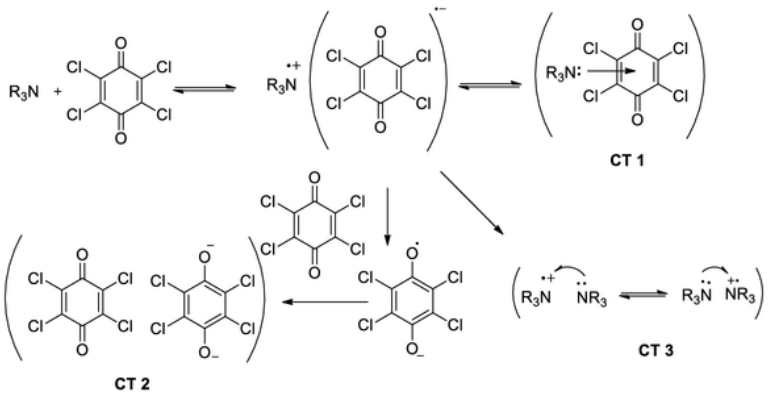

We have developed a simple method for the preparation of polymers containing amine as a pendant group through the reaction of PMMA (polymethylmethacrylate) and 4-hydroxy-2,2,6,6-tetramethylpiperidine. The sterically hindered polymeric 2,2,6,6-tetramethyl-4-piperidinol product reacts with *p*-chloranil to give radical ion intermediates followed by charge transfer complex. The radical ion intermediates gave triplet signal in epr spectroscopy which corresponds to the presence of amine radical cation. Similar results were also obtained in the reaction of 4-hydroxy-2,2,6,6-tetramethylpiperidine and 2,2,6,6-tetramethylpiperidin-4-one with *p*-chloranil.

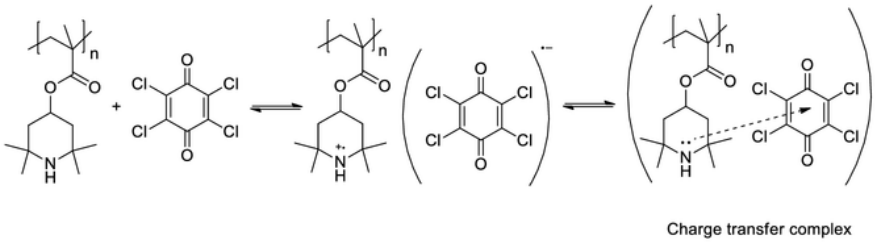

We have briefly studied the reaction between *N, N*-diisopropyl ethylamine, DIPEA with CH_2Cl_2, CH_2Br_2 and $CHCl_3$. The formation of paramagnetic intermediates were confirmed by epr spectroscopy. The epr signal with very weak hyperfine splitting for the

nitrogen radical cation was observed. We have also investigated the reaction of 2,2,6,6-tetramethylpiperidin-4-ol and polymeric 2,2,6,6-tetramethylpiperidine derivatives with CH_2Cl_2, CH_2Br_2 and $CHCl_3$. Similar paramagnetic intermediates with triplet epr signal were observed. The results indicate that the halogenated solvents also behave like acceptor in the presence of strong amine donors.

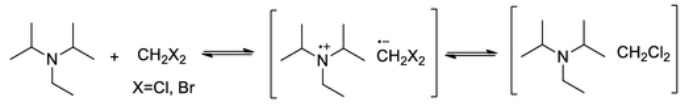

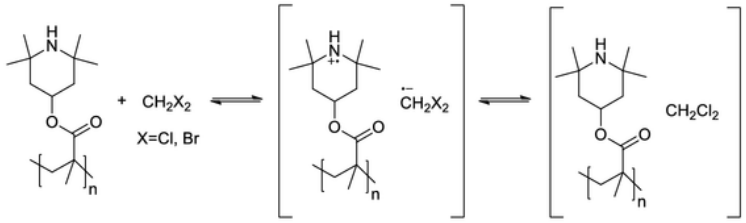

We have also studied the reaction of viologen acceptors with different amines. Again, the formation of paramagnetic intermediates was confirmed by epr spectroscopy. The releatively weak aromatic amine donors did not undergo electron transfer reaction with viologen derivatives.

Chapter 4

Development of Electrochemical cell exploiting reversible electron transfer reaction between tertiary amine donors and *p*-chloranil acceptor

4.1 Introduction

In the previous chapter, we have already discussed that electron transfer readily takes place from donor amines to acceptor quinones resulting the formation corresponding radical cation – anion pair (Scheme 1).

Scheme 1

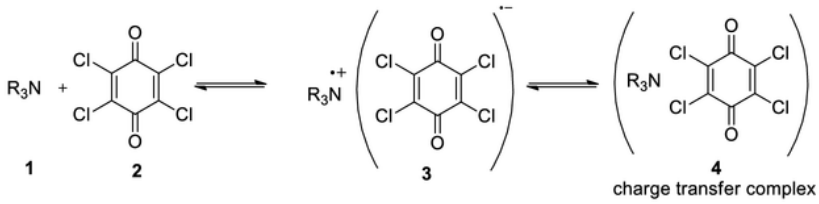

We have also observed that the reaction of tertiary amines with *p*-chloranil gives radical cation-anion pair first followed by formation charge transfer complex (CT complex) in equilibrium with the ion pair (Scheme 2). These reversible reactions take place at ambient temperature conditions in the ground state of the donor and acceptor. Accordingly, energy barrier or activation energy for the formation of the ions and ions is overcome by surrounding heat (Figure 1).

Scheme 2

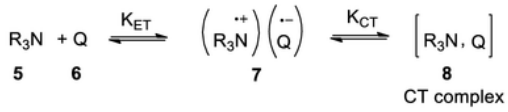

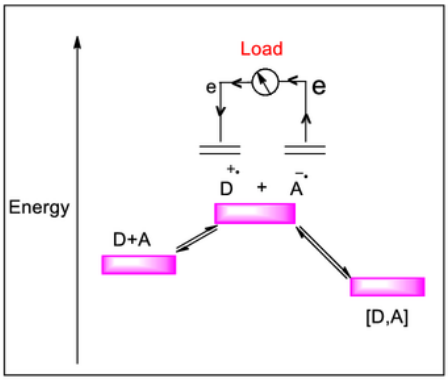

Figure 1. Ground state electron transfer between organic electron donor (D) and acceptor (A) - Construction of an electricity harvesting cell.

We have envisaged the construction of an electrochemical cell that could transport the charge carriers (i.e. electron in $Q^{\cdot-}$ and the hole in $R_3N^{+\cdot}$) formed in such reactions to produce electricity (Figure 1). The difference between such ground state electron transfer process in such cells and the electron transfer involved in donor/acceptor photovoltaic or solar cell is that in the later case the electron transfer from a donor to an acceptor takes place after photoexcitation of the electron from the ground state to excited state. Accordingly, a brief review of reports on the construction of various types of solar cells including donor/acceptor organic photovoltaic cells would facilitate the discussion of the present results.

4.1.1 Photovoltaic cell

Electrochemical cell which produce electric current through chemical reactions are called voltaic or galvanic cell. In a photovoltaic cell or solar cell, the light or solar energy is converted into electrical energy and produces an electric current in the circuit. Solar cells are made up of semiconductors which absorb light in the visible region. The research on solar cell

focused mainly on technologies involving the silicon and other inorganic semiconductors, dyes, perovskites and organic donor/acceptor molecules.

4.1.2 Silicon solar cell

Silicon (Si) solar cell consists of n-type Si and p-type Si semiconductor material. The Addition of atoms (boron or gallium) having one electron less than silicon in their outer energy level produce a p-type silicon. Addition of atoms (phosphorus or arsenic) having one electron more than silicon in their outer energy level produce an n-type silicon. When sunlight (photons) strikes the solar cell the electrons ejected from the silicon moves to the n-type layer and holes moves to the p-type layer. The produced electron and holes will move to the electrodes to produce electricity (Figure 2).

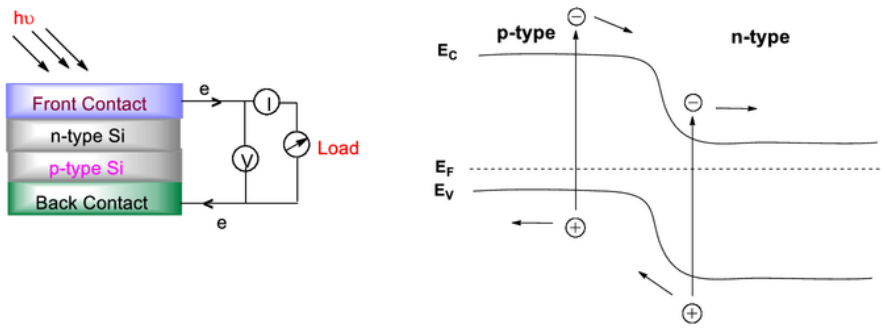

Figure 2. (a) Schematic diagram for crystalline silicon solar cell. (b) Energy level diagram for crystalline silicon solar cell (E_V-Valance band energy level, E_F-Fermi energy level and E_C-Conduction band energy level)

In 1954, scientists in Bell laboratory produced the first practical photovoltaic cell based on silicon semiconductor material with 6% efficiency.[1] The crystalline solar cell

requires complex fabrication process and high production cost even though the efficiency of single crystal silicon solar cell reached up to 25%.[2] At present, amorphous silicon (a-Si), cadmium telluride (CdTe), copper indium gallium selenide (CIGS) and gallium arsenide (GaAs) materials are used in thin film solar cells.

4.1.3 Thin film solar cell or Inorganic solar cell

Thin film solar cells also called as second generation solar cells are made by placing one or more thin layers of photovoltaic material on glass or metal current collector.

4.1.3.1 Amorphous silicon solar cells (a-Si)

Amorphous silicon (a-Si) is an allotrope of silicon and widely used in thin film technology. The absorption of solar radiation by amorphous silicon is 40 times more than that of single crystal silicon solar cell. The thin layer of silicon is coated using a gaseous mixture of silane and hydrogen on transparent conductive oxide (TCO) glass. The basic electronic structure of amorphous silicon solar cell is p-i-n junction (Figure 3).

The efficiency of amorphous silicon solar cell is around 5-7% and lower than that of crystalline solar cell.[3] The efficiency of amorphous silicon solar cell was improved to 10% by stacking the two or more cells together with micro crystalline silicon (μ-c-Si) solar cell. This type of stacking improve the performance of the cell (Figure 3b).

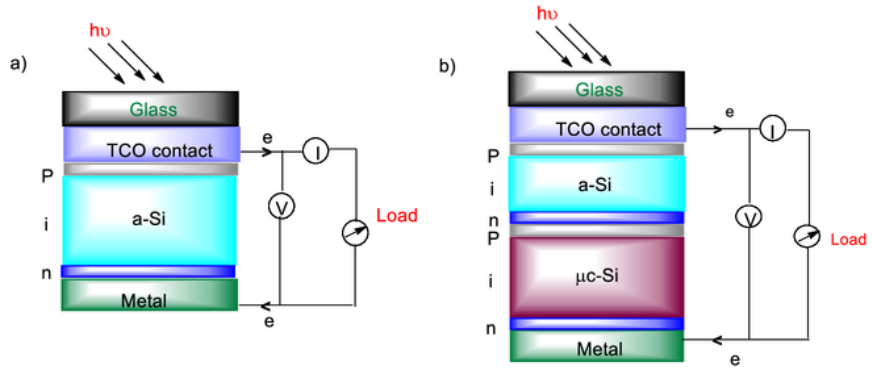

Figure 3. (a) Schematic diagram for thin film amorphous silicon solar cell. (b) Tandem a-Si and μ-c-Si solar cell.

4.1.3.2 Cadium-telluride (CdTe) thin film solar cell

This cell is a simple heterojunction contains p-type CdTe and n-type CdS semiconductors (Figure 4 a).

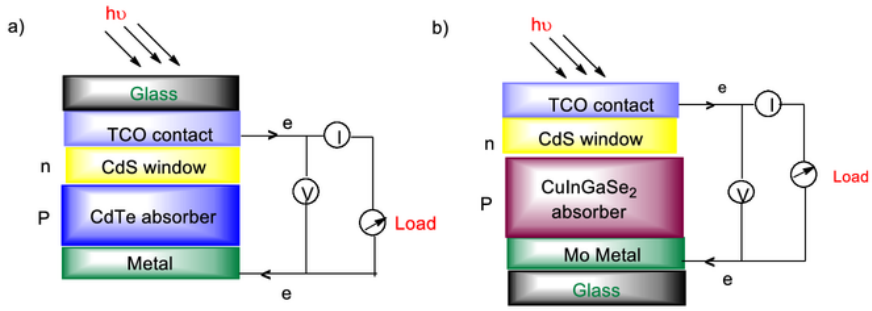

Figure 4. (a) Schematic diagram for thin film CdTe solar cell. (b) Thin film $CuInGaSe_2$ (CIGS) solar cell.

The efficiency of CdTe solar cell varies between 10-16%.[4,5] However, the rare abundance of tellurium and toxicity of cadmium are the main disadvantage of this cell.

4.1.3.3 Copper indium gallium selenide (CIGS) thin film solar cell

The fabricating process of CIGS thin film cell is similar to that of CdTe process but the light conversion efficiency is higher than that of CdTe cell (Figure 4 b). This material absorbs sunlight effectively because it has high absorption coefficient. The efficiency of CIGS solar cell was around 20% and higher than that of other thin film cell.[6]

4.1.4 Dye-sensitized solar cell (DSSC)

In 1968, Gerischer and co-workers[7] developed the electrolytic cell using the p-type perylene organic dyes and with n-type zinc oxide (ZnO). The modern DSSC was invented by O' Regan and Grätzel[8] in 1991. The use of mesoporous titanium dioxide (TiO_2) as photoanode and the electrolyte containing iodide/triiodide redox shuttle leads to the DSSC with up to 12% efficiency. The cell was further improved by the introduction of N3 (cis-Bis(isothiocyanato) bis(2,2'-bipyridyl 4,4'-dicarboxylatoruthenium(II)) dye with efficiency of around 10%.

The DSSC was fabricated by coating TiO_2 on the conductive glass plate. Then the plates were soaked into the organic dye solution. The redox electrolyte couple was drop coated on the organic dye layer and the counter electrode was fixed above the fabricated conductive glass. When the solar radiation (light) strikes the dye molecule and it goes to excited state. The photo induced electron is injected to the conduction band of mesoporous TiO_2. The oxidized dye molecule gets regenerated by electron donation from the electrolyte I^-/I_3^- redox couple. The holes move towards the counter electrode to complete the electronic circuit (Figure 5).

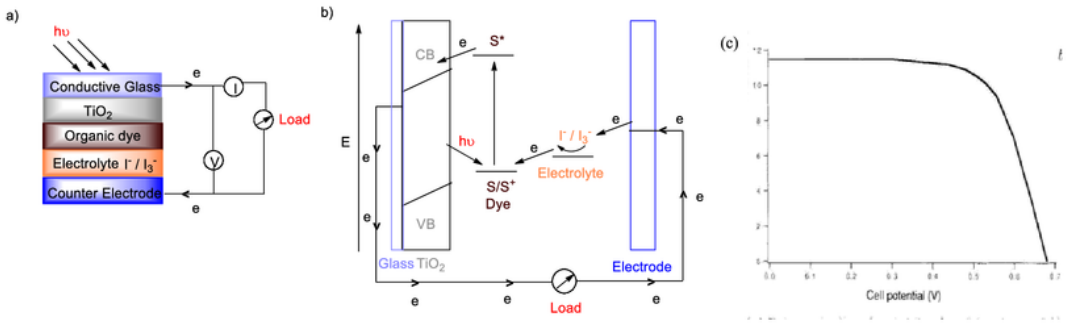

Figure 5. (a) Schematic diagram for DSSC solar cell. (b) Energy level diagram of liquid DSC based on mesoporous TiO_2 photoanode and I^-/I_3^- redox couple (c) Typical current voltage curve for DSSC (Cell efficiency = 7.12% with FF = 0.684, Reference. 8).

In last two decades research efforts were undertaken to improve the performance of DSSC by designing the organic dye molecules with high extinction coefficient and also with modified redox shuttle[9-13] like cobalt (II/III), copper (I/II), ferrocene (Fc)/ferrocinium (Fc^+), Nickel (III/IV), TEMPO/$TEMPO^+$. The redox shuttle can reduce the electron-hole recombination process with efficient electron transport properties.[14-21]

It was reported that the highest efficiency of 13% observed for the cobalt (II/III) electrolyte used in the DSSC.[22] The first solid-state dye sensitized solar cell (sDSSC) using 2,2',7,7'-tetrakis (*N*,*N*-dimethoxyphenylamine)-9,9'-spirobifluorene (spiro-OMeTAD) as hole transporting material (HTM) was also reported. [23] The efficiency of the DSSC was improved to 7.2% by the use of spiro-OMeTAD with the addition of cobalt complex (p-type dopant).[24] The sDSSC was further improved by using other hole transporting material like poly(3-hexylthiophene-2,5-diyl) (P3HT).[25] But, the efficiency is lower than that of liquid DSSC.[26,27]

The decrease in efficiency is due to the higher recombination rate and intrinsic properties of spiro-OMeTAD with TiO_2.

4.1.5 Perovskite solar cell

The perovskite (ABX_3) is hybrid inorganic/organic material with efficient light harvesting structure. The construction of perovskite solar cell is similar to that of dye-sensitized solar cell as shown in Figure 6. In 2009, the first perovskite solar cell was reported with methylammonium lead iodide ($CH_3NH_3PbI_3$) which gave 3.81% power conversion efficiency.[28]

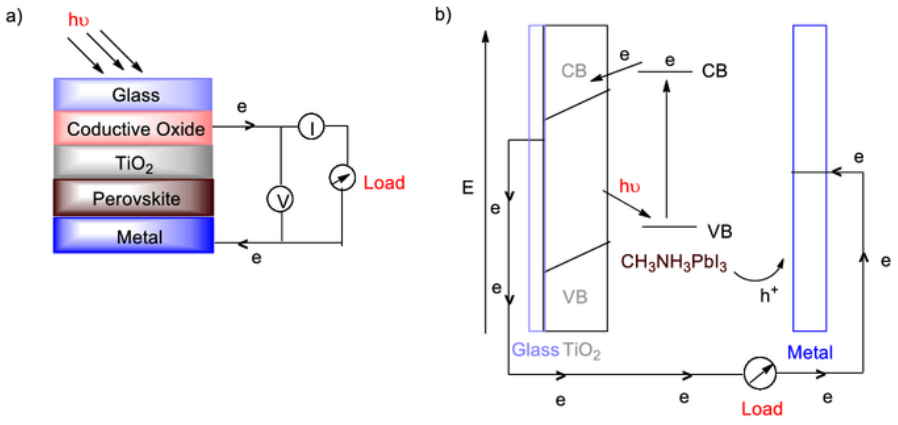

Figure 6. (a) Schematic diagram for perovskite solar cell (b) Energy level diagram of perovskite solar cell without hole transport material.

The iodide redox couple degrades the perovskite that leads to the lower efficiency. The replacement of the liquid electrolyte with solid-state p-type semiconductor spiro-OMeTAD as a hole transport material (HTM) improves the efficiency to 9.7%.[29]

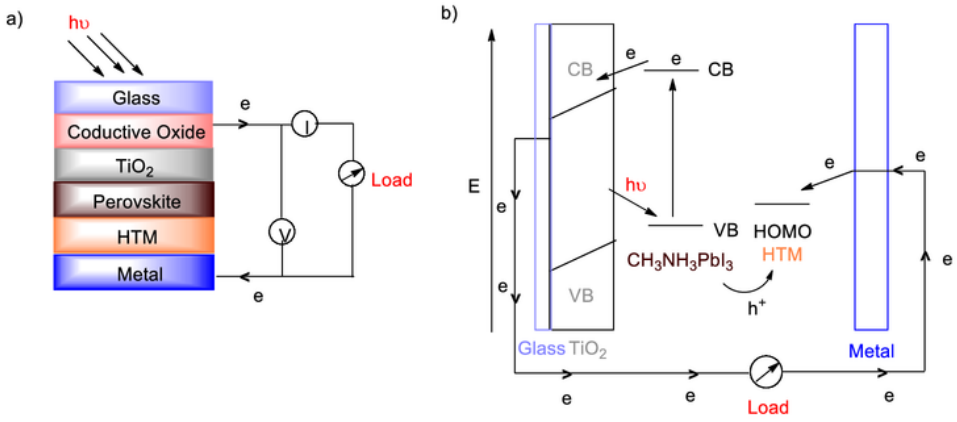

Figure 7. (a) Schematic diagram for perovskite solar cell. (b) Energy level diagram of perovskite solar cell with hole transport material.

Recent reports[30] on mixed lead halogen perovskite solar cell indicated that the efficiency was improved to 20.7%. Some of the hole transporting materials used for the studies on perovskite solar cell are listed in Figure 8. The research efforts on the perovskite solar cells are still under progress.[31-35]

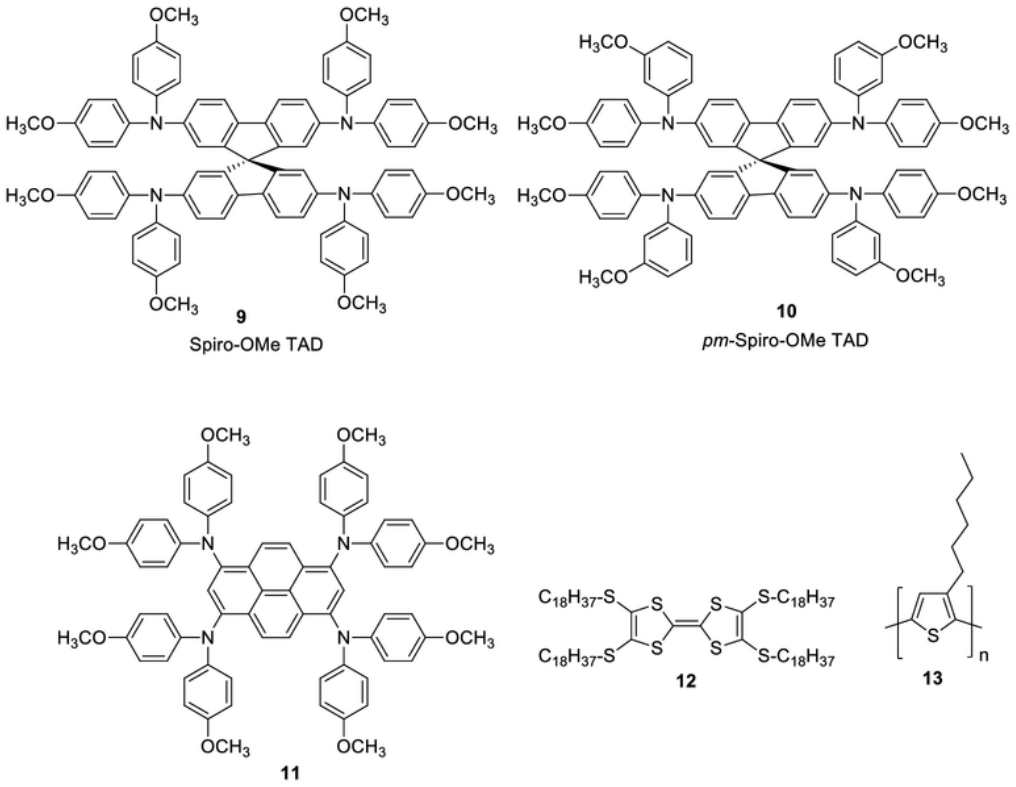

Figure 8. Hole Transporting Material (HTM) used in perovskite solar cell.

4.1.6 Organic solar cell

The organic photovoltaics or solar cells are flexible devices with low manufacturing cost compared to the rigid inorganic solar cells. In organic solar cells, upon excitation of organic material creates positive charge on the donor layer (p-type) and negative charge on the acceptor layer (n-type) like p-n junction.

The operating mechanism of the organic solar cell is almost similar to that of the inorganic solar cell. The photo excitation of the light harvesting organic material produces an exciton (coupled electron-hole pair). The field splits the exciton into the charge carrier (separated electron-hole pair) which then moves to the respective electrodes to produce

electricity. Some typical donor and acceptors used in the organic solar cells are shown in Figure 9.

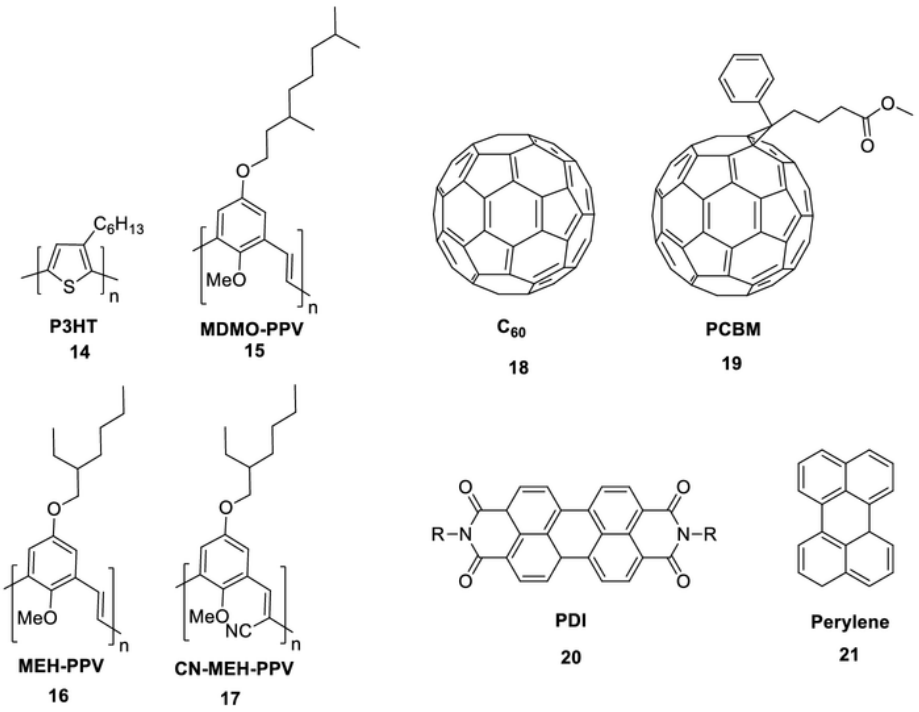

Figure 9. Major donor polymers and acceptors used in the organic solar cells.

4.1.6.1 Single layer organic solar cell

The cell was made by sandwiching an organic material between the two metal conductors having high work function such as ITO and low work function such as aluminum, magnesium or calcium (Figure 10). The organic material absorbs the light which excites the electrons to the LUMO and leaves holes in the HOMO. The potential created by the different work functions of the metals splits the exciton pair. The electrons move to the positive electrode and holes to the negative electrode. The magnesium phthalocyanine (MgPc) used in the single layer solar cell (Al/MgPc/Ag) produces 0.01% efficiency.[36]

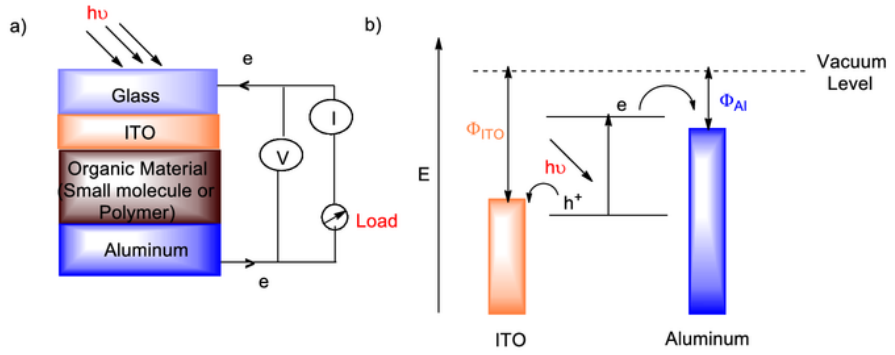

Figure 10. (a) Schematic diagram for single layer organic solar cell (b) Energy level diagram for organic solar cell.

The single layer cell using poly-3-methyl thiophene gave 0.15% power conversion efficiency.[37] Another single layer cell using the conjugated polymer polyacetylene gave 0.3% efficiency.[38] These types of cells produces low quantum efficiency (<1%) and less than 1% power conversion efficiency.

4.1.6.2 Bilayer or Planar donor-acceptor heterojunction

Bilayer cells are constructed by sandwiching two different layers contains donor and acceptor between two conductive electrodes (Figure 11 a). The difference in electron affinity and ionization energy of two layers could generate the electrostatic forces at the interface. The layers having high electron affinity and ionization energy are called as electron acceptor and electron donor, respectively. Tang *et al.* investigated copper phthalocyanine (CuPc) as an electron donor and perylene tetracarboxylic derivative as an acceptor in two layer organic cell which gave 1% power conversion efficiency.[39]

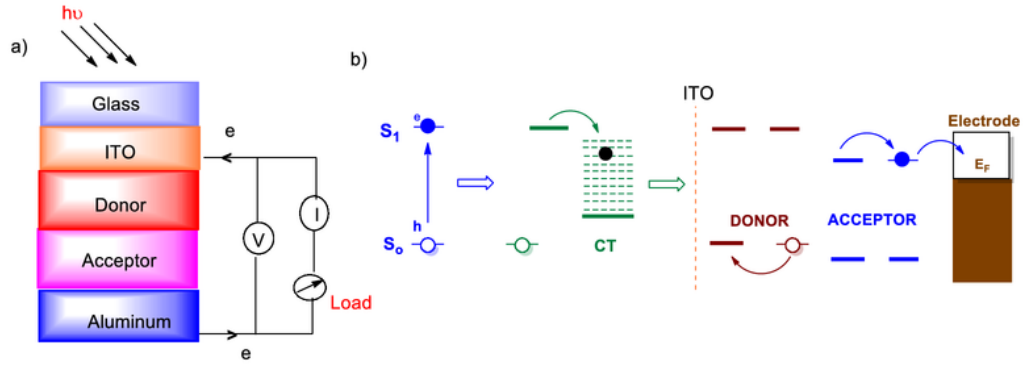

Figure 11. (a) Schematic diagram for Bilayer organic solar cell (b) Energy level diagram for bilayer organic solar cell.

Perylene amide derivatives are chemically stable and have high electron affinity. Sariciftci and co-workers reported[40] that the use of C_{60}/MEH-PPV in double layer cell gave 0.04% power conversion efficiency. Here, C_{60} acts as an acceptor and poly (2-methoxy-5-(2'-ethylhexyloxy- 1,4-phenylene-vinylene), MEH-PPV as a donor. The bilayer cell with donor polymer poly (p-phenylenevinylene), PPV and acceptor C_{60} produces around 9% power conversion efficiency.[41]

4.1.6.3 Bulk heterojunction solar cell

In organic photovoltaics the layer thickness is important for effective absorption of light. The increase of layer thickness increases the exciton diffusion pathway in the donor-acceptor interface. The exciton has shorter life time and it recombines before reaching the electrodes if thickness of the layer is more. In bulk-heterojunction cell, the exciton diffusion pathway is minimized by placing a mixture of electron donor and acceptor blend and it also increases the light absorption efficiency. The light absorbing layer of bulk heterojunction

solar cell consists a blend of donor and acceptor materials. In bulk heterojunction the donor and acceptor are mixed together and deposited over the ITO electrode (Figure 12a).

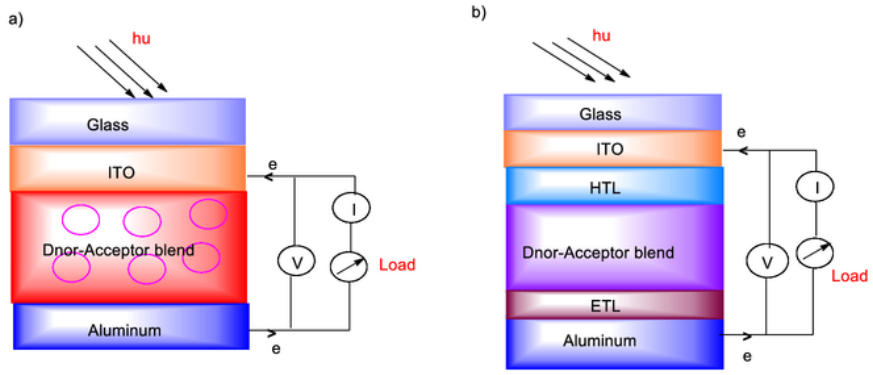

Figure 12. (a) Schematic diagram for Bulk heterojunction solar cell (b) Use of buffer HTL and ETL layers

The active layer consists of conjugated donor and fullerene based acceptor. The efficiency of polymer photovoltaic cell (single layer cell) was improved by the introduction of fullerene based derivatives in bulk heterojunction. The cell with blend polymer MEH-PPV donor and fullerene acceptor as the heterojunction was reported.[42] The device using Ca/MEH-PPV/PCBM/ITO gave 2.9% power conversion efficiency. It was reported that the introduction of poly (3-octylthiophene) P3OT in place of polymer MEH-PPV improved the quantum efficiency as well as power conversion efficiency.[43]

Recently, it was reported[44] that the higher power conversion efficiency of 11% was obtained using thiophene based PTB7-Th polymer and $PC_{71}BM$ as an acceptor. The use of donor MEH-PPV polymer and acceptor CN-PPV polymer in polymer/polymer blend heterojunction cell gave power conversion efficiency of 1% under monochromatic light.[45] It was found that the cell efficiency improved by incorporating hole conducting material such as

PEDOT:PSS.[46] The organic bulk heterojunction was further improved by sandwiching the active layer between the electron and hole transport material.[47,48]

We have decided to examine the possibility of constructing an organic electrochemical cell with ground state electron transfer using readily accessible donor amines and acceptor quinones. The radical cation - radical anion intermediates formed in the reaction could lead to generation of electric current. To construct the cell, we have chosen the readily accessible aluminum foil (Al) and stainless steel or graphite as electrodes/current collectors.

4.2 Results and Discussion

Organic charge transfer complexes and electron transfer reactions from organic donors and acceptors were known for more than 60 years.[49] In recent years, attention was turned towards mostly solid state high conductivity or superconductivity of organic charge transfer salts. For instance, the highly conductive donor-acceptor complex of TTF-TCNQ was called as organic metal.[50] Recent reports reveal that these complexes have interesting and important semiconductor properties useful in the construction of electronic devices.[51]

The charge transfer complexes formed from the donor and acceptor in solution have entirely different properties compared to that of the parent compounds. Mechanistic schemes were proposed involving the formation of charge transfer (CT) complex followed by equilibrium involving formation of radical cation and anion pairs, dissociated ions in such organic electron transfer reactions (eq. 1).[52a] The electron transfer kinetics were reconciled with an electron transfer process and formation of paramagnetic intermediates (eq. 2) without involving initial formation of a CT complex in a manner analogous to self-exchange (SE) of the $D/D^{\cdot+}$ and $A/A^{\cdot-}$ based on two state model.[52b,c] Formation of radical cation and anion pairs followed by slow formation of CT complex was also considered in polar solvent (eq. 3).[52a] The epr spectroscopic results obtained in present work (chapter 3) are in accordance with the initial formation of paramagnetic intermediates followed by formation of diamagnetic CT complexes (eq. 3).

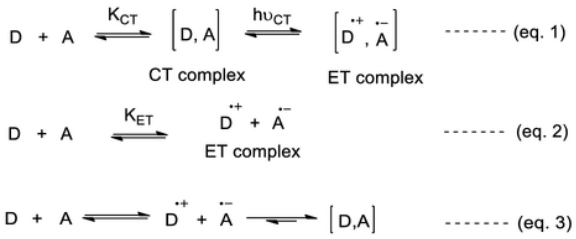

In 1966, it was reported[53] that conductometric titration could be carried out by titrating a donor solution with an acceptor and the conductivity pass through a maximum when the donor and acceptor were present in the stoichiometry required for the formation of the CT complex.

Surprisingly, there was no attempt on the development of an electrochemical device based on transport of charges in these radical cation and anion pair species to the electrodes and regenerating the donor and acceptor for further electron transfer reaction. If the electron transfer from the amine donor to the quionone acceptor could happen reversibly, then the device would be useful in converting the heat around it continuously to electricity. Therefore, we have decided to construct the electrochemical cell using *p*-chloranil acceptor with amine or amide donors.

4.2.1 Construction of Donor and Acceptor Electrochemical Cell

We have selected the readily accessible acceptor quinones and donor amines to construct the electrochemical cell which can produce electricity from the surrounding heat without using visible light (Figure 13). We have already discussed that a variety of readily accessible, inexpensive and simple tertiary amine donors react with quinone acceptors like 1,4-benzoquinone, *p*-chloranil, 1, 4-naphthoquinone and 2,3-dichloro-1,4-naphthoquinone to give paramagnetic intermediates.

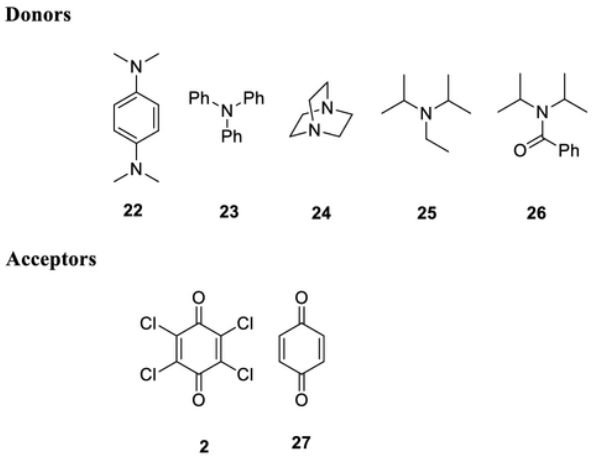

Figure 13. Donors and acceptors used in the electrochemical cell studies.

We have selected the highly electron deficient *p*-chloranil **2** as acceptor for detailed studies as it acts as an acceptor even with tertiary amides (Figure 13). Also, we have selected the donors like *N,N'*-tetramethyl-1,4-phenylenediamine (TMPDA) **22**, triphenylamine (TPA) **23**, 1,4-diazabicyclo[2.2.2]octane (DABCO) **24**, *N, N*-diisopropylethylamine (DIPEA) **25** and *N,N*-diisopropylbenzamide (DiPrBA) **26** for the construction of the electrochemical cell (Figure 13).

4.2.1.1 Two Layer Cell Configuration

After extensive experimentation, we have found that the cells can be easily constructed by making donor and acceptor pastes using TiO_2, polyethylene oxide (PEO) and propylene carbonate (PC) for coating on commercially available Al (0.2mm x 5cm x 5cm) and SS (SS 304, 0.05mm x 5cm x 5cm) foils or graphite sheet (0.4mm x 5cm x 5cm). Initially, a simple two layer cell was constructed using Al and SS foils. The mixture of TiO_2, *p*-chloranil, PC, EC and PEO was coated on Al foil and the mixture of TiO_2, amines, PC, EC and PEO was coated on SS foil. The foils were then sandwiched to construct the electrochemical cell. The configuration of this two layers electrochemical

cell is almost similar to the bi-layer in organic solar cell[54] but the electron transport would have contributions from both ionic conduction and also through exchange reactions involving $D/D^{\cdot+}$ and $A^{\cdot-}/A$ with formation of corresponding charge transfer complexes (CT 1, CT 2 and CT 3). The current (I) and voltage (V) characteristics observed for the cells using different amines are summarized in the experimental section in Table ES1 (ES: Experimental Section), entries 1-3.

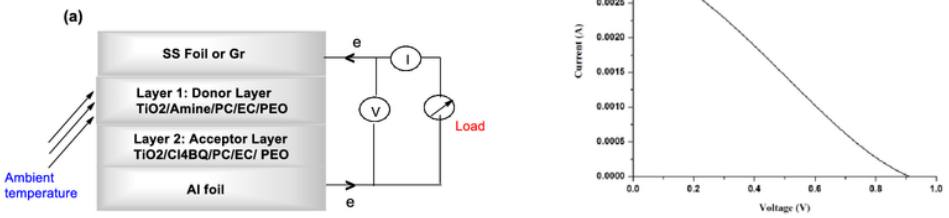

At 28^{0}C, With SS Foil Cathode

DIPEA	Pmax=0.756mW/FF=0.263
DABCO	Pmax=0.665mW/FF=0.233
TPA	Pmax=0.306mW/FF=0.254

With Graphite Cathode:

DIPEA	Pmax=1.415mW/FF=0.235
DABCO	Pmax=0.139mW/FF=0.194
TPA	Pmax=0.794mW/FF=0.240

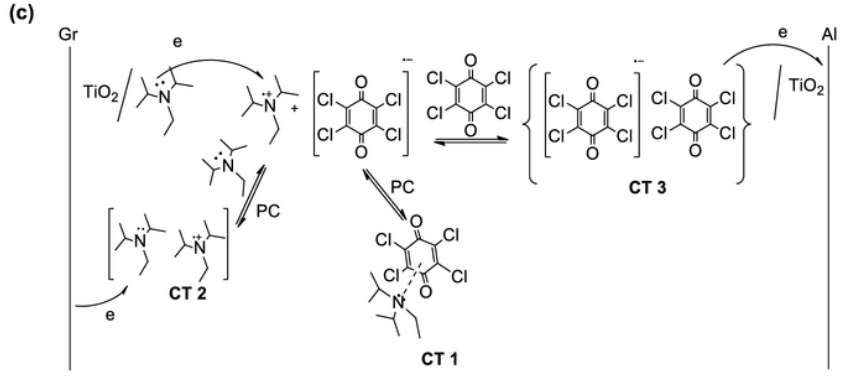

Figure 14. (a) Schematic diagram of cell with two layer configuration (b) Representative IV curve for the two layer cell (Table ES1, entry 1, DIPEA donor). (c) Tentative mechanism for electron transport via $D/D^{\cdot+}$ and $A^{\cdot-}/A$ exchange reactions.

The representative IV curve for this cell is shown in Figure 14b for the cell in (Pmax = 0.756 mW, FF=0.263). Similarly, the cells prepared using amines DABCO and TPA with *p*-chloranil gave power output of 0.665 mW with FF=0.233 and 0.306 mW with FF=0.254, respectively.

However, visible holes were formed on the SS foil indicating corrosion, probably due to the formation of Fe^{2+}-amine species by the reaction of SS foil with the amine radical cation present in the reaction mixture. We then constructed the cell with similar configuration using Al foil (0.2mm x 5cm x 5cm) anode and graphite (0.4mm x 5cm x 5cm) cathode. The results obtained are summarized in the experimental section in Table ES1, entries 4-6. The cells constructed did produce power in these cases (Table ES1, Figure 14), but there was only very little or no power output after 24 h. A possibility is that ionic conduction may lead to the deposition of the radical ion pairs on the respective electrodes which may not dissolve back into the solution preventing reversible equilibrium necessary for continued power generation. Also, the formation of amine-*p*-chloranil CT complex to more extent may lead to reduction in power output, especially if this complex precipitates out of the PC solution.

4.2.1.2 Multi-layer Cell Configuration

We have then decided to construct multi-layer cell to improve the performance of the cell. Recently, there were several reports[55-61] that the stability of the solar cells improved by coating additional buffer layers or electrode interfacial layer using metal oxides like TiO_2.

Accordingly, we have constructed the cells in two different configurations (Figure 15a and 15b) by coating TiO_2/PEO on both electrodes, followed by coating of Cl_4BQ/PEO on TiO_2/PEO/Al and TiO_2/PEO/Gr. Then, the Cl_4BQ/Amine/PC/PEO (Figure 15a) or

Cl_4BQ/Amine/PC/TiO_2/PEO pastes (Figure 15b) coated above the Cl_4BQ/PEO layers. The results are summarized in Table ES2, entries 1-10.

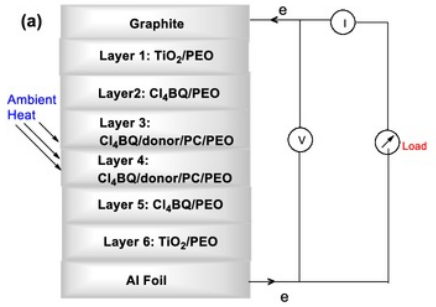

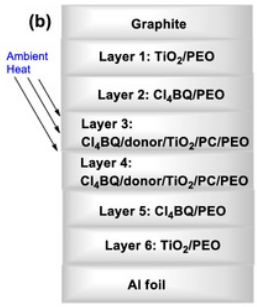

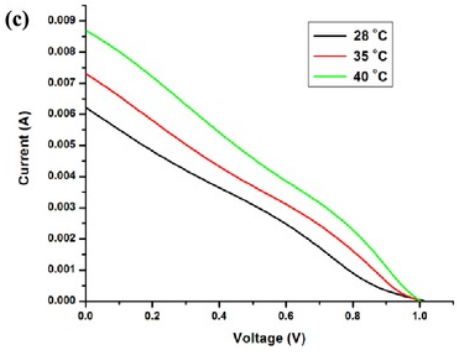

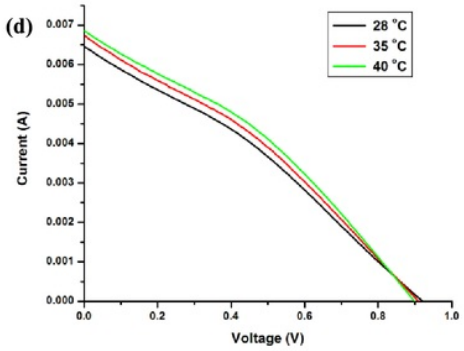

1 h after packing

Donor	Pmax/mW/FF(40 °C)	Donor	Pmax/mW/FF(40 °C)
TMPDA	1.469/0.221	TMPDA	3.099/0.261
TPA	1.333/0.255	TPA	0.375/0.245
DABCO	5.492/0.313	DABCO	6.155/0.206
DIPEA	5.695 /0.296	DIPEA	8.147/0.347
DiPrBA	2.198/0.260	DiPrBA	4.193/0.295

48 h after packing

Donor	Pmax/mW/FF(40 °C)	Donor	Pmax mW/FF(40°C)
TMPDA	0.790/0.309	TMPDA	1.822/0.250
TPA	0.428/0.285	TPA	0.142/0.256
DABCO	**2.320/0.267**	DABCO	1.216/0.249
DIPEA	2.228 /0.347	**DIPEA**	**2.057/0.334**
DiPrBA	1.047/0.261 (35 °C)	DiPrBA	2.969/0.273

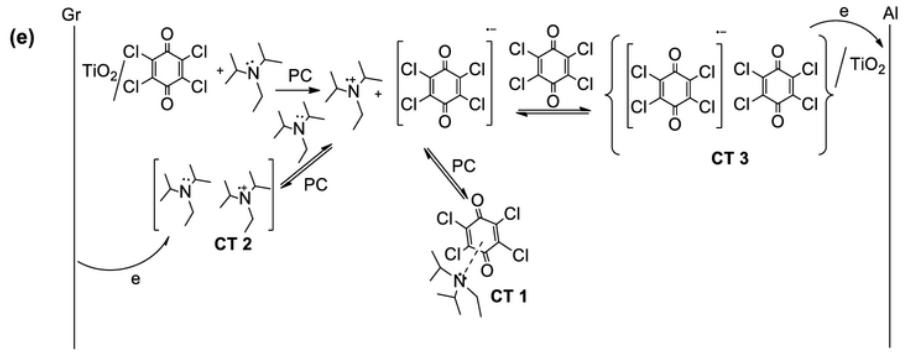

Figure 15. (a) Schematic diagram of multi-layer with Cl_4BQ/donor/PC/PEO configuration and (b) Schematic diagram of multi-layer with Cl_4BQ/donor/PC/TiO_2/ PEO configuration (c) Representative IV curve for the cell (Table ES2, entry 3, DABCO donor) after 48 h packing (d) Representative IV curve for the cell (Table ES2, entry 9, DIPEA donor) after 48 h packing (e) Tentative mechanism for electron transport to the electrodes via D/D.+ and A-/A exchange reactions.

The IV-data were recorded after 1 h and 48 h after packing. The higher power outputs (Pmax) were observed 1 h after packing compared to that observed after 48 h. Presumably, the power output becomes less as the initially formed amine radical cations and *p*-chloranil anions are converted to the corresponding charge transfer complex (CT 1) (Figure 15e). The complexes CT 2 and CT 3 may also contribute to the conduction. The data for the cells with similar configuration with additional TiO_2 in PC layer (Figure 15b) are summarized in Table ES2, entries 6-10.

The data (Table ES2) indicate that increase in the temperature of the cell (from 28 °C to 40 °C) increases the power output due to increase in the rate of electron transfer between the donor-acceptor and also dissociation of formed charge transfer complexes into radical ion pairs. Also, the increase in temperature would help in crossing the activation energy barrier for transport of ions to the electrodes and hence would improve the conductance.

The TiO_2 rutile and TiO_2 and anatase were reported to have very high electron affinities of 4.8eV and 5.1eV, respectively.[62a,b] It was also reported that the TiO_2 surface could donate or accept electrons depending on the nature of the adsorbed molecules.[62c] Accordingly, it was of interest to us to examine whether the donors used in the cell experiments could produce power by interaction with TiO_2 without using *p*-chloranil. Indeed, this was observed and diisopropylbenzamide gave slightly higher power upon interaction with TiO_2 (Figure 16). Presumably, the interactions outlined in Figure 16c may also play a role in the reaction and transport of charge carriers using *p*-chloranil.

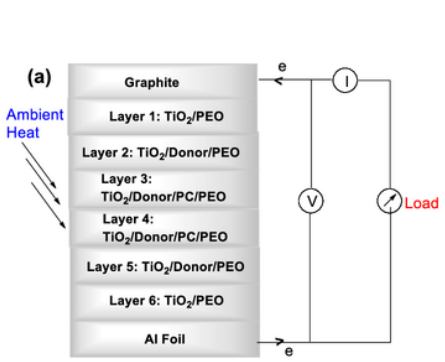

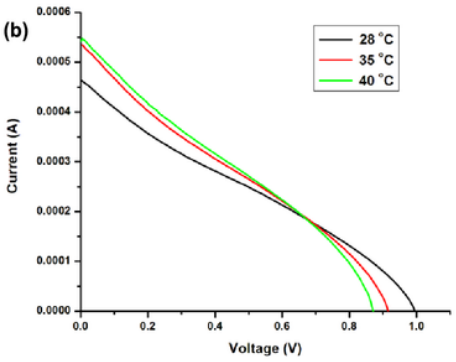

1 h after packing

Donor	**Pmax/mW/FF(40°C)**
TPA	0.004/0.270
DABCO	0.026/0.092
DIPEA	0.005/0.281
DiPrBA	0.235/0.283

48 h after packing

Donor	**Pmax/mW/FF(40°C)**
TPA	0.003/0.287
DABCO	0.019/0.136
DIPEA	0.005/0.305
DiPrBA	**0.136/0.289**

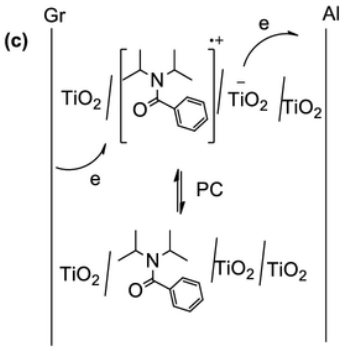

Figure 16. (a) Schematic diagram of multi-layer cell with TiO_2/donor without Cl_4BQ (b) Representative IV curve for the cell (Table ES3, entry 4, DiPrBA donor) (c) Tentative mechanism for electron transport.

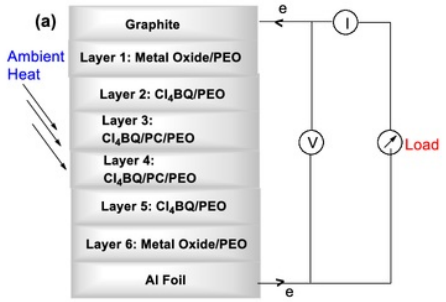

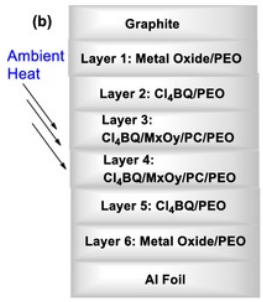

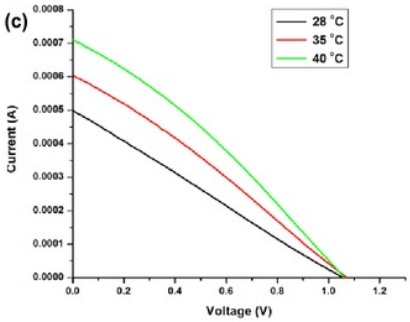

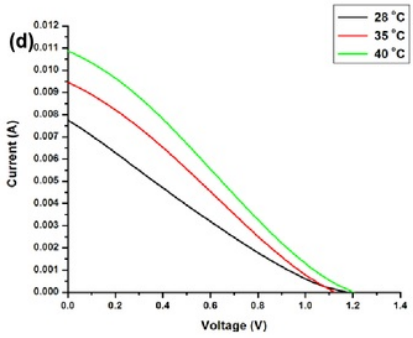

1 h after packing

MxOy	Pmax/MW/FF(40 °C)
TiO_2	1.181/0.270
ZnO	0.492/0.266
Al_2O_3	1.276/0.206

1 h after packing

MxOy	Pmax/mW/FF(40 °C)
TiO_2	3.639/0.261
ZnO	0.584/0.227
Al_2O_3	0.848/0.233

48 h after packing

MxOy	Pmax/MW/FF(40 °C)
TiO_2	**0.228/0.303**
ZnO	0.272/0.260
Al_2O_3	1.049/0.203

48 h after packing

MxOy	Pmax/mW/FF(40 °C)
TiO_2	**3.376/0.258**
ZnO	0.366/0.195
Al_2O_3	1.226/0.286

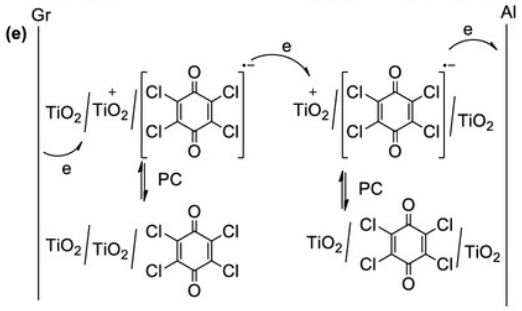

Figure 17. (a) Schematic diagram of multi-layer cell with metal oxide in edge layers (b) multi-layer cell with metal oxide in edge layers and also in PC layer (c) Representative IV curve for the cell (Table ES4, entry 1, TiO_2 donor) (d) Representative IV curve for the cell (Table ES4, entry 4, TiO_2 donor) (e) Tentative mechanism for electron transport.

Previously, there were also reports on the formation paramagnetic intermediates when *p*-chloranil was adsorbed on the surface of TiO_2.[63] Such intermediates may play a role in the electron transport at the interfaces, thus improving the performance of the device. The TiO_2 sample used in the present studies did not give paramagnetic species with *p*-chloranil. However, we have also constructed the cell without using other donors. Interestingly, the cells constructed using the metal oxides TiO_2, Al_2O_3 and ZnO in the configurations shown in Figure 17a and 17b without using donor amines or amide did produce power with TiO_2 giving higher power when it is present in the middle PC layers (Figure 17b). The results indicate that the metal oxides transfer electron to *p*-chloranil as visualized in Figure 17e. This may also play a role in the transport of charges in the cells using donors.

We have observed that in the cells constructed using different donors and *p*-chloranil acceptor (Figure 15 and Figure 17), the power output decreases with time. Possibly, the chloranil radical anion may get deposited on the Al electrode and the *p*-chloranil may not fully dissolve back in the PC solvent (only 0.03 g *p*-chloranil soluble in 1 mL PC), thus preventing the reversible formation of amine or amide radical cation and *p*-chloranil radical anion.

The *p*-chloranil has a very high electron affinity (EA) of 2.78eV.[64] Interestingly, it was reported that anion radicals of molecules with lower electron affinity are solvated to more extent.[64a] Therefore, we have carried out experiments using *p*-benzoquinone (BQ) which has lower electron affinity (EA=1.91eV) to examine whether the chloranil anion radical can transfer electron to BQ to form the corresponding radical anion for further electron transport to the Al electrode. Also, the BQ is more soluble in PC solvent (0.1 g BQ soluble in 1 mL PC) which may be also helpful. We have carried out experiments by

constructing the cell in two different configurations, Figure 18a and 18b. Some improvements were observed in the power outputs, but still the Pmax values decreased with time (Figure 18a and 18b). Presumably, the more soluble BQ accepts electrons from *p*-chloranil anion radical effectively for transporting to the Al electrode improving the power output to some extent. The results of cells 18a and 18b are summarized in Table ES 5, entries 1-10.

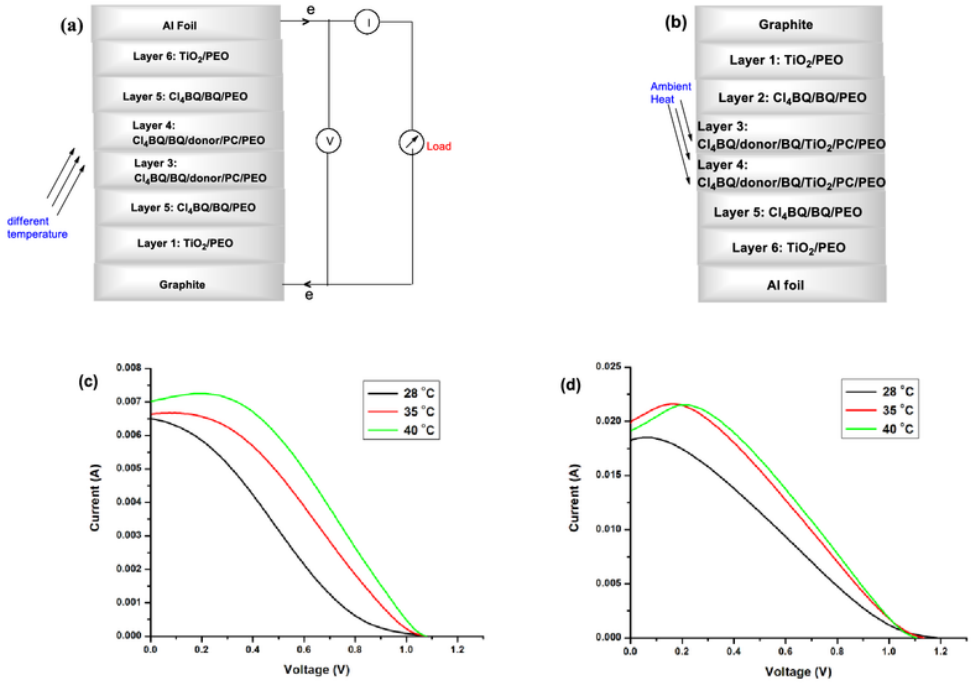

1 h after packing

Donor	Pmax(mW)/FF(40 °C)	Donor	Pmax(mW)/FF(40 °C)
TMPDA	2.175/0.276	TMPDA	1.614/0.282
TPA	1.752/0.240	TPA	0.939/0.219
DABCO	5.391/0.391	DABCO	4.806/0.432
DIPEA	8.229/0.229	DIPEA	11.74/0.296
DiPrBA	1.714/0.243	DiPrBA	1.871/0.232

48 h after packing

Donor	Pmax(mW)/FF(40 °C)	Donor	Pmax(mW)/FF(40 °C)
TMPDA	1.205/0.273	TMPDA	1.299/0.263
TPA	1.216/0.240	TPA	0.728/0.219
DABCO	**3.023/0.399**	DABCO	3.776/0.434
DIPEA	2.074/0.231	**DIPEA**	**8.338/0.394**
DiPrBA	1.534/0.258	DiPrBA	1.411/0.243

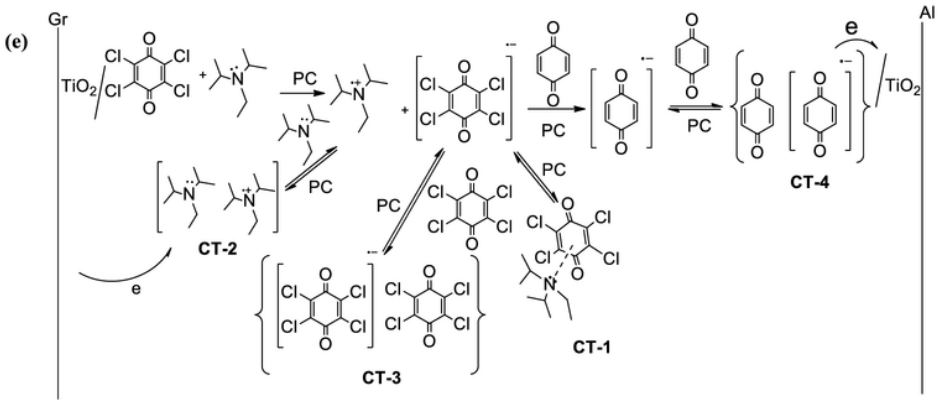

Figure 18. (a) Schematic diagrams of multi-layer cell using BQ along with *p*-chloranil without TiO_2 in PC layer (b) multilayer cell using BQ along with *p*-chloranil with TiO_2 in PC layer (c) Representative IV curve for the cell (Table ES5, entry 3, DABCO donor) and (d) Representative IV curve for the cells (Table ES5, entry 9, DIPEA donor) (e) Tentative mechanism for electron transport to the electrodes via D/D.+ and A-/A exchange reactions.

As discussed in Chapter 3, epr spectral studies indicated that the radical ions are transformed to charge transfer complexes with time. This could account for the reduction of current and Pmax values with time as the concentration of radical ions would be lesser with time. One way to prevent the formation of such charge transfer complexes is to remove the charges from the radical ions by using the cells to charge a rechargeable battery. The results obtained on the performance of the cells while charging a rechargeable Ni-Cd battery is summarized in Table 1.

The performance of the cells with configurations as in Figures 18a and 18b using BQ improved when the cells were used for charging batteries (Table 1, entries 3 and 4) compared to cells with configurations without using BQ (Figures 15a and 15b, Table 1,

entries 1 and 2) indicating that the BQ may transport the electron from the *p*-chloranil radical anion as it is formed thus preventing the formation of the corresponding CT complex which otherwise would reduce the concentration of radical ions with time. The electron acceptor BQ would accept electron from the *p*-chloranil radical anion as the corresponding anion radical formed from these compounds with lower EA are expected to interact with solvents to more extent, preventing the formation of CT complex. In case of DABCO (Table 1, entry 5) there was not much power output was observed. This may be due to the formation of stronger charge transfer complex with *p*-chloranil thus preventing the reversible reaction for charge transport. The donor DIPEA gives higher power output for longer time in these configurations compared to other donors. This may be due to the formation of more amount of radical ion pairs in case reaction of DIPEA with *p*-chloranil as revealed by epr spectroscopic studies. Further, it is sterically hindered and hence formation of CT 1 complex may be also difficult.

Table 1. Performance of Cells by Charging Ni-Cd Battery after packing.[a]

entry	Figure/Donor	Pmax/mW/FF at 40 °C/1 h	Pmax/mW/FF at 40 °C/48 h	Pmax/mW/FF at 40 °C/144 h
1[b]	15(a)/DIPEA	8.988/0.300	2.893/0.473	1.738/0.391
2[b]	15(b)/DIPEA/TiO_2	7.626/0.286	2.911/0.437	2.027/0.366
3[c]	18(a)/DIPEA/BQ	17.49/0.189	13.46/0.239	14.57/0.260
4[c]	18(b)/DIPEA/BQ/TiO_2	13.21/0.172	12.77/0.270	10.65/0.277
5[c]	18(b)/DABCO/BQ/TiO_2	4.022/0.413	2.733/0.316	1.291/0.160
6[c]	18(b)/TMPDA/BQ/TiO_2	1.883/0.279	0.620/0.249	0.373/0.248
7[c]	18(b)/TPA/BQ/TiO_2	0.985/0.255	0.855/0.231	0.698/0.218
8[c]	18(b)/DiPrBA/BQ/TiO_2	2.606/0.238	1.660/0.234	0.592/0.223

[a]After packing the cell was connected immediately to charge a Ni-Cd battery through Zener diode and disconnected while carry out the IV-curve measurement (Table ES6 and ES7). The battery connection was removed from the cell after 48 h. [b]Configuration without BQ. [c]Configuration with BQ.

Also, charging the rechargeable battery would lead to removal of charges from the radical ions, resulting in the recycling of the neutral species for continuous reactions. The donors TMPDA, TPA and DiPrBA which are relatively weak donors and also produce lower power output as concentration of radical ion formed may also be lower (Table 1, entries 6, 7 and 8).

In recent years, there have been several reports on the conversion of low-grade waste heat (<130 °C) to electricity by thermally regenerative electrochemical cycles.[65a,b] A thermoelectrochemical device based on ferrocene-iodine redox couple was also reported, but the device produced only μW/m^2 power with respect to the electrode surface area.[65c] The power density of the cell in this case was calculated by using the amount of power produced with respect to the electrode surface area. The cell constructed from the donor DIPEA (Table 1, entry 3) gave power density at 40 °C was 0.5384 mW/cm^2 or 5.384 W/m^2 (13.46 mW (Pmax)/25 cm^2 (electrode surface area)). The methods reported in the literature for construction of the devices are very complex compared to methods described here. In the present case, the device utilizes very inexpensive materials that are already manufactured in large scale. Further, since there are established methods are available for heating air at even below 0 °C to 40 °C using solar radiation and methods available for storing solar heat in simple chemicals like aq. NaOH, $CaCl_2$ and methods are also available for using these solar heat stored materials for heating the air to 40 °C to 60 °C,[66] the present low/ambient heat harvesting electricity producing cell device has potential for use 24x7 in all seasons, day and night.

4.3 Conclusions

We have developed a simple method and device for constructing the electrochemical cell based on ground state electron transfer reaction of amine or amide donor and *p*-chloranil acceptor in various configurations. These low/ambient heat harvesting electricity producing and air cooling cells can be readily stacked.

The present case, the device utilizes very inexpensive materials and hence has potential for household, automobile and large scale applications. However, long term performance of this cell device remains to be established and there is plenty of scope for further research and developments to improve the performance of this device. Accordingly, the low/ambient heat to electricity converting electrochemical system disclosed here has the potential to meet the increasing energy requirements without having to burn fossil fuels. Further systematic studies on improve the stability of the cells with different electron donors and acceptors are expected to lead to the discovery of cost effective stable electrochemical cells.

Development of Synthetic Methods and Electrochemical Cells Based on Organic Electron Transfer Reactions

ORIGINALITY REPORT

13%	3%	11%	1%
SIMILARITY INDEX	INTERNET SOURCES	PUBLICATIONS	STUDENT PAPERS

PRIMARY SOURCES

1	Mariappan Periasamy, Polimera Obula Reddy, Masilamani Shanmugaraja. "Organoboranes Oxidation and Lewis Base Borane Complexes Preparation Using Oxygen Adsorbed Carbon Materials", ChemistrySelect, 2017 Publication	4%
2	Mariappan Periasamy, Masilamani Shanmugaraja, Polimera Obula Reddy, Modala Ramusagar, Gunda Ananda Rao. "Synthetic Transformations Using Molecular Oxygen-Doped Carbon Materials", The Journal of Organic Chemistry, 2017 Publication	2%
3	uu.diva-portal.org Internet Source	<1%
4	www.ijcep.com Internet Source	<1%
5	Sergiy V. Rosokha, Jay K. Kochi. "Fresh Look at Electron-Transfer Mechanisms via the	<1%

Donor/Acceptor Bindings in the Critical Encounter Complex", Accounts of Chemical Research, 2008
Publication

---

6 Ahmed, K., Q.-L. Zhao, Y. Matsuya, D.-Y. Yu, T. L. Salunga, H. Nemoto, and T. Kondo. "Enhancement of macrosphelide-induced apoptosis by mild hyperthermia", International Journal of Hyperthermia, 2007.
Publication <1%

---

7 Fan, Rundong, Yuan Huang, Ligang Wang, Liang Li, Guanhaojie Zheng, and Huanping Zhou. "The Progress of Interface Design in Perovskite-Based Solar Cells", Advanced Energy Materials, 2016.
Publication <1%

---

8 Serap Günes. "Organic Solar Cells and Their Nanostructural Improvement", Green Energy and Technology, 2011
Publication <1%

---

9 須賀 健雄. "酸化還元ラジカル高分子 : 合成と有機二次電池への展開", [出版者不明], 2009.
Publication <1%

---

10 Xianwu Zeng, Yong X.. "Chapter 8 Nanocomposites for Photovoltaic Energy Conversion", InTech, 2011
Publication <1%

11	Submitted to Institute of Technology, Nirma University Student Paper	<1%
12	Sajjad Dadashi-Silab, Sean Doran, Yusuf Yagci. "Photoinduced Electron Transfer Reactions for Macromolecular Syntheses", Chemical Reviews, 2016 Publication	<1%
13	Roger J. Mortimer. "Electrochromic Polymers", Encyclopedia of Polymer Science and Technology, 03/15/2004 Publication	<1%
14	Submitted to Jamia Milia Islamia University Student Paper	<1%
15	vdocuments.site Internet Source	<1%
16	Xue, Wei Wei, Xiu Qin Zhang, Qiang Chen, Ji Jin, and Guo Yuan Lu. "Synthesis and Crystal Structure Hindered Amine with Methaerylate", Advanced Materials Research, 2015. Publication	<1%
17	Shun-Ichi Mitomo. "The Reactions of Sulfilimines withTCNQ and their Characteristic Charge-Transfer Complexes as Products", Molecular Crystals and Liquid Crystals, 4/1/1998	<1%

Publication

18	Submitted to Jawaharlal Nehru Technological University Student Paper	<1%
19	www.jove.com Internet Source	<1%
20	Duoli Sun, Sergiy V. Rosokha, Jay K. Kochi. " Reversible Interchange of Charge-Transfer versus Electron-Transfer States in Organic Electron Transfer via Cross-Exchanges between Diamagnetic (Donor/Acceptor) Dyads ", The Journal of Physical Chemistry B, 2007 Publication	<1%
21	thieme-connect.de Internet Source	<1%
22	Anees A., M. Alhoshan, M.S. Alsalhi, A.S. Aldwayy. "Chapter 2 Nanostructured Metal Oxides Based Enzymatic Electrochemical Biosensors", InTech, 2010 Publication	<1%
23	MacManus-Spencer, Laura A., Betsy L. Edhlund, and Kristopher McNeill. "Singlet Oxygen Production in the Reaction of Superoxide with Organic Peroxides", The Journal of Organic Chemistry, 2006. Publication	<1%

24	J. W. Verhoeven. "Glossary of terms used in photochemistry (IUPAC Recommendations 1996)", Pure and Applied Chemistry, 1996 Publication	<1%
25	Bai, Yu, Iván Mora-Seró, Filippo De Angelis, Juan Bisquert, and Peng Wang. "Titanium Dioxide Nanomaterials for Photovoltaic Applications", Chemical Reviews Publication	<1%
26	www.pearsonpatents.com Internet Source	<1%
27	www.mdpi.com Internet Source	<1%
28	Michael P. Barham, Peter G. Enticott, Russell Conduit, Jarrad A.G. Lum. "Transcranial electrical stimulation during sleep enhances declarative (but not procedural) memory consolidation: Evidence from a meta-analysis", Neuroscience & Biobehavioral Reviews, 2016 Publication	<1%
29	Submitted to Middle East Technical University Student Paper	<1%
30	Bird, C. L., and A. T. Kuhn. "Electrochemistry of the viologens", Chemical Society Reviews, 1981. Publication	<1%

31	Ljubisa R. Radovic, Bradley Bockrath. "On the Chemical Nature of Graphene Edges: Origin of Stability and Potential for Magnetism in Carbon Materials", Journal of the American Chemical Society, 2005 Publication	<1%
32	Gassner, George, Lihua Wang, Christopher Batie, and David P. Ballou. "Reaction of Phthalate Dioxygenase Reductase with NADH and NAD: Kinetic and Spectral Characterization of Intermediates", Biochemistry, 1994. Publication	<1%
33	Reddy, . "Organic and dye-sensitized solar cells", Solar Power Generation Technology New Concepts & Policy, 2012. Publication	<1%
34	Chunhe Yang, Erjun Zhou, Shoji Miyanishi, Kazuhito Hashimoto, Keisuke Tajima. "Preparation of Active Layers in Polymer Solar Cells by Aerosol Jet Printing", ACS Applied Materials & Interfaces, 2011 Publication	<1%
35	redalyc.uaemex.mx Internet Source	<1%
36	V. Vishnyakov, S. E. Donnelly, G. Carter. "Scanning tunnelling microscopy observations of the evolution of small-scale topography on	<1%

gold surfaces following irradiation with low-energy argon ions", Philosophical Magazine B, 2006
Publication

37	www.freepatentsonline.com Internet Source	<1%
38	Submitted to University of KwaZulu-Natal Student Paper	<1%
39	ubm.opus.hbz-nrw.de Internet Source	<1%
40	Fauzia, Vivi, Akrajas Ali Umar, Muhamad Mat Salleh, and Muhammad Yahaya. "Study Phase Separation of Donor:Acceptor in Inkjet Printed Thin Films of Bulk Heterojunction Organic Solar Cells Using AFM Phase Imaging", Advanced Materials Research, 2011. Publication	<1%
41	Submitted to University of California, Los Angeles Student Paper	<1%
42	Submitted to Heriot-Watt University Student Paper	<1%
43	www.slideshare.net Internet Source	<1%
44	www.solenergi.dk Internet Source	<1%

45	Toki, Susumu, Shintaro Komitsu, Sachiko Tojo, Setsuo Takamuku, Nobuyuki Ichinose, Kazuhiko Mizuno, and Yoshio Otsuji. "Cis-trans isomerization of 1,2-bis(4-methoxyphenyl)-cyclopropanes via a cationic chain mechanism.", Chemistry Letters, 1988. Publication	<1%
46	Sergiy V. Rosokha, Jay K. Kochi. "Continuum of Outer- and Inner-Sphere Mechanisms for Organic Electron Transfer. Steric Modulation of the Precursor Complex in Paramagnetic (Ion-Radical) Self-Exchanges", Journal of the American Chemical Society, 2007 Publication	<1%
47	eprints.nottingham.ac.uk Internet Source	<1%
48	Cui, Zheng. "Printed Organic Thin Film Solar Cells", Printed Electronics, 2016. Publication	<1%
49	K Nakahara. "Rechargeable batteries with organic radical cathodes", Chemical Physics Letters, 20020627 Publication	<1%
50	Submitted to Ewha Womans University Student Paper	<1%
51	Submitted to The Hong Kong Polytechnic	

	University Student Paper	<1%
52	www.thieme-connect.de Internet Source	<1%
53	www.google.com Internet Source	<1%
54	Esmaeilpour, Mohsen, Jaber Javidi, Farzaneh Dehghani, and Saeed Zahmatkesh. "One-pot synthesis of multisubstituted imidazoles catalyzed by Dendrimer-PWAn nanoparticles under solvent-free conditions and ultrasonic irradiation", Research on Chemical Intermediates, 2016. Publication	<1%
55	pesquisa.bvsalud.org Internet Source	<1%
56	en.wikipedia.org Internet Source	<1%
57	高橋 悠輔. "Radical-bearing redox polymers and their application to electrochromic cell", [出版者不明], 2009. Publication	<1%
58	Submitted to Windermere Preparatory School Student Paper	<1%
59	www.omicsonline.com	

Internet Source

<1%

60 www.cheric.org

Internet Source

<1%

Exclude quotes	On	Exclude matches	< 10 words
Exclude bibliography	On		